An investigation of the role of *Arabidopsis thaliana* Plant Natriuretic Peptide *in planta*

by

Lara Elizabeth Donaldson

Thesis presented for the degree of **Doctor of Philosophy**

in the Department of Molecular and Cell Biology

University of Cape Town

May 2009

TABLE OF CONTENTS

CHAPTER 2: SECOND MESSENGER SIGNALLING IN RESPONSE TO WATER AND ION STRESSES

CHAPTER 3: CHARACTERIZATION OF AN AtPNP-A MUTANT

3.1 Introduction

3.2 Materials and methods

CHAPTER 4: *AtPNP-A* TRANSCRIPTOMICS

4.1 Introduction

4.2 Materials and Methods

4.3 Results

4.4 Discussion

CHAPTER 5: GENERAL DISCUSSION

5.1 Contribution to the field

CHAPTER 6: REFERENCES

ACKNOWLEDGEMENTS

I would like to thank my supervisors Katherine Denby, Chris Gehring and Rob Ingle. Katherine, you have inspired me to be a researcher and pursue the study of plant molecular biology. Thank you for your helpful insights, guidance and critical thinking that has helped to become a scientist. To Chris I must say thank you for your constant support and encouragement and for always being available and responsive. I owe a big thank you to Rob Ingle for critical reading of my thesis manuscript and for many helpful discussions. I would also like to thank Helen Irving for the pleasure of working with you and for facilitating my time in Australia and to Dave Cahill for allowing me the opportunity to work in your lab.

I must thank those people that have helped me with my laboratory work Ndiko Ludidi, Oziniel Ruzvidzo, Monique Morse, Yu-Hua Wang, Desma Grice, Paige Dando, Lara Reale, Rene Bastian and Sergey Shabala.

Thank you to my friends in the lab especially Maryke and Lindsay for always understanding. Thank you also to Nicki, Shane, Linda, Joseph, Rachel and Inonge, you have all been wonderful to work together with and been great friends and I will always remember this time we have shared.

To all of my friends outside of university, especially Rod, Marisa, Elm, Jamie, Jacs and Tom, I feel privileged to know you. Each one of you are a special part of my life and I couldn't have done this without all of those much needed breaks in between.

To all of my family, especially Mom and Dad, you have shaped the person that I have become and taught me to believe in myself. Thank you for always being there for me, believing in me and for your endless love and support. Thank you to my brother Peter, for always being strong, logical, supportive and encouraging. Also I must say a big thank you to Andrew and my Uncle John for printing my thesis.

Finally I want to say a very special thank you to Stuart for reading my thesis manuscript, for all the helpful discussions, for your guidance, encouragement, love and for supporting me on so many different levels. Thank you for enduring this process with me. I would not have been able to do it without you. There are not enough words to express my love and gratitude.

PUBLICATIONS

The results presented in chapter 2 have been published:

Donaldson L.E., Ludidi N.N., Knight M.R., Gehring C.A. and Denby K.J. (2004) Salt and osmotic stress cause rapid increases in *Arabidopsis thaliana* cGMP levels. *FEBS Letters* **569** (317-320)

The results presented in chapter 4 have been published:

Meier S.K., Bastian R., Donaldson L.E., Murray S.L., Bajic V.B. and Gehring C.A. Co-expression and promoter content analysis assign a role in biotic and abiotic stress responses to plant natriuretic peptides. *BMC Plant Biology* **8**:24

ABSTRACT

An investigation of the role of *Arabidopsis thaliana* Plant Natriuretic Peptide *in planta*

Lara Elizabeth Donaldson

Thesis presented for the degree of Doctor of Philosophy, May 2009

The sessile nature of plants demands that they respond appropriately to changes in their environment (stresses) in order to survive. Critical to survival is the maintenance of water and ion homeostasis. The mechanisms by which plants achieve this are poorly understood. Traditionally plant stress responses were thought to be communicated by five classical plant hormones – auxin, cytokine, gibberellic acid, absisic acid and ethylene. Nowadays a plethora of other molecules are known to fulfil this function including nitric oxide, salicylic acid, jasmonic acid, brassinosteroids and peptide hormones. Plant natriuretic peptides have been proposed to be peptide hormones involved in maintaining water and ion homeostasis in plants. Evidence for this has been provided by studies of plant responses to exogenous natriuretic peptide treatment, however a demonstration of their function *in planta* remains outstanding. This study was undertaken to gain insight into the mechanisms regulating water and ion homeostasis in *Arabdopsis* by examining second messenger responses to stresses that perturb water and ion homeostasis; characterization of an *Arabidopsis thaliana* plant natriuretic peptide (*atpnp-a*) mutant and transcriptome analysis of *AtPNP-A*, in order to establish whether AtPNP-A plays a role in maintaining water and ion homeostasis *in planta*. Results indicated that recombinant AtPNP-A induces second messenger responses reminiscent of the response to NaCl, suggesting that AtPNP-A may play a signalling role in response to disturbances in water and ion homeostasis. In support of this, characterization of an *atpnp-a* mutant revealed that AtPNP-A is likely to be involved in processes that require adjustments to water and ion homeostasis including cell expansion, stomatal opening and NaCl and osmotic stress responses, consistent with reported responses to natriuretic peptide treatment. Furthermore, the *atpnp-a* mutant revealed a role for AtPNP-A in the defence response. Evidence to support this came from the computational analysis of *AtPNP-A* expression which correlates with genes involved in the defence response. Additionally, the transcriptome response to recombinant AtPNP-A treatment further implicated the involvement of AtPNP-A in the defence response. Therefore AtPNP-A is hypothesized to play a role in growth, abiotic and biotic stress responses that enables the plant to mount an integrated response to the environment.

LIST OF ABBREVIATIONS

°C	degrees Celcius
aa	amino acid(s)
ABA	abscisic acid
ANP	atrial natriuretic peptide
ATP	adenosine 5-triphosphate
AtPNP-A	*Arabidopsis thaliana* PNP-A
Avr	avirulence
BAPTA	bis(2-aminophenoxy)-ethane-*N,N,N',N'*-tetraacetic acid
bp	base pair
BNP	B-type NP
$[Ca^{2+}]_{cyt}$	cytosolic free calcium concentration
CaMV	Cauliflower Mosaic Virus
CC-NB-LRR	coiled-coil nucleotide binding leucine rich repeat
cADPR	cyclic adenosine diphosphate ribose
cAMP	5'3'-cyclic adenosine monophosphate
cDNA	complementary DNA
cGMP	5'3'-cyclic guanosine monophosphate
CHX	cycloheximide
CN	cyclic nucleotide
CNBD	cyclic nucleotide binding domain
CNGC	cyclic nucleotide gated channel
CNP	C-type NP
cfu	colony forming units
DEPC	diethylpyrocarbonate
dH_2O	deionized water
DNA	deoxyribonucleic acid
dNTP	deoxynucleosidetriphosphate
DTT	dithiothreitol
ECGG	expression correlated gene group
EDTA	ethylenediamine tetraacetic acid
EGTA	ethylene glycol tetraacetic acid
ETI	effector-triggered immunity
EtOH	ethanol
FW	fresh weight

g	gram
g	gravity constant (9.81 $m.s^{-1}$)
GA	gibberellic acid
GC	guanylyl cyclase
GO	gene ontology
GOI	gene of interest
hr	hour(s)
HR	hypersensitive response
IP_3	inositol 1,4,5-trisphosphate
irPNP	immunoreactant NP
JA	jasmonic acid
kb	kilobase
kDa	kilodalton
l	litre
LB	Luria Bertani media
LY 83583	6-anilino-5,8-quinolinequinone
LRR RLK	leucine rich repeat receptor like kinase
m	metre
M	molar
MAPK(K)	mitogen activated protein kinase (kinase)
MCP	mesophyll cell protoplasts
MeOH	methanol
min	minute(s)
MOPS	4-morpholinepropanesulfonic acid
mRNA	messenger RNA
MS	Murashige and Skoog media
MW	molecular weight
NO	nitric oxide
NP	natriuretic peptide
NPR	natriuretic peptide receptor
NS 2028	4H-8-bromo-1,2,4-oxadiazolo (3,4-d) benz(b) (1,4) oxazin-a-one
NSCC	non-selective cation channels
nts	nucleotides
OD	optical density
ODQ	1H-[1,2,4] oxadiazolo [4,3-a] quinoxaline-1-one
p	probability
PAMP	pathogen-associated molecular pattern

PCD	programmed cell death
PCR	polymerase chain reaction
PDE	phosphodiesterase
P_i	inorganic phosphate
PKG	cGMP dependent protein kinase
PN	Plant Nutrient media
PNP	plant natriuretic peptide
ppm	parts per million
PR	pathogenesis related
Pst	*Pseudomonas syringae*
PTI	PAMP-triggered immunity
pv.	pathovar
R gene	resistance gene
r	correlation value
ROS	reactive oxygen species
RNA	ribonucleic acid
RT-PCR	reverse transcriptase PCR
s	second(s)
SA	salicylic acid
SAR	systemic acquired resistance
SDS	sodium dodecyl sulphate
SOS	salt overly sensitive
sp.	species
T-DNA	transfer DNA
TIR-NB-LRR	toll-interleukin-1 receptor-type nucleotide binding leucine rich repeat
TFBS	transcription factor binding site
TTSS	type three secretion system
U	units
UBQ	ubiquitin conjugating enzyme 21
UTR	untranslated region
UV	ultraviolet
vol	volume
v/v	volume per volume
WAK	wall-associated kinase
WRKY	WRKY DNA binding protein
w/v	weight per volume
XacPNP	*Xanthomonas axonopodis* pv. *citri* PNP

CHAPTER 1

INTRODUCTION

CHAPTER 1: INTRODUCTION

1.1 ANIMAL NATRIURETIC PEPTIDES

1.1.1 The natriuretic peptide family

Natriuretic peptides (NPs) are a family of structurally related peptide hormones that promote natriuresis and diuresis (renal sodium and water excretion) and vasorelaxation in order to modulate body fluid volume and blood pressure (Pandey, 2005). The NPs are part of a natriuretic/diuretic/vasodilatory hormonal system that is counterbalanced by the opposing actions of antinatriuretic/antidiuretic/vasopressor hormones in order to achieve cardiovascular homeostasis (Richards, 2004). NPs were first discovered from heart atrial extracts that were able to stimulate potent natriuresis and diuresis and lower blood pressure when intravenously injected into rats (de Bold *et al.*, 1981). This established the heart as an endocrine organ and provided the first link between the heart and the kidney. A few years later, the atrial natriuretic factor, now known as atrial NP (ANP), was purified and its structure described (Flynn *et al.*, 1983). Two additional peptides with similar biological activity and structure were then isolated from porcine brain and these were named brain or B-type NP (BNP) and C-type NP (CNP) (Sudoh *et al.*, 1988; Sudoh *et al.*, 1990). The main source of BNP was subsequently found to be the heart ventricle whereas CNP was found in abundance in the vascular endothelium (blood vessel wall) and central nervous system (CNS) (Suga *et al.*, 1992). The NP family is comprised of these three principal members: ANP, BNP and CNP.

1.1.1.1 Processing and structure

ANP, BNP and CNP, are encoded by discreet genes that are similar in their primary structure and processing (McGrath and de Bold, 2005) (Figure 1.1). Each gene is composed of three exons that encode a preprohormone. This is subjected to two rounds of proteolytic processing, firstly to remove the signal peptide yielding the prohormone and secondly to release the mature C-terminal peptide from the N-terminal propeptide (Baxter, 2004b; McGrath and de Bold, 2005). The C-terminal peptide is the biologically active form of the hormone while the N-terminal prohormone fragments are generally considered not to be biologically active (Takei, 2001). However Vesely and colleagues have ascribed some functions to the N-terminal proANP fragments (Vesely *et al.*, 1994) (Figure 1.1). The C-terminal peptide adopts a ring structure that is absolutely required for its biological activity, as a result of an intramolecular disulphide bond between conserved cysteine residues in the –CFGXXXDRIXXXXGLGC- consensus sequence (Cea, 2005; Kuhn, 2004). Most similar in the sequence contained within their rings, ANP, BNP and CNP differ in their flanking sequences which may be involved in receptor recognition (He *et al.*, 2006) (Figure 1.1, inset).

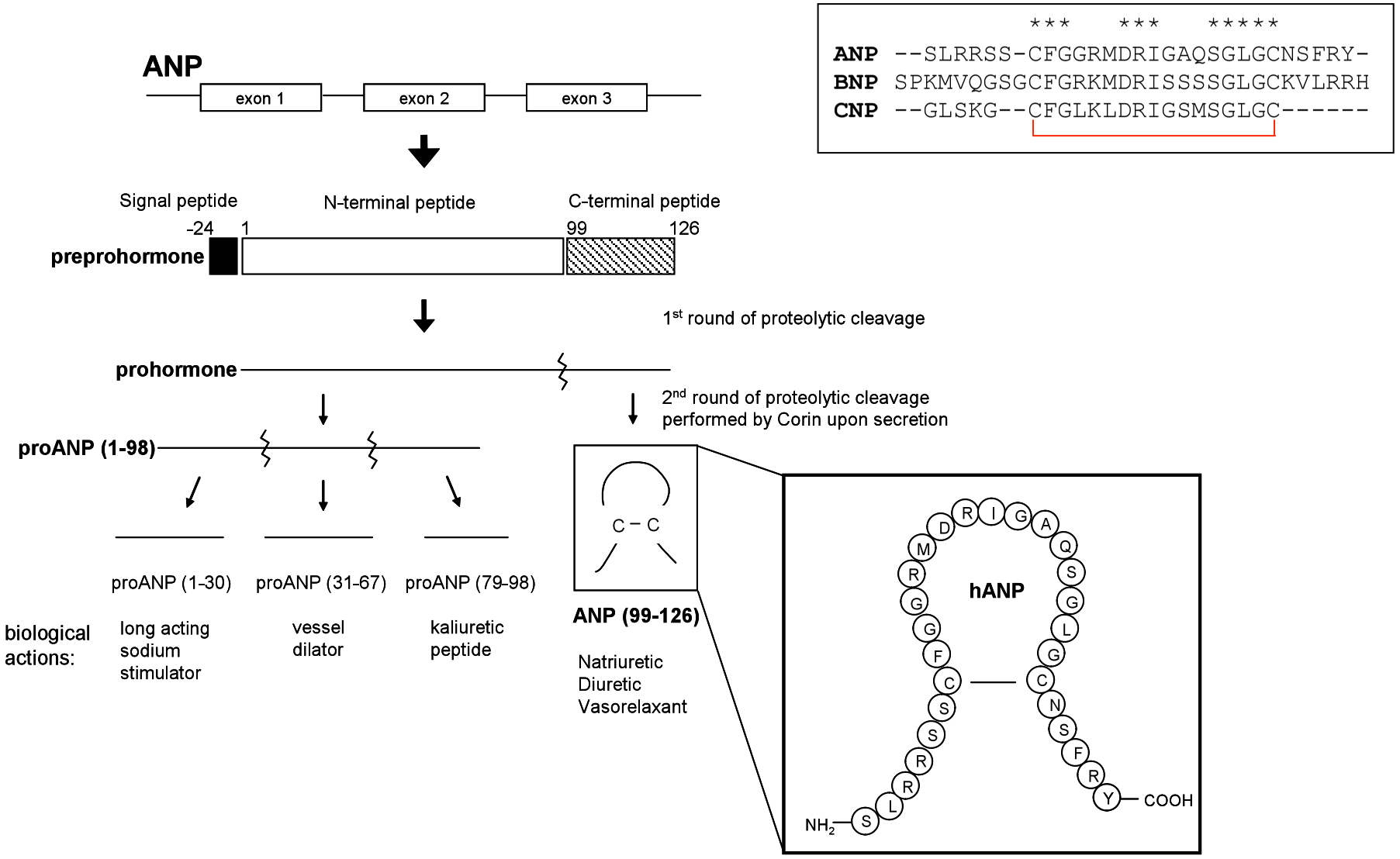

Figure 1.1. Structure and processing of ANP Human ANP, BNP and CNP are aligned in the inset. * denotes conserved aa while the disulphide bond is shown in red.

1.1.1.2 Cardiac NPs: ANP and BNP

The cardiac hormones, ANP and BNP are stored alongside one another in the atrial myocytes (Nakamura *et al.*, 1991). The ANP prohormone is the main stored form of the hormone whereas it is mature BNP that is stored (Baxter, 2004a). Even though BNP levels are higher in the atria compared to the ventricles, the greater size of the ventricle makes this the main site of BNP synthesis and release (LaPointe, 2005). Mature BNP is not stored in the ventricle but is constitutively released (Richards, 2004). ANP and BNP are secreted from the heart atria and ventricle respectively into the bloodstream, resulting in basal levels of ANP (approximately 10 fmol/ml) that are higher than those of BNP (approximately 1 fmol/ml) (Potter *et al.*, 2006). In response to increased blood volume, synthesis and secretion of NPs is further stimulated (Baxter, 2004a). This is most noticeable in cardiac disease states in which ANP and BNP levels are elevated, with the increase in BNP being so dramatic that its concentration can come to exceed that of ANP (Potter *et al.*, 2006). Once in the bloodstream ANP and BNP act in an endocrine manner to induce natriuresis and diuresis in the kidney and vasorelaxation in the blood vessels to lower blood pressure (Ahluwalia *et al.*, 2004). ANP and BNP are primarily cardiac hormones but have also been found to be synthesized, albeit at much lower concentrations, at extracardiac sites (for example the kidney, lung, adrenal gland and brain) where they are believed to exert local effects (Kuhn, 2004). Even though ANP and BNP have similar distributions and elicit similar responses, studies from knockout (KO) mice suggest that they have distinct biological functions (Kuhn, 2004; Potter *et al.*, 2006). In particular ANP KO mice are hypertensive while BNP KO mice are normotensive however display cardiac fibrosis. This suggests that ANP acts as the classic cardiac hormone while BNP plays more of a cardioprotective role in the heart (Kuhn, 2004; Potter *et al.*, 2006).

1.1.1.3 Peripheral CNP

In contrast, the role of CNP is less well understood. Two forms of the peripheral CNP hormone have been isolated: CNP-53 and CNP-22, with the latter being contained within the former (Baxter, 2004a). CNP-22 is generally considered to be the biologically active molecule however there have been some reports that both molecules exert similar effects but differ in their distribution (Chauhan *et al.*, 2004; Pejchalova *et al.*, 2007; Potter *et al.*, 2006). Unlike the cardiac NPs, CNP is barely detected in the heart and circulation and does not induce natriuresis and diuresis (Ahluwalia *et al.*, 2004; Pandey, 2005). Instead CNP is found in the vascular endothelium. Here CNP is not stored but is secreted from endothelial cells in response to endothelial agonists and cytokines (Barr *et al.*, 1996; Chauhan *et al.*, 2004). This induces vasorelaxation and inhibits cell proliferation. Therefore CNP is suggested to be an autocrine/paracrine regulator of vascular remodeling to control local blood flow (Ahluwalia *et*

al., 2004; Kuhn, 2004) Dwarf phenotypes of CNP KO mice suggest that CNP also plays an important role in bone growth (Kuhn, 2005; Pejchalova *et al.*, 2007).

1.1.1.4 Structurally related peptides

In addition to the principal NP family members, other structurally related peptides have been described including: dendroaspis NP (DNP) - a NP isolated from green mamba venom (Schweitz *et al.*, 1992), urodilatin - an alternatively processed form of ANP found exclusively in the kidney (Forssmann *et al.*, 2001), guanylin and uroguanylin - intestinal peptides involved in local fluid and electrolyte balance (Sindic and Schlatter, 2005) and ostecrin - found in bone and muscle where it seems to modify local concentrations of CNP (Potter *et al.*, 2006), however these will not be further discussed here.

1.1.2 Natriuretic peptide receptors

Shortly after their discovery, NPs were shown to stimulate 5'3'-cyclic guanosine monophosphate (cGMP) production (Hamet *et al.*, 1984). Cross-linking studies revealed that NP-binding and guanylyl cyclase (GC) activity reside in the same molecule (Kuno *et al.*, 1986; Paul *et al.*, 1987). Subsequently, three NP receptor types (NPRs) were cloned: NPRA, NPRB and NPRC. In each of these receptors a single transmembrane domain separates the extracellular ligand-binding domain (ECD) from the intracellular region (Pandey, 2005) (Figure 1.2). In the case of NPRA and NPRB the intracellular region consists of a kinase homology domain (KHD), a dimerization domain and a GC catalytic domain (Potthast and Potter, 2005). NPRC differs in that it only has a short 37 amino acid (aa) cytoplasmic tail and lacks GC activity (Fuller *et al.*, 1988).

1.1.2.1 Signal transduction via NPRs

The NPRs exist as dimers that have repressed GC activity in the ligand-unbound state (Potter *et al.*, 2006). One hormone molecule binds per receptor dimer (He *et al.*, 2005; Misono *et al.*, 2005). Unlike other hormone receptors, ligand binding does not induce further dimerization but rather causes a novel hormone-induced rotation that transduces the signal across the membrane (Misono *et al.*, 2005). This rotation exposes an ATP binding site that overlaps with six phosphorylation sites in the intracellular KHD (Duda *et al.*, 2005). No phosphotransferase activity has been reported for the KHD, not surprisingly since it lacks a critical aspartate in the HXD motif that is conserved in all kinases (Potter and Hunter, 2001; Schulz, 2005). Instead the KHD appears to be involved in regulation of the GC domain (Pandey, 2005). Full receptor activation requires ATP binding to the KHD which induces a conformational change exposing the phosphorylation sites (Duda *et al.*, 2005). These sites are maximally phosphorylated in the basal state as is required for hormone responsiveness (Potthast and Potter, 2005).

Dephosphorylation of the exposed sites results in receptor desensitization and hormone dissociation (Potthast and Potter, 2005). However at the same time the ATP-induced conformational change brings the GC domains together allowing them to dimerize via the dimerization domain to form a catalytic site with two active sites per dimer (Duda *et al.*, 2005; Schulz, 2005). The GC then catalyzes the formation of cGMP from 5'-guanosine triphosphate (GTP).

1.1.2.2. The NPR GCs

The intracellular regions of NPRA and NPRB are the most conserved whereas the extracellular regions are less so, reflecting their different ligand-binding affinities but conserved signalling mechanism (Pandey, 2005; Schulz, 2005). Both ANP and BNP bind NPRA, while CNP binds NPRB (He *et al.*, 2006; Schulz, 2005) (Figure 1.2). Consistent with this NPRA is localized in the cardiovascular system and NPRA KO mice are hypertensive whereas NPRB is abundant in the CNS and endothelium and NPRB KO mice are dwarfed (Kuhn, 2004; Kuhn, 2005). Thus NPRA mediates classic cardiac actions of NPs while CNP acting via NPRB plays an important role in growth (Kuhn, 2004). Since most of the biological effects of NPs are mediated by cGMP, NPRA and NPRB are believed to be the main transducers of the NP signals (Baxter, 2004a; Cea, 2005).

1.1.2.3 NPRC and degradation of NPs

The ECD of NPRC is about 30% homologous to that of NPRA and NPRB (He *et al.*, 2006). NPRC is thought to be a clearance receptor that binds and internalizes the NPs for degradation. This is because it binds all NPs fairly indiscriminately, is widely distributed (can account for 95% of NP binding sites) and lacks the GC signalling domain (He *et al.*, 2005; Pandey, 2005). Although NPRC lacks the GC domain it does have G protein recognition sequences in its C-terminal tail that suggests it may signal through inhibition of adenylyl cyclase (AC) and stimulation of phosphatidyl inositol turnover (Anand-Srivastava, 2005). Internalization of NPRC is a constitutive ligand-independent process, after which NPs are degraded by the lysosome and the receptor is recycled to the cell surface (Nussenzveig *et al.*, 1990; Potter *et al.*, 2006). This is important for controlling local NP concentrations and mopping up excesses from circulation, exemplified by the fact that NPRC KO mice have reduced ability to clear I^{125}ANP and concentrate urine as well as being hypotensive and having skeletal deformities (Kuhn, 2005; Matsukawa *et al.*, 1999). In addition to NPRC, neutral endopeptidases (NEPs) degrade NPs. NEPs are ubiquitous and bind and are active against all NPs (Potter *et al.*, 2006). Hypotensive phenotypes of NEP KO mice are consistent with their role in NP clearance however these mice do not exhibit skeletal overgrowth suggesting that NEPs do not degrade CNP in the growth plate (Lu *et al.*, 1995; Potter *et al.*, 2006).

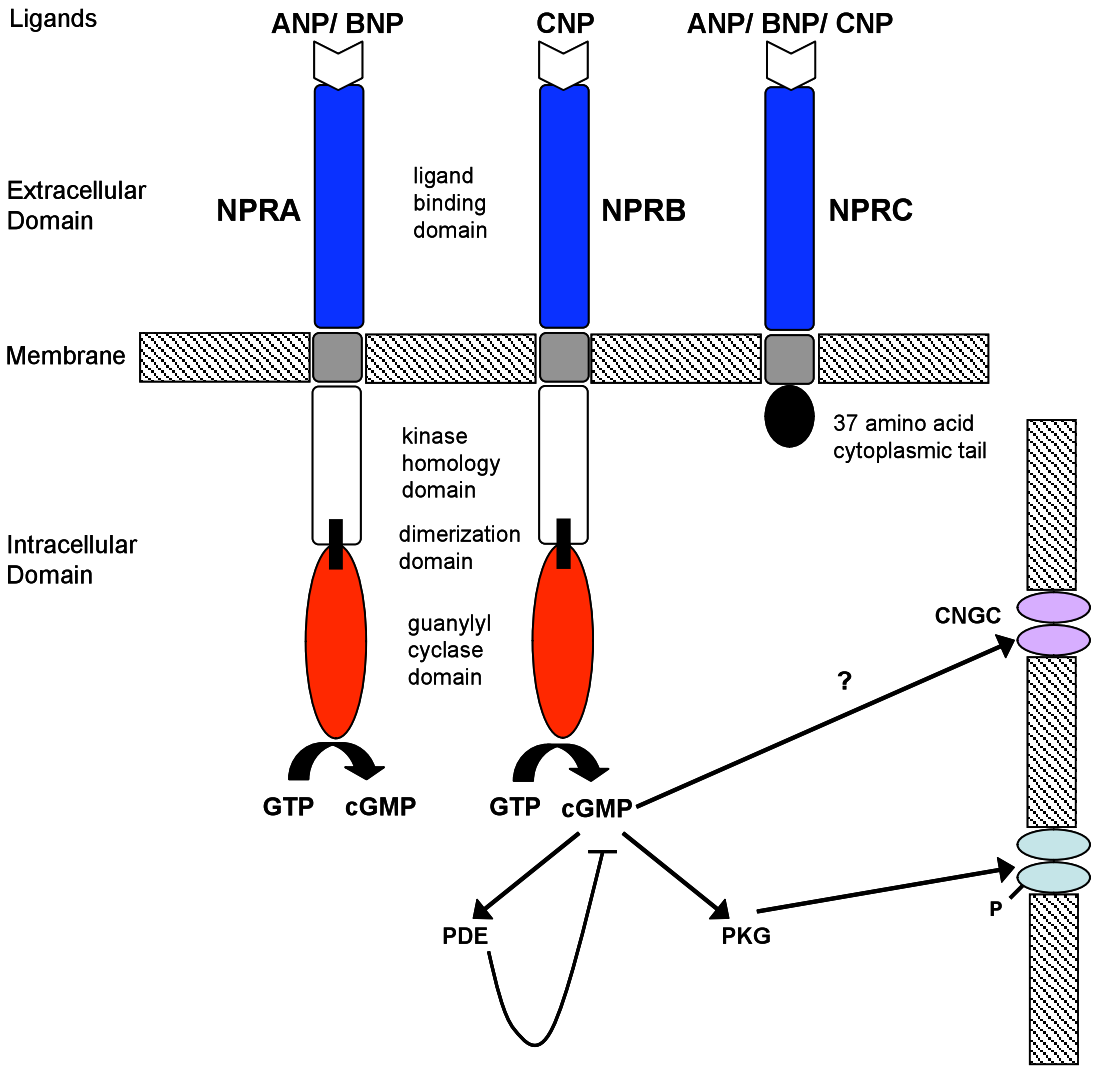

Figure 1.2. NP binding to NPRs initiates cGMP signalling

Ligand binding affinity and domain organization of the NPRs is depicted. Following receptor activation, a downstream cGMP signal transduction cascade is initiated via the cGMP effectors: PKG, PDE and CNGC.

1.1.3 Effectors of cGMP signalling

NPs played an important role in establishing cGMP signal transduction in animals (Duda *et al.*, 2005). In animals cGMP is produced by particulate GCs (NPRs and the guanylin receptor, GC-C) and by nitric oxide (NO)-inducible soluble GCs (Lucas *et al.*, 2000). There is some evidence for cross-talk between these GC types with one being able to compensate for the dysfunction of the other (Ahluwalia *et al.*, 2004; Madhani *et al.*, 2003) since CNP and NO both induce vascular smooth muscle cell (VSMC) relaxation. The cGMP produced acts through binding downstream effectors: cGMP dependent protein kinases (PKGs), phosphodiesterases (PDEs) and cyclic nucleotide gated channels (CNGCs) (Lucas *et al.*, 2000; Potter *et al.*, 2006) (Figure 1.2).

1.1.3.1 PKGs

The PKGs are considered to be the principal mediators of cGMP signalling (Baxter, 2004a). There are two types of PKGs which differ in their distribution and substrate selectivity: PKGI of which there are two alternatively spliced isoforms: α and β, and PKGII (Hofmann *et al.*, 2006; Potter *et al.*, 2006). These PKGs are composed of three domains: an N-terminal, a regulatory and a catalytic domain (Lucas *et al.*, 2000). The N-terminal domain targets the PKG to its substrate, is involved in dimerization and inhibits the catalytic domain in the absence of cGMP through a pseudosubstrate region (Hofmann *et al.*, 2006). Binding of cGMP to the regulatory domain releases this inhibition on the catalytic domain freeing it to catalyze phosphorylation of target proteins on Ser/Thr residues and autophosphorylation to increase basal activity (Hofmann *et al.*, 2006). PKGI is a cytosolic homodimer, expressed in cardiomyocytes, smooth muscle, kidney, brain and platelets (Potter *et al.*, 2006) and PKGI KO mice exhibit loss of cGMP-dependent VSMC relaxation (Hofmann *et al.*, 2006). On the other hand PKGII is a membrane bound homodimer absent from cardiovascular system but found in the brain, intestine, lung, kidney and bone and loss of PKGII results in mice with dwarfism and resistance to *Escherichia coli* enterotoxin (binds GC-C) (Potter *et al.*, 2006). Thus PKGII appears to be involved in NPRB and GC-C responses (Hofmann *et al.*, 2006).

1.1.3.2 PDEs

The PDEs degrade cyclic nucleotides (CNs) to inactive 5'nucleotide monophosphates to modify intracellular CN concentrations (Potter *et al.*, 2006). There are at least 11 different PDE families each with conserved C-terminal catalytic domains and heterogeneous regulatory domains that function as dimers (Feil and Kemp-Harper, 2006; Lucas *et al.*, 2000). Some PDEs hydrolyze both cGMP and 5'3'-cyclic adenosine monophosphate (cAMP) whereas others preferentially cleave cAMP or cGMP (Potter *et al.*, 2006).

PKG and PDEs appear to be the main effectors of NP signal transduction since there are no reports CNGC-mediated NP effects (Potter *et al.*, 2006). Ultimately it is the combination of target proteins, substrate proteins and metabolizing enzymes together with their intracellular co-localization that determines the outcome of the cGMP signal (Lucas *et al.*, 2000; Piggott *et al.*, 2006).

1.1.4 Ion transport

Even though NPs probably do not act on CNGCs, their role in ion and water transport has long been known to underlie their natriuretic and diuretic effects. NPs are thought to regulate channel activity through phosphorylation and affect K^+ channels (calcium-activated K^+ channels, ATP sensitive K^+ channels, inwardly rectifying K^+ channels and outwardly rectifying K^+ channels), Ca^{2+} channels (L-type Ca^{2+} channels), Na^+ channels (Na^+-K^+2Cl^- co-transporter, Na^+-K^+ ATPase and Na^+ channels), Cl^- channels (including cystic fibrosis transmembrane conductance regulator), stretch-activated channels and water channels (aquaporins) (Kourie and Rive, 1999). Furthermore there is some evidence that NPs themselves can form ion channels (Kourie and Rive, 1999).

1.1.4.1 Vasorelaxation

Vasorelaxation is mediated by PKG1-induced phosphorylation of Ca^{2+}-sensitive K^+ channels resulting in K^+ efflux and membrane hyperpolarization. In turn this inhibits Ca^{2+} influx through voltage-gated Ca^{2+} channels thus reducing intracellular Ca^{2+} levels, decreasing Ca^{2+} sensitivity and ultimately causing relaxation (Hofmann *et al.*, 2006; Lucas *et al.*, 2000).

1.1.4.2 Natriuresis and diuresis

The natriuretic and diuretic effects of NPs in the kidney are achieved through inhibition of Na^+ and water re-absorption throughout the nephron (basic structural and functional unit of the kidney). For example in the proximal tubules ANP-induced cGMP inhibits angiotensin II-stimulated Na^+ and water transport; apical Na^+/H^+ exchange and K^+ channels that depolarize the proximal tubule cells and lower the electrical driving force for Na^+ transport (Sindic *et al.*, 2005). In the inner-medullary collecting ducts, NP-induced cGMP reduces apical epithelial Na^+ reabsorption by inhibiting amiloride-sensitive cation channels (Light *et al.*, 1990).

1.1.5 Physiological effects of NPs

The NPs are best known for their role in blood volume and pressure regulation through their vasorelaxant, natriuretic and diuretic effects. Indirectly NPs also exert hypotensive effects including increasing endothelial permeability (lowering intravascular volume); increasing glomerular filtration rate (fluid flow through the kidney); antagonizing the Renin-Angiotensin-

Aldosterone System (RAAS) (to inhibit release of the antinatriuretic hormone aldosterone) as well as suppressing water and salt appetite (Potter *et al.*, 2006). Through their antimitogenic properties, NPs also exert anti-hypertrophic and anti-fibrotic cardioprotective effects in the heart (Kuhn, 2004). Outside of the cardiovascular system NPs have been found to play roles removed from their classic hypotensive actions. In the lung ANP dilates pulmonary airways and blood vessels, reducing pulmonary hypertension and promoting vascular remodeling (Chen, 2005). ANP has also been shown to play a role in fat metabolism by stimulating lipolysis, which may explain the well known link between obesity and hypertension (Lafontan *et al.*, 2008). Finally ANP has been reported to act in the immune system by reducing the production of proinflammatory cytokines (Vollmar, 2005).

1.1.6 Evolution of NPs

NPs have been found throughout the vertebrate kingdom from humans to the most primitive fish. The most conserved family member is CNP being virtually identical across mammals and well conserved between mammals and fish (Takei, 2001). Likewise ANP is well conserved across mammals however is less so between mammals and fish, whereas BNP is poorly conserved even across mammals (Takei, 2001). Fish can have as many as seven NP types which may reflect their diverse osmoregulatory strategies (Trajanovska *et al.*, 2007; Ventura *et al.*, 2006). In addition to ANP, BNP and CNP, a novel ventricular NP (VNP) is found in fish (Takei *et al.*, 1991; Takei *et al.*, 1994a; Takei *et al.*, 1994b; Ventura *et al.*, 2006). The most primitive extant fish have only one NP - hagfish NP (hfNP) in hagfish and CNP in the related lamprey; and the ancestral NP is believed to incorporate properties of both of these (Kawakoshi *et al.*, 2006; Kawakoshi *et al.*, 2003). Primitive bony fish have been found to have four separate CNP genes which lead to the hypothesis that an ancestral CNP molecule underwent gene duplications (Inoue *et al.*, 2003). One of these CNP genes was then further duplicated to yield ANP, BNP and VNP (Inoue *et al.*, 2005). During the evolution of bony fish NP genes have been lost (VNP and in one case ANP) (Inoue *et al.*, 2005). Duplicated CNP genes were then lost or silenced during the evolution of tetrapods so that two CNP genes are found in amphibians while only one remains in mammals. A recent study in chick has revealed that two CNP genes also exist in birds (Trajanovska *et al.*, 2007). This study also reports the loss of ANP from the bird lineage and the discovery of a novel NP, prevalent in the kidney and thus named renal NP (RNP). Throughout vertebrates, the localization of NPs to cardiac and osmoregulatory organs and their effects on fluid and volume composition suggests that they play an integral role in osmoregulation across diverse forms of life (Toop and Donald, 2004).

1.2 PLANT NATRIURETIC PEPTIDES

1.2.1 Early evidence for NPs in plants

The first evidence for the existence of NPs in plants was presented by Vesely and Giordano who showed that radioimmunoassays (RIAs), using antibodies designed to detect animal NPs, recognized molecules from leaf and stem extracts of Florida Beauty (*Dracena godseffiana*) (Vesely and Giordano, 1991). The presence of N-terminal $proANP_{1-98}$, mid portion $proANP_{31-67}$ and C-terminal ANP_{99-126} was reported, at similar levels in leaf and stem tissue and at concentrations intermediary between those present in rat atrial and ventricular tissue.

A follow up study detected immunoreactive $proANP_{1-30}$, $proANP_{31-67}$ and ANP_{99-126} molecules across the plant kingdom, using representatives from angiosperms, gymnosperms, ferns, mosses to *Euglena* (Vesely *et al.*, 1993). The levels reported in this study were somewhat lower than those found in the initial study however high performance gel permeation chromatography (HPGPC) was used to determine that the molecular weights (MWs) and elution profiles of the immunoreactant plant molecules were similar to those of synthetic animal NPs, implying that the plant immunoreactants are similar to their animal counterparts.

A sceptical review by Takei criticized these studies (Takei, 2001). The main reason for this being that RIAs are highly specific and do not cross-react with other NP family members within the same species (even though these share approximately 50% similarity). This would imply that vertebrate and plant NPs (PNPs) share a high degree of sequence conservation (more than 50%), even though ANP is not well conserved across vertebrates (approximately 63% similarity). Moreover, reports of RIAs detecting N-terminal ANP fragments in plants are even more questionable due to their extremely poor degree of sequence conservation even among mammals (approximately 20% similarity). Takei argued that if NPs do exist in plants they would be more like the ancestral CNP molecule than ANP and that one would then expect find NPs in single-celled organisms from which both animals and plants have evolved.

1.2.2 Plant responses to animal NPs

The first report of a plant response to an animal NP came from the study by Vesely and colleagues (Vesely *et al.*, 1993). Treatment of carnations or chrysanthemums with synthetic animal NPs increased the flow of coloured water up the stem to colour flowers earlier than the other half of the same flower that had been left untreated. Both solute absorption and transpiration were enhanced by treatment with N-terminal proANP fragments: $proANP_{1-30}$, $proANP_{31-67}$ and $proANP_{79-98}$ but not C-terminal ANP_{99-126}.

These initial studies piqued the interest of Gehring and colleagues who then demonstrated that rat ANP ($rANP_{99-126}$) induced stomatal opening in a concentration-dependent manner in a number of different plants (*Tradescantia* sp., *Vicia faba* and *Kalanchoë daigremontiana*) (Gehring *et al.*, 1996). This was the first record of a plant response to ANP, the biologically active molecule in animals. Stomatal opening is the driving force for transpiration and so this finding was consistent with those of Vesely (Vesely *et al.*, 1993).

In a follow up pharmacological study, rANP-induced stomatal opening in *Tradescantia albiflora* was found to be conformation and cGMP-dependent (Pharmawati *et al.*, 1998a). S-carboxymethylation-induced linearization of the ring structure of rANP abolished its stomatal opening activity demonstrating that the molecules secondary structure is required for its activity. Since rANP-stimulated stomatal opening could be mimicked by the cell-permeant cGMP analogue, 8-Br-cGMP, and repressed by inhibitors of animal GCs, LY 83583 and methylene blue (MB), this suggests that rANP-induced stomatal opening is mediated by cGMP. This was taken as evidence for a receptor interaction that initiates cGMP signalling.

1.2.3 Animal NP binding activity

Radioactively labelled I^{125}-$rANP_{99-126}$ was demonstrated to bind *Tradescantia* microsomal membranes *in vitro* (Gehring *et al.*, 1996). Binding could be competitively displaced by increasing concentrations of unlabelled rANP implying that it was specific. Similarly I^{125}-rANP specifically bound plasma membranes from leaves and stems of *Tradescantia multiflora* (Suwastika *et al.*, 2000). In both studies the concentration of unlabelled rANP required for 50% displacement was relatively high (0.1-10 μM) compared to animal binding studies, however was in the same range that induced stomatal opening and reasoned to not be unexpected due to the vast evolutionary distance between plants and animals. Furthermore tissue section autoradiography revealed specific binding of I^{125}-$rANP_{99-126}$ to leaf and stem tissue *in situ* (Suwastika *et al.*, 2000). Together with the above findings this suggests that there are NPRs present in plants that are similar to their animal counterparts.

1.2.4 Purification of immunoreactant PNPs

Most importantly, immunoaffinity purified PNPs (irPNPs) were then isolated from ivy (*Hedera helix*) using antibodies raised against human ANP (anti-hANP) (Billington *et al.*, 1997). These irPNPs could induce stomatal opening in a concentration-dependent manner and competitively displace I^{125}-rANP bound to *T. multiflora* plasma membranes (Suwastika *et al.*, 2000). Subsequently it was shown using electrospray mass spectrometry (ESMS) and SDS-polyacrylamide gel electrophoresis (PAGE), that several species of molecules had been purified,

of sizes slightly larger than 11 kDa and approximately 3 kDa (Pharmawati *et al.*, 1998a). This was also later confirmed in tomato leaf and potato tuber using Western blots (Pharmawati *et al.*, 2001). These MWs were in agreement with the findings of Vesely (Vesely *et al.*, 1993) and comparable to those of animal NPs and suggest processing of precursor irPNPs. The fact that anti-hANP could purify plant molecules indicates that NPs have been structurally well conserved.

1.2.5 Plant responses to irPNPs

1.2.5.1 cGMP production

Since rANP-induced stomatal opening appeared to require cGMP (Pharmawati *et al.*, 1998a), cGMP production in response irPNP treatment was examined in maize (*Zea mays*) stele tissue (vascular tissue comprising the xylem and phloem) (Pharmawati *et al.*, 1998b). Treatment with irPNPs elicited a rapid and transient increase in cGMP in maize stele tissue. This occurred within 30 s, reached a maximum of approximately 1.2 pmol/g fresh weight (FW) at 1-2 min and remained elevated for 10 min before returning to control levels after 30 min. This strengthened the evidence for a plant NPR GC.

1.2.5.2 Cross-talk between cGMP and calcium

In *V. faba*, stomatal opening in response to 8-Br-cGMP and irPNPs was inhibited by the extracellular Ca^{2+} chelator, EGTA and inhibitors of cyclic ADP ribose (cADPR)-mediated intracellular calcium release, ruthenium red and procaine (Pharmawati *et al.*, 2001). This indicated that irPNP-induced stomatal opening is also calcium-dependent. Additionally irPNP-induced cGMP increases in potato guard cell protoplasts were inhibited by EGTA, suggesting that cross-talk occurs between cGMP and calcium signalling in the stomatal opening response to irPNPs.

Stomatal opening is the result of swelling of the stomatal guard cells produced by water and ion influx and is mediated by cGMP and calcium. Since animal NPs are well known for their regulatory effect on ion and water transport, it was not surprising to find that irPNPs can also induce water and ion movements in plants.

1.2.5.3 Water movements

At this stage irPNPs had been shown to induce cGMP increases in maize stele however their role in this tissue was unclear. The xylem and phloem are particularly interesting since they are responsible for water and solute transport throughout the plant. Using dye movements and ^{2}H nuclear magnetic resonance (NMR) tissue water exchange techniques, ANP and irPNPs were

shown to significantly increase radial water movement out of the xylem of *T. mulitflora* shoots after 10 min and more so after 30 min of treatment (Suwastika and Gehring, 1998). This could be mimicked by cell-permeant 8-Br-cGMP and inhibited by LY 83583, indicating that cGMP signalling is required for this irPNP-induced water movement. Additionally the aquaporin inhibitor, $HgCl_2$ inhibited NP-induced water movement implicating aquaporins in this process.

The effect of irPNPs on water movement was also examined at a cellular level in potato mesophyll cell protoplasts (MCPs) (Maryani *et al.*, 2001). IrPNPs enhanced osmoticum-induced swelling of MCPs in a concentration and time-dependent manner. This too was probably mediated by aquaporins since the protoplast suspension medium contained no added cations.

1.2.5.4 Ion movements

Guard cell volume changes are controlled by K^+ and Cl^- counter ion fluxes that are driven by the H^+-ATPase.

1.2.5.4.1 H^+-ATPase

The effect of 8-Br-cGMP on the H^+-ATPase was examined *in vitro* in *T. multiflora* leaf and stem-derived plasma membrane vesicles (Suwastika and Gehring, 1999) and in potato guard cell protoplasts (Pharmawati *et al.*, 2001). In both cases, 8-Br-cGMP reduced the rate of H^+ pumping and release of P_i from ATP hydrolysis, consistent with inhibition of the H^+-ATPase.

In contrast, in potato leaf plasma membrane vesicles (Maryani *et al.*, 2000) and potato guard cell protoplasts (Pharmawati *et al.*, 2001) irPNPs inhibited H^+ pumping but stimulated P_i release. These opposing effects suggest that irPNPs cause dissipation of the H^+ gradient rather than direct inhibition the H^+-ATPase. In the plasma membrane vesicles, the reduction in the H^+ gradient only occurred at high external Cl^- concentrations and irPNPs were found to promote Cl^- uptake. Therefore irPNPs were proposed to cause dissipation of the H^+ gradient by activating H^+/Cl^- symporters.

Since neither cGMP nor irPNPs stimulate the H^+-ATPase and yet these are still able to cause stomatal opening, they are more likely to have a direct affect on ion fluxes in the stomata.

1.25.4.2 H^+, K^+ and Na^+ fluxes

Noninvasive ion-selective vibrating microelectrodes were used to measure net ion fluxes in maize stele in response to irPNPs and 8-Br-cGMP treatment (Pharmawati *et al.*, 1999). An immediate (within 2 min) H^+ influx followed by delayed (20 min) K^+ and Na^+ uptake was recorded in response to irPNPs. This is consistent with the proposal that irPNPs activate H^+/Cl^- symporters since direct inhibition of the H^+-ATPase would cause membrane depolarization that

would reflect in an immediate efflux of Na^+ and K^+. In contrast, 8-Br-cGMP did not alter H^+ flux however mimicked irPNPs in that it caused the delayed K^+ influx and a shift towards Na^+ influx.

Therefore irPNPs induce both K^+ and Cl^- uptake which would induce stomatal opening. Since cGMP mimics irPNPs in promoting the stomatal opening and K^+ flux responses, irPNP-induced stomatal opening might occur via cGMP-mediated K^+ influx.

1.2.6 Stress induction

Extractable amounts of irPNPs (relative to the amount of total protein) increased in response to high concentrations of NaCl in both *Erucastrum strigosum* and *Arabidopsis thaliana* suspension cultures (Rafudeen *et al.*, 2003). Iso-osmolar sorbitol imposed less inhibition on growth but resulted in the largest induction of irPNPs. Therefore irPNP levels are elevated in response to osmotic stress and not specifically NaCl stress, possibly as a late adaptive response.

1.2.7 Localization

At this point irPNPs had been purified from leaf tissue but their localization therein and presence in other tissue remained unknown. Antibodies raised against hANP and potato irPNPs were utilized in tissue printing and immunofluorescence labelling to study *in situ* localization of irPNPs in ivy and potato (Maryani *et al.*, 2003). Tissue print localization revealed the presence of immunoreactants in the conductive tissue (phloem and possibly the xylem) of potato stems and ivy leaves, stems and roots. Comparatively immunofluorescence labelling reported the presence of irPNPs in the ivy stomatal ledge wall and guard cells as well as in the vascular bundles (xylem and phloem) of the ivy leaf and stem tissue. In this same study, biologically active (had stomatal opening activity) irPNPs were isolated from the xylem exudates of forest sage, *Plectranthus ciliatus*. Therefore irPNPs are localized in the conductive tissue (xylem and phloem) and stomata.

In summary rANP and irPNPs induce stomatal opening in a cGMP-dependent manner as well as induce water and ion movements that may be responsible for this stomatal opening. Expression of irPNPs is induced in response to NaCl and osmotic stresses and irPNP proteins have been localized to the conductive tissue and extracted from the xylem. Since irPNPs purified from the xylem were able to modify stomatal aperture this suggests that irPNPs could be systemic signalling molecules involved in maintaining water and ion homeostasis.

1.2.8 Cloning the *AtPNP-A* gene

Partial N and C-terminal irPNP sequences from potato were used to search for homologous sequences in *Arabidopsis* (Ludidi *et al.*, 2002). Two sequences were identified: AtPNP-A (AAD08935, At2g18660) and AtPNP-B, with which it shares 37% sequence identity (CAB79756, At4g30380). In turn AtPNP-B is similar (54% identity) to CjBAp12, a blight-induced protein of unknown function from citrus (*Citrus jambhiri*) (Ceccardi *et al.*, 1998). *AtPNP-A* could be reverse transcriptase (RT)-PCR-amplified from uninduced leaf tissue consistent with irPNP purification from leaves (Ludidi *et al.*, 2002). The *AtPNP-A* gene is predicted to encode a 126 aa protein (13.9 kDa) that has an N-terminal signal peptide for directing the molecule to extracellular space.

1.2.8.1 IrPNPs are similar to hANP and expansins

Alignment of AtPNP-A, AtPNP-B and CjBAp12 revealed conserved cysteine residues among these molecules and secondary structure prediction suggests that AtPNP-A and CjBAp12 share a common structure that might imply common function (Ludidi *et al.*, 2002). A number of conserved irPNP sequences were also identified from other plants (both monocots and dicots) but not from yeast or slime mould as would be expected if animal and PNPs were derived from a common ancestor. There is some similarity between hANP and AtPNP-A, as expected (Figure 1.3A). Alignment of the irPNPs with the family of NPs reveals that the irPNPs are most similar to the recently identified RNP from chick rather than ancient NP molecules, as was predicted by Takei (Takei, 2001) (Figure 1.4). A BLAST search with AtPNP-A did not return matches to animal NPs but rather revealed that irPNP-like molecules are most similar to a family of plant expansins (Ludidi *et al.*, 2002).

1.2.8.2 Relatedness of irPNPs and expansins

Expansins induce acid-dependent extension and relaxation of plant cell walls, important for cell elongation (Cosgrove, 2000b). There are two groups of expansins: α and β (the latter are also known as group 1 pollen allergens) (Cosgrove, 2000c). Phylogeny suggests that the irPNP-like molecules form a separate group that has now been classified as γ expansins with AtPNP-A falling in a different subgroup from AtPNP-B and CjBAp12 (Li *et al.*, 2003). The structure of AtPNP-A has subsequently been modelled based on the crystal structure of N-terminal domain of Timothy grass pollen allergen Phl P 1 (Ludidi *et al.*, 2004). These molecules have the same fold pattern (certainty z score > 5) that is a double-ψ β barrel structure. Therefore AtPNP-A and expansins are similar in both sequence and structure.

A.

```
            ** * *         *         *   *    **
AtPNP-A PYTRSACYGTQRETLVVGVKNNLWQNGRACGR-RY
hANP    SLRRSSCFGGRMDR--IGAQS-----GLGCNSFRY
```

B.

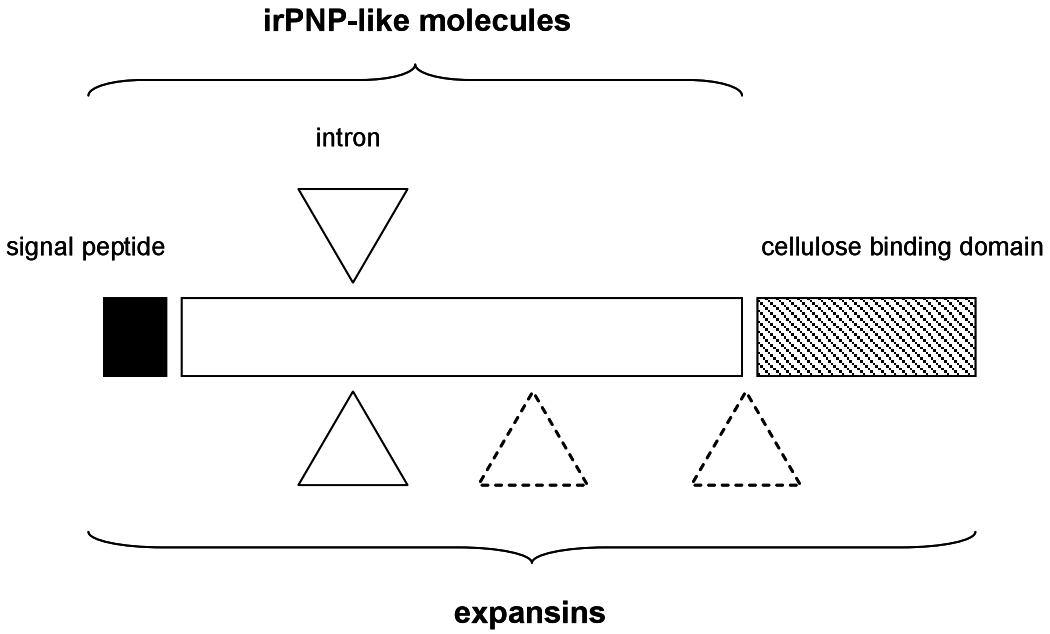

Figure 1.3. Similarity of AtPNP-A to hANP and expansins

Alignment of AtPNP-A (aa 33-66) with human ANP (hANP) reveals that there is some sequence similarity between these molecules. * denotes conserved aa. Importantly, the cysteine residues (shown in red) required for forming the ring structure of ANP are conserved in AtPNP-A. The domain organization of AtPNP-A compared to that of expansins is shown in (B) (Gehring and Irving, 2003). The irPNP-like molecules have lost the cell wall (cellulose) binding domain from the expansins, corresponding to the loss of an intron/exon boundary.

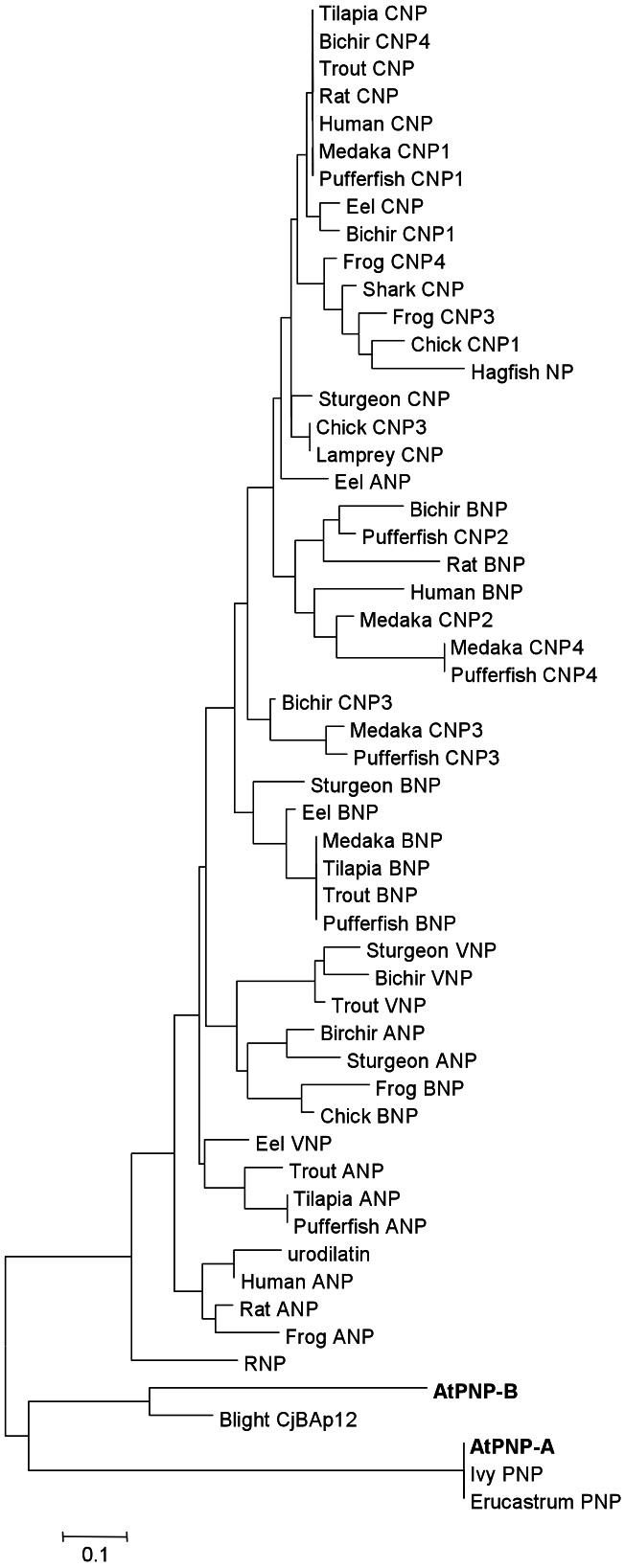

Figure 1.4. Phylogenetic analysis of the vertebrate NP family and the irPNPs

NP protein sequences were obtained from NCBI (www.ncbi.nlm.nih.gov) and aligned by ClustalW using MEGA version 4 (Tamura *et al.*, 2007). IrPNPs are most similar to renal NP (RNP) followed by ANP.

1.2.8.3 IrPNPs have lost the expansin cell wall binding domain

Compared to expansins irPNPs have lost the C-terminal domain that is proposed to bind the cell wall (Cosgrove, 1999). Loss of this domain from the irPNPs corresponds to an intron/exon boundary and has been suggested to allow for the increased mobility of the irPNP molecules (Figure 1.3B). Indeed several lines of evidence suggest that irPNPs do not act on the cell wall but instead are mobile: 1) CjBAp12 does not have expansin activity and is found in the shoots, distally from its site of synthesis in the root (Ceccardi *et al.*, 1998; Gehring and Irving, 2003); 2) irPNPs localize to the conductive tissue and can be isolated from the xylem (Maryani *et al.*, 2003); 3) irPNPs act in systems lacking the cell wall such as protoplasts and membrane vesicles (Maryani *et al.*, 2001; Maryani *et al.*, 2000; Pharmawati *et al.*, 2001) and 4) irPNPs can competitively displace rANP binding to plant plasma membranes (Suwastika *et al.*, 2000) suggesting that irPNPs can act directly on the plasma membrane. Thus irPNPs and expansins are proposed to have evolved from an ancestral glucanase with expansins having diverged to become cell wall loosening agents rather than having hydrolytic activity against the wall and irPNPs having further diverged for a function other than cell wall loosening, possibly extracellular signalling (Ludidi *et al.*, 2002). Therefore AtPNP-A appears to be a heterolog of animal NPs that has arisen by convergent evolution (Gehring and Irving, 2003).

1.2.9 Actions of recombinant AtPNP-A

1.2.9.1 Stomatal opening and protoplast swelling

Recombinant AtPNP-A was able to promote stomatal opening and protoplast swelling in a concentration-dependent manner in *Arabidopsis* (Morse *et al.*, 2004; Rafudeen *et al.*, 2003), as expected. Protoplast swelling was proposed to be the result of compatible solute synthesis since it was inhibited by the translational inhibitor cycloheximide (CHX), implying that it is dependent on rapid *de novo* protein synthesis. Protoplast swelling was cGMP-dependent since it could be mimicked by 8-Br-cGMP and inhibited by GC inhibitors (LY 83583, OQD and NS 2028) while AtPNP-A itself induced a cGMP increase in *Arabidopsis* MCPs (Wang *et al.*, 2007c).

1.2.9.2 Ion fluxes

Recombinant AtPNP-A has also been shown to induce ion fluxes in the mature and elongation zones of the *Arabidopsis* root (Ludidi *et al.*, 2004). In the elongation zone AtPNP-A caused rapid H^+ influx while in the mature zone a rapid H^+ efflux was followed by K^+ and Na^+ efflux. In the mature zone this H^+ flux was an order of magnitude smaller than that of the K^+ and Na^+ fluxes suggesting that it does not drive the K^+ and Na^+ fluxes but rather that AtPNP-A directly or indirectly affects the appropriate transporters. Consistent with K^+ efflux, protoplasts isolated from the mature zone were found to shrink within 5 min AtPNP-A treatment. Over a longer

period, protoplast volumes increased for osmotic reasons but the AtPNP-A-treated samples continued to efflux K^+. Therefore in the presence of AtPNP-A protoplast volume increased even against a K^+ gradient.

1.2.10 Active Site Determination

Full length recombinant AtPNP-A (aa 1-126), AtPNP-A minus the signal peptide (26-126) and a short domain (33-66) that has homology to animal ANP (Figure 1.3A) were all able to cause rapid, concentration-dependent protoplast swelling, whereas other AtPNP-A fragments (26-52), (53-88) and (89-126) could not evoke the swelling response (Morse *et al.*, 2004). Hence the peptide comprised of aa 33-66 contains the active site of AtPNP-A. An investigation of smaller synthetic peptides within the active domain revealed that peptide A (33-66) was the most active molecule while smaller peptides had varying effects that correlated with their degree of secondary structure (Wang *et al.*, 2007c). Consistent with this, only peptide A has two conserved cysteine residues capable of forming a disulphide bond and when linearized by S-carboxymethylation, lost its activity.

1.2.11 ABA and AtPNP-A interaction

The interaction between AtPNP-A and abscisic acid (ABA) was also investigated since both AtPNP-A and ABA are induced in response to NaCl and drought stress and affect plant water status through their actions on stomata (Wang *et al.*, 2007c). As mentioned above, AtPNP-A induced protoplast swelling and cGMP increases in MCPs but ABA did not and neither did it affect the AtPNP-A-induced responses. However ABA inhibited AtPNP-A-induced stomatal opening and visa versa AtPNP-A delayed and reduced ABA-induced stomatal closure. Therefore ABA and AtPNP-A do appear to interact in the stomata.

In summary, AtPNP-A was cloned and found to share similarity with a family of expansins. There was some sequence similarity to hANP and the region of AtPNP-A that is homologous to hANP contains the active domain. Recombinant AtPNP-A elicited the same effects as those documented in response to irPNPs, namely stomatal opening, protoplast swelling and ion fluxes. Since AtPNP-A induces swelling responses, AtPNP-A may act cooperatively with expansins to provide the turgor necessary to drive cell expansion (Morse *et al.*, 2004). AtPNP-A effects appear to be developmental stage and tissue specific, exemplified by the fact that AtPNP-A induces distinct ion fluxes in different zones of the root (Ludidi *et al.*, 2004). Moreover, the fact that ABA antagonized AtPNP-A-induced stomatal opening but did not affect AtPNP-A-induced MCP swelling even though both are swelling responses, suggests that AtPNP-A also exerts cell-type specific effects (Wang *et al.*, 2007c).

1.2.12 Xanthomonas PNP

1.2.12.1 Identification of the XacPNP gene

Shortly after *AtPNP-A* was cloned, a bacterial citrus pathogen *Xanthomonas axonopodis* pv. *citri* was found to contain a gene encoding an irPNP-like protein, which was then named XacPNP (Nembaware *et al.*, 2004). The closest homolog of XacPNP is AtPNP-A and these are similar in both sequence and domain organization. Additionally XacPNP and AtPNP-A share conserved residues in the active site and a common structure that implies that these molecules have a common function. XacPNP has no similarity to other bacterial proteins and incongruent phylogeny suggesting that it may have arisen through an ancient lateral gene transfer. Nembaware and colleagues hypothesized that *X. axonopodis* utilizes XacPNP in a case of molecular mimicry to alter plant host homeostasis, facilitating access to water and nutrients and causing the hyperhydration seen in its symptomatic wet edged lesions that are not a feature of its close relative *X. campestris* that lacking an irPNP has dry corky lesions.

1.2.12.2 XacPNP alters plant homeostasis

Proof of concept has been provided recently in a study that demonstrated that recombinant XacPNP induces stomatal opening and protoplast swelling similarly to AtPNP-A (Gottig *et al.*, 2008). It was observed that XacPNP induced starch degradation in guard cells coincident with stomatal opening, suggestive of solute accumulation in agreement with the idea that AtPNP-A induces swelling by solute synthesis or recompartmentalization (Morse *et al.*, 2004). Importantly both XacPNP and AtPNP-A increased transpiration and photosynthesis and thus alter plant homeostasis (Gottig *et al.*, 2008). Expression of XacPNP was barely detectable under nutrient replete conditions, however was shown to be induced under nutrient poor conditions that mimic the apoplast as well as during infection. The role of XacPNP was then investigated using a XacPNP deletion mutant ($XacPNP^-$). This mutant caused greater necrotic lesions on citrus. Conversely introduction of XacPNP into its close relative *X. axonopodis* pv. *vesicatoria* (a pepper bacterial spot pathogen) ($XavPNP^+$) caused less necrotic lesions on its pepper host. During infection the presence of XacPNP increased net water flux through the leaf and sustained photosynthesis, keeping the plant tissue alive which was advantageous to the biotrophic citrus pathogen however was not advantageous to the necrotrophic pepper pathogen, as reflected in the bacterial numbers. Thus the XacPNP is employed by *X. axonopodis* pv. *citri* to modify host homeostasis and thereby improve bacterial fitness.

1.3 EVIDENCE FOR CYCLIC NUCLEOTIDE SIGNALLING IN PLANTS

The key regulatory role played by CNs in animals and bacteria made it unlikely that they had been lost from plants. Nevertheless CN signalling in plants remained a controversial topic for many decades. IrPNPs helped to establish CN signalling in plants as did their counterparts in animals.

1.3.1 Cyclic GMP as a second messenger in plants

Early evidence for the presence of CNs in plants was criticized for being equivocal, the main reason for this being that 3'5'-cyclic monophosphates could not be easily distinguished from 2'3'-cyclic monophosphate RNA breakdown intermediates (Brown and Newton, 1981). Due to lack of adequate product or substrate identification there was also ambiguity in the identification of the nucleotidyl cyclases and PDEs responsible for CN synthesis and breakdown, respectively. It was not until a rigorous series of fast atom bombardment mass spectrophotometry (FAB/MS) and collision-induced dissociation followed by mass-analyzed kinetic energy spectrum (CID/MIKE) techniques were employed that the molecule was demonstrated irrevocably to be the 3'5'-CN and the presence of CNs in plants became accepted (Newton *et al.*, 1984). Still, compared to animals the levels of CNs in plants were low (often close to the detection limit of methods used) and variable and so people remained cautious (Assmann, 1995; Spiteri *et al.*, 1989). Due to the lack of specific effects elicited by exogenous treatment of plants with cell-permeant CN analogues, sceptics then questioned the function of CNs in plants (Bolwell, 1995; Newton *et al.*, 1999). Unfortunately the early reviews refuting the presence of CNs in plants stifled research in this field and consequently progress has been somewhat lagging (Newton and Smith, 2004). There are still few reports that actually measure CN levels and evidence for their involvement in plant-specific processes is mostly indirect (using cell-permeant CN analogues or activators and inhibitors of mammalian nucleotidyl cyclases and PDEs to infer function) (Meier and Gehring, 2006). Nowadays CN signalling in plants is generally accepted however has been further complicated by the fact that sequencing of a number of plant genomes has not readily identified plant sequences with similarity to animal and bacterial nucleotidyl cyclases and downstream CN binding proteins (Bridges *et al.*, 2005). It seems then that CN signalling in plants has diverged significantly from that in animals.

1.3.2 Measurements of cGMP

Cyclic GMP has been more readily accepted as a second messenger in plants than cAMP, since cGMP levels are higher than those of cAMP and there are more easily drawn functional parallels between cGMP in plants and animals (Newton *et al.*, 1999). The presence of cGMP was first unequivocally established in large scale extracts from French dwarf bean (*Phaseolus*

vulgaris) seedlings (Newton *et al.*, 1984). Since then cGMP has been measured in tobacco bright yellow-2 (BY2) cell culture (Richards *et al.*, 2002); in response to plant hormones - PNPs in maize stele, potato guard cell protoplasts and *Arabidopsis* MCPs, auxin in soybean root and gibberellic acid (GA) in barley aleurone (Hu *et al.*, 2005; Maryani *et al.*, 2001; Penson *et al.*, 1996; Pharmawati *et al.*, 1998b; Pharmawati *et al.*, 2001; Wang *et al.*, 2007c); in oat seedlings in response to light and in *Phartibis nil* during the photoperiod (Dubovskaya *et al.*, 2001; Szmidt-Jaworska *et al.*, 2004); in rice seedlings during anaerobiosis (Reggiani, 1997); in NO-treated spruce needles and soybean roots (Hu *et al.*, 2005; Pfeiffer *et al.*, 1994); in gravistimulated soybean root (Hu *et al.*, 2005); in the response of *Arabidopsis* seedlings to NaCl and osmotic stress (Donaldson *et al.*, 2004) and recently in response to pathogen infection in *Arabidopsis* (Meier *et al.*, 2009).

1.3.3. Guanylyl cyclases

The presence of cGMP in plants meant that GCs responsible for cGMP synthesis must also exist. While GC activity had been reported (Brown *et al.*, 1989; Newton *et al.*, 1984; Volotovski *et al.*, 2003), it was not until recently that the first GC sequence was cloned (Ludidi and Gehring, 2003). In this study a comparison of the *Arabidopsis* genome with eukaryote and cyanobacterium GC sequences did not return any obvious matches, suggesting that plant GC sequences are evolutionarily unrelated or that similarity is restricted to a small catalytic centre. The authors then designed a search motif based on conserved functionally assigned aa in the catalytic centre of annotated GCs [RKS][YFW][GCTH][VIL][FV]X[DNA]X[VIL]XXXX[KR] and used this to query the *Arabidopsis* genome. Seven candidates were returned, one of which contained an adjacent glycine rich domain typical of all known GCs. This was named AtGC1 and was and demonstrated to convert GTP to cGMP *in vitro* (Ludidi and Gehring, 2003). AtGC1 is a soluble GC but lacks the haem binding domain characteristic of the mammalian enzymes and, consistent with this, was insensitive to an NO donor. Furthermore AtGC1 has a unique combination of N-terminal GC and C-terminal protease domain and therefore belongs to a new class of GCs. Similar sequences exist in human, mouse, mosquito and *Drosophila* but these have not been annotated as GCs (Ginalski and Zemojtel, 2004).

In a follow up study by the same group modifications were made to the search motif. Mutation of position seven ([DNA]) that is thought to play a role in dimerization, did not affect the GC activity of AtGC1 (Kwezi *et al.*, 2007). Any residue (X) was then allowed at this position and a new search performed that returned 171 proteins satisfying this criterion. Within this group 88 contained [EQCTDRVHY] two or three aa downstream from the motif that could be involved in metal binding and 27 of these 88 also contained an [R] 5-20 aa upstream from the motif, important for PPi binding. Several of these 27 potential GCs are leucine rich repeat receptor-

like kinases (LRR RLKs) containing cytosolic GC and kinase domains, reminiscent of the domain organization of NPRs. Importantly, one of these LRR RLKs: the bassinosteroid receptor, BRASSINOSTEROID INSENSITIVE 1 (BRI1) was tested for GC activity *in vitro* and found to generate cGMP (Kwezi *et al.*, 2007). In these molecules the GC and kinase domains overlap but the significance of this remains to be determined.

1.3.4 Cyclic GMP binding proteins

Cyclic GMP binding activity has been reported in plants (Dubovskaya *et al.*, 2002). As mentioned above, in animals the targets of cGMP are PDEs, PKGs and CNGCs. A search for the CNBDs in plants returns only CNGCs, shaker-type potassium channels and thioesterases (potentially plant-specific CN targets) but no protein kinases (Bridges *et al.*, 2005).

1.3.4.1 PDEs

Long before the presence of CNs was established in plants, PDE activity was reported (Brown *et al.*, 1975; Brown *et al.*, 1977; Brown *et al.*, 1979). These PDEs had high activity with both 5',3'-cAMP and 5',3'-cGMP substrates and were stimulated by Ca^{2+}, most likely through association with the Ca^{2+} binding protein, calmodulin (CaM) that regulates mammalian PDEs (Trewavas *et al.*, 2002). A PDE was then isolated from *P. vulgaris* chloroplasts which had a 3 fold higher activity with cGMP compared to cAMP (Newton *et al.*, 1984). Subsequently Ca^{2+}/CaM-stimulated PDEs were described in spinach chloroplast (Brown *et al.*, 1989) and in carrot cell cultures (Kurosaki and Kaburaki, 1995). However, little progress has been made in understanding the function of PDEs in plants.

1.3.4.2 PKGs

There are conflicting reports of PKG activity in plants. The best evidence for the presence of PKGs in plants comes from a study in *Phartibis nil* in which a purified protein kinase activity was stimulated by cGMP and cross-reacted with antibodies raised against guinea pig PKG (Szmidt-Jaworska *et al.*, 2003). Additionally evidence was provided for cGMP-stimulated autophosphorylation, a characteristic of mammalian PKGs. On the other hand, a bioinformatics study provided evidence for the lack of CN-regulated kinases in plants since no protein kinase sequences contain CNBDs (Bridges *et al.*, 2005). Of course this does not exclude the possibility of CN regulation of kinase activity through some indirect mechanism or novel binding site (Roelofs *et al.*, 2003).

1.3.4.3 CNGCs

An important finding for the field of CN research in plants was that CNs could directly regulate ion channels and cause ion fluxes (Li *et al.*, 1994; Maathuis, 2006; Pharmawati *et al.*, 1999). This provided an alternative mechanism of action to that mediated by CN-dependent protein kinases. Together with the finding that CNBDs in plants are predominantly associated with CNGCs (Bridges *et al.*, 2005), this suggested that CNGCs are the most likely targets of CN signalling in plants (Talke *et al.*, 2003).

The CNGCs are gated by CN binding to a cytoplasmic CNBD. This domain overlaps with a CaM-binding domain (whereas these domains are discrete in animals) so that CaM antagonizes CN binding (Arazi *et al.*, 2000; Hua *et al.*, 2003a; Kohler and Neuhaus, 2000). Plant CNGCs further differ from animal CNGCs in that their pore region has diverged (Hua *et al.*, 2003b). The first functionally characterized CNGC was AtCNGC2 which facilitated inward-rectifying K^+ and Ca^{2+} currents in three different heterologous systems but did not transport Na^+ making it unique among all other known channels (Leng *et al.*, 2002; Leng *et al.*, 1999). On the other hand, AtCNGC1 facilitated CN-activated K^+ and Na^+ currents (Hua *et al.*, 2003b; Leng *et al.*, 2002). The pore selectivity filter of AtCNGC1 is the most common among the CNGCs and thus the majority of CNGCs are probably poorly selective for these cations (Hua *et al.*, 2003b).

A family of 20 CNGCs is present in *Arabidopsis*, a number of which have been suggested to play a role in important plant processes (Very and Sentenac, 2002). For example several CNGC mutants have altered defence responses - *AtCNGC2*/*defence no death 1* (*dnd1*) (Clough *et al.*, 2000), *AtCNGC4*/*dnd2* (Balague *et al.*, 2003) and *AtCNGC11/12*/*constitutive expressor of PR genes 22* (*cpr22*) (Yoshioka *et al.*, 2006); Ca^{2+} hypersensitivity - *AtCNGC2* (Chan *et al.*, 2003); metal tolerance - *AtCNGC1* (Arazi *et al.*, 1999) and *NtCBP4* (Sunkar *et al.*, 2000); NaCl germination - *AtCNGC3* (Gobert *et al.*, 2006); pollen growth and orientation - *AtCNGC18*; (Frietsch *et al.*, 2007) and development - *AtCNGC10* (Kaplan *et al.*, 2007) and *AtCNGC2*; (Kohler *et al.*, 2001). The distinct phenotypes of the individual CNGC mutants suggest that they each have distinct functions.

1.3.5 Functions of cGMP

1.3.5.1 Light

Cyclic GMP has been implicated in playing a role in light responses in plants, as it does in animals. This began with an elegant study by Bowler who demonstrated that microinjection of cGMP into the phytochrome deficient tomato *aurea* mutant induced anthocyanin biosynthesis and when coinjected with Ca^{2+} could stimulate the development of fully mature chloroplasts, thus mimicking phytochrome and rescuing the mutant phenotype (Bowler *et al.*, 1994a).

The role of cGMP in light responses has since been studied in oat seedlings (Dubovskaya *et al.*, 2001; Dubovskaya *et al.*, 2002; Volotovski *et al.*, 2003). Here red light elevated cGMP levels, stimulated GC activity and cGMP binding while far red light could reverse these effects. Such reversible regulation is consistent with responses that are mediated by phytochrome. Interstingly guanylin increased cGMP levels and induced GC activity in plasma membranes, providing evidence for a receptor GC that can recognize guanylin NPs (Volotovski *et al.*, 2003).

In *Phartibis nil* grown under 12 hr sub-inductive night, cGMP treatment was then demonstrated to stimulate flowering (Szmidt-Jaworska *et al.*, 2004). In the same study it was reported that cGMP levels were constant in light but oscillated during the night. Disruption of the dark cycle by a flash of red light lowered cGMP levels, perturbed the oscillation and prevented flowering.

1.3.5.2 Gene expression

In the *aurea* mutant, cGMP and calcium were shown to act primarily by regulating gene expression (Bowler *et al.*, 1994b). These authors proposed three pathways: a cGMP-mediated pathway that regulates the anthocyanin biosynthetic gene *CHALCONE SYNTHASE* (*CHS*), a calcium-mediated pathway that activates the *RBCS* gene (small subunit of ribulose 1,5-bisphosphate carboxylase, RUBISCO) and a pathway that involves both calcium and cGMP and represses the *ASPARAGINE SYNTHASE 1* (*AS1*) gene (Neuhaus *et al.*, 1997). Follow up studies have since identified *cis* elements in the promoters of these genes responsible for this regulation (Neuhaus *et al.*, 1997; Wu *et al.*, 1996b).

Recently microarrays have been used to look at global changes in gene expression in *Arabidopsis* roots following cGMP treatment, in an attempt to identify cGMP-regulated genes (Maathuis, 2006). It was noteworthy that cGMP treatment resulted in the differential expression of a number of monovalent cation transporters. Therefore not only does cGMP induce ion fluxes but may also affect ion transport at the level of transcription.

It appears that cGMP mediates at least some of its effects via changes in gene expression. While in animals transcription factors have been identified that bind and are regulated by CNs, there is only one report of such a transcription factor in plants (Katagiri *et al.*, 1989).

1.3.5.3 Hormones

Other hormones besides PNP have been found to increase cGMP. In barley aleurone GA treatment induced increases in cGMP levels while LY 83583 prevented: the cGMP increase, GA-induced expression of the GAMYB transcription factor and its target α-amylase as well as

α-amylase synthesis and secretion (Penson *et al.*, 1996). Additionally LY 83583 inhibited GA-induced DNA degradation and programmed cell death (PCD) that is the final step of the developmental programme that promotes successful seedling development (Bethke *et al.*, 1999).

As discussed previously, cGMP plays a role in irPNP-induced stomatal opening (Pharmawati *et al.*, 1998b; Pharmawati *et al.*, 2001). Similarly cGMP has been implicated in auxin-induced stomatal opening responses (Cousson, 2003; Cousson and Vavasseur, 1998) as well as auxin-induced *de novo* root formation (Cousson, 2004) in *Commelina communis*. Furthermore cGMP increases have recently been measured in response to auxin that mediates gravitropic root bending in soybean root (Hu *et al.*, 2005).

1.3.5.4 Nitric oxide (NO)

The high levels of cGMP recorded after exposure of spruce needles to nitric oxide (NO) helped to establish cGMP signalling in plants (Pfeiffer *et al.*, 1994). NO is involved in a number of plant processes including gravitropic root bending and the plant defence response.

Increases in cGMP have since been measured in response to gravistimulation, NO treatment as well as auxin treatment in soybean root (Hu *et al.*, 2005). Evidence was provided that gravistimulation induces auxin redistribution in the root that in turn results in asymmetric NO accumulation and increased cGMP levels to cause root bending.

Infection of resistant but not susceptible tobacco with tobacco mosaic virus (TMV) resulted in enhanced NO synthase (NOS) activity and NO treatment induced an increase in cGMP (Durner *et al.*, 1998). Additionally NO donors, recombinant mammalian NOS, cGMP and cADPR were all shown to induce *PATHOGENESIS RELATED 1* (*PR1*) and *PHENYALANINE AMMONIUM LASYE* (*PAL*) defence gene expression in tobacco. Since NO-induced activation of *PAL* was prevented by GC inhibitors and cGMP-induced *PR1* and *PAL* expression was inhibited by ruthenium red, this suggests that recognition of TMV triggers NO synthesis which acts via cGMP and calcium to stimulate *PR1* and *PAL* expression as part of the defence response.

Avirulent pathogen challenge has also been shown to increase NO in *Arabidopsis* suspension cultures to levels sufficient to cause PCD-type death that could be blocked by a GC inhibitor, suggesting that cGMP is required for NO-induced PCD during the hypersensitive response (HR) that is activated by avirulent pathogens (Clarke *et al.*, 2000). Consistent with the proposed role for cGMP in the response to avirulent pathogens, the pathogen-induced increase in *Arabidopsis* cGMP levels is significantly faster and greater in response to an avirulent *Pseudomonas syringae* strain (*AvrB*) compared to the virulent strain (DC 3000) (Meier *et al.*, 2009).

1.3.6 Summary

In summary the presence of cGMP in plants has now been unequivocally established. Potential GCs have been identified although a demonstration of their activity and biological function *in planta* remains outstanding. In plants, cGMP appears to exert its effects mainly by acting directly on ion channels. Evidence suggests that apart from its role in mediating NP responses, cGMP is also involved in light and growth responses and in the response to pathogens. Multiple points of cross-talk potentially exist between cGMP and calcium signalling pathways, for example in the regulation of PDEs and CNGCs by CaM.

1.4 WATER AND ION HOMEOSTASIS IN PLANTS

The definition of homeostasis is the maintenance of an internal steady state in response to a change in the environment (i.e. stress) (Niu *et al.*, 1995). Therefore water and ion homeostasis are affected in the response to most, if not all, stress conditions. Water and ion status are inextricably linked by the fact that plants take up water and ions together and consequently solute content determines ability to draw water (Gupta *et al.*, 1989; Shabala and Lew, 2002). Essentially cells are assemblies of water, ions and biomolecules contained within semi-permeable membranes. Water and ions constantly flux across the membrane in a controlled manner through water and ion transporters, which can be regulated in order to fine tune homeostasis and are thus the principle determinants of homeostasis (Niu *et al.*, 1995). The movement of water is facilitated by aquaporins (Kjellbom *et al.*, 1999). Ion flux, on the other hand, occurs through a plethora of different transport proteins. These can either be pumps that use the energy generated by ATP hydrolysis to drive active transport; carriers which generally combine the downhill transport of H^+ into the cell with the uphill transport of essential nutrients into or toxic ions out of the cell; or channels which allow passive movement of ions down an electrochemical gradient (Niu *et al.*, 1995). Homeostasis acts at both a cellular level as well as at the level of the whole plant (Bray, 1997; Kjellbom *et al.*, 1999; Munns, 2005). The plant, as a whole, needs to establish the correct balance between roots that take up water, nutrients and ions and shoots that use these to produce photosynthate required for growth (Kaldenhoff *et al.*, 1998; Munns, 2005; van der Weele *et al.*, 2000). Ultimately growth is adjusted to allow the plant time to establish a new equilibrium, minimize exposure to the stress and seek out better environments (Bray, 2004; Munns, 2002; Munns, 2005; Potters *et al.*, 2007; Shabala and Cuin, 2008).

1.4.1 Water homeostasis

Water homeostasis ensures that the cell has the correct amount of water to maintain cell turgor, necessary for expansion growth (Cosgrove, 1993). Should water loss occur (due to increased osmotic potential of the environment) then water will flow out of the cell and the protoplast will shrink (Verslues *et al.*, 2006). If this happens suddenly or if the osmotic solution is able to traverse the cell wall, then the protoplast will shrink without cell wall deformation causing the cell membrane to pull away from the wall and tear in a phenomenon referred to as plasmolysis (Munns, 2002; Verslues *et al.*, 2006). More gradual water loss results in cytorrhesis wherein the cell wall collapses around the shrinking protoplast and cell turgor is maintained (Munns, 2002). Recovery from water loss demands osmotic adjustment in order to draw water back into the protoplast and re-establish turgor (Shabala and Lew, 2002; Xiong and Zhu, 2002b).

1.4.2 Water stress

Water deficit occurs when the rate of transpiration exceeds the rate of water uptake (Bray, 1997). Water stress in plants is thought to be perceived by osmosensors in the plasma membrane in a manner similar to that which occurs in yeast, however the exact mechanism remains elusive at present (Tran *et al.*, 2007; Wohlbach *et al.*, 2008). Stress perception initiates signal transduction cascades involving calcium, inositol 1,4,5-trisphosphate (IP_3), reactive oxygen species (ROS) and kinases (Kaur and Gupta, 2005; Xiong *et al.*, 2002b). ABA is a key hormone involved in the plant response to water deficit stress, although ABA independent pathways also exist (Bray, 2002; Ishitani *et al.*, 1997; Shinozaki and Yamaguchi-Shinozaki, 2000). ABA plays a role in both early and late stress responses (Finkelstein *et al.*, 2002). As an early response to water deficit stress, ABA is rapidly induced in the root and travels to the shoots in the transpiration stream where it causes stomatal closure to prevent further transpirational water loss (Javot and Maurel, 2002; Nilson and Assmann, 2007; Verslues *et al.*, 2006). A second round of ABA signalling is then required for changes in gene expression and adaptation to the water deficit stress (Shinozaki and Yamaguchi-Shinozaki, 1997; Xiong *et al.*, 2002b).

1.4.2.1 Re-establishing homeostasis

Osmotic adjustment involves increasing water permeability, water storage capacity and whole plant water uptake by adjusting aquaporin abundance, localization and activity (Luu and Maurel, 2005; Maurel *et al.*, 2002). In the long term, the plant extends its root system enabling more water absorption from the soil (Kaldenhoff *et al.*, 1998; van der Weele *et al.*, 2000). At a cellular level osmotic adjustment is also vital, although not well understood (Shabala and Cuin, 2008; Shabala and Lew, 2002). Traditionally osmotic adjustment was thought to be achieved by the synthesis of compatible solutes (amino acids, sugars and amides) that can accumulate to

high concentrations in the cytoplasm without impeding metabolism (Cuin and Shabala, 2005; Shabala and Lew, 2002; Verslues *et al.*, 2006). However this is an energy expensive process and growing evidence suggests that compatible solutes do not accumulate to sufficient levels to be able to provide significant osmotic adjustment (Cuin and Shabala, 2005; Munns, 2002; Shabala and Lew, 2002; Xiong and Zhu, 2002b). Instead it has recently been shown that inorganic ion uptake alone can account for up to 90% of osmotic adjustment (Shabala and Lew, 2002).

1.4.2.2 Protection

Compatible solutes have rather been suggested to play a role in protecting membranes and proteins (Munns, 2005; Xiong and Zhu, 2002b). This is crucial for maintenance of cellular structure during water deficit stress since changes in the hydration spheres surrounding macromolecules affects their conformation and charge distributions, thereby disrupting protein interactions (Xiong and Zhu, 2002b). This function has also been attributed to LATE EMBRYOGENESIS ABUNDANT (LEA) proteins as well as the related dehydrins both of which are induced in response to water deficit stress (Bray, 1997; Bray, 2004; Munns, 2005). These hydrophilic proteins can bind water and may also act as chaperones to ensure correct protein folding (Munns, 2005; Verslues *et al.*, 2006). Additionally, unidentified proteins accumulate in the cell wall under conditions of water stress that have been suggested to affect cell wall elasticity to enable the wall to more easily deform around the shrinking protoplast (Bray, 2002).

1.4.2.3 Detoxification

Toxic ROS are continually produced as byproducts of metabolism (photosynthesis and respiration) and must be removed through the action of ROS scavenging enzymes (Apel and Hirt, 2004). Stresses disrupt this balance and cause the rapid accumulation of ROS. This imposes a secondary stress since ROS damage DNA and membranes and so their detoxification is necessary for the resumption of growth (Verslues *et al.*, 2006; Xiong and Zhu, 2002b). Thus expression of ROS scavenging enzymes is induced in response to stress (Bray, 2002; Mittler *et al.*, 2004). Compatible solutes have also been implicated in playing a role in detoxifying ROS (Cuin and Shabala, 2005; Munns, 2005). On the other hand, ROS can also be actively produced in response to water deficit stress to play a positive signalling role (Fujita *et al.*, 2006). Importantly, ROS signalling mediates ABA-induced stomatal closure (Desikan *et al.*, 2004; Kwak *et al.*, 2003). Furthermore ROS signalling may regulate root growth and aquaporin activity while ROS may also cross-link and fortify the cell wall to improve water retention by altering permeability (Luu and Maurel, 2005; Xiong and Zhu, 2002b). Another important aspect of detoxification is the removal of damaged proteins either by degradation or apoptosis

and this has been proposed to be the reason for the observed induction of proteases and ubiquitin genes in response to water stress (Bray, 1997; Bray, 2002; Xiong and Zhu, 2002b).

In summary then the plant response to water stress requires re-establishment of homeostasis through osmotic adjustment. This together with protection of macromolecules, detoxification of ROS and repair of damage incurred allows for recovery of growth.

1.4.3 Ion homeostasis

Ion homeostasis necessitates that the cell maintains high levels of K^+ and Mg^{2+} in the cytosol whilst keeping H^+, Ca^{2+} and Na^+ levels low (Serrano *et al.*, 1999). These ions are essential for basic cellular functioning. Firstly, K^+ is the major inorganic osmoticum crucial for maintenance of turgor pressure, stomatal movements and tropisms (Shabala, 2003). Additionally, K^+ as well as Mg^{2+} bind and are required for enzyme activity during normal metabolism (Serrano *et al.*, 1999). On the other hand, H^+ is actively pumped out of the cell by H^+-ATPases (at both the plasma membrane and tonoplast) in order to establish the proton motif force required for the energization of ion transport and nutrient uptake (Sondergaard *et al.*, 2004). Ca^{2+} is maintained at very low levels in the cytoplasm likely due to its cytotoxic effects and ability to precipitate cytosolic proteins; an ideal feature for its function as a ubiquitous second messenger involved in a number of signal transduction pathways which would be perturbed if Ca^{2+} were to enter the cell inappropriately (Cheng *et al.*, 2003; Serrano *et al.*, 1999). Lastly Na^+, the most common toxic ion in the soil, due to its physiochemical similarity to K^+ is able to compete with K^+ for uptake and binding sites on enzymes and is therefore detrimental to K^+ nutrition and should be excluded from the cytosol (Shabala and Cuin, 2008). Altogether it is the balance of these ions that determines homeostasis and functioning of the cell.

1.4.4 Ion stress

The literature on the topic of ion homeostasis deals largely with the response to NaCl stress that involves excluding toxic Na^+ from the cytosol whilst maintaining K^+ nutrition (Niu *et al.*, 1995; Serrano *et al.*, 1999; Serrano and Rodriguez-Navarro, 2001; Zhu, 2003). In response to NaCl stress Na^+ is prevented from accumulating in the cytoplasm by three techniques: 1) restricting Na^+ uptake, 2) activating Na^+ efflux and 3) compartmentalizing Na^+ in the vacuole (Apse and Blumwald, 2007; Zhu, 2003). At the level of the whole plant, Na^+ taken up from the soil by the root needs to be excluded from the shoot. This is because the shoot has no means of returning Na^+ back to the environment in contrast with the root which can extrude Na^+ back into the soil solution (Munns, 2002; Shabala and Cuin, 2008; Zhu, 2003).

1.4.4.1 Inhibition of Na^+ uptake

Toxic Na^+ is taken up by the cells through low affinity K^+ uptake routes and non selective cation channels (NSCCs), most likely members of the CNGC and glutamate-activated channel (GLR) families since these are poorly selective for K^+ over Na^+ (Apse and Blumwald, 2007; Liu and Zhu, 1997; Tyerman and Skerrett, 1999). The HIGH AFFINITY K^+ TRANSPORTER 1 (HKT1) has also received a lot of attention for its role in Na^+ uptake (Rus *et al.*, 2001). Uptake of Na^+ is restricted through blocking of NSCCs by calcium or CNs (Demidchik and Tester, 2002; Maathuis and Sanders, 1995) and through significant reprogramming of K^+ channels to inhibit the expression of those channels that are susceptible to transporting Na^+ (Shabala, 2003; Very and Sentenac, 2003). For a long time Na^+ uptake was considered to be the most important factor deciding NaCl tolerance and was therefore the major target for the design of transgenic NaCl tolerant crops (Shabala and Cuin, 2008). It has become increasingly apparent that the dogma that reduced Na^+ uptake confers NaCl tolerance, does not hold true because biomass is not well correlated with Na^+ content (Essah *et al.*, 2003; Shabala and Cuin, 2008; Tester and Davenport, 2003). In fact some mutants that have reduced Na^+ uptake are actually more NaCl sensitive (Kim *et al.*, 2007; Zhu *et al.*, 1998). Moreover simply preventing Na^+ uptake does not help the plant deal with the problem of the osmotic stress imposed by NaCl (Shabala and Cuin, 2008).

1.4.4.2 Na^+ efflux and compartmentalization

If Na^+ does enter the cell then it must be actively pumped out or compartmentalized in the vacuole. Na^+ efflux is controlled by Na^+/H^+ antiporters, of which the two best characterized are the plasma membrane SALT OVERLY SENSITIVE 1 (SOS1) which is important for Na^+ efflux from the root and the tonoplast SODIUM PROTON EXCHANGER 1 (NHX1) which is important for vacuolar Na^+ compartmentalization in the shoot (Apse *et al.*, 2003; Shi *et al.*, 2000). Na^+ efflux by the epidermal cells of the root returns the Na^+ back into the soil solution resulting in re-exposure (Shabala and Cuin, 2008) while Na^+ efflux into the apoplast leads to Na^+ deposition in the cell wall and eventual dehydration of the cell wall (Munns, 2005). Compartmentalization is therefore advantageous in that ions incorporated into the vacuole can contribute to the osmotic potential of the cell and allow for more K^+ to be made available to the cytosol (Apse *et al.*, 2003; Shi *et al.*, 2002b; Zhu, 2003). There does however need to be concurrent osmotic adjustment of the cytosol (Munns, 2002; Shabala and Cuin, 2008).

1.4.4.3 Recirculation of Na^+ between the shoot and root

Should Na^+ enter the xylem, it will travel in the transpiration stream until it reaches the actively transpiring leaves. Here it accumulates, attaining toxic levels and causing premature senescence with the leaves that have been transpiring the longest accumulating the most Na^+ and senescing

first (Munns, 2002; Munns, 2005). Once the number of photosynthesizing leaves is too few to sustain the plant it will die (Munns, 2002; Munns, 2005). By loading Na^+ into the phloem it can be translocated back to the root however this is hazardous as it runs the risk of being transported to the actively growing shoot tissue (Munns, 2002). Evidence from measurements of Na^+ loss from the leaves after removal of NaCl stress suggests that very little Na^+ is actually relocated in this way (Munns, 2002). However a number of reports have recently demonstrated that recirculation of Na^+ between the shoot and the root is in fact an important component of NaCl tolerance with transporters involved in xylem and phloem loading and unloading being key to this process. Both SOS1 and HKT1 have been demonstrated to be involved in Na^+ recirculation (Berthomieu *et al.*, 2003; Shi *et al.*, 2002a; Sunarpi *et al.*, 2005).

1.4.4.4 Maintenance of K^+ homeostasis

For a long time the importance of K^+ homeostasis under conditions of NaCl stress has been recognized (Liu and Zhu, 1997; Wu *et al.*, 1996a; Zhu *et al.*, 1998). K^+ uptake is thought to occur by two mechanisms – high and low affinity uptake (Very and Sentenac, 2003; Wu *et al.*, 1996a). Low affinity K^+ uptake operates under K^+-replete conditions down the electrochemical gradient, is poorly selective for K^+ over Na^+ and is prone to allow Na^+ uptake and is therefore inhibited by NaCl stress. In contrast, high affinity K^+ uptake mechanisms are activated when K^+ is limiting and have greater selectivity for K^+ over Na^+ and are therefore induced under conditions of NaCl stress in order to maintain K^+ nutrition (Fu and Luan, 1998; Liu and Zhu, 1997; Niu *et al.*, 1995; Wu *et al.*, 1996a). When Na^+ enters the cell, a massive depolarisation of the membrane occurs that abolishes voltage-driven high affinity K^+ uptake and moreover leads to depolarization-activated K^+ efflux (Shabala and Cuin, 2008). Thus NaCl stress further induces K^+ starvation (Shabala, 2003). Maintaining K^+ nutrition and a high K^+/Na^+ ratio in the face of NaCl stress is imperative for maintaining homeostasis (Hussain *et al.*, 2008; Rus *et al.*, 2004; Shabala and Cuin, 2008; Xiong and Zhu, 2002a).

1.4.4.5 Preventing K^+ efflux

Recently a large study of NaCl sensitive and tolerant varieties of barley has shown that NaCl tolerance is much better correlated ($r^2 > 0.8$) with the magnitude of NaCl-induced K^+ efflux than with any other parameter tested (Chen *et al.*, 2005). Specifically 90% of NaCl tolerant cultivars displayed a superior ability to retain K^+ in the face of NaCl stress while the other 10% were better able to prevent Na^+ accumulation in their shoots (Chen *et al.*, 2007c; Shabala and Cuin, 2008). Although net Na^+ uptake is less in NaCl tolerant varieties, Na^+ influx is not actually reduced implying that Na^+ efflux is enhanced. K^+ efflux, like the K^+/Na^+ ratio, serves as a measure of the loss of K^+ homeostasis after NaCl treatment and has now been proposed to be the best parameter to measure NaCl tolerance (Shabala and Cuin, 2008). Ca^{2+}, amino acids and

compatible solutes have all been demonstrated to reduce the NaCl-induced K^+ efflux consistent with their protective role against NaCl stress (Cuin and Shabala, 2005; Shabala *et al.*, 2007; Shabala *et al.*, 2006).

1.4.4.6 The ameliorative effects of calcium

Calcium has long since been reported to ameliorate the toxic effects of NaCl and NaCl tolerant genotypes have been shown to have higher Ca^{2+} sensitivity (Chen *et al.*, 2007b; Shabala and Cuin, 2008; Shabala *et al.*, 2006). The ameliorative effect of calcium is due to its ability to improve K^+/Na^+ selectivity under conditions of NaCl stress (Liu and Zhu, 1997). Calcium may achieve this by directly modulating ion channels - gating NSCCs responsible for Na^+ uptake and reducing NaCl-induced K^+ efflux (Demidchik and Tester, 2002; Shabala *et al.*, 2006). Additionally calcium can signal via the SALT OVERLY SENSITIVE (SOS) pathway to stimulate Na^+ efflux and compartmentalization. It has been demonstrated that in response to NaCl treatment an intracellular calcium transient is rapidly induced (Knight *et al.*, 1997). Thereafter calcium is thought to bind the calcium sensor calcineurin B like (CBL) protein, SOS3 which in turn binds and activates the CBL-interacting protein kinase (CIPK), SOS2 (Halfter *et al.*, 2000; Ishitani *et al.*, 2000; Liu *et al.*, 2000). The SOS3-SOS2 complex then regulates the activity of Na^+/H^+ antiporters at both the plasma membrane, SOS1, as well as at the tonoplast, NHX1, removing Na^+ from the cytosol and thereby maintaining a favourable K^+/Na^+ ratio (Qiu *et al.*, 2002; Qiu *et al.*, 2004). Certainly, calcium plays an important role in re-establishing ion homeostasis in the face of NaCl stress (Mahajan *et al.*, 2008).

In summary, plants respond to ion stress induced by NaCl by reducing Na^+ influx and increasing Na^+ efflux and compartmentalization. Since K^+ content determines the capacity of the cell for water and nutrient uptake, it is not surprising that maintaining K^+ homeostasis is a major determinant of NaCl tolerance. Additionally Ca^{2+} plays an important protective role.

1.4.5 Stresses that affect water and ion homeostasis

Water and ion stresses are common components of a number of abiotic and biotic stresses. Decreased water availability and thus altered water homeostasis is caused by stresses that reduce the available water in the soil or restrict the plants ability to take up water; for example NaCl and osmotic stresses, nutrient starvation, drought and freezing (Verslues *et al.*, 2006). Water status is also an important component of pathogen infection as the plant attempts to limit the access of water to pathogens as part of its defence (Wright and Beattie, 2004) while the pathogen must use mechanisms to circumvent this and attain water from the plant in order to survive (Melotto *et al.*, 2006). Similarly ion homeostasis is affected in response to stresses such as NaCl, osmotic stress and nutrient starvation since these stresses affect the plants ability to

take up essential ions, most notably K^+ (Niu *et al.*, 1995). Additionally, one of the earliest responses to pathogen infection is ion fluxes that are associated with improved nutrition in the apoplast for the pathogen (Atkinson and Baker, 1987) as well as signal transduction during the plant defence response (Clough *et al.*, 2000). Therefore water and ion homeostasis are both affected by similar stress conditions probably connected by the fact that water and ions move together.

1.4.6 Abiotic stresses – lessons from mutants

Not all mechanisms for dealing with water and ion stress are equally important in determining the stress tolerance phenotype. Arguably the greatest progress in understanding plant mechanisms for maintaining water and ion homeostasis has been gained from studies of mutants and cultivars that present with altered stress sensitive phenotypes (Chen *et al.*, 2007b; Tester and Davenport, 2003). To illustrate the point, a summary of information gained from mutants affected in NaCl and osmotic stress tolerance is discussed briefly.

1.4.6.1 Germination mutants

A large number of mutants have been isolated that are tolerant of NaCl stress during germination. These mutants are primarily osmotolerant since they also show improved germination on media imposing an osmotic stress (Gao *et al.*, 2006; Gonzalez-Guzman *et al.*, 2004; Quesada *et al.*, 2000; Ruggiero *et al.*, 2004; Saleki *et al.*, 1993). Barring a few exceptions, germination mutants are not more tolerant of NaCl or osmotic stress at later stages in development (Ruggiero *et al.*, 2004). In early studies it was established that wildtype seeds did not germinate under stress conditions, however retained their capacity to germinate when transferred onto control media and so it was proposed that mutants that germinate in the presence of stress are actually defective in signalling or perception of the stress (Saleki *et al.*, 1993; Werner and Finkelstein, 1995). If the surrounding environment is not conducive to plant growth germination is inhibited by ABA (Finkelstein *et al.*, 2002). Therefore it is not surprising then that a large number of mutants isolated from these germination assays are ABA mutants (Verslues *et al.*, 2006). For this reason NaCl and osmotic stress germination assays have even been used to isolate ABA mutants (Gonzalez-Guzman *et al.*, 2002).

1.4.6.2 ABA mutants

Not only is ABA important for inhibition of germination under adverse conditions, but it is also involved in stomatal closure to prevent transpirational water loss (Nilson and Assmann, 2007) as well as transcriptome changes (Bray, 2002) for stress adaptation under water deficit conditions. There are two types of ABA mutants – ABA deficient (*aba*) and ABA insensitive mutants (*abi*) (Verslues *et al.*, 2006). Phenotypes of ABA mutants include ABA and sugar-

insensitive germination, defective stomatal closure responses to water deficit stress and stunted, wilted phenotypes of older soil grown plants as a result of turgor loss (Finkelstein *et al.*, 2002). There are many different aspects of ABA signal transduction, all of which can be disrupted to give rise to NaCl and osmotic stress phenotypes including enzymes involved in ABA biosynthesis or downstream components of ABA signalling. The ABA biosynthetic mutants generally display all of the phenotypes described above (Barrero *et al.*, 2005; Gonzalez-Guzman *et al.*, 2004; Gonzalez-Guzman *et al.*, 2002; Ruggiero *et al.*, 2004). There are some reports that different enzymes may catalyze the last step of ABA biosynthesis in the seed and in the leaves in response to water deficit (Seo *et al.*, 2000) while other enzymes involved in ABA biosynthesis may allow ABA-mediated modifications to growth (Barrero *et al.*, 2005; Ruggiero *et al.*, 2004). On the other hand, mutants involved in downstream signalling may specifically display defective stomatal closure responses or aberrant induction of ABA genes (Merlot *et al.*, 2007; Xiong *et al.*, 2001) and have helped to uncover downstream components of the ABA signal transduction pathway. For example the *fiery* (*fry*) mutants, that have altered expression of ABA responsive genes, have revealed the role of IP_3 in ABA signalling (Xiong *et al.*, 2001; Xiong *et al.*, 2002a). Similarly the *open stomata* (*ost*) mutants, that are defective in initial ABA induced stomatal closure, have provided evidence for the importance of the plasma membrane H^+-ATPase (*ost2*) in ABA-induced stomatal closure which had for a long time been proposed although not proven (Merlot *et al.*, 2007; Mueller-Roeber and Dreyer, 2007) while *ost1* together with a *mitogen activated protein kinase kinase* (*mapkk*) mutant, *mkk9* that display ABA-insensitive germination, have demonstrated the importance of kinase cascades in ABA signalling (Alzwiy and Morris, 2007; Yoshida *et al.*, 2006). While ABA is generally thought to be involved in the response to the osmotic component of NaCl stress (Ruggiero *et al.*, 2004), there is also evidence that ABA affects components of the ionic stress pathway (Ohta *et al.*, 2003; Shi and Zhu, 2002).

1.4.6.3 Ion homeostasis mutants

Mutants affected in ion homeostasis have largely been isolated using root bending assays (Verslues *et al.*, 2006). This method identified the *sos* mutants (*sos1-3*) that specifically present NaCl-sensitive phenotypes and are not altered in their response to osmotic stress (Liu and Zhu, 1997; Wu *et al.*, 1996a; Zhu *et al.*, 1998). The *sos* mutants were also reported to be hypersensitive to low K^+ (Liu and Zhu, 1997; Rus *et al.*, 2004; Rus *et al.*, 2001; Wu *et al.*, 1996a; Zhu *et al.*, 1998) and together with the finding that their NaCl-sensitive phenotypes correlated with their reduced K^+ levels rather than their Na^+ content following NaCl exposure (Zhu *et al.*, 1998), revealed the importance of importance of maintaining K^+ nutrition under conditions of NaCl stress. Additionally the NaCl sensitivity of the *sos2* and *sos3* mutants is influenced by the Ca^{2+} levels in the media and lead to the discovery that calcium improves

K^+/Na^+ selectivity under conditions of NaCl stress (Liu and Zhu, 1997; Zhu *et al.*, 1998). Not only does the SOS pathway regulate SOS1, but also the tonoplast Na^+/H^+ antiporter, NHX1 that controls vacuolar Na^+ accumulation in the shoot (Qiu *et al.*, 2004). Therefore the *nhx1* mutant is also an ion homeostasis mutant, compromised in its NaCl tolerance (Apse *et al.*, 2003). Furthermore SOS1 has been found to be involved in the distribution of ions between the shoot and root tissue uncovering the importance of Na^+ recirculation as a mechanism to deal with NaCl stress (Shi *et al.*, 2002a) and altogether suggesting that the SOS1 regulates tissue-specific mechanisms for dealing with NaCl stress. The *sos* mutants have now been used in enhancer and suppressor screens to identify additional genes involved in ion homeostasis. This lead to the identification of *hkt1*, a suppressor of the NaCl-sensitive phenotype of *sos3*. HKT1 has since been reported to be responsible for Na^+ uptake as well as involved in the recirculation of ions between the shoot and root (Berthomieu *et al.*, 2003; Rus *et al.*, 2001; Sunarpi *et al.*, 2005). On the other hand, *enhancer 1* (*enh1*) enhanced the *sos3* mutant phenotype and pointed to the importance of ROS signalling in NaCl stress responses (Zhu *et al.*, 2007).

1.4.6.4 ROS mutants

The first indication that ROS played an important role in NaCl stress responses came from the characterization of a *photoautotrophic salt tolerance 1* (*pst1*) mutant which had lost the light-sensitivity of its NaCl response. These experiments revealed that plants can survive for long periods on NaCl-supplemented media if kept in the dark while seedlings grown on control media die under the same conditions (Tsugane *et al.*, 1999). Additionally, the *pst1* mutant was found to be more tolerant of ROS. This alluded to a NaCl-induced dormancy state and the role of light-induced ROS in NaCl sensitivity. In contrast, the *enh1* mutant, mentioned above, was NaCl hypersensitive, more sensitive to ROS and accumulated higher levels of ROS in response to NaCl stress compared to wildtype plants (Zhu *et al.*, 2007). These phenotypes were also shared by *sos2* although *enh1* did not enhance the NaCl sensitivity of *sos2*, suggesting that ENH1 and SOS2 may act in the same pathway. Furthermore SOS1 has been demonstrated to interact with RADICAL-INDUCED CELL DEATH 1 (RCD1), a regulator of oxidative stress responses (Katiyar-Agarwal *et al.*, 2006). Both *sos1* and *rcd1* display similar phenotypes to *enh1* and *sos2*. Therefore ROS sensitivity and ROS accumulation correlates with NaCl sensitivity, revealing the importance of detoxification of NaCl-induced ROS as a mechanism in determining plant NaCl tolerance.

1.4.6.5 Calcium mutants

Besides *sos3* and *sos2* which carry lesions in the calcium sensor *AtCBL4* and *AtCIPK24* respectively, a number of other mutants involved in calcium signalling also display altered NaCl and osmotic stress responses. These include two other *cbl* mutants: *cbl1* and *cbl10* (Cheong *et*

al., 2003; Kim *et al.*, 2007) as well as *cax1* which is defective in a vacuolar Ca^{2+}/H^{+} antiporter (Cheng *et al.*, 2003; Hirschi, 1999). Potentially these genes could be involved in decoding the NaCl-induced calcium response (Knight *et al.*, 1997). The discovery that CBL10 interacts with SOS2/CIPK24 to regulate vacuolar Na^{+} sequestration in the shoot, was of particular interest (Kim *et al.*, 2007) as this suggests that CIPK24 can interact with multiple CBL partners to regulate different aspects of NaCl tolerance and further implicates the SOS pathway in mediating tissue-specific NaCl tolerance mechanisms.

1.4.6.6 Growth mutants

It was mentioned earlier that ABA plays a role in growth in responses to stress (Barrero *et al.*, 2005; Ruggiero *et al.*, 2004). Additionally, the *nhx1* mutant displays growth defects that revealed the importance of ion homeostasis in development (Apse *et al.*, 2003). Besides these examples, a number of other mutants have been isolated that indicate a role for growth in the response to NaCl stress including *sos5*, *staurosporin and temperature sensitive 3a* (*stt3a*), *complex glycan 1* (*cgl1*), as well as a number of *radially swollen* (*rsw*) mutants, (*rsw1*, *rsw2* and *rsw3*) (Kang *et al.*, 2008; Koiwa *et al.*, 2003; Shi *et al.*, 2003). All of these mutants are hypersensitive to NaCl and display root growth arrest as a result of swelling of the root tip caused by enhanced cell expansion and demonstrate the importance of maintaining root growth in response to NaCl stress. While SOS5 is probably a cell surface adhesion protein involved in cell-to-cell adhesion (Shi *et al.*, 2003), STT3A and CGL1 appear to be involved in protein N-glycosylation that is important for recovery from the unfolded protein response and for cell wall formation under NaCl stress conditions (Kang *et al.*, 2008; Koiwa *et al.*, 2003).

1.4.6.7 Transcription mutants

A large number of genes are differentially regulated in response to NaCl stress (Kreps *et al.*, 2002). While there is some knowledge of ABA-regulated gene transcription, it seems that many NaCl responsive genes are not regulated by ABA (Kreps *et al.*, 2002). NaCl stress induces the expression of a number of transcription factors (Seki *et al.*, 2002), however very few genes involved in transcription have emerged from mutant studies. One that has is *SALT TOLERANCE* (*STO*) encoding a zinc finger transcription factor that when overexpressed in plants improved NaCl tolerance (Nagaoka and Takano, 2003). STO was demonstrated to interact with a H-protein promoter binding factor-1 (HPPBF-1) belonging to the family of MYB transcription factors, suggesting that these act together to induce expression of NaCl stress responsive genes. Recently a bZIP transcription factor, AtbZIP60, has also been implicated as playing a role in NaCl tolerance since an *AtbZIP60* overexpressor mutant was more NaCl tolerant (Fujita *et al.*, 2007). Microarray analysis revealed that *AtbZIP60* overexpression induces of a number of potential target genes; however most of these have not previously been

implicated in salt tolerance. Lastly an activation-tagged mutant screen identified a TATA box-binding protein (TBF)-associated factor, AtTAF10, as playing a positive role in NaCl tolerance possibly through promoter recognition of genes involved in salt tolerance (Gao *et al.*, 2006).

1.4.6.8 Regulation of protein activity and protein-protein interactions

Three other mutants are mentioned briefly whose gene products may regulate the activity of other proteins or facilitate protein interactions in response NaCl stress. These are *sos4*, *tetratricopeptide-repeat-thioredoxin-like 1* (*ttl1*) and *quiescin-sulfhydryl oxidase 2* (*qso2*) (Alejandro *et al.*, 2007; Rosado *et al.*, 2006; Shi *et al.*, 2002b). The *SOS4* gene encodes a pyridoxal kinase that is involved in the biosynthesis of pyridoxal-5-phosphate (vitamin B6) which is a cofactor for many enzymes in animals as well as a ligand for P2X receptor ion channels (Shi *et al.*, 2002b). Since the *sos4* presents with characteristic *sos* phenotypes, SOS4 has been proposed to modulate ion channel activity. The *ttl1* mutant displays reduced NaCl tolerance and impaired ABA-mediated gene expression. TTL1 encodes a structural protein likely to be important for the formation of multi-enzyme complexes that are required for the positive regulation of NaCl-induced ABA signalling (Rosado *et al.*, 2006). The activation-tagged *QSO2* mutant displays improved NaCl tolerance and has increased accumulation of K^+ in its xylem sap and shoot (Alejandro *et al.*, 2007). QSOs oxidize disulfhydryl groups in proteins to disulfides and are thought to participate in the folding of disulfide-containing secreted proteins. Since some channel proteins contain sulfhydryl groups, QSO2 has been proposed to regulate channel activity and thereby control loading of K^+ into xylem.

The study of mutants has revealed important mechanisms determining NaCl tolerance. The role of ABA in the inhibition of germination and stomatal closure in response to NaCl and osmotic stresses is now well known. The SOS signalling pathway has been uncovered as important for maintaining K^+ homeostasis in response to NaCl and additionally revealed the role of calcium and ROS in NaCl signalling. Additionally there are a number of other mutants that display altered NaCl tolerance, whose gene products are less well understood but implicate growth, transcription and the regulation of other proteins as being critical to maintaining ionic and osmotic homeostasis in NaCl stress environments.

1.4.7 Biotic Stresses - competition for water and nutrients

Pathogens must acquire water and nutrients from the plant in order to survive yet astonishingly little is known about how this is actually achieved. The environment inside the plant is harsh for the pathogen since it must compete with the plant for resources as well as avoid the bombardment of plant defences (Gohre and Robatzek, 2008; Greenshields and Jones, 2008). Ultimately any successful pathogen must alter host metabolism to acquire water and nutrients

from the plant and create a more favourable environment (Berger *et al.*, 2007; de Torres-Zabala *et al.*, 2007; Gottig *et al.*, 2008; Lopez *et al.*, 2008). Once a new homeostatic balance is established the infection site becomes a metabolic sink with the pathogen drawing water and nutrients and the plant responding by translocating more nutrients to the infection site, further feeding the pathogen (Berger *et al.*, 2007; Walters and McRoberts, 2006).

1.4.7.1 The plants defence response

The lack of knowledge about plant-pathogen water and nutrient exchange is in stark contrast to the large body of literature describing the plants defence response. This is introduced briefly here in order to understand in context, the pathogens manipulation of host homeostasis and how the plant attempts to prevent this. The manner in which a pathogen obtains water and nutrients depends largely on its lifestyle. Pathogens can broadly be grouped into biotrophic pathogens that survive off living plant tissue, which can in some cases lead to tissue death at later stages of infection (hemi-biotrophic) and necrotrophic pathogens that kill the plant host and feed off dead tissue (Berger *et al.*, 2007; Glazebrook, 2005). Necrotrophic pathogens such as *Botrytis cinerea* directly penetrate the plant, kill it and then feed off the dead tissue using a battery of toxins and lytic enzymes. Biotrophic pathogens like *P. syringae* enter the plant through stomata or wound sites and once inside the plant, they remains in the apoplast where they inject virulence factors into the plant cell to suppress the plants defence response and cause water and nutrients to leak out of the cell. The obligate oomycete *Hyaloperonospora parasitica* is also a biotrophic pathogen but similarly to *B. cinerea* it is able to penetrate the plant. It produces a sophisticated feeding structure - a haustorium that invaginates the host cell membrane and establishes a water and nutrient exchange interface (Slusarenko and Schlaich, 2003; Voegele and Mendgen, 2003).

Plants have distinct defence responses against biotrophic and necrotrophic pathogens. In general, the plant uses salicylic acid (SA)-mediated defences against biotrophic pathogens but jasmonic acid (JA)/ethylene (ET) signalling pathways in defence against necrotrophic pathogens (Glazebrook, 2005). For example, even though the actual lifestyles of *H. parasitica* and *P. syringae* are quite different, the fact that both pathogens require living tissue means that localized cell death at the infection site, known as the HR, effectively contains the spread of these pathogens and limits the supply of water and nutrients to them (Glazebrook, 2005; Knoth *et al.*, 2007). On the other hand the HR aids infection by *B. cinerea* (Govrin and Levine, 2000). This is probably the basis of the antagonism that occurs between SA and JA signalling pathways so as to ensure that cell death is not initiated inappropriately (Loake and Grant, 2007).

The interaction between *Arabidopsis* and *P. syringae* has been well characterized and is therefore discussed in greater detail (Katagiri *et al.*, 2002).

During the initial infection process receptors on the host plasma membrane recognize and bind highly conserved pathogen associated molecular patterns (PAMPs), for example flagellin (Ingle *et al.*, 2006; Schwessinger and Zipfel, 2008). This initiates a signal transduction cascade resulting in the induced defence response known as PAMP-triggered immunity (PTI). One outcome of PTI is reinforcement of the cell wall by callose deposition (Hauck *et al.*, 2003; Shang *et al.*, 2006), and together with the passive defences provided by the waxy cuticle and preformed antimicrobial compounds is the first line of basal defence against pathogens effective against most potential pathogens (Dangl and Jones, 2001; Ham *et al.*, 2007; Lipka *et al.*, 2008).

In order to successfully infect the plant, virulent pathogens must overcome these basal defences (Jones and Dangl, 2006). To this end *P. syringae* enlists a battery of virulence factors which can either be phytotoxins, for example coronatine (COR), or effector proteins (Brooks *et al.*, 2004; de Torres *et al.*, 2006; Kim *et al.*, 2005; Li *et al.*, 2005). As many as 40 effector proteins are injected into the plant cell via the bactrium's type three secretion system (TTSS) (Schechter *et al.*, 2004). These effectors are bacterial virulence factors that target plant proteins in order to suppress basal defence or alter host metabolism to the benefit of the pathogen (de Torres-Zabala *et al.*, 2007; Li *et al.*, 2005).

In some cases the plant has evolved resistance (*R*) genes to recognize these bacterial effectors, either directly or indirectly by sensing modifications made to their host target proteins (Jones and Dangl, 2006). Upon detection the virulence (Vir) factors become avirulence (Avr) factors and recognition of the "pathogen-induced modified self" triggers a second line of inducible defence known as effector-triggered immunity (ETI) or *R* gene-mediated resistance (Jones and Dangl, 2006). This is essentially a rapid, amplified defence response (Jones and Dangl, 2006; Tao *et al.*, 2003) that is thought to be quantitatively rather than qualitatively different from the PTI (Eulgem *et al.*, 2004; Maleck *et al.*, 2000; Navarro *et al.*, 2004; Tao *et al.*, 2003). Often ETI is accompanied by the HR as well as systemic acquired resistance (SAR) that primes defence responses in distal tissues to confer broad spectrum resistance to subsequent pathogen attack (Durrant and Dong, 2004; Glazebrook, 2005). The pathogen is thus rendered avirulent to the plant.

1.4.7.2 Water homeostasis

The main points of entry for the pathogen into the plant are the stomata (Underwood *et al.*, 2007). It has recently been shown that pathogens on the leaf surface can sense and move towards open stomata (Melotto *et al.*, 2006). As part of PTI, the plant closes its stomata in an ABA and SA-dependent manner to prevent further invasion (Melotto *et al.*, 2006). Bacteria

have however evolved mechanisms to re-open stomata to aid their release and re-infection, involving the bacterial toxin COR - a JA mimic that antagonizes SA-mediated signal transduction (Koda *et al.*, 1996; Melotto *et al.*, 2006; Weiler *et al.*, 1994). However some bacterial strains that lack COR are still able to open stomata, therefore it is likely that there are additional virulence factors that open stomata (Melotto *et al.*, 2006; Underwood *et al.*, 2007). Furthermore avirulent pathogens are less effective at re-opening stomata suggesting that recognition of these pathogens by the plant ensures that stomata are kept closed (Melotto *et al.*, 2006). Since the stomata determine whole plant water flux, this is one way that the pathogen manipulates plant water homeostasis and the plant in turn acts to rectify this.

Once inside the plant, the pathogen attempts to modify the water potential of the apoplast to make it more conducive to pathogen growth. Evidence for this was provided in a study by Wright and Beattie who showed that virulent and avirulent pathogens experience different apoplastic water potentials (Wright and Beattie, 2004). This difference is thought to limit the growth of the avirulent pathogen and suggests that the water potential sensed by the pathogen in the apoplastic space is a critical determinant restricting pathogen growth and that virulent pathogens have adapted mechanisms to overcome this by altering plant water status.

Only a few Avr proteins have been characterized, although of the ones that have some have been shown to target ABA or auxin signalling, either by increasing the levels of these hormones or by enhancing the plant's sensitivity to them (Chen *et al.*, 2007a; Cunnac *et al.*, 2009; de Torres-Zabala *et al.*, 2007; Goel *et al.*, 2008). While ABA is best known for its role in abiotic stress responses, auxins are involved in growth. The reason that the pathogen targets these hormones is probably because both of these suppress SA-mediated defence response (Cunnac *et al.*, 2009). Indeed, at first glance it may seem counter-intuitive that pathogens increase ABA levels when ABA closes stomata. Rather it has been proposed that ABA is used by the pathogen to optimize the osmotic pressure in the apoplast (de Torres-Zabala *et al.*, 2007). On the other hand, auxins have been suggested to induce cell wall loosening which would increase membrane leakiness causing water and nutrients to leak from the host cell into the intercellular space for consumption by the pathogen (Beattie and Lindow, 1999). Pathogen manipulation of plant mechanisms to adjust homeostasis is probably the most cost effective and likely way to avoid recognition by the plant.

1.4.7.3 Ion homeostasis

One of the earliest events in the plant defence response are ion fluxes (Balague *et al.*, 2003; Clough *et al.*, 2000). Initial reports described a K^+/H^+ exchange as part of the HR (Atkinson *et al.*, 1985), the magnitude of which correlated with bacterial population growth (Atkinson and

Baker, 1987). Increased pH of the intercellular fluids was associated with improved sucrose availability for the pathogen since reversal of the H^+ gradient inhibits sucrose uptake by the plant cell (Atkinson and Baker, 1987). Therefore pathogens lower plant intracellular K^+ levels and thus induce K^+ starvation in the plant (Clough *et al.*, 2000).

Atkinson also reported a Ca^{2+} increase in response to pathogen infection that was required for the K^+/H^+ response and the subsequent HR (Atkinson *et al.*, 1990). More recently Grant and colleagues have shown that virulent and avirulent pathogens both induce rapid Ca^{2+} transients but that a second delayed Ca^{2+} influx occurs only in response to avirulent pathogens and this is required for the production of H_2O_2 and the HR (Grant *et al.*, 2000). In agreement with this Nemichov and others have recorded similar early Ca^{2+} influxes in response to pathogens; however they also reported a much more delayed Ca^{2+} efflux specific to the HR and possibly important for cell death during the HR (Nemchinov *et al.*, 2008).

As mentioned in the previous section, two *dnd* mutants - *dnd1* and *dnd2* that fail to develop the HR but are still able to initiate *R* gene-mediated resistance, have lesions in *CNGCs*: *CNGC2* and *CNGC4* respectively (Balague *et al.*, 2003; Clough *et al.*, 2000). This was the first link between a plant ion channel and the defence response to pathogens. Since AtCNGC2 has been shown to transport Ca^{2+}, AtCNGC2 was proposed to play a role in calcium signalling during the HR (Clough *et al.*, 2000; Leng *et al.*, 1999) while AtCNGC4 has been shown to transport Na^+ and K^+ and therefore could be responsible for pathogen-induced K^+ leakage (Balague *et al.*, 2003). However these ion channels have not yet been shown to transport ions during the HR.

In summary, both plants and pathogens manipulate water and ion homeostasis and this appears to be critical at early stages of pathogen infection while the pathogen and plant are fighting to establish a new homeostatic balance.

1.5 CONCLUSIONS AND AIMS OF THE CURRENT STUDY

Heterologs of animal NPs, PNPs have probably arisen through convergent evolution presumably to perform some vital function in plants. In plants, NPs act on the stomata which, like the kidneys, control organismal water flux. Additionally PNPs stimulate protoplast swelling, indicating that PNPs also exert cellular effects that involve volume and osmoregulation. Therefore plant responses to PNP treatment suggest that PNPs regulate water and ion homeostasis in plants as do their counterparts in animals. The mechanism of PNP action in plants has yet to be determined however evidence suggests that PNPs induce cGMP signalling and ion fluxes similar to animal NPs. While cGMP signalling in plants is poorly understood, it

seems that cGMP is involved in regulating water and ion homeostasis by directly affecting ion channels, suggesting that CN signalling in plants has diverged from that in animals. Therefore PNPs may exert their effects on water and ion homeostasis via the second messenger cGMP. Water and ion homeostasis in plants is affected by both abiotic stresses that restrict water and nutrient availability in the environment and biotic stresses that involve pathogens competing with the plant for these resources. The aim of the current study was to gain further insight into the role of PNPs *in planta*. In order to achieve this second messenger signalling in response to recombinant AtPNP-A treatment and stresses that perturb water and ion homeostasis was examined; an *atpnp-a* mutant was characterized for its responses to stresses that affect water and ion homeostasis and a computational analysis of *AtPNP-A* expression and the AtPNP-A-induced transcriptome was conducted.

CHAPTER 2

SECOND MESSENGER SIGNALLING IN RESPONSE TO WATER AND ION STRESSES

CHAPTER 2: SECOND MESSENGER SIGNALLING IN RESPONSE TO WATER AND ION STRESSES

2.1 INTRODUCTION

2.1.1 The second messenger concept

The second messenger concept was first described by Sutherland and colleagues in 1971 following their discovery of cAMP (Rall *et al.*, 1957; Robison *et al.*, 1971). Briefly, this entails a mammalian hormone or neurotransmitter that acts as a primary messenger outside of the cell. This binds to a specific receptor on the exterior cell membrane inducing a conformational change that transmits the signal to the cell interior, activating an adenylyl cyclase on the interior cell membrane and thereby causing the rapid synthesis and release of cAMP (which is otherwise maintained at very low levels) inside the cell. Subsequently cAMP stimulates protein kinase A (PKA) which modifies target protein activity. Importantly though, the signal is transient with cAMP being quickly hydrolyzed to AMP by a PDE. The second messenger concept has now been extended to include a number of other molecules. In plants the most ubiquitous and well studied second messenger is calcium (Sanders *et al.*, 2002). Other second messengers that either act independently or in concert with calcium include lipids and phospholipids, cADPR, H^+ ions that change intracellular pH, ROS and CNs (Grant *et al.*, 2000; Irving *et al.*, 1992; Meijer and Munnik, 2003; Newton *et al.*, 1999; Ng and Hetherington, 2001; Wu *et al.*, 1997).

2.1.2 Encoding specificity

There is an abundance of genes encoding receptors and downstream response elements suggesting that these tend toward specificity (Sanders *et al.*, 2002). However a small number of secondary messengers are used to convert a wide range of stress inputs into multiple different response outputs. How then is specificity encoded in the second messenger signal? In the case of calcium, a popular hypothesis is that information is encoded in temporal and spatial aspects of the "calcium signature" which can take the form of oscillations, waves, spikes or biphasic responses (McAinsh and Hetherington, 1998; Ng and McAinsh, 2003; Scrase-Field and Knight, 2003). Additionally, the source of the calcium signal may encode specificity, arising through differential access to the cellular machinery controlling calcium release from extracellular (apoplast) and intracellular (vacuole mainly but also the mitochondria and endoplasmic reticulum) calcium stores (Gao *et al.*, 2004; Logan and Knight, 2003; Ng *et al.*, 2001; Ng and McAinsh, 2003; Pittman and Hirschi, 2003; Sanders *et al.*, 2002). The calcium signature hypothesis is heavily influenced by the animal literature where there is good evidence to support it (Dolmetsch *et al.*, 1997; Hardingham *et al.*, 1997). In plants, the dogma of the calcium signature appears to hold true in the stomata where calcium transients are easily related to

stomatal aperture changes however recent reviews suggest that this is exception rather than the rule (Scrase-Field and Knight, 2003). In fact most of the evidence for the calcium signature is correlative. For the signature to be *bona fide* it is necessary to link differences in the calcium signal to differences in an end response. The efficacy and dynamics of the second messenger signal is also determined by its diffusion properties and the co-localization of sensor and response elements and enzymes for signal termination in microdomains within the cell (Knight and Knight, 2001; Ng *et al.*, 2001; Pittman and Hirschi, 2003; Sanders *et al.*, 2002; Trewavas and Malho, 1997; Trewavas *et al.*, 2002). Cross-talk between signalling pathways may also influence the signal, enabling information from different stresses to be incorporated into a single integrated response (Knight and Knight, 2001). Understanding how specificity is encoded in these initial signalling events is crucial to determining how plants discriminate between stresses.

2.1.3 NaCl and osmotic stress

For reasons discussed in chapter 1, NaCl and osmotic stress affect water and ion homeostasis in plants. Salinity stress accounts for crop losses far greater than those caused by any other stress and arises through irrigation followed by evaporation since irrigation water contains low amounts of NaCl (Boyer, 1982; Serrano *et al.*, 1999). NaCl imposes both an ionic and osmotic stress, therefore the response to NaCl is traditionally examined in parallel with the response to sugars (mannitol or sorbitol) to tease out ionic and osmotic-specific effects (Zhu, 2002). NaCl and drought stress are similar in that both decrease water availability, however differ in that mannitol is thought not to be taken up by the plant so that it induces physiological drought (Knight *et al.*, 1997) whereas Na^+ and Cl^- are taken up and may be used for osmotic adjustment (Verslues *et al.*, 2006). This could explain why dehydration appears to pose less of a problem to plants exposed to NaCl than to those experiencing osmotic stress (Munns, 2005). Physiological experiments suggest that there is little distinction in the early responses to NaCl and osmotic stress (Munns, 2002; Munns, 2005). At the molecular level however, ion fluxes differ and the SOS pathway is only activated by ionic stress (Shabala, 2000; Shabala and Cuin, 2008; Zhu, 2002) suggesting that signal transduction events initiated by these stresses are quite different. The question remains as to whether secondary messengers resolve these stresses. Previous studies demonstrated that calcium increases in response to both NaCl and osmotic stress but concluded that calcium alone cannot discriminate between these stresses (Knight *et al.*, 1997). However calcium is central to the SOS pathway and is thus likely to still play a role (Bressan *et al.*, 1998; Gong *et al.*, 2004). Cyclic GMP has also been implicated in the response to NaCl since cGMP reduces Na^+ uptake and improves salinity tolerance (Maathuis and Sanders, 2001; Rubio *et al.*, 2003), although a cGMP response to NaCl treatment had not been reported. The aim of this study was to further explore the role of calcium and cGMP in the response to NaCl and osmotic stress and to determine whether they can discriminate between these stresses.

2.2 MATERIALS AND METHODS

2.2.1 Chemicals and stock solutions

Coelentrazine (Molecular Probes, Eugene, Oregon, USA) was dissolved in methanol (MeOH) and made up to the desired concentration with water (final concentration of MeOH was 1.25% v/v). Dibutryl cGMP, 1,2-bis(2-aminophenoxy)-ethane-*N,N,N',N'*-tetraacetic acid (BAPTA), neomycin and ruthenium red were all purchased from SIGMA Aldrich (St Louis, USA). Dibutryl cGMP, BAPTA and ruthenium red are all water soluble while neomycin was purchased as a ready made 10 mg/ml stock solution in 0.9% (w/v) NaCl. The GC inhibitor, LY 83583, was a gift from Dr Ndiko Ludidi, who provided a 100 mM stock solution dissolved in dH_2O. Recombinant AtPNP-A was a kind gift from Dr Monique Morse, prepared as described previously (Morse *et al.*, 2004).

2.2.2 Seed sterilization

Seed was sterilized by shaking for 5 min in 70% (v/v) ethanol (EtOH) after which time the EtOH was aspirated and replaced with 10% (v/v) bleach and 0.02% (v/v) Triton X and followed by another 10 min shaking. The sterilized seed was then washed four times in sterile dH_2O before resuspending in sterile 0.1% (w/v) agar. Seeds were stored at 4°C to vernalize prior to sowing.

2.2.3 Plant nutrient media

Plant nutrient (PN) media contains 5 mM KNO_3, 2 mM $MgSO_4.7H_2O$, 2 mM $Ca(NO_3)_2.4H_2O$, 0.5 mM FeNaEDTA and 1 X micronutrients (70 μM H_3BO_3, 14 μM $MnSO_4.H_2O$, 0.5 μM $CuSO_4.5H_2O$, 1 μM $ZnSO_4.6H_2O$, 0.2 μM Na_2MoO_4, 10 μM NaCl and 0.01 μM $CoCl_2.6H_2O$) to which 2.5 mM KPO_4 buffer, pH 5.5 was added after autoclaving (Haugh and Sommerville, 1986).

2.2.4 *Arabidopsis* seedling growth conditions

Transgenic *Arabidopsis* Columbia-0 (Col-0) ecotype seedlings expressing the calcium reporter gene, apoaequorin, expressed under the control of the constitutive cauliflower mosaic virus (CaMV) 35S promoter (Knight *et al.*, 1996) were grown in petri dishes on PN agar (6% w/v) under constant light (100 μM photons m^{-2} s^{-1}) at 24°C for two weeks.

2.2.5 Aequorin reconstitution

Individual seedlings were carefully removed from the PN agar using forceps and placed into 6-well microtitre plates containing 2 ml dH_2O. Aequorin was reconstituted according to the method of Knight and colleagues (Knight *et al.*, 1991). Essentially 2 ml of 5 μM coelentrazine luminophore was added to the microtitre plate wells to a final concentration of 2.5 μM and the plates were then covered in foil and incubated at room temperature overnight in the dark.

2.2.6 Calcium assays

Following aequorin reconstitution, individual seedlings were removed from the coelentrazine solution, placed into cuvettes containing 250 μl dH_2O and allowed to stabilize for 30 min so as to dispel any touch responses. Pretreatments with inhibitors were as follows: 5 mM BAPTA for 5 min, 0.1 mM neomycin for

1 hr, 0.1 mM ruthenium red for 1 hr or 10 μM LY for 15 min. The cuvette was then placed in a luminometer (Luminoskan TL Plus Luminometer, Labsystems, Finland) and background luminescence measured every 5 s for 15 s. Treatments (each of 250 μl) were delivered through a light tight port as double strength solutions and luminescence measured every 5 s until the counts had returned to background levels. In order to calibrate the calcium response with the amount of aequorin in each seedling, the remaining aequorin was discharged with 2 M $CaCl_2$ in 20% (v/v) EtOH (Knight *et al.*, 1997). The concentration of cytosolic free calcium ($[Ca^{2+}]_{cyt}$) was calibrated using the equation pCa = 0.332588(-logk) + 5.5593, where k is a constant equal to luminescence counts per s divided by the total remaining counts (Knight *et al.*, 1996). Since the calcium responses are rapid, occurring within the first 5 s after treatment, and because treatments were added slowly (over a few seconds) so as to minimize any touch responses, the time points of the peak maxima are therefore only approximates. It would have been preferable to record luminometric measurements at sub second intervals to better resolve the peak maxima however 5 s was the smallest interval that could be measured using this particular luminometer.

2.2.7 Cyclic GMP extraction and assays

Seedlings were pooled and treated in microtitre plates exactly as described above. Samples were quickly removed from the treatment solution, blotted dry, then frozen in liquid nitrogen and stored at -70°C. Cyclic GMP was extracted according to the manufacturer's instructions in the cGMP (^{125}I) Assay System (Amersham Biosciences, UK). Briefly, 300 mg frozen tissue was ground in liquid nitrogen to a fine powder and added to 3 ml ice cold 6% (w/v) trichloroacetic acid (TCA). This homogenate was centrifuged at 5000 X *g* for 15 min in a J2-21 Beckman centrifuge (Beckman Coulter, Inc., CA, USA). The aqueous extract was recovered and washed four times with five volumes of diethyl ether, each time centrifuging at 5000 X *g* for 5 min and then discarding the upper diethyl ether phase. Finally the aqueous extract was dried under vacuum at 25°C and stored at -70°C. Cyclic GMP was measured using the cGMP (^{125}I) Assay System (Amersham Biosciences, UK), according to the manufacturer's instructions.

2.2.8 Statistics

Statistics were performed using STATISTICA. In cases where n was < 10 the Mann-Whitney (non-parametric) test was used, while for experiments where $n \geq 10$ a t test was performed.

2.3 RESULTS

2.3.1 Calcium responses to NaCl and osmotic stress treatment

The calcium activated luminescent protein, aequorin has been successfully used to report increases in the cytosolic free calcium concentration ($[Ca^{2+}]_{cyt}$) in response to a number of stimuli (Evans *et al.*, 2005; Grant *et al.*, 2000; Knight *et al.*, 1996; Knight *et al.*, 1997; Knight *et al.*, 1991). In this study transgenic *Arabidopsis* seedlings constitutively expressing aequorin were used to measure changes in $[Ca^{2+}]_{cyt}$ in response to NaCl stress and osmotic stress imposed by iso-osmolar concentrations of sorbitol. Water was used as a control treatment and a small calcium transient was observed immediately (within 5 s) after treatment, due to a touch response. In a NaCl dose response 50 mM NaCl, 150 mM NaCl and 300 mM NaCl treatment all resulted in large, rapid and transient increases in $[Ca^{2+}]_{cyt}$ (Figure 2.1A). These calcium spikes were temporally similar but differed in magnitude. The 50 mM NaCl treatment resulted in a slightly delayed calcium transient that peaked approximately 15 s after treatment at 1.022 ± 0.114 μM. This increased significantly ($p < 0.05$) in response to 150 mM NaCl reaching 1.417 ± 0.102 μM after approximately 10 s. Thereafter the response appeared to have reached a maximum as there was no further increase following 300 mM NaCl treatment which peaked at 1.502 ± 0.074 μM, approximately 10 s after treatment.

A sorbitol dose response using iso-osmolar concentrations was performed to allow for comparison between NaCl and osmotic stress responses. 50 mM NaCl corresponds approximately to an iso-osmolar concentration of 100 mM sorbitol, 150 mM NaCl corresponds approximately to 300 mM iso-osmolar sorbitol and 300 mM NaCl is approximately iso-osmolar to 600 mM sorbitol. This doubling effect occurs because dissociation of NaCl in solution produces two ions, Na^+ and Cl^-, both of which contribute to the osmolarity of the solution whereas sorbitol does not dissociate, thus only one molecule contributes to the osmolarity. Iso-osmolar equivalents are necessarily only approximates because this assumes perfect dissociation of NaCl without accounting for factors such as interionic forces (Maggio *et al.*, 2006). The sorbitol-induced calcium response was similar to that induced by NaCl in timing and duration and also increased in magnitude with increasing sorbitol concentration (Figure 2.1B). In response to 100 mM sorbitol a rapid (within 5 s), very small calcium transient (0.212 ± 0.019 μM) was observed that was not significantly different from the response to water and is therefore also likely to be a touch response. 300 mM sorbitol induced a calcium transient that peaked approximately 10 s following treatment at 0.637 ± 0.092 μM. In comparison, the response to 600 mM sorbitol was temporally similar but significantly ($p < 0.05$) greater in magnitude, reaching 1.089 ± 0.148 μM.

2.1 A.

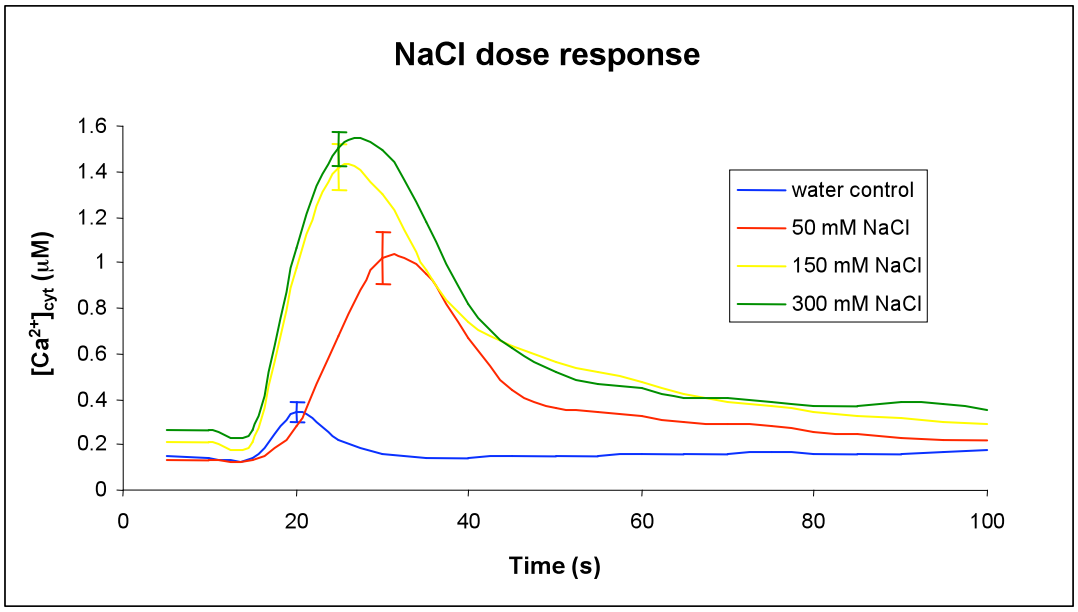
NaCl dose response
[Ca2+]cyt (µM)
1.6
1.4
1.2
1
0.8
0.6
0.4
0.2
0
0
20
40
60
80
100
Time (s)
water control
50 mM NaCl
150 mM NaCl
300 mM NaCl

B.

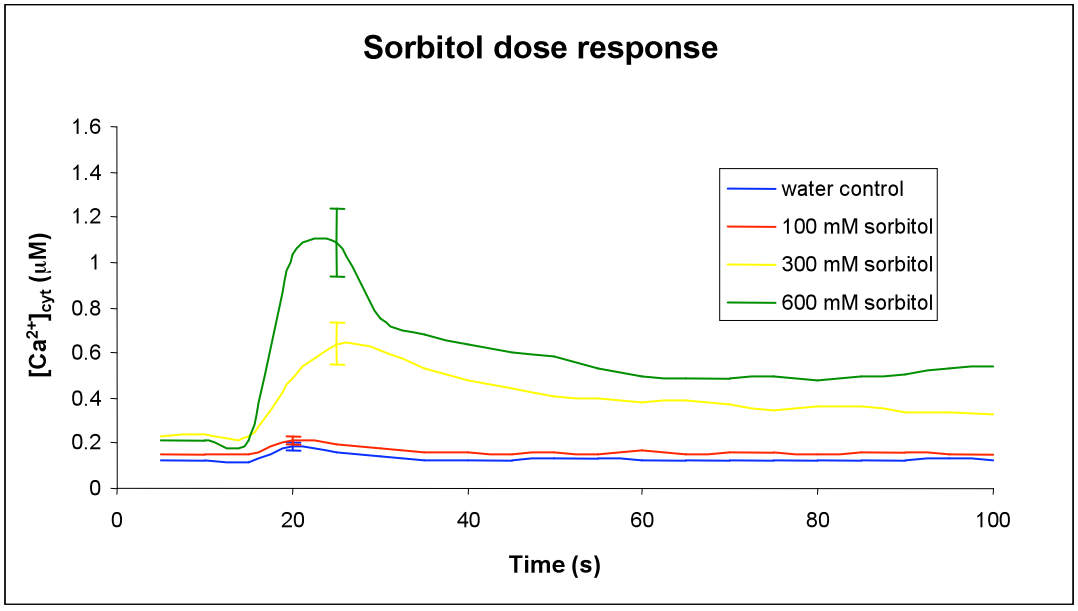
Sorbitol dose response
[Ca2+]cyt (µM)
1.6
1.4
1.2
1
0.8
0.6
0.4
0.2
0
0
20
40
60
80
100
Time (s)
water control
100 mM sorbitol
300 mM sorbitol
600 mM sorbitol

C.

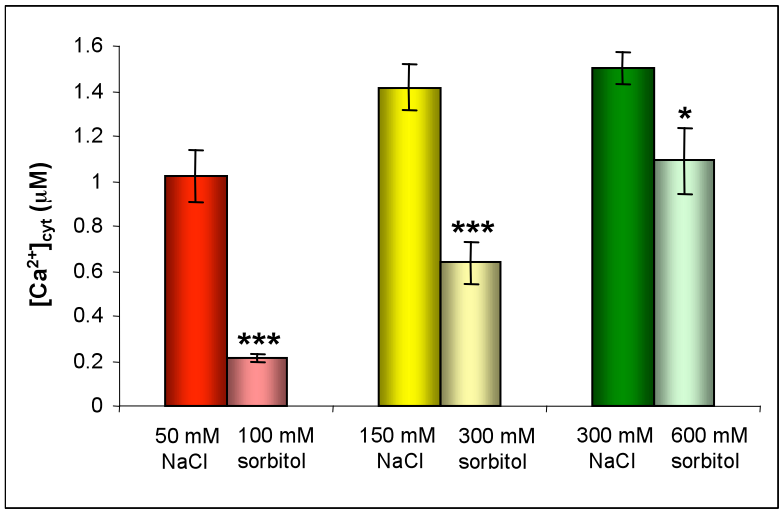

Figure 2.1. NaCl and sorbitol-induced increases in $[Ca^{2+}]_{cyt}$

Two week old *Arabidopsis* Col-0 seedlings expressing the calcium reporter aequorin were treated with increasing doses of NaCl (A) or sorbitol (B). Bioluminescence measurements were recorded over time and $[Ca^{2+}]_{cyt}$ calculated as described by Knight and colleagues (Knight *et al.*, 1996). Each curve is the average of several individual seedling responses. For the NaCl dose response: water n = 5 while for 50 mM NaCl, 150 mM NaCl and 300 mM NaCl n = 10. For the sorbitol dose response each curve is the average response of 10 seedlings. Error bars are the standard error of the mean peak maxima. Mean peak maxima were compared between NaCl and isoosmolar sorbitol concentrations (C). * represents a significant difference of $p < 0.05$ and *** a highly significant difference of $p < 0.001$ when comparing NaCl and the isoosmolar sorbitol-induced $[Ca^{2+}]_{cyt}$ peaks, as calculated using a t test.

Mean peak maxima were compared between NaCl and sorbitol treatments (Figure 2.1C). The NaCl-induced $[Ca^{2+}]_{cyt}$ peaks were greater than those for iso-osmolar sorbitol. This was highly significant ($p < 0.001$) for the 50 mM NaCl compared with 100 mM sorbitol and the 150 mM NaCl compared with 300 mM sorbitol response. The difference between the 300 mM NaCl and 600 mM sorbitol peaks was less pronounced than at lower doses, but still significant ($p < 0.05$).

After the NaCl and sorbitol responses had subsided, the $[Ca^{2+}]_{cyt}$ settled at a new resting level that was higher than before the treatment and dependent on dose. This was significant ($p < 0.05$) for the sorbitol dose response however not for the NaCl response.

Therefore $[Ca^{2+}]_{cyt}$ increased in a concentration-dependent manner in response to NaCl and iso-osmolar sorbitol treatment. The response to NaCl treatment was greater in magnitude than the response to sorbitol indicating that ionic and osmotic stresses induce different calcium signatures. Since 50 mM NaCl induced a large calcium transient whereas iso-osmolar 100 mM sorbitol did not, it appears as if, at this concentration, the NaCl-induced calcium transient is a response specific to the ionic stress.

2.3.2 Inhibitors of the NaCl and sorbitol-induced calcium responses

To explore the possibility that the source of these calcium signals encodes specificity, the effect of inhibitors of calcium release from different calcium stores was investigated on the high (150 mM) and low (50 mM) NaCl and iso-osmolar high (300 mM) sorbitol-induced calcium transients. These concentrations were chosen because they showed the greatest differences between the $[Ca^{2+}]_{cyt}$ peak maxima responses to iso-osmolar NaCl and sorbitol (Figure 2.1C). Three inhibitors of calcium release from different stores were tested: BAPTA - a chelator of extracellular Ca^{2+} that blocks extracellular calcium release, neomycin - an inhibitor of IP_3-mediated calcium release from intracellular stores and ruthenium red - an inhibitor of cADPR-mediated calcium release from intracellular stores. These inhibitors did not affect the (low) 100 mM sorbitol response. Since 100 mM sorbitol failed to induce an osmotic response, this is more an indication that the inhibitors do not affect the touch response therefore the data is not shown.

BAPTA did not have a significant effect on the calcium responses induced by any of the NaCl or sorbitol treatments (Figure 2.2A-F). Neomycin, on the other hand, delayed and significantly ($p < 0.001$) reduced the calcium response to 150 mM NaCl, lowering the peak from 1.143 ± 0.135 μM to 0.638 ± 0.037 μM (Figure 2.2A-B). Likewise neomycin significantly ($p < 0.001$) reduced the 50 mM NaCl peak from 0.947 ± 0.096 μM to 0.391 ± 0.052 μM (Figure 2.2C-D). Neomycin also significantly ($p < 0.001$) reduced the 300 mM sorbitol response from 0.635 ±

2.2 A.

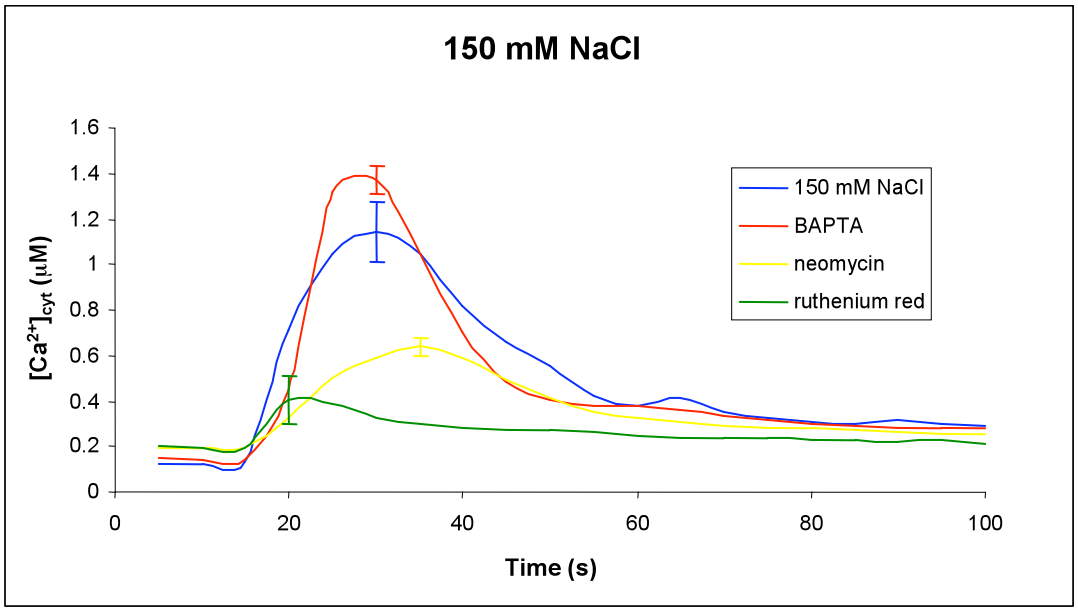
150 mM NaCl
[Ca2+]cyt (µM)
Time (s)
150 mM NaCl
BAPTA
neomycin
ruthenium red

B.

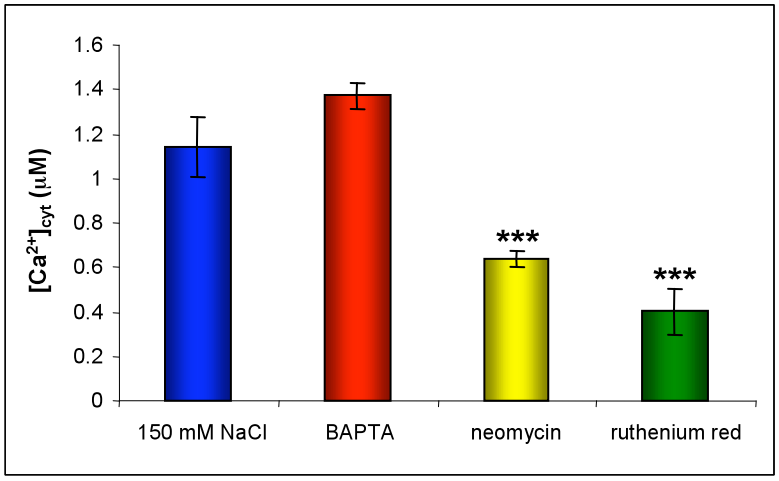
[Ca2+]cyt (µM)
***
***
150 mM NaCl
BAPTA
neomycin
ruthenium red

2.2 C.

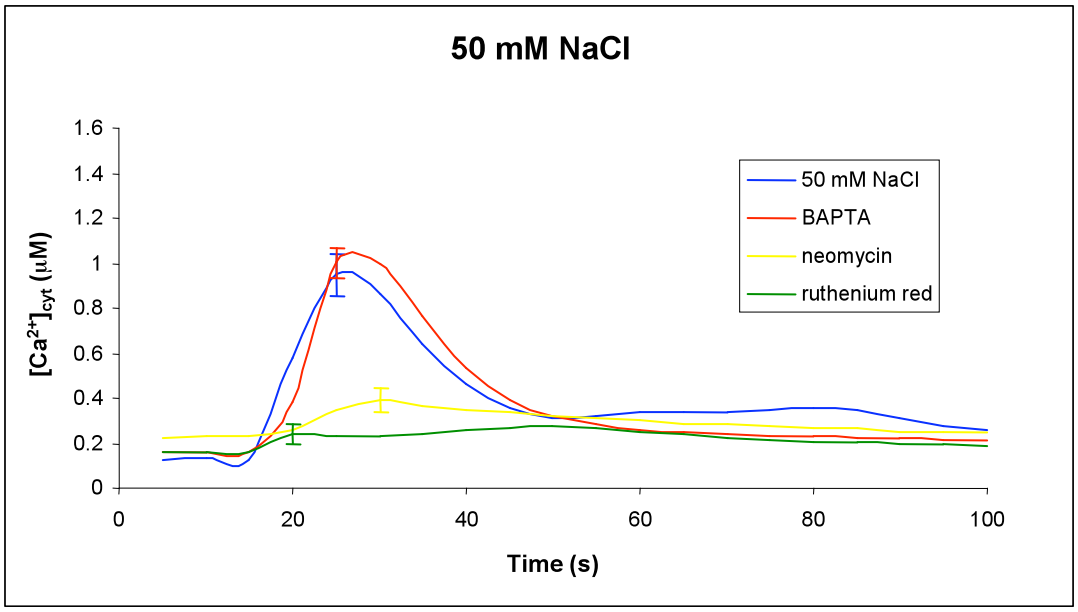
50 mM NaCl
[Ca2+]cyt (µM)
1.6
1.4
1.2
1
0.8
0.6
0.4
0.2
0
0
20
40
60
80
100
Time (s)
50 mM NaCl
BAPTA
neomycin
ruthenium red

D.

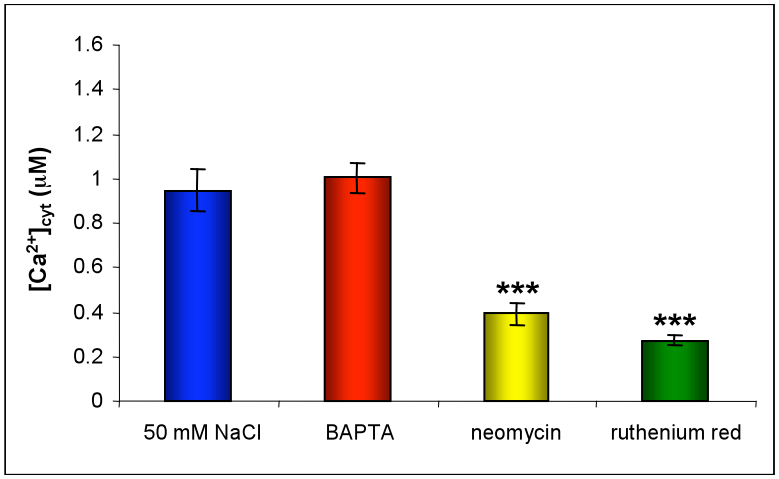
[Ca2+]cyt (µM)
1.6
1.4
1.2
1
0.8
0.6
0.4
0.2
0
***
***
50 mM NaCl
BAPTA
neomycin
ruthenium red

E.

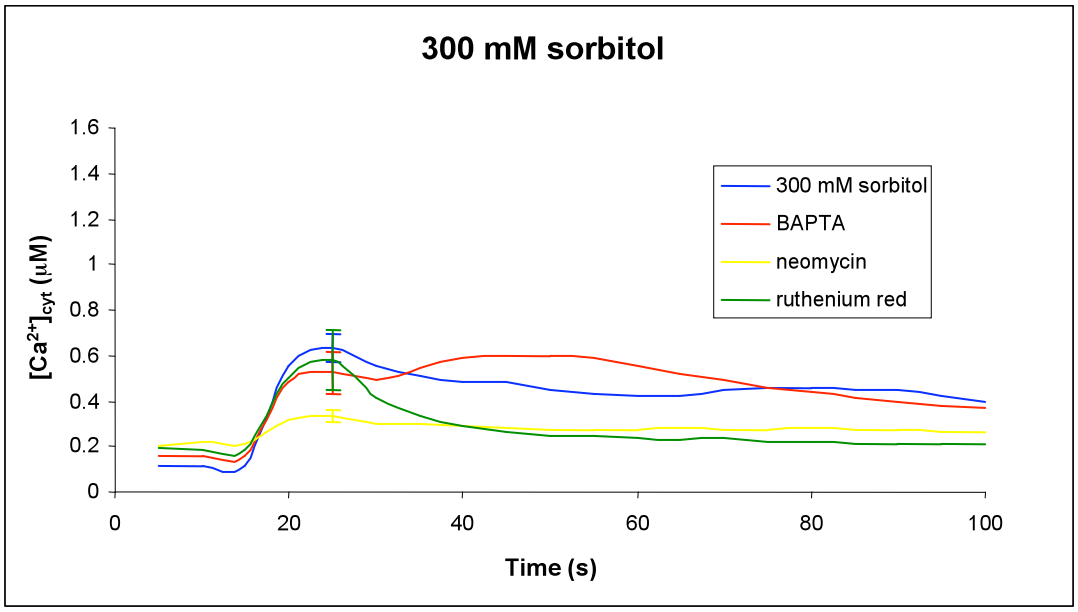

F.

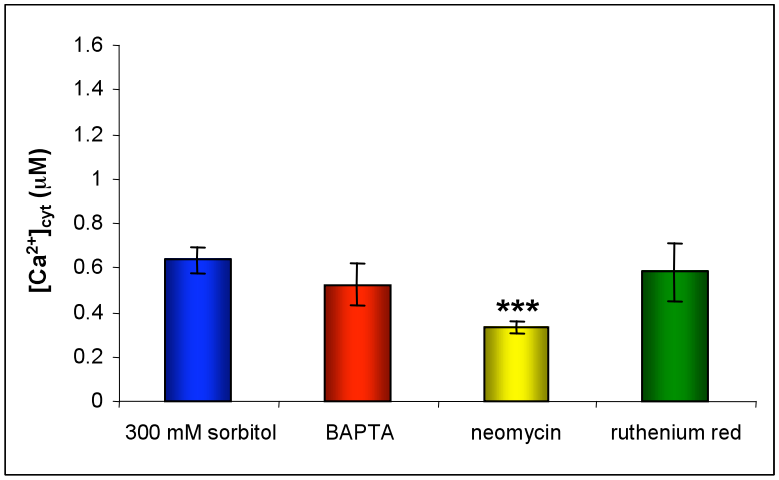

Figure 2.2. Inhibition of the NaCl and sorbitol-induced increases in $[Ca^{2+}]_{cyt}$ by calcium inhibitors
Two week old *Arabidopsis* seedlings were treated with 150 mM NaCl (A), 50 mM NaCl (C) or 300 mM sorbitol (E) and the affect of BAPTA, neomycin and ruthenium red on these responses determined. For all the uninhibited controls n = 10. For the 150 mM and 50 mM NaCl responses with inhibitors n = 15. For the 300 mM sorbitol responses with inhibitors n = 12. Error bars are the standard errors of the mean peak maxima. Mean peak maxima are compared between the control and inhibitor treatments for the 150 mM NaCl (B), 50 mM NaCl (D) and 300 mM sorbitol (F) responses. *** denotes a highly significant difference of $p < 0.001$ according to the t-test.

0.060 μM to 0.333 ± 0.024 μM (Figure 2.2E-F). Comparatively ruthenium red significantly ($p < 0.001$) inhibited the response to both 150 mM NaCl, reducing it from 1.143 ± 0.135 μM to 0.402 ± 0.105 μM (Figure 2.2A-B), and 50 mM NaCl, reducing it from 0.947 ± 0.096 μM to 0.272 ± 0.021 μM (Figure 2.2C-D). Ruthenium red differed from neomycin in that it did not have any significant effect on the 300 mM sorbitol response (Figure 2.2E-F). Therefore neomycin and ruthenium red affect the NaCl and sorbitol-induced calcium responses differently.

In summary, BAPTA had no effect on the NaCl and sorbitol-induced $[Ca^{2+}]_{cyt}$ response suggesting that extracellular calcium stores are not the source of these calcium signals. Instead, neomycin inhibited the NaCl and sorbitol-induced calcium responses suggesting that IP_3-mediated intracellular calcium release is important for the response to both ionic and osmotic stresses. On the other hand ruthenium red only inhibited the NaCl-induced $[Ca^{2+}]_{cyt}$ responses suggesting that cADPR-mediated intracellular calcium release is required for the response to ionic but not osmotic stress.

2.3.3 Cyclic GMP response to NaCl and osmotic stress treatment

Maathuis and Sanders demonstrated that cGMP reduces Na^+ influx into roots and improves salinity tolerance in *Arabidopsis* seedlings (Maathuis and Sanders, 2001). For cGMP to play a role in the response to NaCl *in vivo*, a cGMP signal is expected to precede these effects however this had not been demonstrated. *Arabidopsis* seedlings were treated with NaCl and sorbitol exactly as they were for the calcium assays and samples were harvested immediately (approximately 5 s), 1 min, 5 min and 15 min after treatment with high (150 mM) or low (50 mM) NaCl and iso-osmolar high (300 mM) and low (100 mM) sorbitol. The PDE inhibitor, 3-isobutyl-1-methylxanthine (IBMX) was not added to the samples so that these are actual levels of cGMP at each time point rather than accumulated cGMP levels. Water was again used as a control treatment and did not induce an increase in cGMP over the time points measured (Figure 2.3).

In this experiment the basal levels of cGMP were 0.877 ± 0.020 fmol/mg FW. Levels of cGMP increased significantly ($p < 0.05$) in response to 15 min treatment with both 50 mM NaCl (reaching 2.638 ± 0.208 fmol/mg FW) and 150 mM NaCl (2.894 ± 0.236 fmol/mg FW) as well as in response to 100 mM sorbitol (attaining 3.224 ± 0.104 fmol/mg FW) and 300 mM sorbitol (3.820 ± 0.113 fmol/mg FW) (Figure 2.3). Responses were immediate (within 5 s) and showed a step-wise increase over time with the greatest response being observed after the longest time point. Although the final cGMP levels after 15 min of treatment were similar, earlier time points revealed that the initial rate of cGMP increase was greater in response to higher doses of

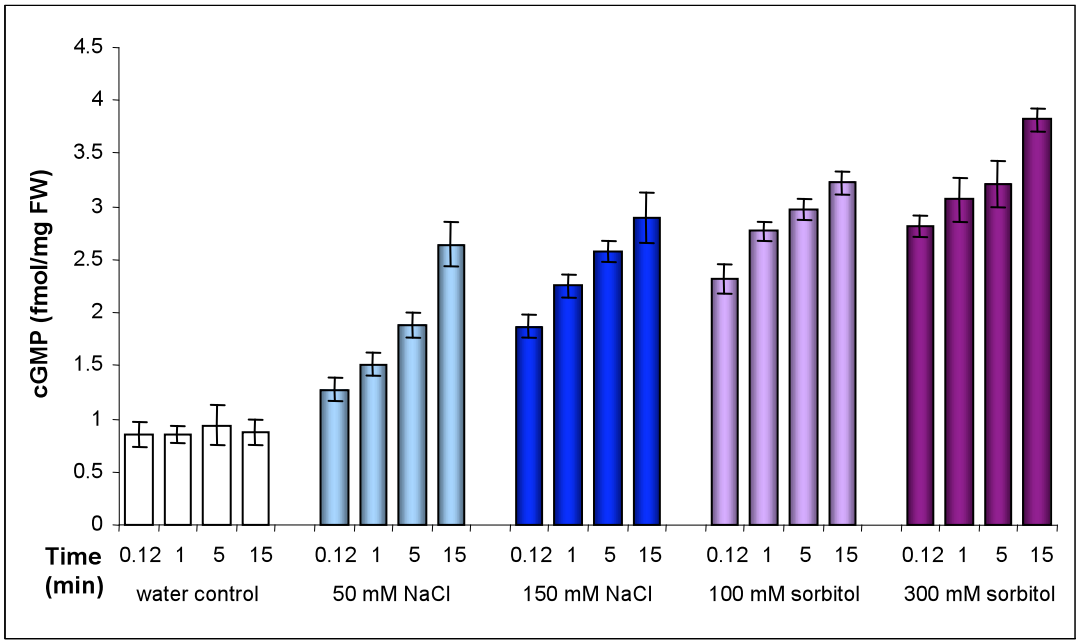

Figure 2.3. NaCl and sorbitol-induced increases in cGMP

Two week old *Arabidopsis* seedlings were treated with 50 mM NaCl, 150 mM NaCl, 100 mM sorbitol or 300 mM sorbitol as for the calcium assays and cGMP was measured 5 s (0.12 min), 1 min, 5 min or 15 min after treatment. Cyclic GMP levels represent the average of a pool of seedlings (approximately 150 plants per pool). Error bars represent the standard error of four replicates.

NaCl and sorbitol in comparison to the response at lower doses. For example, after approximately 5 s cGMP levels reached 1.277 ± 0.110 fmol/mg FW in response to 50 mM NaCl compared to 1.872 ± 0.106 fmol/mg FW with 150 mM NaCl. Similarly immediately after exposure to 100 mM sorbitol cGMP levels reached 2.317 ± 0.142 fmol/mg FW compared to 2.818 ± 0.101 fmol/mg FW with 300 mM sorbitol treatment. From these results it was also apparent that cGMP increases were significantly ($p < 0.05$) greater in response to sorbitol when compared to iso-osmolar NaCl treatments.

An inhibitor of animal particulate GCs, LY 83583, was tested for its affect on the 15 min NaCl and sorbitol-induced cGMP responses. LY 83583 significantly ($p < 0.05$) inhibited these cGMP responses reducing the peak cGMP responses to each treatment to approximately 1.686 ± 0.081 fmol/mg FW (Figure 2.4).

Therefore cGMP is induced in a concentration and time-dependent manner in response to NaCl and sorbitol. The rate of this cGMP increase was dose-dependent as well as greater in response to sorbitol treatment. Additionally, the cGMP increase in response to NaCl and sorbitol was sensitive to the GC inhibitor, LY 83583.

2.3.4 Interplay between the cGMP and calcium responses

There are several reports of processes in which cGMP and calcium interact with each other (Bowler *et al.*, 1994a; Cousson, 2001; Cousson, 2003; Cousson, 2004; Neuhaus *et al.*, 1997; Wu *et al.*, 1996b). This prompted an investigation of the interplay between cGMP and calcium in the response to NaCl and osmotic stresses. Firstly it was tested whether membrane-permeable dibutryl cGMP could induce an increase in $[Ca^{2+}]_{cyt}$ in *Arabidopsis* seedlings. Indeed 50 μM dibutryl cGMP was able to induce a rapid calcium transient that peaked at 0.597 ± 0.063 μM approximately 10 s after treatment (Figure 2.5).

The interaction between cGMP and calcium was then tested by examining the affect of LY 83583, an effective inhibitor of the NaCl and sorbitol-induced cGMP increases, on the calcium transients induced by these compounds. Conversely neomycin, the inhibitor that reduced all of the calcium responses, was tested for its affect on the NaCl and sorbitol-induced cGMP increases. Results showed that LY 83583 significantly ($p < 0.05$) inhibited the calcium response to 50 mM NaCl by delaying and reducing the peak from 0.947 ± 0.096 to 0.630 ± 0.079 μM but did not affect the response to 150 mM NaCl or the 300 mM sorbitol (Figure 2.6A-D). Neomycin, on the other hand, failed to have any affect on the cGMP increases to low or high NaCl or sorbitol (Figure 2.7).

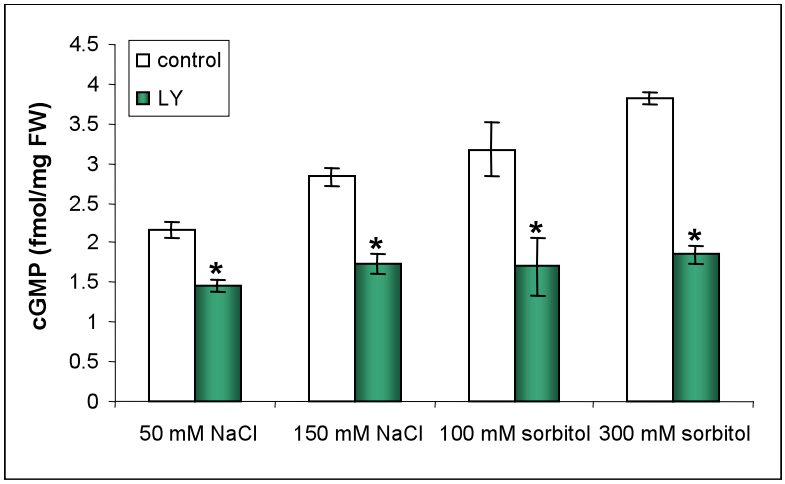

Figure 2.4. Inhibition of the NaCl and sorbitol-induced cGMP increases by LY 83535

Two week old *Arabidopsis* seedlings were treated with 50 mM NaCl, 150 mM NaCl, 100 mM sorbitol or 300 mM sorbitol, as described previously (control samples). The GC inhibitor, LY 83583 was included as a pre-treatment (10 μM LY 83583 for 15 min prior to NaCl or sorbitol treatment) (LY samples) to test whether it could inhibit the NaCl and sorbitol-induced cGMP increases. Error bars represent the standard error of four duplicates. * denotes a $p < 0.05$ according to the Mann-Whitney U test, indicating that LY significantly inhibits the NaCl and sorbitol-induced cGMP increases.

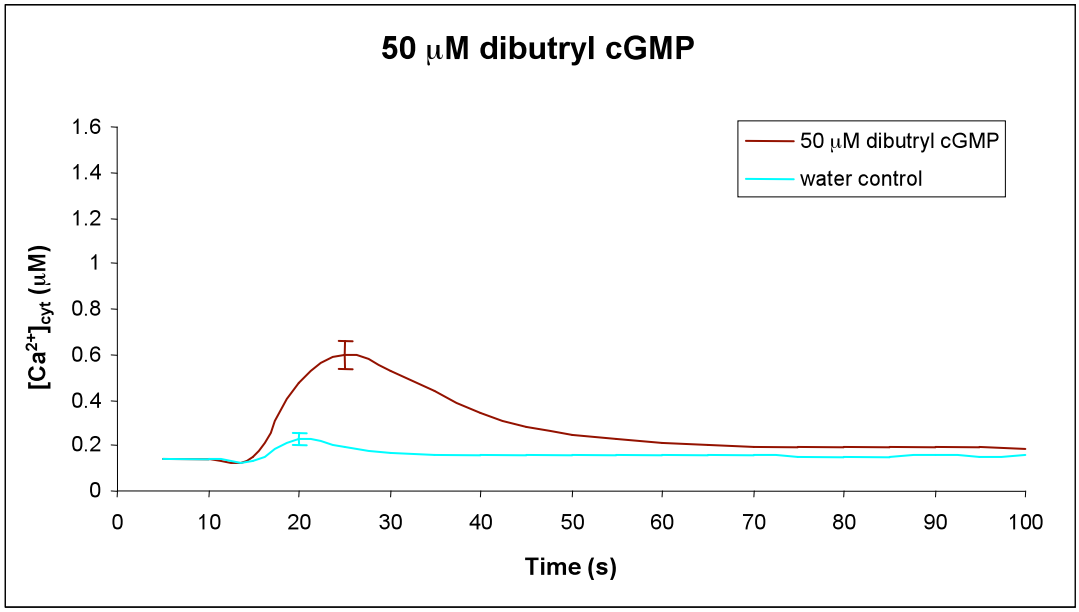

Figure 2.5. Dibutryl cGMP-induced increases in $[Ca^{2+}]_{cyt}$

Two week old *Arabidopsis* seedlings were treated with 50 μM dibutryl cGMP, luminescence measured and $[Ca^{2+}]_{cyt}$ calculated as described previously. The curve represents the average response 20 of individual seedlings. The error bars are standard errors of the mean peak maxima.

2.6 A.

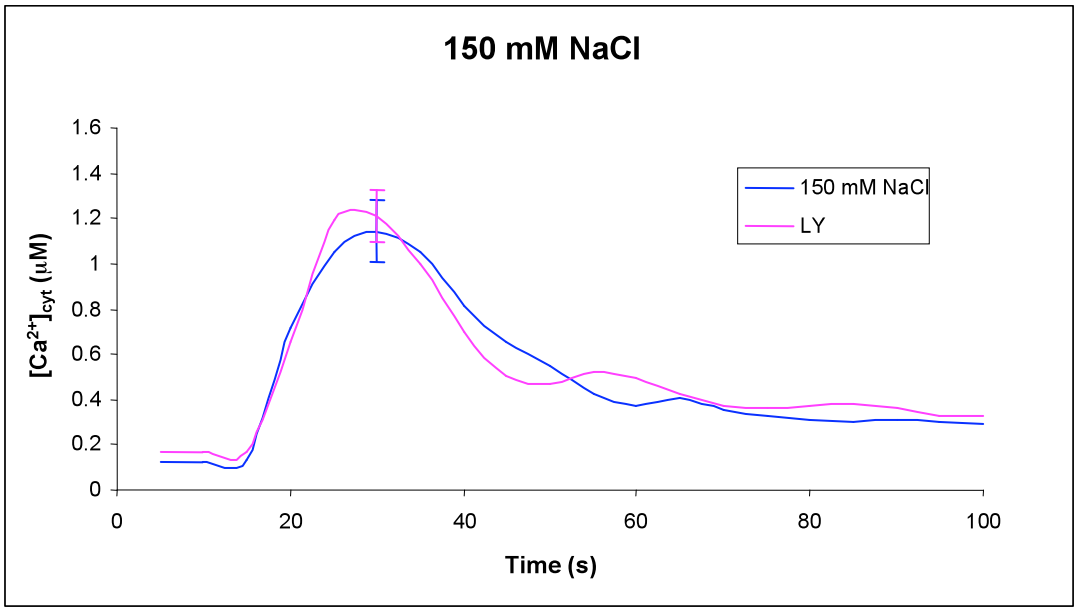
150 mM NaCl
[Ca2+]cyt (µM)
1.6
1.4
1.2
1
0.8
0.6
0.4
0.2
0
0
20
40
60
80
100
Time (s)
150 mM NaCl
LY

B.

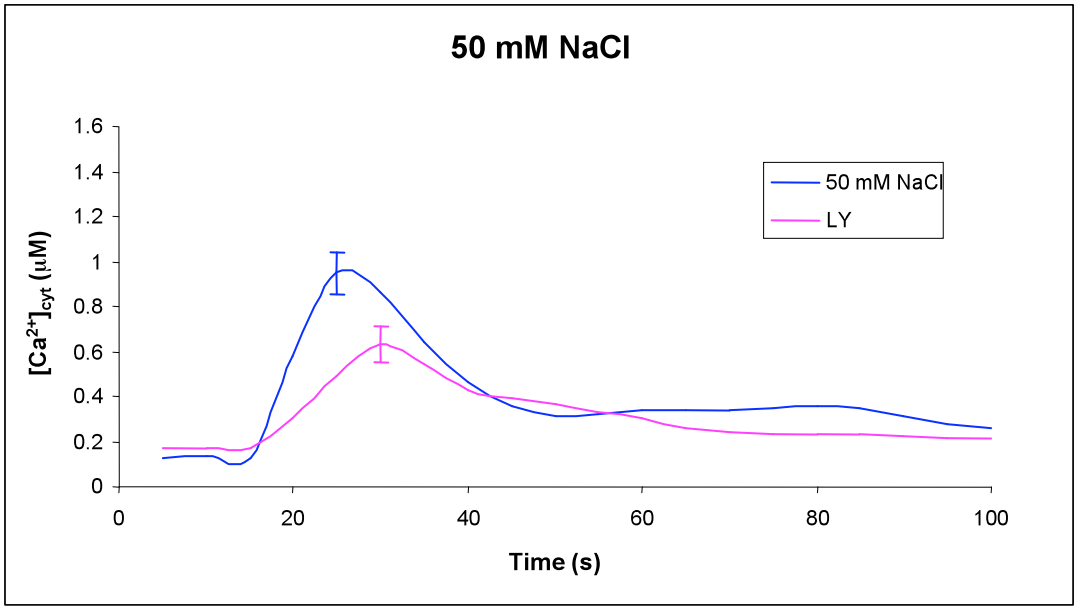
50 mM NaCl
[Ca2+]cyt (µM)
1.6
1.4
1.2
1
0.8
0.6
0.4
0.2
0
0
20
40
60
80
100
Time (s)
50 mM NaCl
LY

C.

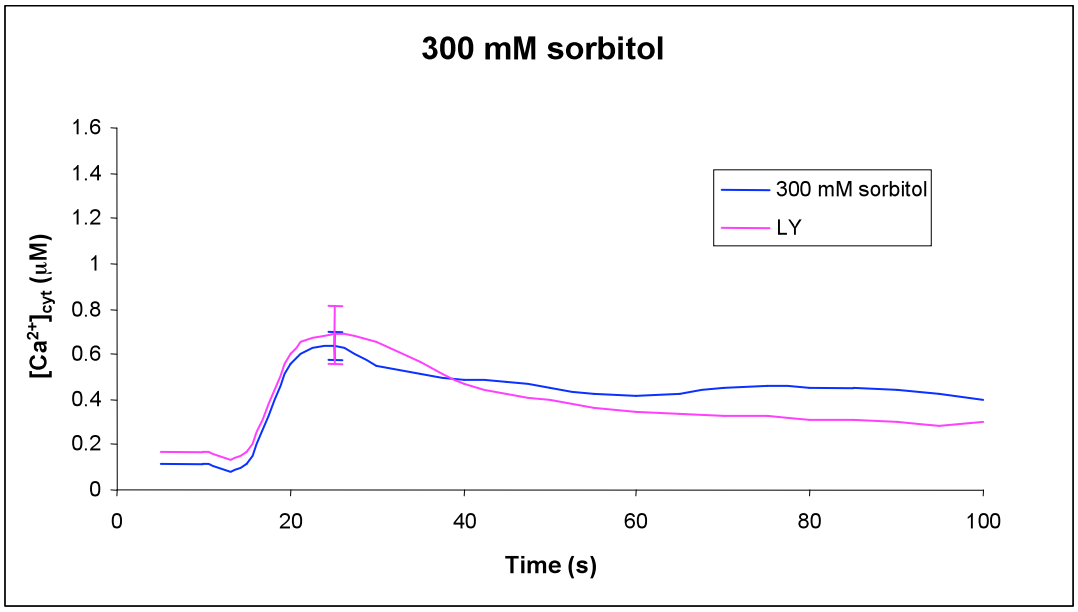

D.

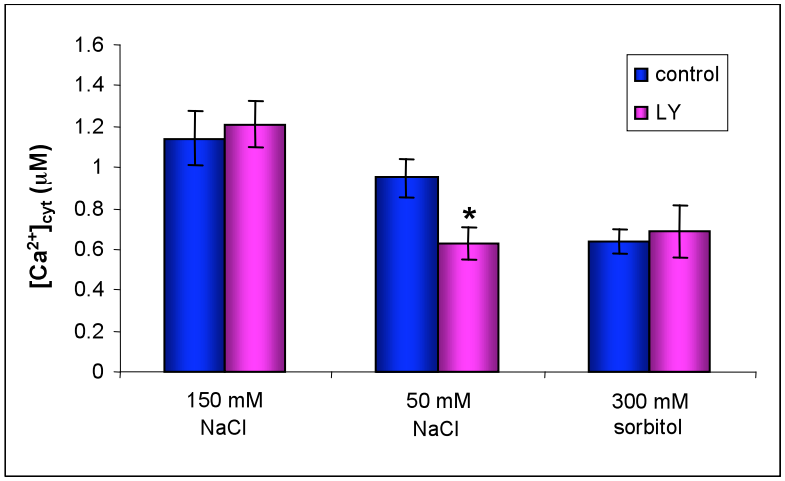

Figure 2.6. Inhibition of the NaCl and sorbitol-induced increases in $[Ca^{2+}]_{cyt}$ by LY 83535

Two week old *Arabidopsis* seedlings were treated with 150 mM NaCl (A), 50 mM NaCl (B) or 300 mM sorbitol (C), as described previously (controls) and the effect of the GC inhibitor, LY 83583 on these responses was determined (LY samples). For all the controls, the curves represent the average response of 10 individual seedlings. For the LY samples n = 15 except for the 300 mM sorbitol response for which n = 10. Error bars are the standard error of the mean peak maxima. Mean peak maxima were compared between the control and inhibitor treatments (D) and* denotes a significant difference of $p < 0.05$ as determined by the t test.

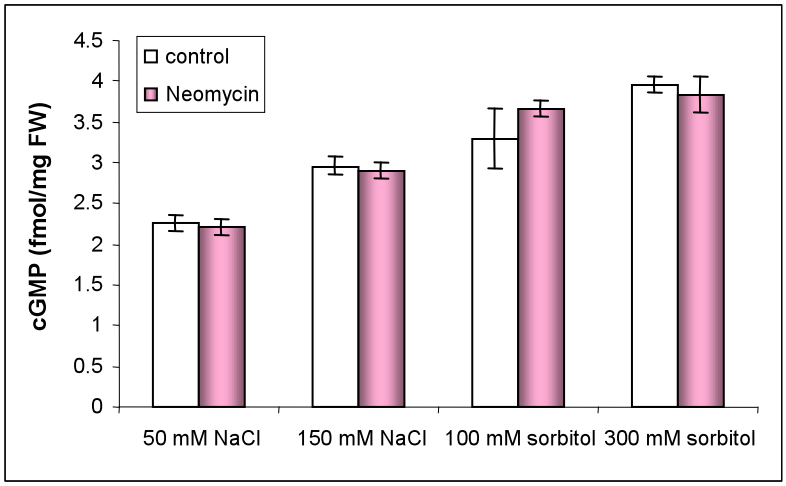

Figure 2.7. Affect of neomycin on the NaCl and sorbitol-induced increases in cGMP

Two week old *Arabidopsis* seedlings were treated with 50 mM NaCl, 150 mM NaCl, 100 mM sorbitol or 300 mM sorbitol, as described previously (control samples). Neomycin, an inhibitor of IP_3-mediated calcium release from intracellular stores, was tested for its ability to inhibit the NaCl and sorbitol-induced cGMP increases (neomycin samples). Error bars represent the standard error of four replicates.

In summary, cGMP induces calcium while GC activity is required for the calcium response to 50 mM NaCl. Therefore a cGMP-induced calcium transient is likely a component of the 50 mM NaCl-induced calcium response. Neomycin had no affect on the 50 mM NaCl-induced cGMP response implying that cGMP is required upstream of calcium in response to ionic stress but not the other way around. As soon as there is an osmotic component to the stress, the calcium response was no longer dependent on GMP while neomycin was still without affect on the cGMP response suggesting that in response to osmotic stress calcium and cGMP act independently.

2.3.5 Calcium response to recombinant AtPNP-A

Previously PNP (irPNP and recombinant AtPNP-A) treatment has been shown to induce transient increases in cGMP that are required for PNP-induced responses (Pharmawati *et al.*, 1998a; Pharmawati *et al.*, 1998b; Wang *et al.*, 2007c). There is indirect evidence that calcium may too be involved in irPNP responses because inhibitors of calcium signalling supress irPNP-stimulated responses (Pharmawati *et al.*, 2001). It was therefore tested whether recombinant AtPNP-A was able to induce an increase in $[Ca^{2+}]_{cyt}$. Indeed 50 ng/ml recombinant AtPNP-A induced a rapid calcium transient that peaked at 0.768 ± 0.100 μM approximately 10 s after treatment (Figure 2.8). After the calcium response had subsided, baseline $[Ca^{2+}]_{cyt}$ levels remained somewhat elevated compared to calcium levels prior to treatment (0.428 ± 0.005 μM after compared to 0.283 ± 0.013 before treatment).

Pharmacological inhibitors were then employed to investigate the calcium source (BAPTA) and cGMP-dependence (LY 83583) of the AtPNP-A-induced calcium response. BAPTA did not have any effect on the AtPNP-A-induced calcium transient, however LY 83583 significantly ($p < 0.05$) reduced the calcium response from 0.768 ± 0.100 to 0.531 ± 0.067 μM (Figure 2.8).

Therefore recombinant AtPNP-A induced a transient increase in calcium that was sensitive to inhibition by LY 83583, suggesting that cGMP lies upstream of calcium in AtPNP-A-induced responses.

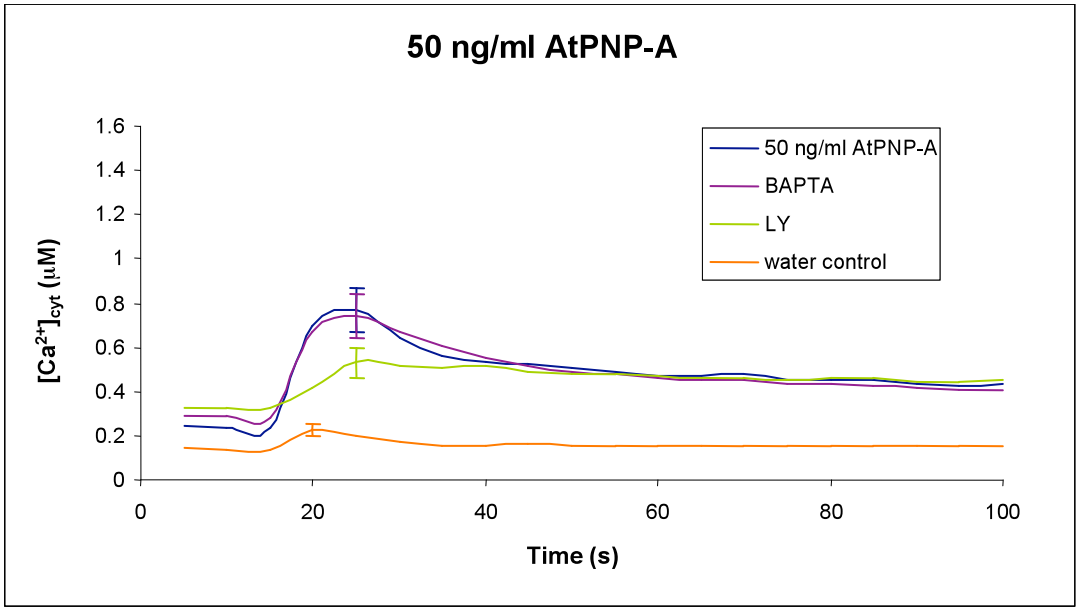

Figure 2.8. Recombinant AtPNP-A-induced increases in $[Ca^{2+}]_{cyt}$

Two week old *Arabidopsis* seedlings were treated with 50 ng/ml recombinant AtPNP-A, luminescence measured and $[Ca^{2+}]_{cyt}$ calculated as described previously. The curve represents the average response 20 of individual seedlings and error bars are standard errors of the mean peak maxima.

2.4 DISCUSSION

2.4.1 NaCl and osmotic stress-induced calcium responses are different

2.4.1.1 Magnitude of the calcium response

Calcium signatures have been recorded in response to a number of stimuli for example touch, cold, elicitors, NaCl and drought stress, pathogen infection and oxidative stress (Evans *et al.*, 2005; Grant *et al.*, 2000; Knight *et al.*, 1996; Knight *et al.*, 1997; Knight *et al.*, 1991). In the current study the calcium response to NaCl and osmotic stress was further explored. The small peak observed following the control treatment with water was probably a result of a touch response even though each treatment was injected carefully so as to minimize any such effect. This response was quite distinct from the dose responses to NaCl and sorbitol. Treatment with NaCl induced a single calcium spike (Figure 2.1A). This increased in a concentration-dependent manner from 50 mM to 150 mM NaCl however appeared to have reached a maximum at 150 mM as there was no further increase in the response to 300 mM NaCl treatment. In each case the calcium response to the iso-osmolar sorbitol concentration was temporally similar however significantly lower in magnitude than the NaCl response (Figure 2.1C). At 100 mM sorbitol, the osmotic stress was apparently insufficient to induce a significant calcium response (Figure 2.1B). The 300 mM sorbitol treatment induced an intermediate calcium response that increased in magnitude in response to 600 mM sorbitol. The quantitatively larger calcium response induced by NaCl compared to that induced by iso-osmolar sorbitol makes it tempting to speculate that these differences in magnitude may reflect the additional ionic component of NaCl stress. This was most obvious at 50 mM NaCl where the calcium response appeared to be induced purely by the ionic component of NaCl stress as there was no corresponding calcium increase in response to iso-osmolar sorbitol. It was noted that the ionic stress-induced calcium response was not specific to 50 mM NaCl as a similar calcium transient was recorded in response to 50 mM KCl treatment which is also iso-osmolar to 100 mM sorbitol (Appendix Figure 2.1). This established a means for looking at calcium responses to the ionic and osmotic stresses imposed by NaCl separately.

Calcium signatures have been reported previously in response to NaCl and iso-osmolar mannitol stress in seven day old *Arabidopsis* roots (Knight *et al.*, 1997). While quantitative differences in $[Ca^{2+}]_{cyt}$ values recorded in these studies may arise from differences in the luminometers, since the detectors are located at different positions in these machines (pers. comm. L. Petersen), it is more likely that this results from differences in the age of the plants and experimental conditions used in these studies. The current study differs in that calcium responses were measured in 14 day old intact seedlings and sorbitol was used to impose the osmotic stress rather than mannitol. It has been reported that in response to NaCl and osmotic stress constitutively expressing aequorin plants display calcium responses that are restricted to the root (Kiegle *et al.*, 2000).

Unless this changes with age, this would imply that the calcium responses measured in the whole plant in the current study are probably also root responses. This does appear to be true since both NaCl and sorbitol induced calcium transients in detached roots of the constitutively expressing aequorin seedlings while there was no appreciable response measured in leaves (Appendix Figure 2.2A-B). Sorbitol and mannitol differ only in that they are different sugar isomers and therefore responses to these sugars are expected to be similar. Indeed mannitol induced a very similar calcium response to that induced by sorbitol (Appendix Figure 2.3) suggesting that differences in these sugars do not account for differences between the results of the current study and those reported by Knight (Knight *et al.*, 1997).

Knight and colleagues found that calcium spikes induced in response to NaCl and iso-osmolar concentrations of mannitol were not different from one another (Knight *et al.*, 1997). This was true for both 333 mM NaCl and iso-osmolar 666 mM mannitol as well as for 166 mM NaCl and iso-osmolar 333 mM mannitol responses. In their study the calcium response increased from 166 mM to 333 mM NaCl and similarly increased from 333 mM to 666 mM mannitol. The results presented above, compared to those of Knight, confirm that there is little difference in the calcium response to high NaCl (300 mM) and high sorbitol (600 mM). In the current study however, significant differences in the calcium responses induced by lower doses of NaCl and iso-osmolar sorbitol (150 mM NaCl compared to 300 mM sorbitol and 50 mM NaCl compared to 100 mM sorbitol) were observed (Figure 2.1C). Additionally the calcium spike reported here in response to 150 mM NaCl did not increase in magnitude in response to 300 mM NaCl, whereas Knight observed an increased response to 333 mM NaCl compared to 166 mM NaCl (Knight *et al.*, 1997). This may be because a signal intensity threshold had been reached within our system. Knight concluded that magnitude of the NaCl and osmotic stress-induced calcium responses could not be used to discriminate between these stresses (Knight *et al.*, 1997). The results presented here suggest that at lower, more physiologically relevant doses, the magnitude of the calcium responses to NaCl and osmotic stress are different and could potentially encode specificity.

2.4.1.2 Source of the calcium response

Inhibitors of animal calcium channels were used to dissect the source of the NaCl and sorbitol-induced calcium signals to determine whether there is potential for encoding specificity in this manner. This pharmacological approach is based on the assumption that calcium signalling in plants is similar to that in animals with the expectation that these inhibitors exert the same effects in plants as they do in animals, despite the fact that most of the channels for calcium release in plants remain unknown (Sanders *et al.*, 2002; Wu *et al.*, 1997). Results showed that BAPTA did not significantly affect the calcium response to high or low NaCl or sorbitol stress

suggesting that extracellular calcium stores are not involved and rather implicating intracellular calcium stores as the source of the calcium signal (Figures 2.2A–D). This was confirmed using neomycin and ruthenium red. Neomycin caused a quantitatively similar reduction in both NaCl-induced calcium responses and delayed them slightly (Figures 2.2A–D). This partially inhibited the 150 mM NaCl-induced response however almost completely reduced the 50 mM NaCl response. Similarly neomycin also almost completely inhibited the 300 mM sorbitol response. Together this suggests that IP_3-mediated calcium release is required for a full calcium response to both ionic (50 mM NaCl) and osmotic (300 mM sorbitol) stresses, but does not exclude contribution from other calcium stores. Ruthenium red had a somewhat different impact on the calcium transients. Ruthenium red almost completely inhibited the calcium response to both 150 and 50 mM NaCl treatments but did not have any affect on the 300 mM sorbitol treatment (Figures 2.2A-D), suggesting that cADPR-mediated calcium release is required for the response to the ionic stress imposed by NaCl but is not required for the sorbitol-induced osmotic stress response. It should be noted however that while ruthenium red is widely used in animal studies to inhibit cADPR-mediated calcium release, its effect in plants is less clear (Allen *et al.*, 1995).

The BAPTA result described above was unexpected because Knight had reported that both EGTA (a chelator of divalent cations) and lanthanum (a channel blocker that inhibits extracellular calcium release) partly reduced the 333 mM NaCl and 666 mM mannitol calcium responses (Knight *et al.*, 1997). They concluded that both extracellular and intracellular calcium stores are the source of the NaCl and osmotic stress-induced calcium signals. Moreover since these inhibitors affected each response similarly, it was concluded that the source of the NaCl and osmotic stress-induced calcium signals are not different and therefore cannot encode specificity. Additionally a study by Gao and colleagues has demonstrated that 100 mM NaCl induces a calcium signal originating from the apoplast that does not occur in response to osmotic stress (Gao *et al.*, 2004). Clearly there are discrepancies in the results generated by these studies. While it is possible that BAPTA may not be acting as an effective Ca^{2+} chelator in the above described experiments, BAPTA has been used successfully in other studies in plants (Polisensky and Braam, 1996) as well as in our laboratory (pers. comm. L. Petersen) to inhibit calcium responses that require extracellular calcium stores. It may be that the lower NaCl and sorbitol doses used in the current study might affect the source of the calcium signatures. However another possibility is that, in the study by Knight, EGTA and lanthanum reduced the calcium responses non-specifically since EGTA does not exclusively chelate Ca^{2+} ions and lanthanides may enter the cell and block intracellular calcium channels. Chelation of other divalent cations by EGTA, such as Mg^{2+} which is required as a cofactor for enzymes, may affect components of the signalling machinery (for example GCs) required to generate the NaCl and osmotic stress induced calcium transients (Ludidi and Gehring, 2003). In contrast BAPTA

is a specific Ca^{2+} chelator and so the fact that it did not inhibit the calcium responses measured here suggests more convincingly that extracellular calcium sources do not account for the calcium responses to NaCl and osmotic stresses and that intracellular calcium stores (vacuolar or other), rather than a calcium induced calcium release, are instead responsible.

Plants expressing aequorin under the control of the constitutive CaMV 35S promoter report calcium changes in the cytosol. Targeted aequorin constructs have also been used to assess the contribution of the vacuole to the mannitol-induced calcium signal (Knight *et al.*, 1997). This revealed that the vacuole is the major source of the calcium signal in response to osmotic stress since the vacuole produced a calcium signature almost identical to that produced by the cytosolic domain. Furthermore this vacuolar calcium release could be reduced using three different inhibitors of IP_3-mediated calcium release (neomycin, U-73122 and lithium). The results presented here confirmed that IP_3-mediated calcium release is an important component of the calcium response to osmotic stress since neomycin could effectively inhibit the calcium responses to both NaCl and sorbitol (Figures 2.2A–F). Additionally the current study has shown that ruthenium red inhibits the NaCl-induced calcium responses but did not affect the sorbitol-induced calcium response (Figures 2.2A–F). This suggests that the NaCl and osmotic stress-induced calcium responses may be discriminated by an additional cADPR-mediated calcium signal in response to NaCl stress and challenges the conclusion drawn by Knight that source of the calcium signature doesn't encode specificity in NaCl and osmotic stress responses.

A later study by the Knight group has since reported subtle differences in the magnitudes of the NaCl and mannitol-induced calcium response of particular cell types in the root (Kiegle *et al.*, 2000). Specifically the pericycle and endodermis responses to NaCl and osmotic stress differ. Kiegle proposed that these tissues are likely to be involved in xylem loading and the regulation of water and ion flow to the shoot and thus may critically influence whole plant responses to these stresses. Such cell type-specific responses would be masked in the constitutively expressing aequorin line.

2.4.2 NaCl and osmotic stresses induce a cGMP response

The present study demonstrates that 50 mM and 150 mM NaCl as well iso-osmolar 100 mM and 300 mM sorbitol all induce increases in cGMP levels (Figure 2.3). These cGMP increases were immediate, occurring 5 s after treatment - the earliest time point that could be measured. The cGMP response increased over time for 15 min, although it was not determined for how long this increase was sustained. The rate of increase was dose-dependent and greater in response to sorbitol than in response to iso-osmolar NaCl treatment. This constitutes the first measure of cGMP in response to abiotic stress. As mentioned in chapter 1, there have been very few

reports measuring cGMP levels in plants. Compared to the rest of those reports, that should be noted span a range of different plants and tissues, the levels measured here (1–4 fmol/mg FW) fall within the range of measurements reported previously (Dubovskaya *et al.*, 2001; Hu *et al.*, 2005; Penson *et al.*, 1996; Pfeiffer *et al.*, 1994; Pharmawati *et al.*, 2001; Reggiani, 1997; Richards *et al.*, 2002; Szmidt-Jaworska *et al.*, 2004).

An inhibitor of particulate GCs in animals, LY 83583, almost completely inhibited the cGMP response to NaCl and osmotic stress proving that LY 83583 is an effective inhibitor of cGMP synthesis in *Arabidopsis* seedlings (Figure 2.4). This is not always the case; for example LY 83583 has no effect on irPNP-induced cGMP transients in maize stele (Pharmawati *et al.*, 1998b). Inhibition by LY 83583 suggests that a receptor GC is responsible for the NaCl and osmotic stress-induced cGMP responses. Potential plant GC sequences have only recently been reported (Ludidi and Gehring, 2003). It does appear that such GC-linked receptors do exist in plants as several putative GC sequences are annotated as LRR-RLKs, one of which (BRI1) has been tested for GC activity *in vitro* and shown to produce cGMP (Kwezi *et al.*, 2007). However it was not determined whether LY 83583 could inhibit this GC activity.

2.4.3 Cross-talk between calcium and cGMP in the response to NaCl

Membrane permeable cGMP analogs have been demonstrated to induce calcium transients in tobacco protoplasts and this has been proposed to be the point of interaction between these secondary messengers (Volotovski *et al.*, 1998). However a cGMP-induced calcium increase has not yet been shown to be required for any specific process in plants. The results of the current study demonstrate that 50 μM dibutryl cGMP induces a calcium spike in *Arabidopsis* seedlings (Figure 2.5). The cGMP-induced calcium spike was somewhat lower in magnitude than the NaCl-induced calcium responses but comparable to the 300 mM sorbitol-induced calcium response. The concentration of dibutryl cGMP used here was slightly higher than that used to induce the calcium response in tobacco protoplasts (10 μM) (Volotovski *et al.*, 1998), however is the same concentration that most effectively reduced Na^+ uptake in *Arabidopsis* seedlings (Maathuis and Sanders, 2001).

Production of cGMP in response to NaCl is presumed to occur inside the cell. Naturally produced GMP is thought to be cell impermeant so that its downstream effects would result from its actions within the cell. Since the cGMP analog used to induce the calcium transient is membrane permeable, it probably traverses the membrane to induce the calcium response. It is therefore possible that the 50 mM NaCl-induced and cGMP-induced calcium transients are related so that NaCl-induced cGMP could similarly stimulate a downstream calcium response. The interplay between calcium and cGMP was investigated in the response to NaCl and osmotic

stress by examining the affect of an inhibitor of the cGMP response on the calcium signal and visa versa, by measuring the cGMP response in the presence of a calcium inhibitor. This approach assumes linearity of the signal transduction cascade where one second messenger lies downstream of and is dependent on the other. Alternatively the signal transduction pathways initiated by these second messengers could be independent of each other and act in parallel. The GC inhibitor, LY 83583, inhibited the 50 mM NaCl-induced calcium transient but did not affect any of the other calcium responses (Figure 2.6A–E). Since the 50 mM NaCl-induced calcium signature is thought to be a response specific to the ionic component of the NaCl stress, it is thus proposed that the calcium response to ionic stress is at least partially dependent on an upstream cGMP signal. At the higher NaCl concentration, a threshold may have been passed whereupon the osmotic stress negates the need for a cGMP-dependent calcium response. Conversely, neomycin had no effect on the NaCl and sorbitol-induced cGMP responses suggesting that IP_3-mediated calcium release is not required for the NaCl and sorbitol-induced cGMP responses, but not excluding the possibility that other calcium stores may be required (Figure 2.7). Salt stress therefore activates two cGMP-mediated pathways, one in response to ionic stress that also involves calcium and the other in response to osmotic stress that is independent of calcium.

2.4.4 Discrimination between ionic and osmotic stress signals

As mentioned before, for the dogma of the calcium signature to hold true it is necessary to link the calcium signal to an end response (Scrase-Field and Knight, 2003). The Knight study reported that NaCl and mannitol-induced calcium transients were not different in magnitude or source but caused quantitative differences gene expression (Knight *et al.*, 1997). Therefore it was concluded that calcium cannot be the factor used to discriminate between NaCl and osmotic stress. Since calcium inhibitors did not always repress NaCl and mannitol-induced gene expression and Ca^{2+} itself did not fully induce gene expression, they concluded that an additional messenger is involved.

There are three potential ways provided here in which discrimination between NaCl and osmotic stresses could occur, namely magnitude and source of the calcium signal and cross-talk between calcium and cGMP signalling. Firstly, at lower doses the magnitudes of the calcium spikes in response to NaCl and osmotic stress are different, being higher for NaCl than for iso-osmolar sorbitol. Thus it is possible that this difference may encode information relating to the additional component of ionic stress-induced by NaCl. Secondly, the NaCl and sorbitol-induced calcium spikes were differently inhibited by ruthenium red which virtually completely inhibited the NaCl-induced responses whilst having no effect on the sorbitol-induced response. Therefore cADPR-mediated calcium release may be specific to NaCl stress. Lastly, the calcium response

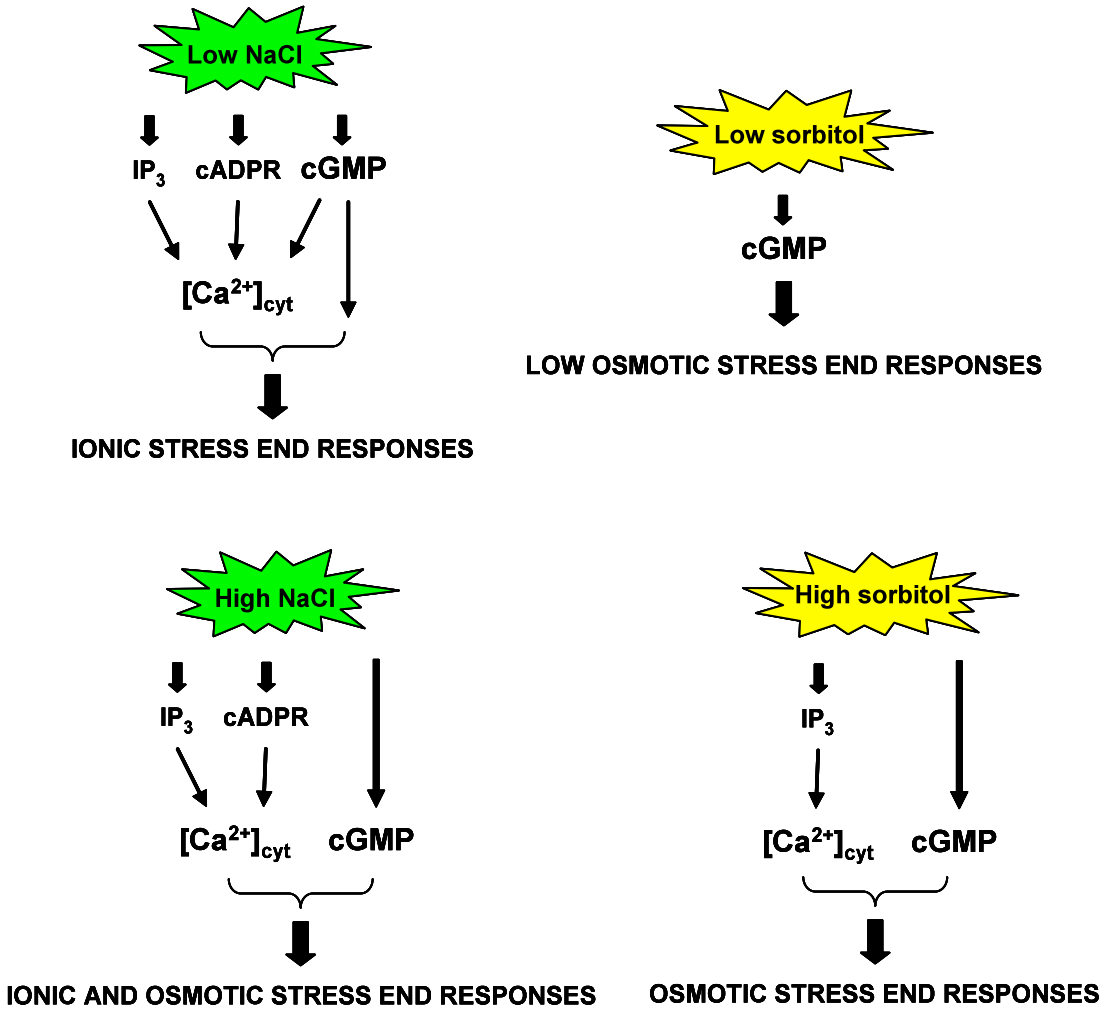

Figure 2.9. Proposed model whereby plants might discriminate between ionic and osmotic stresses using secondary messenger signalling

Ionic stress imposed by low concentrations of NaCl (50 mM) involves signalling via IP_3 and cADPR-mediated calcium release; cGMP-dependent calcium release as well as cGMP signalling alone. High NaCl (150 mM) imposes both an ionic and osmotic stress response that involves IP_3 and cADPR-mediated calcium release as well as cGMP signalling. Low sorbitol concentrations (100 mM) only induce a cGMP signal that is presumably required for end responses, while higher concentrations of sorbitol (300 mM) evoke a stronger osmotic stress response that requires both cADPR-mediated calcium signalling as well as cGMP signalling. Whether these different signal transduction pathways induce disparate end responses has not been determined.

to ionic stress imposed by low concentrations (50 mM) of NaCl was inhibited by LY 83583. Therefore cross-talk between calcium and cGMP may play a role in signalling the ionic component of the NaCl stress. It is thus possible that a combination of these factors can be used to discriminate between high and low NaCl and sorbitol stresses, as illustrated in Figure 2.9. In order to test whether specificity is encoded by these mechanisms (magnitude, source and cross-talk) the affect of dose and inhibitors on an appropriate end response to NaCl and osmotic stress should be examined.

2.4.5 Recombinant AtPNP-A induces a calcium transient

There was previous evidence that calcium is required for irPNP-induced stomatal opening (Pharmawati *et al.*, 2001). For calcium to be involved in irPNP-induced responses, it would be expected that irPNP treatment induces a calcium signal. Indeed 50 ng/ml recombinant AtPNP-A treatment induced a transient increase in $[Ca^{2+}]_{cyt}$ (Figure 2.8). This concentration of AtPNP-A is within the range used to induce other irPNP responses (Morse *et al.*, 2004). The calcium increase was lower than that induced by NaCl stress however comparable to that induced by cGMP itself. Consistent with this idea, LY 83583 reduced the calcium response to AtPNP-A. Since the calcium inhibitors ruthenium red and procaine (another inhibitor of cADPR-mediated calcium release) reduced both irPNP and cGMP-induced stomatal opening (Pharmawati *et al.*, 2001), this suggests that the cGMP-induced calcium response recorded here is indeed important in irPNP signal transduction. BAPTA had no effect on the AtPNP-A-induced calcium transient, suggesting that intracellular calcium stores are the source of the calcium signal, in agreement with the previous findings that ruthenium red and procaine inhibited irPNP-induced responses.

2.4.6 Summary

There is increasing evidence that responses to NaCl and osmotic stress are quite different and that the response to osmotic stress is not merely a subset of the response to NaCl stress (Denby and Gehring, 2005; Gao *et al.*, 2004; Ruggiero *et al.*, 2004). Findings presented here show that there are early differences in secondary messenger signalling in response to NaCl and osmotic stresses. These include differences in magnitude and source of the calcium signal as well as in cross-talk with cGMP signalling that may encode the specificity of the ionic and osmotic stress signals. A model has been proposed that could be used to test whether calcium and cGMP can indeed be used to discriminate between these stresses. This could be used to identify end response genes that are specific to the ionic and osmotic components of NaCl stress. Such stress-specific genes are likely to be better candidates for the design of tolerant crops which historically has met with little success, since these are less likely to produce undesirable non-specific effects such as increased sensitivity to other stresses and growth inhibition that may occur if the gene is involved in more than one cellular process (Denby and Gehring, 2005).

2.5 APPENDIX

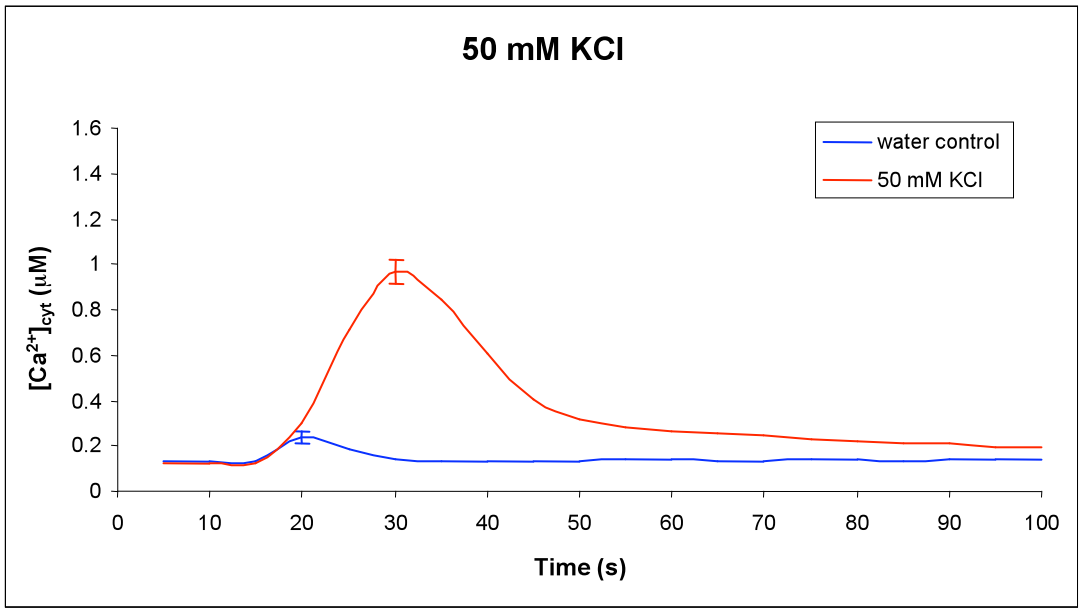

Appendix Figure 2.1. Ionic stress imposed by 50 mM KCl increases $[Ca^{2+}]_{cyt}$

Two week old *Arabidopsis* seedlings treated with 50 mM KCl respond with a calcium transient that is similar in both magnitude and timing to the 50 mM NaCl-induced response (refer to Figure 2.1A). The curve shown is the average response of 20 seedlings. Error bars are standard errors of the mean peak maxima.

A.

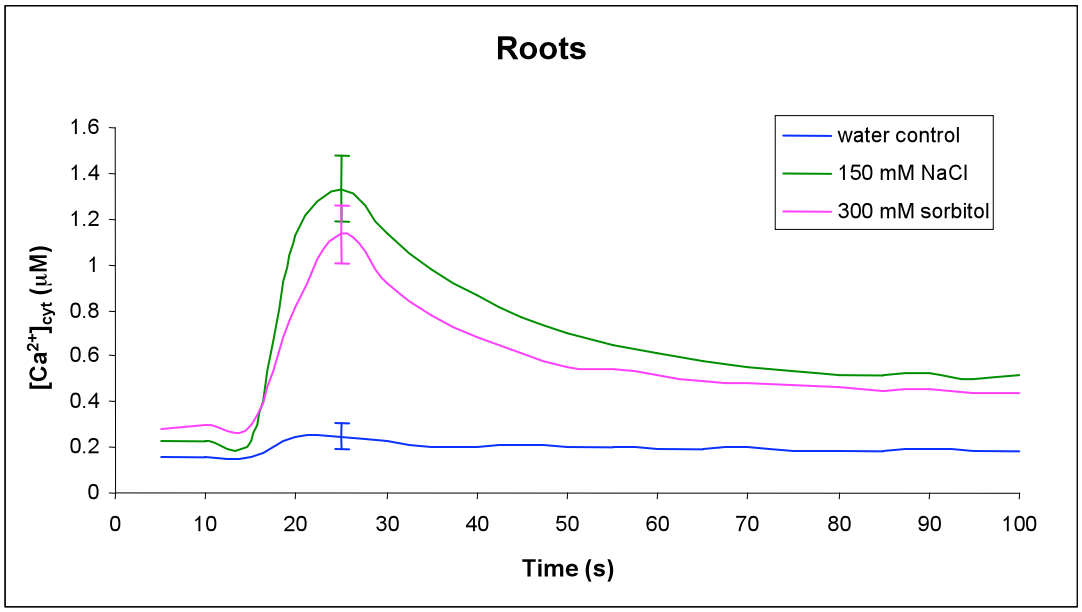

B.

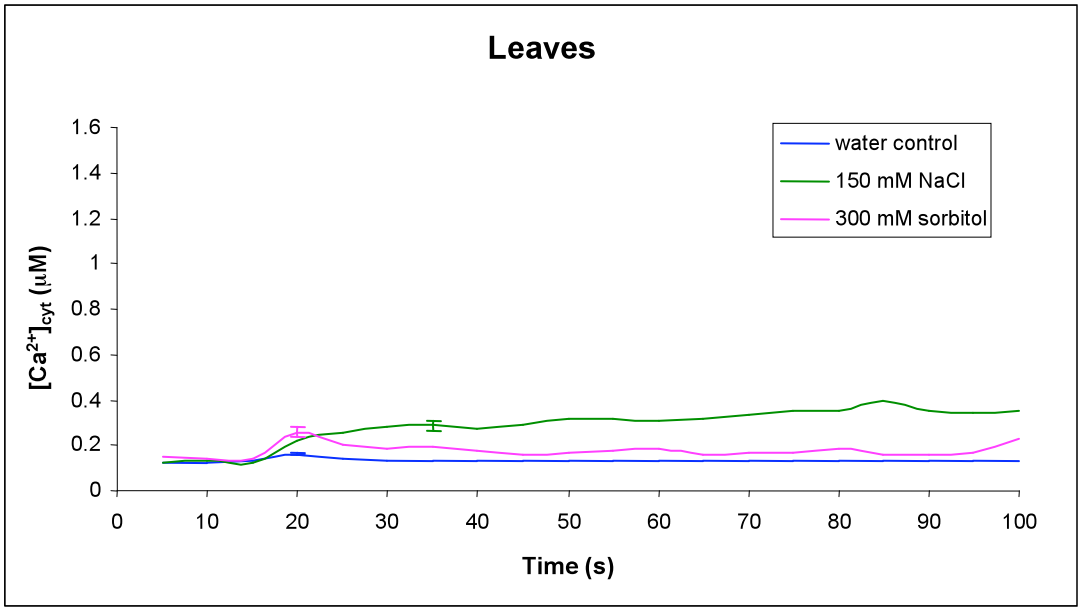

Appendix Figure 2.2. Root and shoot-specific $[Ca^{2+}]_{cyt}$ responses to NaCl and osmotic stress

Detached roots (A) and leaves (B) of *Arabidopsis* seedlings constitutively expressing aequorin were treated with 150 mM NaCl or 300 mM sorbitol and the calcium responses measured as described previously. For the leaf samples treated with water or 300 mM sorbitol n = 5 while for the leaf response to NaCl n = 10. For the root responses each curve represents the average response of 10 seedlings. Error bars are the standard errors of the mean peak maxima.

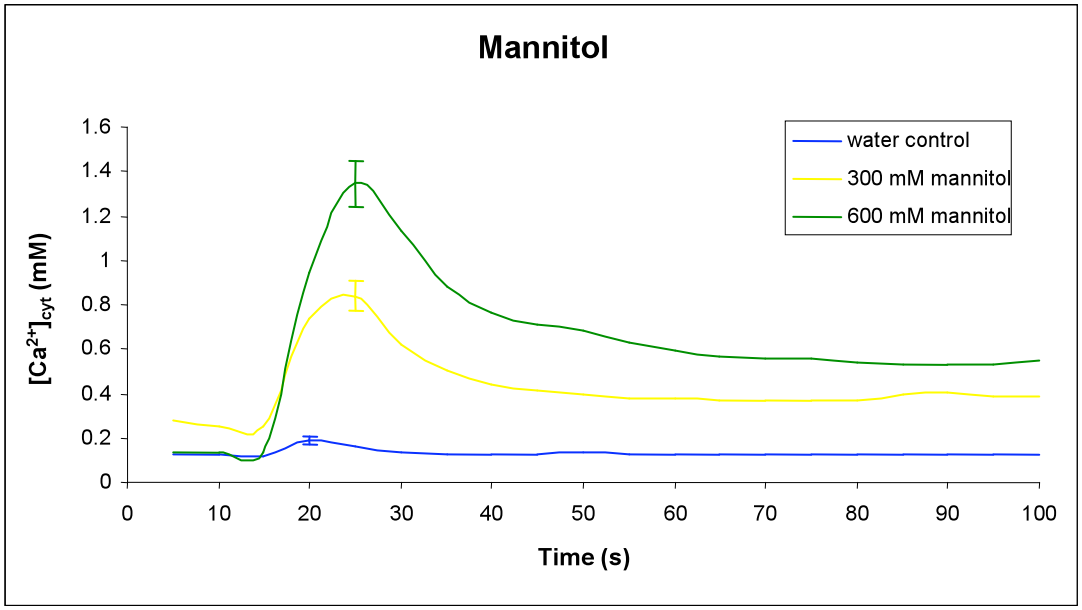

Appendix Figure 2.3. Mannitol induces increases in $[Ca^{2+}]_{cyt}$ similar to those induced by sorbitol
Two week old *Arabidopsis* seedlings treated with 300 mM and 600 mM mannitol respond similarly to seedlings treated with the same concentrations of sorbitol (refer to Figure 2.1B). The curve shown is the average response of 20 seedlings. Error bars are standard errors of the mean peak maxima.

CHAPTER 3

CHARACTERIZATION OF AN *atpnp-a* MUTANT

CHAPTER 3: CHARACTERIZATION OF AN *atpnp-a* MUTANT

3.1 INTRODUCTION

3.1.1 Water and ion homeostasis in plants

As discussed in chapter 1, the preservation of water and ion homeostasis is a fundamental requirement for life. Both abiotic and biotic stresses alter the availability of water and ions to the plant and thus affect water and ion homeostasis. The principal determinants of homeostasis are transport proteins, the activity of which control water and ion flux and can be regulated in order to fine tune homeostasis (Niu *et al.*, 1995). Ultimately in response to stress the plant must establish a new homeostatic state that balances the use of energy resources for growth and stress responses in order to survive. The role of plant hormones in maintaining water and ion homeostasis is not well understood. A likely candidate is ABA as it is induced by stresses that perturb plant water status and acts to promote stomatal closure in response to water deficit stress thus affecting water flux throughout the plant (Shinozaki and Yamaguchi-Shinozaki, 1997; Xiong and Zhu, 2002b). Most probably there are other hormones that act in balance with ABA in order to achieve water and ion homeostasis.

3.1.2 PNPs are proposed to play a role in water and ion homeostasis

It has been proposed that PNPs may play a role in maintaining plant water and ion homeostasis (Gehring and Irving, 2003). The reasons for this are threefold. Firstly irPNPs are induced by stresses that disrupt water and ion homeostasis, namely NaCl and osmotic stresses (Rafudeen *et al.*, 2003). Secondly NP treatment affects plant processes that involve changes in water and ion flux and thus altered homeostasis. For example commercially available animal NPs, irPNPs and recombinant AtPNP-A induce stomatal opening (Billington *et al.*, 1997; Gehring *et al.*, 1996; Morse *et al.*, 2004) and increase transpiration (Gottig *et al.*, 2008; Vesely *et al.*, 1993). Stomatal opening is caused by swelling of the stomatal guard cell pair, as a result of water and ion influx. Similarly, irPNPs and recombinant AtPNP-A induce protoplast swelling (Maryani *et al.*, 2001; Morse *et al.*, 2004). Therefore both stomatal opening and protoplast swelling are processes that involve changes in water and ion fluxes and are affected by PNPs. Thirdly PNPs have been directly shown to induce water and ion fluxes. In particular, irPNPs promote radial water movements out of the xylem while both irPNP and recombinant AtPNP-A treatment stimulate ion fluxes (Ludidi *et al.*, 2004; Pharmawati *et al.*, 1999; Suwastika and Gehring, 1998). In the previous chapter AtPNP-A was found to induce second messenger transients similar to the response to NaCl stress, suggesting that AtPNP-A may be a signalling molecule in water and ion stress responses. Like ABA, irPNPs have been isolated from the xylem and have been demonstrated to exert their affects in the stomata (Maryani *et al.*, 2003). The action of

AtPNP-A in the stomata opposes that of ABA and thus PNP and ABA may in fact be counteracting hormones (Wang *et al.*, 2007c). To date our understanding of PNPs derives entirely from plant responses to exogenous application of PNPs, however their function *in planta* remains elusive.

3.1.3 The *Arabidopsis* model system and mutant approach to inferring gene function

Arabidopsis has been the model plant of choice since the 1980s for a number of reasons (reveiwed in Meinke *et al.*, 1998). In brief, it is easy to grow in culture, on plates or in soil. It is small in size and has a short life cycle. *Arabidopsis* undergoes self fertilization to produce large numbers of progeny but can also be cross-fertilized. There are many different ecotypes that can be used for studies of natural variation and for mapping purposes. Moreover, *Arabidopsis* can be easily mutagenized as well as easily transformed (using *Agrobacterium tumefaciens*) and numerous mutants that have clear phenotypic traits and obey simple Mendelian genetics have already been described (Meinke *et al.*, 1998). By no means least of all, the collaborative efforts of the *Arabidopsis* community have driven the rapid advancement of this field (Pennisi, 2000). The *Arabidopsis* genome sequence was completed in December 2000 (The Arabidopsis Genome Initiative, 2000). Characterization of the coding regions revealed that the function of as few as 9% of genes have been determined experimentally. Approximately 69% of genes were annotated based on their sequence similarity to genes of known function in *Arabidopsis* and other organisms. The remaining 30% of genes could not be assigned any functional classification either because they are plant specific or because they are similar to genes of unknown function in other organisms. Following the genome release, prominent members of the *Arabidopsis* community met to discuss their vision for *Arabidopsis* research in the post genomic era. This culminated in the formation of the 2010 project, the aim of which is to "exploit the revolution in plant genomics in order to assign a function to every gene within its cellular, organismal and evolutionary context" (Chory *et al.*, 2000). To achieve these goals tools were developed to help assign gene function. One approach is the characterization of mutants in genes of unknown function (Alonso *et al.*, 2003). The small number of genes arranged at high density is a feature that makes *Arabidopsis* amenable to near saturation mutagenesis (Ostergaard and Yanofsky, 2004; Parinov and Sundaresan, 2000). Large repositories of T-DNA insertion mutants have now been created, mapped and are stored as seed in stock centres from which they are made publicly available (Alonso *et al.*, 2003). Currently there are about 250 000 sequenced indexed T-DNA inserts in the *Arabidopsis* genome with approximately 90% of genes containing at least one T-DNA- insertion (Daxinger *et al.*, 2008). In this chapter, a commercially available *Arabidopsis* mutant that has a T-DNA insertion in the *AtPNP-A* gene was characterized in an attempt to infer the function of PNPs *in planta*.

3.2 MATERIALS AND METHODS

3.2.1 Chemicals and stock solutions

Antibiotics: kanamycin, rifampicin, tetracylin, gentamicin and ampicillin were all purchased from SIGMA Aldrich (St Louis, USA). Kanamycin and ampicillin are water soluble while gentamycin is provided as a 50 mg/ml solution. Rifampicin is made up as a 10 mg/ml stock solution in 100% MeOH while tetracyclin is dissolved in 70% (v/v) EtOH to make a 10 mg/ml stock solution. DL-phosphinothricin (PPT) and MS medium were purchased from Duchefa (Haarlem, The Netherlands). PPT and is water soluble. Supertherm, Superscript III was acquired from Invitrogen (Paisley, UK). The Wizzard SV Gel and PCR Clean-Up System, T_4 DNA ligase and λ DNA were all supplied by Promega Corporation, (Madison, USA). Restriction enzymes: *EcoRI*, *BamHI* and *PstI* as well as the Super-therm polymerase were obtained from Roche Molecular Biochemicals (Basel, Switzerland). Silwet L-77 was provided by Lehle Seeds (Round Rock, USA). The dNTPs and O'GeneRuler 1 kb DNA Ladder were both purchased from (Fermentas Inc., Maryland, UK). ABA, MS media, bovine serum albumin (BSA) and Sigmaspin columns were all aquired from SIGMA Aldrich (St Louis, USA). ABA is dissolved in 100% EtOH to make a 100 mM stock solution. The Megaprime DNA labelling kit, Hybond N^+ membrane and α-[^{32}P]dCTP were all attained from Amersham Pharmacia Biotech (Little Chalfont, UK). Finally Kodac Biomax ML X-ray film is from Kodak Industrie (Cedex, France) while the developer and fixer solutions are from AGFA-Gevaert Limited (Mortsel, Belgium).

3.2.2 Microorganisms

3.2.2.1 E. coli growth and competent cell preparation

E. coli JM109 was grown on Luria Bertani (LB) (1% w/v tryptone, 0.5% w/v yeast extract, 0.5% w/v NaCl) (Sambrook *et al.*, 1989) agar (1.5% w/v) at 37°C overnight. To make competent cells a single colony was inoculated into 5 ml LB media and grown shaking at 37°C overnight. The following day 2 ml of the overnight culture was subcultured into 250 ml LB media supplemented with 20 mM $MgSO_4$ and grown at 37°C, shaking until OD_{600} was 0.4-0.6, measured using the Beckman DU 650 Spectrophotometer (Beckman Coulter, Inc., CA, USA). The cells were recovered by centrifugation at 5000 X *g* for 5 min at 4°C in a J2-21 Beckman centrifuge (Beckman Coulter, Inc., CA, USA) and the supernatant discarded. The cells were gently resuspended in 100 ml ice cold TFB1 buffer (30 mM potassium acetate, 100 mM RbCl, 10 mM $CaCl_2$, 50 mM $MnCl_2$, 15% v/v glycerol, which had been adjusted to pH 5.8 with glacial acetic acid and then filter sterilized) and incubated on ice for 5 min. The cells were collected again by centrifugation at 5000 X g for 5 min at 4°C and the supernatant discarded. Finally the pellet was gently resupended in 10 ml ice cold TFB2 buffer (10 mM MOPS, 75 mM $CaCl_2$, 10 mM RbCl and 15% v/v glycerol, filter sterilized) and incubated on ice for 15-60 min. Competent cells were dispensed in 100 μl aliquots into pre-cooled 1.5 ml eppendorf tubes, frozen immediately in liquid nitrogen and stored at -70°C.

3.2.2.2 A. tumefaciens growth and competent cell preparation

A. tumefaciens GV3101 (Holsters *et al.*, 1980) was cultured on LB agar (1.5% w/v) containing 150 μg/ml rifampicin and 15 μg/ml gentamicin antibiotic selection and grown at 28°C for two days. To make

competent cells a single colony was inoculated into 10 ml yeat extract peptone (YEP) media (1% w/v peptone; 1% w/v yeast extract and 0.5% w/v NaCl) supplemented with 100 μg/ml rifampicin and incubated shaking at 28°C overnight. The following day 2 ml of the overnight culture was transferred to 50 ml fresh YEP media with antibiotic selection and incubated shaking at 28°C until the OD_{600} reached 0.5–1.0, measured using the Beckman DU 650 Spectrophotometer (Beckman Coulter, Inc., CA, USA). The culture was chilled on ice before the cells were harvested by centrifugation at 3000 X *g* for 5 min at 4°C in a J2-21 Beckman centrifuge (Beckman Coulter, Inc., CA, USA). The supernatant was discarded and the pellet resuspended in 1 ml ice cold 20 mM $CaCl_2$. Aliquots of 100 μl were then dispensed into pre-cooled 1.5 ml eppendorf tubes, immediately frozen in liquid nitrogen and stored at -70°C.

3.2.2.3 Botrytis cinerea

The *B. cinerea* GLUK-1 (pepper) (Kliebenstein *et al.*, 2005) and *Brassica oleracea* (*Brassica*) (Ferrari *et al.*, 2003) isolates were maintained on sugar free apricot halves (Natuurlite, South Africa) at 25°C in the dark. Every four weeks *B. cinerea* was subcultured by inoculating a small piece of infected apricot onto a fresh apricot using a sterile toothpick.

3.2.2.4 Pseudomonas syringae

Virulent *P. syringae* DC 3000 pv. *tomato* (*Pst*) (Whalen *et al.*, 1991) and avirulent *Pst AvrB* (Bisgrove *et al.*, 1994) strains were grown on Kings Broth (KB) (1% w/v glycerol, 1% w/v tryptone, 1% w/v peptone, 0.15% $MgSO_4.7H_2O$, 0.15% K_2HPO_4, pH adjusted to 7.0) (King *et al.*, 1954) agar (1.2% w/v) supplemented with 50 μg/ml rifampicin for *Pst* and 50 μg/ml rifampicin plus 50 μg/ml kanamycin for *Pst AvrB* selection; for two days at 28°C.

3.2.2.5 Hyaloperonospora parasitica

The *H. parasitica* virulent isolate HpNoks1 (Kunz *et al.*, 2008), kindly provided by Prof. David Cahill, Deakin University, Australia was maintained on highly susceptible *Arabidopsis eds1* plants by rubbing previously infected leaves heavily laden with condiophores on to leaves of 3-4 week old uninfected plants (Koch and Slusarenko, 1990; Kunz *et al.*, 2008; Mohr and Cahill, 2003; Parker *et al.*, 1996). The plants were then grown at 16°C under a 10 hr light 14 hr dark photoperiod for seven days in transparent plastic containers to ensure a high humidity optimal for spore formation (Channon, 1981).

3.2.3 Plasmids

3.2.3.1 pGEMT Easy

The pGEMT Easy plasmid is selected for by growing cells transformed with the plasmid on LB agar (1.5% w/v) containing 100 μg/ml ampicillin. The media additionally contained 0.5 M isopropyl-β-D-thiogalactopyranoside (IPTG) and 80 μg/ml 5-bromo-4-chloro-2-indolyl-β-D-galactoside (X-gal) for blue/white colony screening in order to identify transformants containing inserts, according to the manufacturer's instructions (Promega Corporation, Madison, USA).

3.2.3.2 pSMB

The pSMB binary plasmid was a kind gift from Dr Jimmy Botella (Mylne and Botella, 1998) and is maintained as a glycerol stock in *E. coli* DH5α cells. The presence of the plasmid is selected for on LB agar (1.5% w/v) supplemented with 10 μg/ml tetracycline.

3.2.4 Sterilizing seed

As described in chapter 2 (section 2.2.2).

3.2.5 Plant growth conditions

3.2.5.1 Seedlings

Seedlings were grown in Petri dishes on PN media as described in chapter 2 (section 2.2.3-4).

3.2.5.2 Older plants

For experiments conducted on older plants, plants were grown on soil that is a 1:1 mixture of peat (Jiffy Products, International AS, Norway) and vermiculite. Seeds were sown onto soil or in some cases seedlings were transplanted from Petri dishes onto soil and thereafter covered with cling film for one week to ensure high humidity optimal for seedling establishment. Plants were grown under a 16 hr light (100 μM photons m^{-2} s^{-1}) and 8 hr dark cycle at 21 °C. After a week the cling film was removed and the plants were fertilized with Phostrogen (Bayer CropScience Group, Hertfordshire, UK). Thereafter plants were watered every few days, as required, until they reached four weeks of age, at which time experiments were conducted.

3.2.6 Prediction of the site of the T-DNA insertion in the SALK line

The SALK sequence was downloaded from the SALK institute (http://signal.salk.edu/cgi-bin/tdnaexpress) and the *AtPNP-A* gene (At2g18660) sequence was downloaded from TAIR (www.arabidopsis.org). The DNAMAN program was used to align these sequences (Version 4.13, Lynnon Biosoft, Quebec, Canada). The predicted site of T-DNA insertion was the position at which the two sequences aligned.

3.2.7 DNA manipulations

3.2.7.1 DNA extraction

Genomic DNA was extracted from *Arabidopsis* seedlings or leaf tissue using a superquick DNA extraction procedure adapted from the method of Edwards (Edwards *et al.*, 1991). Briefly, a single seedling or leaf was homogenized in 250 μl extraction buffer (200 mM Tris pH 7.5, 250 mM NaCl, 25 mM EDTA pH 8.0 and 0.5% w/v SDS) and then incubated at 60°C for 10 min. An equal volume of chloroform:isoamylalcohol (24:1 v/v) was added to each sample, mixed and then centrifuged at 10 000 X *g* for 10 min in a bench top centrifuge (Heraeus Biofuge Pico, Kendro Laboratory Products, Germany). The aqueous phase was collected and precipitated with 1/10 X vol sodium acetate pH 5.6 and 2 X vol ice cold 100% EtOH at -20°C overnight. The following day the DNA was collected by centrifugation at 10 000 X *g* for 10 min. The pellet was washed with 70% (v/v) EtOH and the centrifugation repeated. The

EtOH was aspirated and the DNA pellet allowed to air dry. Finally the DNA was resuspended in 50 µl TE buffer (10 mM Tris and 1 mM EDTA pH 8.0) and stored at -20°C.

3.2.7.2 Visualization of PCR products by gel electrophoresis

The PCR products were mixed with 6 X loading dye (either bromophenol blue: 0.25% w/v bromophenol blue in 40% w/v sucrose or orange G: 0.15% w/v orange G, 10 mM Tris HCl pH 7.5, 60 mM EDTA, pH 8.0 and 60% v/v glycerol; depending on the expected product size). Products were separated in 1% (w/v) agarose gels made up in 1 X Tris-Acetate (TAE) buffer (40 mM Tris, 20 mM acetic acid and 1 mM EDTA pH 8.0), containing 0.16 µg/ml ethidium bromide (EtBr) and run in the same 1 X TAE buffer. A O'GeneRuler 1 kb DNA Ladder (Fermentas Inc., Maryland, UK) or λ *PstI* DNA ladder (20 µg λ DNA digested with 20 U *PstI* in 20 µl at 37°C overnight, to which 180 µl dH_2O and 40 µl 6 X bromophenol blue loading dye was added) was included on each gel to confirm that products were the expected sizes. Products were then visualized using Gel Doc system and images captured using Quantity One 1D analysis software (both from BioRad Inc., Hercules, CA, USA).

3.2.8 Isolation of the SALK line by PCR

PCR screening was undertaken to identify homozygous wildtype, homozygous mutant or heterozygous individuals from the segregating SALK_000951 seed (Ostergaard and Yanofsky, 2004). Primers for determining the presence of the wildtype *AtPNP-A* gene were: *AtPNP-A* SALK forward: 5' ACGGATCGAAGTGGGTATTCG 3' and *AtPNP-A* SALK reverse: 5' TAGTTGATTTCTGCCGGGAGC 3' while primers for determining the presence of the T-DNA insertion mutant were the same *AtPNP-A* SALK forward primer and T-DNA reverse: 5' GTTCACGTAGTGGGCCATCG 3'. PCR reactions were conducted in 20 µl volumes containing 1 X PCR buffer (provided with enzyme), 1.0 mM $MgCl_2$ (optimal for this PCR reaction), 0.125 mM dNTPs; 0.1 U/µl Super-Term Polymerase (Roche Molecular Biochemicals, Basel, Switzerland) and 0.2 µM each of forward and reverse primers. PCR reactions were performed using the GeneAmp PCR Systems 2700 (Applied Biosystems, Foster City, USA) PCR machine using the following conditions: initial denaturation of 94°C for 5 min followed by 35 cycles of 94°C for 1 min, annealing at 60°C for 1 min and 72°C elongation for 1 min after which a final elongation step of 72°C for 10 min was performed (Table 3.1).

3.2.9 PCR amplification of the kanamycin gene

Primers designed to amplify the *NPT II* marker gene present in the T-DNA insertion sequence were *NPT II* forward: 5' GAGGCTATTCGGCTATGACTG 3' and *NPT II* reverse: 5' ATCGGGAGCGGCGATACCGTA 3'. PCR reactions were the exactly the same as described above (section 3.2.8). The $MgCl_2$ concentration used in the PCR reaction was 1 mM, the annealing temperature was 60°C and the number of cycles performed was 35, as optimized for these primers (Table 3.1).

Table 3.1. Primers and PCR conditions

Primer name	Forward primer	Reverse primer	$MgCl_2$ (mM)	Ta (°C)	# of cyc	Cycling conditions
Screening SALK lines						
AtPNP-A SALK	5' ACGGATCGAAGTGGGTATTCG 3'	5' TAGTTGATTTCTGCCGGGAGC 3'	1.0	60	35	1 min each denaturation, annealing, elongation
T-DNA		5' GTTCACGTAGTGGGCCATCG 3'	1.0	60	35	1 min each denaturation, annealing, elongation
NPT II	5' GAGGCTATTCGGCTATGACTG 3'	5' ATCGGGAGCGGCGATACCGTA 3'	1.0	60	35	1 min each denaturation, annealing, elongation
Expression						
AtPNP-A RT	5' TCTATTACGACCCTCCCTACACT 3'	5' TGTTCTTGACTCCGACTACCA 3'	1.5	62	37	15 s denaturation, 30 s annealing, 1 min elongation
UBQ	5' GGACCGCTCTTATCAAAGGA 3'	5' CTTGAGGAGGTTGCAAAGGA 3'	3.0	65	25	15 s denaturation, 30 s annealing, 1 min elongation
Cloning						
AtPNP-A CLONING	5' AAGAAAATGATAAAAATGGCAG 3'	5' AAGAATGAAACTTACGGTGTGT 3'	1.0	60	35	1 min each denaturation, annealing, elongation
CaMV	5' ACGCACAATCCCACTATCC 3'		1.0	55	35	1 min each denaturation, annealing, elongation
Annotation of *AtPNP-A*						
AtPNP-A ANNOTATION	5' ACTTTGACAGAGCATGCACC 3'	5' GAATCGAAGCGGATCTAACG 3'	3.0	60	40	15 s denaturation, 30 s annealing, 1 min elongation

Each PCR reaction includes an initial denaturation step at 94°C for 5 min followed by the appropriate number of cycles (# of cyc) and cycling times indicated in the table and is concluded with a final elongation step at 72°C for 10 min. During cycling, the denaturation and elongation temperatures are also 94°C and 72°C respectively but the annealing temperatures (Ta) differ depending on the primer pair.

3.2.10 RNA manipulations and cDNA synthesis

3.2.10.1 RNA extraction – LiCl method

RNA was extracted using a LiCl precipitation method modified from the method of Verwoerd (Verwoerd *et al.*, 1989). Briefly, tissue was ground to a fine powder in liquid nitrogen and then added to ice cold 3 ml extraction buffer (100 mM Tris-HCl pH 9.0, 200 mM NaCl, 20 mM EDTA pH 8.0, 1% w/v Sarkosyl and 5 mM DTT, made up in DEPC-treated dH_2O). The aqueous supernatant was extracted by adding 1.4 ml each of phenol pH 4.0 and chloroform: isoamylalcohol (24:1 v/v), mixing and centrifuging for 10 min at 5000 X *g* and 4°C in a J2-21 Beckman centrifuge (Beckman Coulter, Inc., CA, USA). The upper phase was aspirated into a clean tube. This was washed three times, each time by adding an equal volume of chloroform: isoamylacohol (24:1 v/v), then re-centrifuging for 5 min at 5000 X *g* and 4°C and removing the supernatant into a clean tube. Finally the aqueous supernatant was removed into 2 ml eppendorf tubes and made up to 2 M LiCl using an 8 M LiCl stock solution. The RNA was precipitated overnight at 4°C. The following day the RNA was pelleted by centrifugation for 20 min at 10000 X *g* and 4°C in a bench top centrifuge (Heraeus Biofuge Pico, Kendro Laboratory Products, Germany). The pellet was washed twice with 2 M LiCl, each time by resuspending the pellet in 300 µl fresh 2 M LiCl, re-centrifuging and then discarding the supernatant. The final pellet was resuspended in 300 µl DEPC-treated dH_2O. The RNA was precipitated a second time with 1/10 vol 3 M sodium acetate pH 5.2 and 2.5 vol ice cold 100% EtOH overnight at - 20°C. The following day the RNA was collected by centrifugation for 10 min at 10000 X *g* and 4°C. The pellet was then washed with 70% (v/v) EtOH, re-centrifuged and the supernatant aspirated. Finally the RNA pellet was air dried, resuspended in 20 µl of DEPC-treated dH_2O and then stored at -70°C.

3.2.10.2 Determination of RNA quality

The quality of the RNA was analyzed using the Nanodrop (NanoDrop Technologies, Wilmington, USA). An absorbance 260: 280 nm ratio > 1.8 was considered high enough quality to be used for subsequent analysis. Additionally the RNA was visualized using gel electrophoresis. Briefly, 2.5 µg RNA was mixed with 10 µl loading dye (1 X MOPS, 60% v/v formamide, 67 µg/ml EtBr and 9% v/v formaldehyde) and run on a 1.2% (w/v) agarose gel made up in 1X MOPS with 6.2% (v/v) formaldehyde in a 1 X MOPS running buffer. The RNA was then visualized using the Gel Doc system (BioRad Inc., Hercules, CA, USA) described above (section 3.2.7.2).

3.2.10.3 cDNA synthesis for semi quantitative RT-PCR

For the semi-quantitative RT-PCR, cDNA was synthesized using Superscript III Reverse Transcriptase according to the manufacturer's instructions (Invitrogen, Paisley, UK). Briefly, 2.5 µg RNA, together with 1 ul of 500 ng/µl oligo dT_{18} primer and 1 µl of 10 mM dNTPs in a total volume of 13 µl was denatured by heating at 65°C for 5 min and then snap cooling on ice for 2 min. To each reaction 4 µl first strand buffer, 1 µl 0.1 M DTT and 0.5 µl Superscript III enzyme was then added and the volume made up to 20 µl with DEPC treated dH_2O. The reaction was incubated overnight at 46°C and stopped the following day by heating at 70°C for 15 min. The cDNA was diluted 1:10 before using in a PCR.

3.2.11 Expression of *AtPNP-A* determined by semi-quantitative RT-PCR

Semi-quantitative RT-PCR was used to measure the expression of *AtPNP-A* in the *atpnp-a* mutant, wildtype and complemented lines. The *UBIQUITIN-CONJUGATING ENZYME* 21 (*UBQ*) (At5g25760) was used as a control to check that there were comparable amounts of template in each sample.

3.2.11.1 AtPNP-A PCR

The PCR reaction was conducted in 20 µl volumes including 1 X PCR buffer (provided with the enzyme), 1.5 mM $MgCl_2$, 0.125 mM dNTPs, 0.1 U/µl Super-Term Polymerase and 0.2 µM each of *AtPNP-A* RT forward 5' TCTATTACGACCCTCCCTACACT 3' and *AtPNP-A* RT reverse primers 5' TGTTCTTGACTCCGACTACCA 3'. The PCR was performed by the GeneAmp PCR Systems 2700 (Applied Biosystems, Foster City, USA) PCR machine using the following cycling conditions: initial denaturation at 94°C for 5 min, followed by 37 cycles of 94°C denaturation for 15 sec, 62°C annealing for 30 sec and 72°C elongation for 1 min and concluded with a final extension step of 72°C for 10 min (Table 3.1).

3.2.11.2 UBQ PCR

The *UBQ* semi-quantitative RT-PCR was essentially identical except for minor revisions optimized for this primer pair: *UBQ* forward 5' GGACCGCTCTTATCAAAGGA 3' and *UBQ* reverse 5' CTTGAGGAGGTTGCAAAGGA 3'. In this reaction 3 mM $MgCl_2$ was optimal and 25 PCR cycles were performed at an annealing temperature of 65°C (Table 3.1).

3.2.12 Northern blot analysis

3.2.12.1 RNA gel electrophoresis and transfer

RNA was extracted from the homozygous *atpnp-a* mutant and wildtype lines as per the LiCl method (section 3.2.10.1) and quantified on the Nanodrop (section 3.2.10.2). For each sample, 20 µg of RNA was separated by gel electrophoresis (section 3.2.10.2) and then transferred on to Hybond N^+ membrane by capilliary action using 20 X SSC (3 M NaCl and 0.3 M sodium citrate adjusted to pH 7.0 with HCl) transfer buffer and 3 MM Whatman filter paper as a wick, according to standard procedures (Sambrook *et al.*, 1989). The transfer continued overnight and the following day the RNA was UV cross-linked to the membrane at 700 joules using the UV crosslinker (Amersham Pharmacia Biotech, Little Chalfont, UK). The membrane was then stained with methylene blue (0.04% methylene blue in 0.5 M sodium acetate pH 5.2) with gently shaking at room temperature. Excess stain solution was removed by washing with dH_2O and the stained membrane was then photographed using the Syngene gel documentation system (Synoptics Ltd, Cambridge, UK) to visualize whether there had been equal amounts of RNA loaded and transferred for each sample.

3.2.12.2 Preparation of the AtPNP-A probe

The full length *AtPNP-A* gene was PCR amplified from cDNA template using the *AtPNP-A* CLONING primers and PCR conditions described in section 3.2.13.1 below. The PCR product was the purified using the Wizzard SV Gel and PCR Clean-Up System and quantified on the Nanodrop as described below

(section 3.2.13.2). 100 ng of the purified PCR product was ladelled by random priming using the Megaprime DNA labelling kit according to the manufacturer's instructions (Amersham Pharmacia Biotech, Little Chalfont, UK). The labelled probe was then purified from unincorporated α-[^{32}P]dCTP using the SigmaSpin post reaction clean up columns columns according to the manufacturer's instructions (SIGMA Aldrich, St Louis, USA).

3.2.12.3 Northern blot analysis – hybridization and wash procedures

The Northern blot was performed according to the method of Church and Gilbert (Church and Gilbert, 1984). Membranes were first blocked by pre-hybridization in Church buffer (1% w/v BSA, 0.5 M $NaPO_4$ buffer pH 7.2, 1 mM EDTA and 7% w/v SDS) at 42°C for 1 hr, shaking gently in a Hybridization oven/shaker (Amersham Pharmacia Biotech, Little Chalfont, UK). The purified radio-labelled probe was denatured at 95°C for 5 min and snap cooled on ice before it was added to the hybridization buffer (same as the Church buffer). The pre-hybridization buffer was replaced with the hybridization buffer and the membranes were incubated with the probe at 42°C shaking overnight. The following day the hybridization buffer was discarded and the membranes washed in 2 X SSC buffer with 0.1% SDS for 30 min. Subsequent washes of increasing stringency were 0.5 X SSC with 0.1% SDS; 0.2 X SSC with 0.1% SDS and 0.1 X SSC with 0.1% SDS, as required. Each wash was performed for 15 min and the temperature raised (to a maximum 65°C) to increase stringency, as required. When the counts were 2-5 counts per second as determined using a Geiger counter (Mini Instruments Ltd., Essex, UK) the membrane was sealed in a plastic bag to prevent it from drying out. The membrane was then placed in an autoradiography cassette containing intensifying screens and exposed to Biomax ML film (Kodak Industrie, Cedex, France) at -70°C overnight. The following day the X-ray film was developed by incubating in developer solution for 2-3 min with gentle agitation, rinsed in 3% (v/v) acetic acid for 1 min and then fixed in the fixer solution for 2 min after which the membrane was rinsed in water and then allowed to dry. The X-ray image was scanned using an HP scanner.

3.2.13 Complementation of the *atpnp-a* mutant

3.2.13.1 PCR amplification of the wildtype AtPNP-A gene

The wildtype *AtPNP-A* gene was PCR amplified from *Arabidopsis* Col-0 genomic DNA using primers that span the START and STOP codons, a kind gift from Dr Ndiko Ludidi (Ludidi *et al.*, 2002): *AtPNP-A* CLONING forward primer: 5' AAGAAAATGATAAAAATGGCAG 3' *AtPNP-A* CLONING reverse primer: 5' AAGAATGAAACTTACGGTGTGT 3'. For cloning purposes, *BamHI* and *EcoRI* restriction enzyme sites were incorporated on the 5' ends of the forward and reverse primers respectively. PCR reactions were prepared in 100 µl volumes that included 1 X PCR buffer, 1 mM $MgCl_2$, 0.125 mM dNTPs, 0.1 U/µl Super-Term Polymerase, 0.2 µM each of forward and reverse primers and 10 µl of Col-0 genomic DNA template. PCR cycling conditions were: initial denaturation of 94°C for 5 min followed by 35 cycles of 94°C for 1 min, 60°C for 1 min and 72°C for 1 min, then a final elongation step at 72°C for 10 min (Table 3.1).

3.2.13.2 Purification of the AtPNP-A PCR product

The PCR product was separated on a 1% (w/v) agarose TAE gel and visualized on a long wavelength UV light (365 nm) box. A gel slice containing the PCR band was removed using a clean scapal blade and placed into a 1.5 ml eppendorf tube. The gel slice was then purified using the Wizzard SV Gel and PCR Clean-Up System, according to the manufacturer's instructions (Promega Corporation, Madison, USA). The purified PCR product was quantified on the Beckman DU-600 Spectrophotometer (Beckman Coulter, Inc., CA, USA) and visualized again on a 1% (w/v) agarose TAE gel to ensure that no degradation had occurred during the purification process. In this case the purified PCR product recovered was 33.5 ng/μl.

3.2.13.3 Ligation of the AtPNP-A gene sequence into pGEMT Easy

The purified *AtPNP-A* PCR product was then cloned in to pGEMT-Easy vector which contains T-A overhangs, according to the manufacturer's instructions (Promega Corporation, Madison, USA). 20 ng of insert DNA (purified PCR product) and 50 ng vector were used in the ligation reaction so that the ratio of insert to vector is 3:1 (as recommended) according to the following calculation:

$$\frac{\text{amount of vector (ng)} \times \text{size of insert (kb)}}{\text{size of vector (kb)}} \times \text{insert: vector ratio} = \text{amount of insert (ng)}$$

The ligation reaction was performed in 10 μl volume and included 1 μl each of 10 X buffer (provided with the enzyme) and T_4 DNA ligase (Promega Corporation, Madison, USA) along with the appropriate amounts of DNA. This was incubated at 4°C overnight.

3.2.13.4 Transformation of pGEMT Easy containing AtPNP-A into E. coli

The following day 2μl of the ligation reaction was transformed into 100 μl *E. coli* JM109 competent cells (described above). Briefly, the cells were thawed on ice and then the DNA (ligation) was added and left for 1 hr on ice. The cells were then heat shocked at 42°C for 45 s, immediately after which they were placed back on ice for 2 min. 1 ml of LB media (without antibiotic selection) was added to the cells which were then incubated at 37°C shaking for 1 hr. The cells were then plated on LB agar (1.5% w/v) supplemented with 100 μg/ml ampicillin, 0.5 M IPTG and 80 μg/ml X-gal and incubated at 37°C overnight. The following day cells that had been successfully transformed with the insert DNA produced white colonies while the rest of the colonies were blue.

3.2.13.5 Screening for positive transformants

Candidate white colonies were inoculated into sterile PCR tubes for colony PCR as well as into 5 ml overnight cultures containing LB media with appropriate antibiotic selection (in this case 100 μg/ml ampicillin) which were then incubated shaking at 37°C overnight.

3.2.13.5.1 Colony PCR

The colony PCR was exactly the same as that used to originally amplify the wildtype *AtPNP-A* gene from the Col-0 genomic DNA prior to cloning (described in section 3.2.12.1).

3.2.13.5.2 Alkaline lysis plasmid preparation

The following day, the 5ml overnight culture was centrifuged at 10 000 X *g* for 1 min in a bench top centrifuge (Heraeus Biofuge Pico, Kendro Laboratory Products, Germany) to harvest the cells and the

supernatant was discarded. The cell pellet was resuspended in 200 µl solution 1 (25 mM Tris ph 8.0, 50 mM glucose and 10 mM EDTA ph 8.0) and then incubated at room temperature for 10 min. Next 400 µl solution 2 (0.2 M NaOH and 1% w/v SDS) was added to each sample and mixed well by inverting 6 times, then incubated on ice for 10 min. 300 µl pre-cooled solution 3 (3 M sodium acetate and 2 M acetic acid) was then added and again mixed by inversion and left on ice for ice for a further 10 min. After this the samples were centrifuged at 10 000 X *g* for 5 min in the bench top centrifuge and 900 µl supernatant recovered. To precipitate the DNA 600 µl isopropanol was added, mixed and then left at room temperature for 2 min. The DNA was pelleted by centrifugation for 10 min at 10 000 X *g*. Finally the DNA pellet was washed with 500 µl 70% (v/v) EtOH. A short centrifugation step aided aspiration of the supernatant. The DNA was then allowed to air dry before being resuspended in 50 µl TE (section 3.2.7.1). DNA was stored at -20°C.

3.2.13.5.3 Restriction enzyme digestion of plasmid preparations

In order to confirm that the white colonies indeed contained the appropriate sized insert, the plasmid preparation was subjected to restriction enzyme analysis. In this, 1 µl of the plasmid preparation was digested with 5 U each of *EcoRI* and *BamHI* restriction enzymes that should excise the insert, and incubated at 37°C for two hrs. The products of the restriction enzyme digest were analyzed on 1% (w/v) agarose TAE gels.

3.2.13.6 Glycerol stocks

Glycerol stocks were made of positive transformants by adding 500 µl of freshly grown overnight culture and 500 µl of glycerol storage solution (65% v/v glycerol, 0.1 M $MgSO_4.7H_2O$ and 0.025 M Tris HCl pH 8.0) in a 1.5 ml eppendorf tube. Immediately these were frozen in liquid nitrogen and stored at -70°C.

3.2.13.7 Excising the AtPNP-A gene sequence from pGEMT Easy

Once positive transformants had been identified, the plasmid DNA was again digested with restriction enzymes in order to extract the *AtPNP-A* gene for subsequent cloning into the binary vector. The *AtPNP-A* CLONING reverse primer has an *EcoRI* restriction sites incorporated at its 5' end while pGEMT Easy has two *EcoRI* sites, either side of the multiple cloning site (MCS). It was therefore necessary to perform sequential digests, first using *BamHI* and then using *EcoRI* to ensure that *BamHI* definitely cut the insert. Firstly 10 µg of the plasmid was digested with 10 U of *BamHI* and incubated at 37°C overnight. The products of the restriction digest were separated by gel electrophoresis and the linearized plasmid was excised and purified using the Wizzard gel purification system, as described previously. The purified linearized plasmid was then subjected to a second restriction enzyme digestion with *EcoRI*. In this case 17 µl of the linearized plasmid (maximal amount allowed in the 20 µl restriction enzyme digest) was incubated with 10 U of *EcoRI* at 37°C for two hours. Again the products were separated by gel electrophoresis and bands of the expected insert size excised and then purified using the Wizzard gel purification kit. The purified insert that had been cut with *BamHI* and *EcoRI* was quantified to be approximately 2 ng/µl.

3.2.13.8 Plasmid preparation of the pSMB binary plasmid

The glycerol stock of *E. coli* harboring the pSMB plasmid was plated onto LB agar (1.5% w/v) supplemented with 10 μg/ml tetracycline and grown at 37°C overnight. The following day a single colony was inoculated into 5 ml culture of LB media containing antibiotic selection and grown shaking at 37°C overnight. Since the alkaline plasmid preparation method was unsuccessful with this low copy number plasmid, large scale plasmid preparations were performed. In brief, 2.5 ml from overnight cultures was subcultured into 250 ml LB media with appropriate antibiotic selection and grown shaking at 37°C overnight. The following day the cells were harvested by centrifugation at 6000 X *g* for 15 min at 4°C in a J2-21 Beckman centrifuge (Beckman Coulter, Inc., CA, USA). The plasmid DNA was then purified using the QIAGEN-tip 100, columns according to the manufacturer's instructions in the Qiagen very low copy plasmid/cosmid purification protocol (Qiagen, Crawley, UK). The purified plasmid was visualized by gel electrophoresis and quantified on the Beckman DU-600 Spectrophotometer (Beckman Coulter, Inc., CA, USA) and determined to be approximately 1 μg/μl.

3.2.13.9 Restriction enzyme digestion of pSMB

The pSMB plasmid was the digested with *BamHI* and *EcoRI* that each cut pSMB once in the MCS, downstream of the CaMV 35S promoter sequence. 10 μg of purified pSMB plasmid was digested with 10 U of each enzyme and incubated at 37°C overnight. The linearized pSMB plasmid was then separated from uncut plasmid by gel electrophoresis, excised from the gel and purified using the Wizzard gel purification system. Finally the purified DNA fragment was visualized by gel electrophoresis and quantified on the Beckman DU-600 Spectrophotometer (Beckman Coulter, Inc., CA, USA) and found to be approximately 50 ng/μl.

3.2.13.10 Ligation of the AtPNP-A insert into pSMB

The *BamHI* and *EcoRI* digested *AtPNP-A* insert (originally from the pGEMT Easy plasmid) was ligated into the *BamHI* and *EcoRI* digested pSMB plasmid using the T_4 DNA ligase method described previously (section 3.2.13.3). Since the size of insert is approximately 0.4 kb and the vector is 27 kb, 2.2 ng of insert was was ligated with 50 ng of vector to ensure a 3:1 insert to vector ratio.

3.2.13.11 Transforming pSMB containing AtPNP-A into E. coli

Again 2 μl of each ligation reaction was transformed into competent *E. coli* JM109 cells using the heat shock method described previously. The transformed cells were plated onto LB media containing tetracycline selection for the pSMB plasmid. Colonies that grew were potentially positive transformants and were screened by colony PCR. However this produced very faint bands on the gel and so the plasmid was extracted from large scale cultures using the alkaline lysis plasmid preparation method (section 3.2.13.5.2) and the PCR repeated on the purified plasmid as template, yielding positive results.

3.2.13.12 Transformation of pSMB containing AtPNP-A into A. tumefaciens

The purified pSMB plasmid containing the wildtype *AtPNP-A* gene insert under the control of the CaMV 35S promoter (35S::*AtPNP-A*), purified from the positively transformed *E. coli* cells, was transformed

into competent *A. tumefaciens* GV3101 cells (described above in 3.2.2.2). In this 25μl of the plasmid preparation was added to 100 μl of competent *A. tumefaciens* cells. These were then placed in a 37°C water bath for 5 min to both thaw and heat shock the cells. Then 900 μl of LB media (without antibiotic selection) was added and the cells were incubated shaking at 28°C for 6 hrs. Thereafter the cells were plated onto LB agar (1.5% w/v) containing 150 μg/ml rifampicin and 15 μg/ml gentamicin to select for the *A. tumefaciens* and 10 μg/ml tetracyclin to select for the pSMB plasmid, and incubated at 28°C for 2-3 days until colonies appeared. Transformants were screened by colony PCR (as described previously) and overnight cultures were prepared from which glycerol stocks of the positive transformants were generated. These were stored at -70°C.

3.2.13.13 Arabidopsis transformation with Agrobacterium

Based on the floral dip methof of Clough and Bent (Clough and Bent, 1998).

3.2.13.13.1 Plant preperation

From first emergence of primary bolts at about four weeks, bolts were clipped at the base of the rosette to promote secondary bolt formation. This was done every couple of days until all of the plants in that particular tray were at the bolting stage. The plants were then left to flower until there were maximal numbers of flowers with no sliques which took approximately one week further.

3.2.13.13.2 Agrobacterium preparation

Sucessfully transformed 35S::*AtPNP-A A. tumefaciens* (stored as glycerol stocks) were streaked onto LB agar (1.5% w/v) containing the appropriate antibitotic selection (150 μg/ml rifampicin, 15 μg/ml gentamicin and 10 μg/ml tetracycline) and grown at 28°C for 2-3 days. A single colony was then innoculated into 5 ml selective liquid LB media and incubated shaking at 28°C for 2 days. Thereafter the entire 5 ml culture was innoculated into a large scale culture of 500 ml LB media containing antibiotics and incubated shaking at 28°C overnight. The following day the cells were harvested by centrifugation at 3500 X *g* for 15 min at room temperature. Finally the cells were resuspended in 250 ml 5% (w/v) sucrose containing 0.05% (v/v) Silwet L-77 surfactant.

3.2.13.13.3 Floral dip

The aerial parts of the *Arabidopsis* plants were submerged in the *A. tumefaciens* solution for appproximately 5 s. Dipped plants were laid on their side in trays lined with tissue paper, covered in clingfilm and left overnight. The following day the plants were uncovered and placed upright. From then onwards plants were watered from below to prevent loss of the *A. tumefaciens*.

3.2.13.14 Isolation of positive plant transformants

Positive transformants were identified by screening T_0 seed on PN agar (0.6% w/v) containing 10 μg/ml PPT (Duchefa Biochemie, Haarlem, The Netherlands). Resistant individuals were transplanted on to soil and allowed to grow to maturity. Seed from these selfed individuals was collected, dried and then rescreened on PPT plates. This whole procedure was repeated until lines that were 100% PPT resistant were obtained. Finally, these lines were confirmed to be homozygous by PCR.

3.2.14 PCR screening to determine homozygosity of the complemented line

A forward primer in the CaMV 35S promoter 5' ACGCACAATCCCACTATCC 3' and the *AtPNP-A* CLONING reverse primer, were used to amplify the T-DNA containing the 35S::*AtPNP-A* construct that had been introduced into the homozygous *atpnp-a* mutant line. The same PCR conditions as were used as those in the PCR amplification of the wildtype *AtPNP-A* gene (section 3.2.12.1) that were 1 mM $MgCl_2$ in the PCR reaction and 35 cycles of 1 min each for denaturation, annealing and elongation, except in this case the annealing temperature was dropped to 55°C as required for the CaMV 35S primer (Table 3.1).

3.2.15 Sequencing the T-DNA insertion site

The *AtPNP-A* SALK forward and T-DNA reverse primers (designed to isolate the homozygous SALK_000951 line) were used to PCR amplify left border of the T-DNA and flanking genomic DNA sequence from the homozygous *atpnp-a* mutant. The PCR product was then purified using the Wizzard kit, as described previously (section 3.2.13.2). The purified PCR product was sent for sequencing in both directions using the same primers as were amplified the product. The sequencing reaction was performed by Di James (University of Cape Town, South Africa) using the Big Dye terminator v3.1 Cycle Sequencing kit (Applied Biosystems, Foster City, USA). Each reaction was performed in a 10 µl volume containing 1.1 µl Terminator Premix, 2.9 µl Bioline Half Dye Mix (Bioline Ltd., London, UK), 50 ng of the purified PCR product and 1 µl of 5 µM primer. Amplification was performed on the GeneAmp PCR System 9700 (Applied Biosystems, Foster City, USA) with rapid thermal ramping using the cycling conditions: denaturation for 1 min at 96°C, followed by 25 cycles of 96°C for 10 s, 50°C for 20 s and 60°C for 4 min. The clean up and electrophoresis was then performed by the Core DNA Sequencing Facility at the University of Stellenbosch, South Africa, using the 3130 Genetic Analyser DNA Capillary Sequencer (Applied Biosystems, Foster City, USA). The DNAMAN program was used to align the sequences returned with each other and against the *AtPNP-A* gene sequence obtained from TAIR and T-DNA sequence provided by the SALK institute (http://signal.salk.edu/tdna_FAQs.html).

3.2.16 Resolving the annotation of the *AtPNP-A* gene

Primers spanning the putative second intron region were designed in order to resolve the annotation of the *AtPNP-A* gene. The *AtPNP-A* ANNOTATION forward primer 5' ACTTTGACAGAGCATGCACC 3' binds in exon 2 while the *AtPNP-A* ANNOTATION reverse primer 5' GAATCGAAGCGGATCTAACG 3' binds in the 3' untranslated region (UTR). The disputed fragment of the *AtPNP-A* gene was then PCR amplified from Col-0 genomic DNA. The PCR reaction was performed in a 20 µl volume including 1 X PCR buffer (provided with the enzyme), 3 mM $MgCl_2$, 0.125 mM dNTPs, 0.1 U/µl Super-Term Polymerase and 0.2 µM each of the forward and reverse primers. Cycling conditions were initial denaturation at 94°C for 5 min, followed by 40 cycles of 94°C denaturation for 15 sec, 60°C annealing for 30 sec and 72°C elongation for 1 min and concluded with a final extension step of 72°C for 10 min (Table 3.1). PCR products were analyzed by gel electrophoresis, as before.

3.2.17 Microscopic examination of leaves

From a tray of four week old *atpnp-a* mutant and wildtype plants, 7th and 8th rosette leaves of varying sizes were collected. Leaves were prepared by fixing them in 5% (v/v) glutaraldehyde in 100 mM $NaPO_4$ buffer pH 7.0 and were then sent to Dr Lara Reale (Universita di Perugia, Italy) for microscopic analysis. Here, samples were postfixed in 1% (w/v) osmium tetroxide (OsO_4) and then dehydrated in a graded ethanol. Samples were embedded in Epon resin (Epon, 2-dodecenylsuccinic anhydride and methylnadic anhydride mixture) (Loreto *et al.*, 2001). A preinclusion at room temperature in increasing concentrations of resin dissolved in propylene oxide was followed by the final inclusion in freshly prepared resin after which polymerization occurred at 35°C for 12 hrs, 45°C for 12 hrs and 60°C for 12 hrs (Loreto *et al.*, 2001). For the light microscopy semi-thin sections (1-2 μm) were cut with an ultramicrotome (Reichter, Heidelberg, Germany). Samples then were stained in toluidine blue and mounted in Eukitt for light microscopy observation. Photomicrographs were taken using a Lecia DMR HC photomicroscope (Lecia Microsystems, Heerbrugg, Switzerland). For the scanning electron microscopy, samples were treated as described previously until dehydration in the graded ethanol series, after which they were subjected to critical point drying in liquid CO_2, mounted on aluminium stubs, sputter coated with gold and then viewed with the Stereoscan 90B (Cambridge Instruments, Cambridge, UK). For measurements of cell size, light microscopy images were analysed using the Lecia QWin image analysis software (Lecia Microsystems, Heerbrugg, Switzerland) while the total leaf surface was calculated from digital photographs of the leaf obtained using a Nikon Coolpix 950 (Nikon, Tokyo, Japan) and calculated using the Image-Pro Plus image analysis software (Media Cybernetics, Carlsbad, CA).

3.2.18 Statistics

As described in chapter 2 (section 2.2.8).

3.2.19 Germination assays

Seeds were sterilized and vernalized as described in chapter 2 (section 2.2.2) and then sown on PN agar (0.6% w/v) supplemented with the indicated concentrations of NaCl, KCl and sorbitol (included in the media prior to autoclaving). In the case of ABA, PN agar was first autoclaved and the media allowed to cool before adding the appropriate volume of the 100 mM ABA to the final concentration of 1 μM. Seedlings were then grown for two weeks under standard conditions as described previously (section 2.2.4) after which time the number of seedlings (out of the 50 sown per plate) that had fully opened green cotyledons were counted. The number of seedlings that grew on media supplemented with NaCl, KCl or sorbitol was expressed relative to the number of seedlings that grew on control PN media.

3.2.20 Leaf water loss assay

Leaves at different developmental stages were detached from four week old soil grown plants. The FW of each leaf was measured immediately after detachment. Leaves were then placed on filter paper and allowed to dry. The weight of each leaf was then measured every hour thereafter. At each time point the leaf weight was expressed relative to its initial FW at the time of detachment (Verslues *et al.*, 2006).

3.2.21 Seedling growth

3.2.21.1 FW per seedling

Seedlings were germinated on PN media, or PN media supplemented with NaCl. All of the seedlings that grew successfully on a particular plate were removed and weighed. Their collective FW was divided by the number of seedlings that grew on that particular plate in order to attain a measure of the FW per seedling. For each line, the FW per seedling grown on NaCl is expressed relative to the FW per seedling grown on PN media. The data is the average for 10 plates per treatment.

3.2.21.2 Root elongation

Seedlings were germinated and grown horizontally on Petri dishes containing PN media or PN media supplemented with NaCl. The root length of each seedling that grew successfully was measured. The root length was averaged for each line taking in to account all of the seedlings that grew at a particular NaCl concentration. For the *AtPNP-A* wildtype line this was at least 16 seedlings per treatment while for the *atpnp-a* mutant line the minimum was 26 seedlings per treatment.

3.2.22 Stress tolerance of older plants

3.2.22.1 Watering with NaCl and sugar solutions

Plants were grown on soil for 3-4 weeks prior to treatment. Plants were treated with water (control), NaCl or iso-osmolar solutions of sorbitol or mannitol, by watering from above until soil was thoroughly drenched. This was repeated every two days for a week. Alternatively water was withheld for the drought treatment.

3.2.22.2 Leaf disc chlorophyll assay

Leaf discs were punched out of untreated leaves of four week old soil grown plants using the back end of a 200 μl yellow tip that fits a Gilson pipette. The leaf discs were then placed into 6 well microtitre plates containing solutions of either water (control), NaCl (100, 200 or 300 mM) or iso-osmolar mannitol (200, 400 or 600 mM) (Sanan-Mishra *et al.*, 2005). The leaf discs were suspended in these solutions for 48 hrs and incubated under the standard growth conditions. After this time the leaf discs were removed and patted dry on tissue paper and then collected into 1.5 ml eppendorf tubes. To extract chlorophyll, the leaf discs were homogenized in 100% acetone and then stored in the dark until the leaf tissue had completely bleached. The $OD_{661.6}$ and $OD_{644.8}$ of each of the solutions was measured on the Beckman DU 650 Spectrophotometer (Beckman Coulter, Inc., CA, USA). The total chlorophyll content was calculated using the equation Chlorophyll a+b = (7.05 X $OD_{661.6}$) + (18.09 X $OD_{644.8}$). The chlorophyll content of leaf discs treated with NaCl and mannitol solutions was expressed relative to the chlorophyll content of leaf discs treated with water.

3.2.23 Nutrient starvation

All seedlings were germinated vertically in Petri dishes on nutrient replete media [0.25 mM KH_2PO_4, 0.5 mM KOH, 0.75 mM $MgSO_4.7H_2O$, 0.025 mM $CaCl_2.2H_2O$, 0.1 mM FeNaEDTA, 2 mM $Ca(NO_3)_2.4H_2O$ and 2mM NH_4NO_3 with micronutrients (30 μM H_3BO_3, 10 μM $MnSO_4.4H_2O$, 1 μM $ZnSO_4.7H_2O$, 3 μM

$CuSO_4.5H_2O$ and 0.5 μM $Na_2MoO_4.2H_2O$)] for five days under constant light (100 μM photons m^{-2} s^{-1}). Nutrient starvation was induced by transferring five day old seedlings on to media that lacked K, N or P. The K deficient media is exactly the same as the nutrient replete media except that the KH_2PO_4 and KOH were substituted with 0.27 mM $Ca(H_2PO_4)_2$. The N deficient media is exactly the same as the nutrient replete media except the $Ca(NO_3)_2.4H_2O$ and NH_4NO_3 were replaced with 4 mM $CaSO_4.H_2O$. Similarly, the P deficient media is the same as the nutrient replete media except the KH_2PO_4 was replaced with 0.13 mM K_2SO_4. Recipes were kindly provided by Dr John Hammond (Warwick HRI, University of Warwick, UK) (Hammond *et al.*, 2003; Hermans *et al.*, 2006). After transfer on to the nutrient deficient media, seedlings were grown horizontally for a further seven days after which time the root length was used as a measure of stress tolerance. The root length of seedlings grown on the nutrient deficient media was expressed relative to the root length of seedlings grown on nutrient replete media.

3.2.24 Ion accumulation

Seedlings were grown for two weeks on PN agar (0.6% w/v) in Petri dishes under constant light (100 μM photons m^{-2} s^{-1}). Seedlings were then gently removed using forceps. About 250 seedlings were weighed (approximately 700 mg of tissue) prior to being placed into 6 well microtitre plates containing 2 ml each of fresh liquid PN media. The seedlings were allowed to equilibrate for 30 min after which time they were treated with 100 mM NaCl made up as a double strength solution in the same liquid PN media for either 30 min or 24 hrs. Seedlings were harvested by removing them from the treatment solution and patted dry on absorbent tissue paper. The samples were then oven dried at 60°C. The Na^+ and K^+ content of each sample was analyzed using inductively coupled plasma mass spectrometry (ICP-MS) by Dr Andreas Späth (University of Cape Town, South Africa). Samples were first ashed and then acid digested (le Roex *et al.*, 2001). Briefly, 10-50 mg of material was dissolved in a 3:1 HF/HNO_3 acid mixture in a sealed savilex beaker on a hot plate at 60°C for 48 hrs. Thereafter the samples were dried. The samples were then mixed with 2 ml concentrated HNO_3 solution and allowed to evaporate. This last step was repeated. Finally the sample was taken up in 5% HNO3 containing 10 parts per million (ppm) of internal standards - Rh, In, Re and Bi. The Na^+ and K^+ content of each of the sample was then measured in ppm using a Perkin-Elmer ELAN 6000 ICP-MS (Perkin-Elmer, Massachusetts, USA). The Na^+ and K^+ contents were divided by the FW per sample in order to attain the ppm/mg measures indicated in the graphs.

3.2.25 Ion flux measurements

Arabidopsis seedlings were grown for one week on half strength MS media (Ducefa, Haarlem, The Netherlands) containing 1% (w/v) sucrose and 0.35% Phytagel (SIGMA Aldrich, St Louis, USA) at 22°C under a 16 hr light (100 μM photons m^{-2} s^{-1}) 8 hr dark cycle. Ion flux measurements were performed by René Bastian (University of Western Cape, South Africa) and Prof. Sergey Shabala (University of Tasmania, Australia) using non-invasive ion-selective vibrating microelectrodes (MIFE, University of Tasmania, Hobart, Australia) as described previously (Demidchik *et al.*, 2007; Shabala *et al.*, 2005a; Shabala *et al.*, 2006; Shabala and Newman, 1999; Shabala and Shabala, 2002; Shabala and Lew, 2002; Shabala *et al.*, 1997).

Microelectrodes were pulled from borosilicate glass capilliaries (GC150-10, Clark Electromedical Instruments, Pangbourne, UK), oven dried and salinised with tributylchlorsilane. After backfilling, electrodes were filled with commercially available K^+ ionophore cocktail (Cat No. 60031, Fluka, Busch, Switzerland). The electrodes were calibrated before and after use with known standards and those that gave a response less than 50 mV per decade and correlation less than 0.999 discarded. The electrodes were then mounted on a manipulator for 3D positioning (MMT5, Narishige, Tokyo, Japan).

Excised roots of seven day old *Arabidopsis* seedlings were mounted horizontally in a Perspex holder using agar, then placed into the measuring chamber and immersed in the basic measuring solution (BMS) (0.5 mM KCl and 0.1 mM $CaCl_2$, pH 5.5, unbuffered). The chamber was placed on a three-way hydraulic manipulator driven by a computer-controlled stepper motor (MHW-3 Narishige, Tokyo, Japan) and left to equilibrate for 40-50 min.

Electrodes were positioned 20 μm above the root surface. During measurements the electrodes were moved between 20 and 50 μm from the tissue surface at a frequency of 0.1 Hz in a 10 s square wave manner. Measurements were taken for 5 min prior to treatment to ensure steady state basal levels. NaCl was then added as a double strength solutions (made up in BMS) to a final concentration of 100 mM and measurements of transient K^+ fluxes recorded for 50 min thereafter. In a second experiment inhibition of the NaCl-induced K^+ efflux by 1 mM Zn^{2+} (pre-treatment for 30 min) was examined. The recorded potential differences were converted to electrochemical potential differences using the calibrated Nernst slopes of the electrodes and the ion fluxes calculated using the microelectrode ion flux estimation (MIFE) software as described previously (Newman, 2001).

3.2.26 *B. cinerea* infection

Spores were harvested 10–14 days after subculture by adding 3 ml of sterile dH_2O to the Petri dish containing the infected apricot and then gently rubbing the spores with a sterile glass rod until the water appeared cloudy. The concentration of spore suspension was determined by counting on a haemocytometer. The spore suspension was then adjusted to 5 X 10^4 spores/ml made up in half strength (v/v) sterile grape juice (Liquifruit, South Africa). Leaves of four week old plants were detached and placed on to 0.8% (w/v) agar plates. The upper leaf surface was inoculated with 5 μl of the spore suspension or half strength grape juice (control) (Denby *et al.*, 2004). Lesion sizes that developed over the following three days were measured.

3.2.27 *P. syringae* infection

A single colony of *Pst* or *Pst AvrB* was picked from KB agar (1.5% w/v) plates, inoculated into KB liquid media supplemented with appropriate antibiotics and incubated shaking at 28°C overnight. The following day cells were harvested by centrifugation at 10 000 X *g* for 30 s in a bench top centrifuge (Heraeus Biofuge Pico, Kendro Laboratory Products, Germany). The cell pellet was washed once with 10 mM $MgCl_2$ before resuspension in 10 mM $MgCl_2$. The OD_{600} was measured using the Beckman DU 650

Spectrophotometer (Beckman Coulter, Inc., CA, USA) and adjusted to 0.2 that corresponds to a bacterial titre of approximately 1 X 10^8 colony forming units (cfu)/ml (Katagiri *et al.*, 2002).

3.2.27.1 Pressure inoculation

The 1 X 10^8 cfu/ml suspension was diluted 1:100 in 10 mM $MgCl_2$ so that 1 X 10^6 cfu/ml was used to infect plants. Leaves of four week old plants were pressure infiltrated with 10 mM $MgCl_2$ (control) or 1 X 10^6 cfu/ml of either *Pst* or *Pst AvrB* using a 1 ml syringe gently applied to the underside of the leaf until the entire leaf appeared water soaked (Cao *et al.*, 1994). Excess solution was removed using tissue paper after which the plants were covered in clingfilm to aid the infection process. Three leaf discs per plant were harvested 4 hrs (day 0), 24 hrs, 48 hrs or 72 hrs after infection. These leaf discs were homogenized in 1 ml of 10 mM $MgCl_2$, then diluted 1:10 serially after which 10 μl of each dilution was plated on KB agar (1.5% w/v) supplemented with 50 μg/ml rifampicin. These bacterial plates were incubated for 2-3 days at 28°C until colonies formed. The number of colonies that grew was recorded along with the appropriate dilution factor.

3.2.27.2 Spray inoculation

For the spray experiment 1 X 10^8 cfu/ml containing 0.05% (v/v) Silwet L-77 (Melotto *et al.*, 2006) was spray inoculated onto four week old plants ensuring that the leaves were evenly coated with the solution. Again the infected plants were covered with cligfilm to aid the infection process. Leaf discs were collected 4 hrs (day 0), 24 hrs, 48 hrs or 72 hrs after infection. To remove surface bacterial that had not successfully infiltrated the plant, the leaf discs were floated in 70% (v/v) EtOH for 30 s followed by dH_2O for 30 s, patted dry and then placed into 1.5 ml eppendorf tubes containing 10 mM MgCl (Zipfel *et al.*, 2004). The leaf discs were then processed as described above (section 3.2.27.1).

3.2.28 *H. parasitica* infection

Arabidopsis seedlings were grown in MS agar (7.5% w/v) (SIGMA Aldrich; St Louis, USA) containing 3% (w/v) sucrose on Petri dishes for two weeks after which time they were transplanted to soil and grown for one week further. Conidiospores were harvested by placing infected plants into eppendorf tubes containing 1 ml water and then vortexing. The spore suspension was recovered and then counted on a haemocytometer. This was then adjusted to 5 X 10^4 spores/ml and four drops of 2 μl were applied to four leaves per plant. Infected plants were grown in sealed transparent plastic containers at 16°C (under the same conditions as described in section 3.2.2.5) for seven days until spores emerged. Infection was quantified by counting the number of sporangiophores per leaf on both the abaxial and adaxial surfaces, under a dissecting microscope (Warren *et al.*, 1998). For heavily infected leaves the maximal number of sporangiophores counted was 20. Infected leaves were then photographed under the dissecting microscope at 4 X magnification.

3.3 RESULTS

3.3.1 Identification of a T-DNA insertion line

At the onset of this investigation, the SALK database (http://signal.salk.edu/cgi-bin/tdnaexpress) was queried with the *AtPNP-A* (At2g18660) gene sequence and one match was returned. This corresponded to a SALK T-DNA insertion line: SALK_000951 (Alonso *et al.*, 2003). The SALK institute sequenced the region of the *Arabidopsis* genome that flanks the T-DNA insertion and used this to predict that the T-DNA lies within the *AtPNP-A* gene. The SALK sequence aligns with the *AtPNP-A* gene, 36 base pair (bp) upstream from the TGA STOP codon (Figure 3.1). This falls within the second intron of the *AtPNP-A* gene. According to the SALK institute, the T-DNA insertion could lie within 300 bp of this site due to possible errors in the sequencing data (http://signal.salk.edu/tdna_FAQs.html). Immediately it was apparent that the TAIR annotation of the *AtPNP-A* gene (www.arabidopsis.org) (Rhee *et al.*, 2003) used by SALK was different from that published by Ludidi (Ludidi *et al.*, 2002). Ludidi reported that the *AtPNP-A* gene is comprised of two exons and one intron, with exon 2 read through one additional bp before terminating in a TAA STOP codon. If this is true, then the T-DNA insertion is predicted to lie 85 bp downstream of this STOP codon.

3.3.2 Isolation of homozygous wildtype and mutant SALK lines

Segregating T_3 SALK_000951 seed was acquired from the Nottingham Arabidopsis Stock Centre (NASC) (Scholl *et al.*, 2000). Initially the seed was planted on soil and allowed to self fertilize in order to bulk up the seed. This generated 12 parental lines which could then be screened for the presence of the T-DNA insertion. The T-DNA insertion contains within its sequence the *NPT II* marker gene that confers resistance to kanamycin (Kan) (Alonso *et al.*, 2003). All the seed was Kan sensitive however making it impossible to use Kan to screen the segregating SALK_000951 seed. A PCR based approach was therefore employed. Primers were designed to distinguish between wildtype and mutant chromosomes (Ostergaard and Yanofsky, 2004). Gene-specific primers that lie on either side of the T-DNA insertion should only amplify the wildtype chromosome (Figure 3.2). This is because the T-DNA insertion in the mutant chromosome is approximately 6000 bp and therefore too large to PCR amplify across. Instead, a primer within the T-DNA left border was designed to produce a product with the gene-specific forward primer in the mutant chromosome. Two separate PCRs (one with gene-specific forward and reverse primers and the other with the gene-specific forward and T-DNA reverse primers) were performed in order to determine whether individuals were heterozygous or homozygous mutant or homozygous wildtype. Initially four T_4 progeny from each of the 12 parental lines were screened using this method. One of these lines was identified as being potentially homozygous for the T-DNA insertion. Homozygosity was confirmed in the following generation (T_5) through PCR screening of 20 progeny (Figure 3.3).

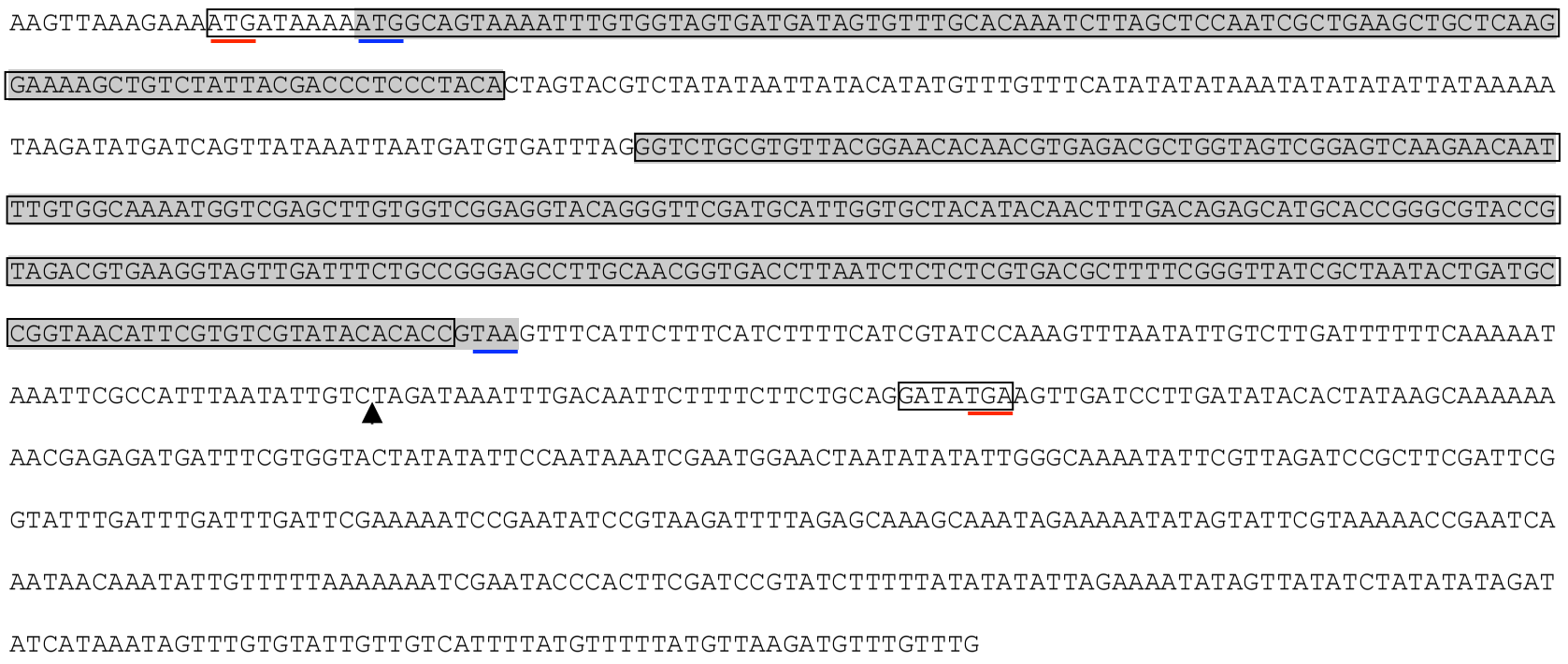

Figure 3.1. *AtPNP-A* gene structure and the predicted site of T-DNA insertion in the SALK_000951 line

The *AtPNP-A* gene sequence was downloaded from TAIR. TAIR annotates the *AtPNP-A* gene as having the START and STOP codons underlined in red and the three exons outlined in boxes that would encode a protein of 130 aa. The TAIR annotation differs from that reported by Ludidi (Ludidi *et al.*, 2002) who predicts that exon 2 is read through one additional bp before terminating in a STOP codon. The exons predicted by Ludidi are highlighted in grey and the START and STOP codons are underlined in blue. This would produce a protein of 126 aa. The T-DNA insertion is predicted to lie 36 bp upstream from the TGA STOP codon annotated by TAIR and 85 bp downstream of the TAA STOP codon predicted by Ludidi, as indicated by the arrow.

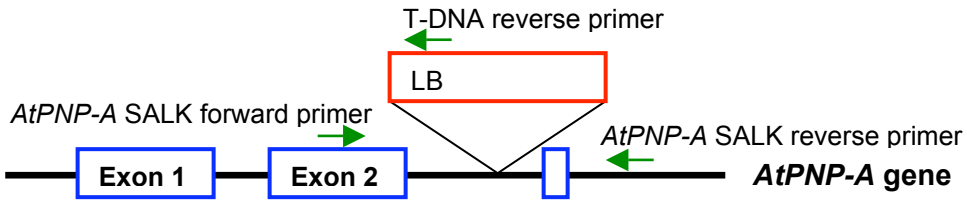

Figure 3.2. Primer design for PCR screening of the segregating SALK_000951 line based on the predicted site of T-DNA insertion

Exons as annotated by TAIR, are depicted by the blue boxes while the predicted site of the T-DNA insertion is shown by the red box with LB indicating the left border of the T-DNA. Primers are represented by the green arrows. The presence of the T-DNA insertion would be reported by a positive PCR result with the *AtPNP-A* SALK forward and T-DNA reverse primers while the wildtype copy of the *AtPNP-A* gene would be amplified by the *AtPNP-A* SALK forward and *AtPNP-A* SALK reverse primers.

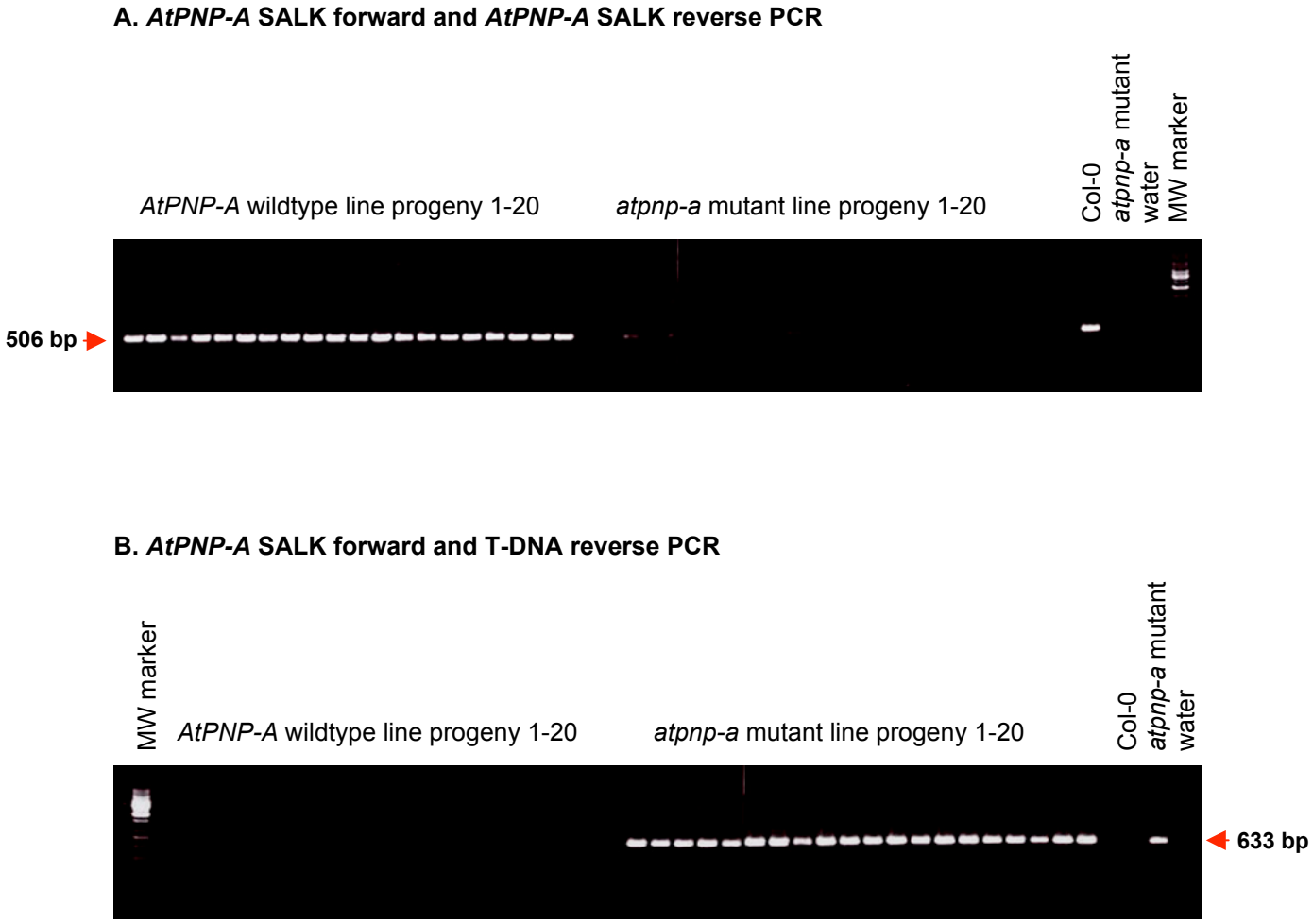

Figure 3.3. PCR screening confirmed homozygosity of the wildtype and *atpnp-a* mutant SALK_000951 lines

Twenty progeny of putative *AtPNP-A* wildtype and *atpnp-a* mutant lines were screened by PCR in order to confirm that they were homozygous. The gene specific *AtPNP-A* SALK forward and *AtPNP-A* SALK reverse primers confirmed the presence of the wildtype copy of the gene in all 20 progeny of the *AtPNP-A* wildtype line (A), while there was no product in any of the progeny of the *atpnp-a* mutant line. The *AtPNP-A* SALK forward primer and T-DNA reverse primer reported the presence of the T-DNA insertion in all twenty progeny of the *atpnp-a* mutant line (B), while there was no product in any of the progeny from the *AtPNP-A* wildtype line. The MW marker indicated is the Fermentas 1 kb gene ladder. The predicted PCR product sizes are indicated by the arrows. Controls were Col-0 DNA as a positive control for the wildtype copy of the gene; DNA from the parent of the *atpnp-a* mutant line as a positive control for the presence of the T-DNA insertion and water as a negative control for both PCRs.

The same technique was used to isolate a homozygous wildtype line. Care was taken to isolate the wildtype line from the background of SALK T-DNA mutagenized seed since it has been established that approximately 50% of the SALK lines carry more than one T-DNA insertion (Alonso *et al.*, 2003). This wildtype line should be segregating for any additional T-DNA insertions and second site mutations that may exist within the *atpnp-a* mutant line. These may quickly segregate out. Importantly however the ecotype of the wildtype and mutant lines is exactly the same, as even Col-0 passaged through several generations in the lab will change. This isolation procedure was performed twice. While the separately isolated mutant lines carry the same mutation in the *AtPNP-A* gene they should be segregating differently for any additional T-DNA insertions and second site mutations. The majority of phenotypes have been tested in both sets of wildtype and mutant lines and are essentially identical.

3.3.3 Kanamycin silencing in the wildtype and mutant SALK lines

Kan sensitivity of the SALK seed was probably the result of silencing of the Kan gene (*NPT II*) in the SALK_000951 line. Approximately 20% of the SALK lines have been reported to be Kan silenced (Ostergaard and Yanofsky, 2004). This is thought to occur over successive generations and more frequently when there are multiple copies of the T-DNA (either at a single site or at distinct sites). The homozygous wildtype and *atpnp-a* mutant lines are indeed Kan silenced because primers specific to the *NPT II* gene amplified products in both lines demonstrating that they do contain the gene for Kan resistance despite not displaying the Kan resistant phenotype (Figure 3.4). This result furthermore showed that the *AtPNP-A* wildtype line contains at least one additional T-DNA insertion at a discrete site since it still carries the marker gene for the T-DNA even though it does not contain a T-DNA insertion in the *AtPNP-A* gene.

3.3.4 *AtPNP-A* expression in the wildtype and mutant SALK lines

It was necessary to determine the expression of *AtPNP-A* in the homozygous SALK_000951 mutant in order to establish whether the T-DNA insertion has any affect on the transcription of *AtPNP-A*. The homozygous SALK_000951 line had lower, but not completely reduced *AtPNP-A* mRNA levels, as determined by both semi-quantitative RT-PCR and Northern blot analysis (Figure 3.5). There is still residual *AtPNP-A* expression in the homozygous SALK_000951 line and therefore it is a knock-down rather than a null mutant.

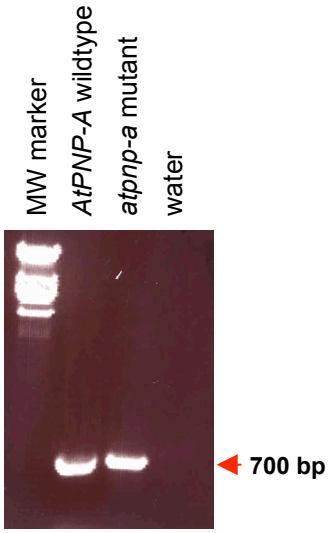

Figure 3.4. Kan silencing in the homozygous wildtype and *atpnp-a* mutant SALK_000951 lines

The homozygous wildtype and *atpnp-a* mutant lines both tested positive for the presence of the *NPT II* marker gene that is contained within the SALK T-DNA sequence and confers resistance to kanamycin (Kan). Neither line displays Kan resistance therefore the *NPT II* gene has been silenced in these lines. The predicted *NPT II* PCR product size is indicated by the arrow. The MW marker is λ DNA digested with *Pst I* and water is the negative control for the PCR.

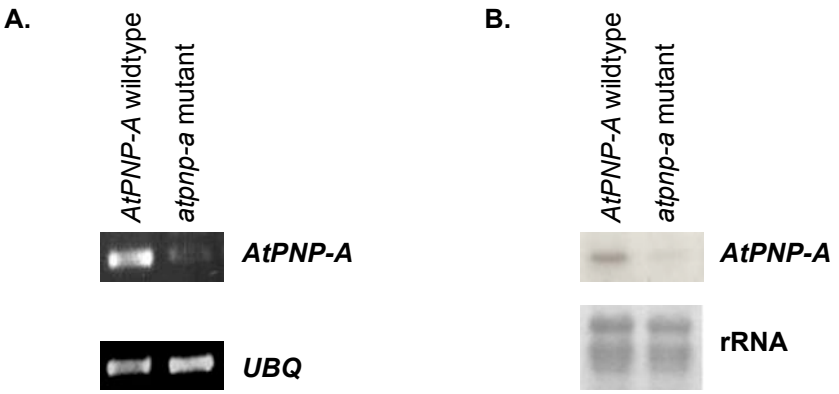

Figure 3.5. *AtPNP-A* expression in the wildtype and *atpnp-a* mutant SALK_000951 lines

Expression of *AtPNP-A* was examined using semi-quantitative RT-PCR (A) and Northern blot analysis (B). Wildtype and *atpnp-a* mutant lines were untreated and so these results show basal *AtPNP-A* expression levels. Primers that bind in exon 1 (*AtPNP-A* RT forward) and exon 2 (*AtPNP-A* RT reverse) of the *AtPNP-A* gene were used for the semi-quantitative RT-PCR amplification (A, upper panel). *UBQ* was the "housekeeping" gene used as a control to show that each sample had similar amounts of template (A, lower panel). The *AtPNP-A* CLONING primers used to PCR amplify *AtPNP-A* from cDNA template and this was used as the probe in the Northern blot analysis. The probe was labelled through random priming with radioactive α-[^{32}P]dCTP. Hybridization of the *AtPNP-A* probe to the membrane was visualized following exposure of the membrane to X-ray film (B, upper panel). The membrane was stained with methylene blue prior to Northern blot analysis in order to show that there had been equal loading and transfer of the RNA samples (B, lower panel).

3.3.5 Complementation of the *atpnp-a* mutant

At the time when the SALK_000951 line was characterized, there were no other mutants in the *AtPNP-A* gene available and so it was not possible to confirm phenotypes in two independent insertion lines (Ostergaard and Yanofsky, 2004). Therefore an attempt was made to complement the *atpnp-a* mutant with a wildtype copy of the *AtPNP-A* gene. This was necessary in order to confirm that any phenotype observed in the SALK_000951 line was the result of the mutation in the *AtPNP-A* gene and not caused by a second site mutation in the background of the SALK line. The wildtype *AtPNP-A* gene sequence was amplified from genomic DNA using primers that encompass the START and STOP codons predicted by Ludidi and cloned into the pSMB binary plasmid under the control of the constitutive CaMV 35S promoter (Ludidi *et al.*, 2002; Mylne and Botella, 1998). This construct was transformed into the homozygous *atpnp-a* mutant. Contained within the borders of this second T-DNA was the BASTA resistance gene, conferring resistance to the herbicide BASTA and the antibiotic PPT. Transformants were screened on media supplemented with PPT. Resistant individuals were selfed and their progeny screened until two independent lines that were 100% PPT resistant were obtained. Twenty progeny of each of these independent lines were then screened by PCR using a forward primer within the CaMV 35S promoter and a reverse primer in the *AtPNP-A* gene to confirm that these two lines were homozygous for the overexpression construct (Figure 3.6).

3.3.6 *AtPNP-A* expression in the homozygous complemented lines

Expression of *AtPNP-A* was examined in the complemented lines in order to test whether the overexpression construct had reverted *AtPNP-A* expression back to wildtype levels. Semi-quantitative RT-PCR revealed that the *atpnp-a* mutant had lower *AtPNP-A* mRNA levels than the wildtype line, as previously demonstrated. However both complementation lines showed *AtPNP-A* expression levels similar to those seen in the *atpnp-a* mutant with neither showing the expected overexpression of *AtPNP-A* (Figure 3.7). The overexpression construct therefore did not appear to be expressed nor complement the *atpnp-a* mutant. This suggests that the transgene either could not be expressed, for example if it lacked important regulatory elements, or that the transgene was silenced. It is unlikely though that silencing would occur at multiple locations, an issue which could have been addressed if more transgenics had been recovered, however it was only possible to obtain two homozygous complemented lines.

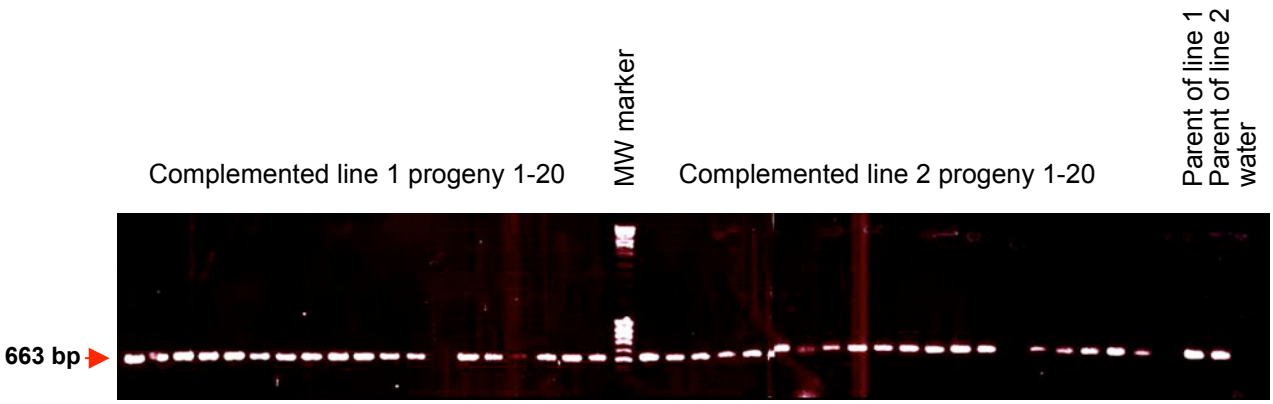

Figure 3.6. PCR screening to confirm homozygosity of two independent complemented lines

Two independently isolated complemented lines were thought to be homozygous for the overexpression construct (T-DNA containing the BASTA resistance gene and a wildtype copy of the *AtPNP-A* gene under the control of the CaMV 35S promoter) because both lines were 100% resistant to phosphinothricin (PPT). Homozygosity of complemented lines was confirmed by PCR screening using a forward primer that binds in the CaMV 35S promoter and the reverse primer used in cloning the *AtPNP-A* gene. For each of the complemented lines 19 out of 20 progeny tested positive for the PCR product indicating that they contained the overexpression construct. Both of these lines were determined to be homozygous for the overexpression construct. The predicted size of the PCR product is indicated by the arrow. The DNA from the parents of each of the complemented lines was used as positive controls for the PCR while water was used as a negative control. The MW marker is the 1 kb ladder from Fermetas.

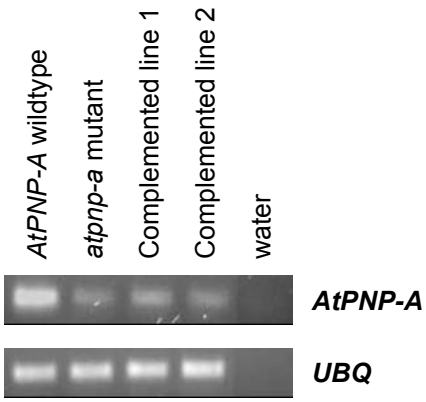

Figure 3.7. Expression of *AtPNP-A* in two independent complemented lines homozygous for the overexpression construct.

Semi-quantitative RT-PCR, described previously, was used to examine *AtPNP-A* expression (upper panel) in the two independent lines that were homozygous for the overexpression construct in order to test whether this construct had complemented the expression of *AtPNP-A* in the *atpnp-a* mutant. *UBQ* was the "housekeeping" gene used as a control to show that the amount of template in each PCR reaction was comparable (lower panel). The complemented lines had similar levels of *AtPNP-A* expression as that seen in the *atpnp-a* mutant.

3.3.7 Sequencing of the T-DNA insertion site in the *AtPNP-A* gene

In order to determine the site of the T-DNA insertion in the *AtPNP-A* gene, the PCR product from the gene-specific (*AtPNP-A* SALK) forward and T-DNA reverse primers (used in screening the segregating SALK_000951 line) was sequenced. Sequencing was performed using both primers and sequence information obtained from both directions. The sequence of the PCR product was then aligned with the *AtPNP-A* gene sequence as well as with the T-DNA sequence which was downloaded from SALK. The actual position of the T-DNA insertion (where the two alignments meet) was determined to be 6-8 bp upstream from the TAIR predicted TGA STOP codon (Figure 3.8). This two bp discrepancy exists because coincidentally the last two bps of the PCR product sequence that align with the T-DNA are the same as the last two bps that align with the *AtPNP-A* gene sequence making it impossible to ascertain from where those two bps actually derive. Therefore sequencing the site of T-DNA insertion confirmed that, according to the TAIR annotation, the T-DNA lies within the second intron of the *AtPNP-A* gene.

3.3.8 Resolving the annotation of the *AtPNP-A* gene

It was necessary to resolve whether the annotation of the *AtPNP-A* gene reported by TAIR or Ludidi (Ludidi *et al.*, 2002) is correct in order to be able to say conclusively whether the T-DNA insertion lies in the second intron of the *AtPNP-A* gene or whether it lies downstream of the TAA STOP codon. Both the TGA STOP codon annotated by TAIR and the TAA STOP codon predicted by Ludidi have AATAAA polyadenylation signals situated approximately 60 bp downstream from either STOP site and therefore there could be alternatively spliced products of the *AtPNP-A* gene. Primers designed to amplify across the putative second intron, were used in a RT-PCR with Col-0 cDNA as a template (Figure 3.9). Products corresponding to the expected sizes predicted by both TAIR (second intron excised) and Ludidi (Ludidi *et al.*, 2002) were present suggesting that both scenarios may be true (Figure 3.10). The lower band that corresponds to the size predicted by TAIR was far more abundant than the faint upper band and thus the major cDNA product is that predicted by TAIR. The larger product which corresponds to the size predicted by Ludidi would be indistinguishable from product formed as a result of genomic DNA contamination (Ludidi *et al.*, 2002). It was therefore necessary to rule out the possibility that the larger product was not the result of genomic DNA contamination in the RNA sample. For this reason a RNA control was included where no reverse transcriptase ("no RT") was added to the cDNA reaction. This produced a positive result for the upper band, indicating genomic DNA contamination in the "no RT" RNA control (Figure 3.10). This suggested that the upper band in the cDNA was also the result of genomic DNA contamination; however does not exclude the possibility that there may still be some product corresponding to the alternatively spliced mRNA predicted by Ludidi (Ludidi *et al.*, 2002).

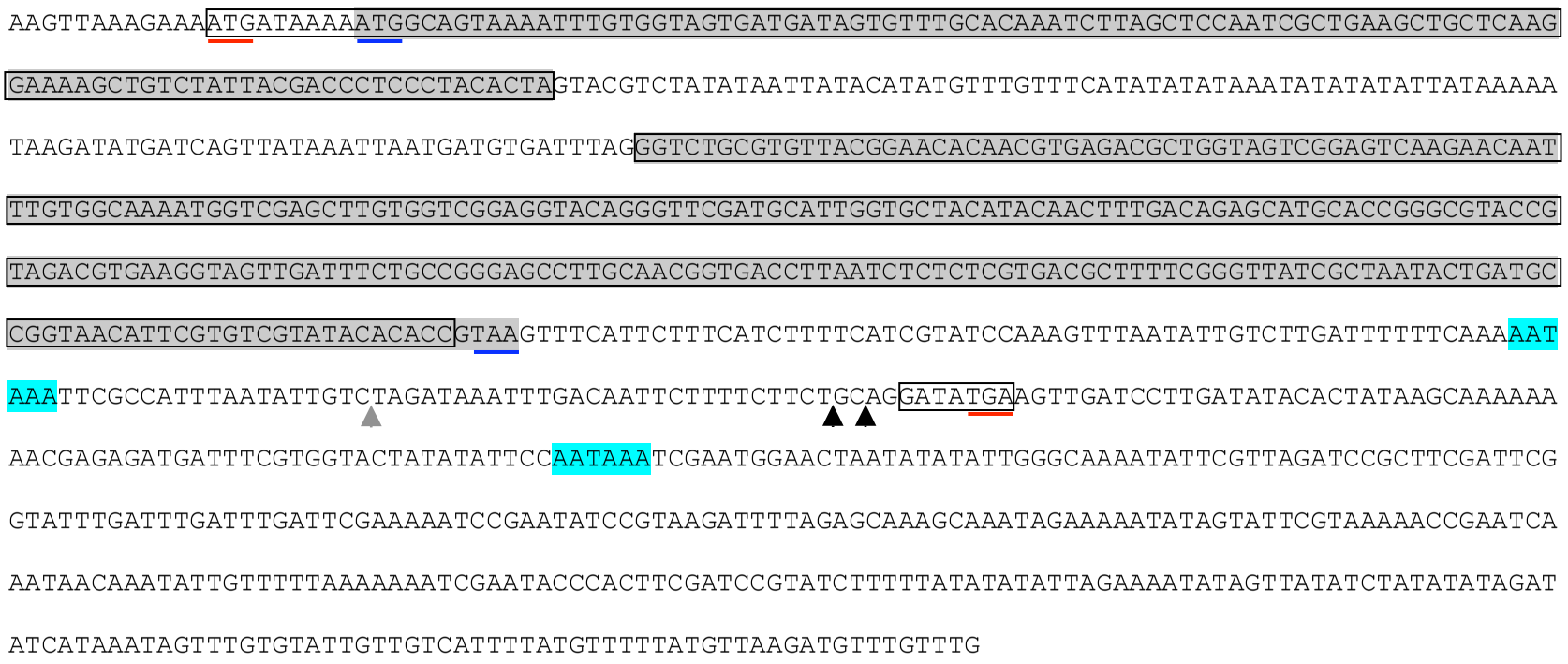

Figure 3.8. Determination of the site of T-DNA insertion in the *atpnp-a* mutant line

The PCR product obtained using the *AtPNP-A* SALK forward primer and the T-DNA reverse primers, was sequenced. The sequence obtained was aligned with the *AtPNP-A* gene sequence and the T-DNA sequence and the actual site of the T-DNA insertion determined to be 6-8 bp upstream from the TAIR annotated TGA STOP codon or 114–116 bp downstream from the TAA STOP codon predicted by Ludidi (Ludidi *et al.*, 2002), as indicated by the two black arrows. The predicted site of T-DNA insertion is shown by the grey arrow. Depending on the annotation of the *AtPNP-A* gene, the T-DNA insertion could either lie in the second intron or downstream of the TAA STOP codon. Both STOP codons have putative polyadenylation signals approximately 60 bp downstream of each STOP site (highlighted in turquoise), making both options possible and suggesting that the *AtPNP-A* gene may be alternately spliced.

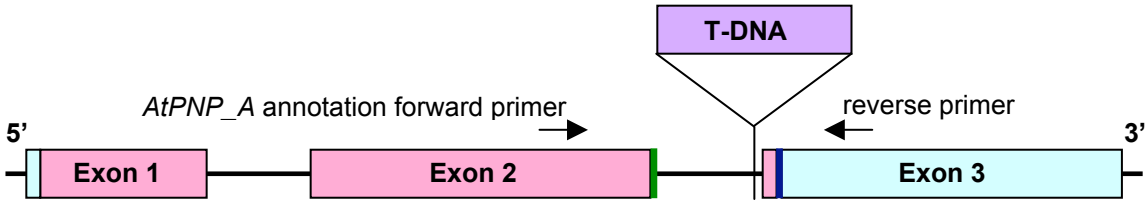

Figure 3.9. Primer design to resolve the annotation of the *AtPNP-A* gene

Schematic representation of the *AtPNP-A* gene showing the exon regions in the boxes of which the coding sequences are depicted in pink and the UTR regions in light blue, according to the TAIR annotation of the *AtPNP-A* gene. The STOP codon predicted by Ludidi is shown in green (Ludidi *et al.*, 2002) while the STOP codon predicted by TAIR is indicated in dark blue. The sequenced site of T-DNA insertion is just upstream of TAIR exon 3 which codes only for one additional aa before terminating in a STOP codon. Primers designed to resolve the annotation of the *AtPNP-A* gene are represented by the arrows. The *AtPNP-A* ANNOTATION forward primer binds in exon 2 while the *AtPNP-A* ANNOTATION reverse primer binds in the 3'UTR annotated by TAIR to span the disputed second intron region. Should the annotation of the *AtPNP-A* gene published on TAIR be correct then the primers are expected to amplify a product of 284 bp from cDNA due to the removal of the second intron from the mRNA. However if Ludidi and colleages are correct and the *AtPNP-A* ANNOTATION reverse primer would either lie downstream of the polyA tail in which case it would not bind or produce a product from the cDNA or the reverse primer would lie in the 3'UTR in which case the primers would amplify a larger product of 405 bp from the cDNA owing to the fact that no intron sequence has been spliced out.

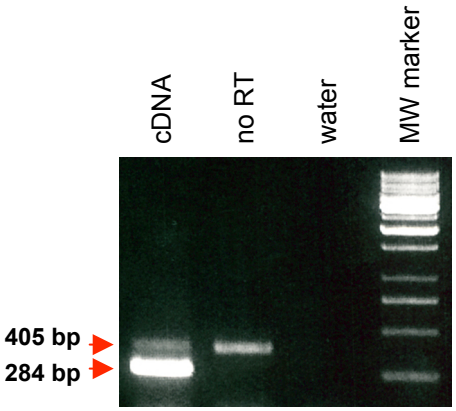

Figure 3.10. Annotation of the *AtPNP-A* gene

Primers that flank the putative second intron of the *AtPNP-A* gene (refer to Figure 3.9) were used in an attempt to resolve whether the annotation of the *AtPNP-A* gene published on TAIR or that reported by Ludidi (Ludidi *et al.*, 2002) is correct. Product obtained from RT-PCR using Col-0 cDNA as a template corresponded to the sizes predicted should both TAIR and Ludidi be correct. TAIR predicts that the intron would be removed to produce a band at 284 bp, while there is no second intron should Ludidi and colleagues be correct and the resultant band would be 405 bp, as indicated by the arrows. It should be noted that RNA was not treated with DNase prior to cDNA synthesis. Since the product predicted by Ludidi would be indistinguishable from genomic DNA (gDNA) contamination, a RNA control was included where the reverse transcriptase enzyme was excluded from the cDNA reaction (no RT). The larger product obtained when this was used as a template in the PCR reaction, indicates gDNA contamination in the RNA. Water was used as a negative control for the PCR and the MW marker is the 1 kb ladder from Fermentas.

The homozygous wildtype and *atpnp-a* mutant lines were screened for altered growth, abiotic and biotic stress response phenotypes that might imply function of the wildtype *AtPNP-A* gene.

3.3.9 Morphology

The *AtPNP-A* gene shows sequence homology to expansins which are cell-wall loosening agents involved in plant growth and development (Cosgrove, 2000b; Ludidi *et al.*, 2002; Sampedro and Cosgrove, 2005). AtPNP-A does not exhibit expansin activity (pers. comm. C. Gehring) however it has been shown to induce protoplast swelling and in this way may act in concert with expansins to provide the turgor pressure necessary for expansion growth (Morse *et al.*, 2004). In order to test this hypothesis, an examination of growth and development was undertaken in the *atpnp-a* mutant.

3.3.9.1 Gross morphology

On the gross morphological scale there are no obvious phenotypic differences between the *atpnp-a* mutant and wildtype lines grown on PN media in Petri dishes or in soil under standard growth conditions (Figure 3.11).

3.3.9.2 Cell size and number and stomatal phenotypes

Leaves of the *atpnp-a* mutant were examined more closely using light and scanning electron microscopy (SEM) (kindly analyzed by Dr Lara Reale, Universita di Perugia, Italy). At first glance, it was apparent that the *atpnp-a* mutant differs from the wildtype in terms of its cell size and stomatal numbers. These phenotypes were clearly visible from light microscopy images of toluidine blue stained sections and from SEM photographs (Figure 3.12). For both the *atpnp-a* mutant and wildtype line a selection of 7th and 8th rosette leaves were collected from a number of plants. For each line the selection of leaves could be divided into two groups: small developing leaves that were approximately 92 mm^2, and large fully developed leaves that were approximately 208mm^2 in size. The *atpnp-a* mutant differs from the wildtype in that it has smaller cell sizes but greater cell numbers in the upper and lower epidermis of its small, developing leaves (Figure 3.13). While the same trend was observed in both the epidermal layers, the differences in cell size and number between the *atpnp-a* mutant and wildtype lines were only significant ($p < 0.05$) in the lower epidermis. There were no differences in the cell sizes or cell numbers of the large, fully expanded leaves of the *atpnp-a* mutant and wildtype lines. Despite a tendency for the large fully developed leaves of the *atpnp-a* mutant to have more stomata per unit leaf area when compared to the wildtype line, this difference was not statistically significant. However the *atpnp-a* mutant did have significantly ($p < 0.05$) smaller stomatal apertures under standard growth conditions than the wildtype plants (Figure 3.14).

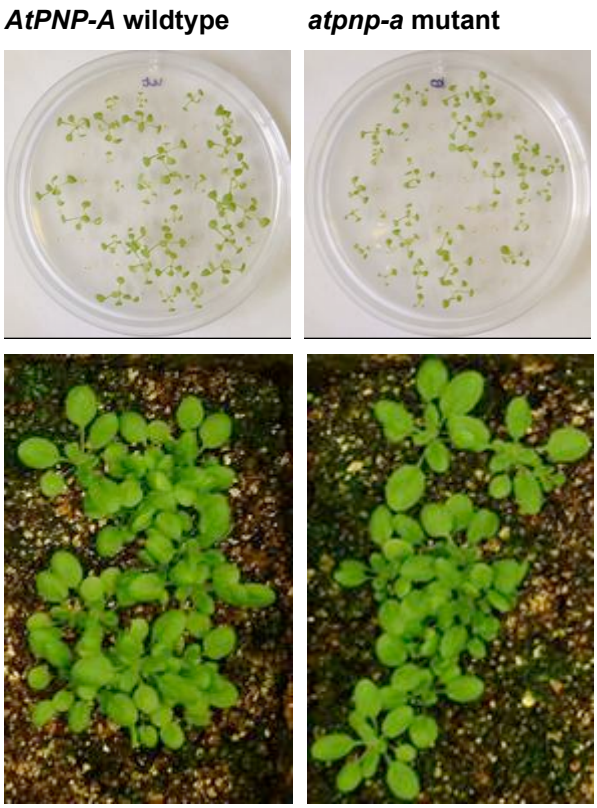

Figure 3.11. Gross morphology of the *atpnp-a* mutant and wildtype lines

Representative photographs of *atpnp-a* mutant and wildtype lines grown in plates on PN media for two weeks (upper panel) or grown on soil for four weeks (lower panel) under standard conditions. There were no obvious phenotypic differences in the *atpnp-a* mutant and wildtype lines.

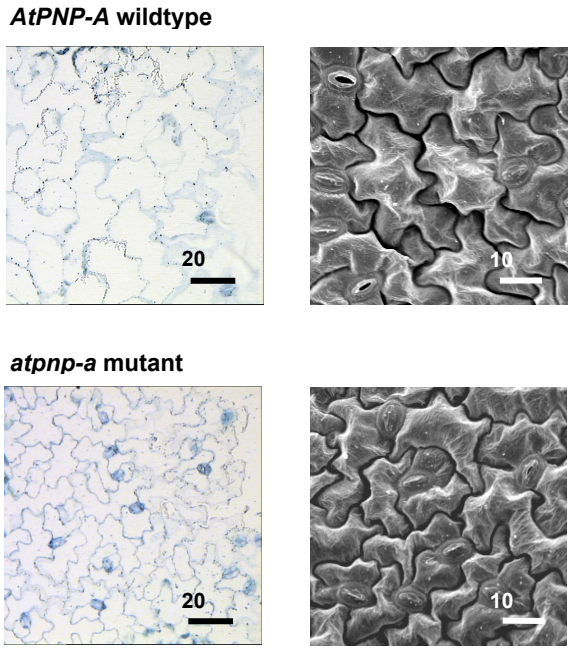

Figure 3.12. Representative images of the upper epidermis of the *atpnp-a* mutant and wildtype lines
Toluidine blue stained light microscopy (left hand panel) and scanning electron microscopy (SEM) (right hand panel) images of the upper epidermis of the *AtPNP-A* wildtype (upper panels) and *atpnp-a* mutant (lower panels). It is clear from the photographs of the toluidine blue stained sections that the *atpnp-a* mutant has smaller cell sizes and greater stomatal numbers when compared to the wildtype. Smaller stomatal apertures of the *atpnp-a* mutant when compared to the wildtype are apparent from the photographs taken by SEM.

3.13 A.

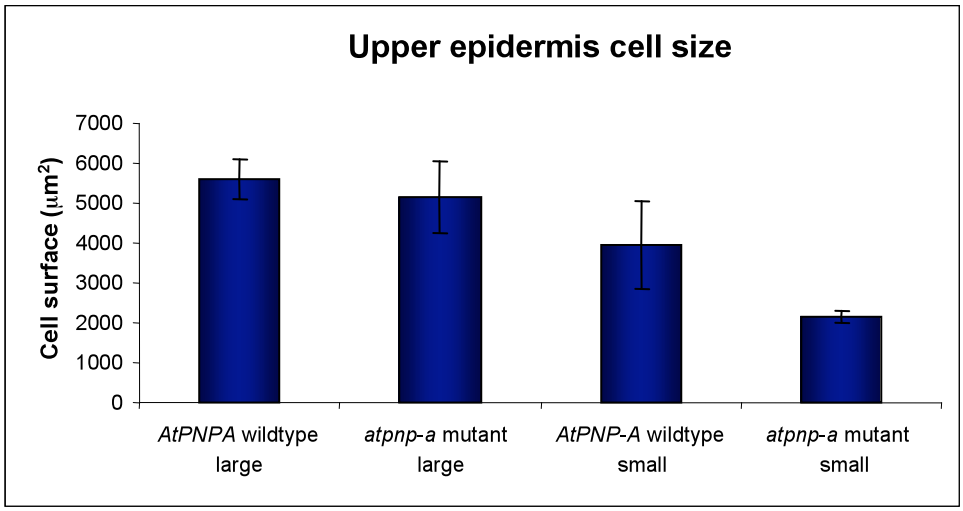
Upper epidermis cell size
Cell surface (µm²)
7000
6000
5000
4000
3000
2000
1000
0
AtPNPA wildtype large
atpnp-a mutant large
AtPNP-A wildtype small
atpnp-a mutant small

B.

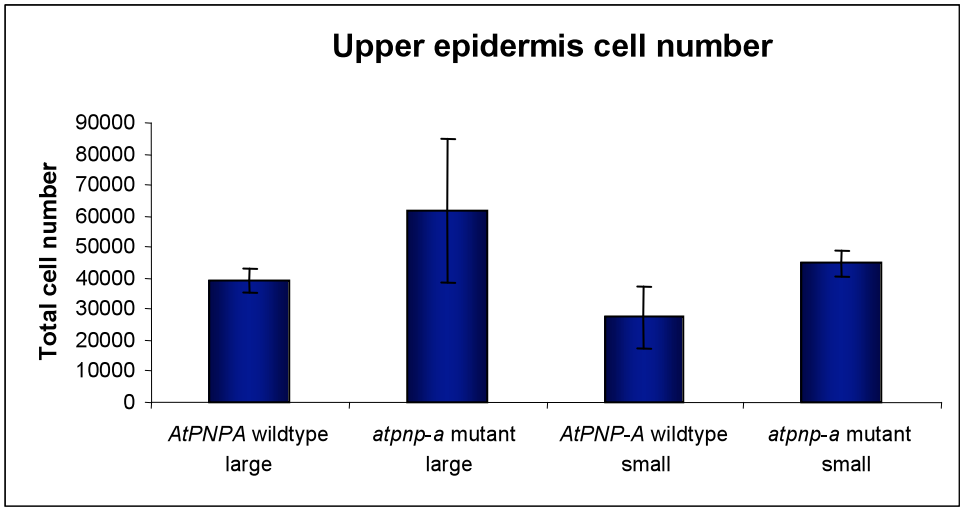
Upper epidermis cell number
Total cell number
90000
80000
70000
60000
50000
40000
30000
20000
10000
0
AtPNPA wildtype large
atpnp-a mutant large
AtPNP-A wildtype small
atpnp-a mutant small

C.

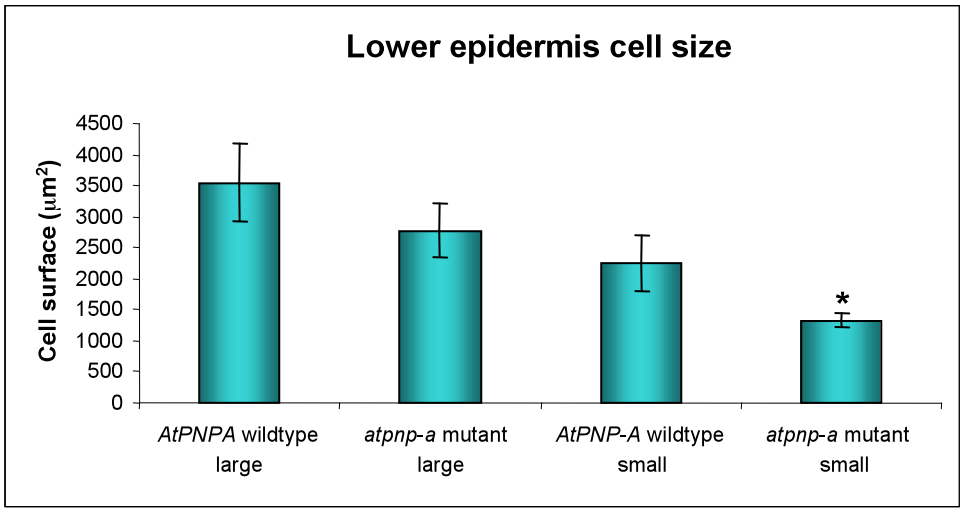

D.

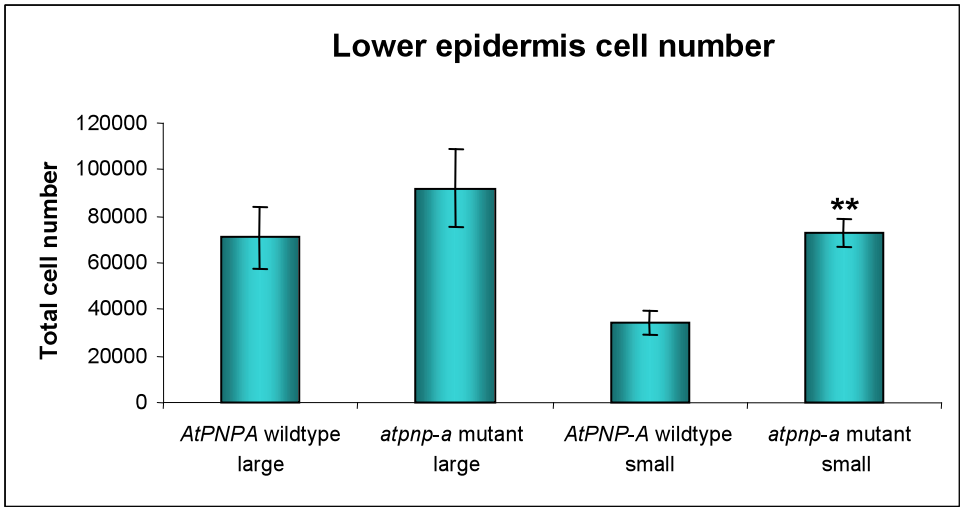

Figure 3.13. Upper and lower epidermal cell sizes and cell numbers of the wildtype and *atpnp-a* mutant lines

The small, developing leaves (approximately 92 mm^2) of the *atpnp-a* mutant have smaller cell surface size (A) and greater cell numbers (B) in the upper epidermis than those of the wildtype line. The same was true for the lower epidermis with the *atpnp-a* mutant having smaller cell sizes (C) and greater cell numbers (D) than the wildtype line. The differences were statistically significant for the lower epidermis but not for the upper epidermis, with * denoting $p < 0.05$ and ** $p < 0.01$ as calculated using a Mann-Whitney U test. There were no differences between the *atpnp-a* mutant and wildtype lines in terms of cell size or number in either epidermal layer of the large, fully developed leaves (approximately 208 mm^2). At least four measurements were recorded per leaf and the data represent the mean value for a minimum of five leaves. Error bars are standard errors of the mean.

A.

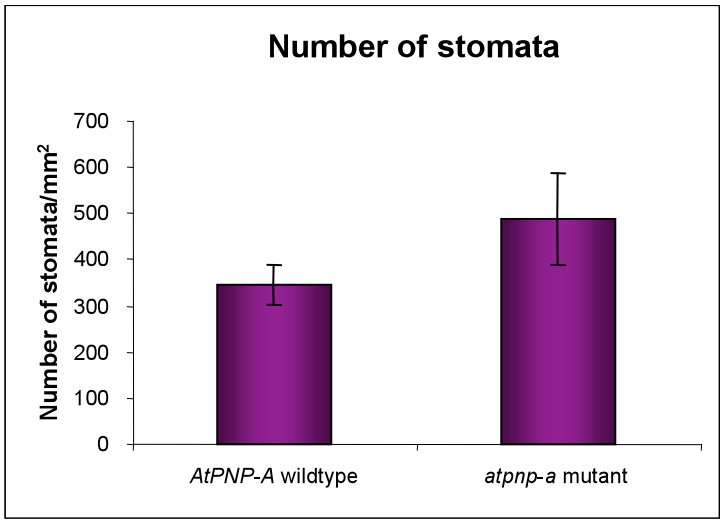

B.

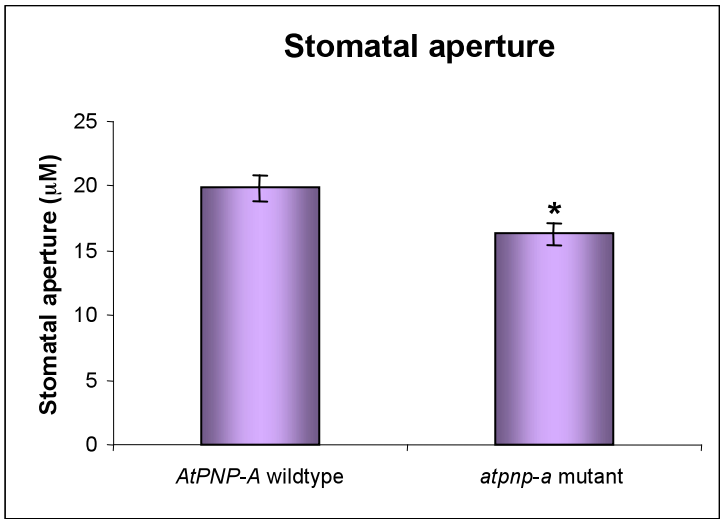

Figure 3.14. Stomatal numbers and apertures of the *atpnp-a* mutant and wildtype lines

Stomatal numbers (A) and apertures (B) were measured in the fully developed (large) *atpnp-a* mutant and wildtype leaves under standard growth conditions. Stomata in the upper epidermis were considered in this analysis. The *atpnp-a* mutant has greater stomatal numbers than the wildtype line. These stomatal numbers are the mean values of at least four individual leaves. Stomatal apertures are the mean values of at least ten measurements and error bars are standard errors of the mean. The *atpnp-a* mutant has smaller stomatal apertures than the wildtype line and this was statistically significant with * denoting a p value of < 0.05 as determined using a t test.

3.3.10 NaCl and Osmotic stress phenotypes

Extractable irPNP protein levels increase after treatment with NaCl and even more so with iso-osmolar sorbitol treatment which might suggest that irPNPs are involved in the response to these stresses (Rafudeen *et al.*, 2003). For this reason NaCl and osmotic stress responses were examined in the *atpnp-a* mutant.

3.3.10.1 Germination responses

Firstly, a germination assay was performed in order to determine whether the *atpnp-a* mutant has altered germination efficiency on media containing various salts and sugars that impose different ionic and osmotic stresses on the seed and seedling after it has germinated. Since calcium can affect NaCl tolerance, it was ensured that the levels of Ca^{2+} (2 mM) used in the basal media were not limiting (Liu and Zhu, 1997; Shabala *et al.*, 2006). Sucrose was also excluded from the media as it imposes an additional osmotic stress and interferes with ABA signalling (Verslues *et al.*, 2006). Germination was considered to be successful when seedlings developed fully expanded green cotyledons (Gao *et al.*, 2006). Representative pictures from two independent experiments are shown in Figure 3.15 and 3.16. NaCl, KCl and sorbitol all reduced germination efficiency in the wildtype line as expected (Quesada *et al.*, 2000; Saleki *et al.*, 1993; Werner and Finkelstein, 1995). Specifically, NaCl reduced germination efficiency across all concentrations tested; KCl was inhibitory at concentrations greater than 50 mM while sorbitol only significantly inhibited germination at 300 mM, the highest concentration tested (Figure 3.17). KCl did not inhibit germination to a greater extent than NaCl as has been reported (Saleki *et al.*, 1993). Rather NaCl and KCl inhibited germination similarly. Comparatively, sorbitol imposed less inhibition on germination than iso-osmolar concentrations of NaCl or KCl in agreement with published reports that ionic stress is more toxic than osmotic stress during germination (Saleki *et al.*, 1993; Werner and Finkelstein, 1995). The *atpnp-a* mutant was more tolerant than the wildtype line of NaCl, KCl and sorbitol in the germination media. In the case of sorbitol, this is less apparent from the photographs however the *atpnp-a* mutant was better able to develop fully expanded leaves and longer roots that translated to significantly greater gains in FW, compared to the wildtype (Fgure 3.17C). In conclusion the *atpnp-a* mutant is more tolerant of both ionic and osmotic stresses imposed at germination.

3.3.10.2 ABA responses

The majority of mutants more tolerant of NaCl and osmotic stress during germination are affected in ABA signalling since ABA inhibits germination under these unfavourable conditions (Gonzalez-Guzman *et al.*, 2002). It was therefore necessary to look at ABA responses in the *atpnp-a* mutant. There are two types of ABA mutant phenotypes – ABA insensitive (*abi*) and ABA deficient (*aba*) (Verslues *et al.*, 2006). ABA sensitivity was tested in a germination assay.

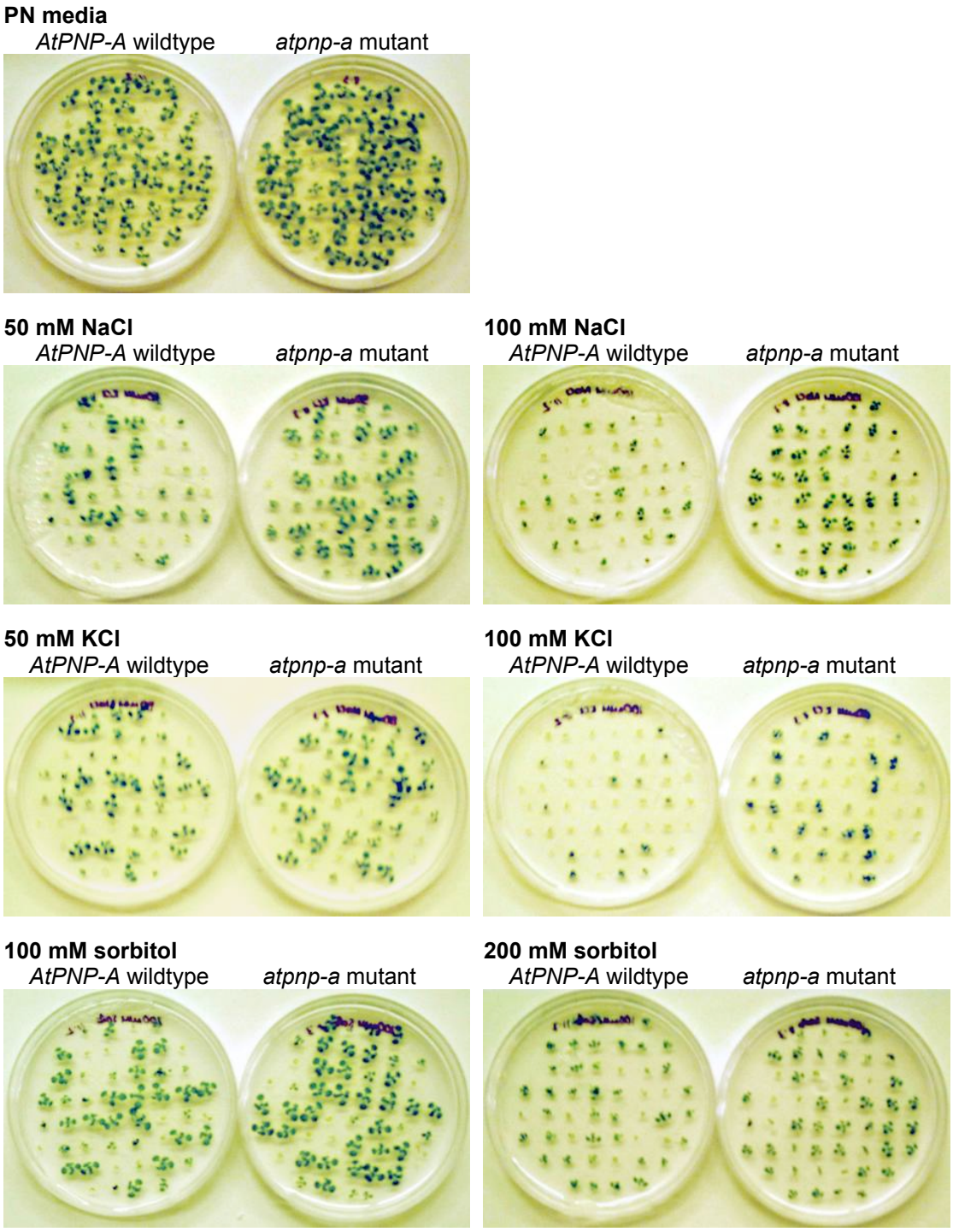

Figure 3.15. Representative photographs of *atpnp-a* mutant and wildtype lines after two weeks growth on NaCl, KCl and sorbitol-supplemented media.

The wildtype (left) and *atpnp-a* mutant (right) are shown alongside each other, following germination on 50 or 100 mM NaCl (top panel, left and right respectively), 50 or 100 mM KCl (middle panel, left and right) or isoosmolar 100 or 200 mM sorbitol (bottom panel, left and right). PN media was the basal media and control for this experiment (extreme top panel). 50 seedlings were planted per plate.

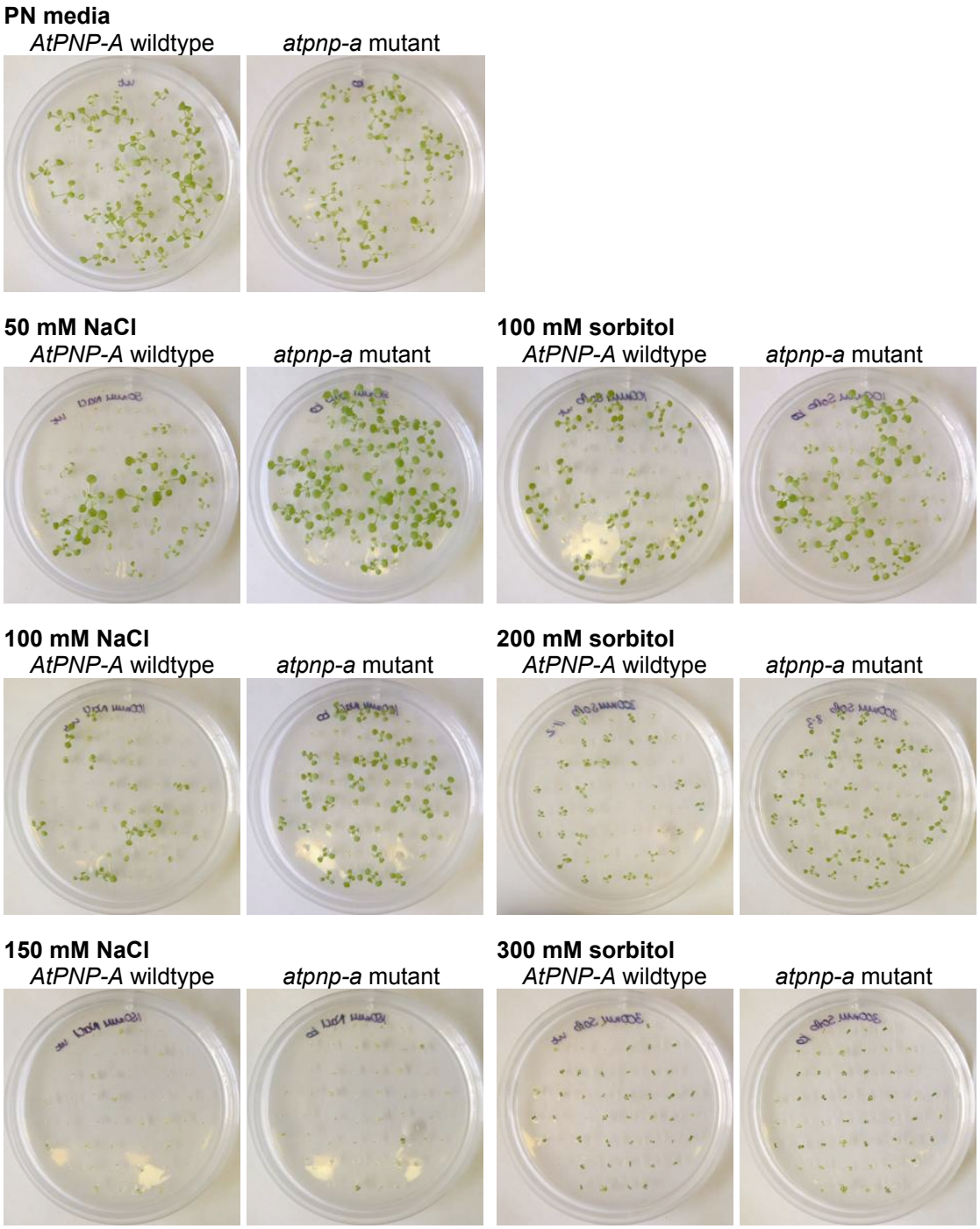

Figure 3.16. Duplicate experiment examining germination of the wildtype and *atpnp-a* mutant lines on NaCl and sorbitol-supplemented media

Second set of representative photographs of wildtype and *atpnp-a* mutant lines germinated on PN media (control, extreme top) supplemented with varying strengths of NaCl and isoosmolar sorbitol (below). The *AtPNP-A* wildtype (left) and *atpnp-a* mutant (right) lines are shown alongside each other for ease of comparison on 50 mM NaCl and isoosmolar 100 mM sorbitol (top panel); 100 mM NaCl and 200 mM sorbitol (middle panel) and 150 mM NaCl and 300 mM sorbitol (bottom panel). 50 seedlings were planted per plate and photographs were taken two weeks after planting.

3.17 A.

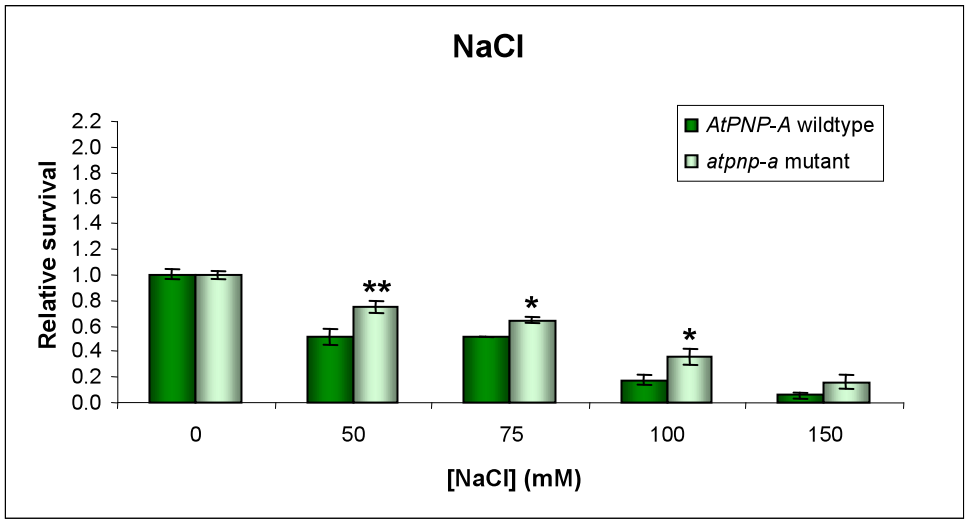
NaCl
AtPNP-A wildtype
atpnp-a mutant
Relative survival
2.2
2.0
1.8
1.6
1.4
1.2
1.0
0.8
0.6
0.4
0.2
0.0
**
*
*
0
50
75
100
150
[NaCl] (mM)

B.

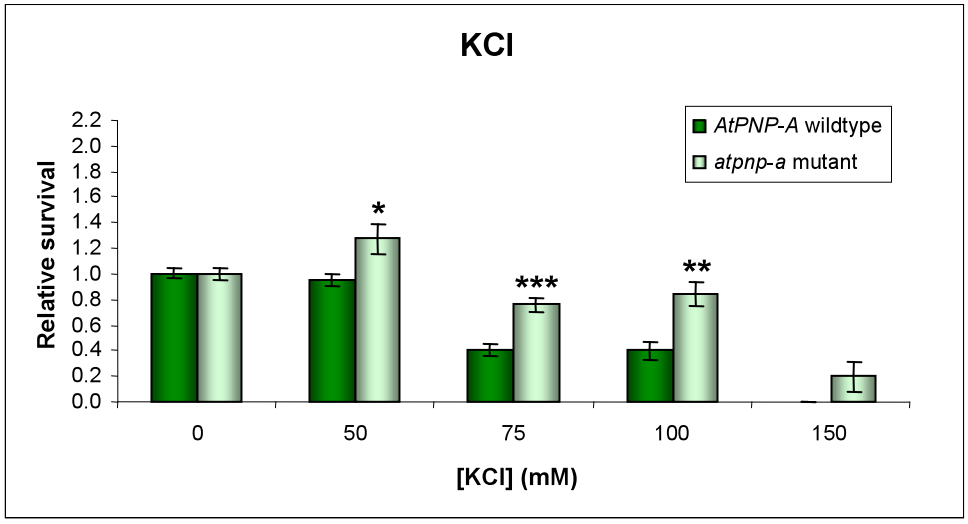
KCl
AtPNP-A wildtype
atpnp-a mutant
Relative survival
2.2
2.0
1.8
1.6
1.4
1.2
1.0
0.8
0.6
0.4
0.2
0.0
*
***
**
0
50
75
100
150
[KCl] (mM)

C.

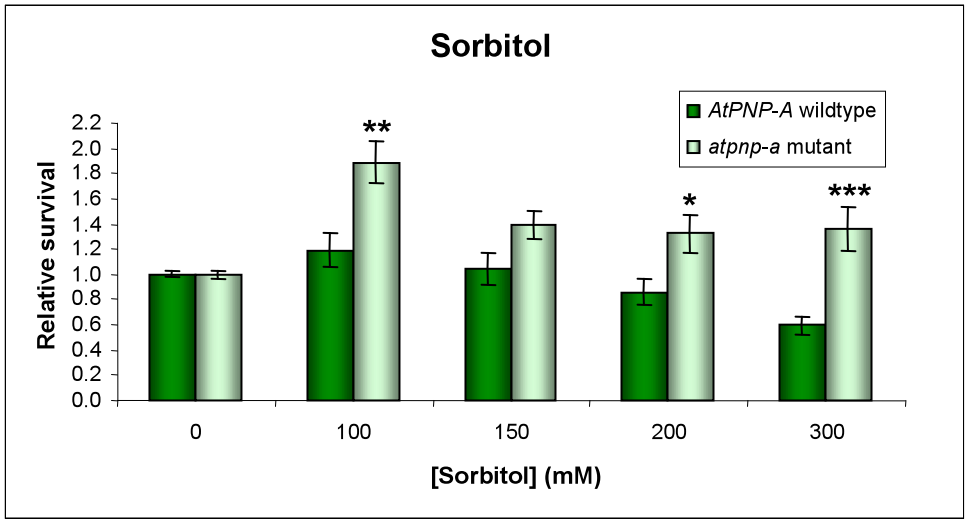
Sorbitol
AtPNP-A wildtype
atpnp-a mutant
Relative survival
2.2
2.0
1.8
1.6
1.4
1.2
1.0
0.8
0.6
0.4
0.2
0.0
**
*
***
0
100
150
200
300
[Sorbitol] (mM)

Figure 3.17. Germination efficiency of the *atpnp-a* mutant and wildtype lines on NaCl, KCl and sorbitol-supplemented media

Germination of the *atpnp-a* mutant and wildtype lines on NaCl, KCl and sorbitol relative to germination on basal media was analyzed two weeks after planting. 50 seedlings were planted per plate. Data are the mean values for several (n) plates. For the NaCl germination assay n = 21 for 0, 50 and 100 mM while n = 2 for 75 mM and n = 11 for 150 mM. For the KCl germination assay n = 7 for 0, 50, 75 and 100 mM while n = 2 for 150 mM. For the sorbitol germination assay n = 11 for 0, 100 and 200 mM while n = 7 for 150 mM and n = 10 for 300 mM. Error bars are standard errors of the mean. Statistically significant differences between the *atpnp-a* mutant and wildtype lines are represented by * for $p < 0.05$; ** for $p < 0.01$ and *** for $p < 0.001$ as determined using a t test.

Wildtype seeds germinated on media supplemented with 1 μM ABA showed radical emergence after two weeks but did not produce fully open green cotyledons or true leaves, as expected (Barrero *et al.*, 2005; Xiong *et al.*, 2002a). The *atpnp-a* mutant was not significantly different from the wildtype in its germination on ABA-supplemented media and therefore is not ABA insensitive (Figure 3.18). To test whether the *atpnp-a* mutant is ABA deficient a leaf water loss assay was performed (Ruggiero *et al.*, 2004; Verslues *et al.*, 2006). This assay measures water loss from a detached leaf as it undergoes dehydration to determine whether ABA is made in response to water deficit stress imposed at later stages in development and identifies both *abi* and *aba* mutants. ABA mutants show altered rates of water loss because ABA regulates stomatal closure under these conditions. Approximately 40–50% water loss was recorded over a 6 hr period in the *AtPNP-A* wildtype line, as expected (Figure 3.19) (Verslues *et al.*, 2006). Despite the stomatal phenotype of the *atpnp-a* mutant, it was not significantly different from the wildtype in the rate of water loss from its dehydrating leaves, suggesting that the *atpnp-a* mutant is not affected in ABA-mediated stomatal closure in response to dehydration. Furthermore ABA mutants are generally stunted and display wilty phenotypes, neither of which are attributes belonging to the *atpnp-a* mutant (Ruggiero *et al.*, 2004; Werner and Finkelstein, 1995). Altogether these results suggest that the *atpnp-a* mutant is not affected in ABA signalling.

3.3.10.3 Seedling responses

Sensitivity to NaCl and osmotic stresses varies depending on developmental stage (Gao *et al.*, 2003) and tissue type (Kiegle *et al.*, 2000; Kim *et al.*, 2007). Most mutants that are tolerant of NaCl and osmotic stress during germination aren't tolerant of these stresses later in development (Quesada *et al.*, 2000; Saleki *et al.*, 1993; Werner and Finkelstein, 1995). The inhibitory effect of NaCl on seedling growth was therefore examined in the wildtype and *atpnp-a* mutant lines to determine whether the *atpnp-a* mutant is more tolerant of NaCl stress at later stages of development. Following germination on NaCl, FW was used as a measure of NaCl tolerance of the seedling (Quesada *et al.*, 2000; Ruggiero *et al.*, 2004), while inhibition of root elongation was used as a measure of NaCl tolerance of the root (Rus *et al.*, 2001; Wu *et al.*, 1996a). NaCl stress significantly inhibited growth in the wildtype line, both in terms of gain in FW (at 50 and 100 mM) and root elongation (at concentrations greater than 50 mM) (Figure 3.20). Thus NaCl stress imposes greater inhibition on shoot growth than on root growth, as expected (Munns, 2002). The *atpnp-a* mutant showed reduced growth inhibition in response to NaCl in terms of gain in seedling FW compared to the wildtype. This was significant ($p < 0.05$) at 50 mM but not at 100 mM. However the *atpnp-a* mutant did not show a significant difference in root elongation growth in the presence of NaCl compared to the wildtype line (Figure 3. 20B). Since the majority of the seedling FW is contributed by the shoot tissue it appears that the *atpnp-a* mutant is more tolerant of NaCl stress at the seedling stage in the shoot but not in the root.

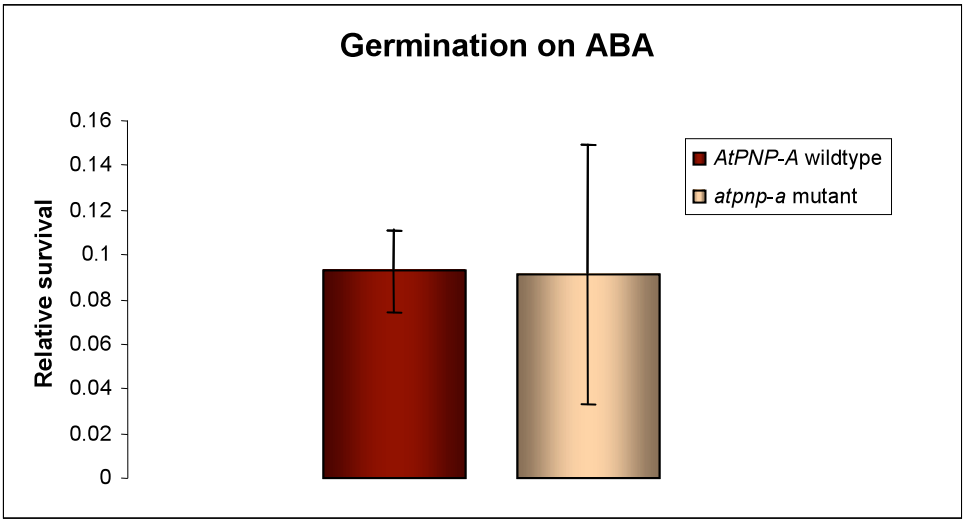

Figure 3.18. Germination of the wildtype and *atpnp-a* mutant lines on PN media supplemented with ABA

Germination assay showing survival of the *atpnp-a* mutant and wildtype lines on 1 μM ABA after two weeks, relative to their survival on PN media. Seedlings were determined to have survived if they developed fully expanded green cotyledons. 25 seeds were sown per plate. Error bars are standard errors of the mean.

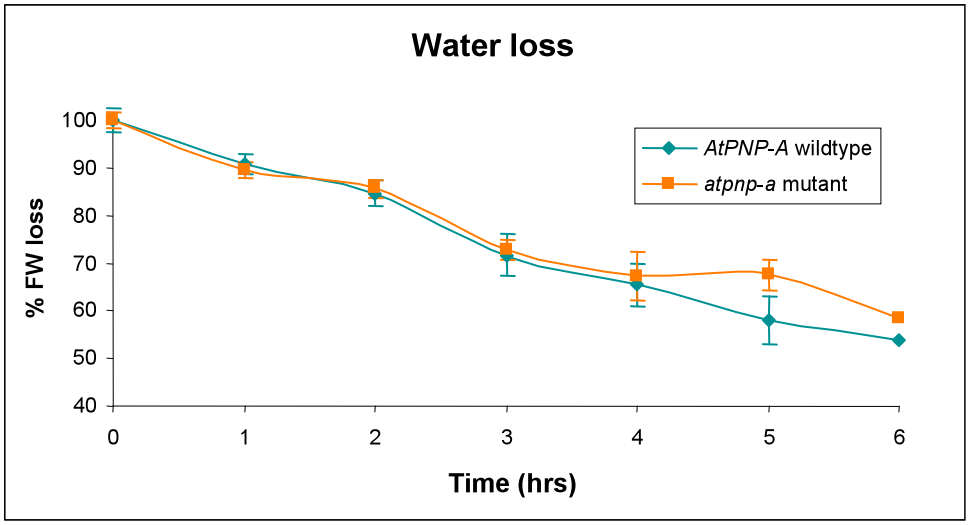

Figure 3.19. Leaf water loss assay to measure ABA-mediated stomatal closure in response to water deficit stress

Leaves were removed from the *atpnp-a* mutant and wildtype plants that had been grown on soil for four weeks. Loss of FW over time was used as a measure of water loss from the detached leaves that were undergoing water deficit stress. For each line n = 12 and error bars are standard errors of the mean. There was no significant difference between the *atpnp-a* mutant and wildtype lines.

A.

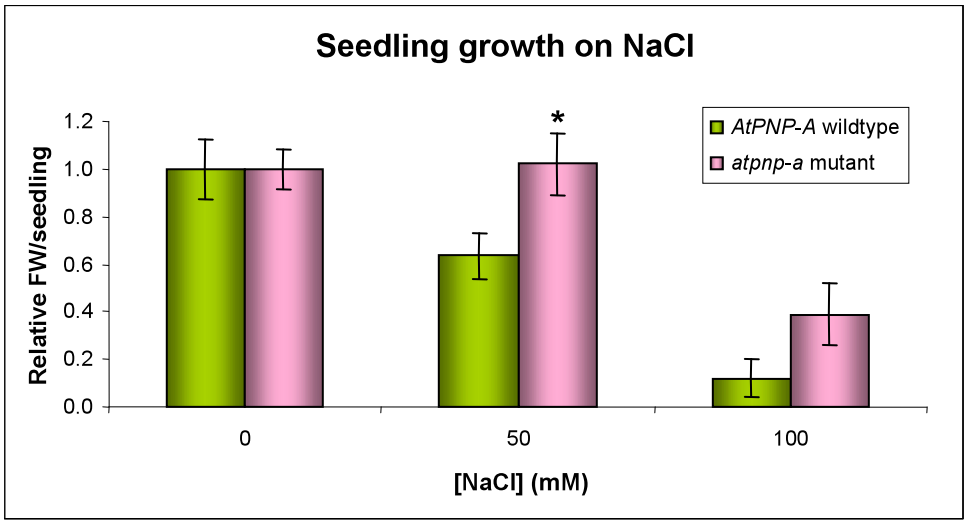

B.

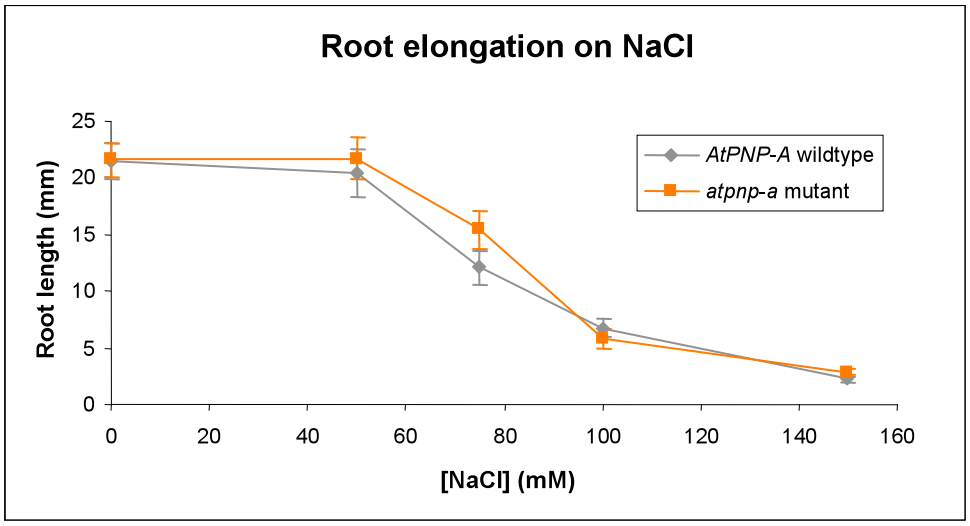

Figure 3.20. Seedling growth and root elongation on NaCl-supplemented media

The FW per seedling is determined by dividing the FW of all the seedlings by the number of seedlings that germinated per plate, after two weeks growth on NaCl-supplemented media (A). Data is the mean for n = 10 plates and error bars are standard errors of the mean. Statistical differences between the *atpnp-a* mutant and wildtype was shown by * which denotes $p < 0.05$, calculated using a t test. Root elongation was used as a measure of root sensitivity of the seedling to NaCl (B). Data points are mean values for several individual seedlings. For NaCl concentrations less than 150 mM, n was a minimum of 38 whereas for 150 mM NaCl n = 16. Error bars are standard errors of the mean. There is no statistical difference in the inhibition of root growth imposed by NaCl on the *atpnp-a* mutant and wildtype lines.

3.3.10.4 Older plant responses

The germination and seedling stages are most sensitive to NaCl and osmotic stresses (Gao *et al.*, 2003). Therefore the older plant may not display the same NaCl and osmotic stress sensitivity as the seedling. Additionally, the phenotype of the seedling may differ from that of the older plant because the high humidity of the closed plate system can mask the stomatal response to stress (Ruggiero *et al.*, 2004). NaCl, osmotic stress and drought phenotypes of soil grown wildtype and *atpnp-a* mutant lines were therefore examined. Firstly, plants were watered with NaCl or isoosmolar mannitol or sorbitol; alternatively water was withheld to simulate drought conditions. All treatments inhibited the growth of *AtPNP-A* wildtype line, as expected (Figures 3.21 and 3.22). Slight yellowing was observed after NaCl treatment indicative of chlorosis while leaves darkened with mannitol and sorbitol treatment probably due to anthocyanin accumulation. Additionally the sugars caused severe wilting suggesting that osmotic stress is more toxic to older plants than NaCl, opposite to the germination stage. Drought induced turgor loss however this is not obvious from the photographs. The *atpnp-a* mutant did not show visibly different phenotypes from the wildtype line. As a second approach to quantify the NaCl and osmotic stress tolerance of older *atpnp-a* mutant and wildtype plants, a leaf disc assay was performed (Sanan-Mishra *et al.*, 2005). Leaf discs were exposed to NaCl or mannitol for 48 hrs and chlorophyll extracted as a measure of the effect of the stress (Figure 3.23). Unexpectedly, NaCl did not reduce chlorophyll content whereas mannitol reduced chlorophyll content in a concentration-dependent manner. This however was not significant because the data is only the average of two pooled leaf disc samples. More replicates may have improved this data and would have allowed for statistical analysis. The results indicate that the *atpnp-a* mutant and wildtype were not different in their response to NaCl and mannitol in the leaf disc assay. Altogether this suggests that older soil grown *atpnp-a* mutant plants are not more tolerant of NaCl or osmotic stress than wildtype plants.

3.3.11 Nutrient starvation

Mutants that are hypersensitive to NaCl stress are, in some cases, also hypersensitive to low external K^+ (Liu and Zhu, 1997; Wu *et al.*, 1996a; Zhu *et al.*, 1998). As discussed in chapter 1, NaCl stress induces K^+ starvation as Na^+ competes with K^+ for uptake and Na^+ uptake causes further K^+ loss (Shabala and Cuin, 2008; Wu *et al.*, 1996a). For this reason it was appropriate to look at phenotypes of the *atpnp-a* mutant in response to K^+ deficiency; and the effect of other nutrient deficiencies was also tested. Seeds were germinated on nutrient replete media since germination is unable to occur on media lacking these essential nutrients. Once seedlings were five days old they were transferred to media lacking either K, N or P (Hammond *et al.*, 2003).

3.21

PRE-TREATMENT **POST-TREATMENT**

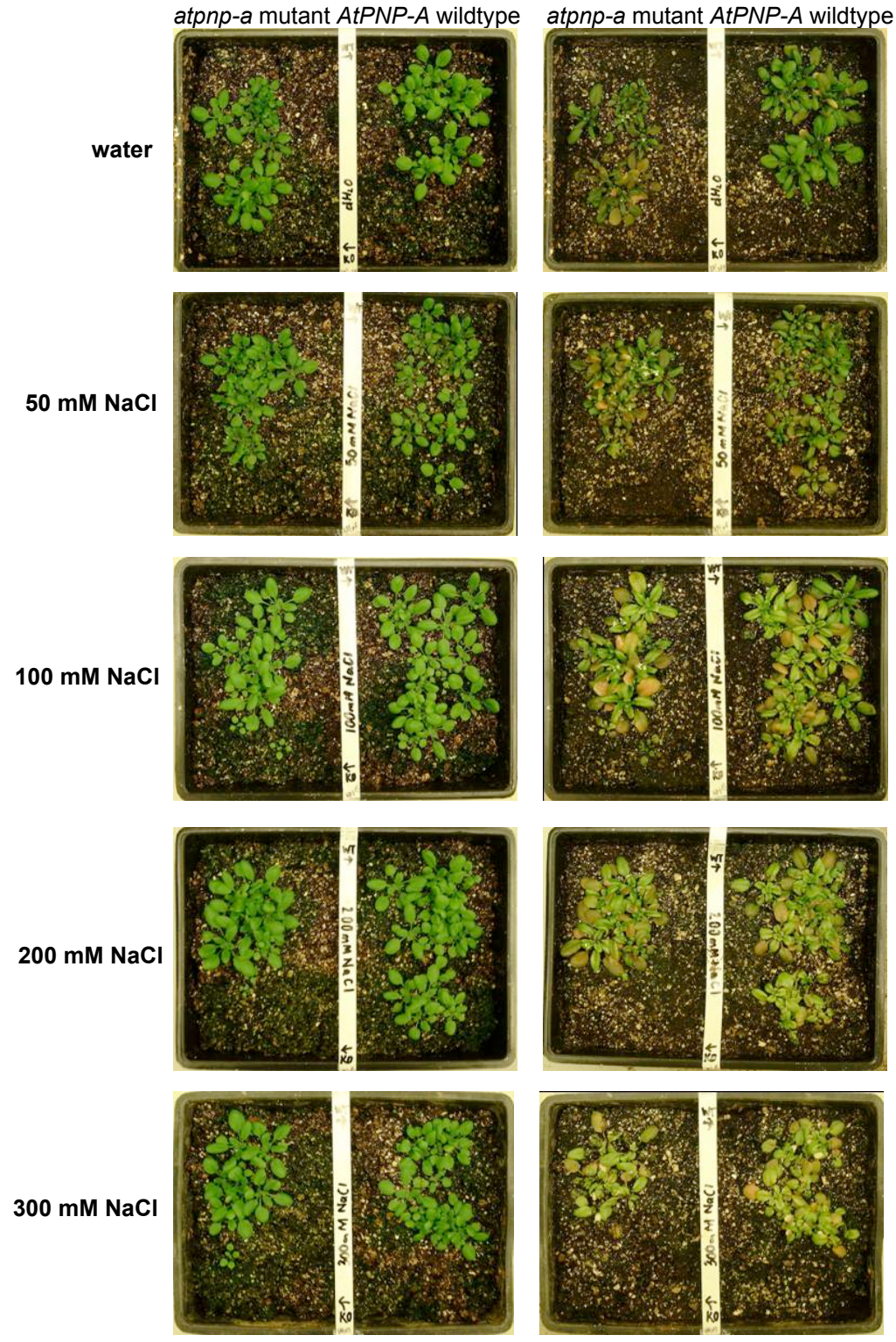

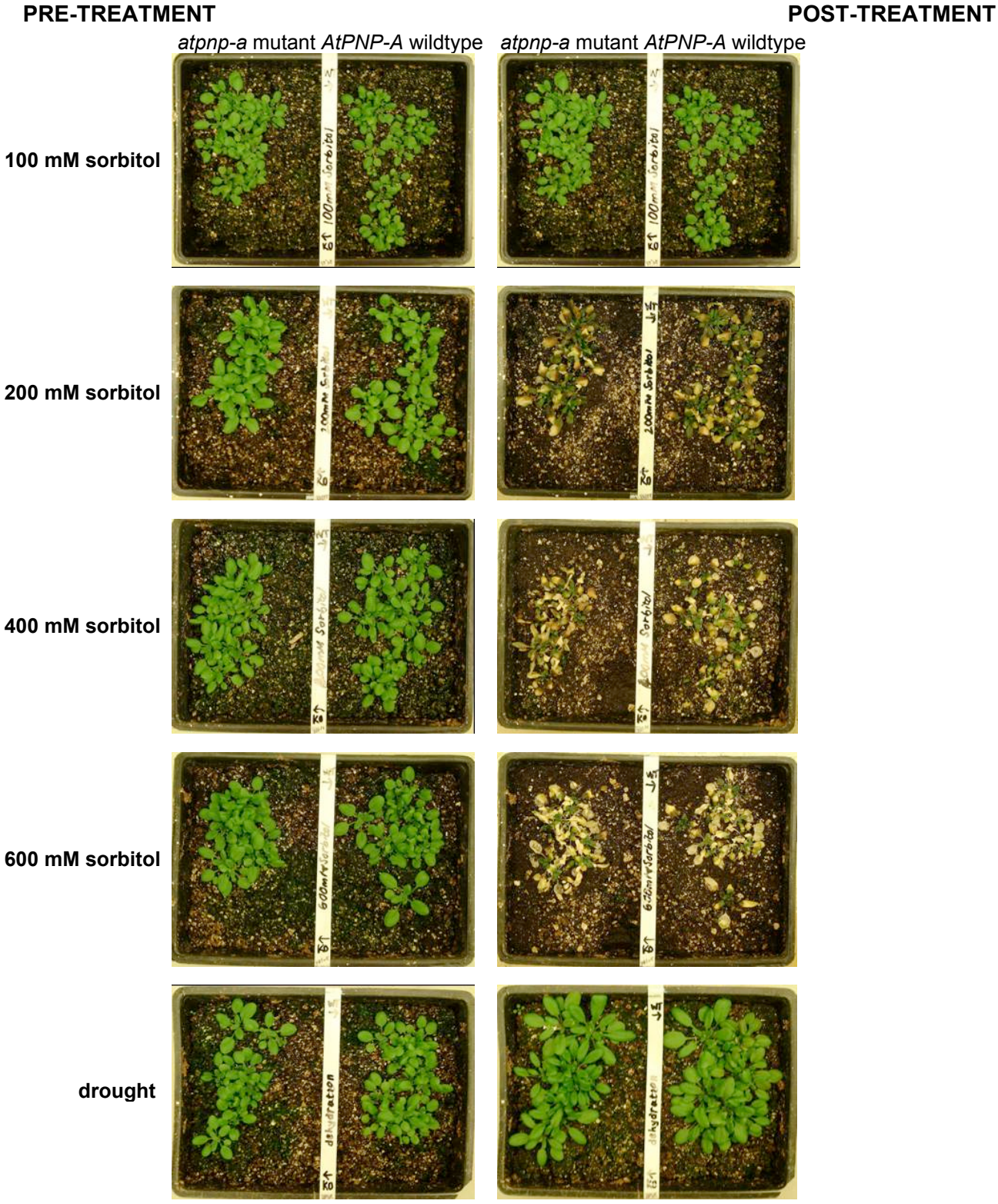

Figure 3.21. Soil-grown wildtype and *atpnp-a* mutant lines before and after stress treatment

Photographs of *atpnp-a* mutant (left) and wildtype (right) plants grown in soil for four weeks before (left hand panels) and seven days after (right hand panels) stress exposure. Water was the control treatment. Stresses included NaCl (50, 100, 200 and 300 mM) and isoosmolar sorbitol (100, 200, 400 and 600 mM respectively) treatment while water was withheld for seven days in the drought treatment.

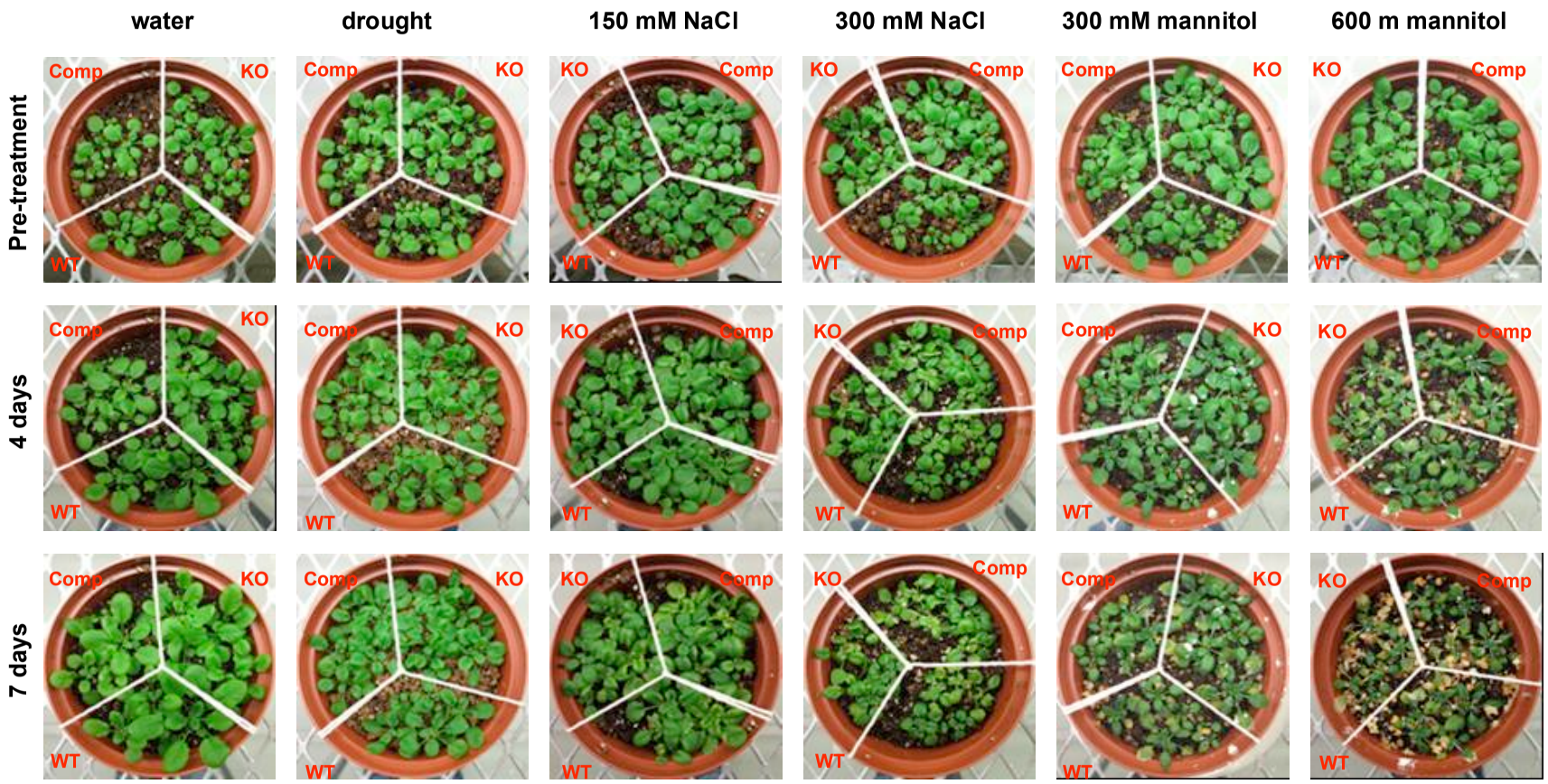

Figure 3.22. Duplicate experiment showing wildtype and *atpnp-a* mutant lines grown on soil and then exposed to NaCl, osmotic stress or drought

A second set of representative photographs of the wildtype and *atpnp-a* mutant lines grown on soil for three weeks, before (0 days) and after (4 and 7 days) treatment with water (control), NaCl or isoosmolar mannitol. Alternatively water was withheld to simulate drought conditions. "WT" is the *AtPNP-A* wildtype line, "KO" the *atpnp-a* mutant line and "Comp" refers to the complemented line which at this stage was homozygous however its expression had yet to be determined.

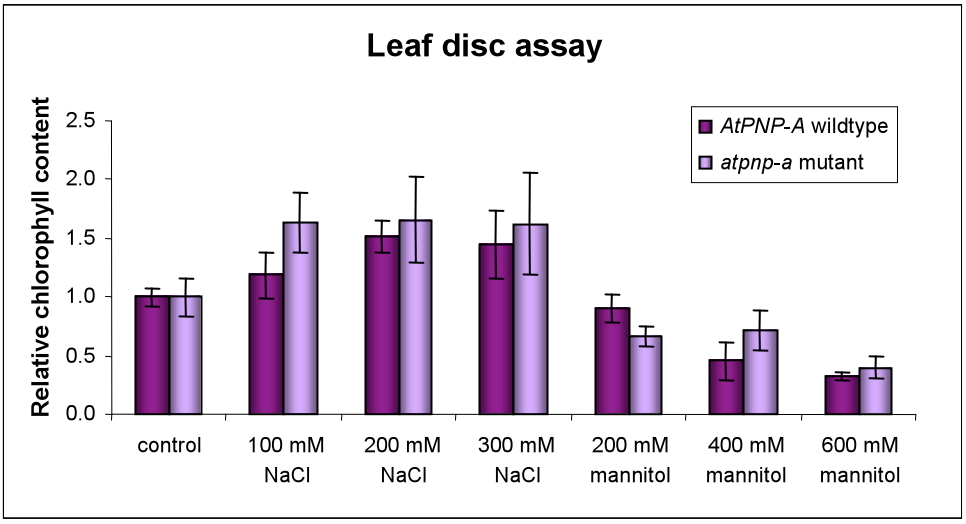

Figure 3.23. Chlorophyll loss from leaf discs of the wildtype and *atpnp-a* mutant lines following exposure to NaCl or mannitol

Leaf discs were punched out of leaves from wildtype and *atpnp-a* mutant lines grown in soil for four weeks under standard conditions. Leaf discs were then placed in microtitre plates and then treated with water (control), NaCl (100, 200 or 300 mM) or isoosmolar mannitol (200, 400 and 600 mM). After 48 hrs, three leaf discs were collected per line per treatment and chlorophyll extracted. This was performed in duplicate. Data is the mean of the duplicates and expressed relative to the chlorophyll content of the control (water) treated samples. Error bars are standard errors of the means. Statistical differences between the wildtype and *atpnp-a* mutant lines could not be calculated due to the small sample size.

Root growth is sustained when nutrients are limiting to enable exploration of the soil environment for better growth conditions (Potters *et al.*, 2007; Shin and Schachtman, 2004). Primary root growth seven days after transfer onto the nutrient limiting media was the parameter used to measure the response of the wildtype and *atpnp-a* mutant lines to nutrient deficiency (Cheong *et al.*, 2007; Rus *et al.*, 2004; Wu *et al.*, 1996a). Nitrogen (N) and potassium (K) deficiency both inhibited root elongation in the *AtPNP-A* wildtype line when compared to root growth on nutrient replete media however this inhibition was only significant in response to the nitrogen deficiency (Figure 3.24). Phosphorous (P) deficiency on the other hand did not inhibit root growth within the time frame of this experiment. The *atpnp-a* mutant grew better than the wildtype line on media lacking K, N or P and its root growth was not significantly inhibited in response to any of the nutrient deficiencies tested. In fact the *atpnp-a* mutant actually grew significantly better on media lacking phosphorous than on nutrient replete media. Again the same trend was observed for its growth on potassium-deficient media however, this was not statistically significant. Therefore the *atpnp-a* mutant therefore is more resistant than the wildtype line to nutrient deficiencies imposed by lack of K, N and P in the media.

3.3.12 Ion accumulation

Other mutants with phenotypes in response to both NaCl stress and K^+ deficiency are affected in ion homeostasis (Rus *et al.*, 2004; Rus *et al.*, 2001; Wu *et al.*, 1996a; Zhu *et al.*, 1998). Therefore ion homeostasis was investigated in the *atpnp-a* mutant. Preserving K^+ nutrition in the face of NaCl stress is of utmost importance for the maintenance of homeostasis (Liu and Zhu, 1997; Wu *et al.*, 1996a; Zhu *et al.*, 1998). Thus the K^+/Na^+ ratio is considered a measure of ion homeostasis (Hussain *et al.*, 2008; Rus *et al.*, 2004; Shabala and Cuin, 2008; Xiong and Zhu, 2002a; Zhu, 2003). Following NaCl and osmotic stress treatment of the *AtPNP-A* wildtype and mutant lines, accumulation of Na^+ and K^+ ions was measured using inductively coupled plasma mass spectrometry (ICP-MS) (Gobert *et al.*, 2006). In response to NaCl treatment, the *AtPNP-A* wildtype seedlings significantly accumulate Na^+ after 30 min treatment and even more so after 24 hrs, as expected (Gobert *et al.*, 2006) (Figure 3.25A-B). On the other hand Na^+ did not accumulate in response to mannitol treatment. There was no significant loss of K^+ after 30 min NaCl or mannitol treatment (Figure 3.25C). However K^+ was lost from both the NaCl and mannitol treated samples following 24 hrs of exposure (Figure 3.25D). The *atpnp-a* mutant had significantly ($p < 0.05$) lower Na^+ and K^+ content after the control treatment with water for 30 min and the same trend was observed after 24 hrs (Figure 3.25A-D). Following NaCl treatment for 30 min or 24 hrs the tendency for the *atpnp-a* mutant to have a lower Na^+ and K^+ content than the wildtype line was again observed however this difference was not statistically significant. The *atpnp-a* mutant did not differ from the wildtype line in terms of its Na^+ and K^+

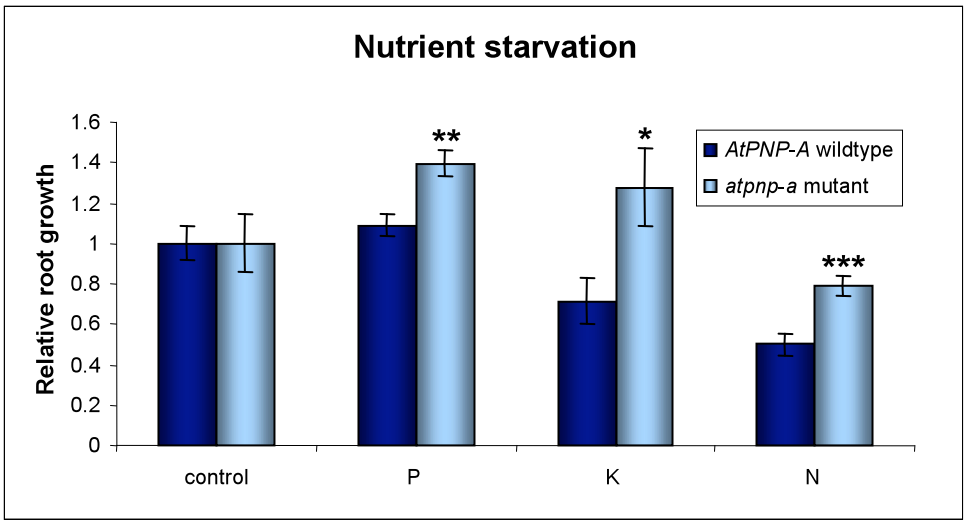

Figure 3.24. Affect of nutrient starvation on the *atpnp-a* mutant and wildtype lines

Seedlings were germinated for five days on nutrient replete media and then transferred on to media lacking phosphorus (P), potassium (K) or nitrate (N). Root elongation was measured seven days after growth on nutrient deficient media. Data is the mean of ten individual seedling measurements and error bars are standard errors of the mean. The statistical difference between the wildtype and *atpnp-a* mutant lines has been calculated using a t test with * denoting $p < 0.05$, ** $p < 0.01$ and *** $p < 0.001$.

3.25 A.

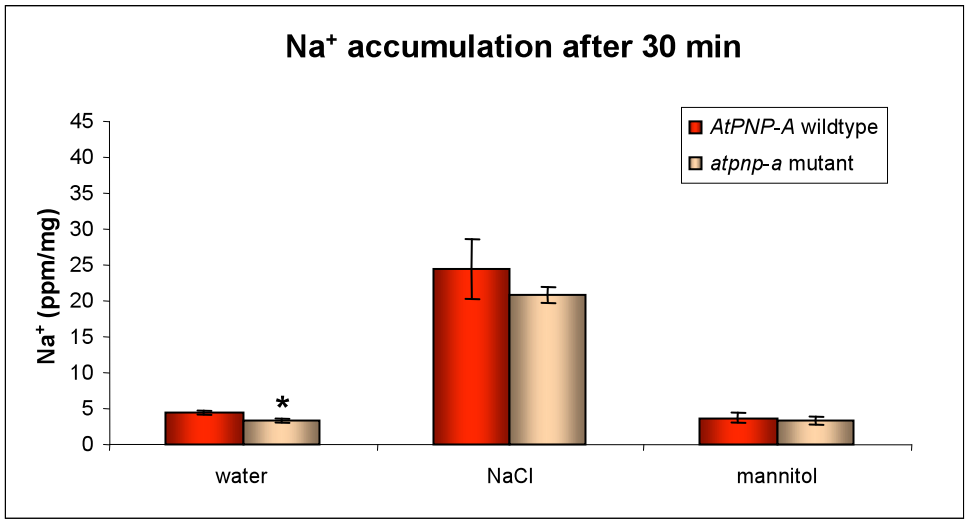
Na+ accumulation after 30 min
AtPNP-A wildtype
atpnp-a mutant
Na+ (ppm/mg)
45
40
35
30
25
20
15
10
5
0
*
water
NaCl
mannitol

B.

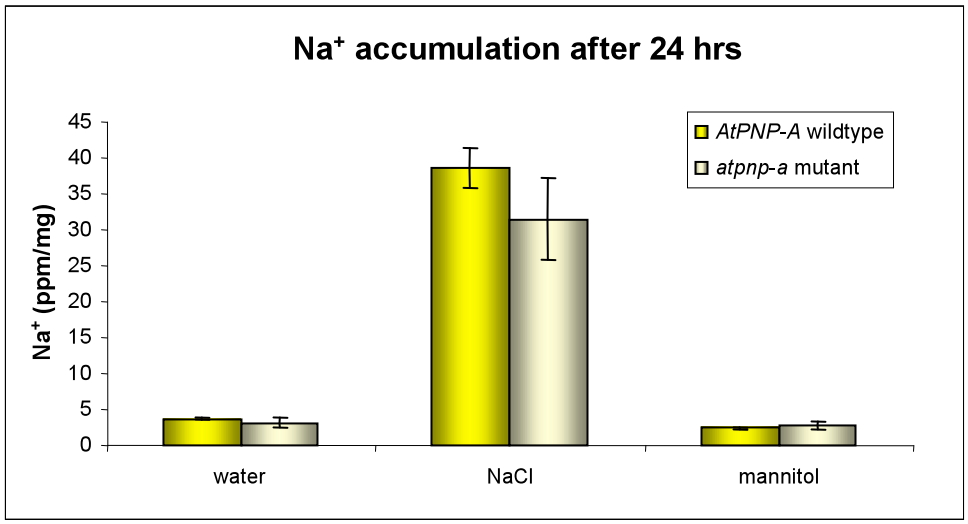
Na+ accumulation after 24 hrs
AtPNP-A wildtype
atpnp-a mutant
Na+ (ppm/mg)
45
40
35
30
25
20
15
10
5
0
water
NaCl
mannitol

3.25 C.

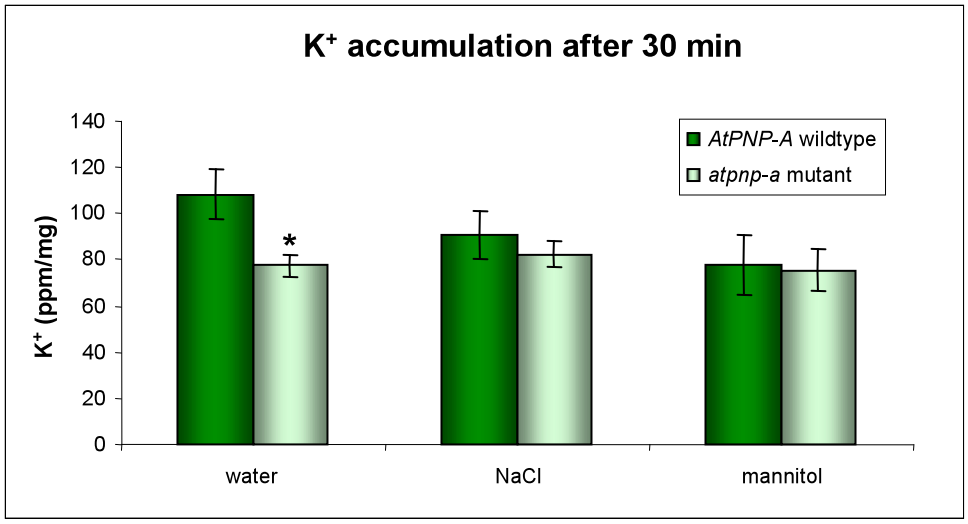
K+ accumulation after 30 min
K+ (ppm/mg)
140
120
100
80
60
40
20
0
*
AtPNP-A wildtype
atpnp-a mutant
water
NaCl
mannitol

D.

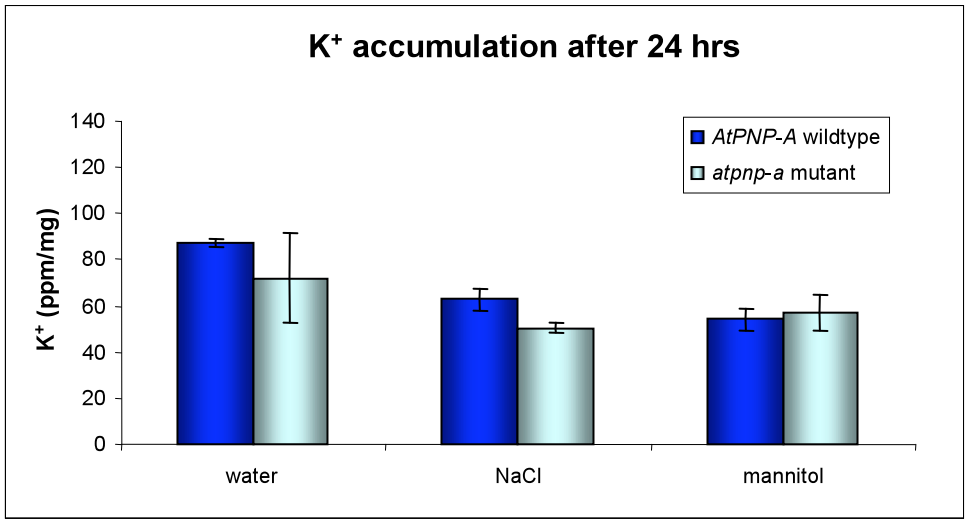
K+ accumulation after 24 hrs
K+ (ppm/mg)
140
120
100
80
60
40
20
0
AtPNP-A wildtype
atpnp-a mutant
water
NaCl
mannitol

E.

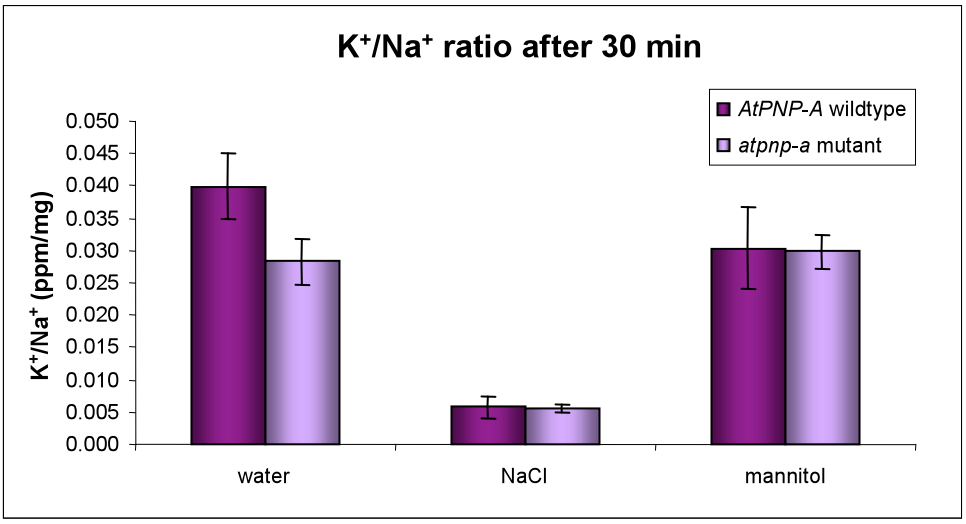

F.

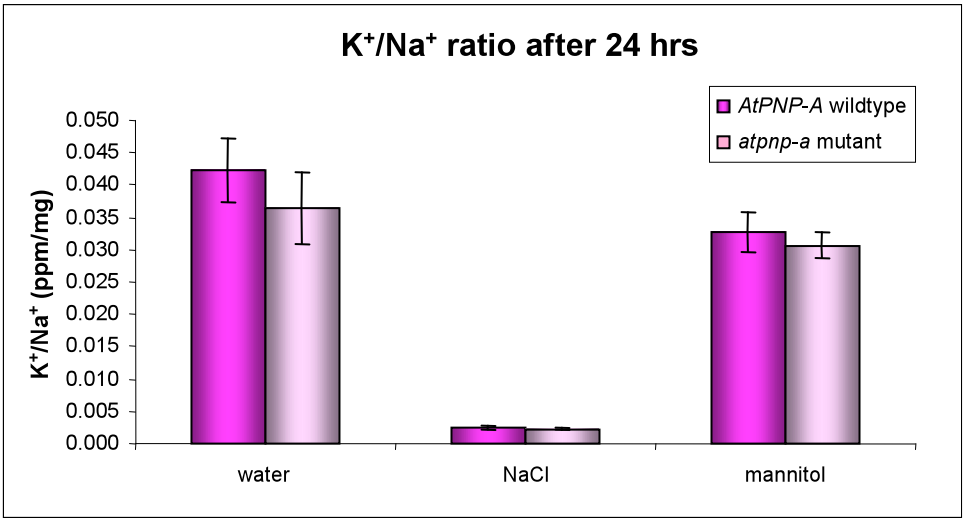

Figure 3.25. Na^+ and K^+ content following short and long-term water, NaCl or mannitol treatment

Ion content was measured in ppm using inductively coupled plasma mass spectrometry (ICP-MS) and expressed per mg tissue in two week old *atpnp-a* mutant and wildtype seedlings in response to treatment with water (control), NaCl or mannitol. Na^+ content was measured after 30 min (A) and 24 hrs (B), K^+ content was measured in the same 30 min (C) and 24 hr (D) samples and the K^+/ Na^+ ratio determined at both time points, 30 min (E) and 24 hrs (F). The data are the mean values for three biological replicates and error bars are standard errors of the mean. Statistical differences between the *atpnp-a* mutant and wildtype lines were analysed using the Mann-Witney U test with * denoting $p < 0.05$.

content after mannitol treatment, irrespective of the exposure time. In the control samples the *atpnp-a* mutant had a lower K^+/Na^+ ratio but this was not statistically significant (Figure 3.25E-F). However after NaCl or mannitol treatment the K^+/Na^+ ratio was the same between the *atpnp-a* mutant and wildtype lines. Since the *atpnp-a* mutant had a significantly lower Na^+ and K^+ content and a lower (albeit not significant) K^+/Na^+ ratio than the wildtype line in the control samples, this suggests that the *atpnp-a* mutant is compromised in terms of its ion homeostasis in the basal state. The fact that the Na^+ and K^+ content of the *atpnp-a* mutant is no longer different from the wildtype after stress treatment, suggests that the *atpnp-a* mutant has taken up more Na^+ and lost less K^+ in response to NaCl and mannitol treatment. Furthermore the reduction of K^+/Na^+ ratio in response to NaCl and mannitol treatment was visibly less for the *atpnp-a* mutant compared to the wildtype line, therefore the *atpnp-a* mutant is better able to maintain its K^+/Na^+ ratio in response to NaCl and osmotic stress, consistent with its stress tolerant phenotype.

3.3.13 Ion flux

Recently it has been proposed that K^+ efflux in response to NaCl stress is the parameter that is best correlated with NaCl tolerance (Shabala and Cuin, 2008). K^+ efflux has been attributed to plasma membrane depolarization as a result of Na^+ influx which would affect voltage dependent inward and outward -rectifying K^+ channels, both reducing K^+ uptake and enhancing K^+ efflux concurrently. A non-invasive MIFE experiment was kindly conducted by René Bastian (University of the Western Cape, RSA) and Prof. Sergey Shabala (University of Tasmania, Australia) in order to measure K^+ efflux from the *atpnp-a* mutant and wildtype lines in response to NaCl treatment. As expected, NaCl treatment induces a rapid net K^+ efflux from the mature and elongation zones of the wildtype roots (Figure 3.26) (Shabala *et al.*, 2005a; Shabala and Cuin, 2008). The *atpnp-a* mutant effluxes more K^+ from the elongation zone and less K^+ from the mature zone of the root in response to NaCl treatment compared to the wildtype. The *atpnp-a* mutant therefore exhibits tissue-specific differences in terms its K^+ efflux response to NaCl. Additionally the NaCl-induced K^+ efflux in the elongation zone of the *atpnp-a* mutant root was found to be more sensitive than the wildtype to inhibition by Zn^{2+}, an inhibitor of NSCCs (Figure 3.27). The *atpnp-a* mutant therefore also has different sensitivity to channel inhibitors when compared to the wildtype. In sum, the *atpnp-a* mutant differs from the wildtype in its ion fluxes in response to NaCl in the different regions of *Arabidopsis* root which may be encoded by differences in its transporters.

A.

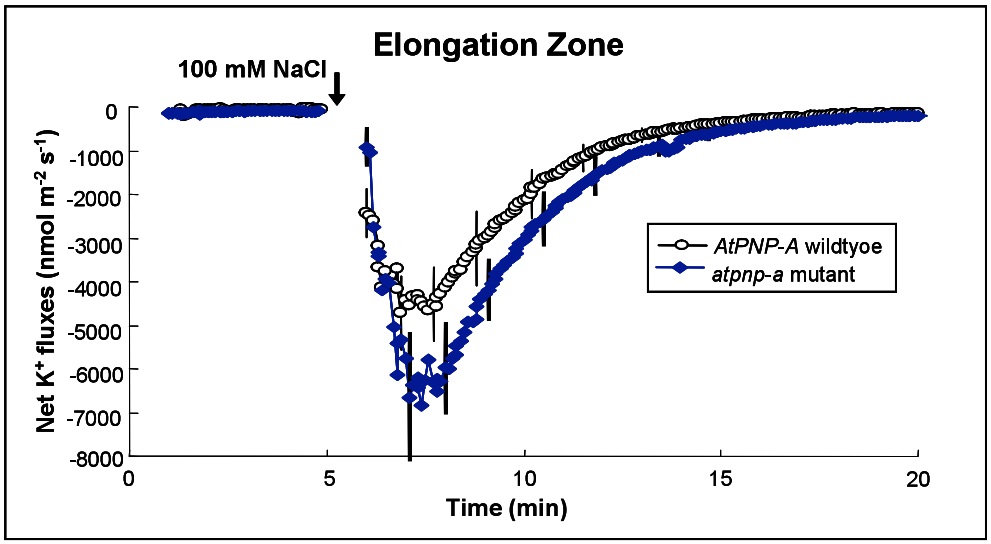

B.

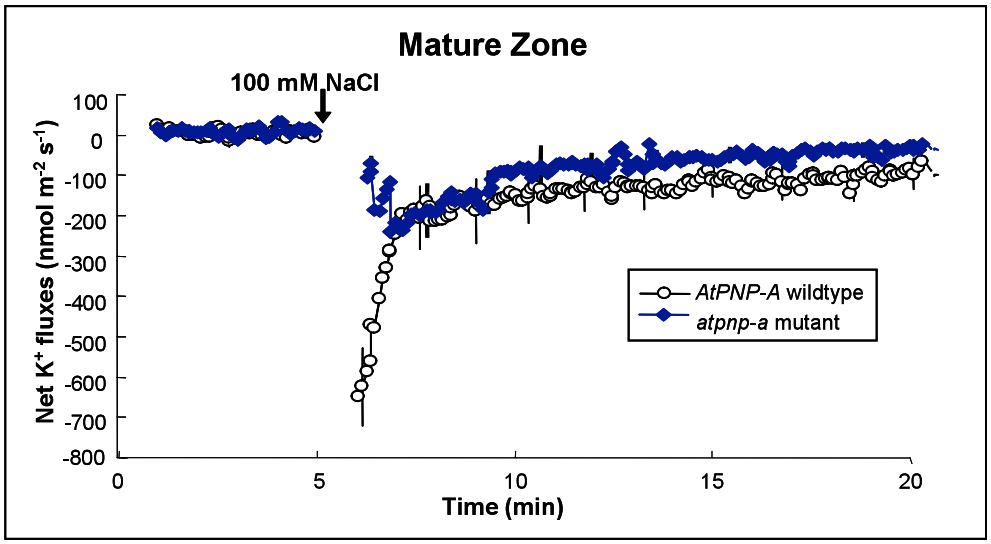

Figure 3.26. K^+ flux in the *atpnp-a* mutant and wildtype lines in response to NaCl treatment

The effect of 100 mM NaCl on K^+ efflux from the elongation (A) and mature (B) zones of *atpnp-a* mutant and wildtype roots of one week old seedlings. Traces are the means for a minimum of five samples and error bars are standard errors of the mean.

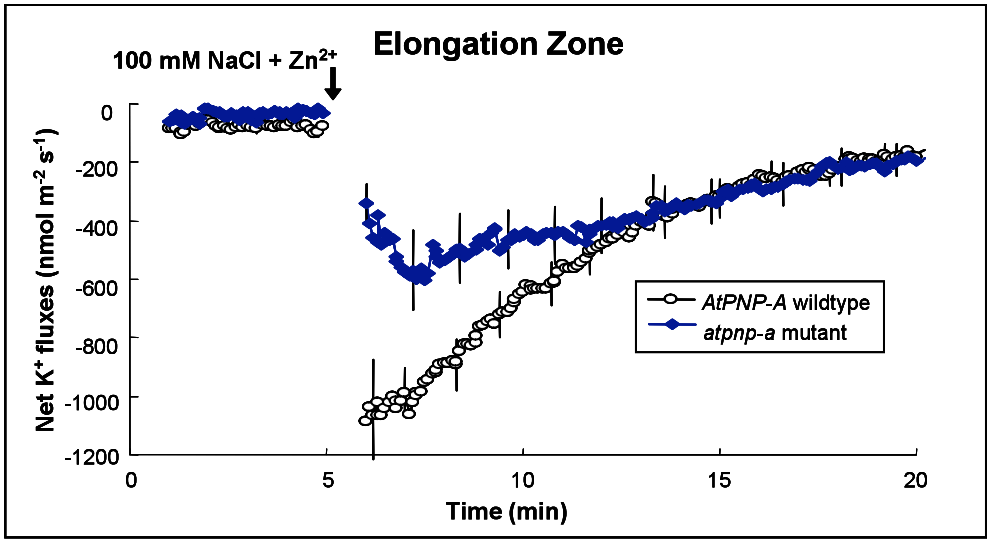

Figure 3.27. Effect of Zn^{2+} on the NaCl-induced K^+ efflux from the elongation zone of the *atpnp-a* mutant and wildtype roots

Inhibition of the 100 mM NaCl-induced K^+ efflux from the elongation zone of the *atpnp-a* mutant and wildtype roots by pre-treatment with 1 mM Zn^{2+}. Traces are the average responses for a minimum of n = 4 individual seedlings and error bars, the standard errors of the mean.

The *atpnp-a* mutant differs from the wildtype in its response to a number of abiotic stresses that disrupt water and ion homeostasis, supporting a role for *AtPNP-A* in maintaining homeostasis *in planta*. Biotic stresses also affect water and ion homeostasis. Therefore the phenotypes of the *atpnp-a* mutant and wildtype lines in response to biotic stresses was examined in order to determine whether *AtPNP-A* could also play a role in biotic stress responses. The biotic stress imposed depends largely on the pathogen employed since pathogens have various strategies for exploiting the host and the plant's defence response against each type of pathogen is quite different (section 1.4.7.1). It was therefore appropriate to test the response of *atpnp-a* mutant and wildtype plants to a range of pathogens including the necrotrophic fungal pathogen *B. cinerea,* the hemi-biotrophic bacterial pathogen *P. syringae* and the obligate oomycete *H. parasitica*.

3.3.14 *B. cinerea*

The *atpnp-a* mutant was tested for its susceptibility to *B. cinerea*. Leaves were detached from four week old soil grown plants. A single droplet of spores was placed on each leaf and the diameter of the watery lesion that develops over the following four days was measured. This detached leaf assay has been shown to correlate with whole plant susceptibility (Denby *et al.*, 2004). Two different *B. cinerea* isolates were tested, namely Brassica and Pepper (Figure 3.28A and B respectively). In the *AtPNP-A* wildtype line, the lesion size increased with increasing time post-infection, as expected (Denby *et al.*, 2004). The *atpnp-a* mutant did not show any difference in its response to either *B. cinerea* isolate when compared to the wildtype. The *atpnp-a* mutant therefore does not differ from the wildtype in its susceptibility to *B. cinerea*.

3.3.15 *P. syringae*

P. syringae can be either virulent or avirulent on *Arabidopsis* depending on the strain of *P. syringae* and the ecotype of *Arabidopsis* (Katagiri *et al.*, 2002). Both virulent and avirulent strains induce PTI. Virulent pathogens however suppress PTI to cause disease (de Torres *et al.*, 2006; Hauck *et al.*, 2003; Kim *et al.*, 2005; Li *et al.*, 2005) while the attempt by avirulent pathogens to suppress PTI is recognized by the plant initiating the second layer of ETI defence that ultimately renders the pathogen avirulent to the plant. The response of the *atpnp-a* mutant and wildtype plants to virulent and avirulent strains of *P. syringae* was tested in order to determine whether *AtPNP-A* could play a role in defence against *P. syringae* and if so to delineate whether it is involved in PTI or ETI.

A.

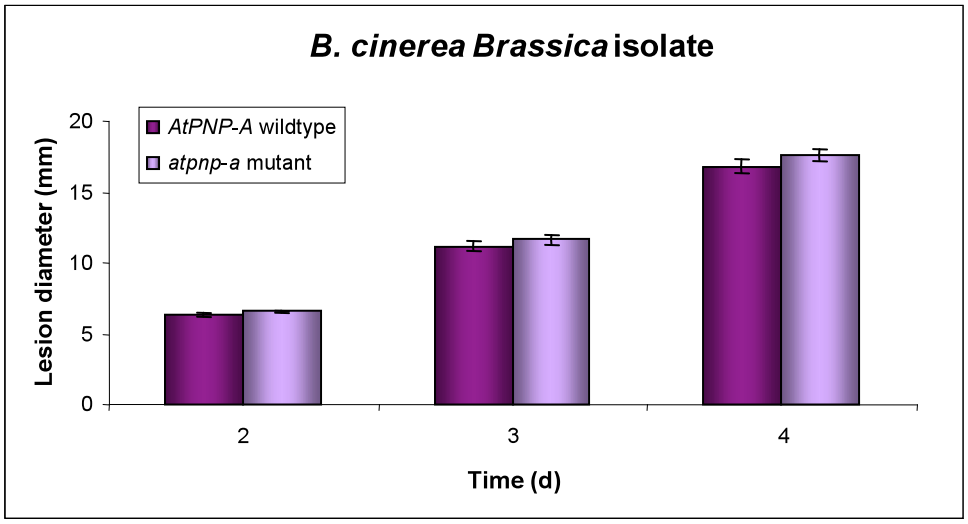

B.

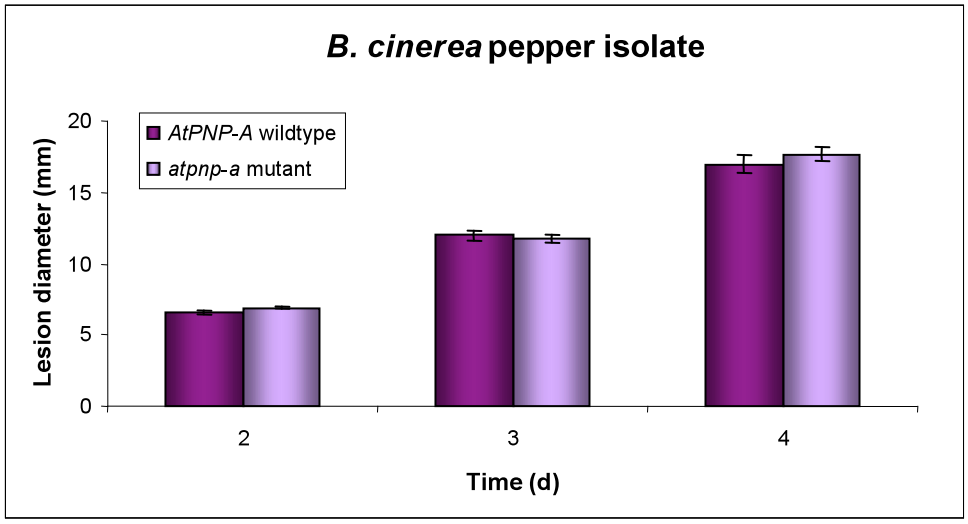

Figure 3.28. *B. cinerea* susceptibility of the *atpnp-a* mutant and wildtype lines

Susceptibility of four week old *atpnp-a* mutant and wildtype lines to *B. cinerea* was tested using two different isolates, namely *Brassica* (A) and pepper (B). Progression of infection was measured in terms of lesion diameter over four days post inoculation. Graphs show the mean values for n = 28 leaves and error bars are standard errors of the mean. The *atpnp-a* mutant was not statistically different from the *AtPNP-A* wildtype line, as determined by using a t test.

3.3.15.1 Pressure inoculation

Firstly avirulent *P. syringae* DC3000 *AvrB* and virulent *P. syringae* DC3000 were pressure infiltrated into leaves of the wildtype and *atpnp-a* mutant plants and the bacterial titre measured over the following three days (Figure 3.29 A and B respectively). After 4 hrs (day 0) similar bacterial numbers were present in the *atpnp-a* mutant and wildtype lines indicating that bacteria had been successfully delivered into the apoplast. Over the following three days bacterial numbers increased as the infection progressed. This increase was faster and greater in response to the virulent pathogen compared to the avirulent pathogen. It has been reported that bacterial titres in response to avirulent *P. syringae* are approximately 100-fold lower than those observed in response to virulent strains (Glazebrook, 2005). Indeed the results of this experiment fall within this range. There were no differences between the bacterial numbers attained during the infection of the wildtype and *atpnp-a* mutant lines with either pathogen for all time points tested, except one - at day 1 of infection with avirulent *P. syringae* the *atpnp-a* mutant had lower bacterial numbers than the wildtype. This did not persist at subsequent time points and was not reproducible in independent experiments and thus was not considered further. Therefore the *atpnp-a* mutant is not affected in its susceptibility to virulent or avirulent *P. syringae* when pressure-inoculated.

3.3.15.2 Spray inoculation

The above technique artificially delivers the pathogen beneath the epidermis, directly into the apoplast (Melotto *et al.*, 2006; Zipfel *et al.*, 2004). In nature *P. syringae* must enter the plant through wound sites or openings like stomata (Beattie and Lindow, 1995; Melotto *et al.*, 2006). The pressure inoculation techniques bypass critical elements of pathogen recognition and the plants PTI defence that results in stomatal closure (Kim *et al.*, 2005; Melotto *et al.*, 2006; Zipfel *et al.*, 2004). Since the *atpnp-a* mutant has greater stomatal numbers and reduced stomatal apertures, the wildtype and *atpnp-a* mutant lines were tested for their susceptibility to virulent (DC3000) and avirulent (*AvrB*) *P. syringae* strains using the more natural spray technique. Even though a higher inoculum was used in this experiment, the bacterial numbers that successfully penetrated the leaf after 4 hrs (day 0) were much lower when compared to those following pressure inoculation (Figure 3.30). Bacterial numbers were similar between the wildtype and *atpnp-a* mutant lines at day 0 demonstrating that the spraying had been even. There were slightly greater bacterial numbers in the *atpnp-a* mutant at day 0 after spraying with virulent *P. syringae* however this was not reproducible over independent experiments. Over the following three days, bacterial numbers increased in the wildtype line as expected. In response to the avirulent pathogen, greater bacterial numbers were observed only after day 2 and day 3 whereas the infection was more rapid in response to virulent *P. syringae* with increases in bacterial titres being noticeable from day 1. The wildtype and *atpnp-a* mutant lines were not

A.

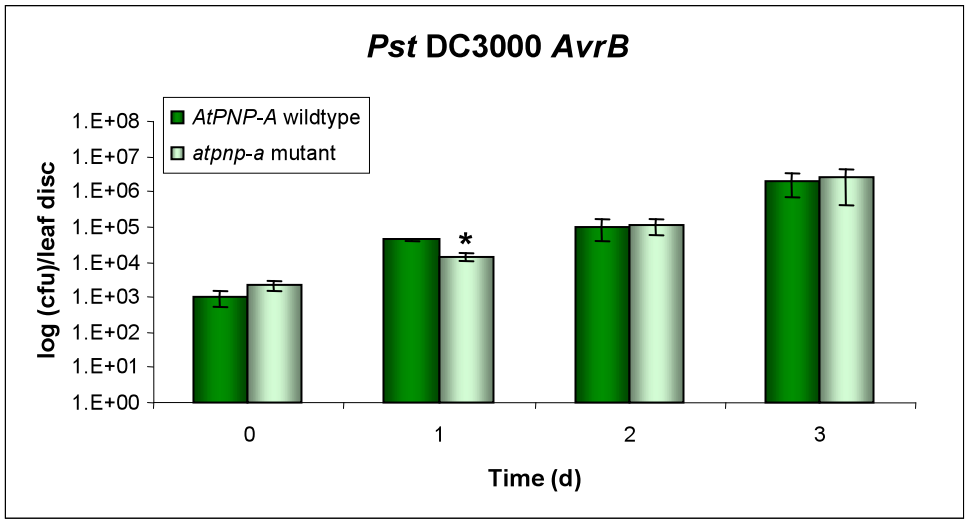

B.

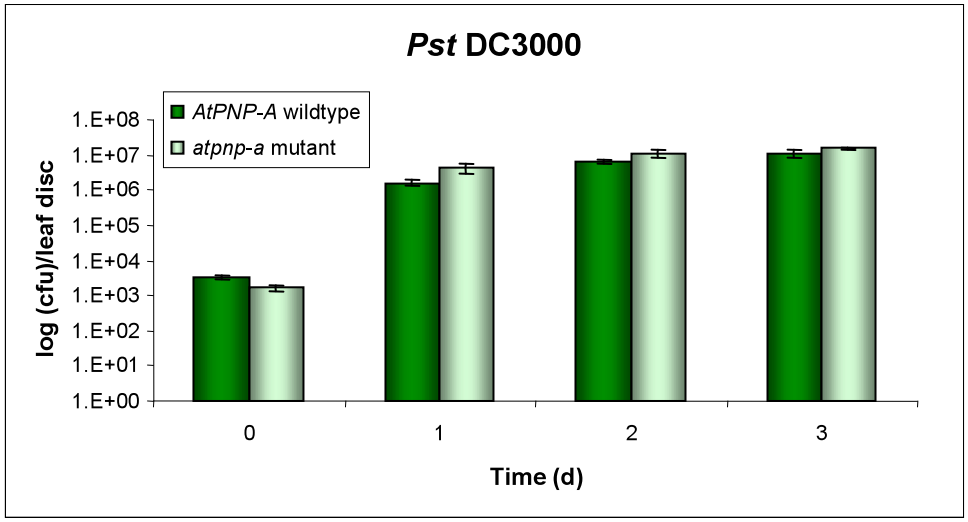

Figure 3.29. Infection of the *atpnp-a* mutant and wildtype lines with *P. syringae* using the pressure inoculation technique

Four week old *atpnp-a* mutant and wildtype plants were infected with avirulent *P. syringae* DC3000 *AvrB* (A) or virulent *P. syrinage* DC3000 (B) by pressure infiltration with 1 x 10^6 cfu/ml. Progression of the infection was measured over the following three days by the number of cfus that were extracted per leaf disc. Single leaf discs were harvested from three different leaves per plant and pooled. Data points are the mean values for three individual plants per time point and error bars are standard errors of the mean. Statistical differences between the susceptibility of the wildtype and *atpnp-a* mutant lines was analyzed using the Mann-Witney U test and * represents a difference of $p < 0.05$.

A.

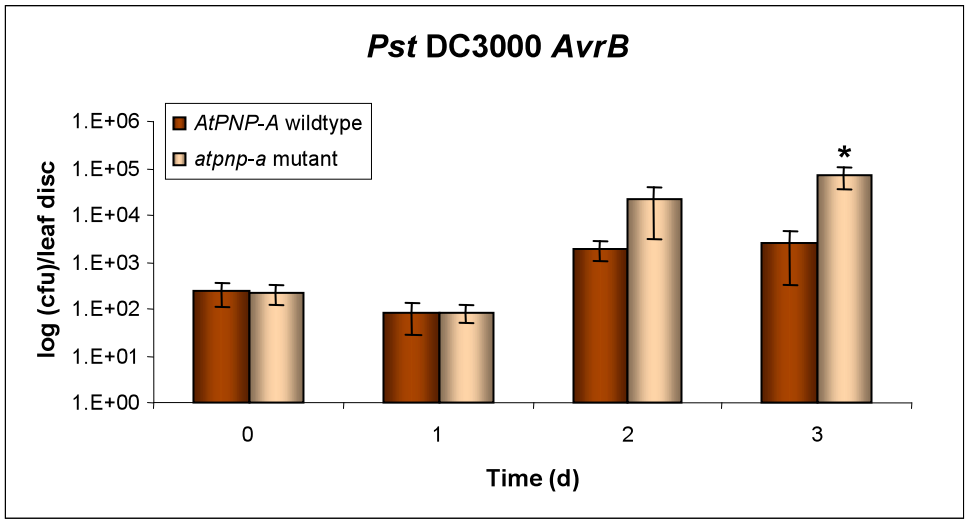

B.

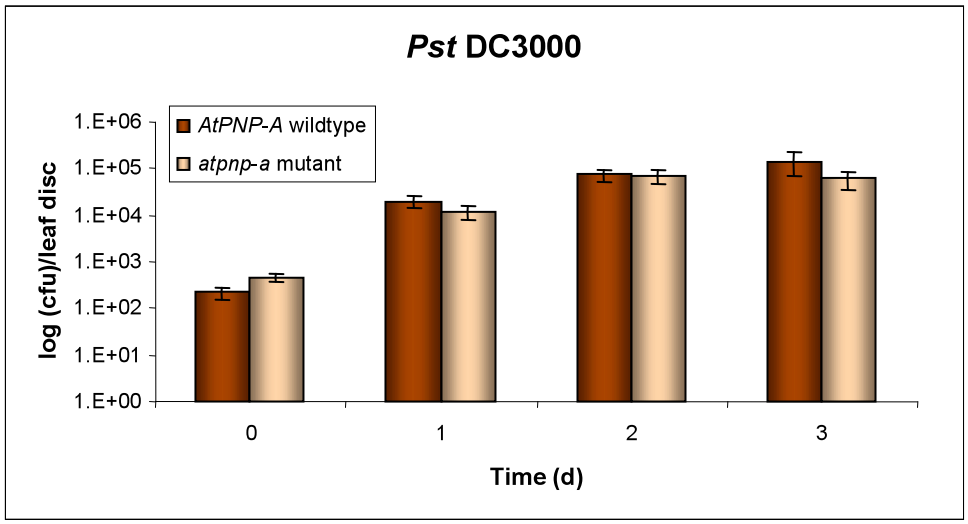

Figure 3.30. Infection of the *atpnp-a* mutant and wildtype lines with *P. syringae* using the spray inoculation technique

The *atpnp-a* mutant and wildtype lines were infected with avirulent *P. syringae* DC3000 *AvrB* (A) or virulent *P. syrinage* DC3000 (B) by spray inoculation with 1 x 10^8 cfu/ml with 0.05% (v/v) silwet. Infection was measured over the following three days by the number of cfus extracted per leaf disc. Single leaf discs were harvested from three different leaves per plant and pooled. These leaf discs were surface sterilized so that only bacteria that had successfully colonized the leaf interior were measured. Data points are the means for three different plants per line per time point and error bars are standard errors. Statistical differences between the susceptibility of the wildtype and *atpnp-a* mutant lines was analyzed using the Mann-Witney U test with * representing a significant difference of $p < 0.05$.

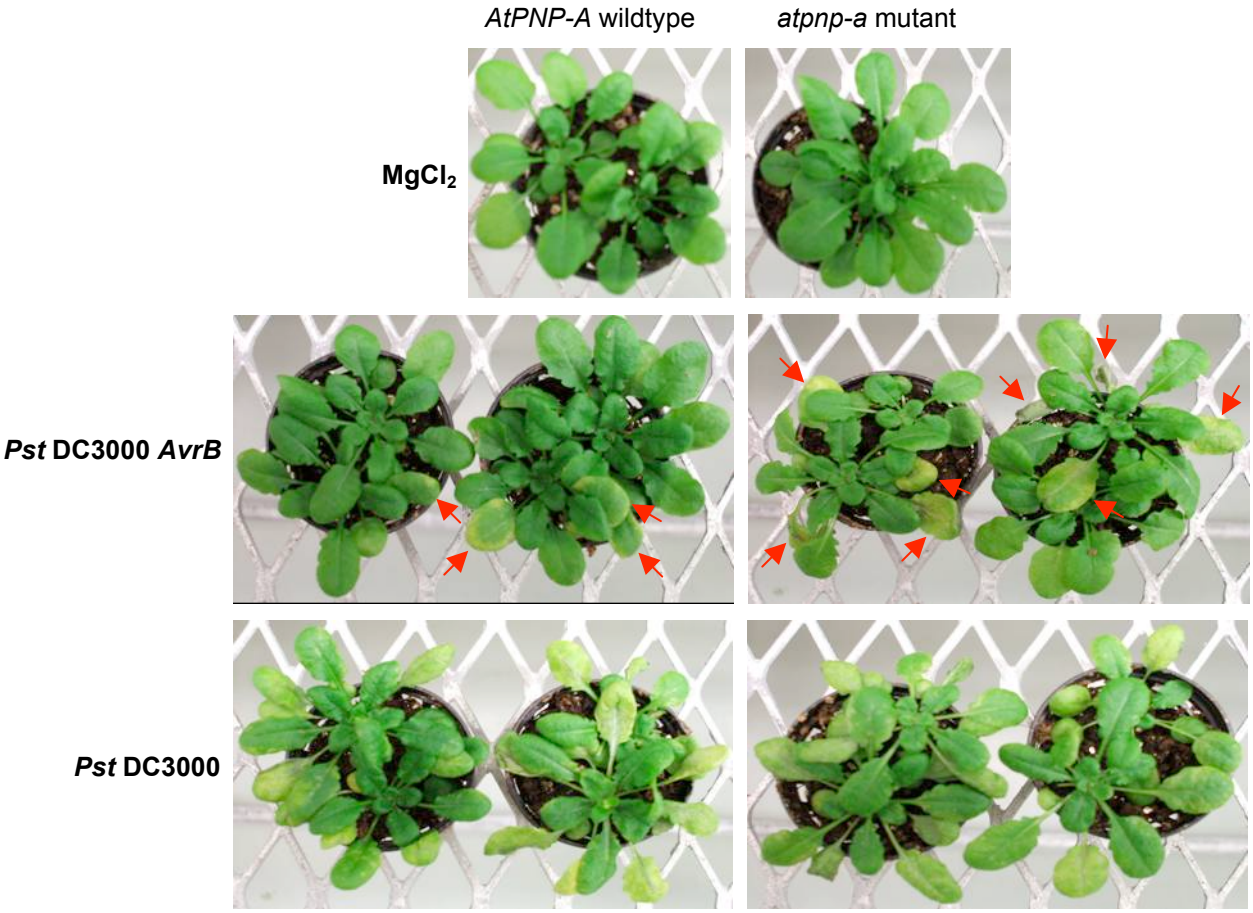

Figure 3.31. Representative photographs of the wildtype and *atpnp-a* mutant lines three days after spray inoculation with avirulent and virulent *P. syringae*

Four week old *AtPNP-A* wildtype (left hand panels) and *atpnp-a* mutant (right hand panels) lines were spray inoculated with 10 mM $MgCl_2$ (control) (top panel) or 1 x 10^8 cfu/ml with 0.05% (v/v) silwet avirulent *P. syringae* DC3000 *AvrB* (middle panel) or virulent *P. syringae* DC3000 (bottom panel). Two plants per line are grown in each pot. Symptoms of infection are chlorosis (yellowing of the leaves). The *atpnp-a* mutant shows more severe symptoms of infection than the *AtPNP-A* wildtype line in response to the avirulent *P. syringae* DC3000 *AvrB*, as indicated by the arrows.

different in terms of their susceptibility to virulent *P. syringae* after spraying. However the *atpnp-a* mutant had greater bacterial titres than the wildtype line in response to spray inoculation with the avirulent pathogen. This phenotype persisted over days 2 and 3 and was significant ($p < 0.05$) at day 3. Importantly this phenotype is robust since it has been observed in independent experiments. In fact the bacterial numbers reached in the *atpnp-a* mutant infected with the avirulent pathogen were equivalent to those attained in response to virulent *P. syringae*. These differences were clearly visible as the *atpnp-a* mutant developed more severe chlorosis than the wildtype (Figure 3.31). Therefore the *atpnp-a* mutant is compromised in its resistance to avirulent *P. syringae* following spray inoculation and appears to have lost the defence response to the avirulent pathogen allowing this pathogen to become virulent to the plant.

3.3.16 *H. parasitica*

In some cases plants that are more susceptible to *P. syringae* infection are also more susceptible to *H. parasitica* (Knoth *et al.*, 2007; Li *et al.*, 2006; Li *et al.*, 2004; Nawrath and Metraux, 1999). For this reason, a preliminary experiment was conducted in order to test whether the *atpnp-a* mutant was altered in its susceptibility to virulent *H. parasitica* isolate, HpNoks1 (Kunz *et al.*, 2008). Seven days after infection with *H. parasitica* sporangiophores emerge from stomates to complete the lifecycle of the pathogen (Glazebrook, 2005; Slusarenko and Schlaich, 2003). The numbers of sporangiophores per leaf, seven days post infection, were used to quantify plant susceptibility. Infection was successful with the wildtype and *atpnp-a* mutant lines developing sporangiophore numbers within the range previously reported (Knoth *et al.*, 2007; Mohr and Cahill, 2003) (Figure 3.32). The *atpnp-a* mutant had more sporangiophores per leaf than the wildtype line. This was also visibly apparent as leaves of the *atpnp-a* mutant looked more heavily infested with white sporangiophores than the wildtype line (Figure 3.33). These preliminary results suggest that *AtPNP-A* may play a role in the defence response to *H. parasitica*.

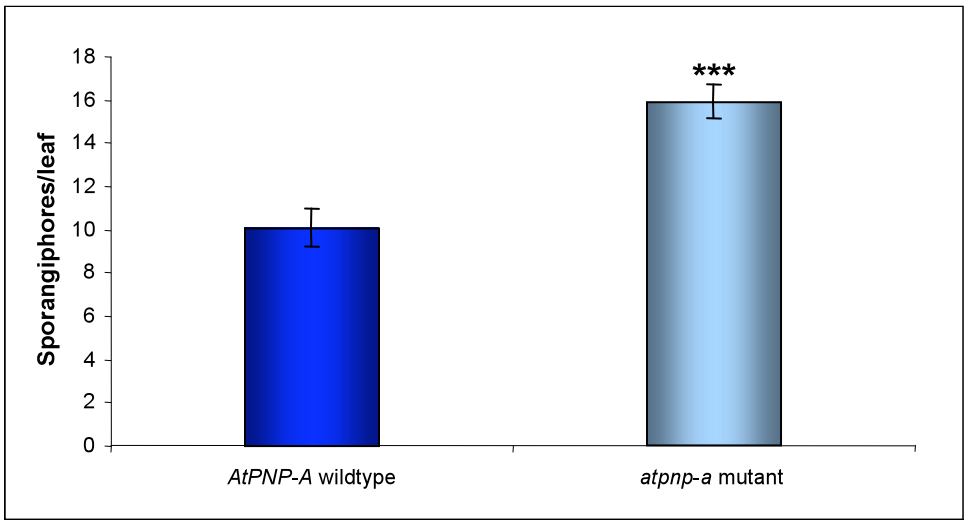

Figure 3.32. *H. parasitica* susceptibility of the wildtype and *atpnp-a* mutant lines

The susceptibility of four week old soil grown wildtype and *atpnp-a* mutant lines was measured seven days after infection with *H. parasitica* virulent NpNoks1 isolate by counting the number of sporangiophores per leaf. Data is the mean of n = 76 and n = 73 leaves for the wildtype and mutant lines respectively. Error bars are standard errors of the means. The statistical difference between the wildtype and *atpnp-a* mutant lines was determined by a t test with *** showing $p < 0.001$.

***AtPNP-A* wildtpe**

***atpnp-a* mutant**

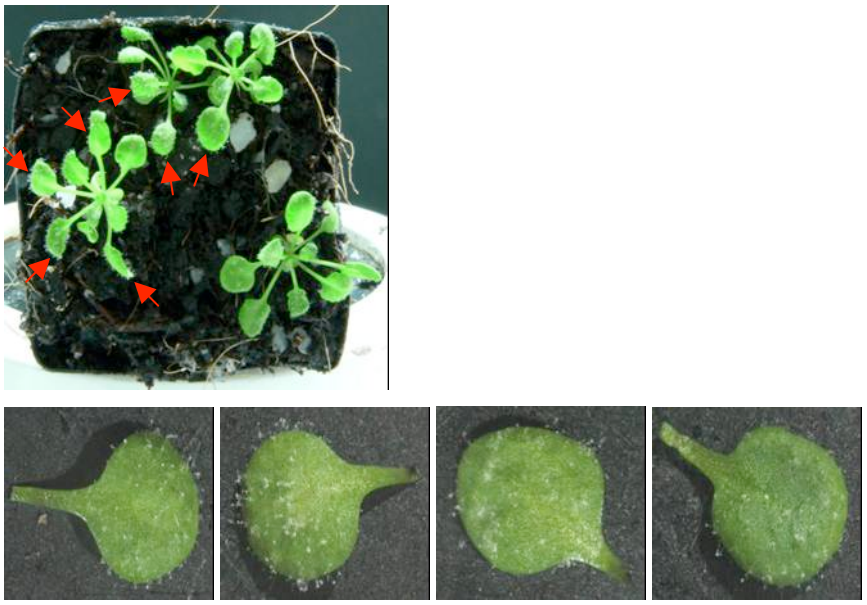

Figure 3.33. Representative photographs of *H. parasitica* infected wildtype and *atpnp-a* mutant plants and individual leaves

AtPNP-A wildtype (upper panels) and *atpnp-a* mutant (lower panels) lines seven days post infection with *H. parasitica* HpNoks1. Pictures of whole infected plants (infected leaves indicated by the arrows) and individual leaves (at 4 X magnification) are shown. Heavier infection of the *atpnp-a* mutant line was clear from the pictures of the individual leaves whose surface was covered with the dense white mass of sporangiophores.

3.4 DISCUSSION

3.4.1 The *atpnp-a* mutant

A homozygous SALK T-DNA insertion mutant in the *AtPNP-A* gene was isolated to test the phenotypic effects of reduced *AtPNP-A* expression. In characterizing this mutant a discrepancy over the annotation of the *AtPNP-A* gene was highlighted. TAIR annotates the *AtPNP-A* gene as having an additional third exon that codes for a single aa before terminating in the TGA STOP codon; whereas Ludidi reports the *AtPNP-A* gene as having two exons with the second exon being read through by one bp before terminating in an immediate TAA STOP codon, however there is no biological evidence to support the latter (Ludidi *et al.*, 2002). It appears that both STOP codons could be authentic since each is followed by a polyadenylation signal approximately 60 bp downstream from the STOP codon suggesting that the *AtPNP-A* mRNA may be alternatively spliced. It should be noted that the polyA tail does not necessarily follow directly after the polyadenylation signal but occurs at some point downstream of this signal. An RT-PCR approach was taken to resolve this and resulted in products that agree with the sizes predicted by both TAIR and Ludidi, however genomic DNA contamination is probably the source of the fainter larger product that corresponds to the size predicted by Ludidi (Ludidi *et al.*, 2002). To completely exclude the possibility of alternative splicing 3' RACE (random amplification of cDNA ends) should be performed. The major cDNA product is that predicted by TAIR, hence the T-DNA insertion is concluded to lie in the second intron of the *AtPNP-A* gene. It is perhaps interesting to note the *AtPNP-A* gene, while dissimilar in sequence is similar in structure to that of the animal NP genes which are also encoded by three exons, the last of which only codes for a single aa (Pandey, 2005). This structure of the *AtPNP-A* gene has some connotations for the published literature. For example, the loss of the expansin cell wall binding domain from the irPNP-like molecules would no longer coincide with the loss of an intron/exon boundary as has been reported (Ludidi *et al.*, 2002; Meier *et al.*, 2008).

Most importantly, the homozygous SALK_000951 T-DNA insertion mutant has reduced *AtPNP-A* expression demonstrating that it truly is an *atpnp-a* mutant. The *atpnp-a* mutant mRNA is missing exon 3 which encodes the last aa, the STOP codon and the 3' UTR of the *AtPNP-A* gene. It is unlikely that a single aa would affect the expression of the *AtPNP-A* gene but more likely that *AtPNP-A* mRNA is less stable in the mutant because it lacks a functional STOP codon and the 3' UTR. Since the T-DNA insertion lies in an intron it is also possible that there may still be some correct splicing of the mRNA (Ostergaard and Yanofsky, 2004; Xiong *et al.*, 2002a).

It is important to characterize a second mutant in the *AtPNP-A* gene in order to confirm that any phenotypes observed in the SALK_000951 line are the result of the mutation in the *AtPNP-A*

gene and not caused by additional T-DNA or second site mutations (not T-DNA tagged) that could be present in the SALK line (Ostergaard and Yanofsky, 2004). Since there were no other mutants available at the time of this study the alternative approach to complement the *atpnp-a* mutant with the wildtype copy of the *AtPNP-A* gene was undertaken. This was not a true complementation as the wildtype gene was placed under the control of the CaMV 35S promoter rather than the native promoter. Unfortunately, the complementation failed because the *AtPNP-A* transgene was not overexpressed in two independent lines that were homozygous for the overexpression construct. The overexpression construct may have integrated into transcriptionally silent regions of the genome in both lines or the overexpression construct may have been silenced as has been observed when there are multiple transgenes containing the same sequences (Daxinger *et al.*, 2008). That is, both the SALK T-DNA and the overexpression construct contain the CaMV 35S promoter sequence. The complementation construct was sequenced during cloning but did not reveal any obvious errors, for example in splice sites, which would explain why it was not expressed. It is more likely that the overexpression construct was not expressed because it is missing some key regulatory elements from the promoter, second intron (the first intron is present since the complementation construct was cloned from genomic DNA), third exon or 3' UTR. Most importantly the complementation construct does not actually contain the sequence that is disrupted in the *atpnp-a* mutant – that of the third exon which encodes the 3' UTR, as it was designed from the sequence predicted by Ludidi and colleagues (Ludidi *et al.*, 2002), prior to the knowledge of their misannotation of the gene. It is therefore not surprising this complementation has not worked, however this does not explain why the transgene was not expressed. Importantly, the fact that the coding sequence predicted by Ludidi was not able to complement *AtPNP-A* expression in the *atpnp-a* mutant further indicates that this sequence does not produce a functional mRNA and supports the notion that the TAIR annotation of the *AtPNP-A* gene is correct. To be sure that the phenotypes seen in the *atpnp-a* mutant are due to reduced *AtPNP-A* expression, a second mutant in the *AtPNP-A* gene must still be characterized or the complementation needs to be repeated successfully. Presently there is another T-DNA insertion line (CSHL_GT12338) available that is predicted to have a T-DNA in the 5' UTR of the *AtPNP-A* gene, just upstream to the START codon. This is expected to produce a null mutation which may make phenotypes easier to interpret (Hirschi, 2003). It is however possible that a null *atpnp-a* mutant could be lethal since it was originally difficult to isolate a homozygous mutant line and it was not possible to re-isolate homozygous *atpnp-a* mutant individuals from a backcross (data not shown). Therefore the complementation should be repeated as well ensuring that the native promoter and 3' UTR are included. Alternatively, one could make an inducible RNAi line which would allow control over the timing and level of *AtPNP-A* silencing.

3.4.2 Phenotypes of the *atpnp-a* mutant

3.4.2.1 Growth phenoptypes

The *atpnp-a* mutant has smaller cells but increased cell numbers in its developing leaves when compared to the wildtype line. This suggests that the *atpnp-a* mutant is compromised in cell expansion which is compensated for by an increase in cell division. Compensation is a phenomenon based on coordinate regulation of cell expansion and cell division and in most cases refers to mutants that have reduced cell division compensated for by increased cell expansion in order to produce leaves of the correct size (Ferjani *et al.*, 2007; Horiguchi *et al.*, 2006). The *atpnp-a* mutant appears to undergo cell division at a reduced cell size, dividing until it reaches the correct number of cells per leaf, after which time the cells recover the ability to expand normally to reach their correct final size. This would suggest that there is a difference between the early expansion process when the cells are still dividing and later postmitotic expansion when cells have finished dividing and are expanding to reach their final size. A recent paper that examined a number of compensation mutants has found that in all cases except one, compensation is a postmitotic event that either involves an increase in the rate or duration of expansion (Ferjani *et al.*, 2007). The exception to this rule was the *KIP-RELATED PROTEIN 2* (*KRP2*) overexpressor mutant in which expansion is enhanced during cell proliferation. It was suggested that this mutant has an increased set point for the cell size at which division occurs. Since the *atpnp-a* mutant presents the opposite phenotype it is conceivable that the set point for cell size at which division occurs is decreased in the *atpnp-a* mutant.

The fact that the *atpnp-a* mutant is affected in its epidermal cell size is interesting because the epidermal cells expand rapidly to drive the expansion of the entire leaf (Shabala, 2003; Van Volkenburgh, 1999). These cells are able to do this because they have very large vacuoles, occupying almost the entire volume of the cell (Karley *et al.*, 2000; Shabala, 2003) using K^+ as their main osmoticum (Fricke *et al.*, 1994; Shabala, 2003). This could be similar to the expansion process that occurs in cells that are rapidly expanding during cell proliferation. That is, inorganic ions may be used as cheap osmotica to provide for turgor for rapid cell expansion whereas at later stages time allows for the production of solutes to fulfil this role (Gonzalez-Guzman *et al.*, 2002; Shabala and Lew, 2002). Thus AtPNP-A may indeed be involved in drawing water and ions into the cell to provide this turgor pressure required for rapid cell expansion, consistent with the hypothesis that AtPNP-A cooperates with expansins during expansive growth (Ludidi *et al.*, 2002; Morse *et al.*, 2004).

The *atpnp-a* mutant has greater stomatal numbers in the mature leaf compared to the *AtPNP-A* wildtype line (albeit not statistically significant). Stomatal density is strictly correlated with

epidermal cell size and number (Masle *et al.*, 2005; Wang *et al.*, 2007b). Since epidermal cell size and number are not different between the *atpnp-a* mutant and wildtype lines in these leaves, this implies that the *atpnp-a* mutant has a higher stomatal density than the wildtype. Stomatal density may not actually have much affect on photosynthetic parameters because differences in stomatal density can be compensated for by changes in stomatal aperture (Bussis *et al.*, 2006). Therefore water usage efficiency and stomatal conductance would need to be measured in the *atpnp-a* mutant in order to determine whether the stomatal phenotype actually affects physiological function (Nilson and Assmann, 2007). Interestingly the stomata of the *atpnp-a* mutant have significantly reduced apertures when compared to the stomata of the wildtype. It appears then that AtPNP-A is in fact involved in stomatal opening *in planta*. Smaller stomatal apertures would allow the *atpnp-a* mutant to compensate for reduced turgor, by preventing further water loss. Both cell expansion and stomatal opening involve increases in cell turgor (Cosgrove, 2000a; Nilson and Assmann, 2007). Therefore the *atpnp-a* mutant is defective in processes that require increases in cell turgor, suggesting that AtPNP-A does increase cell turgor *in planta*.

3.4.2.2 NaCl and osmotic stress phenotypes

The *atpnp-a* mutant is more tolerant than the wildtype line of NaCl, KCl and sorbitol during germination. Sorbitol imposes an osmotic stress while NaCl and KCl both impose an ionic stress in addition to the osmotic stress, therefore the *atpnp-a* mutant can be described as being primarily osmotolerant (Saleki *et al.*, 1993). Since the *atpnp-a* mutant is more tolerant than the wildtype of both NaCl and KCl, the mutant may be more tolerant of the ionic stresses imposed by Na^+ and K^+ or better able to cope with the toxic affects of Cl^-. It is interesting then that irPNP and recombinant AtPNP-A treatment has been shown to induce uptake of all of these ions (Ludidi *et al.*, 2004; Maryani *et al.*, 2000; Pharmawati *et al.*, 1999) and animal NPs exert their natriuretic and diuretic effects by inducing movement of these ions (Kourie and Rive, 1999; Sindic *et al.*, 2005). To further investigate these phenotypes a range of other salts could be tested in the germination media. For example LiCl could be used to test whether AtPNP-A is involved in ionic stress responses since Li^+ imposes a similar ionic stress to Na^+ but is more toxic so that it can be used at concentrations where its osmotic affects are negligible (Gao *et al.*, 2006; Ruggiero *et al.*, 2004; Saleki *et al.*, 1993; Wu *et al.*, 1996a). Similarly Na_2SO_4 and K_2SO_4 can be used to determine whether the tolerance of the *atpnp-a* mutant is specific to the stress imposed by Na^+ and K^+ or Cl^- (Gao *et al.*, 2006; Quesada *et al.*, 2000; Saleki *et al.*, 1993; Wu *et al.*, 1996a).

The *atpnp-a* mutant is unlikely to be affected in germination *per se* because its germination efficiency on basal media was not different from that of the wildtype. Early studies have shown

that wildtype seed that fail to germinate on NaCl-supplemented media retain their ability to germinate when transferred onto basal media, suggesting that mutants that germinate under stress conditions actually lack perception or signal transduction of the stress (Saleki *et al.*, 1993; Werner and Finkelstein, 1995). It has subsequently been shown the majority of mutants that are more tolerant of NaCl and osmotic stress during germination are affected in ABA signalling since ABA inhibits inappropriate germination under stress conditions (Verslues *et al.*, 2006). The *atpnp-a* mutant however does not appear to be compromised in ABA signalling. Thus despite there being evidence for interplay between AtPNP-A and ABA in stomatal closure responses, this probably does not happen *in planta* (Wang *et al.*, 2007c).

The interplay between ABA and germination means that phenotypes at later stages of development may be more telling of true NaCl and osmotic stress tolerance. The *atpnp-a* mutant was able to attain greater FW per seedling than the wildtype line, however did not show any difference in its root growth on NaCl-supplemented media, implying that the *atpnp-a* mutant is also more tolerant of NaCl at the seedling stage and that this tolerance could be specific to the shoot. While similar measurements have been used to assess stress sensitivity of the seedling (Quesada *et al.*, 2000; Ruggiero *et al.*, 2004), it perhaps would have been better to germinate seed on basal media and then transfer seedlings to media supplemented with NaCl (Verslues *et al.*, 2006) to completely exclude any germination effect. The root is better able to cope with NaCl stress than the shoot because it can either return Na^+ back to the soil solution or incorporate Na^+ into the vacuoles of its rapidly elongating cells for use as osmoticum (Dolan and Davies, 2004; Munns, 2002; Munns, 2005). The shoot on the other hand must either load Na^+ into the phloem for transport back to the root running the risk of Na^+ being transported to growing leaves, or it must compartmentalize Na^+ in the vacuole where it accumulates to toxic levels and causes premature senescence (Berthomieu *et al.*, 2003; Munns, 2002; Shi *et al.*, 2002a; Sunarpi *et al.*, 2005). The tissue-specific NaCl tolerance of the *atpnp-a* mutant suggests that it is affected in one of these tissue-specific strategies for coping with NaCl stress. In support of this notion other mutants that display tissue-specific NaCl sensitivity are thus affected. For example a *cbl10* mutant has recently been described that has altered sensitivity to NaCl stress only in the shoot tissue (Kim *et al.*, 2007). CBL10 interacts with SOS2 in the shoot where it is proposed to play a role in Na^+ sequestration. It is notable then that ion sequestration also plays an important role in cell expansion since mutants affected in vacuolar Na^+ compartmentalization have smaller cells like those of the *atpnp-a* mutant (Apse *et al.*, 2003). Addtionally an *hkt1* mutant displays NaCl sensitivity in the shoot but NaCl tolerance in the root and is affected in recirculation of Na^+ between the shoot and root tissue (Maser *et al.*, 2002).

3.4.2.3 The atpnp-a mutant is affected in ion homeostasis

The *atpnp-a* mutant is more tolerant of K^+ deficiency than the wildtype. Since NaCl stress induces K^+ starvation (Shabala and Cuin, 2008), this may be the basis of the NaCl tolerance of the *atpnp-a* mutant. To the best of my knowledge there are no other reports of mutants that have improved tolerance to K^+ starvation. Mutants that are hypersensitive to low K^+ have been suggested to be affected in high affinity K^+ uptake (Wu *et al.*, 1996a) or less efficient at using K^+ (Liu and Zhu, 1997). Conversely the *atpnp-a* mutant may be more effective at high affinity K^+ uptake or better at using the available K^+. High affinity K^+ uptake is important under conditions of low external K^+ and NaCl stress because these transporters are more selective for K^+ over Na^+ (Liu and Zhu, 1997; Rus *et al.*, 2001). This is not in conflict with the fact that the *atpnp-a* mutant is also more tolerant of high concentrations of KCl because different K^+ uptake routes operate at different external K^+ concentrations (low affinity K^+ uptake acts at high external K^+) (Liu and Zhu, 1997; Wu *et al.*, 1996a). Germination assays with CsCl and RbCl in the media could be used to determine whether high affinity K^+ uptake mechanisms are affected in the *atpnp-a* mutant (Gao *et al.*, 2006; Tsugane *et al.*, 1999; Werner and Finkelstein, 1995; Wu *et al.*, 1996a) since these are inhibited by Cs^+ and Rb^+.

Consistent with a possible role for AtPNP-A in ion homeostasis, the *atpnp-a* mutant has altered ion content compared to the wildtype. In particular, the *atpnp-a* mutant had significantly less Na^+ and K^+ as well as a lower K^+/Na^+ ratio (albeit not significant) under control conditions, suggesting that the *atpnp-a* mutant may be affected in its ability to draw ions in its basal state. If not adjusted for (for example by compatible solutes), the *atpnp-a* mutant would have lower turgor which would impede cell expansion, as has been observed. There is no difference however between the *atpnp-a* mutant and wildtype in terms of its Na^+ or K^+ content or K^+/Na^+ ratio following either NaCl or mannitol treatment suggesting that the *atpnp-a* mutant accumulated more Na^+ and retained more K^+ in response to these stresses and that the *atpnp-a* mutant has altered capacity for Na^+ and K^+ uptake. This may be a compensation mechanism if AtPNP-A is used to draw ions and in its absence the plant adjusts the activity of its transporters to better enable it to take up and retain ions and consequently water. This supports the idea that AtPNP-A is involved in ion uptake and agrees with findings that irPNP treatment induces Na^+ and K^+ uptake (Pharmawati *et al.*, 1999). Increased Na^+ uptake in response to NaCl does not negatively impact on the phenotype of the *atpnp-a* mutant which is more tolerant than the wildtype, consistent with the reports that Na^+ uptake is no longer considered to be the major determinant of salinity tolerance (Shabala and Cuin, 2008; Tester and Davenport, 2003). Rather, NaCl tolerance is correlated with K^+ content (Zhu *et al.*, 1998) and specifically the K^+/Na^+ ratio since this reflects K^+ homeostasis in the face of NaCl stress (Gao *et al.*, 2006; Zhu, 2003). The reduction in the K^+/Na^+ ratio in response to stress treatment was less in the *atpnp-a*

mutant compared to the wildtype. Therefore the *atpnp-a* mutant better maintains its K^+/Na^+ ratio in the face of NaCl and osmotic stress and can therefore be considered an ion homeostasis mutant.

K^+ efflux in response to NaCl treatment, similar to the K^+/Na^+ ratio, serves as a measure of K^+ homeostasis under conditions of NaCl stress (Shabala and Cuin, 2008). The *atpnp-a* mutant showed zone-specific differences in K^+ flux in response to NaCl. This is consistent with a report by Ludidi that showed spatially distinct ion fluxes in response to recombinant AtPNP-A treatment and suggests that this holds true *in planta* (Ludidi *et al.*, 2004). Specifically, the *atpnp-a* mutant has greater K^+ efflux in the elongation zone and improved K^+ retention in the mature zone of the root in response to NaCl when compared to the wildtype. Greater Na^+ uptake (as suggested by the ion accumulation results) in the elongation zone of the *atpnp-a* mutant would result in greater membrane depolarization and thereby greater K^+ loss. Cells in the elongation zone are still expanding and may be able to better cope with NaCl stress by incorporating Na^+ into their vacuoles thereby providing osmoticum (Dolan and Davies, 2004; Munns, 2002). Greater K^+ efflux from the elongation zone of the root in the *atpnp-a* mutant points to a positive role for AtPNP-A in preventing K^+ efflux in the wildtype situation consistent with a role for AtPNP-A in drawing ions for turgor in expanding cells and complements the cell size data. The *atpnp-a* mutant effluxes less K^+ from the mature zone than the wildtype in accordance with a role for AtPNP-A in K^+ uptake in this zone, as was reported in response to recombinant AtPNP-A treatment (Ludidi *et al.*, 2004). Reduced ion fluxes at this location (where ions can't be incorporated into expanding cells) may prevent ions being loaded into the transpiration stream, considering that irPNPs have also been shown to induce ion fluxes in the stele (Maryani *et al.*, 2003; Pharmawati *et al.*, 1999).

In the *atpnp-a* mutant, K^+ efflux from the root elongation zone in response to NaCl stress is more sensitive to inhibition by Zn^{2+} than the wildtype. Zn^{2+} inhibits NSCCs which are thought to be the main points of entry for Na^+ and Zn^{2+} has also been found to inhibit the activity or gating of K^+ transporters (Shabala *et al.*, 2005b). Thus the *atpnp-a* mutant may have a higher abundance of NSCCs or Zn^{2+}-sensitive K^+ channels in the elongation zone of its root, or its channels may be more sensitive to Zn^{2+}. Therefore the difference in the K^+ fluxes from the *atpnp-a* mutant and wildtype roots may be encoded by the abundance, distribution or activity of its transporters which could also account for differences in magnitude of the NaCl induced K^+ fluxes from the different zones of the *atpnp-a* mutant and wildtype roots.

The fact that the *atpnp-a* mutant is more resistant than the wildtype to all nutrient deficiencies, ionic and osmotic stresses tested suggests that the *atpnp-a* mutant is better adapted to dealing

with homeostatic disturbances and that the function of AtPNP-A in the wildtype situation is as a negative regulator of ionic and osmotic stress tolerance. This supports a role for AtPNP-A as a regulator of water and ion homeostasis. Based on the phenotypes of the mutant, AtPNP-A is proposed modulate Na^+ and K^+ uptake and retention probably by regulating ion transport; for example AtPNP-A may act on ion channels such as NSCCs that are capable of transporting both of these ions. While ion uptake may not be advantageous to the plant under stress conditions, it is crucial in the normal case for the maintenance of turgor required for cell expansion and growth which would explain why AtPNP-A function has been retained over the evolution of plants.

3.4.2.4 Biotic stress phenotypes reveal a potentially novel role for AtPNP-A:

Not only does AtPNP-A play a role in the response to abiotic stress but it is also involved in biotic stress responses since the *atpnp-a* mutant was more susceptible to the biotrophic pathogens, *P. syringae* and *H. parasitica*. The fact that the *atpnp-a* mutant was tolerant of abiotic stresses but compromised in its defence against biotrophic pathogens and unaffected in its response to the necrotroph *B. cinerea* suggests that AtPNP-A is not simply involved in a common response to both abiotic and biotic stress but that AtPNP-A plays a specific role in the defence against biotrophic pathogens. The finding that the *atpnp-a* mutant is more susceptible to avirulent but not virulent *P. syringae* speaks against a role for AtPNP-A in the basal defence responses commonly initiated by both pathogens. More likely AtPNP-A is involved in ETI that is specifically induced by the avirulent pathogen. The *atpnp-a* mutant only presents its phenotype when spray inoculated implying that AtPNP-A does not play a role in downstream ETI defences but instead it is involved in the early recognition of the avirulent pathogen likely involving the stomatal defence response. This does not appear to be linked to the stomatal phenotype of the *atpnp-a* mutant as this would influence resistance to both the virulent and avirulent pathogens. Virulent *P. syringae* reopens stomata through the action of the phytotoxin COR (Melotto *et al.*, 2006). COR is probably one of many such virulence factors since *P. syringae* mutants that don't have COR are still able to open stomata (Melotto *et al.*, 2006). Avirulent bacteria are less effective at stomatal reopening suggesting that there are either Avr factors that promote stomatal reopening that are recognized by the plant triggering ETI and stomatal closure or that the ETI response to the avirulent pathogen specifically acts to close stomata by a mechanism removed from the PTI response (Melotto *et al.*, 2006). The *atpnp-a* mutant appears to have lost the avr-R gene for gene recognition of the avirulent pathogen following spray inoculation since the avirulent pathogen becomes virulent on the host. Therefore AtPNP-A may play a role in this early recognition of the Avr pathogen and resultant inhibition of stomatal reopening. The more susceptible phenotype of the *atpnp-a* mutant implies a positive role for AtPNP-A in pathogen defence, whether this involves AtPNP-A being

used by the plant in defence or being manipulated by the pathogen triggering recognition by the plant, remains to be unravelled.

Preliminary results suggest that AtPNP-A also plays a role in defence again *H. parasitica*. In this case the *H. parasitica* strain tested was virulent and may suggest a more general role for AtPNP-A in the defence against this pathogen. This could involve some aspect of SA signalling which is commonly induced by both *H. parasitica* and *P. syringae*. Alternatively the more susceptible phenotype of the *atpnp-a* mutant may be linked to its greater stomatal density since sporangiophore density has been reported to correlate with stomatal density (Slusarenko and Schlaich, 2003). Finally, it is interesting to note also that there is evidence for a role for ANP in the animal immune system (Vollmar, 2005). These results reveal a previously unconsidered role for AtPNP-A in the response to pathogens.

3.4.3 Summary

Reduced *AtPNP-A* expression results in plants that have smaller cell sizes in the developing leaves and reduced stomatal apertures. The *atpnp-a* mutant plants also display increased NaCl and osmotic stress tolerance and alterations to their ion homeostasis. These phenotypes are consistent with a role for AtPNP-A in cell expansion and water and ion homeostasis as has been suggested from the literature. Furthermore characterization of *atpnp-a* mutant revealed a potential role for AtPNP-A in the response to pathogens. Specifically AtPNP-A may be involved in the stomatal response to avirulent pathogens. These phenotypes while interesting need to be confirmed in a second mutant or by complementation. In total these results suggest that AtPNP-A plays an important role in both growth and in the response to abiotic and biotic stresses.

CHAPTER 4

AtPNP-A TRANSCRIPTOMICS

CHAPTER 4: *AtPNP-A* TRANSCRIPTOMICS

4.1 INTRODUCTION

There are a number of ways to explore gene function. In the previous chapter insight was gained into the function of AtPNP-A through the characterization of an *atpnp-a* mutant. The *atpnp-a* mutant had smaller cells in its developing leaves and greater NaCl tolerance than the wildtype, supporting the proposed role for AtPNP-A in cell expansion and maintenance of water and ion homeostasis (Morse *et al.*, 2004; Rafudeen *et al.*, 2003). Additionally the *atpnp-a* mutant revealed a role for AtPNP-A in the response to pathogens that had not before been considered. The mutant analysis however was hampered in that the *atpnp-a* mutant phenotypes could not be confirmed in a second mutant, neither could they be complemented.

4.1.1 Exploring gene function in *Arabidopsis*

The study of mutants while useful has certain limitations. For example null mutation of some genes does not result in any obvious phenotype, probably due to compensation by redundant genes or genes that have been recruited to perform the function of the missing gene in the mutant (Hirschi, 2003). In fact as many as 65% of *Arabidopsis* genes can be placed into gene families based on sequence similarity, leading to the suggestion that only around 10% of genes will produce a loss of function mutant phenotype (Meinke *et al.*, 1998). Furthermore phenotypes of mutants may not truly reflect the function of the wildtype gene as pleiotrophic effects may be associated with loss of gene function (Hirschi, 2003). In contrast gene expression studies look at the natural behaviour of the gene. It is assumed that if expression of a gene is induced under a particular set of conditions, then its gene product is functionally important in the adaptation to those conditions. Thus inferences of gene function can be made from gene expression data. Not long after the *Arabidopsis* genome was sequenced, whole genome microarrays were developed to allow global transcript profiling (Allemeersch *et al.*, 2005; Redman *et al.*, 2004). The use of standardized microarray platforms and processing methods such as those provided by Affymetrix and the requisite that microarray data be made publicly available has made the data generated across many diverse experiments comparable and resulted in the development of a large number of freely available web-based tools that can be used to analyze this data (Zimmermann *et al.*, 2004).

4.1.2 Mining expression data for inferences of gene function

An initial approach to exploring microarray expression data is to screen the expression profile of a particular gene of interest (GOI) across a large number of diverse experiments in order to identify conditions under which the GOI is highly differentially expressed and thus may play an

important function. It is becoming increasingly apparent that genes do not act in isolation but rather function together coherently to elicit common biological responses (Eisen *et al.*, 1998). It has been demonstrated that genes that function together or that have interacting protein products are co-ordinately expressed (or co-expressed) (Eisen *et al.*, 1998) and that there is evolutionary pressure to maintain this co-regulation (Fraser *et al.*, 2004). Co-expression is assumed to be orchestrated by a common set of transcription factors that bind conserved motifs in the promoters of co-expressed genes (Allocco *et al.*, 2004). Within a single microarray experiment co-expression is complicated by the fact that multiple transcription regulatory pathways may be activated in response to a particular treatment and therefore the co-expression of genes may be coincidental. However when considered across multiple, diverse experimental conditions it becomes more likely that consistently co-expressed genes are functionally related and regulated by a common mechanism (Allocco *et al.*, 2004; Meier and Gehring, 2008). A number of computational tools are available to perform correlation analysis to identify genes that frequently co-express with a defined GOI. Correlation analysis calculates the similarity between the expression pattern of every gene relative to the GOI and assigns this a correlation value (*r*-value). Genes are then ranked according to their *r*-values in order to generate an expression correlated gene group (ECGG) that is the group of genes most highly co-expressed with the GOI. Correlation analysis has been used to infer gene function in cases where genes of unknown function are correlated with genes of well defined function (Persson *et al.*, 2005). The ECGG can be examined visually for genes of known function, however this is limited by an individual's knowledge of the biological systems (Manfield *et al.*, 2006). A superior and unbiased approach is to perform an in depth computational analysis of the ECGG in order to infer the function of the ECGG. Meier and Gehring (2008) suggest the use of three complementary techniques to characterize the ECGG. Firstly a gene ontology (GO) analysis is used to determine functional enrichment in GO terms associated with the ECGG compared to the genome. Second a promoter content analysis is performed to identify over-representation of transcription factor binding sites (TFBSs) in the ECGG compared to the genome that may regulate the co-expression of the ECGG. Finally an expression analysis is used to identify conditions under which the ECGG is highly expressed and thus likely to function. The aim of this study was to infer the function of AtPNP-A from a 'systems' perspective, using a computational analysis to explore the expression profile of *AtPNP-A* and to generate an *AtPNP-A* ECGG. The *AtPNP-A* ECGG was then subjected to GO, promoter and expression analyses to assign function to the ECGG and consequently AtPNP-A. Finally a microarray experiment was conducted to investigate the affect of recombinant AtPNP-A treatment on the *Arabidopsis* transcriptome. The results were assessed in the context of the *atpnp-a* mutant phenotypes and physiological responses to PNPs to ascertain whether they provide any additional evidence to support a role for AtPNP-A in growth, abiotic and biotic stress responses.

4.2 METHODS

4.2.1 Correlation analysis: The *Arabidopsis* Co-expression Tool (ACT)

The *Arabidopsis* Co-expression Tool (ACT) which is part of the Arabidopsis Co-expression Data Mining Tools (ACDMT) (www.arabidopsis.leeds.ac.uk/act) (Manfield *et al.*, 2006) was used to perform a correlation analysis using *AtPNP-A* as the driver gene. The *AtPNP-A* gene (At2g18660) is represented by a single probe, 266070_at, on the Affymetrix ATH1 22 k arrays. ACT calculates a Pearson correlation (*r*-value) based on the hybridization signal intensity for each probe across the 322 Affymetrix ATH1 22 k microarrays in its database. The *r*-value reflects the strength and direction of the relationship between every represented gene and the driver gene ranging from 1 to -1 (perfect positive or negative correlation respectively). Genes are ranked in descending order according to their *r*-values to generate an ECGG. A list of the 100 probes whose expression is most positively correlated with that of *AtPNP-A* was extracted. This list was edited to remove probes that hybridize more than one gene as their expression profile is unreliable. From the unique probes that remained, the genes corresponding to the 50 probes whose expression is most positively correlated with that of *AtPNP-A* was used to compile the ECGG. The *AtPNP-A* ECGG refers to these 50 genes whose expression is most positively correlated with *AtPNP-A*.

4.2.2 Gene ontology analysis: Fast Assignment and Transference of Information using Gene Ontology (FatiGO)

The FatiGO compare tool within the Babelomics suite (http://www.babelomics.org/) (Al-Shahrour *et al.*, 2004; Al-Shahrour *et al.*, 2007; Al-Shahrour *et al.*, 2005) was used to identify functional enrichment in GO terms associated with the *AtPNP-A* ECGG compared to the genome, across GO levels 3-9. At higher levels in the GO hierarchy the GO annotations become more precise with fewer genes being annotated. FatiGO uses a Fisher exact test to generate a p value that is then adjusted to correct for multiple testing using the False Discovery Rate (FDR) procedure of Benjamini and Hochberg. The analysis was run selecting all three GO categories: GO biological process, GO molecular function and GO cellular component; as well as KEGG pathways and SwissProt Keywords which can be searched for simultaneously. Other settings used were: never to remove duplicates and to return overrepresented terms in list one (*AtPNP-A* ECGG). KEGG pathways returned were blasted against the KEGG database (http://www.genome.ad.jp/kegg/pathway.html). GO terms that were only represented by one *AtPNP-A* ECGG gene were not reported since these are unlikely to reflect the function of the group as whole. The same parameters were used to analyze the four lists of differentially expressed genes identified in the recombinant AtPNP-A microarray experiment (genes upregulated and downregulated by 1 hr recombinant AtPNP-A treatment and genes induced and repressed by 24 hr AtPNP-A treatment).

4.2.3 Promoter content analysis

4.2.3.1 Arabidopsis thaliana Expression Network Analysis (Athena)

The Athena (http://www.bioinformatics2.wsu.edu/Athena) (O' Conner *et al.*, 2005) database contains the promoter sequences for all *Arabidopsis* genes as well as the consensus sequences for all 105 known TFBSs. Athena was used to visualize the distribution of TFBSs in the promoters of the *AtPNP-A* ECGG and to compute enrichment in TFBSs in these promoters compared against all the promoters in the

genome. A Bonferroni correction method that corrects for multiple testing has been used to determine that the p value threshold for significant enrichment is $p < 10^{-4}$. Promoter regions of 1000 bp were evaluated and it was chosen not to cut off at adjacent genes. Athena was also used to determine enrichment in TFBSs in the promoters of the differentially expressed genes identified in the recombinant AtPNP-A microarray experiment (the same four lists of genes as those specified above in section 3.2.2).

Two different enumerative methods were used to calculate enrichment in computationally-derived motifs in the 1000 bp promoter regions of the ECGG compared against the promoters of the genome. Both methods analyze the promoter region upstream of the ATG START site rather than that transcription start site (TSS) because the latter is often poorly defined and in some cases the 5'UTR has been shown to alter transcription (Toufighi *et al.*, 2005).

4.2.3.2 Motif analysis

The motif analysis tool available on TAIR (http://www.arabidopsis.org/tools/bulkmotiffinder/index.jsp) was used to find enrichment in 6mer motifs in the *AtPNP-A* ECGG. Since this program does not account for multiple testing (Coulibaly and Page, 2008) only the motifs with the highest unadjusted p values ($p < 0.001$) were considered further.

4.2.3.3 Pronomer

The Pronomer tool within the Botany Array Resource (BAR) suite, was used to find enrichment in the frequency of motifs ranging from 4 to 10 nts in length in the *AtPNP-A* ECGG (http://bar.utoronto.ca) (Toufighi *et al.*, 2005) compared their frequency across the promoters in the genome. Default parameters were used that require the element to occur in a minimum of 75% of the genes.

4.2.3.4 POBO

The seven motifs that commonly emerged from the Motif Analysis and Pronomer results were analysed by POBO to verify their enrichment in the *AtPNP-A* ECGG (www.pobo.org) (Kankainen and Holm, 2004). POBO calculates the frequency of the motif in a group of promoters and compares this against its frequency in the genome promoters using a bootstrapped analysis to detect over or under representation with statistical confidence. POBO was used to evaluate the 1000 bp promoter sequences (downloaded from TAIR, http://www.arabidopsis.org/tools/bulk/sequences/index.jsp) (Rhee *et al.*, 2003) of the *AtPNP-A* ECGG. The parameters selected were: 50 for the number of sequences to pick out, 1000 for the number of samples to generate and the sequence length was 1000 bp. POBO was also used to examine enrichment in motifs known to be associated with defence genes in this same set of promoters including core (TTGAC) and stringent W box motifs (TTGACT, TTGACC and TTGACA), the TGA motif (TGACG) and the Whirly motif (GTCAAAA) (Desveaux *et al.*, 2004; Mahalingam *et al.*, 2003).

4.2.3 5 TRANSFAC

The seven motifs that commonly emerged from the Motif Analysis and Pronomer results were blasted against the TRANSFAC database (http://www.gene-regulation.com/pub/database.html) (Fogel *et al.*,

2005) using the PATCH tool (Matys *et al.*, 2006) in order to test whether they correspond to any known TFBSs. The motifs were queried against the set of plant transcription factors contained in the database, using the parameters: minimum length of site 4, maximum number of mismatches 1, mismatch penalty 100 and lower score boundary 87.5.

4.2.3.6 Scatter plot

The Scatter Plot tool in the ACDMT suite maps the correlation coefficients of all genes represented on the ATH1 22k microarrays relative to two user defined query genes (Manfield *et al.*, 2006). This was used to visualize the correlation between *AtPNP-A* and *WRKY DNA binding protein 70* (*WRKY70)*. Additional genes of interest that were selected to be highlighted included *PATHOGENESIS RELATED* (*PR*) genes: *PR1, PR2, PR5, ENHANCED DISEASE SUSCEPTIBILITY 1* (*EDS1*), *WALL-ASSOCIATED KINASE 1 (WAK1), NON-EXPRESSOR OF PR GENES 1* (*NPR1*), *MAP KINASE/ ERK KINASE 1* (*MEK1*), and *MAP KINASE KINASE 2* (*MKK2)*.

4.2.4 Expression analysis: Microarray data

Genevestigator V3 was used as a screening tool to identify experiments in which *AtPNP-A* is highly differentially expressed (https://www.genevestigator.ethz.ch) (Hruz *et al.*, 2008; Zimmermann *et al.*, 2004). This analysis examined the expression of the *AtPNP-A* probe (266070_at) across 3110 high quality ATH1 arrays (Redman *et al.*, 2004) from the NASC Tanscriptomics Service (NASCArrays) (Craigon *et al.*, 2004) (816), the Functional Genomics Centre Zurich (FGCZ) (55), Gene Expression Omnibus (GEO) at the National Centre for Biotechnology Information (NCBI) (Edgar *et al.*, 2002) (621), ArrayExpress at the European Bioinformatics Institute (EBI) (Brazma *et al.*, 2003) (412), AtGenExpress (1122), TAIR (57) and other sources (27) (Hruz *et al.*, 2008). The Meta-Profile Analysis tool was used to generate the expression profile of *AtPNP-A* in various anatomical parts, at different stages of development, in response to various stimuli and in the background of different mutations.

4.2.4.1 Growth

The following normalized microarray data was downloaded from NASCArrays (http://affymetrix.arabidopsis.info/narrays/experimentbrowse.pl) (Craigon *et al.*, 2004): the AtGenExpress development series (Schmid *et al.*, 2005) for examining expression in the sepal (NASC-152) and senescent leaf (NASC-150); the *N*-(1-naphthyl) phthalamic acid (NPA) (NASC-428) and isoxaben (NASC-27) treatments as well as the *continuous vascular ring 1* (*cov1*) (NASC-54) mutant array. The unprocessed microarray data for the *elongata 3* (*elo3*) mutant (E-MEXP-300) and the GA deficient *ga1* and *ga1-3 gai-t6 rga-t2 rgl1-1 rgl2-1* (*ga1 della*) (additionally lacks four DELLA proteins) mutants (E-MEXP-849) was obtained from Array Express (www.ebi.ac.uk/microarray-as/ae) (Brazma *et al.*, 2003) and normalized using RMA express (http://rmaexpress.bmbolstad.com/) (Bolstad *et al.*, 2003).

4.2.4.2 Abiotic stress

NASCArrays was also used to download the normalized data for the abiotic stress experiments including: NaCl (NASC-140), osmotic stress (NASC-139) and UV-B (NASC-144) time courses and the respective

controls (NASC-137) that are all part of the AtGenExpress Stress series (Kilian *et al.*, 2007); the ozone treatment (NASC-26) and K^+ starvation (NASC-105) (Hampton *et al.*, 2004) experiments as well as the phostphate starved *pho1* (NASC-102) and *pho3* (NASC-49) abiotic stress mutants.

4.2.4.3 Pathogen infection

Some of the data for generating the expression profiles of the *AtPNP-A* ECGG in the response to pathogens was also obtained from NASCArrays including the *P. syringae* ES 2346 and *Rpt2* (NASC-198) and the half leaf infection (NASC-168), *Erysiphe orontii* (NASC-169), *Phytophthora infestans* (NASC-123) and *B. cinerea* (NASC-167) treatments. While the data for the *Bemisia tabaci* (GSE6516) and *Erysiphe chichoracearum* (GDS1785) experiments were obtained from GEO (www.ncbi.nlm.nih.gov/geo) (Edgar *et al.*, 2002) and that for the *P. syringae Rpm1* and *Rps4* experiment was retrieved from Array Express (E-MEXP-546).

4.2.4.4 Defence response mutants

Array data for the defence response mutants was also downloaded from NASCArrays including *constitutive expression of PR genes 5* (*cpr5*) (NASC-355), *NahG* that expresses the bacterial salicylate hydroxylase (NASC-52), *npr1* (NASC-392) and *suppressor of NPR1, inducible 1* (*sni1*) (NASC-389). The remaining data from this set was obtained from Array Express including that for the *map kinase 4* (*mpk4*) (E-MEXP-174), *eds1* (E-MEXP-546) and *flagellin sensitive 2* (*fls2*) (E-MEXP-81) experiments, while the normalized data from the *WRKY70* overexpressor mutant was kindly provided by Dr Stuart Meier (SANBI) (through his correspondence with Dr Günter Brader, Univeristy of Helsinki).

4.2.4.5 Chemicals and hormones

NASCArrays contained the microarray data for the AtGenExpress Hormone series (Goda *et al.*, 2008) from which the SA (NASC-192), JA (NASC-174) and ABA (NASC-176) data was extracted. The expression data for the benzothiadiazole S-methylester (BTH) (NASC392) and CHX (NASC-189) microarrays was also retrived from NASCArrays.

Expression values were calculated by log2 transforming the fold change values. The fold change was calculated by dividing the signal intensity value for the probe corresponding to a GOI in the treated sample by its signal intensity in the appropriate control sample.

4.2.4.6 NaCl and osmotic stress response genes

The NaCl and osmotic stress responsive genes chosen for the analysis of tissue-specific expression in response to NaCl and osmotic stress were: the *SOS* genes (*SOS1, SOS2* and *SOS3*) that specifically play a role in the ionic stress response with SOS3 interacting with SOS2 in the root to regulate Na^+ exclusion and long distance Na^+ transport via the Na^+/ H^+ antiporter, SOS1 (Shi *et al.*, 2002a; Zhu, 2003); *CBL10* that interacts with SOS2 in the shoot to regulate *NHX1*, a Na^+/ H^+ antiporter responsible for shoot Na^+ compartmentalization (Apse *et al.*, 2003; Kim *et al.*, 2007); *HKT1* a Na^+ transporter involved in recirculating Na^+ between the shoot and root (Berthomieu *et al.*, 2003; Rus *et al.*, 2001; Sunarpi *et al.*,

2005); *9-CIS-EPOXYCAROTENOID DIOXYGENASE 3* (*NCED3*), *ABSCISIC ALDEHYDE OXIDSASE 3* (*AAO3*), *ABA DEFICIENT 1* (*ABA1*) and *ABSCISIC ACID INSENTIVE 1* (*ABI1*), all of which are components of the ABA signalling pathway that is induced by osmotic stress (Barrero *et al.*, 2005; Gonzalez-Guzman *et al.*, 2004; Quesada *et al.*, 2000; Ruggiero *et al.*, 2004); *RESPONSIVE TO DESSICATION 29* (*RD29A*), a marker gene responsive to a number of abiotic stresses (Xiong and Zhu, 2002b); Δ^1-PYRROLINE-5-CARBOXYLATE SYNTHETASE (*P5CS*), a gene involved in compatible solute synthesis for osmotic adjustment (Munns, 2005) and finally an osmosensor *HISTIDINE KINASE 1* (*HK1*) that regulates NaCl and osmotic stress responses (Tran *et al.*, 2007).

4.2.5 Chemicals and stock solutions

Most of the chemicals used have been described previously in section 3.2.1. SA, Na-SA and CHX were all purchase from SIGMA Aldrich St Louis, USA. Stock solutions of 200 mM SA were dissolved in 100% EtOH while the CHX was provided as a 100 mg/ml stock solution made up in DMSO. TRIzol was purchased from Invitrogen (Paisley, UK) while the RNA purification columns were taken from the RNeasy kit (Qiagen, Crawley, UK).

4.2.6 Plant growth

Arabidopsis Col-0 seedlings were grown in Petri dishes on PN agar (0.6% w/v) as described in section 2.2.4 for the validation of the publicly available microarray data. Plants infected with pathogens were grown in soil as described in section 3.2.5.2. *Arabidopsis* Col-0 seedlings used in the microarray experiment were grown on Petri dishes in MS agar (0.6% w/v) (Murashige and Skoog, 1962) containing 0.75% (w/v) sucrose under a 16 hr light (100 μM photons m^{-2} s^{-1}) 8 hr dark cycle at 24°C.

4.2.7 Pathogen growth

Growth of *P. syringae* and *B. cinerea* has been described in sections 3.2.2.4 and 3.2.2.3 respectively.

4.2.8 Plant treatments

4.2.8.1 Validation of the microarray results

Microarray experiments selected for validation included NaCl, osmotic stress, K^+ starvation, SA, UV-B and CHX treatments. Seedlings were treated exactly as described in the original microarray experiments (Goda *et al.*, 2008; Hampton *et al.*, 2004; Kilian *et al.*, 2007). Where the original microarray experiment had been conducted over a time course (NaCl, osmotic stress and UV-B treatments), the time point at which *AtPNP-A* expression was most highly induced were chosen for the treatment time. For the NaCl and osmotic stress treatments, the seedlings were gently removed from the Petri dishes using forceps and placed into 6 well microtitre plates containing liquid PN media. After allowing touch responses to dispel for approximately 30 min, seedlings were treated with water (control), 150 mM NaCl or 300 mM mannitol (osmotic stress). Samples were harvested 6 hrs post treatment by quickly blotting the seedlings on tissue paper and then snap freezing in liquid nitrogen and storing at -70°C. K^+ starvation was induced by transferring five day old seedlings germinated on nutrient replete media (described in section 3.2.23) on to fresh nutrient replete media (control) or K^+ deficient media (described in section 3.2.23). Seedlings

were harvested after seven days growth on the K^+ deficient media. For the SA treatment, seedlings were removed into microtitre plates described previously. Seedlings were treated with 1mM Na-SA or the equivalent concentration (0.5% v/v) of EtOH (control) and harvested 3 hrs after treatment as described previously. UV-B exposure was performed by removing the lids from the Petri dishes and exposing seedlings to a hand-held UV light (310 nm) for 15 min. The lids were then replaced and plates returned to the growth chamber in continuous light for a further 6 hrs before harvesting. Finally, seedlings were treated in microtitre plates as described above, for 3 hrs with 10 μM CHX or the equivalent concentration (0.003% v/v) of DMSO (control). All of the samples were snap frozen in liquid nitrogen and then stored at -70°C until the RNA was extracted.

4.2.8.2 Confirmation of co-expression of the select ECGG genes

For the SA time course leaves of four week old soil grown plants were detached and placed in 6 well microtitre plates. The leaves were floated in 1 mM SA solution or 0.5% (v/v) EtOH (control) for 30 min after which time the leaves were removed, quickly blotted dry and placed into fresh microtitre plates in which they were suspended in water for the remaining treatment time. *P. syringae* infection was performed using the pressure inoculation technique described in section 3.2.27.1 while the *B. cinerea* infection proceeded as described in section 3.2.26. Samples were harvested 1, 3, 6, 12, 24 and 48 hrs after each treatment, snap frozen in liquid nitrogen and then stored at -70°C until the RNA was extracted. For examining the expression of the selected ECGG genes in the *atpnp-a* mutant and wildtype lines, the above experiment was repeated and samples were collected at 12 and 24 hrs post infection.

4.2.8.3 Microarray analysis of the response to recombinant AtPNP-A treatment

Recombinant AtPNP-A, a kind gift from Yu-Hua Wang (Monash University, Australia), had been confirmed to be active in both a protoplast swelling and stomatal opening assay (Wang *et al.*, 2007c). Two week old seedlings were placed into 6 well microtitre plates containing liquid MS media and left for 30 min prior to treatment to dispel any touch responses. Seedlings were treated for either 1 hr or 24 hrs with 1 μM recombinant AtPNP-A. For the confirmation of the microarray data, recombinant AtPNP-A was kindly provided by Oziniel Ruzvidzo (University of the Western Cape, South Africa). Seedlings were treated exactly as described for the microarray experiment.

4.2.9 RNA manipulations

4.2.9.1 RNA extraction for semi-quantitative RT-PCR

RNA was extracted according to the LiCl method described in section 3.2.10.1.

4.2.9.2 RNA extraction for microarray analysis

The RNA was extracted from six biological repeats of control and treated samples using TRIzol, according to the manufacturer's instructions (Invitrogen, Paisley, UK). The RNA was then cleaned using the spin columns from the RNeasy Plant total RNA kit, according to the manufacturer's instructions (Qiagen, Crawley, UK), as is the standard operating procedure requirement for samples sent to the microarray facility at Warwick HRI University, UK. Here the RNA quality was evaluated using the

Bioanalyzer (Agilent Technologies, Inc., CA, USA) and the four best control and treated samples were chosen for the microarray experiment (28S:18S ratio not less than 1:1).

4.2.9.3 cDNA synthesis for semi-quantitative RT-PCR

For these experiments, cDNA was synthesized as described in section 3.2.10.3.

4.2.9.4 RNA amplification, cDNA synthesis and labelling for the microarray

Total RNA (1 μg) was amplified using the Message Amp^{TM} II aRNA amplification kit (Ambion, UK) according to the manufacturer's instructions. For Cy3 and Cy5 labelling, cDNA was synthesized from 5 μg of amplified RNA (aRNA) using Superscript II according to the manfacturer's instructions (Invitrogen, Paisley, UK). Briefly, 5 μg of aRNA, 0.75 μl of 2μg/μl random nonamers and 0.5 μl RNaseOUT in a final volume of 10.5 μl was denatured by incubating at 70°C for 10 min and then snap cooled on ice for 2 min. To this 4 μl of first strand buffer, 2 μl 0.1 M DTT, 1 μl dNTPs (10 mM each of dATP, dGTP, dTTP and 2 mM dCTP) and 1 μl Superscript II enzyme was added. Finally 1.5 μl of 25 mM Cy3-dCTP or Cy5-dCTP was added and mixed well by pipetting gently. The samples were then incubated at 42°C for 2.5 hrs. Following cDNA synthesis 2 μl of 2.5 M NaOH was added to each reaction which was then incubated at 37°C for 15 min. After this time 10 μl of 2 M MOPS buffer was added and samples were placed on ice. Finally the cDNA was purified using the QiaQuick PCR purification column according to the manufacturer's instructions (Qiagen, Crawley, UK). The appropriate Cy3 and Cy5 labelled control and treated samples were combined and freeze-dried until just dry prior to being used for hybridization to the microarray slides.

4.2.10 Semi-quantitative RT-PCR

Semi-quantitative RT-PCR was used to measure the expression of *AtPNP-A* for validation of the publicly available microarray experiments, to examine co-expression of the select ECGG genes as well as to confirm the expression of candidate genes identified in the recombinant AtPNP-A microarray experiment. *UBQ* was used as a control to confirm visually that there were comparable amounts of template in each of the samples. Each of the primer pairs was optimized for semi-quantitative PCR. Briefly, the $MgCl_2$ concentration and annealing temperatures were optimized for each primer pair as per usual. PCR amplification was then performed for 40 cycles, removing samples at regular intervals. The cycle number that gave product formation in a good linear range was then confirmed to be semi-quantitative by showing that a dilution series of template produced the expected dilution of product. The optimized $MgCl_2$ concentrations, annealing temperatures and cycle numbers for each of the primer pairs are shown in Table 4.1. Reactions were conducted in 20 μl volumes including 1 X PCR buffer (provided with the enzyme), the appropriate $MgCl_2$ concentration (Table 4.1), 0.125 mM dNTPs, 0.1 U/μl Super-Term Polymerase and 0.2 μM each of forward and reverse primers. PCR reactions were performed by the GeneAmp PCR Systems 2700 (Applied Biosystems, Foster City, USA) using the following cycling conditions: initial denaturation at 94°C for 5 min, followed by the optimized number of cycles for each primer pair of 94°C for 15 sec, the appropriate annealing temperature for 30 sec and 72°C for 1 min and concluded with a final extension step of 72°C for 10 min. PCR products were visualized as described in section 3.2.7.2.

Table 4.1. Primers and optimization conditions for semi-quantitative RT-PCR

Gene	AGI ID	Forward Primer	Reverse Primer	[$MgCl_2$] in mM	Annealing temperature	number of cycles
Validation of Expression Results						
AtPNP-A	At2g18660	5' TCTATTACGACCCTCCCTACACT 3'	5' TGTTCTTGACTCCGACTACCA 3'	1.5	62 °C	37
WAK1	At1g21250	5' GCTTCATCAATAATGCTTTGCT 3'	5' CCAATGGGAATTACAAACATG 3'	3.0	62 °C	30
PR1	At2g14610	5' AGACTCGGATGTGCCAAAGT 3'	5' ACATAATTCCCACGAGGATCA 3'	3.0	62 °C	27
WRKY70	At3g56400	5' CCAGTTACGTCAATGGGAAA 3'	5' CACCTCCAAACACCATGAGA 3'	3.0	62 °C	27
Ubiquitin-conjugating enzyme	At5g25760	5' GGACCGCTCTTATCAAAGGA 3'	5' CTTGAGGAGGTTGCAAAGGA 3'	3.0	65 °C	25
Microarray Confrimation						
pseudogene, NADH dehydrogenase	At2g07600	5' CGGCCATTTTAATAGGAACA 3'	5' TTGTCTGATTCATGCGGATA 3'	3.0	62 °C	33
Structural constituent of ribosome	At2g28820	5' AAACACTTGAACCAGCTTGGA 3'	5' ACGCGTTTCAGGAGGTCTTA 3'	2.0	62 °C	29
AtCEL2	At1g02800	5' TTGTTGGAGCTTTGGCTTATC 3'	5' GGACAATCTTGGCCATTCAT 3'	3.0	62 °C	33
protease inhibitor/seed storage/lipid transfer protein	At4g12500	5' GCGGCTATCCATACTCTTCA 3'	5' CGGGAAACGTTTACAAAATG 3'	2.0	62 °C	24
Peroxidase	At5g64120	5' TGTTTCCGGCACTAGGATTG 3'	5' AGTATTCCGGGTGCGATTCT 3'	2.0	62 °C	24

4.2.11 Microarray experiment

4.2.11.1 Hybridization, wash and scanning conditions

The microarray experiment kindly conducted by Dr Priya Madhou (Warwick HRI, University of Warwick, UK) using the CATMA microarray platform (Allemeersch *et al.*, 2005). Four microarray sides were used for each treatment time point. Firstly, the CATMA array slides were incubated in pre-hybridization buffer (10 mg/ml BSA, 5 X SSC and 0.1% SDS) at 42°C for 1 hr. The slides were then washed five times in dH_2O and then once briefly in isopropanol after which they were allowed to air dry. The freeze-dried labelled combined control and treated cDNA samples (30 pmol) were resuspended in 50 µl hybridization buffer (25% formamide, 5 X SSC, 0.1% SDS and 0.5 µg/µl Yeast tRNA) and incubated at 95°C for 5 min. The labelled sample was then hybridized to the CATMA array and incubated at 42°C overnight. The following day the arrays were washed first in 2 X SSC and 0.1% SDS at 42°C, then in 1 X SSC and 0.1% SDS shaking on an orbital shaker for 10 min and finally in 0.1 X SSC shaking for 1 min. The last wash step was repeated four times. Thereafter the slides were briefly immersed in isopropanol, placed into a 50 ml tube and centrifuged for 1 min at 2000 rpm to dry. The arrays were scanned on the Afymetrix 428^{TM} Array Scanner at 532 nm for the Cy3 reading and 635 nm for the Cy5 reading.

4.2.11.2 Microarray data analysis

The signal intensity data from the two channel microarrays was extracted using Imagene software. This data was analyzed using limmaGUI, a graphical interface for the limma statistical package for R (Wettenhall and Smyth, 2004). LimmaGUI was used to graphically display the microarray results, normalize the data, extract M (log_2 ratio of expression) and to generate lists of differentially expressed genes. Diagnostic graphs were generated for each slide to evaluate the spread of the data and requirement for normalization. The M box plots for each print tip group demonstrate the need to normalize the data within the slide (Appendix Figure 4.1). Print tip loess normalization was used to normalize the data within each slide, to correct for sub-array spatial variations and intensity based trends (Smyth and Speed, 2003), and the M box plots were regenerated to demonstrate that the data had effectively been normalized. An example is shown for Slide 1 of the 1 hr AtPNP-A microarray experiment (Appendix Figure 4.1). The M box plots that show the spread of the data across each slide as a whole demonstrated the need to normalize the data between the slides. Again an example is shown for the 1hr recombinant AtPNP-A microarray experiment (Appendix Figures 4.2). Quantile normalization was used to normalize the data between the slides and the M box plots were regenerated to ensure that the data had been effectively normalized (Appendix Figures 4.2). Following normalization lists of differentially expressed genes that include p values and adjusted p values (calculated using the Benjamini and Hochberg method) were extracted for both the 1 hr and 24 hr AtPNP-A treated microarray experiments. The CATMA IDs were ranked according to their log_2 M values. The AtPNP-A microarray did not show good statistical reproducibility across slides as none of the adjusted p values were returned as being significant. The significant analysis of microarrays (SAM) tool was therefore used to explore statistical significance in the microarray data (Tusher *et al.*, 2001). SAM takes into account the change in gene expression relative to the standard deviation and uses combinations of repeated measurements to estimate the FDR.

4.3 RESULTS

4.3.1 Correlation analysis

A correlation analysis was performed using the ACT tool and a list of the 50 genes whose expression is most highly correlated with that of *AtPNP-A* was extracted (Table 4.2). This group of genes is hereafter referred to as the *AtPNP-A* ECGG. Previously functional relatedness has been ascribed to groups of genes that have correlation (*r*) values from 0.7 to 0.9 (Manfield *et al.*, 2006). Therefore *r* values returned for the *AtPNP-A* ECGG were considered moderate, ranging from 0.707 to 0.570.

4.3.2 Functional enrichment

In order to identify whether there was any functional bias in GO terms associated with the *AtPNP-A* ECGG, a GO analysis was performed using FatiGO. This returned a significant (adjusted p values < 0.005) enrichment of GO terms associated with GO biological processes at GO levels 3 through 7 (Table 4.3). These included enrichment of the terms "defence response" (adjusted p = 1.15 X 10^{-6}), "immune response" (adjusted p = 9.54 X 10^{-4}), "response to biotic stimulus" (adjusted p = 1.11 X 10^{-3}) and "cell communication" (adjusted p = 2.12 X 10^{-3}) at level 3; "innate immune response" (adjusted p = 1.78 X 10^{-3}) and "response to other organisms" (adjusted p = 1.78 X 10^{-3}) at level 4; "defence response, incompatible interaction" (adjusted p = 1.83 X 10^{-3}) at level 6 and "systemic acquired resistance" (adjusted p = 6.29 X10^{-6}) at level 7. The most significant enrichments were of the terms defence response at level 3 and SAR at level 7. In particular, 30 of the *AtPNP-A* ECGG genes have been assigned a GO biological process annotation at level 3, 11 of which are annotated as being involved in the defence response. Thus 36.67% of the *AtPNP-A* ECGG are annotated defence response genes, compared to 4.18% of genes in the genome which is a significant enrichment (adjusted p = 1.15 X 10^{-6}). These 11 *AtPNP-A* ECGG defence response genes inlcude: three *DISEASE RESISTANCE* genes (At2g32680, *r* = 0.653; At3g11010, *r* = 0.572 and At3g04210, *r* = 0.572); a gene with similarity to *ACTIVATED DISEASE RESISTANCE 1* (*ADR1*) (*r* = 0.597); a MAPKK - *MEK1* (*r* = 0.623); *EDS1* (*r* = 0.650); *WRKY70* (*r* = 0.630) and its closest homology *WRKY54* (*r* = 0.591) and three *PR* genes - *PR1* (*r* = 0.636), *PR2* (*r* = 0.672) and *PR5* (*r* = 0.640). At level 7, 19 of the *AtPNP-A* ECGG have GO biological process annotations and five of these genes are associated with the GO term SAR, namely *EDS1*, *WRKY70*, *PR1*, *PR2* and *PR5*. This is particularly striking when considering that there are only 21 genes in genome that are annotated at this level as being involved in SAR. Therefore 26.32% of *AtPNP-A* ECGG genes are annotated as being involved in SAR compared to 0.39% of genes in the genome, that is a significant enrichment (adjusted p = 6.29 X 10^{-6}). Therefore the *AtPNP-A* ECGG is statistically enriched in terms associated with the defence response and specifically SAR.

Table 4.2. The *AtPNP-A* ECGG

Gene	Description	*r*-value
AT3G56710	SIB1 (SIGMA FACTOR BINDING PROTEIN 1); binding	0.707
AT5G27830	hypothetical protein	0.702
AT5G10760	aspartyl protease family protein	0.695
AT5G64000	SAL2; 3'(2'),5'-bisphosphate nucleotidase/ inositol or phosphatidylinositol phosphatase	0.692
AT2G40600	appr-1-p processing enzyme family protein	0.685
AT1G08450	CRT3 (CALRETICULIN 3); calcium ion binding	0.675
AT3G57260	**BGL2 (PATHOGENESIS-RELATED PROTEIN 2); glucan 1,3-beta-glucosidase/ hydrolase, hydrolyzing O-glycosyl compounds**	**0.672**
AT5G52760	heavy-metal-associated domain-containing protein	0.667
AT2G14560	unknown protein	0.663
AT2G32680	disease resistance family protein	0.653
AT5G52740	heavy-metal-associated domain-containing protein	0.651
AT1G21270	WAK2 (wall-associated kinase 2); protein serine/threonine kinase	0.650
AT3G48090	**EDS1 (ENHANCED DISEASE SUSCEPTIBILITY 1); signal transducer/ triacylglycerol lipase**	**0.650**
AT5G10380	zinc finger (C3HC4-type RING finger) family protein	0.648
AT1G23840	unknown protein	0.644
AT1G75040	**PR5 (PATHOGENESIS-RELATED GENE 5)**	**0.640**
AT1G76960	unknown protein	0.637
AT2G14610	**PR1 (PATHOGENESIS-RELATED GENE 1)**	**0.636**
AT5G24530	oxidoreductase, 2OG-Fe(II) oxygenase family protein	0.635
AT2G02360	ATPP2-B10 (Phloem protein 2-B10); carbohydrate binding	0.633
AT3G26600	armadillo/beta-catenin repeat family protein	0.631
AT3G56400	**WRKY70 (WRKY DNA-binding protein 70); transcription factor**	**0.630**
AT1G13470	unknown protein	0.630
AT2G26440	pectinesterase family protein	0.627
AT5G52750	heavy-metal-associated domain-containing protein	0.624
AT4G26070	MEK1 (mitogen-activated protein kinase kinase 1); MAP kinase kinase/ kinase	0.623
AT1G21250	WAK1 (CELL WALL-ASSOCIATED KINASE); kinase	0.622
AT5G12890	UDP-glucoronosyl/UDP-glucosyl transferase family protein	0.621
AT1G03400	2-oxoglutarate-dependent dioxygenase, putative	0.616
AT1G67970	AT-HSFA8 (Arabidopsis thaliana heat shock transcription factor A8); DNA binding / transcription factor	0.614
AT3G08870	lectin protein kinase, putative	0.613
AT4G23320	protein kinase family protein	0.612
AT5G55420	Encodes a Protease inhibitor/seed storage/LTP family protein and	0.610
AT5G60900	RLK1 (RECEPTOR-LIKE PROTEIN KINASE 1); carbohydrate binding / kinase	0.609
AT4G04500	protein kinase family protein	0.606
AT1G73800	calmodulin-binding protein similar to calmodulin-binding protein TCB60 GI:1698548 from [Nicotiana tabacum]	0.601
AT4G33300	ADR1-L1 (ADR1-LIKE 1); ATP binding / protein binding	0.597
AT1G78200	protein phosphatase 2C, putative / PP2C, putative	0.597
AT3G26210	CYP71B23 (cytochrome P450, family 71, subfamily B, polypeptide 23); oxygen binding	0.594
AT2G40750	WRKY54 (WRKY DNA-binding protein 54); transcription factor	0.591
AT5G02630	unknown protein	0.589
AT5G55450	protease inhibitor/seed storage/lipid transfer protein (LTP) family protein	0.588
AT4G36210	unknown protein	0.586
AT4G28490	HAESA (RECEPTOR-LIKE PROTEIN KINASE 5); ATP binding / kinase/ protein serine/threonine kinase	0.586
AT4G29810	ATMKK2 (MAP KINASE KINASE 2); MAP kinase kinase/ kinase	0.583
AT5G18470	curculin-like (mannose-binding) lectin family protein	0.580
AT1G78620	integral membrane family protein	0.579
AT3G04210	disease resistance protein (TIR-NBS class), putative	0.572
AT3G11010	disease resistance family protein / LRR family protein	0.572
AT3G63420	AGG1 (ARABIDOPSIS GGAMMA-SUBUNIT 1)	0.570

The group of the 50 genes whose expression is most positively correlated with that of *AtPNP-A* is considered to be the *AtPNP-A* ECGG. Genes shown in boldface are genes annotated as being involved in SAR.

Table 4.3. FatiGO analysis of the *AtPNP-A* ECGG

Term	Genes in ECGG containing term	ECGG vs. genome	p value	Adjusted p value
GO BIOLOGICAL PROCESS				
Level 3				
defence response (GO:0006952)	AT4G33300,AT2G32680,AT2G40750, AT3G57260,AT3G11010,AT3G04210, AT3G48090,AT2G14610,AT4G26070, AT3G56400,AT1G75040	89.78% 10.22%	1.92E-08	1.15E-06
immune response (GO:0006955)	AT3G57260,AT3G48090,AT2G14610, AT3G56400,AT1G75040	93.2% 6.8%	3.18E-05	9.54E-04
response to biotic stimulus (GO:0009607)	AT3G57260,AT3G48090,AT2G14610, AT4G26070,AT3G56400,AT5G55450, AT1G75040	87.3% 12.7%	5.55E-05	1.11E-03
cell communication (GO:0007154)	AT4G28490,AT2G32680,AT3G11010, AT1G21250,AT3G48090,AT2G14610, AT4G26070,AT3G56400,AT4G29810	81.24% 18.76%	1.42E-04	2.12E-03
Level 4				
innate immune response (GO:0045087)	AT3G57260,AT3G48090,AT2G14610, AT3G56400,AT1G75040	93.51% 6.49%	2.45E-05	1.78E-03
response to other organism (GO:0051707)	AT3G57260,AT3G48090,AT2G14610, AT4G26070,AT3G56400,AT5G55450, AT1G75040	88.58% 11.42%	2.47E-05	1.78E-03
response to salicylic acid stimulus (GO:0009751)	AT1G21270,AT1G21250,AT3G48090, AT3G56400	94.02% 5.98%	1.26E-04	6.04E-03
signal transduction (GO:0007165)	AT4G28490,AT2G32680,AT3G11010, AT1G21250,AT3G48090,AT4G26070, AT3G56400,AT4G29810	81.49% 18.51%	3.09E-04	1.11E-02
regulation of response to stimulus (GO:0048583)	AT3G56400,AT2G40750	97.92% 2.08%	9.65E-04	2.78E-02
Level 5				
innate immune response (sensu Viridiplantae) (GO:0002226)	AT2G14610,AT3G56400,AT1G75040, AT3G57260,AT3G48090	93.77% 6.23%	1.90E-05	6.10E-03
Level 6				
defence response, incompatible interaction (GO:0009814)	AT3G57260,AT3G48090,AT2G14610, AT3G56400,AT1G75040	95.27% 4.73%	4.56E-06	1.83E-03
protein kinase cascade (GO:0007243)	AT4G26070,AT4G29810	99.41% 0.59%	1.04E-04	2.09E-02
Level 7				
systemic acquired resistance (GO:0009627)	AT3G57260,AT3G48090,AT2G14610, AT3G56400,AT1G75040	98.55% 1.45%	1.47E-08	6.29E-06
MAPKKK cascade (GO:0000165)	AT4G26070,AT4G29810	99.46% 0.54%	9.25E-05	1.98E-02

4.3.3 Promoter content analysis

In order to identify whether there was any enrichment of *cis* elements in the promoters of the *AtPNP-A* ECGG that could be responsible for its co-expression a promoter analysis was performed. The *AtPNP-A* ECGG was first examined for enrichment of known TFBSs. Currently only 105 TFBSs have been experimentally determined whereas there are approximately 1500 transcription factors annotated in *Arabidopsis* (Riechmann *et al.*, 2000) so there are potentially many more as of yet undiscovered TFBSs that could control the co-expression of the *AtPNP-A* ECGG. Therefore the *AtPNP-A* ECGG was also tested for enrichment of computer derived motifs that may or may not be TFBSs.

4.3.3.1 Experimentally derived motifs

Athena was used to visualize the *AtPNP-A* ECGG promoters and query them for known TFBSs. Firstly, the *AtPNP-A* promoter was visualized and found to contain three TATA-box motifs, three GAREATs, two W-box promoter motifs, two MYB4 binding site motifs and single copies each of MYB1AT, MYB1 binding site motif, CCA1 binding site motif, MYB binding site promoter and ARF binding site motif (Figure 4.1). The *AtPNP-A* promoter itself was not enriched in TFBSs when compared to the rest of the promoters in the genome (Table 4.4). The *AtPNP-A* ECGG, on the other hand, was enriched in W-box promoter motifs (TTGACY where Y = C/T; $p < 10^{-3}$) and LS7 promoter elements (ACGTCATAGA; $p < 10^{-3}$) (Table 4.5). The number of promoters that contain each motif should be kept in mind since motifs that are present in few promoters are unlikely to influence the expression of the *AtPNP-A* ECGG as a whole. For example the LS7 promoter element only occurs in two *AtPNP-A* ECGG promoters and is therefore less likely to regulate the co-expression of the *AtPNP-A* ECGG than the W-box promoter motifs that occur in the majority (41/50) of promoters. Secondly, the number of copies of the motif per promoter is important because multiple copies of a TFBS, particularly when arranged in palindromes or direct repeats, leads to cooperative binding and stronger transcriptional activation (Maleck *et al.*, 2000). Visualization of the *AtPNP-A* ECGG promoters revealed that 30 out of these 41 promoters had more than one W-box motif including *AtPNP-A* and the annotated defence response genes: *MEK1*, *EDS1*, *PR1, PR2*, *PR5*, the three disease resistance genes and the gene that is similar to *ADR1*. In most of these cases (22/30) multiple W box promoter motifs were found in close proximity, true for *AtPNP-A*, *MEK1*, *EDS1*, *PR1*, two out of the three disease resistance genes and the gene that is similar to *ADR1* (Figure 4.2). W-box promoter motifs bind WRKY transcription factors and have consistently been reported to be the most prominent TFBS present in the promoters of defence response genes, including those induced by SAR, *R* gene-mediated resistance and basal defence (Eulgem *et al.*, 2004; Maleck *et al.*, 2000; Navarro *et al.*, 2004). It is therefore pertinent that *AtPNP-A* ECGG genes annotated as defence response genes contain multiple copies of W-box promoter motifs in close proximity.

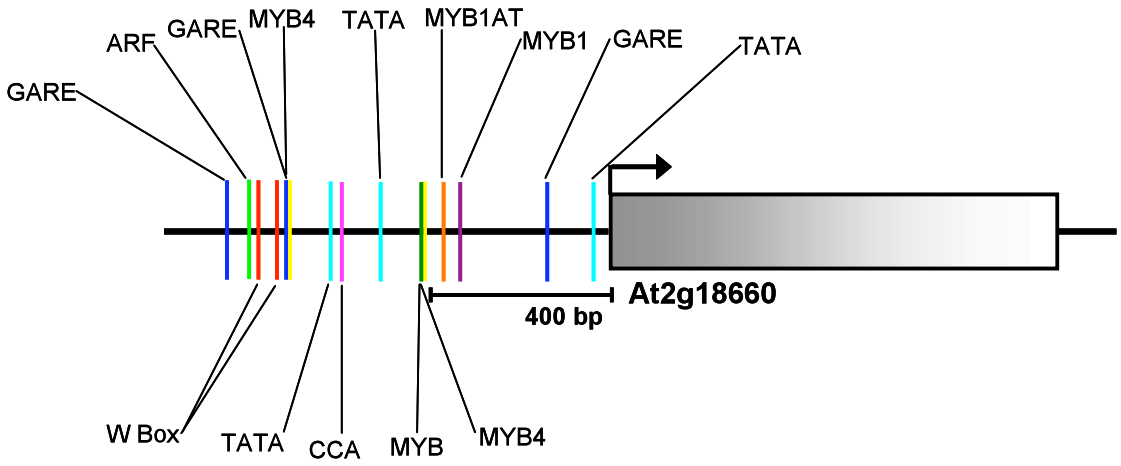

Figure 4.1. Visualization of the *AtPNP-A* promoter

The 1000 bp promoter region of the *AtPNP-A* gene (depicted by the grey box) is shown above. The positions of known TFBSs are show by the coloured lines.

Table 4.4. TFBSs in the *AtPNP-A* promoter

Motif	# P	# S	p value	Consensus sequence
MYB1 binding site motif	1	1	0.0478	MTCCWACC
CCA1 binding site motif	1	1	0.2353	AAMAATCT
MYB binding site promoter	1	1	0.2465	MACCWAMC
ARF binding site motif	1	1	0.3074	TGTCTC
MYB1AT	1	1	0.7377	WAACCA
W-box promoter motif	1	2	0.5803	TTGACY
MYB4 binding site motif	1	2	0.6402	AMCWAMC
GAREAT	1	3	0.4761	TAACAAR
TATA-box Motif	1	3	0.7552	TATAAA

P is the number of promoters with the particular TFBS and # S that is the number of times that the TFBS occurs in the *AtPNP-A* promoter diagrammatically represented above. M = A/C; W = A/T; Y = C/T and R = A/G.

Table 4.5. ATHENA analysis of the *AtPNP-A* ECGG

Motif	# P	# S	p value	Consensus sequence
Enriched TF sites				
W-box promoter motif	41	94	$<10^{-3}$	TTGACY
LS7 promoter element	2	2	$<10^{-3}$	ACGTCATAGA
Non-Enriched sites				
AGL2ATCONSENSUS	3	3	0.0201	NNWNCCAWWWWTRGWWAN
ARF binding site motif	23	29	0.0215	TGTCTC
CCA1 binding site motif	18	22	0.0388	AAMAATCT
GAREAT	33	49	0.0103	TAACAAR
GCC-box promoter motif	7	7	0.0171	GCCGCC
MYB1 binding site motif	6	6	0.0340	MTCCWACC
P1 promoter motif	2	4	0.0465	GTGATCAC
SV40 core promoter motif	13	15	0.0404	GTGGWWHG
T-box promoter motif	30	43	0.0444	ACTTTG

P is the number of promoters with the particular TFBS and # S that is the number of times that the TFBS occurs in the *AtPNP-A* ECGG. Y = C/T; R = A/G; W = A/T; M = A/C and H = A/C/T

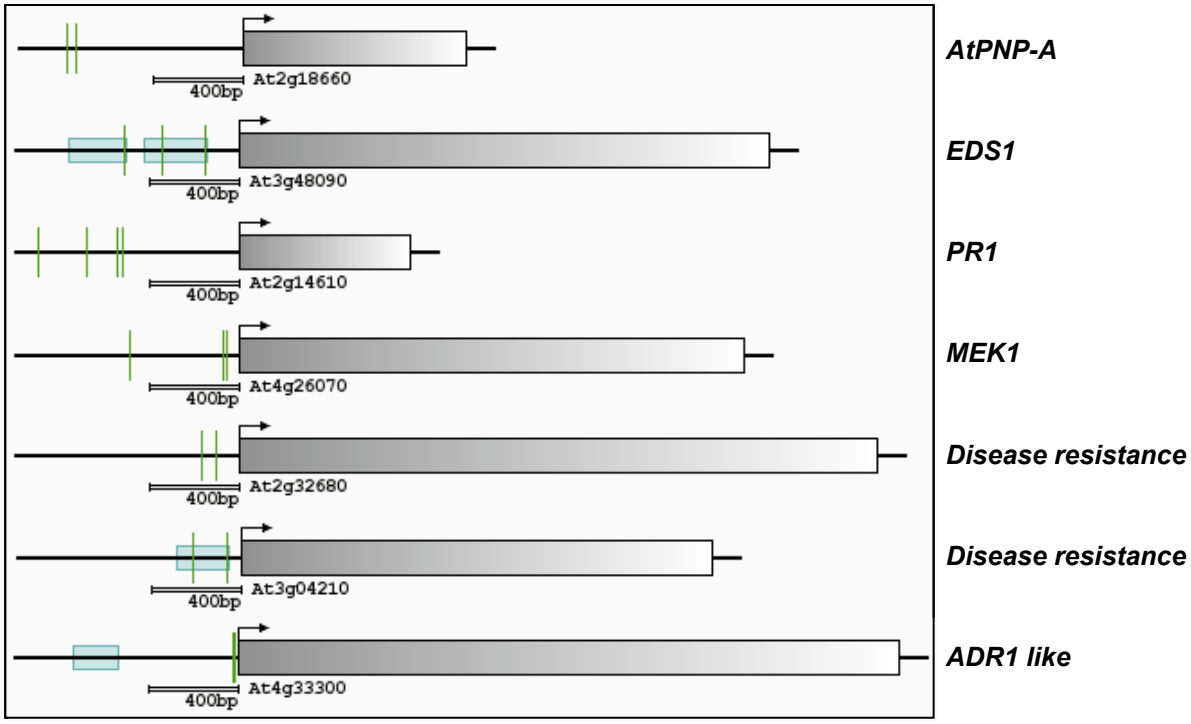

Figure 4.2. Multiple W-box promoter motifs are found in close proximity in disease resistance genes Schematic representation of the 1000 bp promoter regions of *AtPNP-A* (At2g18660), *ENHANCED DISEASE SUSCEPTIBILITY 1* (*EDS1*) (At3g48090), *PR1* (At2g14620), *MAP KINASE/ ERK KINASE 1* (*MEK1*) (At4g26070), the two disease resisance genes (At2g23680 and At3g04210) and the *ACTIVATED DISEASE RESISTANCE 1* (*ADR1*) like gene (At4g33300). W-box promoter motifs are indicated by the green lines. This shows that the genes among the *AtPNP-A* ECGG that are annotated as playing a role in defence have multiple copies of the W-box promoter motifs within close proximity of one another.

4.3.3.2 Computationally derived motifs

Motif Analysis and Pronomer tools were used for motif discovery in the *AtPNP-A* ECGG. The 16 most significantly enriched motifs ($p < 0.001$) returned by Motif Analysis were compared to 4mer and 5mers that emerged from the Pronomer analysis (Table 4.6). These 16 motifs correspond to eight potential TFBSs since each sequence and its reverse compliment are present. Seven of these eight motifs had Pronomer matches and were thus analysed further.

POBO uses a rigorous statistical approach to verify whether motifs generated using other tools are enriched in terms of their frequency (copy number per promoter) in a group of genes compared to in the promoters in the genome. POBO results revealed that six out of the seven motifs are twice as prevalent in the *AtPNP-A* ECGG as in the genome with sample distributions that show almost complete separation (Table 4.6, Figure 4.3). For example GACGTA/TACGTC is found at a frequency of 0.47 copies per promoter in the *AtPNP-A* ECGG compared to 0.17 copies per promoter in the genome; CAAGTC/GACTTG is present at a frequency of 1.00 copies per promoter in the *AtPNP-A* ECGG compared to 0.46 in the genome and ACGTAG/CTACGT at 0.40 versus 0.18 copies per promoter. The GACATC/GATGTC motif yielded the poorest POBO result at a frequency of 0.39 in the *AtPNP-A* ECGG compared to 0.33 in the genome, reflected in less separation in the sample distributions on the graph. For each motif the t value returned by POBO was used to calculate a p value, all of which were < 0.0001, verifying that these seven motifs are enriched in their frequency in the *APNP-A* ECGG.

The same seven motifs were then queried against the TRANSCFAC database to determine whether they bind any known transcription factors. Four of the motifs returned matches; two of which were to WRKY TFBSs and the other two were to COMMON PLANT REGULATORY FACTOR 1 (CPRF1) TFBSs (Table 4.6). Like the WRKY TFBSs, CPFR1 has also been reported regulate pathogen responses (Logemann and Hahlbrock, 2002). The fact that the motif discovery returned matches to known TFBSs, gives confidence that the remaining three motifs are potentially novel TFBSs.

The defence transcriptome has been well studied with many TFBSs and motifs involved in its regulation having been identified (Eulgem, 2005; Mahalingam *et al.*, 2003; Maleck *et al.*, 2000; Navarro *et al.*, 2004; Wang *et al.*, 2005). The three potentially novel TFBSs arising from the motif discovery, were therefore checked against the literature for matches to other motifs (not necessarily TFBSs) that have been previously associated with defence response genes. Two of these three motifs contain within their sequence the GACTT 5mer that has been reported to be a WRKY-like motif (Mahalingam *et al.*, 2003) and one of these motifs (GACTTG) has previously been identified as being overrepresented in a group of genes upregulated in the *mpk4* mutant

Table 4.6. Comparative analysis of computer generated motifs over represented in the *AtPNP-A* ECGG

MOTIF ANALYSIS		PRONOMER		POBO						TRANSFAC PATCH		
Oligomer	p value	nmer	significance	# P in ECGG/ 50	# P in genome /31353	# of X in ECGG	# of X in genome	P mean in ECGG	P mean in genome	Identifier	Binding factor	Search pattern
CGTTAG/ CTAACG	5.36E-05	-	-	-	-	-	-	-	-	-	-	-
CTTGAC/ GTCAAG	9.01E-05	TCAA GTCA	0.050 0.005	28	10236	39	12814	0.79	0.40	AT$RLK4_01 PARS$PR12_02 PARS$PR12_02	WRKY18 WRKY1,WRKY2, WRKY3 WRKY1,WRKY2, WRKY3	TTGAC TGAC GTCA
GACGTA/ TACGTC	9.37E-05	ACGT TACG CGTC	0.050 0.050 0.050	18	4568	24	5153	0.48	0.16	PARS$CPRF1_01 RICE$GLUB1_05	CPRF-1	ACGT ACGT
AAGTCT/ AGACTT	1.56E-04	GACTT AGTC GACT AGAC	0.001 0.010 0.001 0.001	35	14281	66	19874	1.31	0.63			
AGTCAA/ TTGACT	5.21E-04	TCAA AGTC GTCA GACT TGAC	0.050 0.010 0.005 0.001 0.050	37	15567	67	22767	1.34	0.73	NT$CHN50_01 PARS$PR12_02 PARS$PR12_02 AT$RLK4_01	WRKY1,WRKY3, WRKY4 WRKY1,WRKY2, WRKY3 WRKY1,WRKY2, WRKY3 WRKY18	AGTCA GTCA TGAC TTGAC
GACATC/ GATGTC	6.36E-04	ATGT TGTC	0.050 0.050	23	8453	26	10268	0.52	0.33			
CAAGTC/ GACTTG	7.37E-04	GACTT AGTC GACT CTTG	0.001 0.010 0.001 0.050	28	11081	47	14302	0.94	0.46			
ACGTAG/ CTACGT	7.60E-04	ACGT TACG	0.050 0.050	17	4873	20	5608	0.41	0.18	PARS$CPRF1_01 RICE$GLUB1_05	CPRF-1	ACGT ACGT

# of P denotes the number of promoters containing a particular motif in the *AtPNP-A* ECGG or in the genome; # of X denotes the number of times a particular motif occurs among the *AtPNP-A* ECGG or genome. P mean indicates the number of copies of the motif per promoter.

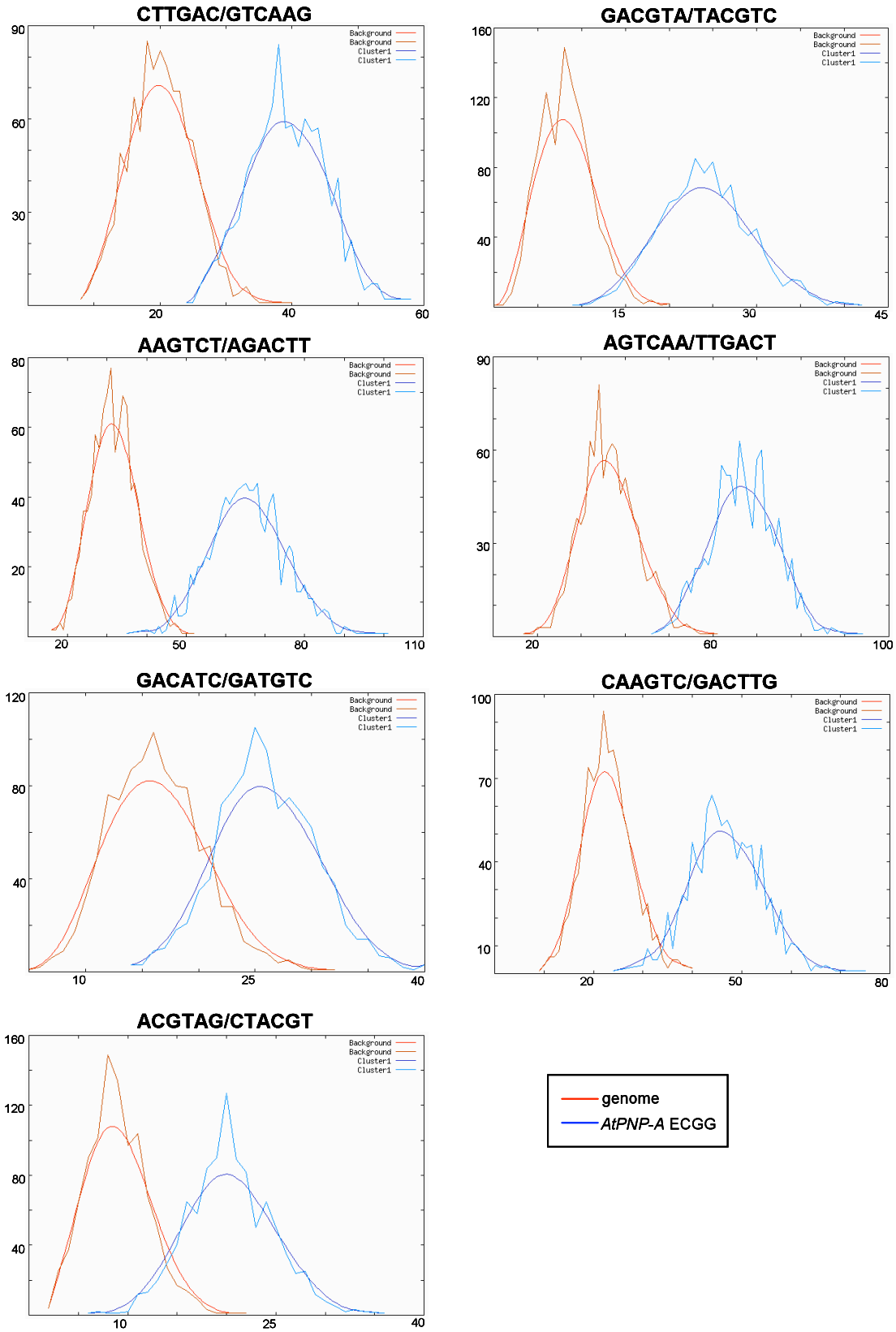

Figure 4.3. POBO plots of the frequency of discovered motifs in the *AtPNP-A* ECGG and genome

Computer generated motifs (Table 4.6) were confirmed by POBO to be statistically enriched. Smooth plots are best fits for the raw data. Good separation of sample distributions is indicative of enrichment.

(Petersen *et al.*, 2000). These authors suggested that this motif is similar to the LS10 motif (GGACTTTTC) identified in the *PR1* promoter (Lebel *et al.*, 1998). The last remaining motif (GACATC/GATGTC) is not similar to any previously described motifs associated with defence response genes, although also gave the poorest POBO result.

Since the *AtPNP-A* ECGG was enriched in TFBSs and motifs known to be affiliated with defence response genes, the frequency of TFBSs that bind key transcription factors involved in the defence response was examined (Figure 4.4). Firstly, POBO was used to examine the frequency of the core (TTGAC) and stringent (TTGAC[C/T/A]) W-box promoter motifs in the *AtPNP-A* ECGG relative to the genome. The *AtPNP-A* ECGG was enriched in the frequency of the core TTGAC motif (2.78 copies per promoter in the *AtPNP-A* ECGG versus 2.24 copies per promoter in the genome) and the stringent TTGACT motif (1.34 copies per promoter in the *AtPNP-A* ECGG compared to 0.72 in the genome). However the TTGACC motif was not enriched (0.46 copies per promoter in the *AtPNP-A* ECGG compared to 0.44 in the genome) and the TTGACA site was actually under represented in the *AtPNP-A* ECGG compared to the genome (0.50 versus 0.76 copies per promoter respectively). Next, the frequency of TGA and Whirly TFBSs was examined in the *AtPNP-A* ECGG relative to the genome. The TGA TFBS (TGACG) was over represented in the *AtPNP-A* ECGG (1.12 copies per promoters compared to 0.88 in the genome). In contrast the Whirly TFBS (GTCAAAA) was not considerably enriched in the *AtPNP-A* ECGG (0.26 copies per promoter compared to 0.30 in the genome). Since TGA transcription factors mediate the *NPR1*-dependent output of the SA signalling pathway while Whirly transcription factors have been proposed to control *NPR1*-independent output from the SA signalling pathway (Desveaux *et al.*, 2004; Durrant and Dong, 2004; Glazebrook, 2005) this suggests that the *AtPNP-A* ECGG may be regulated in an *NPR1*-dependent manner.

In summary, the *AtPNP-A* ECGG is enriched in TFBSs (W-box promoter motifs, CPRF1 and TGA) and motifs that are known to regulate defence response genes. Therefore the promoters of the *AtPNP-A* ECGG have hallmark features of other sets of defence response genes.

4.3.3.3 Scatter plot

The enrichment of WRKY TFBSs in the *AtPNP-A* ECGG suggests that WRKY transcription factors regulate the co-expression of the *AtPNP-A* ECGG. An attractive candidate is *WRKY70* since its expression is highly correlated with that of *AtPNP-A* (26^{th} most highly correlated gene $r = 0.630$) and *WRKY70* has previously been reported to regulate the expression of the *PR* genes among the *AtPNP-A* ECGG (Li *et al.*, 2004). The relationship between *AtPNP-A* and *WRKY70* was explored in a scatter plot (Figure 4.5). The results show that *AtPNP-A* and *WRKY70* are highly correlated (since the slope of the graph is very near to 1). The annotated defence genes

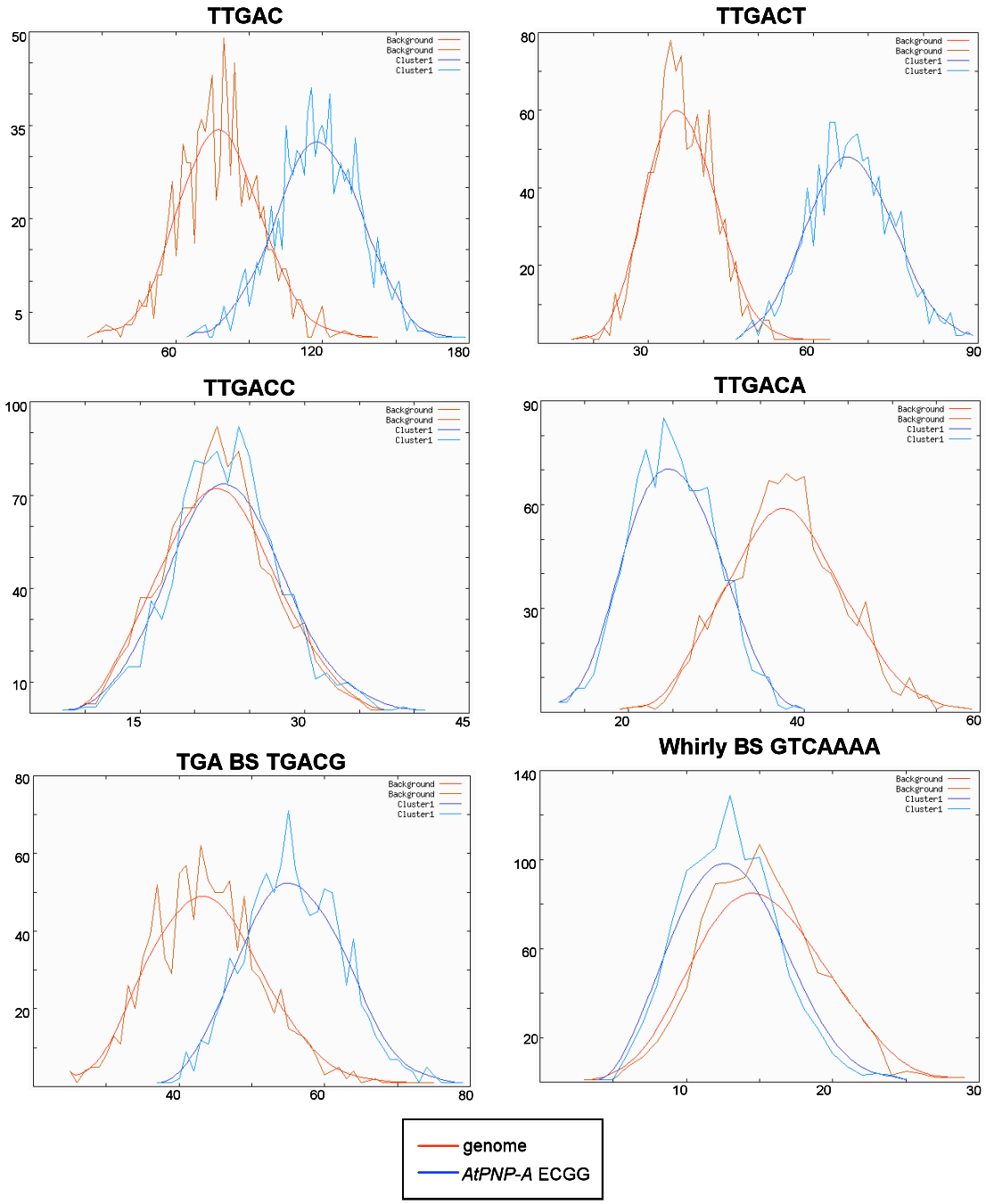

Figure 4.4. POBO distributions for TFBSs known to be associated with genes involved defence, in the *AtPNP-A* ECGG

POBO plots of core and stringent W-box promoter motifs, TGA and Whirly TFBSs in the *AtPNP-A* ECGG relative to the genome. Smooth plots are best fits for the raw data shown.

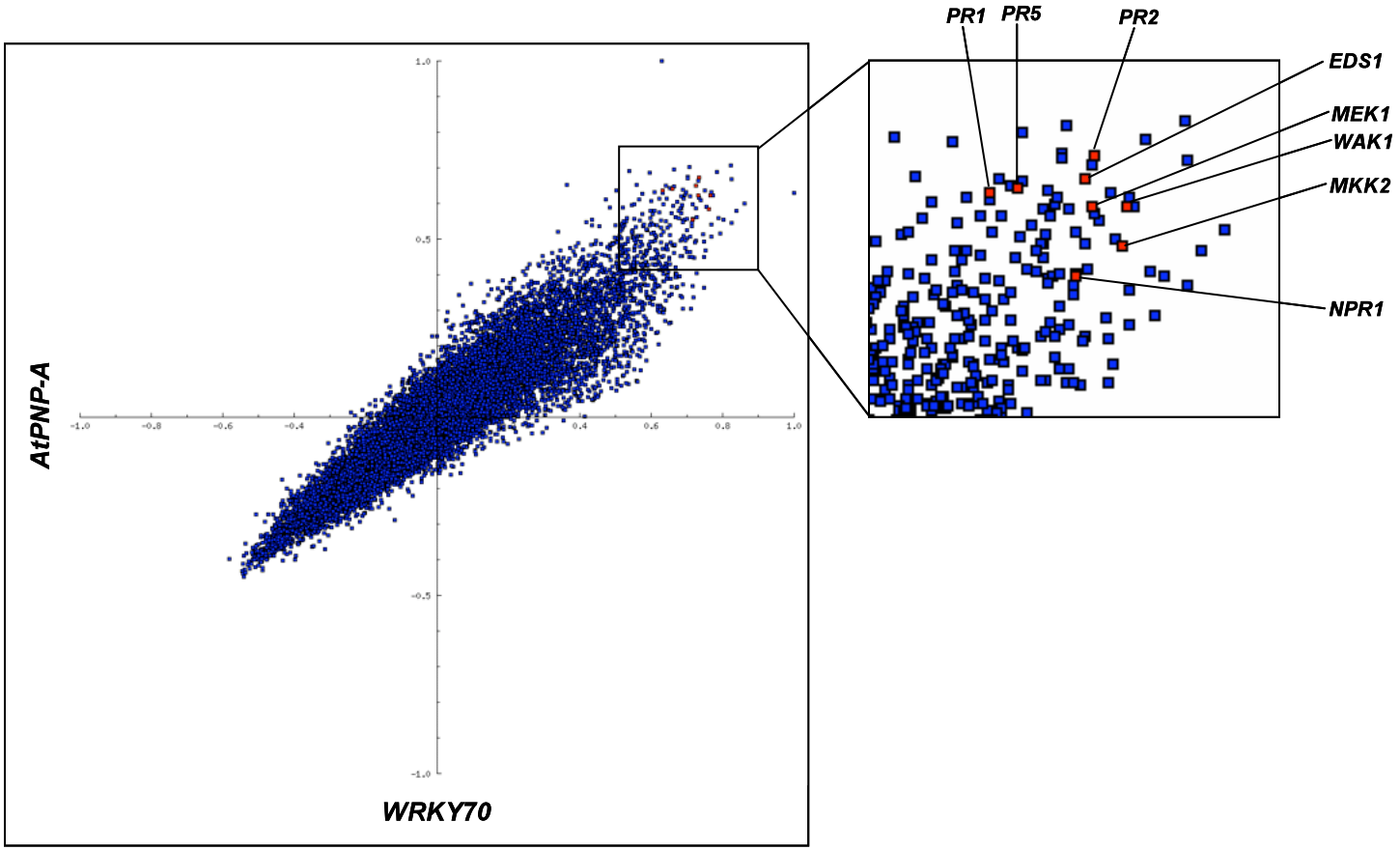

Figure 4.5. Scatter plot mapping the correlation of every gene to both *AtPNP-A* and *WRKY70*

Values on each axis are correlation (*r*) values. On the Y axis the correlation of every gene to *AtPNP-A* is plotted while on the X axis the correlation of every gene is plotted relative to *WRKY70*. Genes highlighted in red are the known defence genes that were present in the *AtPNP-A* ECGG. The genes that surround the highlighted defence genes are listed in Table 4.7.

Table 4.7. Genes emerging from the scatter plot

AGI ID	Gene Name	TTGACY	WRKY70 oex microarray
Highlighted genes			
AT2G14610	**PR1 (PATHOGENESIS-RELATED GENE 1)**	**4**	**0.142**
AT3G57260	**BGL2 (PATHOGENESIS-RELATED PROTEIN 2); glucan 1,3-beta-glucosidase/ hydrolase, hydrolyzing O-glycosyl compounds**	**2**	**3.199**
AT1G75040	**PR5 (PATHOGENESIS-RELATED GENE 5)**	**2**	**3.021**
AT3G48090	**EDS1 (ENHANCED DISEASE SUSCEPTIBILITY 1); signal transducer/ triacylglycerol lipase**	**3**	**0.889**
AT1G64280	NPR1 (NONEXPRESSER OF PR GENES 1); protein binding	0	0.949
AT1G21250	WAK1 (CELL WALL-ASSOCIATED KINASE); kinase	0	2.320
AT4G26070	**MEK1 (mitogen-activated protein kinase kinase 1); MAP kinase kinase/ kinase**	**3**	**1.285**
AT4G29810	ATMKK2 (MAP KINASE KINASE 2); MAP kinase kinase/ kinase	4	1.055
AT3G56710	SIB1 (SIGMA FACTOR BINDING PROTEIN 1); binding	0	-0.038
AT5G39670	calcium-binding EF hand family protein	2	0.709
AT5G52760	heavy-metal-associated domain-containing protein	4	2.427
AT5G27830	hypothetical protein	3	0.907
AT1G08450	CRT3 (CALRETICULIN 3); calcium ion binding	2	1.410
AT2G46430	ATCNGC3 (CYCLIC NUCLEOTIDE GATED CHANNEL 3); calmodulin binding / cyclic nucleotide binding / ion channel	2	2.030
AT2G14560	unknown protein	2	1.049
AT5G24530	oxidoreductase, 2OG-Fe(II) oxygenase family protein	0	1.456
AT3G26600	armadillo/beta-catenin repeat family protein	2	1.518
AT2G31890	hypothetical protein	0	2.301
AT2G40750	**WRKY54 (WRKY DNA-binding protein 54); transcription factor**	**1**	**-0.422**
AT5G60900	RLK1 (RECEPTOR-LIKE PROTEIN KINASE 1); carbohydrate binding / kinase	3	2.308
AT1G03400	2-oxoglutarate-dependent dioxygenase, putative	1	1.301
AT1G72930	TIR (TOLL/INTERLEUKIN-1 RECEPTOR-LIKE); transmembrane receptor	3	0.743
AT5G02290	NAK; kinase	3	1.035
AT2G02360	ATPP2-B10 (Phloem protein 2-B10); carbohydrate binding	1	0.804
AT5G52750	heavy-metal-associated domain-containing protein	2	3.158
AT5G12890	UDP-glucoronosyl/UDP-glucosyl transferase family protein	1	0.794
AT1G67970	AT-HSFA8 (Arabidopsis thaliana heat shock transcription factor A8); DNA binding / transcription factor	2	0.921
AT5G10380	zinc finger (C3HC4-type RING finger) family protein	1	1.404
AT1G23840	unknown protein	3	2.923
AT1G21270	WAK2 (wall-associated kinase 2); protein serine/threonine kinase	3	1.322
AT1G13470	unknown protein	3	2.745
AT4G33300	**ADR1-L1 (ADR1-LIKE 1); ATP binding / protein binding**	**2**	**1.478**
AT4G36210	unknown protein	3	1.035
AT1G14870	Uncharacterized protein	2	3.090
AT2G23680	stress-responsive protein, putative	0	1.381
AT3G08870	lectin protein kinase, putative	2	1.524
AT1G78200	protein phosphatase 2C, putative / PP2C, putative	1	0.299
AT1G33720	CYP76C6 (cytochrome P450, family 76, subfamily C, polypeptide 6); oxygen binding	0	0.866
AT4G11840	PLDGAMMA3 (phospholipase D gamma 3); phospholipase D	1	1.444
AT3G26210	CYP71B23 (cytochrome P450, family 71, subfamily B, polypeptide 23); oxygen binding	2	2.646
AT4G28490	HAESA (RECEPTOR-LIKE PROTEIN KINASE 5); ATP binding / kinase/ protein serine/threonine kinase	5	2.253
AT1G21240	WAK3 (WALL ASSOCIATED KINASE 3); kinase/ protein serine/threonine kinase	1	

Number of W-box promoter motifs (TTGACY) and the fold change (log2) values in the WRKY70 overexpressor (oex) microarray experiment are indicated.

from the *AtPNP-A* ECGG are among the genes that are most highly correlated with both *AtPNP-A* and *WRKY70* (highlighted in the figure). From the group of genes that fall within the plot area of these highlighted defence genes (area blocked in Figure 4.5 and corresponding genes listed in Table 4.7), most of the genes are found within the *AtPNP-A* ECGG and all of them are among the 100 genes whose expression is most positively correlated with *AtPNP-A*. Out of these 42 genes, 28 were induced more than two fold in a *WRKY70* overexpressor, including *PR2* and *PR5* that are known to be regulated by *WRKY70* and many of them contain multiple copies of the W-box promoter motif in their promoters. This suggests that *WRKY70* regulates at least a subset of the *AtPNP-A* ECGG including the well known defence genes.

4.3.4 Microarray expression data

Genevestigator was used to screen the publicly available microarray data to identify experiments in which *AtPNP-A* and the *AtPNP-A* ECGG are differentially expressed. For experiments of interest the original microarray data was obtained for better resolution of the expression profiles because Genevestigator combines data across tissue types, time points and experiments. Since correlation is based on directional changes in gene expression and not necessarily on quantitative changes, it is possible that the *AtPNP-A* ECGG may not be as strongly induced as *AtPNP-A* across all experiments. Furthermore the moderate correlation values might arise from the *AtPNP-A* ECGG being well correlated with *AtPNP-A* in some experiments but not in others. Experiments where *AtPNP-A* and the *AtPNP-A* ECGG are both highly expressed are likely to be conditions under which AtPNP-A and the *AtPNP-A* ECGG function together. On the other hand, experiments where expression of *AtPNP-A* is induced without that of the *AtPNP-A* ECGG may be conditions under which AtPNP-A has a unique function. Therefore the expression profile of *AtPNP-A* was compared to the mean expression of the *AtPNP-A* ECGG. Additionally the mean expression profile of the SAR annotated genes among the *AtPNP-A* ECGG (*PR1, PR2, PR5* and *EDS1*, termed the SAR ECGG) was considered separately in order to determine whether *AtPNP-A* behaves more similarly to these functionally annotated genes than to the *AtPNP-A* ECGG as a whole. Expression of *WRKY70* (also annotated as being involved in SAR) was considered individually to explore the possibility that *WRKY70* could regulate the co-expression of the *AtPNP-A* ECGG. The original microarray data revealed that in some of the controls *AtPNP-A* was lowly expressed. Expression of *AtPNP-A* was however highly induced in response to a number of treatments and different mutants.

4.3.4.1 Growth

An initial screen using Genevestigator suggested that transcription of *AtPNP-A* increases during development, reaching a maximum during bolting followed by a second smaller peak in the flower while in the anatomy *AtPNP-A* appeared to be most highly expressed in the sepal and the

senescent leaf. Previously irPNPs have been localized to the vasculature and proposed to play a role in cell expansion. Therefore the expression of *AtPNP-A*, the *AtPNP-A* ECGG, SAR ECGG and *WRKY70* was examined at these developmental stages, in these tissues and in response to treatments including mutants that are related to the vasculature and cell expansion (Figure 4.6A). In agreement with the Genevestigator results, expression of *AtPNP-A*, the *AtPNP-A* ECGG, SAR ECGG and *WRKY70* was induced in the 35 day old senescent leaf relative to a healthy 17 day old rosette leaf and in the sepal relative to the entire floral organ. It was then found that expression of *AtPNP-A* and the SAR ECGG was induced by treatment with NPA, an auxin transport inhibitor that induces vascular overgrowth (Wenzel *et al.*, 2008), relative to the control and in the *cov1* mutant, that displays increased vascular development (Parker *et al.*, 2003), relative to the wildtype; whereas expression of the *AtPNP-A* ECGG and *WRKY70* are only slightly induced under the same conditions. Therefore *AtPNP-A* and the SAR ECGG are strongly expressed in the vascular tissue where both irPNP and PR proteins are localized (Maryani *et al.*, 2003; van Loon *et al.*, 2006). The *elo3* mutant, that has altered cell expansion as a result of a decreased cell division rate (Nelissen *et al.*, 2005), displays elevated *AtPNP-A* expression relative to the wildtype control. While *WRKY70* expression was also upregulated in *elo3*, neither the *AtPNP-A* ECGG nor the SAR ECGG were induced, suggesting that AtPNP-A may play a unique role in coordination between cell expansion and cell division. GA is a key hormone involved in cell expansion well known for its role in germination and flowering (Olszewski *et al.*, 2002); processes mediated by GA-induced degradation of the growth repressor DELLA proteins (Cao *et al.*, 2006). Expression of *AtPNP-A*, the SAR ECGG, *WRKY70* and the *AtPNP-A* ECGG to a lessor extent, was induced in the GA deficient *ga1-3* mutant, relative to the wildtype and in all cases this elevated expression was reverted back to wildtype levels in a *ga1-3 della* mutant that lacks four of the DELLA proteins. This implies that expression of *AtPNP-A*, the *AtPNP-A* ECGG and SAR ECGG is repressed by GA and activated by the DELLA proteins. The manufacture of new cell wall components is key to the process of cell expansion (Cosgrove, 1993). Therefore it was also interesting to find that suspension cultures habituated with isoxaben, a cellulose synthesis inhibitor that induces cell wall remodelling (Manfield *et al.*, 2004), had lower levels of *AtPNP-A* expression relative to mock-treated controls. In this experiment the *AtPNP-A* ECGG and *WRKY70* had a similar expression pattern to that of *AtPNP-A*, however the SAR ECGG did not follow suit. Thus *AtPNP-A* expression is modified by multiple processes that regulate cell expansion. The transcript profile of *WRKY70* matched that of the *AtPNP-A* remarkably well, even when the *AtPNP-A* ECGG genes did not, indicating that *WRK70* has the potential to regulate *AtPNP-A* mediated growth effects.

A.

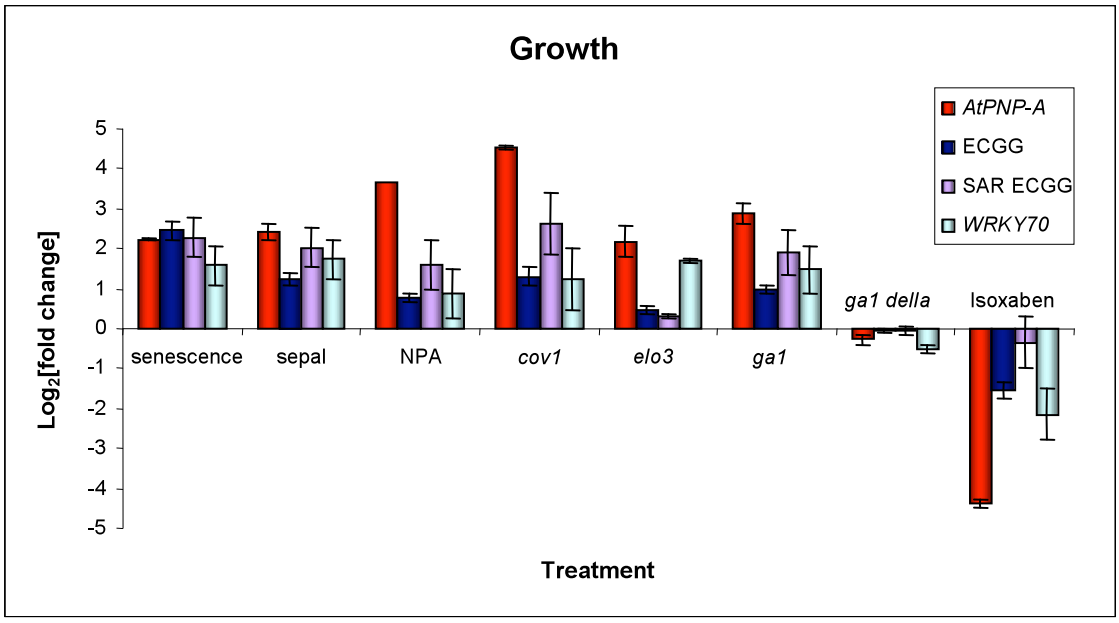

Figure 4.6A. Expression of *AtPNP-A* the *AtPNP-A* ECGG, SAR ECGG and *WRKY70* during development, growth and in related mutants

The expression of *AtPNP-A*, the *AtPNP-A* ECGG (ECGG - mean expression of the 50 genes most positively correlated with *AtPNP-A*), the SAR ECGG (mean expression of *PR1, PR2, PR5* and *EDS1*) and *WRKY70* in response to various treatments that affect growth are presented as $\log_2$[fold change] values relative to the appropriate controls. Treatments included: senescence (35 day old senescent leaves relative to 17 day old rosette leaf 4) (n = 3); sepal (relative to total expression in the whole flower at stage 12) (n = 3); *N*-(1-naphthyl) phthalamic acid (NPA) (n = 1); the *continuous vascular ring 1* (*cov1*) mutant (n = 2); the *elongata 3* (*elo3*) mutant (n = 3); the GA deficient *ga1* mutant and *ga1 della* mutants (floral tissue) (n = 6 in both cases) and isoxaben habituated suspension cultures (n = 3). Error bars are standard errors of the mean.

4.3.4.2 Abiotic stress

Initial Genevestigator results suggested that *AtPNP-A* expression is strongly induced in response to a number of abiotic stresses. In fact osmotic stress and ozone treatment appeared to be the most potent inducers of *AtPNP-A* expression. This together with reports that irPNP protein levels increase after NaCl and osmotic stress treatments (Rafudeen *et al.*, 2003), prompted an in depth investigation into the transcriptional response of *AtPNP-A*, the *AtPNP-A* ECGG, SAR ECGG and *WRKY70* to various abiotic stresses and in mutants that are compromised in their abiotic stress responses (Figure 4.6B). The data shown are late time points after treatment since it was noted that *AtPNP-A* expression generally increased with increasing time post treatment. Firstly NaCl, osmotic stress and K^+ starvation augmented *AtPNP-A* expression compared to the appropriate controls. The *AtPNP-A* ECGG and SAR ECGG were also induced in response to osmotic stress and K^+ starvation with the expression profile of the SAR ECGG closely matching that of *AtPNP-A*. However *WRKY70* expression was not induced by either treatment. In response to NaCl stress the *AtPNP-A* ECGG was not appreciably induced while expression of the SAR ECGG and *WRKY70* was slightly upregulated. Therefore even though NaCl stress has an osmotic component and induces K^+ starvation, the transcriptional responses of *AtPNP-A* and the *AtPNP-A* ECGG genes to these stresses are quite different. NaCl stress also induces a secondary oxidative stress (Katiyar-Agarwal *et al.*, 2006). It is therefore interesting that UV-B and ozone treatments that induce oxidative stress also greatly increased expression of *AtPNP-A*, the *AtPNP-A* ECGG, SAR ECGG and *WRKY70* relative to the controls. The transcript profile of the SAR ECGG in response to UV-B treatment was more similar than that of the *AtPNP-A* ECGG to *AtPNP-A*, whereas in response to ozone the SAR ECGG and *AtPNP-A* ECGG behaved similarly. Two phosphate starved mutants, *pho1* and *pho3* were found to display high levels of *AtPNP-A* expression relative to their wildtype controls. Expression of the *AtPNP-A* ECGG, SAR ECGG and *WRKY70* in *pho3* closely matched that of *AtPNP-A* while in *pho1* *AtPNP-A* expression was higher that that of the ECGG groups and *WRKY70*. Therefore the SAR ECGG displayed a higher degree of co-expression with *AtPNP-A* compared to the *AtPNP-A* ECGG in response to osmotic stress, K^+ starvation and UV-B treatment. Expression of *WRKY70* was not induced by osmotic stress or K^+ starvation suggesting that *WRKY70* does not play a role in these responses.

B.

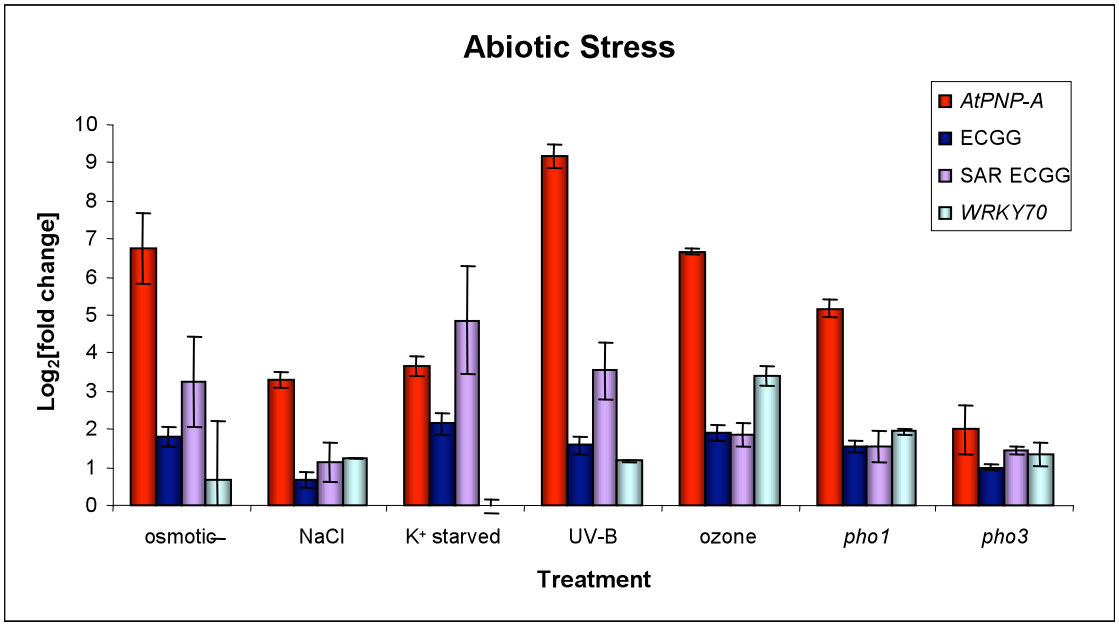

Figure 4.6B. Expression of *AtPNP-A*, the *AtPNP-A* ECGG, SAR ECGG and *WRKY70* in the response to abiotic stress

The expression profile of *AtPNP-A* is compared to the mean expression of the *AtPNP-A* ECGG (ECGG - described above), the SAR ECGG (described above) and *WRKY70*. Expression values are presented as $\log_2$[fold change] values relative to the appropriate controls. Treatments were 300 mM mannitol for 24 hrs (shoot tissue) (n = 2); 150 mM NaCl for 24 hrs (root tissue) (n = 2); K^+ starvation for 7 days (shoot tissue) (n = 3); 24 hrs following UV-B exposure (15 min exposure to 1.18 W m^{-2} UV-B, 310 nm light), (shoot tissue) (n = 2); ozone treatment (500 parts per billion (ppb) ozone fumigation) for 6 hrs (n = 3) and the phostphate starved *pho1* and *pho3* mutants (n = 3 in both cases). Error bars are standard errors of the mean.

In cases where expression was assayed separately in the shoot and root it was noted that, in general, *AtPNP-A* expression was induced in the shoot. However in response to NaCl treatment, *AtPNP-A* was expressed in the root. In fact *AtPNP-A* expression in response to NaCl stress was root-specific whereas in response to iso-osmotic stress *AtPNP-A* expression was induced specifically in the shoot. This suggests that AtPNP-A responds and possibly functions quite differently in the response to NaCl and osmotic stresses. In order to determine whether this is a feature unique to *AtPNP-A* or whether it is shared by other genes known for their role in NaCl and osmotic stress responses, the tissue specific expression pattern of *AtPNP-A* and selected NaCl and osmotic stress response genes was compared (Figure 4.6C-D). While there was a tendency for *AAO3*, *NCED3* and *ABI1* to be more strongly induced in the shoot in response to osmotic stress than in response to NaCl stress and more strongly induced in the root in response to NaCl stress compared to osmotic stress, none of these genes showed the restricted tissue specific expression profile observed for *AtPNP-A*. On the other hand the *AtPNP-A* ECGG and SAR ECGG genes behaved similarly to *AtPNP-A* (Figure 4.6E) although neither of these were as strongly induced as *AtPNP-A* in response to NaCl treatment. The expression of *WRKY70* did not show the same tissue specific expression pattern as that of *AtPNP-A* and the ECGG, since *WKRY70* was not induced in the shoot in response to osmotic stress, however its expression in the root in response to NaCl stress was consistent with that of *AtPNP-A*. Therefore the expression of the other WRKY transcription factors whose expression were correlated with *AtPNP-A* was examined in the shoot and root in response to NaCl and osmotic stress in order to determine whether any of these could be responsible for the tissue-specific expression pattern of *AtPNP-A* (Figure 4.6F-G). Included in this analysis was *WRKY54*, a member of the *AtPNP-A* ECGG as well as *WRKY60* (160^{th} gene most positively correlated with *AtPNP-A*; $r = 0.480$) and *WRKY46* (180^{th} gene most expression correlated with *AtPNP-A*; $r = 0.468$). It was found that *WRKY46* was more strongly induced than *WRKY70* in the root in response to NaCl stress and in response to K^+ starvation but *WRKY46* was not appreciably induced in the shoot in response to osmotic stress. On the other hand *WRKY60* showed the strongest shoot-specific induction in response to osmotic stress and was also induced in response to K^+ starvation, but was not induced by NaCl stress in the root. Therefore it does not seem that a single *WRKY* transcription factor is responsible for the tissue-specific induction of *AtPNP-A* expression in response to the NaCl and osmotic stresses but rather that different *WRKY*s may be responsible in each tissue.

C.

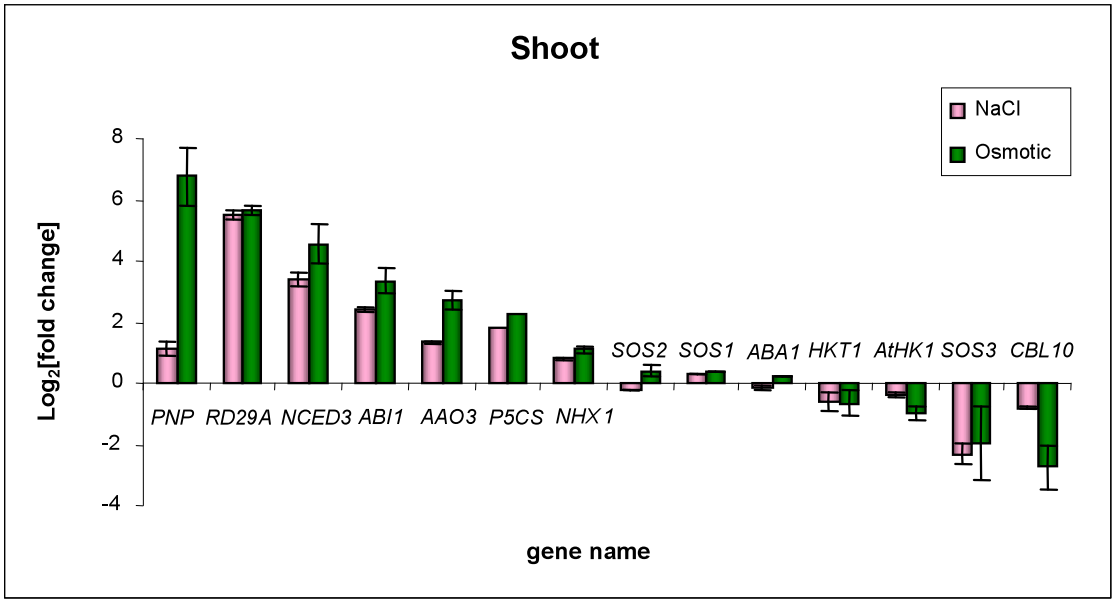

D.

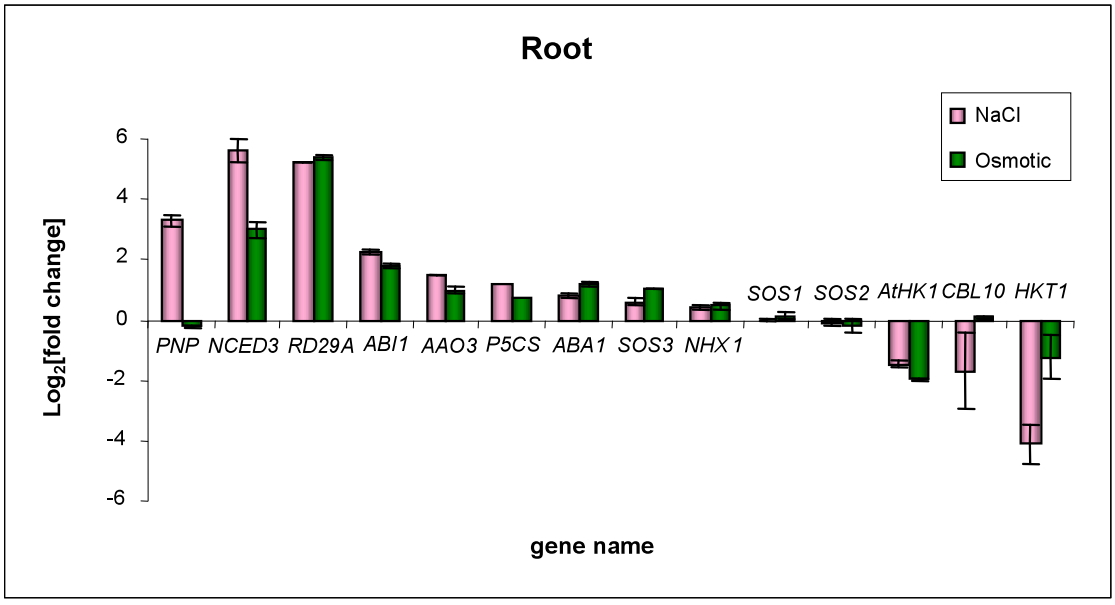

Figure 4.6C and D. Expression of *AtPNP-A* and genes known for their role in NaCl and osmotic stress responses in the shoot and root in response to NaCl and osmotic stress treatments

Expression of *AtPNP-A* (refered to as *PNP* in the figure) and the NaCl and osmotic stress response genes is shown as $\log_2$[fold change] values relative to the appropriate controls in the shoot (C) and in the root (D) in response to 150 mM NaCl for 24 hrs (n = 2) and 300 mM mannitol for 24 hrs (n = 2). Error bars are standard errors of the mean.

E.

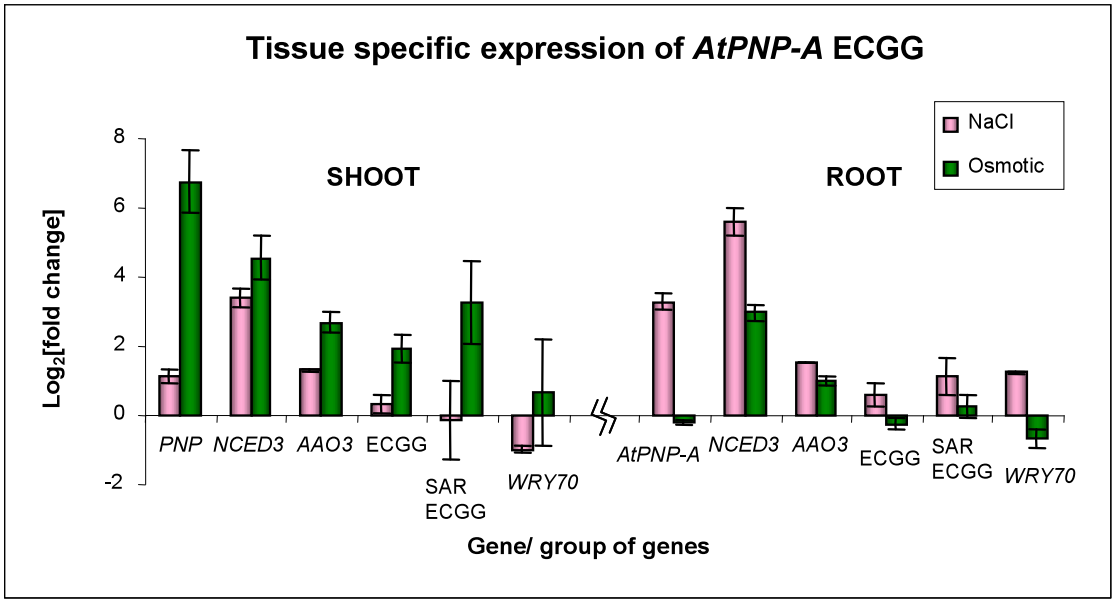

Figure 4.6E. Tissue specific expression of *AtPNP-A*, the *AtPNP-A* ECGG, SAR ECGG and *WRKY70* in response to NaCl and osmotic stress

Expression of *AtPNP-A* (referred to as *PNP* in the figure), the *AtPNP-A* ECGG, the SAR ECGG and *WRKY70* is shown alongside that of *9-CIS-EPOXYCAROTENOID DIOXYGENASE 3* (*NCED3*) and *ABSCISIC ALDEHYDE OXIDSASE 3* (*AAO3*) - the genes that showed the best tendency toward shoot expression in response to osmotic stress and root expression in response to NaCl stress (refer to Figures 3C and 3D above). Expression is shown as $\log_2$[fold change] values relative to the appropriate control (water) in the shoot and in the root in response to 150 mM NaCl for 24 hrs (n = 2) and 300 mM mannitol for 24 hrs (n = 2). Error bars are standard errors of the mean.

F.

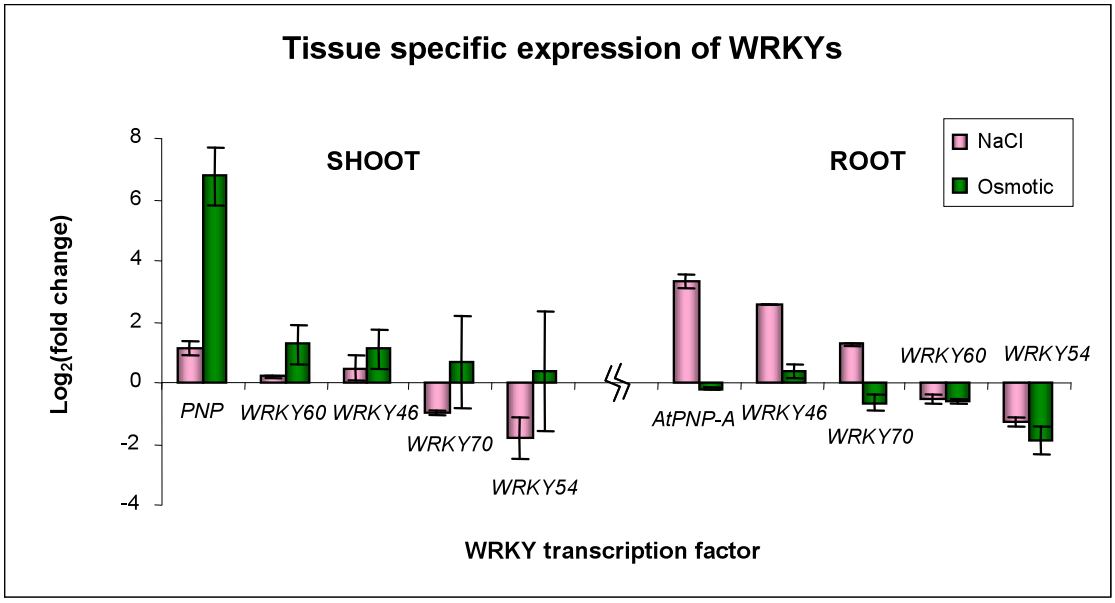

G.

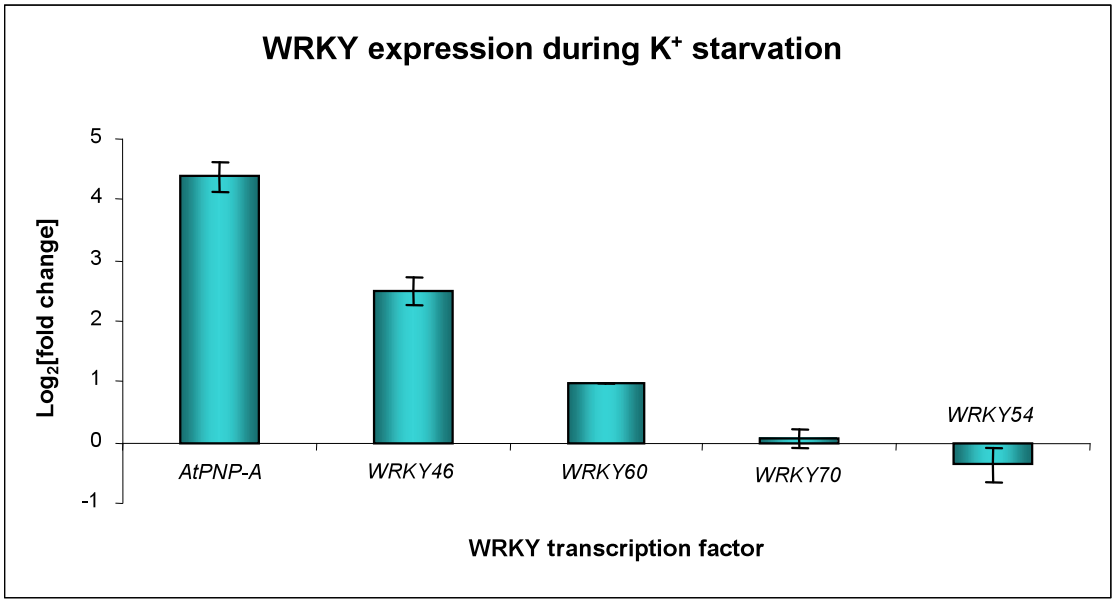

Figure 4.6F and G. The tissue specific expression pattern of the *WRKYs* in response to NaCl and osmotic stress and K^+ starvation

Shoot and root expression of WRKY transcription factors whose expression is correlated with that of *AtPNP-A*, in response to NaCl and osmotic stress is shown in 3F. Expression is $\log_2$ of the fold change. For the NaCl treatment samples were treated for 24 hrs with 150 mM NaCl and for the osmotic stress plants were treated with isoosmolar 300 mM mannitol for 24 hrs. In both cases n = 2. For the K^+ starvation, expression was analysed seven days after plants were transferred to K^+ deficient media (3G). The data shown is that of the shoot tissue and n = 3. Error bars represent the standard error of the mean.

4.3.4.3 Biotic stress

Genevestigator results suggested that, in addition to abiotic stresses, biotic stresses imposed by pathogens strongly induced *AtPNP-A* expression. Expression of *AtPNP-A*, the *AtPNP-A* ECGG, SAR ECGG and *WRKY70* was therefore examined in response to a number of biotic stresses, presented in Figure 4.6H. Expression of *AtPNP-A*, the *AtPNP-A* ECGG, SAR ECGG and *WRKY70* was upregulated in response to infection with both virulent (ES 4326) and avirulent strains of the biotrophic bacterial pathogen *P. syringae* relative to the mock-infected control. The avirulent strains included those containing the *Rpt2*, *Rpm1* and *Rps4* avirulence genes. *AtPNP-A* expression was most strongly induced in response to avirulent *P. syringae Rps4* and *Rpm1* while the *AtPNP-A* ECGG and SAR ECGG were not as strongly induced. However in response to the virulent (ES 4326) and *Rpt2* avirulent strains, the expression pattern of the *AtPNP-A* ECGG, SAR ECGG and *WRKY70* closely matched that of *AtPNP-A*. Expression of *AtPNP-A* was also induced in response to two biotrophic obligate oomycete *Erysiphe* sp. (*E. orontii* and *E. cichoracearum*), the non host fungal pathogen, *Phytophthora infestans*, and the phloem feeding insect herbivore, *Bemisia tabaci* compared to the respective uninfected controls. In response to the *Erysiphe* sp. and *B. tabaci*, the induced expression of the SAR ECGG was more strongly correlated with *AtPNP-A* than that of the *AtPNP-A* ECGG whereas *WRKY70* expression was not appreciably induced. However following *P. infestans* treatment the upregulated expression of the *AtPNP-A* ECGG, SAR ECGG and *WRKY70* was highly congruent with that of *AtPNP-A*. In contrast, induction of *AtPNP-A*, the *AtPNP-A* ECGG, SAR ECGG and *WRKY70* expression in response to the necrotrophic fungal pathogen, *Botrytis cinerea*, was negligible. Therefore *AtPNP-A* expression is induced by biotrophic pathogens but not by the necrotrophic pathogen *B. cinerea*.

The Genevestigator screen also suggested that *AtPNP-A* expression is altered in a number of mutants that are affected in their defence response. The expression of *AtPNP-A*, the *AtPNP-A* ECGG, SAR ECGG and *WRKY70* in some of these mutants is depicted in Figure 4.6I. Expression of *AtPNP-A* was found to be induced in mutants that show constitutive activated defence responses including the *cpr5*, *mpk4*, *sni1* and in a *WRKY70* overexpressor, relative to their respective wildtype controls. In *cpr5*, *mpk4* and *sni1* the induced expression of the SAR ECGG matches that of *AtPNP-A* remarkably well, while expression of the *AtPNP-A* ECGG is not as strongly induced. In the *cpr5* and *mpk4* mutants, induced expression of *WRKY70* is similar to that of the *AtPNP-A* ECGG while in the *sni1* mutant *WRKY70* expression is not induced. Remarkably, in the *WRKY70* mutant, *AtPNP-A* expression is more strongly induced that that of *WRKY70* itself while the induced expression of the *AtPNP-A* ECGG and SAR ECGG is similar to that of *WRKY70*. In contrast, *AtPNP-A* expression was repressed in mutants that are compromised in their defence responses, in particular the SA-depleted *NahG* mutant as

H.

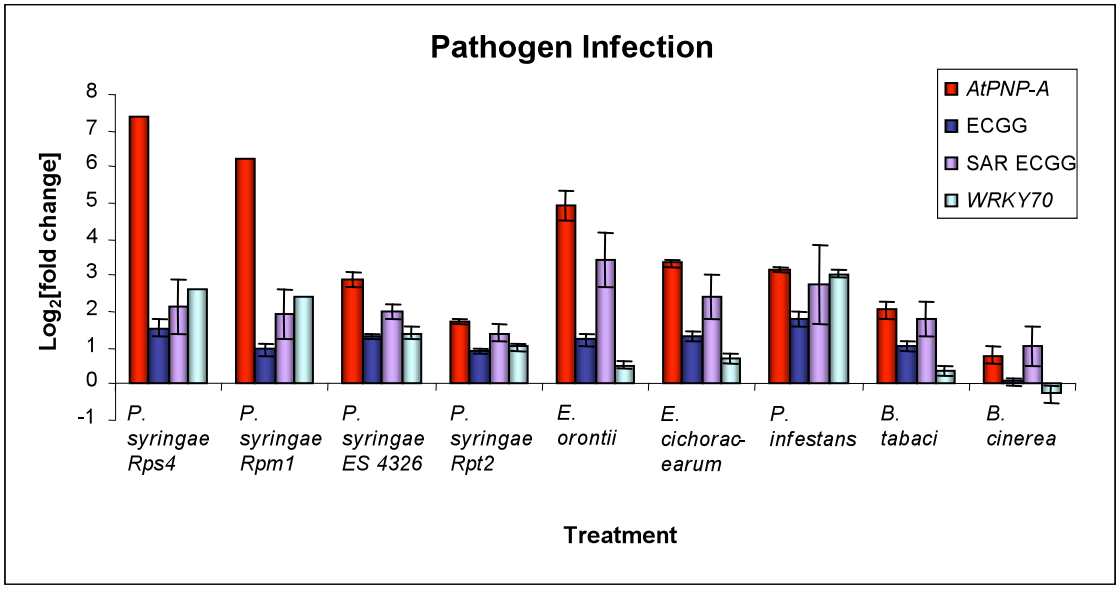

Figure 4.6H. Expression of *AtPNP-A*, the *AtPNP-A* ECGG, SAR ECGG and *WRKY70* in response to pathogen infection

Expression of *AtPNP-A*, the *AtPNP-A* ECGG (ECGG), SAR ECGG and *WRKY70* in response to infection by various pathogens is shown as $\log_2$ fold change values. Treatments were: *P. syringae Rps4* and *Rpm1* avirulent strains n = 1 for both; *P. syringae Rpt2* (avirulent) and *ES 4326* (virulent) strains for which n = 2; virulent *Erisyphe* species: *E. orontii* (n = 2) and *E. cichoracearum* (n = 4); the non-host pathogen *P. infestans* (n = 3); silverleaf whitefly *B. tabaci* (n = 2) and the necrotrophic fungal pathogen *B. cinerea* (n = 3). Error bars are standard errors of the mean.

I.

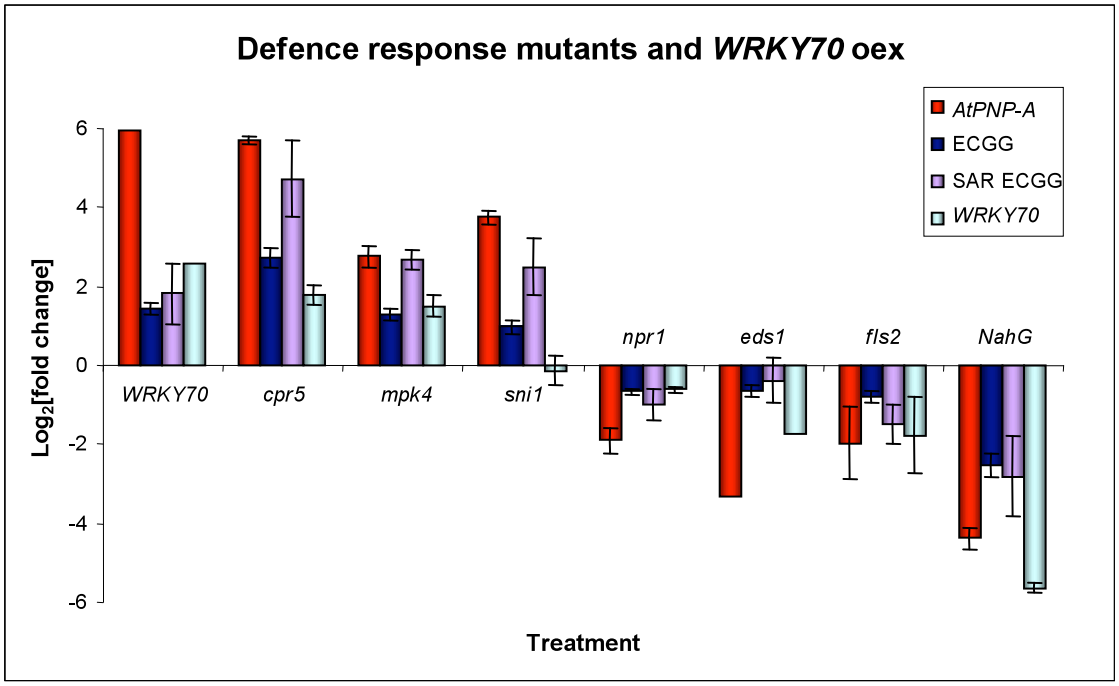

Figure 4.6I. Expression of *AtPNP-A*, the *AtPNP-A* ECGG, SAR ECGG and *WRKY70* in defence response mutants and the *WRKY70* overexpressor (oex)

Expression changes in various mutants affected in their defence response against pathogens are shown as $\log_2$ fold change values relative to the corresponding wildtype controls. Mutants included were the constitutive SAR mutants: *constitutive expression of PR genes 5* (*cpr5*) (n = 2); *map kinase 4* (*mpk4*) (n = 3) and *suppressor of NPR1, inducible 1* (*sni1*) (n = 3); while mutants that are compromised in SA-mediated signalling included *non-expressor of PR genes 1* (*npr1*) (n = 3); *eds1* (n = 1) and the SA depleted mutant *NahG* (n = 2). Finally the *flagellin sensitive 2* (*fls2*) mutant is compromised in basal defence (n = 2). Also shown is the expression profile in a *WRKY70* overexpressor (n = 1). Error bars are standard errors of the mean.

well as mutants in key genes in the SA signalling pathway - *npr1* and *eds1* relative to their wildtype controls. Expression of the *AtPNP-A* ECGG, SAR ECGG and most of all *WRKY70* was also strongly repressed in the *NahG* mutant. In the *npr1* and *eds1* mutants, however, expression of the *AtPNP-A* ECGG, SAR ECGG and *WRKY70* is not as strongly repressed as that of *AtPNP-A*. It was noted that *EDS1* expression was repressed in the *eds1* mutant ($\log_2$ = -1.87) as expected. Expression of *AtPNP-A* was additionally repressed in the *fls2* mutant that is compromised in its basal defence against bacterial pathogens, compared to the wildtype. The expression profiles of *AtPNP-A*, the *AtPNP-A* ECGG, SAR ECGG and *WRKY70* were qualitatively similar to that of *AtPNP-A* in this mutant. Altogether these results suggest that expression of the *AtPNP-A* ECGG is dependent on *FLS2*, *EDS1*, SA and *NPR1* while its expression is induced by *WRKY70* and repressed by *SNI1*.

Expression of the *AtPNP-A* ECGG is well correlated with that of *AtPNP-A* in the response to pathogens. In this series *AtPNP-A* expression is better correlated with that of the SAR ECGG than the *AtPNP-A* ECGG as a whole implying that *AtPNP-A* behaves like the SAR ECGG genes in response to pathogens. The induction of the *AtPNP-A* ECGG in the *WRKY70* overexpressor supports the notion that *WRKY70* may regulate the co-expression of the *AtPNP-A* ECGG.

4.3.4.4 Chemicals and hormones

Finally, *AtPNP-A* expression was examined in response to hormones that are known to play a role in abiotic and biotic stress signalling (Figure 4.6J). Elevated *AtPNP-A* expression was observed following treatment with SA as well as its less toxic functional analog BTH relative to mock-treated controls. Expression of the *AtPNP-A* ECGG and *WRKY70* was also strongly induced in response to SA and BTH. Unexpectedly however, the SAR ECGG was not induced in response to SA because *PR5* expression was down-regulated in this microarray experiment. Probably the treatment time of 3 hrs was too short to induce *PR5* expression, since the expression of the *PR* genes is generally examined after longer times of SA treatment (Murray *et al.*, 2007). In accordance with this, expression of all the *PR* genes were highly induced by 24 hr BTH treatment. The BTH induction of *AtPNP-A*, the *AtPNP-A* ECGG, SAR ECGG and *WRKY70* was found to be NPR1-dependent since BTH did not induce the expression of these genes in the background of the *npr1* mutant. This suggests that the *AtPNP-A* ECGG is induced by SA in an NPR1-dependent manner. On the other hand JA, another hormone involved in biotic stress signalling did not induce expression of *AtPNP-A*, the *AtPNP-A* ECGG, SAR ECGG or *WRKY70* and neither did the abiotic stress hormone ABA, consistent with reports that JA and ABA antagonize the SA signalling pathway (Loake and Grant, 2007). Lastly, treatment with the translational inhibitor CHX that is required for the induction of the defence secretome during

J.

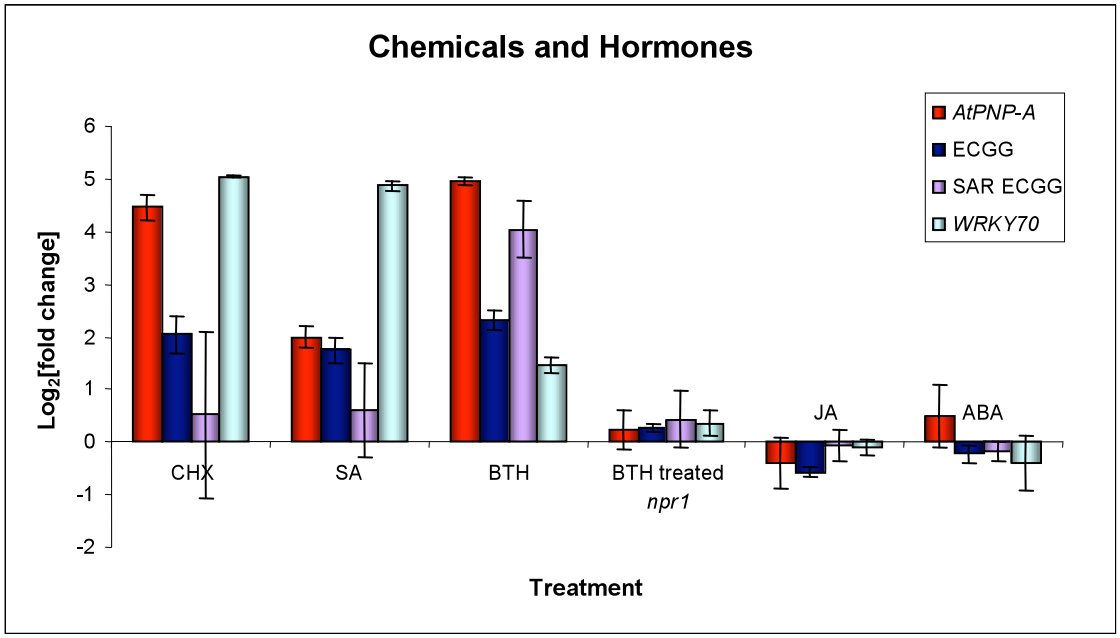

Figure 4.6J. Expression of *AtPNP-A* and the ECGG in response to chemical and hormone treatment
The effect of chemical and hormone treatments on the expression of *AtPNP-A*, the ECGG, SAR ECGG and *WRKY70* is shown. Expression values are $\log_2$ fold changes. Treatments are CHX (n =2); SA treatment for 3 hrs (n = 2), treatment of wildtype and *npr1* mutant plants with the SA functional analog benzothiadiazole S-methylester (BTH) (n = 3 in both cases) and finally JA and ABA treatments for which n = 2. Error bars are standard errors of the mean.

SAR (Wang *et al.*, 2005) augmented the expression of *AtPNP-A*, the *AtPNP-A* ECGG and the *WRKY70* however did not increase the expression of the SAR ECGG. Therefore the *AtPNP-A* ECGG is specifically induced by SA and chemicals that induce defence response genes involved in the SA signalling pathway.

4.3.5 Experimental validation of the microarray data

4.3.5.1 Semi-quantitative RT-PCR validation of select experiments

From the above microarray results, a few experiments were chosen for validation by semi-quantitative RT-PCR based on the fact that *AtPNP-A* expression was highly induced in these experiments and they could be easily replicated in the laboratory. This included NaCl, osmotic stress and K^+ starvation treatments as a selection of abiotic stresses; SA and UV-B treatments as these induce the plant's immune response mimicking biotic stress and CHX treatment since the microarray data showed this to be a potent inducer of *AtPNP-A* expression. Expression of *AtPNP-A* was induced in response to all of these treatments relative to the appropriate controls (Figure 4.7). Therefore *AtPNP-A* expression behaves as predicted by the 266070_at probe, indicating that computational analysis of *AtPNP-A* based on the expression profile of 266070_at across the microarray experiments is meaningful. This serves to validate the microarray data for these select experiments and instils confidence in the data obtained from the remaining microarray experiments in which *AtPNP-A* expression has not yet been confirmed.

4.3.5.2 Expression of AtPNP-A and select ECGG genes in response to pathogens

Results of the correlation analysis and subsequent GO, promoter content and expression analyses of the *AtPNP-A* ECGG point to a role for AtPNP-A in the response to pathogens. In order to confirm that expression of *AtPNP-A* is induced in response to pathogens and that the *AtPNP-A* ECGG is indeed co-expressed with *AtPNP-A*, the expression of *AtPNP-A* and select *AtPNP-A* ECGG genes was investigated in response to SA treatment and pathogen infection. The select *AtPNP-A* ECGG genes chosen for this analysis were *WAK1*, *PR1* which also serves as a positive control and *WRKY70* to further explore the possibility that it regulates the co-expression of the *AtPNP-A* ECGG. It could be argued that co-expression of a transcription factor and its targets is unlikely since some delay would be expected between their expression to allow for the transcription factor to be translated and translocated to the nucleus. Although this highlights a limitation of the correlation analysis, the majority of microarray experiments are not well dissected time courses but rather single time point treatments or mutant studies, therefore subtle temporal patterns of gene expression may not greatly affect this type of analysis. The best time course of transcription in response to pathogen infection is a *P. syringae* half leaf infection experiment conducted by the AtGENExpress Consortium. In this time course transcriptome changes were examined 4 - 48 hrs post infection (Figure 4.8). From this

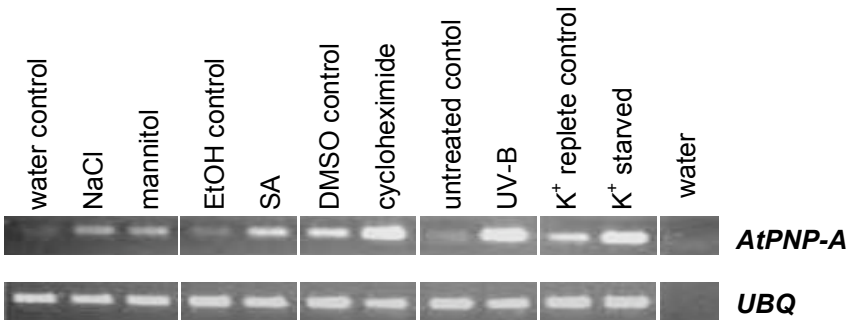

Figure 4.7. Validation of the publicly available microarray data

Semi-quantitative RT-PCR confirmed the induction of *AtPNP-A* expression in response to NaCl and osmotic stress (mannitol) relative to the water control; SA relative to the EtOH control; CHX relative to the DMSO control; UV-B relative to the untreated control and K^+ starved relative to the K^+ replete control. Treatments were 150 mM NaCl treatment and 300 mM mannitol for 6 hrs; 1 mM SA treatment for 3 hrs; 10 μM CHX for 3 hrs; 15 min UV-B (310 nm) followed by 6 hrs recovery under the normal light regime and seven days K^+ starvation in K^+ deficient media. Primers that amplify the *AtPNP-A* gene span the intron to ensure that product formed is the result of cDNA and not the result of genomic DNA contamination. *UBQ* was used as the control gene to show that there was approximately equal amount of template in each sample, while water was the negative control for the PCR reaction.

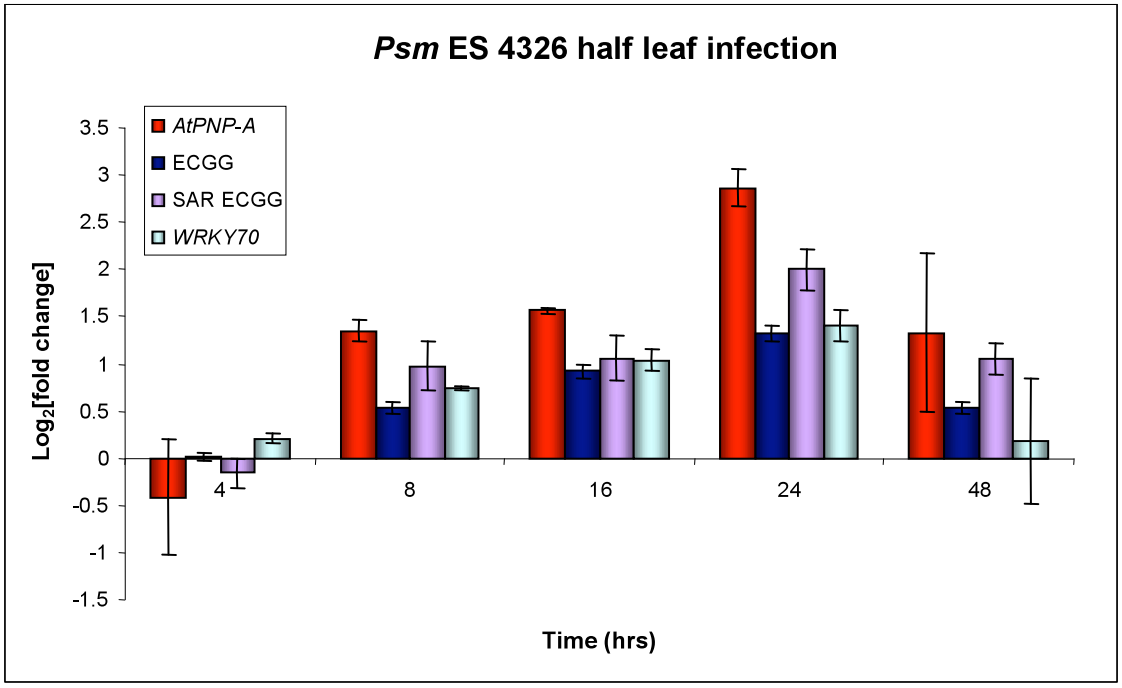

Figure 4.8. Expression of *AtPNP-A*, the *AtPNP-A* ECGG, SAR ECGG and *WRKY70* in the *Psm* ES 4326 half leaf infection microarray experiment

Time course of *AtPNP-A* and *WRKY70* transcription in response to virulent *P. syringae* pv. *maculicola* (*Psm*) ES 4326 infection, expressed as $\log_2$ fold change values. For each time point n = 2 and error bars are standard errors of the mean. *WRKY70* expression may precede that of *AtPNP-A*, the *AtPNP-A* ECGG and SAR ECGG as is expected for a transcription factor and its target genes, however this is not clear.

experiment it could not be resolved whether *WRKY70* expression preceded that of the *AtPNP-A* ECGG. Therefore a time course experiment including earlier time points was conducted to monitor temporal changes in gene expression in response to SA treatment and pathogen infection, in an attempt to delineate *WRKY70* expression from that of the *AtPNP-A* ECGG.

Expression of *AtPNP-A, WAK1, PR1* and *WRKY70* were all induced over a 48 hr time course of SA treatment relative to the EtOH control (Figure 4.9A). Expression of *AtPNP-A* was induced relative to the control 6, 12 and 24 hrs following treatment. At 48 hrs and 24 hrs, *AtPNP-A* expression was induced in both the control and treated samples relative to the earlier time points. This have may be the result of a wound response or osmotic effect. Induction of *WAK1* expression was apparent earlier at 3, 6, 12 and 24 hrs after treatment and was similarly induced in the control sample at 48 hr. Expression of *PR1*, like that of *WAK1*, was induced earlier than *AtPNP-A*, from 3 hrs after treatment, however unlike the other two genes the induced expression of *PR1* was prolonged, remaining clearly elevated over the control samples at all subsequent time points, as expected (Murray *et al.*, 2007). In contrast *WRKY70* expression was induced from the earliest time point post treatment, 1 hr and was clearly up-regulated over the control in the 3, 6, and 12 hr treatments. At later time points *WRKY70* expression was also induced in the control samples, at both 24 and 48 hrs following treatment. Therefore the transcript profile of *AtPNP-A* and *WAK1* mirrored that of *WRKY70* but was temporally delayed, allowing for the possibility that *WRKY70* regulates the co-expression of these genes in response to SA.

In the *P. syringae* time course, expression of *AtPNP-A* and the select *AtPNP-A* ECGG genes was induced in response to both avirulent and virulent *P. syringae* strains relative to mock infection with $MgCl_2$ (Figure 4.9B). The transcript profiles of *AtPNP-A, WAK1* and *WRKY70* were nearly identical. Each was induced 1 hr after treatment with both avirulent and virulent *P. syringae* with expression returning to baseline levels at 3 hrs post infection, following which a second induction was observed 6 hrs after treatment with the avirulent pathogen and 12 hrs after treatment with the virulent pathogen. At 48 hrs post infection with both *P. syringae* strains the expression of all three genes was somewhat reduced. This biphasic expression pattern has previously been reported for defence response genes following pathogen infection (Murray *et al.*, 2007). On the other hand, *PR1* had a slightly different transcript profile as it did not show the initial phase of induction but was induced at the later time points, displaying high expression at 12, 24 and 48 hrs after treatment with the avirulent pathogen and moderate expression after 12 hrs of treatment with the virulent pathogen that was increased further at 24 and 48 hrs. Expression of *PR1* was again prolonged compared to the other genes and did not wane at later time points, as expected (Murray *et al.*, 2007). The earlier and quantitatively larger induction of gene expression in response to the avirulent pathogen compared to virulent pathogen is expected

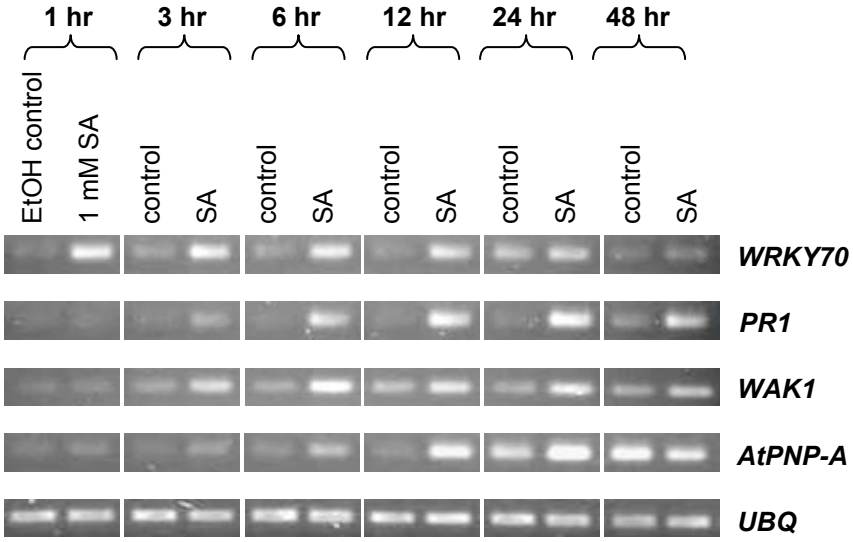

Figure 4.9A. Expression of *AtPNP-A* and select *AtPNP-A* ECGG genes in response to SA treatment
Leaves of four week old plants were treated with 1 mM SA or the equivalent concentration of EtOH as a control for the times indicated. The expression of *AtPNP-A*, *WAK1*, *PR1* and *WRKY70* was investigated using semi-quantitative RT-PCR. The "housekeeping" gene was *UBQ*, used to show the relative amount of template in each sample. Expression of all of these genes was induced by SA, most notably at 6 and 12 hrs following treatment.

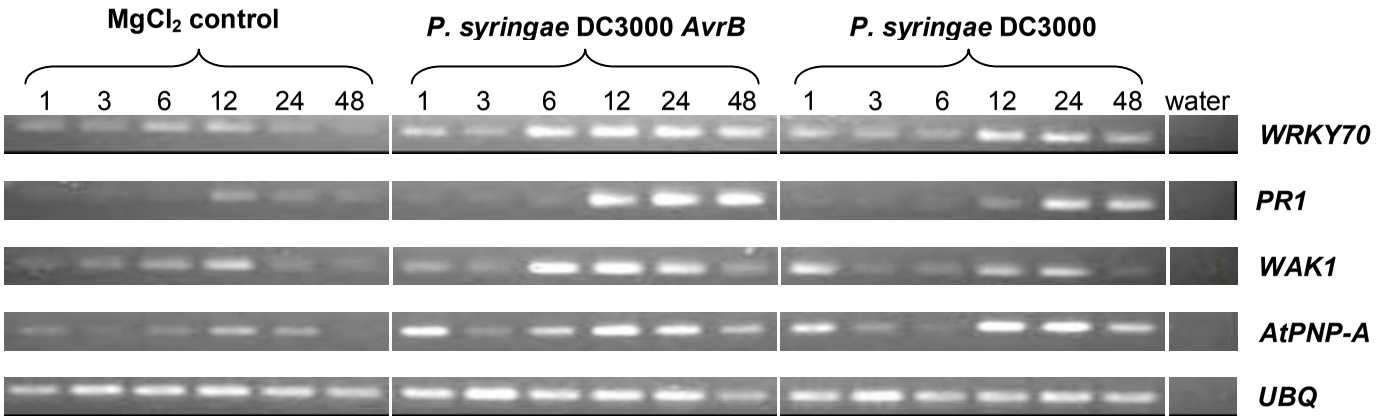

Figure 4.9B. Expression of *AtPNP-A* and select *AtPNP-A* ECGG genes in response to *P. syringae* infection

Leaves of four week old plants were pressure infiltrated with 1 X 10^6 cfu/ ml of *P. syringae* DC3000 (virulent strain); *P. syrinage* DC3000 *AvrB* (avirulent strain) or 10 mM $MgCl_2$ (control). Samples were harvested at the times (in hrs) indicated post infection. The expression of *AtPNP-A*, *WAK1*, *PR1* and *WRKY70* was investigated using semi-quantitative RT-PCR. Again *UBQ* is the "housekeeping" gene used to show the relative amount of template in each sample. Expression of these genes was induced by *P. syringae* infection. A biphasic pattern of expression is apparent for *AtPNP-A*, *WAK1* and WRKY70, however not for *PR1*. In each case the induced expression was faster and stronger in response to the avirulent pathogen as is expected for the incompatible interaction (Tao *et al.*, 2003).

for defence response genes (Tao *et al.*, 2003). Since *WRKY70*, *AtPNP-A* and *WAK1* expression was induced at the earliest time point measured, it is impossible to draw any conclusions as to whether *WRKY70* expression precedes that of the other genes in this case.

Finally, the *B. cinerea* time course revealed that *AtPNP-A, WAK1* and *WRKY70* expression was induced 24 and 48 hrs after both grape juice (control) and *B. cinerea* treatments (Figure 4.9C). Again *PR1* expression was somewhat different from the rest as it was not induced in the control samples but appeared to be specifically induced 48 hrs after *B. cinerea* infection. However this is in agreement with the published data (Ferrari *et al.*, 2003). Since *B. cinerea* is thought to induce JA-mediated defence responses, this suggests that *AtPNP-A, WAK1* and *WRKY70* are specifically induced by pathogens that initiate SA-mediated defence responses. The fact that *WRKY70, WAK1* and *AtPNP-A* expression was induced non-specifically in control and treated samples at late time points in both the SA and *B. cinerea* time courses could result from the detached leaf assay method. It is possible that at 48 hrs the detached leaves have begun to senesce which, according to the microarray data, would account for their induced expression.

Importantly, *AtPNP-A*, *WAK1*, *PR1* and *WRKY70* have been confirmed to be co-expressed in the response to SA treatment and *P. syringae* infection (He *et al.*, 1998; Li *et al.*, 2004). Expression of *WAK1* was best correlated with that of *AtPNP-A* while *PR1* was the most dissimilar since its induced expression was always maintained for longer however, it did serve to confirm that the treatments had been successful. *WRKY70* expression preceded that of the other genes in response to SA, allowing for the possibility that it regulates the co-expression of these select *AtPNP-A* ECGG genes. These results give confidence that the remaining *AtPNP-A* ECGG genes are co-expressed in response to SA and SA-inducing treatments.

4.3.5.3 Expression of the select AtPNP-A ECGG in the atpnp-a mutant

A preliminary experiment was conducted to investigate the interaction between *AtPNP-A* and the select *AtPNP-A* ECGG genes. In order to test whether the expression of any of these genes is dependent on *AtPNP-A* during the pathogen response, their expression was examined in the *atpnp-a* mutant post infection with *P. syringae* at 12 and 24 hrs (time points at which these genes were strongly induced in the *P. syringae* time course). Expression of *AtPNP-A* was lower in the *atpnp-a* mutant compared to the wildtype in all samples, as expected (Figure 4.10). The pattern of *PR1* and *WRKY70* expression was identical in the *atpnp-a* mutant and wildtype lines. In contrast, induced expression of *WAK1* was lower in the *atpnp-a* mutant after 12 hr treatment with the avirulent pathogen, however this phenotype did not persist at 24 hrs. Furthermore there was no difference in *WAK1* expression in the *atpnp-a* mutant and wildtype lines in response to the virulent pathogen. Therefore this result may not be reproducible and should be repeated.

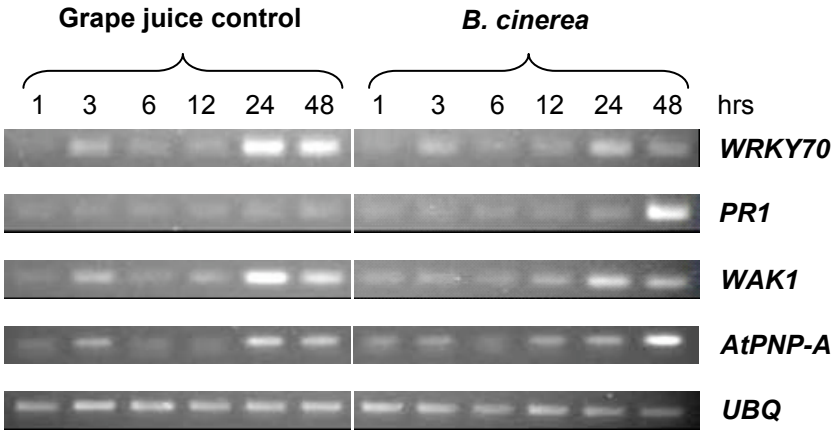

Figure 4.9C. Expression of *AtPNP-A* and select *AtPNP-A* ECGG genes in response to *B. cinerea*
Leaves of four week old plants were inoculated with 5 X 10^4 spores/ml *B. cinerea* (pepper isolate) or half strength grape juice (control) and samples collected at the times indicated post infection. The expression of *AtPNP-A*, *WAK1*, *PR1* and *WRKY70* was investigated using semi-quantitative RT-PCR. As before, *UBQ* is the "housekeeping" gene used to show the relative amount of template in each sample. Expression of these genes was induced in both the control and treated samples at late time points, except in the case of *PR1* whose expression was induced by *B. cinerea*.

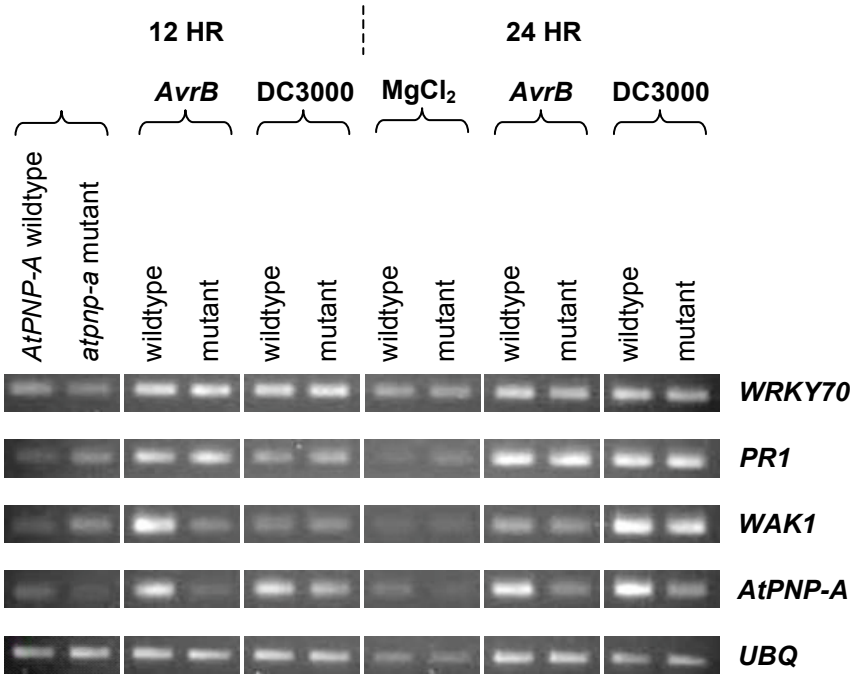

Figure 4.10. Expression of *AtPNP-A* and select *AtPNP-A* ECGG in the wildtype and *atpnp-a* mutant in response to *P. syringae* infection

Leaves of four week old plants were pressure infiltrated with 1 X 10^6 cfu/ml of *P. syringae* DC3000 (virulent strain); *P. syringae* DC3000 *AvrB* (avirulent strain) or 10 mM $MgCl_2$ (control) for either 12 or 24 hrs as indicated. The expression of *AtPNP-A*, *WAK1*, *PR1* and *WRKY70* was investigated using semi-quantitative RT-PCR. *UBQ* is the "housekeeping" gene used to show the relative amount of template in each sample. Expression of each of these genes was induced at both time points as seen previously the *P. syringae* timecourse (Figure 4.9B). Expression of *AtPNP-A* was reduced in the *atpnp-a* mutant. Expression of the selected ECGG genes was unaltered in the *atpnp-a* mutant when compared to the wildtype.

In sum, expression of *PR1* and *WRKY70* is not dependent on wildtype expression levels of *AtPNP-A* while early *WAK1* expression in response to the avirulent pathogen might require prior *AtPNP-A* expression. Therefore the induction of the select *AtPNP-A* ECGG genes is not considerably altered in the *atpnp-a* mutant. Since the *atpnp-a* mutant is not a null mutant this does not completely exclude the possibility that some level of *AtPNP-A* expression is required for the expression of these select *AtPNP-A* ECGG genes, however *AtPNP-A* expression levels in the mutant suffice.

4.3.6 Microarray analysis of recombinant AtPNP-A treatment

The molecular response to recombinant AtPNP-A treatment was measured at 1 hr and 24 hrs following treatment in a microarray experiment kindly conducted by Dr Priya Madhou (Warwick HRI, University of Warwick, UK). The early time point is within the time frame of physiological responses to recombinant AtPNP-A treatment (Ludidi *et al.*, 2004; Morse *et al.*, 2004). However these physiological responses mostly involve changes in water and ion fluxes that may not be orchestrated at the level of gene transcription. Therefore a later time point was included to measure the effect of long term recombinant AtPNP-A exposure. Four replicate dual channel microarray slides were analyzed for each time point.

In response to 1 hr recombinant AtPNP-A treatment, expression of only 28 genes was induced more than two fold ($\log_2 > 1$) while the expression of nine genes was repressed more than two fold ($\log_2 < -1$). Larger lists of differentially expressed genes were obtained by considering genes that showed a greater than 1.5 fold change in expression. Satisfying this criterion, 270 genes were induced more than 1.5 fold ($\log_2 > 0.6$) (Table 4.8A) and 256 genes were repressed by more than 1.5 fold ($\log_2 < -0.6$) (Table 4.8B). Fewer genes were differentially expressed following 24 hr recombinant AtPNP-A treatment. Only three genes were induced and five genes repressed more than two fold at 24 hrs after treatment while 74 genes were induced and 83 genes repressed more than 1.5 fold at this time point (Table 4.8C and D respectively).

4.3.6.1 Functional enrichments in differentially expressed gene lists

These four lists of differentially expressed genes that are either induced or repressed more than 1.5 fold by 1 hr or 24 hr recombinant AtPNP-A treatment, were subjected to FatiGO analysis to determine whether there was any enrichment of GO terms associated with these genes compared to the genome. None of the lists returned significant enrichment of GO terms, according to their adjusted p values (adjusted in FatiGO using the FDR procedure of Benjamini and Hochberg). However when considering terms that had unadjusted p values < 0.05 some interesting observations could be made, although should be interpreted with caution.

Table 4.8A. Genes induced more than 1.5 fold by 1 hr recombinant AtPNP-A treatment

Locus	Name and description	log2 ratio	p value
At2g07600	pseudogene, NADH dehydrogenase	**2.11**	1.76E-04
At3g33002	pseudogene, ribosomal protein S2p family	**2.09**	3.69E-03
At5g06050	dehydration-responsive protein-related	**1.87**	8.70E-02
At2g28820	structural constituent of ribosome	**1.76**	1.61E-03
At3g33000	pseudogene, AtP synthase A subunit	**1.64**	3.66E-04
At1g34680	pseudogene, ribosomal maturase	**1.61**	8.34E-04
At2g11200	F-box family protein	**1.54**	9.23E-02
At3g32990	pseudogene, AtP synthase C subunit	**1.50**	8.02E-03
At2g21650	MEE3 (maternal effect embryo arrest 3); DNA binding / transcription factor	**1.46**	2.13E-02
At3g33004	pseudogene, DNA-directed RNA polymerase beta-chain	**1.43**	5.55E-03
At2g07783	pseudogene, similar to Ccl1	**1.40**	5.53E-03
At2g07732	pseudogene, similar to ribulose-1,5-bisphosphate carboxylase/oxygenase large subunit	**1.33**	7.93E-04
At5g49220	unknown protein	**1.28**	1.37E-03
At2g36700	pectinesterase family protein	**1.15**	2.34E-02
At1g67460	GTP binding / GTPase	**1.15**	3.83E-02
At2g01510	pentatricopeptide (PPR) repeat-containing protein	**1.12**	1.12E-03
At1g33350	pentatricopeptide (PPR) repeat-containing protein	**1.11**	6.58E-02
At5g40450	unknown protein	**1.10**	5.15E-02
At2g07717	pseudogene, similar to NADH-ubiquinone oxidoreductase chain 4	**1.08**	2.63E-02
At3g15860	unknown protein	**1.06**	7.93E-02
At5g35660	expressed protein	**1.06**	9.63E-02
At3g52460	hydroxyproline-rich glycoprotein family protein	**1.05**	1.58E-01
At5g58510	unknown protein	**1.05**	4.71E-03
At4g21865	unknown protein	**1.04**	8.60E-03
At5g22550	unknown protein	**1.04**	5.12E-04
At5g59520	ZIP2 (ZINC TRANSPORTER 2 PRECURSOR); transferase, transferring glycosyl groups / zinc ion transmembrane transporter	**1.04**	1.50E-01
At2g23380	CLF (CURLY LEAF); transcription factor	**1.02**	1.37E-01
At3g49520	F-box family protein	**1.01**	1.62E-02
At1g02800	AtCEL2 (Arabidopsis thaliana Cellulase 2); hydrolase, hydrolyzing O-glycosyl compounds	**0.99**	3.21E-04
At2g32270	ZIP3 (ZINC TRANSPORTER 3 PRECURSOR); zinc ion transmembrane transporter	**0.97**	6.17E-03
At4g17570	zinc finger (GAtA type) family protein	**0.97**	9.12E-04
At1g63020	NRPD1a (NUCLEAR RNA POLYMERASE D 1A); DNA binding / DNA-directed RNA polymerase	**0.97**	2.00E-01
At1g23520	unknown protein	**0.97**	2.69E-02
At2g15590	unknown protein	**0.97**	1.30E-03
At1g11720	AtSS3 (STARCH SYNTHASE 3); starch synthase/ transferase, transferring glycosyl groups	**0.95**	3.09E-02
At1g63070	pentatricopeptide (PPR) repeat-containing protein	**0.95**	2.69E-02
At4g22730	leucine-rich repeat transmembrane protein kinase, putative	**0.94**	4.48E-02
At3g08660	phototropic-responsive protein, putative	**0.94**	3.53E-03
At2g40935	unknown protein	**0.94**	2.22E-04
At3g48670	XH/XS domain-containing protein / XS zinc finger domain-containing protein	**0.94**	2.21E-01
At5g23960	terpene synthase/cyclase family protein	**0.94**	2.88E-04
At2g46980	unnamed protein product	**0.94**	3.94E-02
At5g21030	PAZ domain-containing protein / piwi domain-containing protein	**0.94**	5.36E-02
At1g66100	thionin, putative	**0.93**	1.18E-01
At4g09140	AtMLH1 (ARABIDOPSIS THALIANA MUTL-HOMOLOGUE 1)	**0.93**	1.10E-01
At3g26616	unknown protein	**0.92**	2.59E-01
At2g26970	exonuclease family protein	**0.91**	3.39E-01
At2g20170	unknown protein	**0.90**	3.35E-04
At1g63870	disease resistance protein (TIR-NBS-LRR class), putative	**0.89**	7.46E-03
At5g37690	GDSL-motif lipase/hydrolase family protein	**0.89**	3.09E-03
At5g15290	integral membrane family protein	**0.88**	7.35E-02
At5g03350	legume lectin family protein	**0.88**	6.94E-02
At2g33230	flavin-containing monooxygenase, putative / FMO, putative	**0.88**	1.70E-03
At3g48650	pseudogene, At14a-related protein	**0.88**	8.51E-03
At4g20235	pseudogene of cytochrome P450	**0.88**	1.37E-01
At1g67960	unnamed protein product	**0.88**	1.12E-01
At3g46220	unnamed protein product	**0.88**	2.10E-03
At4g15450	senescence/dehydration-associated protein-related	**0.87**	8.51E-03
At5g26730	unknown protein	**0.87**	1.22E-01
At3g23950	F-box family protein	**0.87**	1.54E-01
At3g03400	calmodulin-related protein, putative	**0.87**	1.20E-02
At5g07980	dentin sialophosphoprotein-related	**0.86**	5.76E-03
At1g09880	Lyase	**0.86**	3.11E-03
At5g22980	SCPL47 (serine carboxypeptidase-like 47); serine carboxypeptidase	**0.86**	2.03E-03

Table 4.8A. Genes induced by 1 hr recombinant AtPNP-A treatment continued

Locus	Name and description	log2 ratio	p value
At5g47960	SMG1 (SMALL MOLECULAR WEIGHT G-PROTEIN 1); GTP binding	**0.85**	7.14E-03
At5g61430	ANAC100/AtNAC5 (Arabidopsis NAC domain containing protein 100); transcription factor	**0.85**	3.85E-04
At5g39020	protein kinase family protein	**0.84**	9.48E-03
At3g43835	transposable element gene	**0.84**	1.60E-02
At5g20150	SPX (SYG1/Pho81/XPR1) domain-containing protein	**0.84**	8.69E-02
At4g13870	WRNEXO (WERNER SYNDROME-LIKE EXONUCLEASE); 3'-5' exonuclease/ nucleic acid binding / protein binding	**0.83**	1.05E-01
At3g59680	hypothetical protein	**0.83**	4.32E-04
At1g72416	heat shock protein binding	**0.82**	1.13E-02
At3g14150	(S)-2-hydroxy-acid oxidase, peroxisomal, putative / glycolate oxidase, putative / short chain alpha-hydroxy acid oxidase, putative	**0.82**	3.85E-02
At4g29285	LCR24 (Low-molecular-weight cysteine-rich 24)	**0.82**	1.30E-02
At5g60740	ABC transporter family protein	**0.82**	6.03E-02
At1g11655	unknown protein	**0.82**	2.49E-01
At2g36380	AtPDR6/PDR6 (PLEIOTROPIC DRUG RESISTANCE 6); AtPase, coupled to transmembrane movement of substances	**0.81**	2.36E-02
At3g25240	unknown protein	**0.81**	1.32E-02
At1g32780	alcohol dehydrogenase, putative	**0.81**	8.95E-02
At4g35770	SEN1 (DARK INDUCIBLE 1)	**0.81**	9.55E-03
At2g45760	BAP2 (BON ASSOCIAtION PROTEIN 2)	**0.81**	6.35E-02
At2g03740	late embryogenesis abundant domain-containing protein / LEA domain-containing protein	**0.80**	1.22E-02
At3g60640	AtG8G (AUTOPHAGY 8G); microtubule binding	**0.80**	4.57E-03
At5g17950	unknown protein	**0.80**	3.41E-02
At3g49050	lipase class 3 family protein / calmodulin-binding heat-shock protein, putative	**0.80**	1.82E-01
At3g46520	ACT12 (ACTIN-12); structural constituent of cytoskeleton	**0.79**	6.47E-03
At1g55035	pseudogene, putative importin alpha	**0.79**	1.95E-02
At2g38823	unknown protein	**0.79**	2.15E-01
At4g16195	self-incompatibility protein-related	**0.79**	4.14E-03
At5g53910	(S)-2-hydroxy-acid oxidase, peroxisomal, putative / glycolate oxidase, putative / short chain alpha-hydroxy acid oxidase, putative	**0.79**	3.06E-03
At5g23955	transposable element gene	**0.79**	6.32E-02
At5g63930	leucine-rich repeat transmembrane protein kinase, putative	**0.78**	3.17E-03
At1g12180	heat shock protein-related	**0.78**	4.91E-02
At3g07450	protease inhibitor/seed storage/lipid transfer protein (LTP) family protein	**0.78**	3.97E-02
At1g18350	AtMKK7 (MAP KINASE KINASE7); kinase	**0.78**	1.24E-02
At3g48330	PIMT1 (PROTEIN-L-ISOASPARTAtE METHYLTRANSFERASE 1); protein-L-isoaspartate (D-aspartate) O-methyltransferase	**0.78**	1.92E-02
At5g63200	tetratricopeptide repeat (TPR)-containing protein	**0.77**	2.12E-02
At2g03620	magnesium transporter CorA-like family protein (MRS2-5)	**0.77**	2.39E-02
At3g53390	transducin family protein / WD-40 repeat family protein	**0.77**	5.22E-03
At1g79780	UPF0497 membrane protein	**0.77**	3.45E-03
At1g04180	flavin-containing monooxygenase family protein / FMO family protein	**0.77**	1.35E-01
At4g04990	unknown protein	**0.77**	1.36E-03
At1g28690	pentatricopeptide (PPR) repeat-containing protein	**0.77**	5.54E-02
At1g63780	IMP4	**0.76**	8.35E-03
At3g04160	hypothetical protein	**0.76**	2.60E-03
At3g53570	AFC1 (ARABIDOPSIS FUS3-COMPLEMENTING GENE 1); kinase	**0.76**	2.29E-03
At4g14250	UBX domain-containing protein	**0.76**	3.99E-03
At1g63860	pseudogene, disease resistance protein, similar to disease resistance protein RPP1-WsC	**0.75**	1.03E-01
At2g03770	sulfotransferase family protein	**0.75**	9.61E-04
At3g13080	AtMRP3 (Arabidopsis thaliana multidrug resistance-associated protein 3)	**0.75**	6.56E-02
At2g01960	TET14 (TETRASPANIN14)	**0.75**	5.76E-02
At1g73800	calmodulin binding protein	**0.75**	5.10E-02
At5g62420	aldo/keto reductase family protein	**0.75**	2.01E-02
At4g04614	unnamed protein product	**0.75**	4.53E-03
At5g50480	CCAAt-box binding transcription factor Hap5a, putative	**0.75**	2.36E-03
At5g28523	transposable element gene	**0.74**	2.33E-03
At5g09290	3'(2'),5'-bisphosphate nucleotidase, putative / inositol polyphosphate 1-phosphatase, putative	**0.74**	2.46E-01
At1g11880	unnamed protein product	**0.74**	2.32E-03
At1g58390	disease resistance protein (CC-NBS-LRR class), putative	**0.74**	1.07E-02
At5g16630	DNA repair protein Rad4 family	**0.74**	2.88E-02
At3g30147	pseudogene, hypothetical protein	**0.74**	3.24E-02
At4g27657	unknown protein	**0.73**	4.42E-03
At1g23140	C2 domain-containing protein	**0.73**	9.71E-02
At1g62820	calmodulin, putative	**0.73**	2.26E-03
At3g60420	unknown protein	**0.73**	1.68E-02
At5g40710	zinc finger (C2H2 type) family protein	**0.73**	1.07E-02

Table 4.8A. Genes induced by 1 hr recombinant AtPNP-A treatment continued

Locus	Name and description	log2 ratio	p value
At2g18110	elongation factor 1-beta, putative / EF-1-beta, putative	**0.72**	6.82E-03
At3g10530	Transducin family protein / WD-40 repeat family protein	**0.72**	5.85E-03
At4g14280	Binding	**0.72**	6.39E-02
At5g09270	hypothetical protein	**0.72**	1.56E-01
At4g08040	ACS11 (1-Amino-cyclopropane-1-carboxylate synthase 11); 1-aminocyclopropane-1-carboxylate synthase	**0.72**	4.22E-03
AtMG00260	Uncharacterized mitochondrial protein AtMg00260	**0.72**	2.15E-03
At5g53980	AtHB52 (ARABIDOPSIS THALIANA HOMEOBOX PROTEIN 52); transcription factor	**0.71**	6.34E-02
At1g10790	hydroxyproline-rich glycoprotein family protein	**0.71**	2.10E-02
At4g00830	RNA recognition motif (RRM)-containing protein	**0.71**	5.40E-02
At2g22210	transposable element gene	**0.71**	1.61E-01
At3g56400	WRKY70 (WRKY DNA-binding protein 70); transcription factor	**0.71**	1.34E-01
At2g33030	leucine-rich repeat family protein	**0.71**	5.33E-02
At5g07490	unknown protein	**0.71**	1.09E-02
At2g37720	unknown protein	**0.71**	3.88E-02
At1g49030	unknown protein	**0.71**	8.52E-02
At3g02040	SRG3 (SENESCENCE-RELAtED GENE 3); glycerophosphodiester phosphodiesterase	**0.71**	2.57E-02
At2g40370	LAC5 (laccase 5); copper ion binding / oxidoreductase	**0.71**	1.00E-03
At3g05790	Lon protease, putative	**0.70**	7.37E-03
At4g15280	UDP-glucoronosyl/UDP-glucosyl transferase family protein	**0.70**	8.82E-03
At1g33870	avirulence-responsive protein, putative / avirulence induced gene protein, putative / AIG protein, putative	**0.70**	1.29E-03
At3g01880	unknown protein	**0.70**	1.79E-01
At2g41050	PQ-loop repeat family protein / transmembrane family protein	**0.70**	1.78E-01
At2g11730	transposable element gene	**0.70**	3.22E-02
At4g24640	APPB1; pectinesterase inhibitor	**0.70**	8.50E-02
At3g13130	hypothetical protein	**0.70**	5.47E-02
At5g64060	ANAC103 (Arabidopsis NAC domain containing protein 103); transcription factor	**0.70**	6.22E-03
At5g24170	unknown protein	**0.70**	8.42E-02
At2g07751	NADH-ubiquinone oxidoreductase chain 3, putative	**0.70**	6.92E-03
At4g38410	dehydrin, putative	**0.70**	5.83E-03
At2g27220	BLH5 (BELL1-LIKE HOMEODOMAIN 5); DNA binding / transcription factor	**0.70**	1.81E-03
At4g21300	pentatricopeptide (PPR) repeat-containing protein	**0.70**	1.47E-02
At2g20630	protein phosphatase 2C, putative / PP2C, putative	**0.70**	3.34E-02
At3g03847	auxin-responsive family protein	**0.69**	5.37E-02
At1g36395	transposable element gene	**0.69**	7.65E-03
At3g50690	leucine-rich repeat family protein	**0.69**	9.50E-02
At1g31680	copper amine oxidase family protein	**0.69**	5.82E-03
At5g04850	VPS60.2	**0.69**	9.20E-02
At3g12770	pentatricopeptide (PPR) repeat-containing protein	**0.69**	5.02E-03
At3g03050	CSLD3 (CELLULOSE SYNTHASE-LIKE 3); cellulose synthase/ transferase, transferring glycosyl groups	**0.69**	1.60E-02
At1g03620	phagocytosis and cell motility protein ELMO1-related	**0.69**	2.04E-01
At2g04032	ZIP7 (ZINC TRANSPORTER 7 PRECURSOR); cation transmembrane transporter	**0.69**	3.95E-02
At5g40100	disease resistance protein (TIR-NBS-LRR class), putative	**0.69**	1.72E-01
At3g53470	unnamed protein product	**0.69**	6.01E-02
At4g11230	respiratory burst oxidase, putative / NADPH oxidase, putative	**0.69**	1.45E-02
At1g59720	pentatricopeptide (PPR) repeat-containing protein	**0.68**	9.98E-02
At1g74170	protein binding	**0.68**	1.58E-02
At1g34490	membrane bound O-acyl transferase (MBOAt) family protein / wax synthase-related	**0.68**	1.80E-02
At5g05960	protease inhibitor/seed storage/lipid transfer protein (LTP) family protein	**0.68**	1.94E-02
At1g13460	serine/threonine protein phosphatase 2A (PP2A) regulatory subunit B', putative	**0.68**	7.63E-02
At5g17890	LIM domain-containing protein / disease resistance protein-related	**0.68**	5.13E-02
At4g10470	unknown protein	**0.68**	2.08E-01
At2g26660	SPX (SYG1/Pho81/XPR1) domain-containing protein	**0.68**	2.38E-03
At4g00950	MEE47 (maternal effect embryo arrest 47); transcription factor	**0.68**	2.21E-02
At2g04750	fimbrin-like protein, putative	**0.67**	1.84E-02
At5g54720	ankyrin repeat family protein	**0.67**	8.49E-03
At4g27900	unknown protein	**0.67**	2.94E-01
At3g56020	60S ribosomal protein L41 (RPL41g)	**0.67**	1.49E-03
At5g51340	Binding	**0.67**	6.74E-02
At3g13210	crooked neck protein, putative / cell cycle protein, putative	**0.67**	1.59E-02
At5g55330	membrane bound O-acyl transferase (MBOAt) family protein / wax synthase-related	**0.67**	5.55E-02
At1g23680	contains InterPro domain Protein of unknown function DUF220	**0.67**	1.27E-01
At3g17160	unknown protein	**0.67**	1.03E-02
At4g00040	chalcone and stilbene synthase family protein	**0.67**	9.82E-03

Table 4.8A. Genes induced by 1 hr recombinant AtPNP-A treatment continued

Locus	Name and description	log2 ratio	p value
At4g11660	At-HSFB2B (Arabidopsis thaliana heat shock transcription factor B2B); transcription factor	**0.67**	2.00E-02
At1g20240	metal ion binding	**0.66**	8.80E-02
At3g02310	SEP2 (SEPALLAtA2); DNA binding / transcription factor	**0.66**	1.05E-01
At4g26350	F-box family protein	**0.66**	1.73E-02
At1g08300	AtP binding	**0.66**	1.76E-02
At5g44280	protein binding / zinc ion binding	**0.66**	4.73E-02
At4g19630	heat shock factor protein-related / heat shock transcription factor-related	**0.66**	1.37E-01
At5g52940	unknown protein	**0.65**	6.07E-02
At1g60180	unknown protein	**0.65**	1.40E-02
At5g38070	zinc finger (C3HC4-type RING finger) family protein	**0.65**	1.12E-01
At4g21870	26.5 kDa class P-related heat shock protein (HSP26.5-P)	**0.65**	7.07E-02
At1g29290	hypothetical protein	**0.65**	5.64E-03
At1g76650	CML38; calcium ion binding	**0.65**	7.94E-02
At1g28300	LEC2 (LEAFY COTYLEDON 2); transcription factor	**0.65**	2.18E-02
At1g14080	FUT6 (fucosyltransferase 6); fucosyltransferase/ transferase, transferring glycosyl groups	**0.65**	1.40E-02
At5g12280	RNA binding	**0.65**	6.71E-02
At5g10530	lectin protein kinase, putative	**0.65**	1.30E-01
At1g52950	replication protein-related	**0.65**	4.31E-03
At2g41910	protein kinase family protein	**0.64**	1.72E-02
At1g64000	WRKY56 (WRKY DNA-binding protein 56); transcription factor	**0.64**	2.02E-02
At5g59700	protein kinase, putative	**0.64**	1.77E-01
At1g10880	unknown protein	**0.64**	2.48E-03
At5g55620	unknown protein	**0.64**	1.20E-01
At5g37980	NADP-dependent oxidoreductase, putative	**0.64**	3.85E-03
At3g29764	pseudogene, DNA-directed RNA polymerase Beta chain (fragment)	**0.64**	1.04E-01
At1g59780	disease resistance protein (CC-NBS-LRR class), putative	**0.64**	4.68E-02
At1g70030	paired amphipathic helix repeat-containing protein	**0.64**	2.95E-03
At4g38700	disease resistance-responsive family protein	**0.64**	9.70E-02
At3g29739	transposable element gene	**0.64**	4.15E-03
At3g17200	transposable element gene	**0.64**	9.15E-02
At4g04740	CPK23 (calcium-dependent protein kinase 23); calmodulin-dependent protein kinase/ kinase	**0.64**	4.32E-03
At5g49200	WD-40 repeat family protein / zfwd4 protein (ZFWD4)	**0.63**	8.98E-04
At5g43120	tetratricopeptide repeat (TPR)-containing protein	**0.63**	2.91E-03
At5g29020	transposable element gene	**0.63**	3.43E-03
At5g33280	chloride channel-like (CLC) protein, putative	**0.63**	1.46E-02
At1g71030	AtMYBL2 (Arabidopsis myb-like 2); DNA binding / transcription factor	**0.63**	1.35E-02
At5g64780	unknown protein	**0.63**	1.02E-02
At2g06550	transposable element gene	**0.63**	1.36E-01
At2g21650	MEE3 (maternal effect embryo arrest 3); DNA binding / transcription factor	**1.46**	2.13E-01
At5g01390	DNAJ heat shock protein, putative	**0.63**	6.40E-02
At1g19850	MP (MONOPTEROS); transcription factor	**0.63**	3.92E-02
At4g18180	glycoside hydrolase family 28 protein / polygalacturonase (pectinase) family protein	**0.63**	2.61E-02
At2g20465	unknown protein	**0.63**	2.68E-03
At3g42570	peroxidase-related	**0.63**	6.56E-02
At1g62580	flavin-containing monooxygenase family protein / FMO family protein	**0.62**	6.03E-02
At4g12090	cornichon family protein	**0.62**	4.28E-02
At1g14750	SDS (SOLO DANCERS); cyclin-dependent protein kinase	**0.62**	1.27E-02
At1g05400	unknown protein	**0.62**	1.97E-02
AtMG01000	Uncharacterized mitochondrial protein AtMg01000	**0.62**	8.79E-03
At1g64460	phosphatidylinositol 3- and 4-kinase family protein	**0.62**	3.52E-02
At5g60760	2-phosphoglycerate kinase-related	**0.62**	3.48E-03
At2g39805	integral membrane Yip1 family protein	**0.62**	6.95E-02
At4g25750	ABC transporter family protein	**0.62**	1.92E-02
At4g14370	disease resistance protein (TIR-NBS-LRR class), putative	**0.62**	3.63E-01
At2g27140	heat shock family protein	**0.62**	7.84E-03
At1g59800	cullin-related	**0.62**	2.17E-02
At1g20050	HYD1 (Hydra 1)	**0.61**	3.59E-02
At2g42900	unnamed protein product	**0.61**	1.91E-01
At3g51620	nucleotidyltransferase family protein	**0.61**	1.26E-02
At4g26200	ACS7 (1-Amino-cyclopropane-1-carboxylate synthase 7); 1-aminocyclopropane-1-carboxylate synthase	**0.61**	1.90E-02
At1g74120	mitochondrial transcription termination factor-related / mTERF-related	**0.61**	2.09E-03
At2g16380	SEC14 cytosolic factor family protein / phosphoglyceride transfer family protein	**0.61**	1.12E-02
At2g20290	XIG (Myosin-like protein XIG); motor/ protein binding	**0.61**	2.30E-01
At4g01360	BPS1 (BYPASS 1)	**0.61**	1.97E-03
At3g18180	unknown protein	**0.61**	1.35E-03
At1g61060	F-box family protein	**0.61**	1.67E-02
At2g43390	unknown protein	**0.61**	1.83E-03

Table 4.8A. Genes induced by 1 hr recombinant AtPNP-A treatment continued

Locus	Name and description	log2 ratio	p value
At1g54440	3'-5' exonuclease/ nucleic acid binding	**0.61**	6.44E-02
At2g41360	F-box family protein	**0.61**	5.13E-02
At1g60760	invertase/pectin methylesterase inhibitor family protein	**0.61**	1.06E-01
At1g71450	AP2 domain-containing transcription factor, putative	**0.61**	1.08E-01
At2g20270	glutaredoxin family protein	**0.61**	1.26E-02
At5g06950	AHBP-1B (bZIP transcription factor HBP-1b homolog); DNA binding / transcription factor/ transcription repressor	**0.60**	4.78E-02
At1g47280	unknown protein	**0.60**	8.17E-02
At3g15354	SPA3 (SPA1-RELAtED 3); signal transducer	**0.60**	1.37E-01
At2g27120	POL2B/TIL2 (TILTED2); DNA-directed DNA polymerase	**0.60**	2.53E-03
At1g55320	Ligase	**0.60**	6.68E-02
At3g11860	unknown protein	**0.60**	4.94E-02
At3g45170	zinc finger (GAtA type) family protein	**0.60**	3.92E-02
At1g69040	ACR4 (ACT REPEAt 4); amino acid binding	**0.60**	2.58E-02
At3g22820	allergen-related	**0.60**	5.09E-02

Table 4.8B. Genes repressed more than 1.5 fold by 1 hr recombinant AtPNP-A treatment

Locus	Name and description	log2 ratio	p value
At3g53130	LUT1 (LUTEIN DEFICIENT 1); oxygen binding	**-1.18**	2.34E-02
At5g38880	unnamed protein product	**-1.15**	3.83E-02
At1g74650	AtMYB31/AtY13 (myb domain protein 31); DNA binding / transcription factor	**-1.13**	3.56E-03
At1g08340	rac GTPase activating protein, putative	**-1.13**	5.15E-02
At2g29250	lectin protein kinase, putative	**-1.11**	1.58E-01
At3g29180	unknown protein	**-1.04**	6.17E-03
At4g11510	RALFL28 (RALF-LIKE 28)	**-1.03**	2.00E-01
At5g02730	allergen V5/Tpx-1-related family protein	**-1.03**	2.69E-02
At2g27505	F-box family protein	**-1.01**	2.69E-02
At3g17620	F-box family protein	**-1.00**	3.53E-03
At1g32020	F-box family protein	**-0.99**	2.21E-01
At1g67720	leucine-rich repeat family protein / protein kinase family protein	**-0.99**	2.88E-04
At1g63060	unknown protein	**-0.99**	3.94E-02
At5g67050	lipase class 3 family protein	**-0.99**	5.36E-02
At4g22230	unknown protein	**-0.98**	1.18E-01
At2g19330	leucine-rich repeat family protein	**-0.98**	1.10E-01
At5g04220	ATSYTC/NTMC2T1.3/NTMC2TYPE1.3/SYTC	**-0.96**	7.46E-03
At1g75450	CKX5 (CYTOKININ OXIDASE 5); cytokinin dehydrogenase	**-0.95**	3.89E-03
At2g45490	ATAUR3 (ATAURORA3); ATP binding / histone serine kinase(H3-S10 specific) / protein kinase	**-0.94**	1.22E-01
At5g47300	F-box family protein	**-0.93**	3.11E-03
At2g47290	unknown protein	**-0.92**	9.48E-03
At1g10095	protein prenyltransferase	**-0.91**	1.60E-02
At2g14060	S-adenosyl-L-methionine:carboxyl methyltransferase family protein	**-0.90**	1.13E-02
At2g17040	ANAC036 (Arabidopsis NAC domain containing protein 36); transcription factor	**-0.89**	1.30E-02
At2g42240	nucleic acid binding	**-0.89**	6.03E-02
At2g37500	arginine biosynthesis protein ArgJ family	**-0.89**	2.36E-02
At3g61730	unknown protein	**-0.88**	1.32E-02
At5g65460	kinesin motor protein-related	**-0.88**	6.35E-02
At2g04675	unknown protein	**-0.87**	1.49E-02
At1g47885	leucine-rich repeat family protein	**-0.86**	3.06E-03
At4g36180	leucine-rich repeat family protein	**-0.86**	6.32E-02
At2g43290	MSS3 (MULTICOPY SUPPRESSORS OF SNF4 DEFICIENCY IN YEAST 3); calcium ion binding	**-0.86**	3.97E-02
At1g43667	protease inhibitor/seed storage/lipid transfer protein (LTP) family protein	**-0.85**	2.05E-02
At1g80730	ZFP1 (ARABIDOPSIS THALIANA ZINC-FINGER PROTEIN 1); nucleic acid binding / transcription factor/ zinc ion binding	**-0.85**	1.40E-03
At4g25510	unknown protein	**-0.85**	5.22E-03
At3g11920	glutaredoxin-related	**-0.84**	2.38E-02
At5g02900	CYP96A13 (cytochrome P450, family 96, subfamily A, polypeptide 13); oxygen binding	**-0.84**	3.45E-03
At3g07650	COL9 (CONSTANS-LIKE 9); transcription factor/ zinc ion binding	**-0.83**	8.35E-03
At4g04220	disease resistance family protein	**-0.83**	2.60E-03
At4g22753	SMO1-3 (STEROL 4-ALPHA METHYL OXIDASE); catalytic	**-0.83**	2.29E-03
At5g44510	disease resistance protein (TIR-NBS-LRR class), putative	**-0.83**	1.05E-01
At5g65685	soluble glycogen synthase-related	**-0.83**	1.03E-01
At1g21650	ATP binding	**-0.83**	9.61E-04
At2g41590	unknown protein	**-0.83**	6.56E-02
At4g09100	zinc finger (C3HC4-type RING finger) family protein	**-0.82**	5.76E-02
At1g22140	unnamed protein product	**-0.82**	2.01E-02
At2g02955	MEE12 (maternal effect embryo arrest 12); zinc ion binding	**-0.82**	3.76E-03
At1g70040	unknown protein	**-0.82**	2.36E-03
At4g23980	ARF9 (AUXIN RESPONSE FACTOR 9); transcription factor	**-0.82**	2.33E-03
At3g60060	Male sterility, NAD-binding	**-0.82**	2.46E-01
At1g47390	F-box family protein	**-0.82**	2.32E-03
At5g46300	unknown protein	**-0.82**	1.51E-01
At3g14150	(S)-2-hydroxy-acid oxidase, peroxisomal, putative / glycolate oxidase, putative / short chain alpha-hydroxy acid oxidase, putative	**-0.81**	2.88E-02
At5g59480	haloacid dehalogenase-like hydrolase family protein	**-0.81**	3.24E-02
At3g01970	WRKY45 (WRKY DNA-binding protein 45); transcription factor	**-0.81**	9.71E-02
At2g44030	kelch repeat-containing F-box family protein	**-0.81**	2.26E-03
At5g46880	HB-7 (homeobox-7); DNA binding / transcription factor	**-0.81**	1.68E-02
At1g54470	RPP27 (RESISTANCE TO PERONOSPORA PARASITICA 27); protein binding	**-0.81**	1.07E-02
At4g21460	unknown protein	**-0.81**	5.85E-03
At4g03060	AOP2 (ALKENYL HYDROXALKYL PRODUCING 2); oxidoreductase, acting on paired donors, with incorporation or reduction of molecular oxygen, 2-oxoglutarate as one donor, and incorporation of one atom each of oxygen into both donors	**-0.80**	8.95E-03
At3g60260	phagocytosis and cell motility protein ELMO1-related	**-0.80**	1.61E-01
At4g37470	hydrolase, alpha/beta fold family protein	**-0.80**	1.34E-01
At1g01710	acyl-CoA thioesterase family protein	**-0.79**	7.37E-03

Table 4.8B. Genes repressed by 1 hr recombinant AtPNP-A treatment continued

Locus	Name and description	log2 ratio	p value
At1g70890	MLP43 (MLP-LIKE PROTEIN 43)	**-0.79**	1.29E-03
At1g10180	unknown protein	**-0.79**	1.79E-01
At1g43760	unknown protein	**-0.79**	3.22E-02
At3g60920	beige/BEACH domain-containing protein	**-0.79**	5.47E-02
At2g42080	DNAJ heat shock N-terminal domain-containing protein	**-0.79**	6.22E-03
At3g07360	armadillo/beta-catenin repeat family protein / U-box domain-containing protein	**-0.78**	5.83E-03
At3g59370	contains domain PTHR22683	**-0.78**	2.47E-02
At5g43130	TAF4 (TBP-ASSOCIATED FACTOR 4); transcription initiation factor	**-0.77**	9.50E-02
At5g15840	CO (CONSTANS); transcription factor/ zinc ion binding	**-0.77**	1.45E-02
At4g05631	unknown protein	**-0.77**	1.58E-02
At2g40300	ATFER4 (FERRITIN 4); ferric iron binding	**-0.77**	4.85E-02
At1g18780	zinc finger (C3HC4-type RING finger) family protein	**-0.76**	5.13E-02
At1g13470	unknown protein	**-0.76**	2.38E-03
At1g44780	unknown protein	**-0.76**	2.04E-02
At3g18000	NMT1 (N-METHYLTRANSFERASE 1); phosphoethanolamine N-methyltransferase	**-0.76**	2.21E-02
At4g33980	unknown protein	**-0.76**	1.84E-02
At2g32670	ATVAMP725 (Arabidopsis thaliana vesicle-associated membrane protein 725)	**-0.76**	2.94E-01
At4g16740	ATTPS03 (Arabidopsis thaliana terpene synthase 03)	**-0.76**	6.74E-02
At5g03495	nucleotide binding	**-0.75**	5.79E-02
At2g01130	ATP binding / helicase/ nucleic acid binding	**-0.75**	8.80E-02
At1g04760	ATVAMP726 (VESICLE-ASSOCIATED MEMBRANE PROTEIN)	**-0.75**	1.18E-01
At3g16895	unknown protein	**-0.75**	1.15E-01
At4g34550	F-box family protein	**-0.75**	4.73E-02
At5g53370	ATPMEPCRF; pectinesterase	**-0.75**	2.20E-02
At5g54000	oxidoreductase, 2OG-Fe(II) oxygenase family protein	**-0.75**	3.36E-03
At5g07380	unnamed protein product	**-0.75**	1.37E-01
At5g44960	F-box family protein	**-0.74**	3.96E-02
At5g02430	WD-40 repeat family protein	**-0.74**	6.07E-02
At4g33430	BAK1 (BRI1-ASSOCIATED RECEPTOR KINASE); kinase	**-0.74**	1.12E-01
At4g09870	F-box family protein	**-0.74**	2.44E-02
At1g24390	unknown protein	**-0.74**	2.18E-02
At1g43665	protease inhibitor/seed storage/lipid transfer protein (LTP) family protein	**-0.74**	1.30E-01
At5g07970	dentin sialophosphoprotein-related	**-0.74**	1.31E-02
At5g60620	phospholipid/glycerol acyltransferase family protein	**-0.74**	2.02E-02
At3g29791	unknown protein	**-0.73**	1.77E-01
At5g22020	strictosidine synthase family protein	**-0.73**	1.04E-01
At5g58630	hypothetical protein	**-0.73**	9.22E-03
At3g50720	protein kinase, putative	**-0.73**	4.15E-03
At5g50910	unknown protein	**-0.73**	4.32E-03
At4g22910	signal transducer	**-0.73**	2.91E-03
At1g30350	pectate lyase family protein	**-0.72**	1.46E-02
At5g63540	hypothetical protein	**-0.72**	1.35E-02
At5g53460	GLT1 (NADH-dependent glutamate synthase 1 gene)	**-0.72**	1.36E-01
At5g40280	ERA1 (ENHANCED RESPONSE TO ABA 1); protein farnesyltransferase	**-0.72**	6.03E-02
At4g03380	ATNAF1/NAF1	**-0.72**	2.48E-02
At1g52420	glycosyl transferase family 1 protein	**-0.72**	3.16E-02
At3g28570	AAA-type ATPase family protein	**-0.71**	3.52E-02
At2g39430	disease resistance-responsive protein-related / dirigent protein-related	**-0.71**	1.37E-01
At3g16550	DEGP12; serine-type peptidase/ trypsin	**-0.71**	3.63E-01
At1g32690	unknown protein	**-0.71**	2.17E-02
At5g57840	transferase family protein	**-0.71**	5.13E-03
At2g42955	unknown protein	**-0.71**	3.59E-02
At3g53380	lectin protein kinase family protein	**-0.71**	1.91E-01
At1g71830	SERK1 (SOMATIC EMBRYOGENESIS RECEPTOR-LIKE KINASE 1); kinase	**-0.71**	1.12E-02
At1g54920	hypothetical protein	**-0.71**	1.38E-01
At1g16515	unknown protein	**-0.70**	1.35E-03
At3g12690	protein kinase, putative	**-0.70**	1.83E-03
At3g56320	nucleotidyltransferase family protein	**-0.70**	6.26E-02
At1g06930	unknown protein	**-0.70**	4.78E-02
At1g53450	unknown protein	**-0.70**	8.17E-02
At3g43170	unknown protein	**-0.70**	2.53E-03
At2g45750	dehydration-responsive family protein	**-0.70**	6.68E-02
At3g53400	CPuORF47	**-0.69**	3.68E-03
At1g50750	unknown protein	**-0.69**	7.72E-02
At5g15300	pentatricopeptide (PPR) repeat-containing protein	**-0.69**	1.84E-02
At1g45207	remorin family protein	**-0.69**	1.57E-01
At1g30420	ATMRP12 (Arabidopsis thaliana multidrug resistance-associated protein 12)	**-0.69**	8.91E-03
At4g37950	Lyase	**-0.68**	1.61E-02
At5g39240	unknown protein	**-0.68**	2.76E-02
At1g49120	AP2 domain-containing transcription factor, putative	**-0.68**	1.37E-02
At2g18100	unknown protein	**-0.68**	4.37E-02

Table 4.8B. Genes repressed by 1 hr recombinant AtPNP-A treatment continued

Locus	Name and description	log2 ratio	p value
At1g79460	GA2 (GA REQUIRING 2); ent-kaurene synthase	**-0.68**	7.26E-03
At3g49930	zinc finger (C2H2 type) family protein	**-0.68**	6.89E-03
At3g09340	amino acid transporter family protein	**-0.68**	1.00E-02
At3g45095	transposable element gene	**-0.68**	1.38E-02
At1g47660	unknown protein	**-0.68**	5.84E-02
At5g35930	AMP-dependent synthetase and ligase family protein	**-0.68**	4.73E-02
At3g52950	CBS domain-containing protein / octicosapeptide/Phox/Bemp1 (PB1) domain-containing protein	**-0.68**	2.52E-02
At5g47600	heat shock protein-related	**-0.68**	3.65E-02
At2g27200	GTP-binding family protein	**-0.68**	1.52E-01
At4g05470	F-box family protein (FBL21)	**-0.67**	2.63E-02
At5g45840	leucine-rich repeat transmembrane protein kinase, putative	**-0.67**	2.34E-02
At4g32510	anion exchanger	**-0.67**	6.20E-02
At1g34140	PAB1 (POLY(A) BINDING PROTEIN 1); RNA binding / translation initiation factor	**-0.67**	4.17E-03
At2g37880	unknown protein	**-0.67**	7.45E-02
At3g28153	transposable element gene	**-0.67**	3.86E-03
At3g13960	AtGRF5 (GROWTH-REGULATING FACTOR 5)	**-0.67**	3.67E-02
At2g14870	RNA recognition motif (RRM)-containing protein	**-0.67**	4.79E-02
At3g57410	VLN3 (VILLIN 3); actin binding	**-0.67**	1.71E-02
At3g28153	transposable element gene	**-0.67**	1.06E-02
At5g54990	zinc finger (C3HC4-type RING finger) family protein	**-0.67**	2.75E-02
At1g49440	transposable element gene	**-0.67**	1.52E-02
At1g63860	pseudogene, disease resistance protein	**-0.67**	5.21E-02
At2g10250	transposable element gene	**-0.67**	4.12E-02
At3g47110	leucine-rich repeat transmembrane protein kinase, putative	**-0.67**	4.71E-03
At4g26980	unnamed protein product	**-0.67**	1.62E-01
At1g14930	major latex protein-related / MLP-related	**-0.67**	5.11E-02
At2g15030	Pseudogene	**-0.66**	1.40E-02
At5g17360	ATP dependent DNA ligase family protein	**-0.66**	1.84E-02
At1g13710	CYP78A5 (cytochrome P450, family 78, subfamily A, polypeptide 5); oxygen binding	**-0.66**	1.77E-01
At1g75060	unknown protein	**-0.66**	1.49E-01
At3g30845	unknown protein	**-0.66**	1.00E-01
At3g09660	MCM8; ATP binding / DNA binding / DNA-dependent ATPase	**-0.66**	7.04E-02
At5g09710	magnesium transporter CorA-like family protein	**-0.66**	5.02E-02
At5g06100	ATMYB33/MYB33 (myb domain protein 33); DNA binding / transcription factor	**-0.66**	8.44E-02
At3g48010	ATCNGC16 (cyclic nucleotide gated channel 16); calmodulin binding / cyclic nucleotide binding / ion channel	**-0.65**	6.05E-02
At5g35331	transposable element gene	**-0.65**	4.29E-02
At1g76190	auxin-responsive family protein	**-0.65**	1.23E-01
At5g59530	2-oxoglutarate-dependent dioxygenase, putative	**-0.65**	3.08E-03
At5g40750	F-box family protein	**-0.65**	4.93E-02
At1g27860	ATP binding / aminoacyl-tRNA ligase	**-0.65**	5.21E-02
At3g03200	ANAC045 (Arabidopsis NAC domain containing protein 45); transcription factor	**-0.64**	1.16E-02
At4g19720	glycosyl hydrolase family 18 protein	**-0.64**	1.68E-01
At1g48090	C2 domain-containing protein	**-0.64**	5.89E-03
At3g44235	unknown protein	**-0.64**	4.15E-02
At1g67910	unknown protein	**-0.64**	6.13E-02
At2g44800	oxidoreductase, 2OG-Fe(II) oxygenase family protein	**-0.64**	1.17E-02
At2g42190	unknown protein	**-0.64**	2.66E-01
At5g39560	kelch repeat-containing F-box family protein	**-0.64**	2.53E-01
At3g31395	transposable element gene	**-0.64**	1.46E-01
At5g39200	unknown protein	**-0.64**	5.23E-02
At3g61230	LIM domain-containing protein	**-0.64**	8.74E-02
At3g13030	hAT dimerisation domain-containing protein	**-0.63**	2.05E-02
At4g19490	protein binding	**-0.63**	1.69E-02
At1g60080	3' exoribonuclease family domain 1-containing protein	**-0.63**	1.48E-02
At4g23370	unknown protein	**-0.63**	3.39E-02
At1g03310	ATISA2/BE2/DBE1/ISA2 (DEBRANCHING ENZYME 1); alpha-amylase/ isoamylase	**-0.63**	1.05E-02
At5g65210	TGA1; DNA binding / calmodulin binding / transcription factor	**-0.63**	2.63E-02
At2g03000	zinc finger (C3HC4-type RING finger) family protein	**-0.63**	1.08E-01
At4g33720	pathogenesis-related protein, putative	**-0.63**	2.51E-02
At1g51900	unknown protein	**-0.63**	2.74E-03
At5g29560	Ca+2-binding EF hand family protein	**-0.63**	4.31E-02
At1g67920	unknown protein	**-0.63**	8.65E-02
At5g44950	F-box family protein	**-0.63**	2.60E-02
At5g35670	IQD33 (IQ-domain 33); calmodulin binding	**-0.63**	1.35E-01
At4g18690	unknown protein	**-0.63**	4.54E-02
At2g15380	transposable element gene	**-0.63**	6.32E-03
At1g73840	ESP1 (ENHANCED SILENCING PHENOTYPE 1)	**-0.63**	1.72E-02

Table 4.8B. Genes repressed by 1 hr recombinant AtPNP-A treatment continued

Locus	Name and description	log2 ratio	p value
At1g31460	unknown protein	**-0.63**	9.32E-02
At1g15050	IAA34 (indoleacetic acid-induced protein 34); transcription factor	**-0.63**	1.51E-01
At1g51320	F-box family protein (FBX11)	**-0.63**	1.63E-01
At3g01380	phosphatidylinositolglycan class N (PIG-N) family protein	**-0.63**	6.80E-02
At5g52990	vesicle-associated membrane protein-related	**-0.63**	5.27E-02
At5g30520	unknown protein	**-0.63**	1.08E-01
At2g06140	transposable element gene	**-0.63**	6.74E-02
At5g62940	Dof-type zinc finger domain-containing protein	**-0.62**	1.67E-02
At3g12580	HSP70 (heat shock protein 70); ATP binding	**-0.62**	6.51E-02
At2g30810	gibberellin-regulated family protein	**-0.62**	3.70E-02
At4g22030	F-box family protein	**-0.62**	1.88E-01
At1g53600	pentatricopeptide (PPR) repeat-containing protein	**-0.62**	2.54E-02
At1g76770	heat shock protein-related	**-0.62**	1.46E-02
At4g02170	unknown protein	**-0.62**	1.55E-02
At5g19980	integral membrane family protein	**-0.62**	8.28E-02
At3g18540	unknown protein	**-0.62**	1.42E-02
At1g52640	pentatricopeptide (PPR) repeat-containing protein	**-0.62**	3.42E-03
At1g67600	Catalytic	**-0.62**	6.92E-02
At1g77550	protein binding / tubulin-tyrosine ligase	**-0.62**	1.14E-02
At5g44785	OSB3; single-stranded DNA binding	**-0.62**	7.60E-03
At5g66500	pentatricopeptide (PPR) repeat-containing protein	**-0.62**	8.17E-03
At2g29250	lectin protein kinase, putative	**-0.62**	1.96E-02
At1g67820	protein phosphatase 2C, putative / PP2C, putative	**-0.62**	6.67E-03
At5g28650	WRKY74 (WRKY DNA-binding protein 74); transcription factor	**-0.62**	1.02E-01
At1g63640	kinesin motor protein-related	**-0.62**	1.59E-02
At5g56410	F-box family protein	**-0.61**	1.05E-02
At5g20490	XIK (Myosin-like protein XIK); motor/ protein binding	**-0.61**	1.04E-02
At1g08360	60S ribosomal protein L10A (RPL10aA)	**-0.61**	1.78E-02
At3g18260	reticulon family protein (RTNLB9)	**-0.61**	5.21E-02
At1g43150	transposable element gene	**-0.61**	1.13E-02
At1g51770	unknown protein	**-0.61**	8.02E-03
At1g22240	APUM8 (ARABIDOPSIS PUMILIO 8); RNA binding	**-0.61**	6.22E-02
At2g15370	FUT5 (Fucosyltransferase 5); fucosyltransferase/ transferase, transferring glycosyl groups	**-0.61**	4.89E-02
At5g59430	ATTRP1 (TELOMERE REPEAT BINDING PROTEIN 1); DNA binding	**-0.61**	1.08E-02
At1g77480	nucellin protein, putative	**-0.61**	4.85E-02
At3g03170	hypothetical protein	**-0.61**	1.33E-01
At2g34890	CTP synthase, putative / UTP--ammonia ligase, putative	**-0.61**	1.76E-02
At2g38025	OTU-like cysteine protease family protein	**-0.61**	2.05E-02
At4g09760	choline kinase, putative	**-0.61**	1.08E-01
At4g04980	proline-rich family protein	**-0.61**	6.91E-02
At2g21540	SEC14 cytosolic factor / phosphoglyceride transfer protein, putative	**-0.61**	4.42E-02
At5g28773	transposable element gene	**-0.61**	2.49E-01
At3g02570	MEE31 (maternal effect embryo arrest 31); mannose-6-phosphate isomerase	**-0.61**	1.63E-02
At5g44360	FAD-binding domain-containing protein	**-0.61**	1.72E-01
At5g49190	SUS2 (SUCROSE SYNTHASE 2); UDP-glycosyltransferase/ sucrose synthase/ transferase, transferring glycosyl groups	**-0.61**	2.67E-02
At5g41430	zinc finger (C3HC4-type RING finger) family protein	**-0.61**	8.81E-02
At5g62850	ATVEX1 (VEGETATIVE CELL EXPRESSED1)	**-0.61**	9.10E-02
At3g53410	zinc finger (C3HC4-type RING finger) family protein	**-0.61**	7.08E-02
At2g45550	CYP76C4 (cytochrome P450, family 76, subfamily C, polypeptide 4); oxygen binding	**-0.60**	7.76E-02
At5g18160	F-box family protein	**-0.60**	7.39E-02
At3g43302	transposable element gene	**-0.60**	6.55E-02
At1g22130	AGL104; DNA binding / transcription factor	**-0.60**	1.97E-01
At2g42480	meprin and TRAF homology domain-containing protein / MATH domain-containing protein	**-0.60**	2.43E-02
At5g07800	flavin-containing monooxygenase family protein / FMO family protein	**-0.60**	4.20E-02
At1g59740	proton-dependent oligopeptide transport (POT) family protein	**-0.60**	1.39E-01

Table 4.8C. Genes induced more than 1.5 fold by 24 hr recombinant AtPNP-A treatment

Locus	Name and description	log2 ratio	p value
AT3G59590	jacalin lectin family protein, similar to F-box family protein	**1.17**	2.21E-02
AT3G21000	unknown protein	**1.12**	2.38E-01
AT4G16900	ATP binding / protein binding / transmembrane receptor, similar to SNC1 (SUPPRESSOR OF NPR1-1, CONSTITUTIVE 1)	**1.05**	2.17E-01
AT4G36280	ATP-binding region, ATPase-like domain-containing protein	**0.93**	2.28E-01
AT2G39790	mitochondrial glycoprotein family protein / MAM33 family protein	**0.93**	3.57E-02
AT4G12500	protease inhibitor/seed storage/lipid transfer protein (LTP) family protein	**0.92**	1.96E-04
AT5G15080	protein kinase, putative	**0.92**	1.04E-01
AT5G48430	aspartic-type endopeptidase/ pepsin A	**0.91**	3.71E-03
AT5G52340	ATEXO70A2 (exocyst subunit EXO70 family protein A2); protein binding	**0.91**	8.57E-02
AT5G09910	ATP binding / GTP binding / transcription factor binding	**0.90**	5.61E-02
AT3G55050	serine/threonine protein phosphatase 2C (PP2C6)	**0.89**	3.49E-02
AT2G24350	RNA recognition motif (RRM)-containing protein	**0.88**	2.57E-01
AT5G49670	hypothetical protein	**0.87**	9.34E-02
AT5G64120	peroxidase, putative	**0.86**	1.03E-03
AT2G46430	ATCNGC3 (CYCLIC NUCLEOTIDE GATED CHANNEL 3); calmodulin binding / cyclic nucleotide binding / ion channel	**0.83**	9.36E-03
AT1G07960	ATPDIL5-1 (PDI-LIKE 5-1); thiol-disulfide exchange intermediate	**0.83**	5.46E-03
AT4G19730	glycosyl hydrolase family 18 protein	**0.82**	1.10E-01
AT5G56060	ATP binding / nucleotide binding / phenylalanine-tRNA ligase	**0.82**	5.74E-03
AT3G56270	unknown protein	**0.81**	1.57E-02
AT5G51950	glucose-methanol-choline (GMC) oxidoreductase family protein	**0.81**	4.49E-02
AT4G12490	protease inhibitor/seed storage/lipid transfer protein (LTP) family protein	**0.80**	3.06E-04
AT2G25160	CYP82F1 (cytochrome P450, family 82, subfamily F, polypeptide 1); oxygen binding	**0.80**	1.80E-01
AT5G25260	unknown protein	**0.80**	3.69E-03
AT1G60470	ATGOLS4 (ARABIDOPSIS THALIANA GALACTINOL SYNTHASE 4); transferase, transferring glycosyl groups / transferase, transferring hexosyl groups	**0.79**	2.98E-02
AT1G09310	unknown protein	**0.78**	6.20E-04
AT1G12180	heat shock protein-related	**0.78**	1.31E-03
AT1G23210	ATGH9B6 (ARABIDOPSIS THALIANA GLYCOSYL HYDROLASE 9B6); hydrolase, hydrolyzing O-glycosyl compounds	**0.78**	6.42E-02
AT3G46340	leucine-rich repeat protein kinase, putative	**0.76**	1.26E-02
AT2G32660	disease resistance family protein / LRR family protein	**0.76**	9.72E-02
AT2G30460	transporter-related	**0.75**	1.08E-01
AT5G36670	PHD finger family protein	**0.72**	1.12E-01
AT5G54745	DegP protease family	**0.71**	5.53E-02
AT1G58320	unknown protein	**0.70**	4.77E-04
AT2G10270	transposable element gene	**0.70**	3.22E-03
AT4G22470	protease inhibitor/seed storage/lipid transfer protein (LTP) family protein	**0.69**	4.26E-03
AT1G28630	unknown protein	**0.69**	4.11E-02
AT5G67290	FAD-dependent oxidoreductase family protein	**0.68**	9.88E-02
AT4G29400	oxidoreductase/ transition metal ion binding	**0.68**	3.14E-02
AT3G17080	self-incompatibility protein-related	**0.68**	2.50E-01
AT1G21310	ATEXT3 (EXTENSIN 3); structural constituent of cell wall	**0.68**	4.41E-03
AT4G25530	FWA; DNA binding / transcription factor	**0.68**	9.10E-04
AT1G23350	invertase/pectin methylesterase inhibitor family protein	**0.68**	9.33E-03
AT5G53430	SDG29 (SET DOMAIN GROUP 29); DNA binding	**0.67**	1.38E-02
AT3G07560	APM2/PEX13 (ABERRANT PEROXISOME MORPHOLOGY 2); protein binding	**0.67**	4.44E-03
AT3G56870	unnamed protein product	**0.67**	2.37E-03
AT3G44730	kinesin motor protein-related	**0.67**	2.15E-02
AT3G49130	RNA binding	**0.66**	2.76E-03
AT5G41000	YSL4 (YELLOW STRIPE LIKE 4); oligopeptide transporter	**0.66**	5.86E-03
AT4G20790	leucine-rich repeat family protein	**0.65**	2.21E-02
AT4G14365	zinc finger (C3HC4-type RING finger) family protein / ankyrin repeat family protein	**0.65**	1.77E-03
AT4G21670	CPL1 (FIERY 2); double-stranded RNA binding	**0.64**	2.00E-03
AT3G17390	MTO3 (S-adenosylmethionine synthase 3); methionine adenosyltransferase	**0.64**	1.57E-02
AT1G47210	CYCA3;2; cyclin-dependent protein kinase	**0.64**	1.94E-02
AT5G35760	beta-galactosidase	**0.64**	1.41E-01
AT1G03982	RIC6 (ROP-INTERACTIVE CRIB MOTIF-CONTAINING PROTEIN 6)	**0.64**	7.81E-03
AT1G37030	transposable element gene	**0.64**	9.68E-02
AT3G52950	CBS domain-containing protein / octicosapeptide/Phox/Bemp1 (PB1) domain-containing protein	**0.64**	2.47E-02
AT5G09210	DNA binding / transcription factor	**0.63**	3.62E-03
AT3G53930	protein kinase family protein	**0.63**	7.28E-02
AT5G20470	myosin, putative	**0.63**	6.30E-02
AT4G35180	LHT7 (LYS/HIS TRANSPORTER 7); amino acid transmembrane transporter	**0.63**	1.23E-03
AT5G06810	mitochondrial transcription termination factor-related / mTERF-related	**0.63**	8.54E-03
AT1G17940	unknown protein	**0.62**	2.37E-02
AT1G26250	proline-rich extensin, putative	**0.62**	1.91E-03

Table 4.8C. Genes induced by 24 hr recombinant AtPNP-A treatment cont inued

Locus	Name and description	log2 ratio	p value
AT1G60220	cysteine-type peptidase	**0.62**	1.33E-01
AT2G33190	F-box family protein	**0.61**	3.66E-03
AT1G75500	nodulin MtN21 family protein	**0.61**	5.09E-02
AT4G08830	transposable element gene	**0.61**	4.09E-03
AT1G64100	pentatricopeptide (PPR) repeat-containing protein	**0.60**	1.55E-02
AT2G01250	60S ribosomal protein L7 (RPL7B)	**0.60**	1.01E-01
AT4G23100	RML1 (ROOT MERISTEMLESS 1); glutamate-cysteine ligase	**0.60**	3.24E-02
AT4G04700	CPK27 (calcium-dependent protein kinase 27); kinase	**0.60**	1.49E-02
AT3G16880	F-box protein-related	**0.60**	3.33E-02
AT5G28823	zinc knuckle (CCHC-type) family protein	**0.60**	4.74E-02

Table 4.8D. Genes repressed more than 1.5 fold by 24 hr recombinant AtPNP-A treatment

Locus	Name and description	log2 ratio	p value
AT2G28820	structural constituent of ribosome	**-1.50**	8.34E-02
AT1G10770	invertase/pectin methylesterase inhibitor family protein	**-1.28**	1.74E-01
AT3G01860	unknown protein	**-1.24**	7.80E-02
AT4G14145	unknown protein	**-1.04**	1.54E-01
AT3G03060	ATPase	**-1.03**	1.18E-02
AT3G32990	pseudogene, ATP synthase C subunit	**-0.93**	1.65E-01
AT4G39753	kelch repeat-containing F-box family protein	**-0.92**	1.49E-01
AT1G55290	oxidoreductase, 2OG-Fe(II) oxygenase family protein	**-0.91**	1.07E-01
AT4G31400	unnamed protein product	**-0.91**	3.36E-02
AT3G29620	transposable element gene	**-0.88**	2.21E-01
AT2G07739	Uncharacterized mitochondrial protein AtMg00370	**-0.86**	4.52E-02
AT3G50460	HR2 (HOMOLOG OF RPW8 2)	**-0.85**	2.98E-03
AT2G33790	pollen Ole e 1 allergen and extensin family protein	**-0.84**	5.09E-04
AT2G30490	ATC4H/C4H/CYP73A5 (CINNAMATE 4-HYDROXYLASE, CINNAMATE-4-HYDROXYLASE); trans-cinnamate 4-monooxygenase	**-0.80**	2.81E-04
AT3G43920	DCL3 (DICER-LIKE 3); RNA binding / ribonuclease III	**-0.80**	1.81E-02
AT2G15380	transposable element gene	**-0.80**	5.68E-04
AT1G23650	unknown protein	**-0.78**	7.05E-02
AT5G47960	SMG1 (SMALL MOLECULAR WEIGHT G-PROTEIN 1); GTP binding	**-0.78**	5.82E-02
AT5G03070	Binding	**-0.77**	2.96E-02
AT3G21055	PSBTN (photosystem II subunit T)	**-0.75**	1.57E-02
AT2G41390	unknown protein	**-0.74**	1.66E-01
AT1G21150	mitochondrial transcription termination factor family protein / mTERF family protein	**-0.74**	5.68E-02
AT1G67865	unknown protein	**-0.74**	1.47E-03
AT3G12440	extensin family protein	**-0.73**	1.71E-01
AT4G22060	F-box family protein	**-0.73**	1.42E-02
AT4G30670	contains domain PROKAR_LIPOPROTEIN	**-0.73**	1.43E-03
AT2G19300	unknown protein	**-0.73**	1.24E-01
AT3G55590	GDP-mannose pyrophosphorylase, putative	**-0.72**	6.08E-02
AT5G55310	TOP1alpha (TOPOISOMERASE I)	**-0.72**	1.58E-03
AT2G25260	unknown protein	**-0.71**	3.36E-02
AT5G56540	AGP14 (ARABINOGALACTAN PROTEIN 14)	**-0.70**	8.52E-04
AT3G58430	meprin and TRAF homology domain-containing protein / MATH domain-containing protein	**-0.70**	3.83E-02
AT3G12345	similar to Os06g0484500	**-0.70**	6.73E-02
AT5G65400	unknown protein	**-0.69**	8.55E-02
AT3G01015	unknown protein	**-0.68**	2.12E-02
AT3G53240	leucine-rich repeat family protein	**-0.68**	2.17E-01
AT1G51355	hypothetical protein	**-0.68**	2.47E-01
AT3G23450	pseudogene, similar to unnamed protein product	**-0.68**	6.24E-03
AT4G38860	auxin-responsive protein, putative	**-0.68**	6.17E-03
AT5G41835	transposable element gene	**-0.68**	1.14E-03
AT1G03106	unknown protein	**-0.67**	7.89E-02
AT3G03430	polcalcin, putative / calcium-binding pollen allergen, putative	**-0.67**	2.90E-03
AT4G29370	kelch repeat-containing F-box family protein	**-0.67**	3.16E-02
AT1G20930	CDKB2;2 (CYCLIN-DEPENDENT KINASE B2;2); kinase	**-0.67**	5.40E-02
AT3G52020	SCPL39 (serine carboxypeptidase-like 39); serine carboxypeptidase	**-0.67**	1.48E-01
AT4G19470	disease resistance protein-related	**-0.67**	5.93E-02
AT4G00540	ATMYB3R2/MYB3R-2/PC-MYB2 (MYB DOMAIN PROTEIN 3R2, PUTATIVE C-MYB-LIKE TRANSCRIPTION FACTOR); DNA binding / transcription factor	**-0.67**	6.94E-03
AT2G40880	FL3-27; cysteine protease inhibitor	**-0.66**	4.61E-03
AT1G80910	unknown protein	**-0.66**	3.33E-03
AT5G15180	peroxidase, putative	**-0.66**	9.38E-03
AT3G05780	Lon protease, putative	**-0.66**	3.93E-03
AT2G30280	unnamed protein product	**-0.66**	2.12E-01
AT3G47070	unknown protein	**-0.65**	1.05E-02
AT2G13090	transposable element gene	**-0.65**	9.62E-02
AT3G44680	HDA9 (histone deacetylase 9); histone deacetylase	**-0.65**	1.11E-01
AT3G49520	F-box family protein	**-0.65**	1.06E-01
AT5G47290	myb family transcription factor	**-0.65**	2.24E-03
AT4G15710	unknown protein	**-0.64**	9.47E-02
AT5G09980	PROPEP4 (Elicitor peptide 4 precursor)	**-0.64**	1.17E-02
AT4G26840	SUM1 (SMALL UBIQUITIN-LIKE MODIFIER 1)	**-0.64**	5.50E-02
AT2G46740	FAD-binding domain-containing protein	**-0.64**	7.73E-03
AT1G56030	MIF4G domain-containing protein / U-box domain-containing protein	**-0.64**	4.78E-02
AT2G02970	nucleoside phosphatase family protein / GDA1/CD39 family protein	**-0.64**	8.70E-02
AT1G67860	unknown protein	**-0.64**	1.35E-02
AT4G13430	aconitase family protein / aconitate hydratase family protein	**-0.64**	1.95E-02

Table 4.8D. Genes repressed by 24 hr recombinant AtPNP-A treatment continued

Locus	Name and description	log2 ratio	p value
AT2G15960	unknown protein	**-0.63**	1.25E-02
AT2G03180	unknown protein	**-0.63**	3.48E-02
AT2G15110	pseudogene, hypothetical protein	**-0.63**	8.11E-03
AT1G03600	photosystem II family protein	**-0.63**	6.53E-02
AT2G41650	unknown protein	**-0.63**	3.67E-03
AT4G29110	unknown protein	**-0.62**	2.61E-02
AT1G22710	SUC2 (SUCROSE-PROTON SYMPORTER 2); carbohydrate transmembrane transporter/ sucrose transmembrane transporter/ sucrose:hydrogen symporter/ sugar:hydrogen ion symporter	**-0.62**	1.49E-02
AT2G47540	pollen Ole e 1 allergen and extensin family protein	**-0.62**	5.27E-03
AT5G27800	ATP binding / aminoacyl-tRNA ligase/ nucleotide binding	**-0.61**	1.23E-02
AT5G35940	jacalin lectin family protein	**-0.61**	6.18E-02
AT1G08830	CSD1 (COPPER/ZINC SUPEROXIDE DISMUTASE 1); copper, zinc superoxide dismutase	**-0.61**	2.55E-02
AT1G65170	ubiquitin carboxyl-terminal hydrolase family protein	**-0.61**	1.33E-02
AT1G53885	senescence-associated protein-related	**-0.61**	4.39E-03
AT2G21640	unknown protein	**-0.60**	1.55E-02
AT2G44580	protein binding / zinc ion binding	**-0.60**	3.59E-03
AT5G22720	F-box family protein	**-0.60**	4.89E-03
AT2G24210	TPS10 (TERPENE SYNTHASE 10); myrcene/(E)-beta-ocimene synthase	**-0.60**	7.64E-03
AT5G65000	nucleotide-sugar transporter family protein	**-0.60**	2.15E-01

4.3.6.1.1 GO analysis of genes induced by 1 hr AtPNP-A *treatment*

The list of genes induced more than 1.5 fold by 1 hr recombinant AtPNP-A treatment returned some enrichment of GO biological process terms associated with the "defence response" at level 3, "SA mediated signalling pathway" at level 6; "systemic acquired resistance" at level 7 and the most significant enrichment was in the term "systemic acquired resistance, SA mediated signalling pathway" at level 8 (Table 4.9A) all as a result of the presence of *WRKY70, MAPKK 7* (*MKK7*) and the bZIP family transcription factor, *TGA2*. Modest enrichment of the GO terms "RNA biosynthetic process" at level 6, "transcription, DNA dependent" at level 7 and "regulation of transcription, DNA dependent" at level 8 was the result of a number of transcription factors that are found in the list of genes induced by short-term AtPNP-A treatment. Enrichment of the GO term "ethylene biosynthetic process" at level 9 was due to two ethylene biosynthesis genes, *1-AMINOCYCLOPROPANE-1-CARBOXYLATE-SYNTHASE 7* and *11* (*ACS7* and *ACS11*), while enrichment of the term "zinc ion transport" at level 9 was due to the presence of two zinc transporters, *ZIP2* and *ZIP3*, among the list of genes induced by 1 hr recombinant AtPNP-A treatment. Therefore short-term AtPNP-A treatment induces genes involved in SA signalling and SAR, transcription, ethylene biosynthesis and ion transport.

4.3.6.1.2 GO analysis of genes repressed by 1 hr AtPNP-A *treatment*

The GO analysis of the list of genes repressed by 1 hr recombinant AtPNP-A treatment revealed a number of GO biological process terms with low p values (Table 4.9B). There was some enrichment of the GO term "response to gibberellic acid stimulus" at level 5 as a result of the presence of *MYB31* and *MYB33* transcription factors, *GA REQUIRING 2* (*GA2*), a gibberellin-regulated family protein and the *TELOMERE REPEAT BINDING PROTEIN 1* (*ATTRP1*) in the list of genes that were downregulated by 1 hr AtPNP-A treatment. Modest enrichment of the term "vesicle mediated transport" at level 5 was associated with *VESICLE-ASSOCIATED MEMBRANE PROTEINS* (*VAMP*s) - *VAMP725*, *VAMP726*, a *VAMP*-related protein and a phagocytosis and cell motility protein that were present in this list. There was also some enrichment of the GO biological process term "protein prenylation" at level 9 and the GO molecular function term "protein prenyltransferase activity" at level 6, both of which are associated with the presence of a protein prenyltransferase gene and *ENHANCED RESPONSE TO ABA 1* (*ERA1*) in the list of genes repressed by short-term AtPNP-A treatment. Lastly there was enrichment of the GO cellular component term "endosome" at level 8 as a result of *BRI1-ASSOCIATED RECEPTOR KINASE 1* (*BAK1*), *VAMP725* and *VAMP726* that were found in the list of genes repressed by 1 hr AtPNP-A treatment. Therefore short-term AtPNP-A treatment represses genes involved in GA and ABA responses as well as genes involved in vesicle trafficking.

Table 4.9A. GO analysis of genes induced by 1 hr AtPNP-A treatment

Term	PNP 1hr vs genome	p value	Adjusted p value
GO BIOLOGICAL PROCESS			
level 3			
defence response (GO:0006952)	70.05% 29.95%	7.96E-03	4.78E-01
level 4			
alkene metabolic process (GO:0043449)	93.56% 6.44%	9.85E-03	1
response to salicylic acid stimulus (GO:0009751)	81.41% 18.59%	1.44E-02	1
sulfur metabolic process (GO:0006790)	82.96% 17.04%	2.55E-02	1
level 5			
alkene biosynthetic process (GO:0043450)	94.45% 5.55%	7.37E-03	1
RNA metabolic process (GO:0016070)	64.28% 35.72%	1.21E-02	1
regulation of cellular metabolic process (GO:0031323)	60.76% 39.24%	3.85E-02	1
hormone biosynthetic process (GO:0042446)	86.81% 13.19%	3.96E-02	1
level 6			
salicylic acid mediated signalling pathway (GO:0009863)	93.93% 6.07%	1.20E-03	4.41E-01
RNA biosynthetic process (GO:0032774)	70.11% 29.89%	2.20E-03	4.41E-01
ethylene metabolic process (GO:0009692)	94.96% 5.04%	6.07E-03	8.12E-01
regulation of nucleobase, nucleoside, nucleotide and nucleic acid metabolic process (GO:0019219)	62.66% 37.34%	2.04E-02	1
defence response, incompatible interaction (GO:0009814)	79.08% 20.92%	4.69E-02	1
level 7			
transcription, DNA-dependent (GO:0006351)	70.35% 29.65%	1.67E-03	3.67E-01
systemic acquired resistance (GO:0009627)	93.09% 6.91%	1.72E-03	3.67E-01
regulation of transcription (GO:0045449)	63.21% 36.79%	1.42E-02	1
sulfur amino acid metabolic process (GO:0000096)	87.78% 12.22%	3.36E-02	1
metal ion transport (GO:0030001)	75.58% 24.42%	4.14E-02	1
level 8			
systemic acquired resistance, salicylic acid mediated signalling pathway (GO:0009862)	95.37% 4.63%	5.55E-04	2.65E-01
regulation of transcription, DNA-dependent (GO:0006355)	68.63% 31.37%	2.82E-03	6.72E-01
methionine metabolic process (GO:0006555)	90.01% 9.99%	2.26E-02	1
transition metal ion transport (GO:0000041)	86.5% 13.5%	4.12E-02	1
level 9			
zinc ion transport (GO:0006829)	97.74% 2.26%	1.31E-03	4.66E-01
ethylene biosynthetic process (GO:0009693)	95.81% 4.19%	3.98E-03	7.08E-01
covalent chromatin modification (GO:0016569)	90.88% 9.12%	1.79E-02	1
GO CELLULAR COMPONENT			
level 8			
nucleus (GO:0005634)	61.11% 38.89%	6.24E-03	3.93E-01
GO MOLECULAR FUNCTION			
level 3			
transcriptional repressor activity (GO:0016564)	87.4% 12.6%	3.70E-02	1
level 4			
Carbon-sulfur lyase activity (GO:0016846)	86.89% 13.11%	4.00E-02	1
level 6			
zinc ion transporter activity (GO:0005385)	96.59% 3.41%	3.24E-03	1
exonuclease activity (GO:0004527)	89.47% 10.53%	6.12E-03	1
level 7			
3'-5' exonuclease activity (GO:0008408)	91.36% 8.64%	1.73E-02	1
KEGG			
ath00941: flavonoid biosynthesis	96.41% 3.59%	2.84E-03	3.35E-01
ath00561: glycerolipid metabolism	91.88% 8.12%	1.37E-02	8.08E-01

Table 4.9B. GO analysis of genes repressed by 1 hr AtPNP-A treatment

Term	AtPNP-A 1hr vs genome	p value	Adjusted p value
GO BIOLOGICAL PROCESS			
level 3			
cell communication (GO:0007154)	65.32% 34.68%	1.38E-02	8.25E-01
secondary metabolic process (GO:0019748)	70.06% 29.94%	3.21E-02	9.62E-01
level 4			
signal transduction (GO:0007165)	66.45% 33.55%	1.14E-02	1
gametogenesis (GO:0007276)	85.76% 14.24%	4.66E-02	1
level 5			
response to gibberellic acid stimulus (GO:0009739)	84.98% 15.02%	2.22E-03	5.36E-01
vesicle-mediated transport (GO:0016192)	83.68% 16.32%	3.34E-03	5.36E-01
male gametophyte development (GO:0009555)	89.74% 10.26%	5.67E-03	6.06E-01
cellular lipid metabolic process (GO:0044255)	69.26% 30.74%	2.69E-02	1
male gamete generation (GO:0048232)	87.65% 12.35%	3.50E-02	1
gamete generation (sensu Magnoliophyta) (GO:0009552)	87.07% 12.93%	3.83E-02	1
biopolymer modification (GO:0043412)	59.48% 40.52%	4.90E-02	1
level 6			
lipid biosynthetic process (GO:0008610)	73.75% 26.25%	1.30E-02	1
protein modification (GO:0006464)	61.69% 38.31%	1.94E-02	1
male gamete generation (sensu Magnoliophyta) (GO:0048234)	87.91% 12.09%	3.34E-02	1
level 7			
cytoskeleton-dependent intracellular transport (GO:0030705)	84.99% 15.01%	1.73E-02	1
gibberellic acid mediated signalling (GO:0009740)	90.11% 9.89%	2.25E-02	1
terpenoid metabolic process (GO:0006721)	81.33% 18.67%	3.34E-02	1
isoprenoid biosynthetic process (GO:0008299)	80.5% 19.5%	3.81E-02	1
level 8			
glutamine family amino acid biosynthetic process (GO:0009084)	91.76% 8.24%	1.60E-02	1
terpenoid biosynthetic process (GO:0016114)	84.56% 15.44%	1.89E-02	1
regulation of abscisic acid mediated signalling (GO:0009787)	90.27% 9.73%	2.20E-02	1
glycerophospholipid metabolic process (GO:0006650)	88.48% 11.52%	3.07E-02	1
level 9			
protein prenylation (GO:0018342)	98.31% 1.69%	1.03E-03	3.65E-01
glycerophospholipid biosynthetic process (GO:0046474)	91% 9%	1.86E-02	1
GO CELLULAR COMPONENT			
level 8			
endosome (GO:0005768)	91.28% 8.72%	3.40E-03	2.15E-01
cytoskeleton (GO:0005856)	79.37% 20.63%	9.99E-03	3.15E-01
level 9			
cytoskeletal part (GO:0044430)	80.28% 19.72%	1.59E-02	8.58E-01
microtubule cytoskeleton (GO:0015630)	78.86% 21.14%	4.61E-02	8.74E-01
chloroplast (GO:0009507)	56.54% 43.46%	4.86E-02	8.74E-01
GO MOLECULAR FUNCTION			
level 4			
cyclic nucleotide binding (GO:0030551)	88.81% 11.19%	2.92E-02	1
level 5			
prenyltransferase activity (GO:0004659)	87.81% 12.19%	3.45E-02	1
adenyl nucleotide binding (GO:0030554)	64.23% 35.77%	3.55E-02	1
oxidoreductase activity, acting on paired donors, with incorporation or reduction of molecular oxygen, 2-oxoglutarate as one donor, and incorporation of one atom each of oxygen into both donors (GO:0016706)	81.01% 18.99%	3.58E-02	1
level 6			
protein prenyltransferase activity (GO:0008318)	98.14% 1.86%	1.27E-03	7.41E-01
KEGG			
ath00051: fructose and mannose metabolism	89.47% 10.53%	2.34E-02	1

4.3.6.1.3 GO analysis of genes induced by 24 hr AtPNP-A *treatment*

The list of genes induced by 24 hrs recombinant AtPNP-A treatment returned moderate enrichment of GO biological process terms involved in "lipid transport" at level 5 as a result of the presence of three *LIPID TRANSFER PROTEINS* (*LTP*s) (Table 4.9C). There was also some enrichment of the GO term "sulphur compound biosynthetic process" at level 5 as a result of *ROOT MERISTEMLESS 1* (*RML1*) and *S-ADENOSYLMETHIONINE SYNTHASE 3* (*MTO3*) that were found within the list of genes induced by long-term AtPNP-A treatment. Enrichment of the GO terms "response to fungus" at level 5 and "defence response to fungus" at level 6 are due to *RML1*, a putative peroxidase and one of the *LTP*s among the list of genes. Lastly there was modest enrichment of the GO molecular function term "structural constituent of the cell wall" at level 3 as a result of *EXTENSIN 3* (*AtEXT3*) and another putative extensin that were present in the list of genes induced by 24 hr AtPNP-A treatment. Therefore long-term AtPNP-A treatment induces the expression of genes that are involved in lipid transport, the defence response to fungus and cell wall modification.

4.3.6.1.4 GO analysis of genes repressed by 24 hr AtPNP-A *treatment*

From the list of genes repressed by 24 hr AtPNP-A treatment, GO biological process terms that emerged as being modestly enriched included "response to stress" at level 3 as a result of the presence of *SMALL UBIQUITIN-LIKE MODIFIER 1* (*SUM1*), an unknown protein that is a marker of the oxidative stress response, a putative peroxidase, *CINNAMATE-4-HYDROXYLASE* (*ATC4H*), *TERPENE SYNTHASE 10* (*TPS10*) and *COPPER/ZINC SUPEROXIDE DISMUTASE 1* (*CSD1*) (Table 4.9D). Enrichment of the GO term "oxygen and reactive oxygen species metabolic process" at level 4 was the due to a subset of these genes including the oxidative stress response marker, the putative peroxidase and *CSD1*. Therefore long-term AtPNP-A treatment represses genes involved in stress responses and ROS signalling.

4.3.6.2 Promoter content analysis of differentially expressed gene lists

Significant enrichment of known TFBSs was only returned for the list of genes induced by 1 hr recombinant AtPNP-A treatment. Non-enriched TFBSs that had p values < 0.005 among each of the lists of differentially expressed genes are mentioned briefly.

The promoters of the genes induced by 1 hr recombinant AtPNP-A treatment were enriched in three known TFBSs, namely TATA-box motif (p value < 10^{-6}) and ARF and MYB1 binding site motifs, both of which had p values < 10^{-5} (Table 4.10A) while non-enriched TFBSs included LEAFYATAG, MYB1AT and MYB4 binding site motif (p values < 10^{-3}) and AtMYC2 BS in RD22, Box II promoter motif, GAREAT, MYCATERD1, T-box promoter motif and W-box promoter motif (p < 0.005).

Table 4.9C. GO analysis of gene induced by 24 hr AtPNP-A treatment

Term	AtPNP-A 24hr vs genome	p value	Adjusted p value
GO BIOLOGICAL PROCESS			
level 3			
establishment of localization (GO:0051234)	67.35% 32.65%	1.91E-02	8.63E-01
defence response (GO:0006952)	74.29% 25.71%	2.88E-02	8.63E-01
level 4			
transport (GO:0006810)	67.19% 32.81%	1.98E-02	1
sulfur metabolic process (GO:0006790)	88.96% 11.04%	2.65E-02	1
level 5			
lipid transport (GO:0006869)	91.05% 8.95%	3.38E-03	6.48E-01
sulfur compound biosynthetic process (GO:0044272)	95.71% 4.29%	4.04E-03	6.48E-01
response to fungus (GO:0009620)	88.86% 11.14%	6.55E-03	7.00E-01
GO:0018409	76.41% 23.59%	3.46E-02	1
level 6			
defence response to fungus (GO:0050832)	92.89% 7.11%	1.67E-03	5.60E-01
lipoprotein metabolic process (GO:0042157)	76.22% 23.78%	3.52E-02	1
cellulose and pectin-containing cell wall organization and biogenesis (GO:0009664)	86.03% 13.97%	4.26E-02	1
level 7			
protein amino acid acylation (GO:0043543)	78.59% 21.41%	2.18E-02	1
lipoprotein biosynthetic process (GO:0042158)	78.17% 21.83%	2.37E-02	1
peptidyl-amino acid modification (GO:0018193)	77.94% 22.06%	2.47E-02	1
level 8			
N-terminal protein amino acid modification (GO:0031365)	75.33% 24.67%	3.82E-02	1
protein amino acid lipidation (GO:0006497)	74.77% 25.23%	4.19E-02	1
level 9			
protein myristoylation (GO:0018377)	77.43% 22.57%	1.96E-02	1
GO CELLULAR COMPONENT			
level 8			
cytoskeleton (GO:0005856)	85.16% 14.84%	4.67E-02	1
level 9			
cytoskeletal part (GO:0044430)	84.73% 15.27%	4.81E-02	8.65E-01
GO MOLECULAR FUNCTION			
level 3			
structural constituent of cell wall (GO:0005199)	94.11% 5.89%	7.57E-03	5.42E-01
lipid binding (GO:0008289)	86.55% 13.45%	1.18E-02	5.42E-01
level 6			
ATP binding (GO:0005524)	77.34% 22.66%	4.88E-02	1

Table 4.9D. GO analysis of gene repressed by 24 hr AtPNP-A treatment

Term	AtPNP-A 24hr vs genome	p value	Adjusted p value
GO BIOLOGICAL PROCESS			
level 3			
response to stress (GO:0006950)	77.11% 22.89%	7.20E-03	4.32E-01
response to chemical stimulus (GO:0042221)	73.55% 26.45%	1.76E-02	5.28E-01
level 4			
oxygen and reactive oxygen species metabolic process (GO:0006800)	88.52% 11.48%	6.84E-03	9.85E-01
response to wounding (GO:0009611)	91.24% 8.76%	1.61E-02	1
level 5			
response to oxidative stress (GO:0006979)	89.59% 10.41%	5.02E-03	1
carbohydrate transport (GO:0008643)	94.18% 5.82%	7.04E-03	1
DNA metabolic process (GO:0006259)	80.91% 19.09%	3.28E-02	1
GO MOLECULAR FUNCTION			
level 3			
carbohydrate transporter activity (GO:0015144)	89.16% 10.84%	2.51E-02	1
level 4			
oxidoreductase activity, acting on paired donors, with incorporation or reduction of molecular oxygen (GO:0016705)	89.19% 10.81%	2.48E-02	1
level 5			
serine-type peptidase activity (GO:0008236)	89.36% 10.64%	2.39E-02	1
nuclease activity (GO:0004518)	86.2% 13.8%	4.09E-02	1
KEGG			
ath00360: phenylalanine metabolism	90.74% 9.26%	1.58E-02	1

Table 4.10. Athena results of genes differentially expressed in response to AtPNP-A

A. AtPNP-A 1 HR INDUCED	p value	# P	# S	consensus sequence
Enriched sites:				
TATA-box Motif	$<10^{-6}$	230	688	TATAAA
ARF binding site motif	$<10^{-5}$	114	151	TGTCTC
MYB1 binding site motif	$<10^{-5}$	30	31	MTCCWACC
Non-enriched sites:				
LEAFYATAG	$<10^{-3}$	37	42	CCAATGT
MYB1AT	$<10^{-3}$	218	555	WAACCA
MYB4 binding site motif	$<10^{-3}$	192	400	AMCWAMC
GAREAT	0.0015	149	227	TAACAAR
T-box promoter motif	0.0020	144	216	ACTTTG
Ibox promoter motif	0.0022	108	146	GATAAG
MYCATERD1	0.0034	98	136	CATGTG
AtMYC2 BS in RD22	0.0034	98	136	CACATG
BoxII promoter motif	0.0036	117	162	GGTTAA
W-box promoter motif	0.0047	173	312	TTGACY
MYB2AT	0.0125	78	90	TAACTG
MYB1LEPR	0.0238	50	58	GTTAGTT
MYB binding site promoter	0.0452	77	101	MACCWAMC

B. AtPNP-A 1 HR REPRESSED	p value	# P	# S	consensus sequence
Non-enriched sites:				
MYB4 binding site motif	$<10^{-3}$	186	383	AMCWAMC
TATA-box Motif	$<10^{-3}$	213	613	TATAAA
W-box promoter motif	$<10^{-3}$	171	302	TTGACY
RAV1-B binding site motif	0.0020	38	39	CACCTG
EveningElement promoter motif	0.0024	28	30	AAAATATCT
ARF binding site motif	0.0045	97	139	TGTCTC
MYB1AT	0.0051	203	490	WAACCA
GAREAT	0.0079	139	219	TAACAAR
Ibox promoter motif	0.0100	100	131	GATAAG
T-box promoter motif	0.0106	134	192	ACTTTG
Hexamer promoter motif	0.0128	30	33	CCGTCG
ABRE-like binding site motif	0.0146	60	91	BACGTGKM
BoxII promoter motif	0.0178	108	143	GGTTAA
CARGCW8GAT	0.0193	152	516	CWWWWWWWWG
SV40 core promoter motif	0.0196	51	59	GTGGWWHG
ACGTABREMOTIFA2OSEM	0.0221	44	57	ACGTGKC
MYCATERD1	0.0235	89	124	CATGTG
AtMYC2 BS in RD22	0.0235	89	124	CACATG
LEAFYATAG	0.0269	30	31	CCAATGT

C. AtPNP-A 24 HR INDUCED	p-value	# P	# S	consensus sequence
Non-enriched sites:				
MYB4 binding site motif	$<10^{-3}$	61	128	AMCWAMC
W-box promoter motif	0.0034	54	95	TTGACY
CCA1 binding site motif	0.0132	26	33	AAMAATCT
TATA-box Motif	0.0178	63	203	TATAAA
GAREAT	0.0345	43	62	TAACAAR
GCC-box promoter motif	0.0383	8	17	GCCGCC
TELO-box promoter motif	0.0416	11	13	AAACCCTAA
MYB2AT	0.0454	24	30	TAACTG

D. AtPNP-A 24 HR REPRESSED	p-value	# P	# S	consensus sequence
Non-enriched sites:				
MYB1 binding site motif	0.0014	11	13	MTCCWACC
Hexamer promoter motif	0.0086	13	15	CCGTCG
MYB4 binding site motif	0.0132	61	122	AMCWAMC
MYB binding site promoter	0.0136	29	38	MACCWAMC
ATHB2 binding site motif	0.0258	14	15	TAATMATTA
ARF binding site motif	0.0298	33	43	TGTCTC
RAV1-B binding site motif	0.0336	13	13	CACCTG
T-box promoter motif	0.0414	45	63	ACTTTG
MYB2AT	0.0440	26	31	TAACTG
AtMYC2 BS in RD22	0.0475	31	45	CACATG
MYCATERD1	0.0475	31	45	CATGTG

M = A/C; W = A/T; R = A/G; Y = C/T; B = C/G/T; K = G/T and H = A/C/T

Non-enriched TFBSs associated with the list of genes repressed by 1 hr recombinant AtPNP-A treatment included MYB4 binding site motif, TATA-box motif and W-box promoter motifs, which had p values < 10^{-3}, while ARF binding site motif, EveningElement promoter motif and RAV1-B binding site motifs had p values < 0.005 (Table 4.10B).

The promoters of the genes induced by 24 hr AtPNP-A treatment (Table 4.10C) had two TFBSs with low p values - MYB4 binding site motif ($p < 10^{-3}$) and W-box promoter motif ($p < 0.005$). Similarly only two TFBSs from the group of genes repressed by 24 hr AtPNP-A treatment - AGL3 and MYB1 binding site motifs, had p values < 0.005 (Table 4.10D).

4.3.6.3 Validation of the microarray data

Genes were chosen to validate the microarray data based on their fold change values and statistical reproducibility, determined using SAM. For the 1 hr AtPNP-A treatment these included an NADH dehydrogenase (At2g07600), a structural constituent of the ribosome (At2g28820) and *CELLULASE 2* (*AtCEL2*) (At1g02800). For the 24 hr microarray experiment an *LTP* (At4g12500) and peroxidase (At5g64120) gene were chosen. The semi-quantitative RT-PCR results show that the expression of the NADH dehydrogenase and structural constituent of the ribosome was not induced by 1 hr recombinant AtPNP-A treatment (Figure 4.11). However expression of *AtCEL2* was induced in two out of the three biological replicates. Following 24 hr AtPNP-A treatment, induced expression of the *LTP* gene was confirmed however the expression of the peroxidase appeared to be unchanged. Therefore the validation of the microarray results was poor with only two out of five genes tested being confirmed: *AtCEL2* and *LTP* which were induced by 1 hr and 24 hr AtPNP-A treatment respectively.

In summary, treatment with AtPNP-A does not induce large changes in the transcriptome. However there was some enrichment of GO terms and TFBSs associated with the lists of differentially expressed genes. The validation of the microarray results was not met with much success. One explanation for this could be that the microarray and validation experiments were conducted in different laboratories, with different batches of recombinant AtPNP-A, using different RNA extraction techniques. In order to distinguish whether the poor correlation between the microarray and semi-quantitative PCR results arose due to differences in two techniques used to measure gene expression or whether this was caused by variation between the experimental samples, it would be necessary to conduct the PCR validation on the same RNA used for the microarray. It is possible that the detection of these small changes in expression may be beyond the sensitivity of the semi-quantitative RT-PCR technique.

A. 1 hr AtPNP-A treated Microarray

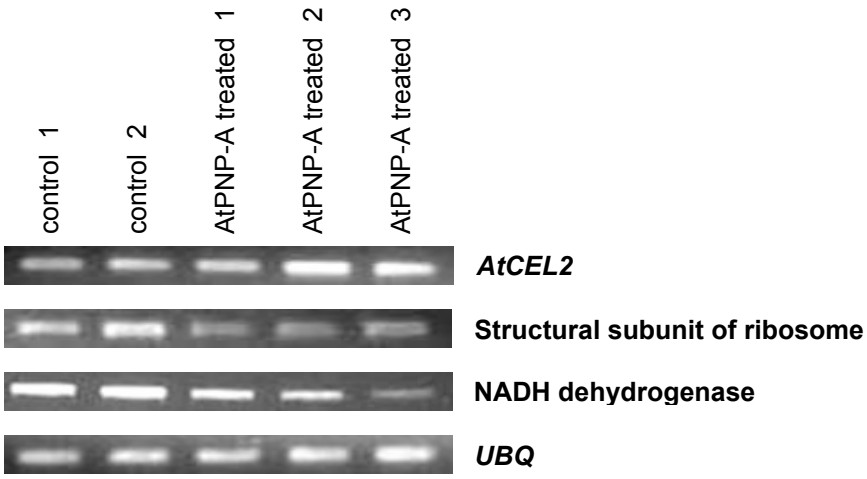

B. 24 hr AtPNP-A treated Microarray

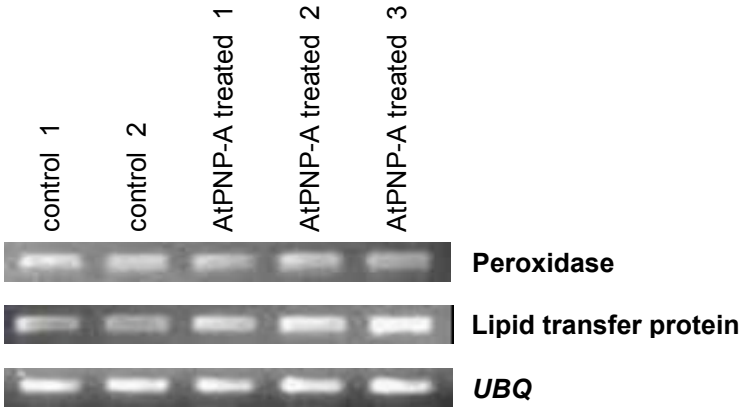

Figure 4.11. Validation of the microarray results in the response to recombinant AtPNP-A treatment

Semi-quantitative RT-PCR was used to confirm the expression of genes induced in response to AtPNP-A treatment in the 1 hr (A) and 24 hr (B) microarray experiment. The 1 μM recombinant AtPNP-A treatments were performed in triplicate while control treatments (water) were done in duplicate. *UBQ* is the "housekeeping" gene used to show the relative amount of template in each sample. NADH dehydrogenase, a structural subunit of the ribosome and *CELLULASE 2* (*AtCEL2*) were chosen to confirm the results of the 1 hr AtPNP-A treated microarray. Only the expression of *AtCEL2* could be confirmed to be induced in response to 1 hr AtPNP-A treatment. The *LIPID TRANSFER PROTEIN* (*LTP*) and peroxidase were were chosen to confirm the results of the 24 hr AtPNP-A treated microarray. Only the expression of the *LTP* gene could be confirmed to be induced in response to 24 hr AtPNP-A treatment while there was no change in the expression of the peroxidase.

4.4 DISCUSSION

In this chapter a computational analysis was conducted in an attempt to further elucidate biological processes in which AtPNP-A may function. A correlation analysis generated a list of the 50 genes with which *AtPNP-A* is most consistently co-expressed, termed the *AtPNP-A* ECGG. A GO analysis then identified enrichment of genes involved in pathogen defence response in the *AtPNP-A* ECGG. Furthermore promoter content analysis revealed an enrichment of *cis* elements known to be overrepresented in defence response genes, in the promoters of the *AtPNP-A* ECGG. The expression profile of *AtPNP-A* and the *AtPNP-A* ECGG across a broad range of experiments indicated that their transcription is generally induced under conditions where the *atpnp-a* mutant displayed phenotypes. Finally a microarray experiment was performed to measure global changes in transcription in response to recombinant AtPNP-A treatment and revealed potentially interesting genes that may help to understand how AtPNP-A exerts its effects. These results support a role for AtPNP-A in growth and abiotic and biotic stress responses *in planta*.

4.4.1 The *AtPNP-A* ECGG

The correlation values of the *AtPNP-A* ECGG are moderate, ranging from 0.707 to 0.570 (Table 4.2). While there is no absolute guide as to what are "good" correlation values, *r*-values of 0.9 have been associated with genes involved in a single pathway; *r*-values of 0.84 have been described for genes that share *cis* elements and *r*-values of 0.7 have been associated with enrichments of functional annotations provided by gene ontology (Allocco *et al.*, 2004; Manfield *et al.*, 2006). The moderate correlation values of the *AtPNP-A* ECGG could imply that the *AtPNP-A* ECGG is subject to complex combinatorial control by multiple promoter motifs that integrate signals from a number of potentially antagonistic pathways (Meier and Gehring, 2008). The fact that GO analysis of the *AtPNP-A* ECGG identified statistically significant enrichment of genes involved in the defence response, specifically SAR and that the promoter content analysis revealed statistically significant enrichment of W-box promoter motifs, implies that the correlation analysis has indeed extracted a biologically relevant set of genes with which *AtPNP-A* is consistently co-expressed.

4.4.2 A role for AtPNP-A in biotic stress responses

4.4.2.1 SAR

SAR is an inducible secondary defence response that is primed throughout the plant following a local primary infection and confers long lasting and broad spectrum resistance against subsequent pathogen attack (Durrant and Dong, 2004; Eulgem, 2005). The SAR response is characterized by increased SA levels and production of PR proteins in systemic tissue (Weigel

et al., 2001). Traditionally SAR is explained alongside the HR as a defence response induced by avirulent pathogens (Vlot *et al.*, 2008). While SAR is probably most effective in response to avirulent pathogens against which the plant survives to fight another day, SAR is actually commonly induced in by all local defence responses that initiate SA signalling (Eulgem, 2005; Mishina and Zeier, 2007).

4.4.2.2 Biotic stresses that induce AtPNP-A expression induce SA and SAR

Analysis of the microarray data revealed that expression of *AtPNP-A* and the *AtPNP-A* ECGG was induced by infection with virulent and avirulent strains of *P. syringae*; two virulent *Erisyphe* sp.; *P. infestans* and *B. tabaci* (Figure 4.6H). Additionally semi-quantitative RT-PCR confirmed that expression of *AtPNP-A* and select *AtPNP-A* ECGG genes is induced in response to virulent and avirulent *P. syringae*. With the exception of *B. tabaci*, infection by all these pathogens initiates a PTI response that forms part of the basal defence. This is sufficient to prevent infection by the non-host pathogen, *P. infestans*. However the virulent *P. syringae* pathogen that successfully colonizes the plant must overcome these basal defences using phytotoxins and effectors which it injects into the plant through its TTSS (Jones and Dangl, 2006). In the case of the avirulent *P. syringae*, plant *R* genes recognize these effectors or their activities, inducing an amplified ETI defence response that effectively curtails pathogen growth. Both of these PTI and ETI responses are signalled via SA and induce, SAR (Eulgem, 2005; Mishina and Zeier, 2007; Tsuda *et al.*, 2008). The response to *Erisyphe* is less well understood however is also mediated by SA (Dewdney *et al.*, 2000; Glazebrook, 2005; Wildermuth *et al.*, 2001). On the other hand the defence response against insect herbivores such as *B. tabaci* is thought to be mediated via JA (Howe and Jander, 2008). Recently however it has been shown that *B. tabaci* can activate SA signalling to improve insect fitness since SA antagonizes JA-mediated defences (Zarate *et al.*, 2007). Additionally there are some reports that *B. tabaci* induces SAR (Durrant and Dong, 2004). Therefore the common response to all of these pathogens is the induction of SA signalling and SAR (Koornneef and Pieterse, 2008) in which AtPNP-A and the *AtPNP-A* ECGG may be involved.

4.4.2.3 SA induces SAR and expression of the AtPNP-A ECGG

SAR is integrally connected to SA signalling since SA is an essential signal for SAR and is itself sufficient to induce SAR (Wildermuth *et al.*, 2001). In accordance with the enrichment of SAR annotated genes in the *AtPNP-A* ECGG, transcription of *AtPNP-A* and the *AtPNP-A* ECGG, is induced by SA and its functional analog BTH (Figure 4.6J). Furthermore, the induced expression of *AtPNP-A* and select *AtPNP-A* ECGG genes in response to SA has been confirmed by semi-quantitative RT-PCR (Figure 4.9A). Therefore the *AtPNP-A* ECGG is not only enriched in SAR annotated genes but is also induced by SA treatment that stimulates SAR.

4.4.2.4 The SAR annotated AtPNP-A ECGG genes are not limited to their role in SAR

Importantly, there was an enrichment of genes annotated as being involved in innate immunity as well as in incompatible interactions (that is ETI) among the *AtPNP-A* ECGG, in addition to the enrichment of SAR annotated genes. Importantly, enrichment in all of these terms (innate immunity, incompatible interactions and SAR) is associated with the same set of genes (*PR1*, *PR2*, *PR5*, *EDS1* and *WRKY70*) suggesting that these are more general components of the SA signalling pathway rather than limited to their role in SAR. The SA signalling pathway (illustrated in Figure 4.12) was therefore considered further in order to understand how the *AtPNP-A* ECGG genes fit in to the signal transduction cascade and to determine whether other genes in this pathway are co-expressed with *AtPNP-A*.

4.4.2.5 The SA signalling pathway

As described above, expression of the *AtPNP-A* ECGG is induced by pathogens that initiate PTI (Figure 4.6H). Furthermore expression of *AtPNP-A* is correlated with genes involved in the PTI response, in particular a MAPK cascade that relays PTI initiated by flagellin binding to *FLS2*. This begins with *MEKK1*, a MAPKKK that interacts with two MAPKKs, *MEK1* and *MKK2*, and culminates in the activation of the MAPK *MPK4*, a negative regulator of SAR and positive regulator of JA-mediated gene expression (Ichimura *et al.*, 1998; Petersen *et al.*, 2000; Suarez-Rodriguez *et al.*, 2007). *MEK1* and *MKK2* (r = 0.583) are both members of the *AtPNP-A* ECGG (Table 4.2) while expression of the *AtPNP-A* ECGG is repressed in the *fls2* mutant and induced in the *mekk1* (Suarez-Rodriguez *et al.*, 2007) and *mpk4* mutants (Figure 4.6I). This suggests that AtPNP-A is involved in PTI via *FLS2* consistent with the compromised resistance of the *atpnp-a* mutant when spray inoculated with *P. syringae*. Recently *EDS1* and *PAD4* have been identified as downstream effectors of *MPK4*; even though they oppose *MPK4* by activating SA and repressing JA signalling (Brodersen *et al.*, 2006).

The *EDS1* and *PAD4* proteins interact to mediate SA accumulation in response to toll-interleukin-1 receptor (TIR)-type nucleotide binding leucine-rich repeat (NB-LRR) type R protein recognition (Aarts *et al.*, 1998; Feys *et al.*, 2001). Expression of *AtPNP-A* ECGG is induced by avirulent *P. syringae* (*Rps4*) that are recognized by TIR-NB-LRR R proteins (Figure 4.6H). Additionally *AtPNP-A* expression is highly correlated with that of *EDS1* and modestly with *PAD4* (428th gene most correlated with *AtPNP-A*; r = 0.390) while expression of the *AtPNP-A* ECGG is repressed in *eds1* (Table 4.2, Figure 4.6I) and *pad4* mutants ($\log_2$ = -1.82; data not shown). On the other hand, coiled-coil (CC)-NB-LRR type R proteins act via *NON-RACE-SPECIFIC DISEASE RESISTANCE 1* (*NDR1*) to activate SA accumulation (Aarts *et al.*, 1998). Expression of the *AtPNP-A* ECGG is also induced by avirulent *P. syringae* (*Rpm1*, *AvrB* and *Rpt2*) that are recognized by CC-NB-LRR R genes (Figure 4.6H). Furthermore expression

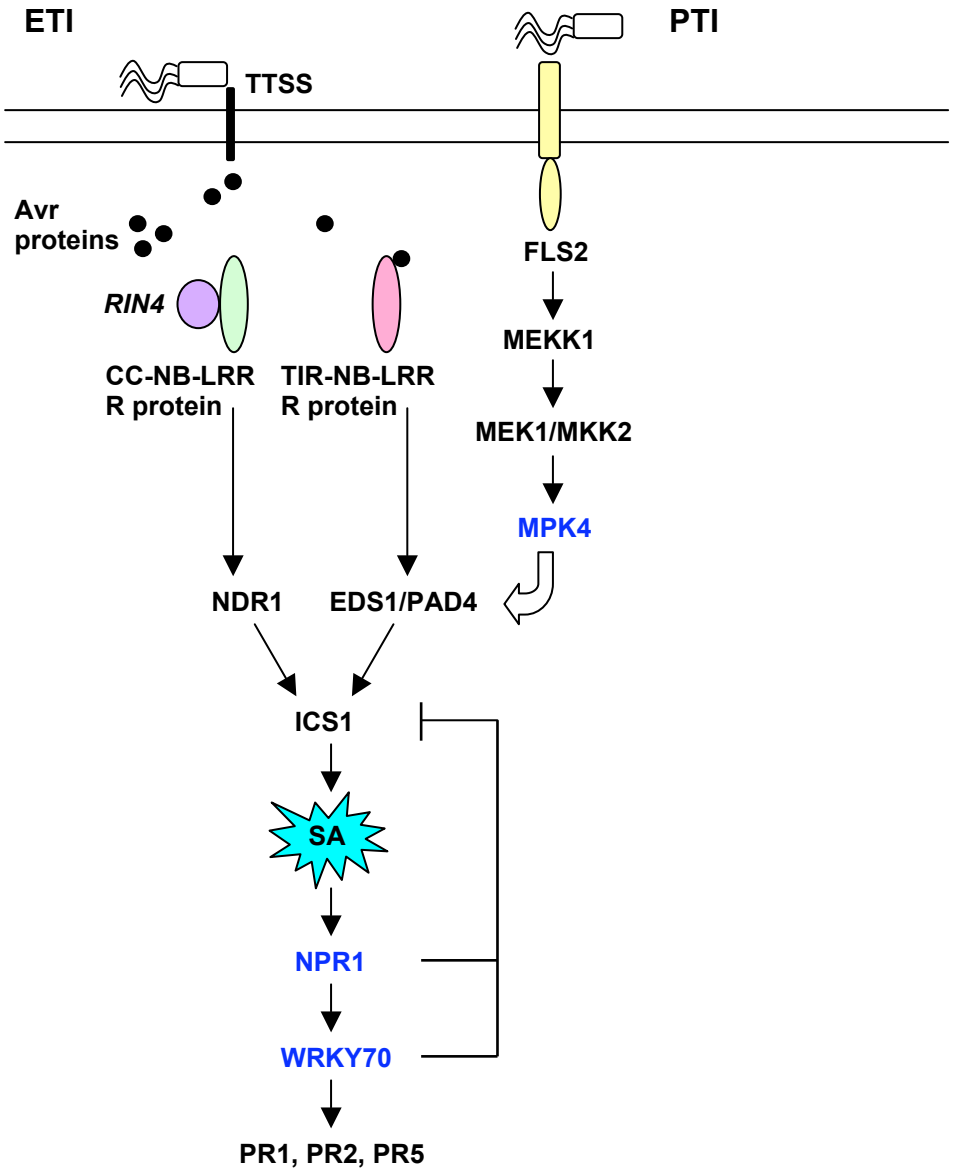

Figure 4.12. The SA signalling pathway in the plant defence response

Both PTI and ETI pathways converge on the SA signalling pathway. In the figure RIN4 is the RPM1-INTERACTING PROTEIN and ICS1 is the SA biosynthesis enzyme, ISOCHORISMATE SYNTHASE 1. Genes that are points of cross talk between SA and JA signalling pathways are shown in blue font.

of *AtPNP-A* is correlated with *NDR1* (169th gene most correlated with *AtPNP-A*; r = 0.475) as well as modestly correlated with *RPM1-INTERACTING PROTEIN 4* (*RIN4*) (308th gene most correlated with *AtPNP-A*; r = 0.428) that interacts with *NDR1* (Day *et al.*, 2006) and is a negative regulator of PTI and point of cross talk between PTI and ETI (Kim *et al.*, 2005). Therefore *AtPNP-A* expression is associated with both types of *R*-gene mediated ETI responses, those that act via *EDS1*/*PAD4* and *NDR1*, consistent with the compromised resistance of the *atpnp-a* mutant to avirulent *P. syringae*.

The *EDS1/PAD4* and *NDR1* arms of the SA signalling pathway converge on *ISOCHORISMATE SYNTHASE 1* (*ICS1)*, the enzyme responsible for SA synthesis (Wildermuth *et al.*, 2001). Importantly, *AtPNP-A* expression is correlated with that of *ICS1* (128th gene most correlated with *AtPNP-A*; r = 0.495). As mentioned previously, expression of *AtPNP-A* and the *AtPNP-A* ECGG is also induced by SA. Additionally expression of the *AtPNP-A* ECGG is repressed in the *NahG* mutant that expresses a bacterial salicylate hydroxylase that depletes SA (Figure 4.6I). This suggests that *AtPNP-A* expression lies downstream of and is dependent on SA.

Downstream of SA, *NPR1* is a key positive regulator of SAR and another point of cross talk between SA and JA signalling pathways through its novel function in the cytosol (Cao *et al.*, 1994; Dong, 2004; Koornneef and Pieterse, 2008; Spoel *et al.*, 2003). Again *AtPNP-A* expression is correlated with that of *NPR1* (61st gene most correlated with *AtPNP-A*; r = 0.554) and expression of the *AtPNP-A* ECGG is repressed in an *npr1* mutant (Figure 4.6I). Furthermore the induced expression of *AtPNP-A* and the *AtPNP-A* ECGG in response to BTH is *NPR1*-dependent suggesting that *AtPNP-A* lies downstream of *NPR1* in the SA signalling.

NPR1 interacts with *NPR1/NIM1 INTERACTING PROTEIN 1* (*NIMIN1)* proteins which are hypothesized to be transcription factors (Weigel *et al.*, 2001). Expression of *AtPNP-A* is correlated with *NIMIN1* (95th gene most correlated with *AtPNP-A*; r = 0.524), that has been shown to interact with *NPR1* to regulate the expression of *PR1* (Weigel *et al.*, 2005). Far better characterized is the interaction between *NPR1* and *TGA* bZIP family transcription factors. A change in redox causes NPR1 translocation into the nucleus where it interacts with TGA transcription factors to positively regulate SA-mediated changes in gene expression (Despres *et al.*, 2003; Fan and Dong, 2002; Kinkema *et al.*, 2000; Mou *et al.*, 2003). Expression of *AtPNP-A* is correlated with that of *TGA3* (139th gene most correlated with *AtPNP-A*; r = 0.490), that has been shown to associate with *NPR1* to positively regulate the expression of *PR1* (Johnson *et al.*, 2003). Moreover the promoters of the *AtPNP-A* ECGG are enriched in *TGA* TFBSs suggesting that the *AtPNP-A* ECGG may be regulated in an *NPR1*-depedent manner via *TGA* transcription factors.

NPR1 translocation to the nucleus results in the upregulated expression of eight WRKY transcription factors including *WRKY70* and its closest homolog *WRKY54* (Wang *et al.*, 2006), both of which are correlated with *AtPNP-A* (Table 4.2). Moreover expression of the *AtPNP-A* ECGG is upregulated in a *WRKY70* overexpressor (Figure 4.6I) and the *AtPNP-A* ECGG is enriched in WRKY TFBSs suggesting that *WRKY70* could activate the expression of the *AtPNP-A* ECGG. *WRKY70* is another node of convergence between JA and SA signalling pathways acting as a positive regulator of SA gene expression but negative regulator of JA genes (Li *et al.*, 2004). Another regulator of the SA signalling pathway that lies downstream of *NPR1* is *SNI1*, a negative regulator of the SAR response (Li *et al.*, 1999). Expression of the *AtPNP-A* ECGG was induced in the *sni1* mutant suggesting that the *AtPNP-A* ECGG is repressed by *SNI1*. Since the expression of *WRKY70* was unchanged in *sni1* (Figure 4.6I), this implies that *SNI1* lies downstream of *WRKY70* in the SA signal transduction cascade.

Ultimately the read out of the SA signalling pathway is the expression of *PR* genes and it is currently thought that it is the combination of PR proteins, and not any one PR protein in particular, that confers resistance to pathogens (van Loon *et al.*, 2006). Since their discovery *PR1, PR2* and *PR5* have become commonly used markers of SAR (Ryals *et al.*, 1996; Weigel *et al.*, 2001). These three *PR* genes are among the genes most highly correlated with *AtPNP-A* (Table 4.2). Additionally expression of the *AtPNP-A* ECGG is induced in mutants that constitutively express *PR* genes, including *cpr5* and *mpk4*, but repressed in mutants that do not express *PR* genes, including the *npr1* and *NahG*. Constitutive *PR* gene expression confers a constitutive SAR phenotype while mutants that do not express the *PR* genes are compromised in SAR. Therefore *AtPNP-A* expression is induced when SAR is constitutively active (in the *cpr5* and *mpk4* mutants) and repressed when SAR is compromised (in the *npr1* and *NahG* mutants).

Therefore expression of *AtPNP-A* is correlated with key genes involved in SA signalling, suggesting that AtPNP-A is intimately involved in this pathway. The correlation analysis has extracted genes whose protein products interact further supporting its validity. Expression of *AtPNP-A* has been associated with genes involved in PTI, ETI and SAR responses that all signal via SA, as well as with genes that act as points of cross-talk between the SA and JA signalling pathways. AtPNP-A appears to be an end point of the pathway as it is induced by SA in *NPR1*-dependent manner, like the PR genes. In support of this *WRKY70* and *PR1* expression is unaltered in *atpnp-a* mutant suggesting that AtPNP-A does not lie upstream of these genes.

4.4.2.6 AtPNP-A could be a PR gene

It is interesting to note that *AtPNP-A* shares a number of features in common with the *PR* genes. These include low basal expression levels and high induction in response to SA, pathogen

infection and CHX treatment (van Loon *et al.*, 2006; Wang *et al.*, 2005). Furthermore the *AtPNP-A* gene shares common promoter elements, for example W box promoter motifs, with the *PR* genes that may account for this similarity in expression (Meier and Gehring, 2008). Additionally AtPNP-A and the PR proteins are secreted proteins that contain N-terminal signal peptides, directing them to the extracellular space where they have been extracted together from the apoplast (Boudart *et al.*, 2005; Wang *et al.*, 2005). The PR proteins, like AtPNP-A, also share structural similarity to pollen allergens (Hoffmann-Sommergruber, 2002; Ludidi *et al.*, 2004; van Loon and van Strien, 1999). In fact the citrus blight protein that has the greatest sequence similarity to the irPNP proteins was originally reported to be a PR protein (Ceccardi *et al.*, 1998; Ludidi *et al.*, 2002). It is therefore tempting to speculate that AtPNP-A may be a PR-like protein. While expression of the *PR* genes has been studied extensively, surprisingly little is known about their function (van Loon and van Strien, 1999) although there is some evidence that they may act on cell wall (Kauffmann *et al.*, 1987; Legrand *et al.*, 1987).

4.4.2.7 WRKY70 is a candidate regulator of the AtPNP-A ECGG

Both the search for experimentally determined motifs and computer derived motifs returned significant enrichment of W-box promoter motifs in the *AtPNP-A* ECGG suggesting that co-expression of the *AtPNP-A* ECGG is regulated by WRKY transcription factors. Several lines of evidence support *WRKY70* as a candidate regulator of the co-expression of the *AtPNP-A* ECGG. Firstly, expression of *AtPNP-A* was highly correlated with *WRK70* (Table 4.2). Indeed *WRKY70* and *AtPNP-A* co-expression was confirmed by semi-quantitative RT-PCR (Figures 4.9A-C). Secondly the *AtPNP-A* ECGG is enriched in genes annotated as playing a role in SAR including *WRKY70* and the *PR* genes that it is known to regulate. Thirdly *WRKY70* overexpression results in the elevated expression of *AtPNP-A* and the *AtPNP-A* ECGG (Figure 4.6I). While overexpression of transcription factors could induce the expression of non-target genes, the fact that genes that are induced by *WRKY70* overexpression are also highly correlated with *WRKY70* suggests that these are more likely to be true *WRKY70* targets (Figure 4.5, Table 4.7). Fourthly, experimental evidence has been provided that *WRKY70* expression does precede that of *AtPNP-A* and the select *AtPNP-A* ECGG genes in response to SA, allowing for the possibility that *WRKY70* regulates the SA-induced expression of the *AtPNP-A*. In sum, promoter content, coexpression, mutant and PCR analysis all provide evidence that *WRKY70* could regulate the expression of the *AtPNP-A* ECGG.

It was interesting to find that AtPNP-A treatment stimulated expression of *WRKY70* (Table 4.8A). This could suggest that AtPNP-A may lie upstream of and induce expression of *WRKY70* in the signalling pathway. However together with the above evidence for *WRKY70* regulating the *AtPNP-A* ECGG, the fact that *WRKY70* expression was unaltered in the *atpnp-a*

mutant in response to pathogen infection suggests that this is not the case. It is possible that *AtPNP-A* expression could feedback regulate the SA signalling pathway through further induction of *WRKY70*. There are a number of such feedback loops within the SA signalling pathway (Figure 4.12). In fact *WRKY70* itself negatively feedback regulates the pathway by repressing *ICS1* expression and inhibiting SA production, probably to alleviate the toxic effects of SA (Wang *et al.*, 2006).

4.4.2.8 Transcriptome responses to AtPNP-A and the defence response

Together with *WRKY70*, two other genes annotated as being involved in SA signalling and SAR (*MKK7* and *TGA2*) were induced in response to 1 hr recombinant AtPNP-A treatment resulting in enrichment of genes annotated as being involved in SAR (Table 4.8A and 4.9A). The *TGA2* transcription factor interacts with *NPR1* to positively control the expression of SA responsive genes (Fan and Dong, 2002) while *MKK7* is a positive regulator of basal defence and SAR (Zhang *et al.*, 2007). This suggests not only is *AtPNP-A* correlated with genes involved in SAR, but AtPNP-A itself can induce SA signalling and SAR. At the same 1 hr time point, AtPNP-A treatment repressed genes annotated as being involved in vesicle-associated membrane transport as well as *BAK1* (Table 4.8B and 4.9B). Vesicle trafficking plays an important role in the transport of callose and antimicrobial componds to the invasion site as part of the basal defence response (Hoefle and Huckelhoven, 2008; Kwon *et al.*, 2008) while *BAK1* associates with *FLS2* to initiate the PTI response (Chinchilla *et al.*, 2007). Therefore 1 hr AtPNP-A treatment may feedback regulate basal defence. The coincident induction of SAR and repression of basal defence is consistent with reports that elements of the SA signalling pathway suppress basal defence (Kim *et al.*, 2005). This antagonism might exist because an activated SA signalling pathway overrides the need for an induced basal defence response (PTI).

In response to long term AtPNP-A exposure there was an enrichment of genes involved in the defence response to fungus (*RML1*, *LTP*s and a peroxidase) and genes that encode cell wall components (extensins) (Table 4.9C). Importantly, the expression of one of these *LTPs* was confirmed by semi-quantitative RT-PCR. Additionally, at the 24 hr time point, genes involved in ROS metabolism were repressed (including *CDS1*) (Table 4.9D). Inhibition of such ROS scavenging enzymes would promote ROS accumulation (Torres *et al.*, 2006). Since ROS and cell wall reinforcement play an important role in the defence response against fungus and ROS can furthermore cause cross-linking of the cell wall (Hoefle and Huckelhoven, 2008; Xiong and Zhu, 2002b), it is possible that these events are connected and act to maintain the defence response at the later time point. On this point, it is also interesting to note that expression of *AtPNP-A* is correlated with *WAK1* that has long since been proposed to play a role in the response to pathogens, by relaying signals from the wall to the cell interior (He *et al.*, 1998).

4.4.3 A role for AtPNP-A in abiotic stress responses

4.4.3.1 SA and its role in abiotic stress responses

The elevated expression of *AtPNP-A* and the *AtPNP-A* ECGG in response to ozone and UV-B, abiotic stresses is consistent with reports that these stresses increase SA levels and *PR* gene expression (Sharma *et al.*, 1996; Surplus *et al.*, 1998; Yalpani *et al.*, 1994). Furthermore UV-B stress induces a type of SAR response since pre-exposure of plants to UV-B confers resistance against subsequent attack by virulent pathogens (Kunz *et al.*, 2008). Although SA is best known for its role in the defence response, SA levels have also been documented to increase in response to a number of abiotic stresses as has expression of the SAR genes (Swindell, 2006; Yalpani *et al.*, 1994). Furthermore it has recently been reported that SA treatment can confer tolerance to abiotic stresses (Horvath *et al.*, 2007; Szepesi *et al.*, 2009). Therefore SA and SAR genes may also play a role in abiotic stress responses.

4.4.3.2 A unique role for AtPNP-A *in NaCl and osmotic stress responses*

The induced expression of *AtPNP-A* in response to NaCl and osmotic stress was confirmed by RT-PCR (Figure 4.6B and 4.7) and is consistent with reports that irPNP protein levels increase in response to NaCl and osmotic stresses (Rafudeen *et al.*, 2003) and the improved tolerance phenotype of the *atpnp-a* mutant under these conditions. *AtPNP-A* is expressed specifically in the root in response to NaCl stress and in the shoot in response to osmotic stress (Figure 4.6C-D) even though both stresses were applied to the hydroponic media in contact with the root (Kilian *et al.*, 2007). This tissue specific expression pattern of *AtPNP-A* in response to NaCl and osmotic stress is particularly interesting considering that other genes involved in NaCl and osmotic stress responses do not behave in a similar fashion. This suggests that AtPNP-A plays a distinct role in the response to NaCl and osmotic stresses. While the *AtPNP-A* ECGG and SAR ECGG display a similar tissue-specific pattern of expression to *AtPNP-A*, neither are strongly induced in the root in response to NaCl stress (Figure 4.6E) despite there being some evidence of a role for SA and the PR genes in response to NaCl (Borsani *et al.*, 2001; Seo *et al.*, 2008). Thus AtPNP-A may play a unique role in the root in response to NaCl stress.

4.4.3.3 AtPNP-A *and* ABA *– counteracting hormones in water flux?*

The only NaCl and osmotic stress response genes that showed a tendency toward the same tissue-specific expression pattern observed for *AtPNP-A* were the ABA biosynthesis genes *AAO3*, *ABI1* and *NCED3*. Mutants in these genes have similar NaCl and osmotic stress phenotypes to that of the *atpnp-a* mutant (Gonzalez-Guzman *et al.*, 2004; Quesada *et al.*, 2000; Ruggiero *et al.*, 2004). ABA signals between the shoot and root to regulate whole plant water status (Javot and Maurel, 2002; Nilson and Assmann, 2007; Verslues *et al.*, 2006) and this may be coordinated by the tissue-specific expression of these genes. In the stomata at least, AtPNP-

A and ABA have opposing actions (Wang *et al.*, 2007c). It is conceivable then that AtPNP-A may too regulate whole plant water flux, counter-balancing ABA to maintain homeostasis, especially considering evidence that AtPNP-A is a systemic signal that promotes transpiration and stomatal opening (Gehring and Irving, 2003; Gottig *et al.*, 2008; Maryani *et al.*, 2003; Morse *et al.*, 2004). Interestingly, expression of these ABA biosynthetic genes is induced by pathogens (de Torres-Zabala *et al.*, 2007), possibly as a way of antagonising SA-mediated defence responses or altering plant water homeostasis. Conversely AtPNP-A may be involved counteracting ABA by inducing SA-mediated defence responses and altering water homeostasis. Consistent with this idea, two genes that are involved in ABA signalling were repressed in response to 1 hr AtPNP-A treatment, *ERA1* and *MYB33* (Table 4.8B and 4.9B).

4.4.3.4 Nutrient starvation and ion transport

NaCl induces osmotic stress and K^+ starvation, however the transcriptional responses of *AtPNP-A*, the *AtPNP-A* ECGG, SAR ECGG and *WRKY70* to osmotic and K^+ starvation stresses is similar while the NaCl response is quite different. The elevated expression of *AtPNP-A* in response to K^+ starvation was also confirmed by semi-quantitative RT-PCR (Figure 4.6B and 4.7) and together with the high level of *AtPNP-A* expression in phosphate starved mutants, *pho1* and *pho3* (Figure 4.6B) indicates that *AtPNP-A* expression is induced under hypo-osmotic and nutrient starvation conditions where the *atpnp-a* mutant displays improved tolerance. The *PHO1* gene is thought to play a role in long distance phosphate transport (Hamburger *et al.*, 2002) while the *pho3* mutant is actually disrupted in the gene encoding the sucrose transporter, SUC2 (Lloyd and Zakhleniuk, 2004). Since AtPNP-A can induce ion fluxes and the *atpnp-a* mutant appears to have altered distributions of ion transporters in the root, it is possible that AtPNP-A is involved in ion and thereby nutrient transport and is induced in order to improve ion and nutrient uptake under these stress conditions. This may also be the reason for the enrichment in ZIP transporters among the group of genes induced by 1 hr AtPNP-A treatment.

4.4.3.5 The commonality between abiotic and biotic stresses

The *AtPNP-A* ECGG and SAR ECGG were strongly induced in response to the abiotic stresses imposed by osmotic stress, K^+ starvation and UV-B treatment. These may be linked to the fact that pathogen infection induces osmotic stress and nutrient starvation as the pathogen draws water and nutrients from the plant cells (Clough *et al.*, 2000; Wright and Beattie, 2004). Indeed the expression of defence genes in response osmotic stresses and K^+ starvation has been previously reported (Armengaud *et al.*, 2004; Swindell, 2006). Further some genes involved in the defence response play a dual role in osmotic stress responses; for example *MEKK1* (Covic *et al.*, 1999). While this may be a response to a common stress imposed by both the abiotic and biotic stress, these genes may also confer common protection against these stresses.

4.4.4 A role for AtPNP-A in growth and development

4.4.4.1 Stress responses impact plant growth

Cross-talk between growth and stress responses exists so that the plant can effectively mount an integrated response to the environment. In response to stress the plant can either switch off growth so as to not waste resources by growing further before adapting to the stress (Bray, 2004; Munns, 2005) or it can increase growth selectively in an attempt to grow out of the stress environment (Potters *et al.*, 2007). Reduced growth in the response to pathogens is exemplified by the dwarfed phenotypes of constitutive defence mutants (Petersen *et al.*, 2000; Suarez-Rodriguez *et al.*, 2007), although it is unclear whether this is a true growth effect or whether this is the result of the fitness cost incurred by having constitutively active defences (Heidel *et al.*, 2004; Tian *et al.*, 2003). Conversely positive signals for growth negatively regulate defence gene induction and in some cases this is manipulated by pathogens (Chen *et al.*, 2007a).

4.4.4.2 Vasculature

The elevated expression of *AtPNP-A*, the *AtPNP-A* ECGG and the SAR ECGG in response to NPA treatment and in the *cov1* mutant relative to the wildtype control indicates that expression of *AtPNP-A* and the ECGG is induced under conditions where there is enrichment of vascular tissue (Figure 4.6A). These results are consistent studies that have localized irPNPs to the vasculature and extracted irPNPs from the xylem of citrus blight-infected trees and uninfected forest sage (Ceccardi *et al.*, 1998; Maryani *et al.*, 2003). The induced expression of the SAR ECGG in vasculature is also not unexpected since PR proteins have also been isolated from the xylem sap of both infected and uninfected plants (Kehr *et al.*, 2005; Rep *et al.*, 2002). In both cases the localization of irPNPs and PR proteins to the xylem has been proposed to confer protection against diseases that cause wilt.

4.4.4.3Cell expansion

The high level of *AtPNP-A*, the *AtPNP-A* ECGG and the SAR ECGG expression in the sepal (Figure 4.6A) is interesting because the sepal has giant cells that can extend up to half its length adjacent to much smaller cells (Smyth *et al.*, 1990). How this specialised cell enlargement occurs is currently unknown, making it tempting to suggest that the ability of recombinant AtPNP-A to cause protoplast swelling (Morse *et al.*, 2004), may generate the turgor required for this specialized cell expansion. The elevated expression of the SAR ECGG in the sepal may also be related to a role for SA in cell enlargement since there is evidence that SA stimulates endoreduplication (DNA replication without division) that enables specialized cell enlargements (Melaragno *et al.*, 1993; Vanacker *et al.*, 2001). Therefore expression of *AtPNP-A* and the SAR ECGG in the sepal may be related to a function for SA-mediated cell enlargement in this tissue.

The induced expression of the *AtPNP-A,* the *AtPNP-A* ECGG and the SAR ECGG in the *ga1-3* mutant relative to the control, that was rescued in the *ga1-3 della* mutant, suggests that expression of *AtPNP-A* and the *AtPNP-A* ECGG is repressed by GA through the action of the DELLA proteins (Figure 4.6A). In the case of *AtPNP-A*, this phenotype was observed in both the seed and in the flower (data not shown). However GA-mediated DELLA-dependent expression of the *AtPNP-A* ECGG and SAR ECGG was specific to the flower (data not shown). This implies that AtPNP-A may be involved in a common process mediated by GA in both the flower and the seed, for example epidermal cell expansion (Cao *et al.*, 2006), consistent with the phenotype of the *atpnp-a* mutant that is compromised in epidermal cell expansion in its developing leaves. On the other hand the *AtPNP-A* ECGG and SAR ECGG may be involved more specifically processes mediated by GA in the flower, possibly conferring disease resistance at this sensitive growth stage. Furthermore the induced expression of *AtPNP-A* in the *ga1-3* mutant may be a compensatory mechanism to improve its cell expansion ability. In this way AtPNP-A and GA may have overlapping functions that are not required simultaneously so that the presence of the one hormone antagonizes the other. In support of this idea 1 hr AtPNP-A treatment repressed genes involved in "GA-mediated signalling" (Table 4.9B).

The fact that the *atpnp-a* mutant has reduced cell size but increased cell numbers in the developing leaf was used to suggest that the *atpnp-a* mutant compensates for reduced cell expansion by increasing cell division (chapter 3). Opposite to this phenotype, the *elo3* mutant has a reduced cell division rate (Nelissen *et al.*, 2005). The induced expression of *AtPNP-A* in *elo3* (that is not matched by the *AtPNP-A* ECGG and the SAR ECGG) (Figure 4.6A) implies a unique role for AtPNP-A in *elo3*. It is possible that *AtPNP-A* expression is increased in the *elo3* mutant to promote expansion in order to compensate for the decreased rate of cell division.

4.4.4.4 Mechanisms of cell expansion

The correlated expression of *AtPNP-A* with a number of *WAKs* (*WAK1*; $r = 0.622$ and *WAK2*; $r = 0.650$) is interesting because both *WAKs* and *AtPNP-A* have been suggested to act together with cell wall loosening expansins during cell expansion (Table 4.2) (Cosgrove, 2001; Morse *et al.*, 2004). Co-expression of *AtPNP-A* and *WAK1* was confirmed by semi-quantitative RT-PCR (Figures 4.9A-C). WAKs are thought to communicate between the cell wall and cytoplasm in early cell expansion (Wagner and Kohorn, 2001) while AtPNP-A has been proposed to promote water influx and protoplast swelling to generate the turgor pressure required for expansive growth (Cosgrove, 2001; Morse *et al.*, 2004). An antisense mutant that abolishes the expression of all of the five WAK proteins displays a reduced cell size phenotype similar to that of the *atpnp-a* mutant suggesting that both of these mutants are compromised in their ability to expand

(Lally *et al.*, 2001; Wagner and Kohorn, 2001) and allowing for the possiblity that AtPNP-A, WAKs and expansins do function co-ordinately to mediate cell expansion.

Loosening of the cell wall can also be achieved enzymatically. For example cellulose degrading enzymes, cellulases have been implicated in facilitating cell expansion (Nicol *et al.*, 1998). It is therefore noteworthy that 1 hr recombinant AtPNP-A treatment induced expression of *AtCEL2* and that this was confirmed by semi-quantitative RT-PCR (Table 4.8A and Figure 4.11). Thus AtPNP-A may directly cause cell wall loosening to evoke protoplast swelling. The enrichment of genes associated with structural constituents of the cell wall after 24 hr AtPNP-A treatment suggests that AtPNP-A may also exert long term effects on the cell wall that could be required for growth (Table 4.9C). This might also be the reason for the reduced expression of *AtPNP-A* following treatment with isoxaben that modifies the cell wall and inhibits growth (Figure 4.6A).

4.4.4.5 Senescence

The induced expression of *AtPNP-A*, the *AtPNP-A* ECGG and SAR ECGG in the senescent leaf suggests that AtPNP-A functions together with the SAR genes during senescence (Figure 4.6A). Senescence is important during development for the redistribution of nutrients to the growing tissue as well as during the HR defence response (Greenberg and Yao, 2004; Himelblau and Amasino, 2001; Lim *et al.*, 2003). The repressed expression of *AtPNP-A* and the SAR ECGG in the *NahG* mutant compared to the wildtype that were both undergoing senescence (Figure 4.6I) suggests that expression of *AtPNP-A* and the ECGG during senescence is in fact SA-dependent. In accordance with this the *cpr5* mutant that has constitutively elevated SA levels and displays accelerated senescence has elevated expression of *AtPNP-A* and the SAR ECGG (Figure 4.6I) (Jing *et al.*, 2007) Therefore AtPNP-A may play a role in SA-mediated senescence.

4.4.5 Summary

Microarray data shows that *AtPNP-A* is expressed under conditions where the *atpnp-a* mutant phenotype is observed and this was confirmed in a number of cases. A role for AtPNP-A in the SA-mediated defence response, was suggested by the correlation analysis. Importantly, expression of *AtPNP-A* and co-expression of *AtPNP-A* with select *AtPNP-A* ECGG genes was confirmed in response to SA and *P. syringae*. *AtPNP-A* expression was also induced alongside defence genes within the *AtPNP-A* ECGG during abiotic stresses and development which may be linked to a role for SA in these responses. Transcriptome analysis of the response to AtPNP-A treatment further implicated a role for AtPNP-A in SA signalling. Although the microarray requires further validation, two marker genes for the response to AtPNP-A treatment have been identified - *AtCEL2* and a *LTP*. These results support a role for AtPNP-A in growth and abiotic stress responses and strengthen the proposed role for AtPNP-A in the defence response.

4.5 APPENDIX

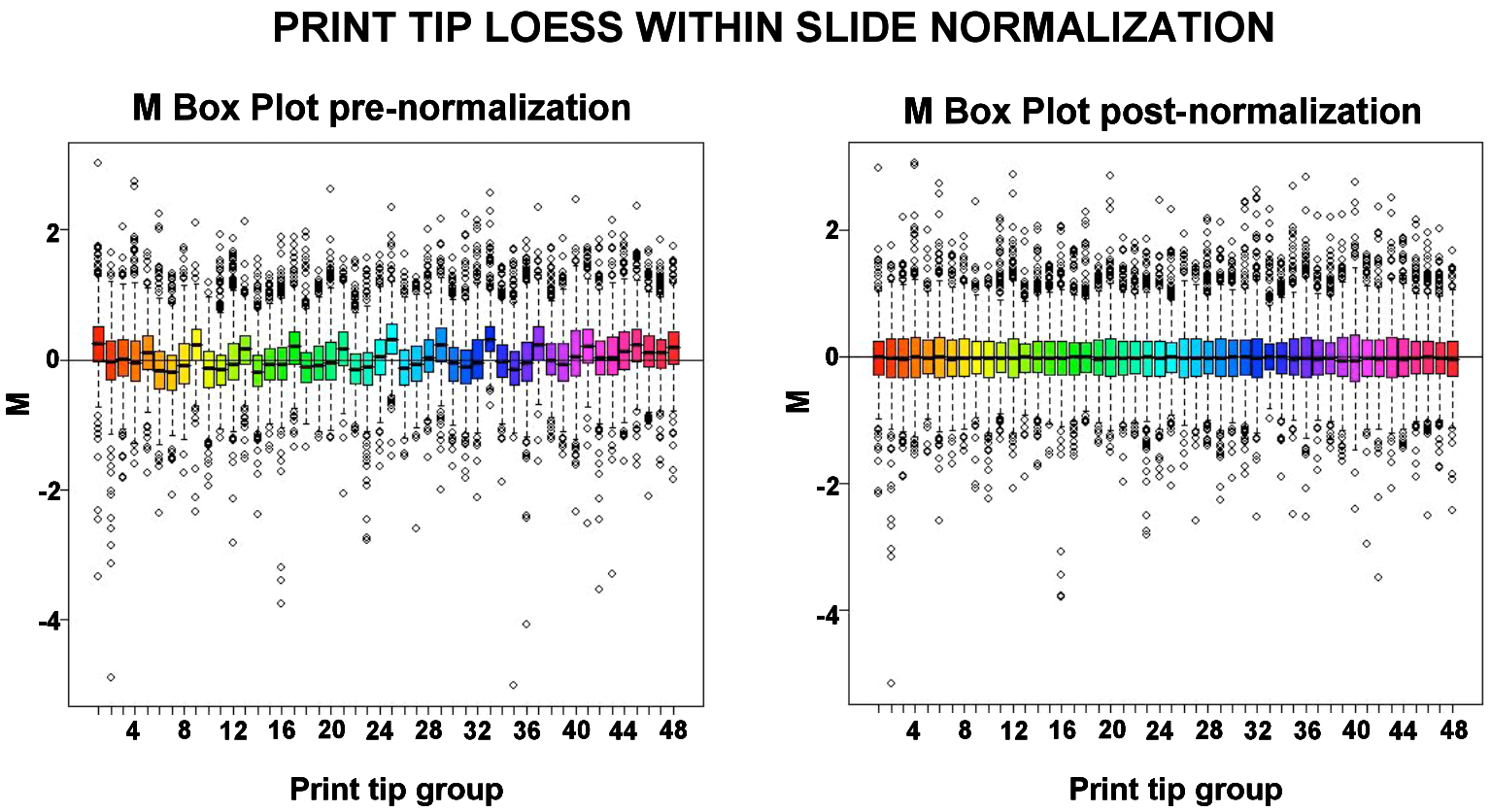

Appendix Figure 4.1. Print tip loess normalization between microarray slides

An example is shown for the M box plots for each print tip group of the fist replicate slide (of four in total) of the 1 hr recombinant AtPNP-A treatment experiment. The left hand panel shows the spread of the data within each print tip group prior to normalization demonstrating the need to normalize the data while the left hand panel shows the same plot after print tip loess normalization to show that the data has effectively been normalized.

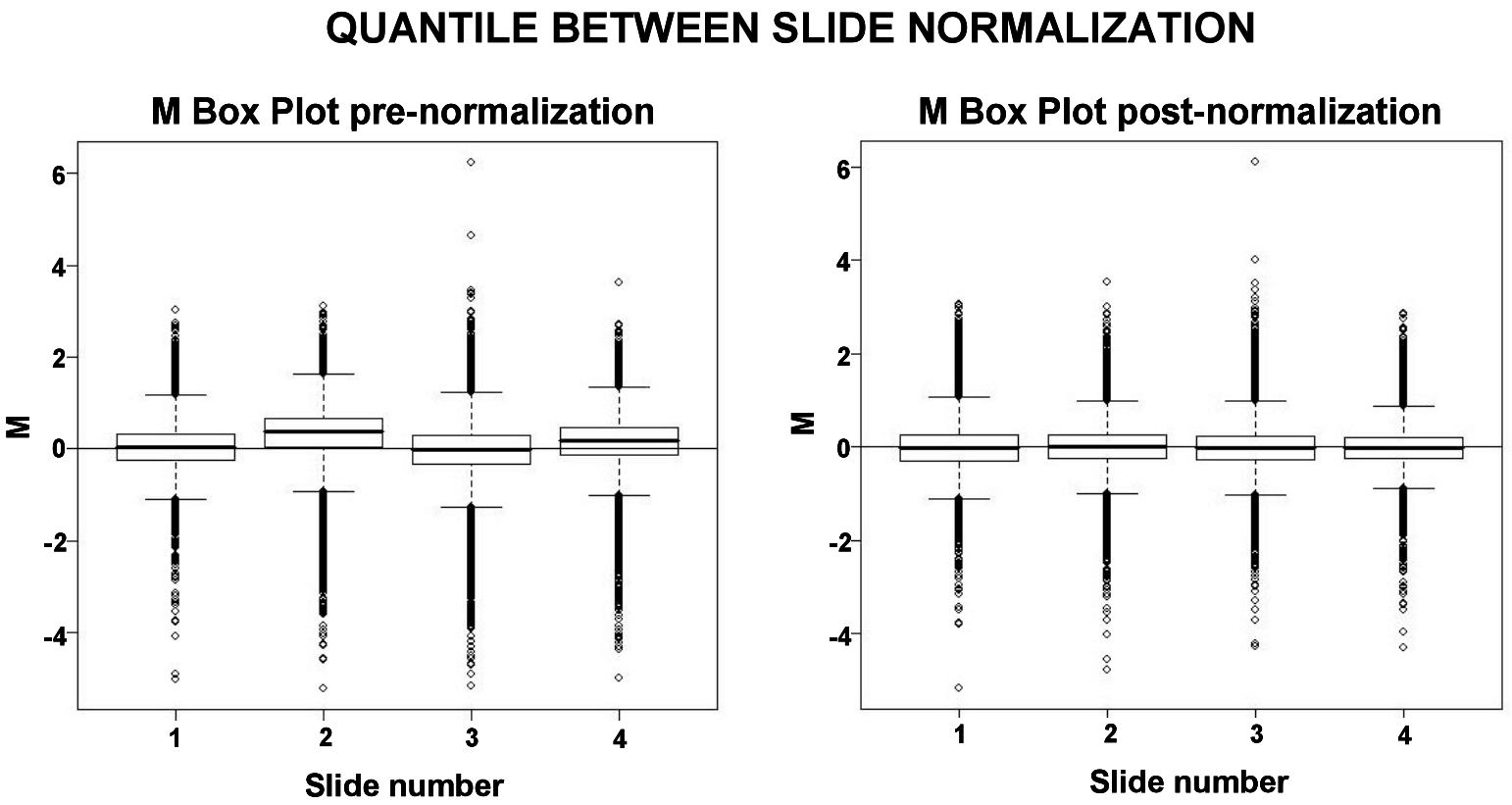

Appendix Figure 4.2. Quantile normalization between microarray slides

An example of the M box plots for each slide of the four replicates of the response to 1 hr recombinant AtPNP-A treatment. The left hand panel shows the plot prior to normalization, demonstrating the need to normalize the data while the right hand panel shows the same plot after quantile normalization to show that the data has been effectively normalized.

CHAPTER 5

GENERAL DISCUSSION

CHAPTER 5: GENERAL DISCUSSION

5.1 CONTRIBUTIONS TO THE FIELD

The results presented here provide the first description of an *atpnp-a* mutant. In order to be able to be able to say with conviction that AtPNP-A has an important function in a particular process *in planta*, it is necessary to demonstrate that responses to AtPNP-A treatment or increases in *AtPNP-A* mRNA or protein levels are associated with phenotypes of an *atpnp-a* mutant. While a number of phenotypes have been revealed that imply function of the wildtype *AtPNP-A* gene, the major drawback has been that these phenotypes have neither been confirmed in a second mutant nor complemented. First and foremost this issue needs to be addressed by characterizing a second *atpnp-a* mutant or by repeating the complementation. Additionally, although *AtPNP-A* mRNA levels have been shown to be reduced in the *atpnp-a* mutant, AtPNP-A protein levels have not been quantified which should be done in order to determine the exact effect of the mutation on AtPNP-A expression. The phenotypes of the *atpnp-a* mutant do however support a role for AtPNP-A in cell expansion and in NaCl and osmotic stress responses as has been proposed previously based on responses to recombinant AtPNP-A treatment and measures of AtPNP-A proteins levels following stress exposure (Morse *et al.*, 2004; Rafudeen *et al.*, 2003). Furthermore the transcript profile of *AtPNP-A* revealed that *AtPNP-A* expression is induced under the same conditions where the *atpnp-a* mutant displays its phenotype, strengthening the argument that AtPNP-A does play a role in the adaptation to these conditions. The *atpnp-a* mutant additionally revealed a role for AtPNP-A in the defence response that had not before been considered. Further evidence for this was provided by a computational analysis that found *AtPNP-A* expression to be correlated with genes involved in SA signalling and SAR, which was confirmed experimentally. Moreover microarray analysis indicated that recombinant AtPNP-A treatment induces the expression of defence response genes, suggesting that *AtPNP-A* coexpression with SAR annotated genes is not coincidental but rather that AtPNP-A is intimately associated with the defence response. In the very least, this study has identified a number of phenotypes of an *atpnp-a* mutant that can rapidly be tested and confirmed in the future and so has helped to establish the function of AtPNP-A *in planta*. Insights have also been gained to inform further experimentation that may help to unravel the mechanism of AtPNP-A action *in planta*.

5.1.1 Second messengers may discriminate between ionic and osmotic stresses

Salinity imposes both an ionic and osmotic stress on the plant. Here it has been shown that NaCl and osmotic stresses produce distinct calcium and cGMP responses suggesting that discrimination between ionic and osmotic stresses might be encoded in three ways: 1) in the

magnitude and 2) in the source of the calcium signal and 3) in cross-talk between calcium and cGMP signalling. A model has been proposed that would allow one to test whether these second messengers can discriminate between the ionic and osmotic components of NaCl stress through manipulating treatment dose and employing inhibitors of calcium and cGMP signalling (Figure 2.9). In order to prove that specificity is encoded in the second messenger signatures, it is necessary to show that perturbations in these signatures result in measurable differences in an appropriate end response (Scrase-Field and Knight, 2003). This has been attempted previously using gene expression outputs that were quantitatively different in response to NaCl and osmotic stresses, however was not successful (Knight *et al.*, 1997). It may be more appropriate to test a gene that has a more distinct transcriptional response to NaCl and osmotic stresses. An ideal candidate is *AtPNP-A* since it is expressed specifically in the shoot in response to osmotic stress and in the root in response to NaCl stress (Figure 4.6C-D). For example, if *AtPNP-A* expression is an output of the ionic stress-induced calcium signalling pathway it is expected that its root-specific induction in response to NaCl would be inhibited by ruthenium red and LY 83583, that have no affect on the osmotic stress-induced calcium response. Should this model hold true then not only will it help to understand stress perception and signal transduction in response to ionic and osmotic stresses but it could be used for gene discovery to identify genes specifically involved in the response to ionic and osmotic components of NaCl stress. Targeting specific components of stress responses has been suggested to be the best approach toward the design of stress tolerant crops without detrimentally affecting other processes which historically has proven problematic (Denby and Gehring, 2005; Meier and Gehring, 2006).

5.1.2 AtPNP-A could play a signalling role in the response to NaCl

5.1.2.1 A role for AtPNP-A *in second messenger signalling in response to NaCl*

Induction of *AtPNP-A* mRNA and protein expression in response to NaCl and osmotic stress implies a role for AtPNP-A in NaCl and osmotic stress responses (Figure 4.7) (Rafudeen *et al.*, 2003). This was supported by the NaCl tolerant phenotype of the *atpnp-a* mutant (Figure 3.17) which suggest that AtPNP-A is a negative regulator of NaCl tolerance. AtPNP-A has been proposed to function as a negative regulator of NaCl tolerance by modulating ion transport through regulation of ion channel activity. Additionally recombinant AtPNP-A treatment induced a cGMP-dependent calcium transient reminiscent of the response to ionic stress (Figure 2.8), suggesting that AtPNP-A may play a signalling role in the response to NaCl. In order to test whether AtPNP-A is involved in the signalling the ionic component of the NaCl-induced calcium response, the *atpnp-a* mutant would have to be crossed to the constitutively expressing aequorin line in order to report calcium responses to NaCl and osmotic stresses in the background of the *AtPNP-A* mutation. This would enable one to determine whether AtPNP-A lies upstream of the calcium signal in response to NaCl treatment which would be expected if

AtPNP-A initiates the cGMP signal that has been shown to lie upstream of the calcium response to NaCl (Figure 2.6 B and E).

5.1.2.2 Potential targets of AtPNP-A *in the response to NaCl*

Both NaCl and AtPNP-A signal via cGMP and calcium and cross talk between these second messengers occurs in both of these responses (Figure 2.1, 2.3, 2.6 and 2.8) (Wang *et al.*, 2007c). In plants, CNGCs have been suggested to be the main targets of CN signalling as well as points of cross talk between cGMP and calcium signalling since they have overlapping CaM and CN binding domains (Talke *et al.*, 2003; Trewavas *et al.*, 2002). There is evidence to suggest that in response to NaCl, cGMP acts to block CNGCs thereby prevent Na^+ uptake (Maathuis and Sanders, 2001). It is possible that in response to NaCl, AtPNP-A, via cGMP and calcium, targets a CNGC to alter ion fluxes and adjust homeostasis in adaptation to the stress. Indeed AtPNP-A as well as cGMP have been shown to induce ion fluxes (Na^+ and K^+) that are similar and have stoichiometry consistent with that described for the CNGCs (Demidchik *et al.*, 2002; Ludidi *et al.*, 2004; Pharmawati *et al.*, 1999). In support of this notion, the *atpnp-a* mutant takes up more Na^+ and effluxes more K^+ in response to NaCl than the wildtype (Figure 3.25 and 3.26). Moreover these K^+ fluxes were more susceptible to inhibition by Zn^{2+} that blocks NSCCs including CNGCs (Figure 3.27). This suggests that the *atpnp-a* mutant is specifically affected in its abundance or regulation of NSCCs involved in ion flux responses to NaCl. Whether this is a compensatory mechanism in order to better draw ions in the absence of AtPNP-A is unclear. Out of the family of 20 CNGCs in *Arabidopsis*, only one has been implicated in functioning in NaCl responses - *CNGC3* (Gobert *et al.*, 2006). The *cngc3* mutant has a similar phenotype to the *atpnp-a* mutant in that it displays improved tolerance to both NaCl and KCl. This KCl tolerance phenotype is quite unusual among NaCl-tolerant mutants. It has been demonstrated that *CNGC3* is involved in Na^+ and K^+ uptake while irPNPs and AtPNP-A also affect the movement of these ions (Gobert *et al.*, 2006; Ludidi *et al.*, 2004; Pharmawati *et al.*, 1999). Therefore it is interesting to consider that in response to NaCl, AtPNP-A may induce the formation of cGMP and the influx of calcium that would then act on *CNGC3* to cause Na^+ and K^+ fluxes. In support of this idea *CNGC3* was one of the genes most strongly upregulated in response to 24 hr AtPNP-A treatment (Table 4.8C). Additionally expression of *AtPNP-A* was highly correlated with a probe that recognizes *CNGC3*, however this probe was not unique and therefore was excluded from further computational analysis. It would be worthwhile to confirm the upregulation of *CNGC3* expression in response to AtPNP-A treatment, especially considering that verification of the microarray experiment yielded poor results. Measurements of AtPNP-A-induced ion fluxes in a *cngc3* mutant would reveal whether AtPNP-A does in fact induce ion fluxes via CNGC3.

5.1.2.3 AtPNP-A *and systemic signalling in response to NaCl*

A signalling role for AtPNP-A in the response to NaCl stress is also consistent with reports that irPNPs are xylem mobile systemic signalling molecules that affect the stomata (Maryani *et al.*, 2003). Similarly to ABA, AtPNP-A may be involved in systemic signalling between the root and the shoot in response to NaCl stress in order to regulate stomatal aperture and whole plant responses to NaCl stress. In accordance with a role for AtPNP-A in stomatal opening, the decreased stomatal apertures in the *atpnp-a* mutant (Figure 3.14) would be advantageous under conditions of NaCl stress and confer the observed NaCl tolerant phenotype. Furthermore this stomatal function would affect whole plant water and ion uptake which is supported by the fact that the *atpnp-a* mutant had reduced Na^+ and K^+ content under normal conditions, suggesting that it is less effective at ion uptake (Figure 3.25), again consistent with the NaCl tolerant phenotype. However, these phenotypes of the *atpnp-a* mutant do not affect its growth under normal conditions (Figure 3.11) so that the *atpnp-a* mutant may compensate for the reduced ion content and therefore lower osmoticum with improved osmotic adjustment, for example by the synthesis of compatible solutes. A signalling function for AtPNP-A between the shoot and root could account for the observed tissue-specific differences in the NaCl tolerance of the *atpnp-a* mutant (the roots of the *atpnp-a* mutant are not more NaCl tolerant whereas the shoots are) (Figure 3.20). It is possible that differences in the ion fluxes of the epidermal cells of the root (that are are critically involved in uptake of Na^+ into the plant) observed in the *atpnp-a* mutant may affect whole plant ion flux in response to NaCl if these differences are translated into altered xylem loading which is possible since irPNPs have been shown to induce ion fluxes in the stele (Pharmawati *et al.*, 1999). Indeed the *atpnp-a* mutant did take up more K^+ and Na^+ than the wildtype in response to NaCl treatment suggesting that these root phenotypes do translate into whole plant ion movements (Figure 3.25). In a sense then, increased osmoticum of the environment may actually benefit the *atpnp-a* mutant by increasing the ions available to it, improving its ability to take up these ions and rescuing the mutant phenotype. This would explain why the *atpnp-a* mutant sometimes fairs better on media containing high osmoticum than on basal media (Figure 3.17). In accordance with this, the increased uptake of K^+ and Na^+ in the *atpnp-a* mutant in response to NaCl does not negatively impact its growth and final K^+ and Na^+ levels reached are not different between the *atpnp-a* mutant and wildtype lines. In order to test whether the *atpnp-a* mutant is indeed perturbed in signalling between the shoot and root in response to NaCl and osmotic stresses, it would be necessary to examine the stomatal response, as well as to measure the ion content of the shoot and root separately in the mutant in response to NaCl. Additionally the generation of AtPNP-A-tagged GFP lines would enable one to visualize any movement of the AtPNP-A protein in response to NaCl stress.

5.1.2.4 Interplay between AtPNP-A *and* ABA

Besides the parallels between ABA and AtPNP-A in their xylem localization and site of action in the stomata, *AtPNP-A* and ABA biosynthetic genes show similar root/shoot specific expression in response to NaCl and osmotic stresses. These tissue specific expression patterns may coordinate signalling between the root and shoot to regulate stomata in response to NaCl and osmotic stress. Previously Wang and colleagues have reported that the actions of AtPNP-A and ABA are antagonistic in the stomata (Wang *et al.*, 2007c). While the results of the AtPNP-A microarray supported this by showing that AtPNP-A treatment represses the expression of genes involved in ABA signalling (Table 4.8B and 4.9B), the phenotype of the *atpnp-a* mutant does not suggest that interaction occurs between AtPNP-A and ABA *in planta* (Figure 3.18).

In summary, the role of AtPNP-A in the response to NaCl and osmotic stresses while likely remains unclear. AtPNP-A may be an early signalling molecule involved in stress perception and possibly in signalling between the root and shoot, affecting whole plant water and ion fluxes in response to NaCl stress. However it may also be a later adaptive response to the stress since *AtPNP-A* expression increases with increasing time of NaCl and osmotic stress exposure.

5.1.3 Why would the plant need a gene that renders it less fit?

The improved NaCl tolerance phenotype of the *atpnp-a* mutant raises the question as to why the plant would retain a gene that renders it less fit under stress conditions. One possibility is that AtPNP-A is critically required in other processes. Indeed the observation that the *atpnp-a* mutant is compromised in its cell expansion suggests that AtPNP-A plays a positive role in growth (Figure 3.12 and 3.13). Reciprocal regulation between growth and stress responses is necessary to ensure that the plant does not continue growing inappropriately in the presence of stress (Bray, 2004). On this note the issue needs to be raised as to whether improved growth under stressed conditions, which is usually the measure of stress tolerance, truly reflects improved stress tolerance. This idea was first questioned in studies of mutants that germinate under conditions of stress and lead to the suggestion that these mutants actually lack perception or signal transduction of the stress (Saleki *et al.*, 1993; Werner and Finkelstein, 1995). Longer term survival experiments are therefore probably a more indicative of stress tolerance. The idea that the *atpnp-a* mutant continues to grow inappropriately in response to stress and does not properly initiate its stress responses may also explain why the *atpnp-a* mutant is instead compromised in its resistance to pathogens (Figure 3.30-3.33).

5.1.4 A role for AtPNP-A in the defence response

The *atpnp-a* mutant is compromised in its resistance to avirulent *P. syringae* and virulent *H. parasitica* while *AtPNP-A* expression is induced in response to a number of pathogens, thus

implying a positive role for AtPNP-A in promoting plant resistance to pathogens. Two possible ideas explaining the positive role of AtPNP-A in the plant's defence response are explored fully below. Firstly AtPNP-A may be part of the plant's defence response mediated by the SA signalling pathway; and secondly AtPNP-A may be targeted by the pathogen, triggering pathogen recognition by the plant which then sets the defense response into motion.

5.1.4.1 The involvement of AtPNP-A *in the* SA *signalling pathway*

Several lines of evidence suggest that AtPNP-A may play a role in SA-mediated defence responses. Firstly, the *atpnp-a* mutant is compromised in its resistance to avirulent *P. syringae* and *H. parasitica* that both activate SA-mediated defences (Figures 3.30-3.33) (Slusarenko and Schlaich, 2003), secondly *AtPNP-A* expression is induced by SA as well as several pathogens to which resistance is acquired through the SA signalling pathway (Figure 4.6H and 4.9A) and thirdly *AtPNP-A* expression is correlated with key genes involved in the SA signalling pathway and co-expression of a subset of these has been validated experimentally (Table 4.2 and Figure 4.9). The expression analysis revealed that the *AtPNP-A* transcript is induced by SA but that this is blocked in an *npr1* mutant while *AtPNP-A* expression is induced in a *WRKY70* overexpressor. This suggests that AtPNP-A may lie downstream of NPR1 and WRKY70 in the SA signalling pathway. Moreover the overrepresentation of TGA and WRKY TFBSs in the *AtPNP-A* ECGG suggests that co-expression of the *AtPNP-A* ECGG may be directly regulated by NPR1 and WRKY70. Therefore AtPNP-A may be an end point in the SA signalling pathway like the *PR* genes and indeed AtPNP-A shares a number of features in common with these (as discussed in section 4.4.2.6). While it is possible that *AtPNP-A* may be a type of *PR* gene, the fact that the *atpnp-a* mutant presents with a phenotype in response to pathogens sets it apart from the *PR* genes (Seo *et al.*, 2008). Furthermore the AtPNP-A treatment microarray revealed that as an early response to AtPNP-A treatment, genes annotated as being involved in SAR including *WRKY70* and *TGA2* were upregulated (Table 4.8A and 4.8B). Therefore AtPNP-A itself appears to induce or amplify the defence response. Known downstream targets of these transcription factors, for example the *PR* genes, were not identified at the late time point (24 hr) in this experiment, although perhaps this was too delayed to detect transcriptional responses mediated by the early upregulation of these transcription factors and this might be resolved in a more rigorous time course. Furthermore, because the plant response to AtPNP-A treatment may not truly reflect the function of endogenous AtPNP-A, it may be more meaningful to conduct the microarray experiment on the *atpnp-a* mutant compared to the wildtype. If this microarray was performed after pathogen infection it could help to elucidate how the *atpnp-a* mutant differs from the wildtype in its defence response and may explain the compromised resistance of the *atpnp-a* mutant and the mechanism of AtPNP-A action during plant defence.

5.1.4.2 Establishing whether AtPNP-A *is involved in* SA *signalling*

Whether AtPNP-A is actually involved in the SA signalling pathway remains to be established. Since the SA signalling pathway is well understood this presents a range of ways to explore this possibility. For instance, one could test SA levels in the *atpnp-a* mutant in response to pathogen infection as well as generate double mutants with other key genes involved in SA signalling. This would help to position AtPNP-A in the SA pathway. The microarray experiment suggests that, like SA, AtPNP-A induces the expression of genes involved in the SAR response. At this point it is interesting to note that SAR requires a systemic signal that remains at large (Suzuki *et al.*, 2004). Recent evidence suggests that the elusive signal may be a peptide (Vlot *et al.*, 2008). It is therefore tempting to speculate that AtPNP-A could play such a role. In support of this, irPNPs have been extracted from the xylem in response to pathogen infection suggesting that they could be mobile signalling molecule induced in response to pathogens (Ceccardi *et al.*, 1998). An examination of the SAR response in the *atpnp-a* mutant may therefore be revealing. Again an AtPNP-A-tagged GFP line would be useful to examine any movement of AtPNP-A in response to pathogen attack. It would also be interesting to further explore the link between AtPNP-A and WRKY70. Both *wrky70* mutant and *WRKY70* overexpressor lines are available that could be used for this purpose. This may help to better understand whether *AtPNP-A* is in fact regulated by WRKY70 and visa versa.

The *atpnp-a* mutant presents with an unusual phenotype in that it is compromised in its resistance to avirulent *P. syringae* when spray inoculated (Figure 3.30 and 3.31). The avirulent pathogen loses its avirulence on the *atpnp-a* mutant so that it becomes as virulent as the DC3000 strain, implying that loss of *AtPNP-A* coincincides with loss of recognition of the avirulent pathogen. This suggests that AtPNP-A is somehow involved in the early recognition of the avirulent pathogen.

5.1.4.3 Plant hormones are targeted by pathogens

Both *AtPNP-A* mRNA and irPNP protein levels increase in response to pathogen infection (Figure 4.9B) (Ceccardi *et al.*, 1998). It was therefore interesting to note that pathogen Avr proteins have been shown to increase the levels of two other plant hormones, namely ABA and auxin (Chen *et al.*, 2007a; de Torres-Zabala *et al.*, 2007). In the first case expression of ABA biosynthetic genes and resultant ABA levels increase in response to pathogen infection and Avr proteins have also been found to enhance plant sensitivity to ABA (de Torres-Zabala *et al.*, 2007; Goel *et al.*, 2008). Additionally exogenous ABA treatment increases plant susceptibility to pathogens while *aba* mutants are more resistant to pathogen infection (de Torres-Zabala *et al.*, 2007; Mohr and Cahill, 2003). Therefore the presence of ABA during pathogen infection is detrimental to the plant. This may be because ABA suppresses SA-mediated plant defences so

that ABA responses to abiotic stress can take precedence (Loake and Grant, 2007). This seems plausible considering two observations: 1) crop losses caused by water deficit far exceed those caused by pathogens and so the response to water stress is more critical to plant survival than the response to pathogens and 2) many pathogens require high humidity for the infection process which probably means that the risk of pathogen infection under conditions of water deficit is low, negating the need to expend resources on the defence response when energy is required for coping with the water deficit (Mohr and Cahill, 2003). Since ABA is required for the plants stomatal closure in response to pathogens, it may seem counter-intuitive that the pathogen would induce ABA (Melotto *et al.*, 2006). Instead ABA has been suggested to be used by the pathogen to adjust the water status of the apoplast which is a critical determinant of pathogen growth (de Torres-Zabala *et al.*, 2007; Wright and Beattie, 2004). In the second case, the induction of auxin in response to pathogen infection may also be related to auxin/SA antagonism (Navarro *et al.*, 2006; Wang *et al.*, 2007a). However auxin has also been proposed to be used by the pathogen to induce cell wall loosening and thereby water and nutrient leak into the apoplast (Goel *et al.*, 2008). Additionally auxins may be used by the pathogen to induce stomatal reopening to aid bacterial release and re-infection (Goel *et al.*, 2008). It is becoming increasingly apparent from these studies that pathogens manipulate plant hormone cross-talk in order to alter homeostasis.

5.1.4.4 Could AtPNP-A *be targeted by pathogens?*

The *atpnp-a* mutant is compromised in its resistance against avirulent *P. syringae* suggesting that AtPNP-A is positively involved in the plants defence response. Again it may seem counter-intuitive that the plant would induce expression of a gene that promotes stomatal opening during pathogen attack. Instead *AtPNP-A* expression may be induced by the pathogen. It is possible that avirulent *P. syringae* targets AtPNP-A for some virulence function that then is recognized by the plant, for example if AtPNP-A is guarded by an R protein, triggering the ETI. This idea is consistent with recent findings that a bacterial plant pathogen has an irPNP-like gene, *XacPNP* and this appears to be used by the pathogen as a virulence factor to alter host homeostasis (Gottig *et al.*, 2008; Nembaware *et al.*, 2004). There are several ways in which AtPNP-A may be used by the pathogen to manipulate plant homeostasis that are similar to the ideas presented above for ABA and auxin. Firstly, AtPNP-A may be used by the pathogen to open stomata. The fact that avirulent *P. syringae* are less effective at stomatal reopening suggests that there may be Avr factors that promote stomatal reopening that are recognized by the plant (Melotto *et al.*, 2006). In support of this idea XacPNP has been demonstrated to induce stomatal opening in plants and pathogens containing the *XacPNP* gene enhance plant transpiration and photosynthesis during infection, keeping the plant tissue alive and healthy and suppressing necrosis to the benefit of the biotrophic pathogen, altogether suggesting that

XacPNP promotes stomatal opening *in planta* (Gottig *et al.*, 2008). This XacPNP would promote the infection site becoming a sink tissue, drawing water and nutrients from the rest of the plant (Berger *et al.*, 2007). Secondly, AtPNP-A could be targeted by the pathogen to induce the swelling response and cell wall loosening (Cosgrove, 1993) and subsequently water and nutrient leakage into the apoplast. In support of this XacPNP has been shown to promote protoplast swelling (Gottig *et al.*, 2008). Lastly, AtPNP-A may be used by the pathogen to induce water and ion fluxes to draw water and nutrients away from the plant and improve the apoplastic water potential sensed by the pathogen as was suggested for ABA. On this same note the pathogen may target AtPNP-A for degradation in order to prevent the plant from drawing water and nutrients, thereby making more water and nutrients available to the pathogen. Induction of both ABA and AtPNP-A by the pathogen could be used in balance to readjust plant water homeostasis to suit the pathogen. It is interesting to note then that the ABA biosynthetic genes that showed the same tissue-specific expression pattern as *AtPNP-A* are also targeted by pathogens (de Torres-Zabala *et al.*, 2007). If these genes do regulate whole plant water and ion fluxes, it indeed makes them attractive targets for manipulation by pathogens. However the actions of XacPNP and AtPNP-A during pathogen attack are not necessarily the same.

5.1.4.5 Resolving the function of AtPNP-A *in the P. syringae defence response*

In order to better understand the role of AtPNP-A in the response to pathogens, it would be informative to examine stomatal aperture changes in response to avirulent and virulent *P. syringae* in the *atpnp-a* mutant. Another approach would be to test whether the *atpnp-a* mutant displays altered susceptibility to the TTSS-defective *hrcC*$^{-}$ *P. sringae* mutant when spray inoculated in order to determine whether the compromised resistance of the *atpnp-a* mutant to the avirulent pathogen requires effectors to be injected into the plant. It would also be interesting to investigate different avirulent *P. syringae* strains to determine whether the *atpnp-a* mutant phenotype is the result of the *AvrB-RPM1* interaction or whether the *atpnp-a* mutant is also compromised in its resistance to other avirulent pathogens which would then suggest that AtPNP-A is the target of a common Avr mechanism. Finally, the use of the *P. syringae* bacterial strains that report the apoplastic water potential (Wright and Beattie, 2004) would reveal whether AtPNP-A does influence the apoplastic water potential sensed by the bacterium. The role of AtPNP-A in the response to pathogens is intriguing and should be pursued further.

5.1.5 Commonalities between growth, abiotic and biotic stress responses

The induced co-expression of *AtPNP-A* and the *AtPNP-A* ECGG genes annotated as being involved in the defence response was observed not only in response to biotic stresses but also in response to abiotic stresses as well as during development (Figure 4.6). This suggests that *AtPNP-A* and the defence genes are commonly involved in growth and development as well as

in the response to abiotic and biotic stresses. Indeed phenotypes of the *atpnp-a* mutant support a role for AtPNP-A in growth, abiotic and biotic stress responses. Again several possibilities arise when considering a common role of AtPNP-A in these processes. In particular, AtPNP-A could be involved in sensing a common homeostatic disturbance; initiating a common signalling event or involved in a common response to all of these conditions (Zhu, 2001). Furthermore, AtPNP-A may be involved in cross-talk between signal transduction pathways and the integration of signals that influence growth and communicate stress, into an appropriate end response. Finally the proposed role for AtPNP-A in systemic signalling could imply a function for AtPNP-A in co-ordinating whole plant growth and stress responses.

5.1.5.1 Stress perception, signal transduction and end responses

In the first instance, AtPNP-A could be involved in perception of the homeostatic state or some common component of the stress. For example abiotic stress and biotic stresses both alter plant water status as well as induce osmotic imbalance and K^+ starvation (Armengaud *et al.*, 2004; Shabala and Cuin, 2008; Verslues *et al.*, 2006; Wright and Beattie, 2004), while in order to grow the cell requires uptake of water and osmotica, particularly K^+ to promote cell expansion (Cosgrove, 1993; Shabala, 2003; Shabala and Lew, 2002). Therefore AtPNP-A could be involved in sensing the osmotic state and/or K^+ content of the cell. Downstream of stress perception, AtPNP-A could be involved in initiating ion fluxes or calcium and cGMP signalling that are common components of abiotic and biotic stress responses (Donaldson *et al.*, 2004; Grant *et al.*, 2000; Knight *et al.*, 1997; Maathuis and Sanders, 1999; Maathuis and Sanders, 2001; Meier *et al.*, 2009; Nemchinov *et al.*, 2008) as well as play an important role in growth (Dolan and Davies, 2004; Hu *et al.*, 2005; Shabala, 2003). Thus AtPNP-A may be involved in the transduction of the growth and stress signals. Growth, abiotic and biotic stress responses may then commonly require the induction of genes involved in cell wall modification (Bray, 2002; Cosgrove, 2005; Hauck *et al.*, 2003) or the protection against ROS damage since ROS are involved growth and stress responses (Fujita *et al.*, 2006; Katiyar-Agarwal *et al.*, 2006; Potters *et al.*, 2007; Shin and Schachtman, 2004; Torres and Dangl, 2005; Tsugane *et al.*, 1999; Zhu *et al.*, 2007). In fact growth itself can be a stress response (Potters *et al.*, 2007). Most likely this balance between growth and the stress response is imperative for the distribution of resources (photosynthate) and timing of stress response that ultimately determine plant survival (Anderson *et al.*, 2004). In support of this a number of mutants affected in genes assigned to growth functions are compromised in their NaCl tolerance (Barrero *et al.*, 2005; Kang *et al.*, 2008; Koiwa *et al.*, 2003; Shi *et al.*, 2003) and pathogens have been found to induce growth hormones to suppress plant defence (Goel *et al.*, 2008; Robert-Seilaniantz *et al.*, 2007).

5.1.5.2 Hormone cross-talk

The idea that plant hormones are limited in function to one type of response, for example auxin in growth and ABA in the abiotic stress responses clearly needs refinement as it is becoming increasingly apparent that elaborate cross-talk exists between plant hormones (Fujita *et al.*, 2006). Interestingly, much of the evidence for this has been gained from the studies of pathogens that have evolved to manipulate these communications (Chen *et al.*, 2007a; de Torres-Zabala *et al.*, 2007; Goel *et al.*, 2008). It is perhaps interesting then that *AtPNP-A* expression is correlated with a number of genes that serve as points of cross-talk between the SA and other hormone signalling; for example *WRKY70, EDS1* and *NPR1*. This could suggest that the *AtPNP-A* ECGG potentially integrates signals from a number of different pathways involved in growth and stress responses. Additionally the AtPNP-A microarray revealed that AtPNP-A may induce SA signalling and antagonize GA and ABA signalling, therefore AtPNP-A itself could directly cross-talk between these different signalling pathways.

Altogether the results of the current work suggest that AtPNP-A plays a role in growth, abiotic and biotic stress responses. Positive and negative actions of AtPNP-A on growth, abiotic and biotic stress responses are consistent with the idea that AtPNP-A is involved in establishing homeostatic balance as is required in each of these circumstances. Even moderately reduced levels of *AtPNP-A* expression alter plant growth and stress responses implying the importance of AtPNP-A to the plant. Therefore it is proposed that AtPNP-A regulates homeostasis by integrating growth, abiotic and biotic stress responses so that the plant can mount an effective response to the environment that contributes to survival.

CHAPTER 6

REFERENCES

CHAPTER 6: REFERENCES

The Arabidopsis Genome Iniative (2000) Analysis of the genome sequence of the flowering plant *Arabidopsis thaliana*. *Nature*, **408**, 796-815.

Aarts, N., Metz, M., Holub, E., Staskawicz, B.J., Daniels, M.J. and Parker, J.E. (1998) Different requirements for EDS1 and NDR1 by disease resistance genes define at least two *R* gene-mediated signaling pathways in *Arabidopsis*. *Proc Natl Acad Sci U S A*, **95**, 10306-10311.

Ahluwalia, A., MacAllister, R.J. and Hobbs, A.J. (2004) Vascular actions of natriuretic peptides. Cyclic GMP-dependent and -independent mechanisms. *Basic Res Cardiol*, **99**, 83-89.

Al-Shahrour, F., Diaz-Uriarte, R. and Dopazo, J. (2004) FatiGO: a web tool for finding significant associations of Gene Ontology terms with groups of genes. *Bioinformatics*, **20**, 578-580.

Al-Shahrour, F., Minguez, P., Tarraga, J., Medina, I., Alloza, E., Montaner, D. and Dopazo, J. (2007) FatiGO +: a functional profiling tool for genomic data. Integration of functional annotation, regulatory motifs and interaction data with microarray experiments. *Nucleic Acids Res*, **35**, W91-96.

Al-Shahrour, F., Minguez, P., Vaquerizas, J.M., Conde, L. and Dopazo, J. (2005) BABELOMICS: a suite of web tools for functional annotation and analysis of groups of genes in high-throughput experiments. *Nucleic Acids Res*, **33**, W460-464.

Alejandro, S., Rodriguez, P.L., Belles, J.M., Yenush, L., Garcia-Sanchez, M.J., Fernandez, J.A. and Serrano, R. (2007) An *Arabidopsis* quiescin-sulfhydryl oxidase regulates cation homeostasis at the root symplast-xylem interface. *Embo J*, **26**, 3203-3215.

Allemeersch, J., Durinck, S., Vanderhaeghen, R., Alard, P., Maes, R., Seeuws, K., Bogaert, T., Coddens, K., Deschouwer, K., Van Hummelen, P., Vuylsteke, M., Moreau, Y., Kwekkeboom, J., Wijfjes, A.H., May, S., Beynon, J., Hilson, P. and Kuiper, M.T. (2005) Benchmarking the CATMA microarray. A novel tool for *Arabidopsis* transcriptome analysis. *Plant Physiol*, **137**, 588-601.

Allen, G.J., Muir, S.R. and Sanders, D. (1995) Release of Ca^{2+} from individual plant vacuoles by both $InsP_3$ and cyclic ADP-ribose. *Science*, **268**, 735-737.

Allocco, D.J., Kohane, I.S. and Butte, A.J. (2004) Quantifying the relationship between co-expression, co-regulation and gene function. *BMC Bioinformatics*, **5**, 18.

Alonso, J.M., Stepanova, A.N., Leisse, T.J., Kim, C.J., Chen, H., Shinn, P., Stevenson, D.K., Zimmerman, J., Barajas, P., Cheuk, R., Gadrinab, C., Heller, C., Jeske, A., Koesema, E., Meyers, C.C., Parker, H., Prednis, L., Ansari, Y., Choy, N., Deen, H., Geralt, M., Hazari, N., Hom, E., Karnes, M., Mulholland, C., Ndubaku, R., Schmidt, I., Guzman, P., Aguilar-Henonin, L., Schmid, M., Weigel, D., Carter, D.E., Marchand, T., Risseeuw, E., Brogden, D., Zeko, A., Crosby, W.L., Berry, C.C. and Ecker, J.R. (2003) Genome-wide insertional mutagenesis of *Arabidopsis thaliana*. *Science*, **301**, 653-657.

Alzwiy, I.A. and Morris, P.C. (2007) A mutation in the *Arabidopsis MAP kinase kinase 9* gene results in enhanced seedling stress tolerance. *Plant Sci*, **173**, 302-308.

Anand-Srivastava, M.B. (2005) Natriuretic peptide receptor-C signaling and regulation. *Peptides*, **26**, 1044-1059.

Anderson, J.P., Badruzsaufari, E., Schenk, P.M., Manners, J.M., Desmond, O.J., Ehlert, C., Maclean, D.J., Ebert, P.R. and Kazan, K. (2004) Antagonistic interaction between abscisic acid and jasmonate-ethylene signaling pathways modulates defense gene expression and disease resistance in *Arabidopsis*. *Plant Cell*, **16**, 3460-3479.

Apel, K. and Hirt, H. (2004) Reactive oxygen species: metabolism, oxidative stress, and signal transduction. *Annu Rev Plant Biol*, **55**, 373-399.

Apse, M.P. and Blumwald, E. (2007) Na^+ transport in plants. *FEBS Lett*, **581**, 2247-2254.

Apse, M.P., Sottosanto, J.B. and Blumwald, E. (2003) Vacuolar cation/H^+ exchange, ion homeostasis, and leaf development are altered in a T-DNA insertional mutant of *AtNHX1*, the *Arabidopsis* vacuolar Na^+/H^+ antiporter. *Plant J*, **36**, 229-239.

Arazi, T., Kaplan, B. and Fromm, H. (2000) A high-affinity calmodulin-binding site in a tobacco plasma-membrane channel protein coincides with a characteristic element of cyclic nucleotide-binding domains. *Plant Mol Biol*, **42**, 591-601.

Arazi, T., Sunkar, R., Kaplan, B. and Fromm, H. (1999) A tobacco plasma membrane calmodulin-binding transporter confers Ni^{2+} tolerance and Pb^{2+} hypersensitivity in transgenic plants. *Plant J*, **20**, 171-182.

Armengaud, P., Breitling, R. and Amtmann, A. (2004) The potassium-dependent transcriptome of *Arabidopsis* reveals a prominent role of jasmonic acid in nutrient signaling. *Plant Physiol*, **136**, 2556-2576.

Assmann, S.M. (1995) Cyclic AMP as a second messenger in higher plants. *Plant Physiol*, **108**, 885-889.

Atkinson, M.M. and Baker, C.J. (1987) Alteration of plasmalemma sucrose transport in *Phaseolus vulgaris* by *Pseudomonas syringae* pv. *syringae* and its association with K^+/H^+ exchange. *Phytopathology*, **77**, 1573-1578.

Atkinson, M.M., Huang, J.-S. and Knopp, J.A. (1985) The Hypersensitive Reaction of Tobacco to *Pseudomonas syringae* pv. *pisi*. Activation of a Plasmalemma K^+/H^+ Exchange Mechanism *Plant Physiol*, **79**, 843-847.

Atkinson, M.M., Keppler, L.D., Orlandi, E.W., Baker, C.J. and Mischke, C.F. (1990) Involvement of Plasma Membrane Calcium Influx in Bacterial Induction of the K^+/H^+ and Hypersensitive Responses in Tobacco. *Plant Physiol*, **92**, 215-221.

Balague, C., Lin, B., Alcon, C., Flottes, G., Malmstrom, S., Kohler, C., Neuhaus, G., Pelletier, G., Gaymard, F. and Roby, D. (2003) HLM1, an essential signaling component in the hypersensitive response, is a member of the cyclic nucleotide-gated channel ion channel family. *Plant Cell*, **15**, 365-379.

Barr, C.S., Rhodes, P. and Struthers, A.D. (1996) C-type natriuretic peptide. *Peptides*, **17**, 1243-1251.

Barrero, J.M., Piqueras, P., Gonzalez-Guzman, M., Serrano, R., Rodriguez, P.L., Ponce, M.R. and Micol, J.L. (2005) A mutational analysis of the *ABA1* gene of *Arabidopsis thaliana* highlights the involvement of ABA in vegetative development. *J Exp Bot*, **56**, 2071-2083.

Baxter, G.F. (2004a) The natriuretic peptides. *Basic Res Cardiol*, **99**, 71-75.

Baxter, G.F. (2004b) Natriuretic peptides and myocardial ischaemia. *Basic Res Cardiol*, **99**, 90-93.

Beattie, G.A. and Lindow, S.E. (1995) The secret life of foliar bacterial pathogens on leaves. *Annu Rev Phytopathol*, **33**, 145-172.

Beattie, G.A. and Lindow, S.E. (1999) Bacterial colonization of leaves: a spectrum of strategies. *Phytopathology*, **89**, 353-359.

Berger, S., Sinha, A.K. and Roitsch, T. (2007) Plant physiology meets phytopathology: plant primary metabolism and plant-pathogen interactions. *J Exp Bot*, **58**, 4019-4026.

Berthomieu, P., Conejero, G., Nublat, A., Brackenbury, W.J., Lambert, C., Savio, C., Uozumi, N., Oiki, S., Yamada, K., Cellier, F., Gosti, F., Simonneau, T., Essah, P.A., Tester, M., Very, A.A., Sentenac, H. and Casse, F. (2003) Functional analysis of AtHKT1 in Arabidopsis shows that Na^+ recirculation by the phloem is crucial for salt tolerance. *Embo J*, **22**, 2004-2014.

Bethke, P.C., Lonsdale, J.E., Fath, A. and Jones, R.L. (1999) Hormonally regulated programmed cell death in barley aleurone cells. *Plant Cell*, **11**, 1033-1046.

Billington, T., Pharmawati, M. and Gehring, C.A. (1997) Isolation and immunoaffinity purification of biologically active plant natriuretic peptide. *Biochem Biophys Res Commun*, **235**, 722-725.

Bisgrove, S.R., Simonich, M.T., Smith, N.M., Sattler, A. and Innes, R.W. (1994) A disease resistance gene in *Arabidopsis* with specificity for two different pathogen avirulence genes. *Plant Cell*, **6**, 927-933.

Bolstad, B.M., Irizarry, R.A., Astrand, M. and Speed, T.P. (2003) A comparrison of normalization methods for high density oligonucleotide array data based on bias and variance. *Bioinformatics*, **19**, 185-193.

Bolwell, P.G. (1995) Cyclic AMP, the reluctant messenger in plants. *Trends Biochem Sci*, **20**, 492-495.

Borsani, O., Valpuesta, V. and Botella, M.A. (2001) Evidence for a role of salicylic acid in the oxidative damage generated by NaCl and osmotic stress in *Arabidopsis* seedlings. *Plant Physiol*, **126**, 1024-1030.

Boudart, G., Jamet, E., Rossignol, M., Lafitte, C., Borderies, G., Jauneau, A., Esquerre-Tugaye, M.T. and Pont-Lezica, R. (2005) Cell wall proteins in apoplastic fluids of *Arabidopsis thaliana* rosettes: identification by mass spectrometry and bioinformatics. *Proteomics*, **5**, 212-221.

Bowler, C., Neuhaus, G., Yamagata, H. and Chua, N.H. (1994a) Cyclic GMP and calcium mediate phytochrome phototransduction. *Cell*, **77**, 73-81.

Bowler, C., Yamagata, H., Neuhaus, G. and Chua, N.H. (1994b) Phytochrome signal transduction pathways are regulated by reciprocal control mechanisms. *Genes Dev*, **8**, 2188-2202.

Boyer, J.S. (1982) Plant Productivity and Environment. *Science*, **218**, 443-448.

Bray, E. (1997) Plant responses to water deficit. *Trends Plant Sci*, **2**, 48-54.

Bray, E.A. (2002) Classification of genes differentially expressed during water-deficit stress in *Arabidopsis thaliana*: an analysis using microarray and differential expression data. *Ann Bot (Lond)*, **89 Spec No**, 803-811.

Bray, E.A. (2004) Genes commonly regulated by water-deficit stress in *Arabidopsis thaliana*. *J Exp Bot*, **55**, 2331-2341.

Brazma, A., Parkinson, H., Sarkans, U., Shojatalab, M., Vilo, J., Abeygunawardena, N., Holloway, E., Kapushesky, M., Kemmeren, P., Lara, G.G., Oezcimen, A., Rocca-Serra, P. and Sansone, S.A. (2003) ArrayExpress--a public repository for microarray gene expression data at the EBI. *Nucleic Acids Res*, **31**, 68-71.

Bressan, R.A., Hasegawa, P.M. and Pardo, J.M. (1998) Plants use calcium to resolve salt stress. *Trends Plant Sci*, **3**, 411-412.

Bridges, D., Fraser, M.E. and Moorhead, G.B. (2005) Cyclic nucleotide binding proteins in the *Arabidopsis thaliana* and *Oryza sativa* genomes. *BMC Bioinformatics*, **6**, 6.

Brodersen, P., Petersen, M., Bjorn Nielsen, H., Zhu, S., Newman, M.A., Shokat, K.M., Rietz, S., Parker, J. and Mundy, J. (2006) *Arabidopsis* MAP kinase 4 regulates salicylic acid- and jasmonic acid/ethylene-dependent responses via EDS1 and PAD4. *Plant J*, **47**, 532-546.

Brooks, D.M., Hernandez-Guzman, G., Kloek, A.P., Alarcon-Chaidez, F., Sreedharan, A., Rangaswamy, V., Penaloza-Vazquez, A., Bender, C.L. and Kunkel, B.N. (2004) Identification and characterization of a well-defined series of coronatine biosynthetic mutants of *Pseudomonas syringae* pv. *tomato* DC3000. *Mol Plant Microbe Interact*, **17**, 162-174.

Brown, E.G., Al-Najafi, T. and Newton, R.P. (1975) Partial purification of adenosine 3',5'-cyclic monophosphate phosphodiesterase from *Phaseolus vulgaris* L.: associated activator and inhibitors. *Biochem. Soc. Trans.*, **3**, 393–395.

Brown, E.G., Al-Najafi, T. and Newton, R.P. (1977) Cyclic nucleotide phosphodiesterase activity in *Phaseolus vulgaris* L. . *Phytochemistry*, **16**, 1333–1337.

Brown, E.G., Edwards, M.J., Newton, R.P. and Smith, C.J. (1979) Plurality of cyclic nucleotide phosphodiesterases in *Spinacea oleracea* L.; subcellular distribution, partial purification and properties. *Phytochemistry*, **18**, 1943–1948.

Brown, E.G. and Newton, R.P. (1981) Cyclic AMP and higher plants. *Phytochemistry*, **20**, 2453-2463.

Brown, E.G., Newton, R.P., Evans, D.E., Walton, T.J., Younis, L.M. and Vaughan, J.M. (1989) Influence of light on cyclic nucleotide metabolism in plants; effect of dibutyryl cyclic nucleotides on chloroplast components. . *Phytochemistry*, **28**, 2559-2563.

Bussis, D., van Groll, U., Fisahn, J. and Altman, T. (2006) Stomatal aperture can compensate altered stomatal density in *Arabidopsis thaliana* at growth light conditions. *Funct Plant Biol*, **33**, 1037-1043.

Cao, D., Cheng, H., Wu, W., Soo, H.M. and Peng, J. (2006) Gibberellin mobilizes distinct DELLA-dependent transcriptomes to regulate seed germination and floral development in *Arabidopsis*. *Plant Physiol*, **142**, 509-525.

Cao, H., Bowling, S.A., Gordon, A.S. and Dong, X. (1994) Characterization of an *Arabidopsis* Mutant That Is Nonresponsive to Inducers of Systemic Acquired Resistance. *Plant Cell*, **6**, 1583-1592.

Cea, L.B. (2005) Natriuretic peptide family: new aspects. *Curr Med Chem Cardiovasc Hematol Agents*, **3**, 87-98.

Ceccardi, T.L., Barthe, G.A. and Derrick, K.S. (1998) A novel protein associated with citrus blight has sequence similarities to expansin. *Plant Mol Biol*, **38**, 775-783.

Chan, C.W., Schorrak, L.M., Smith, R.K., Jr., Bent, A.F. and Sussman, M.R. (2003) A cyclic nucleotide-gated ion channel, CNGC2, is crucial for plant development and adaptation to calcium stress. *Plant Physiol*, **132**, 728-731.

Channon, A.G. (1981) *Downy mildew of Brassicas*. London: Academic Press.

Chauhan, S.D., Hobbs, A.J. and Ahluwalia, A. (2004) C-type natriuretic peptide: new candidate for endothelium-derived hyperpolarising factor. *Int J Biochem Cell Biol*, **36**, 1878-1881.

Chen, Y.F. (2005) Atrial natriuretic peptide in hypoxia. *Peptides*, **26**, 1068-1077.

Chen, Z., Agnew, J.L., Cohen, J.D., He, P., Shan, L., Sheen, J. and Kunkel, B.N. (2007a) *Pseudomonas syringae* type III effector AvrRpt2 alters *Arabidopsis thaliana* auxin physiology. *Proc Natl Acad Sci U S A*, **104**, 20131-20136.

Chen, Z., Newman, I., Zhou, M., Mendham, N., Zhang, G. and Shabala, S. (2005) Screening plants for salt tolerance by measuring K^+ flux: a case study for barley. *Plant Cell Environ*, **28**, 1230-1246.

Chen, Z., Pottosin, II, Cuin, T.A., Fuglsang, A.T., Tester, M., Jha, D., Zepeda-Jazo, I., Zhou, M., Palmgren, M.G., Newman, I.A. and Shabala, S. (2007b) Root plasma membrane transporters controlling K^+/Na^+ homeostasis in salt-stressed barley. *Plant Physiol*, **145**, 1714-1725.

Chen, Z., Zhou, M., Newman, I.A., Mendham, N.J., Zhang, G. and Shabala, S. (2007c) Potassium and sodium relations in salinised barley tissues as a basis of differential salt tolerance. *Funct Plant Biol*, **34**, 150-162.

Cheng, N.H., Pittman, J.K., Barkla, B.J., Shigaki, T. and Hirschi, K.D. (2003) The *Arabidopsis* cax1 mutant exhibits impaired ion homeostasis, development, and hormonal responses and reveals interplay among vacuolar transporters. *Plant Cell*, **15**, 347-364.

Cheong, Y.H., Kim, K.N., Pandey, G.K., Gupta, R., Grant, J.J. and Luan, S. (2003) CBL1, a calcium sensor that differentially regulates salt, drought, and cold responses in *Arabidopsis*. *Plant Cell*, **15**, 1833-1845.

Cheong, Y.H., Pandey, G.K., Grant, J.J., Batistic, O., Li, L., Kim, B.G., Lee, S.C., Kudla, J. and Luan, S. (2007) Two calcineurin B-like calcium sensors, interacting with protein kinase CIPK23, regulate leaf transpiration and root potassium uptake in *Arabidopsis*. *Plant J*, **52**, 223-239.

Chinchilla, D., Zipfel, C., Robatzek, S., Kemmerling, B., Nurnberger, T., Jones, J.D., Felix, G. and Boller, T. (2007) A flagellin-induced complex of the receptor FLS2 and BAK1 initiates plant defence. *Nature*, **448**, 497-500.

Chory, J., Ecker, J.R., Briggs, S., Caboche, M., Coruzzi, G.M., Cook, D., Dangl, J., Grant, S., Guerinot, M.L., Henikoff, S., Martienssen, R., Okada, K., Raikhel, N.V., Somerville, C.R. and Weigel, D. (2000) National Science Foundation-Sponsored Workshop Report: "The 2010 Project" functional genomics and the virtual plant. A blueprint for understanding how plants are built and how to improve them. *Plant Physiol*, **123**, 423-426.

Church, G.M. and Gilbert, W. (1984) Genomic sequencing. *Proc Natl Acad Sci U S A*, **81**, 1991-1995.

Clarke, A., Desikan, R., Hurst, R.D., Hancock, J.T. and Neill, S.J. (2000) NO way back: nitric oxide and programmed cell death in *Arabidopsis thaliana* suspension cultures. *Plant J*, **24**, 667-677.

Clough, S.J. and Bent, A.F. (1998) Floral dip: a simplified method for *Agrobacterium*-mediated transformation of *Arabidopsis thaliana*. *Plant J*, **16**, 735-743.

Clough, S.J., Fengler, K.A., Yu, I.C., Lippok, B., Smith, R.K., Jr. and Bent, A.F. (2000) The *Arabidopsis dnd1* "*defense, no death*" gene encodes a mutated cyclic nucleotide-gated ion channel. *Proc Natl Acad Sci U S A*, **97**, 9323-9328.

Cosgrove, D.J. (1993) Water uptake by growing cells: an assessment of the controlling roles of wall relaxation, solute uptake, and hydraulic conductance. *Int J Plant Sci*, **154**, 10-21.

Cosgrove, D.J. (1999) Enzymes and other agents that enhance cell wall extensibility. *Annu Rev Plant Physiol Plant Mol Biol*, **50**, 391-417.

Cosgrove, D.J. (2000a) Expansive growth of plant cell walls. *Plant Physiol Biochem*, **38**, 109-124.

Cosgrove, D.J. (2000b) Loosening of plant cell walls by expansins. *Nature*, **407**, 321-326.

Cosgrove, D.J. (2000c) New genes and new biological roles for expansins. *Curr Opin Plant Biol*, **3**, 73-78.

Cosgrove, D.J. (2001) Plant cell walls: wall-associated kinases and cell expansion. *Curr Biol*, **11**, R558-559.

Cosgrove, D.J. (2005) Growth of the plant cell wall. *Nat Rev Mol Cell Biol*, **6**, 850-861.

Coulibaly, I. and Page, G.P. (2008) Bioinformatic Tools for Inferring Functional Information from Plant Microarray Data II: Analysis Beyond Single Gene. *Int J Plant Genomics*, **2008**, 893941.

Cousson, A. (2001) Pharmacological evidence for the implication of both cyclic GMP-dependent and -independent transduction pathways within auxin-induced stomatal opening in *Commelina communis* L. *Plant Sci*, **161**, 249-258.

Cousson, A. (2003) Pharmacological evidence for a positive influence of the cyclic GMP-independent transduction on the cyclic GMP-mediated Ca^{2+}-dependent pathway within the *Arabidopsis* stomatal opening in response to auxin. *Plant Sci*, **164**, 759–767.

Cousson, A. (2004) Pharmacological evidence for a putative mediation of cyclic GMP and cytosolic Ca^{2+} within auxin-induced de novo root formation in the monocot plant Commelina communis L. *Plant Sci*, **166**, 1117–1124.

Cousson, A. and Vavasseur, A. (1998) Putative involvement of cytosolic Ca^{2+} and GTP-binding proteins in cyclic-GMP-mediated induction of stomatal opening by auxin in Commelina communis L. *Planta*, **206**, 308-314.

Covic, L., Silva, N.F. and Lew, R.R. (1999) Functional characterization of ARAKIN (ATMEKK1): a possible mediator in an osmotic stress response pathway in higher plants. *Biochim Biophys Acta*, **1451**, 242-254.

Craigon, D.J., James, N., Okyere, J., Higgins, J., Jotham, J. and May, S. (2004) NASCArrays: a repository for microarray data generated by NASC's transcriptomics service. *Nucleic Acids Res*, **32**, D575-577.

Cuin, T.A. and Shabala, S. (2005) Exogenously supplied compatible solutes rapidly ameliorate NaCl-induced potassium efflux from barley roots. *Plant Cell Physiol*, **46**, 1924-1933.

Cunnac, S., Lindeberg, M. and Collmer, A. (2009) *Pseudomonas syringae* type III secretion system effectors: repertoires in search of functions. *Curr Opin Microbiol*, **12**, 53-60.

Dangl, J.L. and Jones, J.D. (2001) Plant pathogens and integrated defence responses to infection. *Nature*, **411**, 826-833.

Daxinger, L., Hunter, B., Sheikh, M., Jauvion, V., Gasciolli, V., Vaucheret, H., Matzke, M. and Furner, I. (2008) Unexpected silencing effects from T-DNA tags in *Arabidopsis*. *Trends Plant Sci*, **13**, 4-6.

Day, B., Dahlbeck, D. and Staskawicz, B.J. (2006) NDR1 interaction with RIN4 mediates the differential activation of multiple disease resistance pathways in *Arabidopsis*. *Plant Cell*, **18**, 2782-2791.

de Bold, A.J., Borenstein, H.B., Veress, A.T. and Sonnenberg, H. (1981) A rapid and potent natriuretic response to intravenous injection of atrial myocardial extract in rats. *Life Sci*, **28**, 89-94.

de Torres-Zabala, M., Truman, W., Bennett, M.H., Lafforgue, G., Mansfield, J.W., Rodriguez Egea, P., Bogre, L. and Grant, M. (2007) *Pseudomonas syringae* pv. *tomato* hijacks the *Arabidopsis* abscisic acid signalling pathway to cause disease. *Embo J*, **26**, 1434-1443.

de Torres, M., Mansfield, J.W., Grabov, N., Brown, I.R., Ammouneh, H., Tsiamis, G., Forsyth, A., Robatzek, S., Grant, M. and Boch, J. (2006) *Pseudomonas syringae* effector AvrPtoB suppresses basal defence in *Arabidopsis*. *Plant J*, **47**, 368–382.

Demidchik, V., Davenport, R.J. and Tester, M. (2002) Nonselective cation channels in plants. *Annu Rev Plant Biol*, **53**, 67-107.

Demidchik, V., Shabala, S.N. and Davies, J.M. (2007) Spatial variation in H_2O_2 response of *Arabidopsis thaliana* root epidermal Ca^{2+} flux and plasma membrane Ca^{2+} channels. *Plant J*, **49**, 377-386.

Demidchik, V. and Tester, M. (2002) Sodium fluxes through nonselective cation channels in the plasma membrane of protoplasts from Arabidopsis roots. *Plant Physiol*, **128**, 379-387.

Denby, K. and Gehring, C. (2005) Engineering drought and salinity tolerance in plants: lessons from genome-wide expression profiling in *Arabidopsis*. *Trends Biotechnol*, **23**, 547-552.

Denby, K.J., Kumar, P. and Kliebenstein, D.J. (2004) Identification of *Botrytis cinerea* susceptibility loci in *Arabidopsis thaliana*. *Plant J*, **38**, 473-486.

Desikan, R., Cheung, M.K., Bright, J., Henson, D., Hancock, J.T. and Neill, S.J. (2004) ABA, hydrogen peroxide and nitric oxide signalling in stomatal guard cells. *J Exp Bot*, **55**, 205-212.

Despres, C., Chubak, C., Rochon, A., Clark, R., Bethune, T., Desveaux, D. and Fobert, P.R. (2003) The *Arabidopsis* NPR1 disease resistance protein is a novel cofactor that confers redox regulation of DNA binding activity to the basic domain/leucine zipper transcription factor TGA1. *Plant Cell*, **15**, 2181-2191.

Desveaux, D., Subramaniam, R., Despres, C., Mess, J.N., Levesque, C., Fobert, P.R., Dangl, J.L. and Brisson, N. (2004) A "Whirly" transcription factor is required for salicylic acid-dependent disease resistance in *Arabidopsis*. *Dev Cell*, **6**, 229-240.

Dewdney, J., Reuber, T.L., Wildermuth, M.C., Devoto, A., Cui, J., Stutius, L.M., Drummond, E.P. and Ausubel, F.M. (2000) Three unique mutants of *Arabidopsis* identify *eds* loci required for limiting growth of a biotrophic fungal pathogen. *Plant J*, **24**, 205-218.

Dolan, L. and Davies, J. (2004) Cell expansion in roots. *Curr Opin Plant Biol*, **7**, 33-39.

Dolmetsch, R.E., Lewis, R.S., Goodnow, C.C. and Healy, J.I. (1997) Differential activation of transcription factors induced by Ca^{2+} response amplitude and duration. *Nature*, **386**, 855-858.

Donaldson, L., Ludidi, N., Knight, M.R., Gehring, C. and Denby, K. (2004) Salt and osmotic stress cause rapid increases in *Arabidopsis thaliana* cGMP levels. *FEBS Lett*, **569**, 317-320.

Dong, X. (2004) NPR1, all things considered. *Curr Opin Plant Biol*, **7**, 547-552.

Dubovskaya, L.V., Molchan, O.V. and Volotovsky, I.D. (2001) Photoregulation of the Endogenous cGMP Content in Oat Seedlings. *Russ. J. Plant Physiol.*, **48**, 19-22.

Dubovskaya, L.V., Molchan, O.V. and Volotovsky, I.D. (2002) Cyclic GMP-binding activity in *Avena sativa* seedlings. *Russ. J. Plant Physiol.*, **49**, 216–220.

Duda, T., Venkataraman, V., Ravichandran, S. and Sharma, R.K. (2005) ATP-regulated module (ARM) of the atrial natriuretic factor receptor guanylate cyclase. *Peptides*, **26**, 969-984.

Durner, J., Wendehenne, D. and Klessig, D.F. (1998) Defense gene induction in tobacco by nitric oxide, cyclic GMP, and cyclic ADP-ribose. *Proc Natl Acad Sci U S A*, **95**, 10328-10333.

Durrant, W.E. and Dong, X. (2004) Systemic acquired resistance. *Annu Rev Phytopathol*, **42**, 185-209.

Edgar, R., Domrachev, M. and Lash, A.E. (2002) Gene Expression Omnibus: NCBI gene expression and hybridization array data repository. *Nucleic Acids Res*, **30**, 207-210.

Edwards, K., Johnstone, C. and Thompson, C. (1991) A simple and rapid method for the preparation of plant genomic DNA for PCR analysis. *Nucleic Acids Res*, **19**, 1349.

Eisen, M.B., Spellman, P.T., Brown, P.O. and Botstein, D. (1998) Cluster analysis and display of genome-wide expression patterns. *Proc Natl Acad Sci U S A*, **95**, 14863-14868.

Essah, P.A., Davenport, R. and Tester, M. (2003) Sodium influx and accumulation in *Arabidopsis*. *Plant Physiol*, **133**, 307-318.

Eulgem, T. (2005) Regulation of the *Arabidopsis* defense transcriptome. *Trends Plant Sci*, **10**, 71-78.

Eulgem, T., Weigman, V.J., Chang, H.S., McDowell, J.M., Holub, E.B., Glazebrook, J., Zhu, T. and Dangl, J.L. (2004) Gene expression signatures from three genetically separable resistance gene signaling pathways for downy mildew resistance. *Plant Physiol*, **135**, 1129-1144.

Evans, N.H., McAinsh, M.R., Hetherington, A.M. and Knight, M.R. (2005) ROS perception in *Arabidopsis thaliana*: the ozone-induced calcium response. *Plant J*, **41**, 615-626.

Fan, W. and Dong, X. (2002) In vivo interaction between NPR1 and transcription factor TGA2 leads to salicylic acid-mediated gene activation in *Arabidopsis*. *Plant Cell*, **14**, 1377-1389.

Feil, R. and Kemp-Harper, B. (2006) cGMP signalling: from bench to bedside. Conference on cGMP generators, effectors and therapeutic implications. *EMBO Rep*, **7**, 149-153.

Ferjani, A., Horiguchi, G., Yano, S. and Tsukaya, H. (2007) Analysis of leaf development in *fugu* mutants of *Arabidopsis* reveals three compensation modes that modulate cell expansion in determinate organs. *Plant Physiol*, **144**, 988-999.

Ferrari, S., Plotnikova, J.M., De Lorenzo, G. and Ausubel, F.M. (2003) *Arabidopsis* local resistance to *Botrytis cinerea* involves salicylic acid and camalexin and requires EDS4 and PAD2, but not SID2, EDS5 or PAD4. *Plant J*, **35**, 193-205.

Feys, B.J., Moisan, L.J., Newman, M.A. and Parker, J.E. (2001) Direct interaction between the *Arabidopsis* disease resistance signaling proteins, EDS1 and PAD4. *Embo J*, **20**, 5400-5411.

Finkelstein, R.R., Gampala, S.S. and Rock, C.D. (2002) Abscisic acid signaling in seeds and seedlings. *Plant Cell*, **14 Suppl**, S15-45.

Flynn, T.G., de Bold, M.L. and de Bold, A.J. (1983) The amino acid sequence of an atrial peptide with potent diuretic and natriuretic properties. *Biochem Biophys Res Commun*, **117**, 859-865.

Fogel, G.B., Weekes, D.G., Varga, G., Dow, E.R., Craven, A.M., Harlow, H.B., Su, E.W., Onyia, J.E. and Su, C. (2005) A statistical analysis of the TRANSFAC database. *Biosystems*, **81**, 137-154.

Forssmann, W., Meyer, M. and Forssmann, K. (2001) The renal urodilatin system: clinical implications. *Cardiovasc Res*, **51**, 450-462.

Fraser, H.B., Hirsh, A.E., Wall, D.P. and Eisen, M.B. (2004) Coevolution of gene expression among interacting proteins. *Proc Natl Acad Sci U S A*, **101**, 9033-9038.

Fricke, W., Leigh, R.A. and Tomos, A.D. (1994) Concentrations of inorganic and organic solutes in extracts from individual epidermal, mesophyll and bundle sheath cells of barley leaves. *Planta*, **192**, 310-316.

Frietsch, S., Wang, Y.F., Sladek, C., Poulsen, L.R., Romanowsky, S.M., Schroeder, J.I. and Harper, J.F. (2007) A cyclic nucleotide-gated channel is essential for polarized tip growth of pollen. *Proc Natl Acad Sci U S A*, **104**, 14531-14536.

Fu, H.H. and Luan, S. (1998) AtKuP1: a dual-affinity K^+ transporter from *Arabidopsis*. *Plant Cell*, **10**, 63-73.

Fujita, M., Fujita, Y., Noutoshi, Y., Takahashi, F., Narusaka, Y., Yamaguchi-Shinozaki, K. and Shinozaki, K. (2006) Crosstalk between abiotic and biotic stress responses: a current view from the points of convergence in the stress signaling networks. *Curr Opin Plant Biol*, **9**, 436-442.

Fujita, M., Mizukado, S., Fujita, Y., Ichikawa, T., Nakazawa, M., Seki, M., Matsui, M., Yamaguchi-Shinozaki, K. and Shinozaki, K. (2007) Identification of stress-tolerance-related transcription-factor genes via mini-scale Full-length cDNA Over-eXpressor (FOX) gene hunting system. *Biochem Biophys Res Commun*, **364**, 250-257.

Fuller, F., Porter, J.G., Arfsten, A.E., Miller, J., Schilling, J.W., Scarborough, R.M., Lewicki, J.A. and Schenk, D.B. (1988) Atrial natriuretic peptide clearance receptor. Complete sequence and functional expression of cDNA clones. *J Biol Chem*, **263**, 9395-9401.

Gao, D., Knight, M.R., Trewavas, A.J., Sattelmacher, B. and Plieth, C. (2004) Self-reporting *Arabidopsis* expressing pH and [Ca^{2+}] indicators unveil ion dynamics in the cytoplasm and in the apoplast under abiotic stress. *Plant Physiol*, **134**, 898-908.

Gao, X., Ren, F. and Lu, Y.T. (2006) The *Arabidopsis* mutant *stg1* identifies a function for TBP-associated factor 10 in plant osmotic stress adaptation. *Plant Cell Physiol*, **47**, 1285-1294.

Gao, X., Ren, Z., Zhao, Y. and Zhang, H. (2003) Overexpression of SOD2 increases salt tolerance of *Arabidopsis*. *Plant Physiol*, **133**, 1873-1881.

Gehring, C.A. and Irving, H.R. (2003) Natriuretic peptides--a class of heterologous molecules in plants. *Int J Biochem Cell Biol*, **35**, 1318-1322.

Gehring, C.A., Khalid, K.M., Toop, T. and Donald, J.A. (1996) Rat natriuretic peptide binds specifically to plant membranes and induces stomatal opening. *Biochem Biophys Res Commun*, **228**, 739-744.

Ginalski, K. and Zemojtel, T. (2004) ECEPE proteins: a novel family of eukaryotic cysteine proteinases. *Trends Biochem Sci*, **29**, 524-526.

Glazebrook, J. (2005) Contrasting mechanisms of defense against biotrophic and necrotrophic pathogens. *Annu Rev Phytopathol*, **43**, 205-227.

Gobert, A., Park, G., Amtmann, A., Sanders, D. and Maathuis, F.J. (2006) *Arabidopsis thaliana* cyclic nucleotide gated channel 3 forms a non-selective ion transporter involved in germination and cation transport. *J Exp Bot*, **57**, 791-800.

Goda, H., Sasaki, E., Akiyama, K., Maruyama-Nakashita, A., Nakabayashi, K., Li, W., Ogawa, M., Yamauchi, Y., Preston, J., Aoki, K., Kiba, T., Takatsuto, S., Fujioka, S., Asami, T., Nakano, T., Kato, H., Mizuno, T., Sakakibara, H., Yamaguchi, S., Nambara, E., Kamiya, Y., Takahashi, H., Hirai, M.Y., Sakurai, T., Shinozaki, K., Saito, K., Yoshida, S. and Shimada, Y. (2008) The AtGenExpress hormone and chemical treatment data set: experimental design, data evaluation, model data analysis and data access. *Plant J*, **55**, 526-542.

Goel, A.K., Lundberg, D., Torres, M.A., Matthews, R., Akimoto-Tomiyama, C., Farmer, L., Dangl, J.L. and Grant, S.R. (2008) The *Pseudomonas syringae* type III effector HopAM1 enhances virulence on water-stressed plants. *Mol Plant Microbe Interact*, **21**, 361-370.

Gohre, V. and Robatzek, S. (2008) Breaking the barriers: microbial effector molecules subvert plant immunity. *Annu Rev Phytopathol*, **46**, 189-215.

Gong, D., Guo, Y., Schumaker, K.S. and Zhu, J.K. (2004) The SOS3 family of calcium sensors and SOS2 family of protein kinases in *Arabidopsis*. *Plant Physiol*, **134**, 919-926.

Gonzalez-Guzman, M., Abia, D., Salinas, J., Serrano, R. and Rodriguez, P.L. (2004) Two new alleles of the *abscisic aldehyde oxidase 3* gene reveal its role in abscisic acid biosynthesis in seeds. *Plant Physiol*, **135**, 325-333.

Gonzalez-Guzman, M., Apostolova, N., Belles, J.M., Barrero, J.M., Piqueras, P., Ponce, M.R., Micol, J.L., Serrano, R. and Rodriguez, P.L. (2002) The short-chain alcohol dehydrogenase ABA2 catalyzes the conversion of xanthoxin to abscisic aldehyde. *Plant Cell*, **14**, 1833-1846.

Gottig, N., Garavaglia, B.S., Daurelio, L.D., Valentine, A., Gehring, C., Orellano, E.G. and Ottado, J. (2008) *Xanthomonas axonopodis* pv. *citri* uses a plant natriuretic peptide-like protein to modify host homeostasis. *Proc Natl Acad Sci U S A*, **105**, 18631-18636.

Govrin, E.M. and Levine, A. (2000) The hypersensitive response facilitates plant infection by the necrotrophic pathogen *Botrytis cinerea*. *Curr Biol*, **10**, 751-757.

Grant, M., Brown, I., Adams, S., Knight, M., Ainslie, A. and Mansfield, J. (2000) The *RPM1* plant disease resistance gene facilitates a rapid and sustained increase in cytosolic calcium that is necessary for the oxidative burst and hypersensitive cell death. *Plant J*, **23**, 441-450.

Greenberg, J.T. and Yao, N. (2004) The role and regulation of programmed cell death in plant-pathogen interactions. *Cell Microbiol*, **6**, 201-211.

Greenshields, D.L. and Jones, J.D. (2008) Plant pathogen effectors: getting mixed messages. *Curr Biol*, **18**, R128-130.

Gupta, A.S., Berkowitz, G.A. and Pier, P.A. (1989) Maintenance of Photosynthesis at Low Leaf Water Potential in Wheat : Role of Potassium Status and Irrigation History. *Plant Physiol*, **89**, 1358-1365.

Halfter, U., Ishitani, M. and Zhu, J.K. (2000) The *Arabidopsis* SOS2 protein kinase physically interacts with and is activated by the calcium-binding protein SOS3. *Proc Natl Acad Sci U S A*, **97**, 3735-3740.

Ham, J.H., Kim, M.G., Lee, S.Y. and Mackey, D. (2007) Layered basal defenses underlie non-host resistance of *Arabidopsis* to *Pseudomonas syringae* pv. *phaseolicola*. *Plant J*, **51**, 604-616.

Hamburger, D., Rezzonico, E., MacDonald-Comber Petetot, J., Somerville, C. and Poirier, Y. (2002) Identification and characterization of the *Arabidopsis PHO1* gene involved in phosphate loading to the xylem. *Plant Cell*, **14**, 889-902.

Hamet, P., Tremblay, J., Pang, S.C., Garcia, R., Thibault, G., Gutkowska, J., Cantin, M. and Genest, J. (1984) Effect of native and synthetic atrial natriuretic factor on cyclic GMP. *Biochem Biophys Res Commun*, **123**, 515-527.

Hammond, J.P., Bennett, M.J., Bowen, H.C., Broadley, M.R., Eastwood, D.C., May, S.T., Rahn, C., Swarup, R., Woolaway, K.E. and White, P.J. (2003) Changes in gene expression in *Arabidopsis* shoots during phosphate starvation and the potential for developing smart plants. *Plant Physiol*, **132**, 578-596.

Hampton, C.R., Bowen, H.C., Broadley, M.R., Hammond, J.P., Mead, A., Payne, K.A., Pritchard, J. and White, P.J. (2004) Cesium toxicity in *Arabidopsis*. *Plant Physiol*, **136**, 3824-3837.

Hardingham, G.E., Chawla, S., Johnson, C.M. and Bading, H. (1997) Distinct functions of nuclear and cytoplasmic calcium in the control of gene expression. *Nature*, **385**, 260-265.

Hauck, P., Thilmony, R. and He, S.Y. (2003) A *Pseudomonas syringae* type III effector suppresses cell wall-based extracellular defense in susceptible *Arabidopsis* plants. *Proc Natl Acad Sci U S A*, **100**, 8577-8582.

Haugh, G.W. and Sommerville, C. (1986) Sulfonylurea-resistant mutants of *Arabidopsis thaliana*. *Mol Gen Genetics*, **204**, 430-434.

He, X.L., Dukkipati, A. and Garcia, K.C. (2006) Structural determinants of natriuretic peptide receptor specificity and degeneracy. *J Mol Biol*, **361**, 698-714.

He, X.L., Dukkipati, A., Wang, X. and Garcia, K.C. (2005) A new paradigm for hormone recognition and allosteric receptor activation revealed from structural studies of NPR-C. *Peptides*, **26**, 1035-1043.

He, Z.H., He, D. and Kohorn, B.D. (1998) Requirement for the induced expression of a cell wall associated receptor kinase for survival during the pathogen response. *Plant J*, **14**, 55-63.

Heidel, A.J., Clarke, J.D., Antonovics, J. and Dong, X. (2004) Fitness costs of mutations affecting the systemic acquired resistance pathway in *Arabidopsis thaliana*. *Genetics*, **168**, 2197-2206.

Hermans, C., Hammond, J.P., White, P.J. and Verbruggen, N. (2006) How do plants respond to nutrient shortage by biomass allocation? *Trends Plant Sci*, **11**, 610-617.

Himelblau, E. and Amasino, R.M. (2001) Nutrients mobilized from leaves of *Arabidopsis thaliana* during leaf senescence. *J Plant Physiol*, **158**, 1317-1323.

Hirschi, K.D. (1999) Expression of *Arabidopsis* CAX1 in tobacco: altered calcium homeostasis and increased stress sensitivity. *Plant Cell*, **11**, 2113-2122.

Hirschi, K.D. (2003) Insertional mutants: a foundation for assessing gene function. *Trends Plant Sci*, **8**, 205-207.

Hoefle, C. and Huckelhoven, R. (2008) Enemy at the gates: traffic at the plant cell pathogen interface. *Cell Microbiol*, **10**, 2400-2407.

Hoffmann-Sommergruber, K. (2002) Pathogenesis-related (PR)-proteins identified as allergens. *Biochem Soc Trans*, **30**, 930-935.

Hofmann, F., Feil, R., Kleppisch, T. and Schlossmann, J. (2006) Function of cGMP-dependent protein kinases as revealed by gene deletion. *Physiol Rev*, **86**, 1-23.

Holsters, M., Silva, B., Van Vliet, F., Genetello, C., De Block, M., Dhaese, P., Depicker, A., Inze, D., Engler, G., Villarroel, R. and et al. (1980) The functional organization of the nopaline *A. tumefaciens* plasmid pTiC58. *Plasmid*, **3**, 212-230.

Horiguchi, G., Ferjani, A., Fujikura, U. and Tsukaya, H. (2006) Coordination of cell proliferation and cell expansion in the control of leaf size in *Arabidopsis thaliana*. *J Plant Res*, **119**, 37-42.

Horvath, E., Szalai, G. and Janda, T. (2007) Induction of abiotic stress tolerance by salicylic signalling. *J Plant Growth Regul*, **26**, 290-300.

Howe, G.A. and Jander, G. (2008) Plant immunity to insect herbivores. *Annu Rev Plant Biol*, **59**, 41-66.

Hruz, T., Laule, O., Szabo, G., Wessendorp, F., Bleuler, S., Oertle, L., Widmayer, P., Gruissem, W. and Zimmermann, P. (2008) Genevesigator V3: A reference expression database for the meta-analysis of transcriptomes. *Adv Bioinformatics*, **2008**, 420747.

Hu, X., Neill, S.J., Tang, Z. and Cai, W. (2005) Nitric oxide mediates gravitropic bending in soybean roots. *Plant Physiol*, **137**, 663-670.

Hua, B.-G., Mercier, R.W., Zielinski, R.E. and Berkowitz, G.A. (2003a) Functional interaction of calmodulin with a plant cyclic nucleotide gated cation channel. *Plant Physiol Biochem*, **41**, 945-954.

Hua, B.G., Mercier, R.W., Leng, Q. and Berkowitz, G.A. (2003b) Plants do it differently. A new basis for potassium/sodium selectivity in the pore of an ion channel. *Plant Physiol*, **132**, 1353-1361.

Hussain, T.M., Chandrasekhar, T., Hazara, M., Sultan, Z., Saleh, B.K. and Gopal, G.R. (2008) Recent advances in salt stress biology – a review. *Biotech Mol Biol Rev*, **3**, 8-13.

Ichimura, K., Mizoguchi, T., Irie, K., Morris, P., Giraudat, J., Matsumoto, K. and Shinozaki, K. (1998) Isolation of ATMEKK1 (a MAP kinase kinase kinase)-interacting proteins and analysis of a MAP kinase cascade in *Arabidopsis*. *Biochem Biophys Res Commun*, **253**, 532-543.

Ingle, R.A., Carstens, M. and Denby, K.J. (2006) PAMP recognition and the plant-pathogen arms race. *Bioessays*, **28**, 880-889.

Inoue, K., Naruse, K., Yamagami, S., Mitani, H., Suzuki, N. and Takei, Y. (2003) Four functionally distinct C-type natriuretic peptides found in fish reveal evolutionary history of the natriuretic peptide system. *Proc Natl Acad Sci U S A*, **100**, 10079-10084.

Inoue, K., Sakamoto, T., Yuge, S., Iwatani, H., Yamagami, S., Tsutsumi, M., Hori, H., Cerra, M.C., Tota, B., Suzuki, N., Okamoto, N. and Takei, Y. (2005) Structural and functional evolution of three cardiac natriuretic peptides. *Mol Biol Evol*, **22**, 2428-2434.

Irving, H.R., Gehring, C.A. and Parish, R.W. (1992) Changes in cytosolic pH and calcium of guard cells precede stomatal movements. *Proc Natl Acad Sci U S A*, **89**, 1790-1794.

Ishitani, M., Liu, J., Halfter, U., Kim, C.S., Shi, W. and Zhu, J.K. (2000) SOS3 function in plant salt tolerance requires N-myristoylation and calcium binding. *Plant Cell*, **12**, 1667-1678.

Ishitani, M., Xiong, L., Stevenson, B. and Zhu, J.K. (1997) Genetic analysis of osmotic and cold stress signal transduction in *Arabidopsis*: interactions and convergence of abscisic acid-dependent and abscisic acid-independent pathways. *Plant Cell*, **9**, 1935-1949.

Javot, H. and Maurel, C. (2002) The role of aquaporins in root water uptake. *Ann Bot (Lond)*, **90**, 301-313.

Jing, H.C., Anderson, L., Sturre, M.J., Hille, J. and Dijkwel, P.P. (2007) *Arabidopsis CPR5* is a senescence-regulatory gene with pleiotropic functions as predicted by the evolutionary theory of senescence. *J Exp Bot*, **58**, 3885-3894.

Johnson, C., Boden, E. and Arias, J. (2003) Salicylic acid and NPR1 induce the recruitment of trans-activating TGA factors to a defense gene promoter in *Arabidopsis*. *Plant Cell*, **15**, 1846-1858.

Jones, J.D. and Dangl, J.L. (2006) The plant immune system. *Nature*, **444**, 323-329.

Kaldenhoff, R., Grote, K., Zhu, J.J. and Zimmermann, U. (1998) Significance of plasmalemma aquaporins for water-transport in *Arabidopsis thaliana*. *Plant J*, **14**, 121-128.

Kang, J.S., Frank, J., Kang, C.H., Kajiura, H., Vikram, M., Ueda, A., Kim, S., Bahk, J.D., Triplett, B., Fujiyama, K., Lee, S.Y., von Schaewen, A. and Koiwa, H. (2008) Salt tolerance of *Arabidopsis thaliana* requires maturation of N-glycosylated proteins in the Golgi apparatus. *Proc Natl Acad Sci U S A*, **105**, 5933-5938.

Kankainen, M. and Holm, L. (2004) POBO, transcription factor binding site verification with bootstrapping. *Nucleic Acids Res*, **32**, W222-229.

Kaplan, B., Sherman, T. and Fromm, H. (2007) Cyclic nucleotide-gated channels in plants. *FEBS Lett*, **581**, 2237-2246.

Karley, A.J., Leigh, R.A. and Sanders, D. (2000) Differential ion accumulation and ion fluxes in the mesophyll and epidermis of barley. *Plant Physiol*, **122**, 835-844.

Katagiri, F., Lam, E. and Chua, N.H. (1989) Two tobacco DNA-binding proteins with homology to the nuclear factor CREB. *Nature*, **340**, 727-730.

Katagiri, F., Thilmonv, R. and He, S.Y. (2002) *The Arabidopsis thaliana-Pseudomonas syringae interaction*. Rockville, MD: American Society of Plant Biologists.

Katiyar-Agarwal, S., Zhu, J., Kim, K., Agarwal, M., Fu, X., Huang, A. and Zhu, J.K. (2006) The plasma membrane Na^+/H^+ antiporter SOS1 interacts with RCD1 and functions in oxidative stress tolerance in *Arabidopsis*. *Proc Natl Acad Sci U S A*, **103**, 18816-18821.

Kauffmann, S., Legrand, M., Geoffroy, P. and Fritig, B. (1987) Biological function of ;pathogenesis-related' proteins: four PR proteins of tobacco have 1,3-beta-glucanase activity. *Embo J*, **6**, 3209-3212.

Kaur, N. and Gupta, A.K. (2005) Signal transduction pathways under abiotic stresses in plants. *Curr Sci*, **88**, 1771-1780.

Kawakoshi, A., Hyodo, S., Nozaki, M. and Takei, Y. (2006) Identification of a natriuretic peptide (NP) in cyclostomes (lamprey and hagfish): CNP-4 is the ancestral gene of the NP family. *Gen Comp Endocrinol*, **148**, 41-47.

Kawakoshi, A., Hyodo, S., Yasuda, A. and Takei, Y. (2003) A single and novel natriuretic peptide is expressed in the heart and brain of the most primitive vertebrate, the hagfish (Eptatretus burgeri). *J Mol Endocrinol*, **31**, 209-220.

Kehr, J., Buhtz, A. and Giavalisco, P. (2005) Analysis of xylem sap proteins from *Brassica napus*. *BMC Plant Biol*, **5**, 11.

Kiegle, E., Moore, C.A., Haseloff, J., Tester, M.A. and Knight, M.R. (2000) Cell-type-specific calcium responses to drought, salt and cold in the *Arabidopsis* root. *Plant J*, **23**, 267-278.

Kilian, J., Whitehead, D., Horak, J., Wanke, D., Weinl, S., Batistic, O., D'Angelo, C., Bornberg-Bauer, E., Kudla, J. and Harter, K. (2007) The AtGenExpress global stress expression data set: protocols, evaluation and model data analysis of UV-B light, drought and cold stress responses. *Plant J*, **50**, 347-363.

Kim, B.G., Waadt, R., Cheong, Y.H., Pandey, G.K., Dominguez-Solis, J.R., Schultke, S., Lee, S.C., Kudla, J. and Luan, S. (2007) The calcium sensor CBL10 mediates salt tolerance by regulating ion homeostasis in Arabidopsis. *Plant J*, **52**, 473-484.

Kim, M.G., da Cunha, L., McFall, A.J., Belkhadir, Y., DebRoy, S., Dangl, J.L. and Mackey, D. (2005) Two *Pseudomonas syringae* type III effectors inhibit RIN4-regulated basal defense in *Arabidopsis*. *Cell*, **121**, 749-759.

King, E.O., Ward, M.K. and Raney, D.E. (1954) Two simple media for the demonstration of pyocyanin and fluorescin. *J Lab Clin Med*, **44**, 301-307.

Kinkema, M., Fan, W. and Dong, X. (2000) Nuclear localization of NPR1 is required for activation of *PR* gene expression. *Plant Cell*, **12**, 2339-2350.

Kjellbom, P., Larsson, C., Johansson, I.I., Karlsson, M. and Johanson, U. (1999) Aquaporins and water homeostasis in plants. *Trends Plant Sci*, **4**, 308-314.

Kliebenstein, D.J., Rowe, H.C. and Denby, K.J. (2005) Secondary metabolites influence *Arabidopsis*/*Botrytis* interactions: variation in host production and pathogen sensitivity. *Plant J*, **44**, 25-36.

Knight, H. and Knight, M.R. (2001) Abiotic stress signalling pathways: specificity and cross-talk. *Trends Plant Sci*, **6**, 262-267.

Knight, H., Trewavas, A.J. and Knight, M.R. (1996) Cold calcium signaling in *Arabidopsis* involves two cellular pools and a change in calcium signature after acclimation. *Plant Cell*, **8**, 489-503.

Knight, H., Trewavas, A.J. and Knight, M.R. (1997) Calcium signalling in *Arabidopsis thaliana* responding to drought and salinity. *Plant J*, **12**, 1067-1078.

Knight, M.R., Campbell, A.K., Smith, S.M. and Trewavas, A.J. (1991) Transgenic plant aequorin reports the effects of touch and cold-shock and elicitors on cytoplasmic calcium. *Nature*, **352**, 524-526.

Knoth, C., Ringler, J., Dangl, J.L. and Eulgem, T. (2007) *Arabidopsis* WRKY70 is required for full RPP4-mediated disease resistance and basal defense against *Hyaloperonospora parasitica*. *Mol Plant Microbe Interact*, **20**, 120-128.

Koch, E. and Slusarenko, A. (1990) *Arabidopsis* is susceptible to infection by a downy mildew fungus. *Plant Cell*, **2**, 437-445.

Koda, Y., Takahashi, K., Kikuta, Y., Greulich, F., Toshima, H. and Ichihara, A. (1996) Similarities of the biological activities of coronatine and coronafacic acid to those of jasmonic acid. *Phytochemistry*, **41**, 93-96.

Kohler, C., Merkle, T., Roby, D. and Neuhaus, G. (2001) Developmentally regulated expression of a cyclic nucleotide-gated ion channel from *Arabidopsis* indicates its involvement in programmed cell death. *Planta*, **213**, 327-332.

Kohler, C. and Neuhaus, G. (2000) Characterisation of calmodulin binding to cyclic nucleotide-gated ion channels from *Arabidopsis thaliana*. *FEBS Lett*, **471**, 133-136.

Koiwa, H., Li, F., McCully, M.G., Mendoza, I., Koizumi, N., Manabe, Y., Nakagawa, Y., Zhu, J., Rus, A., Pardo, J.M., Bressan, R.A. and Hasegawa, P.M. (2003) The STT3a subunit isoform of the *Arabidopsis* oligosaccharyltransferase controls adaptive responses to salt/osmotic stress. *Plant Cell*, **15**, 2273-2284.

Koornneef, A. and Pieterse, C.M. (2008) Cross talk in defense signaling. *Plant Physiol*, **146**, 839-844.

Kourie, J.I. and Rive, M.J. (1999) Role of natriuretic peptides in ion transport mechanisms. *Med Res Rev*, **19**, 75-94.

Kreps, J.A., Wu, Y., Chang, H.S., Zhu, T., Wang, X. and Harper, J.F. (2002) Transcriptome changes for *Arabidopsis* in response to salt, osmotic, and cold stress. *Plant Physiol*, **130**, 2129-2141.

Kuhn, M. (2004) Molecular physiology of natriuretic peptide signalling. *Basic Res Cardiol*, **99**, 76-82.

Kuhn, M. (2005) Cardiac and intestinal natriuretic peptides: insights from genetically modified mice. *Peptides*, **26**, 1078-1085.

Kuno, T., Andresen, J.W., Kamisaki, Y., Waldman, S.A., Chang, L.Y., Saheki, S., Leitman, D.C., Nakane, M. and Murad, F. (1986) Co-purification of an atrial natriuretic factor receptor and particulate guanylate cyclase from rat lung. *J Biol Chem*, **261**, 5817-5823.

Kunz, B.A., Dando, P.K., Grice, D.M., Mohr, P.G., Schenk, P.M. and Cahill, D.M. (2008) UV-induced DNA damage promotes resistance to the biotrophic pathogen *Hyaloperonospora parasitica* in *Arabidopsis*. *Plant Physiol*, **148**, 1021-1031.

Kurosaki, F. and Kaburaki, H. (1995) Phosphodiesterase isoenzymes in cell extracts of cultured carrot. *Phytochemistry*, **40**, 685-689.

Kwak, J.M., Mori, I.C., Pei, Z.M., Leonhardt, N., Torres, M.A., Dangl, J.L., Bloom, R.E., Bodde, S., Jones, J.D. and Schroeder, J.I. (2003) NADPH oxidase AtrbohD and AtrbohF genes function in ROS-dependent ABA signaling in *Arabidopsis*. *Embo J*, **22**, 2623-2633.

Kwezi, L., Meier, S., Mungur, L., Ruzvidzo, O., Irving, H. and Gehring, C. (2007) The *Arabidopsis thaliana* brassinosteroid receptor (AtBRI1) contains a domain that functions as a guanylyl cyclase in vitro. *PLoS ONE*, **2**, e449.

Kwon, C., Neu, C., Pajonk, S., Yun, H.S., Lipka, U., Humphry, M., Bau, S., Straus, M., Kwaaitaal, M., Rampelt, H., El Kasmi, F., Jurgens, G., Parker, J., Panstruga, R., Lipka, V. and Schulze-Lefert, P. (2008) Co-option of a default secretory pathway for plant immune responses. *Nature*, **451**, 835-840.

Lafontan, M., Moro, C., Berlan, M., Crampes, F., Sengenes, C. and Galitzky, J. (2008) Control of lipolysis by natriuretic peptides and cyclic GMP. *Trends Endocrinol Metab*, **19**, 130-137.

Lally, D., Ingmire, P., Tong, H.Y. and He, Z.H. (2001) Antisense expression of a cell wall-associated protein kinase, *WAK4*, inhibits cell elongation and alters morphology. *Plant Cell*, **13**, 1317-1331.

LaPointe, M.C. (2005) Molecular regulation of the brain natriuretic peptide gene. *Peptides*, **26**, 944-956.

le Roex, A.P., Spath, A. and Zartman, R.E. (2001) Lithospheric thickness beneath the southern Kenya Rift: implications from basalt geochemistry. *Contrib. Mineral. Petrol.*, **142**, 89-106.

Lebel, E., Heifetz, P., Thorne, L., Uknes, S., Ryals, J. and Ward, E. (1998) Functional analysis of regulatory sequences controlling *PR-1* gene expression in *Arabidopsis*. *Plant J*, **16**, 223-233.

Legrand, M., Kauffmann, S., Geoffroy, P. and Fritig, B. (1987) Biological function of pathogenesis-related proteins: Four tobacco pathogenesis-related proteins are chitinases. *Proc Natl Acad Sci U S A*, **84**, 6750-6754.

Leng, Q., Mercier, R.W., Hua, B.G., Fromm, H. and Berkowitz, G.A. (2002) Electrophysiological analysis of cloned cyclic nucleotide-gated ion channels. *Plant Physiol*, **128**, 400-410.

Leng, Q., Mercier, R.W., Yao, W. and Berkowitz, G.A. (1999) Cloning and first functional characterization of a plant cyclic nucleotide-gated cation channel. *Plant Physiol*, **121**, 753-761.

Li, J., Brader, G., Kariola, T. and Palva, E.T. (2006) WRKY70 modulates the selection of signaling pathways in plant defense. *Plant J*, **46**, 477-491.

Li, J., Brader, G. and Palva, E.T. (2004) The WRKY70 transcription factor: a node of convergence for jasmonate-mediated and salicylate-mediated signals in plant defense. *Plant Cell*, **16**, 319-331.

Li, W., Luan, S., Schreiber, S.L. and Assmann, S.M. (1994) Cyclic AMP stimulates K^+ channel activity in mesophyll cells of *Vicia faba* L. *Plant Physiol*, **106**, 957-961.

Li, X., Lin, H., Zhang, W., Zou, Y., Zhang, J., Tang, X. and Zhou, J.M. (2005) Flagellin induces innate immunity in nonhost interactions that is suppressed by *Pseudomonas syringae* effectors. *Proc Natl Acad Sci U S A*, **102**, 12990-12995.

Li, X., Zhang, Y., Clarke, J.D., Li, Y. and Dong, X. (1999) Identification and cloning of a negative regulator of systemic acquired resistance, SNI1, through a screen for suppressors of *npr1-1*. *Cell*, **98**, 329-339.

Li, Y., Jones, L. and McQueen-Mason, S. (2003) Expansins and cell growth. *Curr Opin Plant Biol*, **6**, 603-610.

Light, D.B., Corbin, J.D. and Stanton, B.A. (1990) Dual ion-channel regulation by cyclic GMP and cyclic GMP-dependent protein kinase. *Nature*, **344**, 336-339.

Lim, P.O., Woo, H.R. and Nam, H.G. (2003) Molecular genetics of leaf senescence in *Arabidopsis*. *Trends Plant Sci*, **8**, 272-278.

Lipka, U., Fuchs, R. and Lipka, V. (2008) *Arabidopsis* non-host resistance to powdery mildews. *Curr Opin Plant Biol*, **11**, 404-411.

Liu, J., Ishitani, M., Halfter, U., Kim, C.S. and Zhu, J.K. (2000) SOS3 function in plant salt tolerance requires N-myristoylation and calcium binding. *Plant Cell*, **12**.

Liu, J. and Zhu, J.K. (1997) An *Arabidopsis* mutant that requires increased calcium for potassium nutrition and salt tolerance. *Proc Natl Acad Sci U S A*, **94**, 14960-14964.

Lloyd, J.C. and Zakhleniuk, O.V. (2004) Responses of primary and secondary metabolism to sugar accumulation revealed by microarray expression analysis of the *Arabidopsis* mutant, *pho3*. *J Exp Bot*, **55**, 1221-1230.

Loake, G. and Grant, M. (2007) Salicylic acid in plant defence--the players and protagonists. *Curr Opin Plant Biol*, **10**, 466-472.

Logan, D.C. and Knight, M.R. (2003) Mitochondrial and cytosolic calcium dynamics are differentially regulated in plants. *Plant Physiol*, **133**, 21-24.

Logemann, E. and Hahlbrock, K. (2002) Crosstalk among stress responses in plants: pathogen defense overrides UV protection through an inversely regulated ACE/ACE type of light-responsive gene promoter unit. *Proc Natl Acad Sci U S A*, **99**, 2428-2432.

Lopez, M.A., Bannenberg, G. and Castresana, C. (2008) Controlling hormone signaling is a plant and pathogen challenge for growth and survival. *Curr Opin Plant Biol*, **11**, 420-427.

Loreto, F., Mannozzi, M., Maris, C., Nascetti, P., Ferranti, F. and Pasqualini, S. (2001) Ozone quenching properties of isoprene and its antioxidant role in leaves. *Plant Physiol*, **126**, 993-1000.

Lu, B., Gerard, N.P., Kolakowski, L.F., Jr., Bozza, M., Zurakowski, D., Finco, O., Carroll, M.C. and Gerard, C. (1995) Neutral endopeptidase modulation of septic shock. *J Exp Med*, **181**, 2271-2275.

Lucas, K.A., Pitari, G.M., Kazerounian, S., Ruiz-Stewart, I., Park, J., Schulz, S., Chepenik, K.P. and Waldman, S.A. (2000) Guanylyl cyclases and signaling by cyclic GMP. *Pharmacol Rev*, **52**, 375-414.

Ludidi, N. and Gehring, C. (2003) Identification of a novel protein with guanylyl cyclase activity in *Arabidopsis thaliana*. *J Biol Chem*, **278**, 6490-6494.

Ludidi, N., Morse, M., Sayed, M., Wherrett, T., Shabala, S. and Gehring, C. (2004) A recombinant plant natriuretic peptide causes rapid and spatially differentiated K^+, Na^+ and H^+ flux changes in *Arabidopsis thaliana* roots. *Plant Cell Physiol*, **45**, 1093-1098.

Ludidi, N.N., Heazlewood, J.L., Seoighe, C., Irving, H.R. and Gehring, C.A. (2002) Expansin-like molecules: novel functions derived from common domains. *J Mol Evol*, **54**, 587-594.

Luu, D.-T. and Maurel, C. (2005) Aquaporins in a challenging environment: molecular gears for adjusting plant water status. *Plant cell environ*, **28**, 85-96.

Maathuis, F.J. (2006) cGMP modulates gene transcription and cation transport in *Arabidopsis* roots. *Plant J*, **45**, 700-711.

Maathuis, F.J. and Sanders, D. (1995) Contrasting roles in ion transport of two K^+-channel types in root cells of *Arabidopsis thaliana*. *Planta*, **197**, 456-464.

Maathuis, F.J. and Sanders, D. (1999) Plasma membrane transport in context - making sense out of complexity. *Curr Opin Plant Biol*, **2**, 236-243.

Maathuis, F.J. and Sanders, D. (2001) Sodium uptake in *Arabidopsis* roots is regulated by cyclic nucleotides. *Plant Physiol*, **127**, 1617-1625.

Madhani, M., Scotland, R.S., MacAllister, R.J. and Hobbs, A.J. (2003) Vascular natriuretic peptide receptor-linked particulate guanylate cyclases are modulated by nitric oxide-cyclic GMP signalling. *Br J Pharmacol*, **139**, 1289-1296.

Maggio, A., Zhu, J.K., Hasegawa, P.M. and Bressan, R.A. (2006) Osmogenetics: Aristotle to *Arabidopsis*. *Plant Cell*, **18**, 1542-1557.

Mahajan, S., Pandey, G.K. and Tuteja, N. (2008) Calcium- and salt-stress signaling in plants: shedding light on SOS pathway. *Arch Biochem Biophys*, **471**, 146-158.

Mahalingam, R., Gomez-Buitrago, A., Eckardt, N., Shah, N., Guevara-Garcia, A., Day, P., Raina, R. and Fedoroff, N.V. (2003) Characterizing the stress/defense transcriptome of *Arabidopsis*. *Genome Biol*, **4**, R20.

Maleck, K., Levine, A., Eulgem, T., Morgan, A., Schmid, J., Lawton, K.A., Dangl, J.L. and Dietrich, R.A. (2000) The transcriptome of *Arabidopsis thaliana* during systemic acquired resistance. *Nat Genet*, **26**, 403-410.

Manfield, I.W., Jen, C.H., Pinney, J.W., Michalopoulos, I., Bradford, J.R., Gilmartin, P.M. and Westhead, D.R. (2006) *Arabidopsis* Co-expression Tool (ACT): web server tools for microarray-based gene expression analysis. *Nucleic Acids Res*, **34**, W504-509.

Manfield, I.W., Orfila, C., McCartney, L., Harholt, J., Bernal, A.J., Scheller, H.V., Gilmartin, P.M., Mikkelsen, J.D., Paul Knox, J. and Willats, W.G. (2004) Novel cell wall architecture of isoxaben-habituated *Arabidopsis* suspension-cultured cells: global transcript profiling and cellular analysis. *Plant J*, **40**, 260-275.

Maryani, M.M., Bradley, G., Cahill, D.M. and Gehring, C.A. (2001) Natriuretic peptides and immunoreactants modify osmoticum-dependent volume changes in *Solanum tuberosum* L. mesophyll cell protoplasts. *Plant Sci*, **161**, 443–452.

Maryani, M.M., Morse, M.V., Bradley, G., Irving, H.R., Cahill, D.M. and Gehring, C.A. (2003) In situ localization associates biologically active plant natriuretic peptide immuno-analogues with conductive tissue and stomata. *J Exp Bot*, **54**, 1553-1564.

Maryani, M.M., Shabala, S.N. and Gehring, C.A. (2000) Plant natriuretic peptide immunoreactants modulate plasma-membrane H^+ gradients in *Solanum tuberosum* L. leaf tissue vesicles. *Arch Biochem Biophys*, **376**, 456-458.

Maser, P., Eckelman, B., Vaidyanathan, R., Horie, T., Fairbairn, D.J., Kubo, M., Yamagami, M., Yamaguchi, K., Nishimura, M., Uozumi, N., Robertson, W., Sussman, M.R. and Schroeder, J.I. (2002) Altered shoot/root Na^+ distribution and bifurcating salt sensitivity in *Arabidopsis* by genetic disruption of the Na^+ transporter AtHKT1. *FEBS Lett*, **531**, 157-161.

Masle, J., Gilmore, S.R. and Farquhar, G.D. (2005) The *ERECTA* gene regulates plant transpiration efficiency in *Arabidopsis*. *Nature*, **436**, 866-870.

Matsukawa, N., Grzesik, W.J., Takahashi, N., Pandey, K.N., Pang, S., Yamauchi, M. and Smithies, O. (1999) The natriuretic peptide clearance receptor locally modulates the physiological effects of the natriuretic peptide system. *Proc Natl Acad Sci U S A*, **96**, 7403-7408.

Matys, V., Kel-Margoulis, O.V., Fricke, E., Liebich, I., Land, S., Barre-Dirrie, A., Reuter, I., Chekmenev, D., Krull, M., Hornischer, K., Voss, N., Stegmaier, P., Lewicki-Potapov, B., Saxel, H., Kel, A.E. and Wingender, E. (2006) TRANSFAC and its module TRANSCompel: Transcriptional gene regulation in eukaryotes. *Nucleic Acids Res*, **34**, D108-D110.

Maurel, C., Javot, H., Lauvergeat, V., Gerbeau, P., Tournaire, C., Santoni, V. and Heyes, J. (2002) Molecular physiology of aquaporins in plants. *Int Rev Cytol*, **215**, 105-148.

McAinsh, M.R. and Hetherington, A.M. (1998) Encoding specificity in calcium signalling systems. *Trends Plant Sci*, **3**, 32-36.

McGrath, M.F. and de Bold, A.J. (2005) Determinants of natriuretic peptide gene expression. *Peptides*, **26**, 933-943.

Meier, S. and Gehring, C. (2006) Emerging roles in plant biotechnology for the second messenger cGMP - guanosine 3', 5'-cyclic monophosphate. *African J Biotechnology*, **5**, 1687-1692.

Meier, S. and Gehring, C. (2008) A guide to the integrated application of on-line data mining tools for the inference of gene functions at the systems level. *Biotechnol J*, **3**, 1375-1387.

Meier, S., Irving, H. and Gehring, C. (2008) *Plant natriuretic peptides - emerging roles in fluid and salt balance*. Kerala, India: Transworld Research Network.

Meier, S., Madeo, L., Ederli, L., Donaldson, L., Pasqualini, S. and Gehring, C. (2009) Deciphering cGMP signatures and cGMP-dependent pathways in plant defence. *Plant Signaling & Behavior*, **4**, 1-3.

Meijer, H.J. and Munnik, T. (2003) Phospholipid-based signaling in plants. *Annu Rev Plant Biol*, **54**, 265-306.

Meinke, D.W., Cherry, J.M., Dean, C., Rounsley, S.D. and Koornneef, M. (1998) *Arabidopsis thaliana*: a model plant for genome analysis. *Science*, **282**, 662, 679-682.

Melaragno, J.E., Mehrotra, B. and Coleman, A.W. (1993) Relationship between Endopolyploidy and Cell Size in Epidermal Tissue of *Arabidopsis*. *Plant Cell*, **5**, 1661-1668.

Melotto, M., Underwood, W., Koczan, J., Nomura, K. and He, S.Y. (2006) Plant stomata function in innate immunity against bacterial invasion. *Cell*, **126**, 969-980.

Merlot, S., Leonhardt, N., Fenzi, F., Valon, C., Costa, M., Piette, L., Vavasseur, A., Genty, B., Boivin, K., Muller, A., Giraudat, J. and Leung, J. (2007) Constitutive activation of a plasma membrane H^+-ATPase prevents abscisic acid-mediated stomatal closure. *Embo J*, **26**, 3216-3226.

Mishina, T.E. and Zeier, J. (2007) Pathogen-associated molecular pattern recognition rather than development of tissue necrosis contributes to bacterial induction of systemic acquired resistance in *Arabidopsis*. *Plant J*, **50**, 500-513.

Misono, K.S., Ogawa, H., Qiu, Y. and Ogata, C.M. (2005) Structural studies of the natriuretic peptide receptor: a novel hormone-induced rotation mechanism for transmembrane signal transduction. *Peptides*, **26**, 957-968.

Mittler, R., Vanderauwera, S., Gollery, M. and Van Breusegem, F. (2004) Reactive oxygen gene network of plants. *Trends Plant Sci*, **9**, 490-498.

Mohr, P.G. and Cahill, D.M. (2003) Abscisic acid influences the susceptibility of *Arabidopsis thaliana* to *Pseudomonas syringae* pv. *tomato* and *Peronospora parasitica*. *Funct plant biol*, **30**, 461-469.

Morse, M., Pironcheva, G. and Gehring, C. (2004) AtPNP-A is a systemically mobile natriuretic peptide immunoanalogue with a role in *Arabidopsis thaliana* cell volume regulation. *FEBS Lett*, **556**, 99-103.

Mou, Z., Fan, W. and Dong, X. (2003) Inducers of plant systemic acquired resistance regulate NPR1 function through redox changes. *Cell*, **113**, 935-944.

Mueller-Roeber, B. and Dreyer, I. (2007) Ion homeostasis: plants feel better with proper control. *EMBO Rep*, **8**, 735-736.

Munns, R. (2002) Comparative physiology of salt and water stress. *Plant Cell Environ*, **25**, 239-250.

Munns, R. (2005) Genes and salt tolerance: bringing them together. *New Phytol*, **167**, 645-663.

Murashige, T. and Skoog, F. (1962) A revised medium for rapid growth and bioassays with tobacco tissue culture. *Physiol. Plant.*, **15**, 473-497.

Murray, S.L., Ingle, R.A., Petersen, L.N. and Denby, K.J. (2007) Basal resistance against *Pseudomonas syringae* in *Arabidopsis* involves WRKY53 and a protein with homology to a nematode resistance protein. *Mol Plant Microbe Interact*, **20**, 1431-1438.

Mylne, J. and Botella, J.R. (1998) Binary vectors for sense and antisense expression of *Arabidopsis* ESTs. *Plant Mol Biol Rep*, **19**, 257-262.

Nagaoka, S. and Takano, T. (2003) Salt tolerance-related protein STO binds to a Myb transcription factor homologue and confers salt tolerance in Arabidopsis. *J Exp Bot*, **54**, 2231-2237.

Nakamura, S., Naruse, M., Naruse, K., Kawana, M., Nishikawa, T., Hosoda, S., Tanaka, I., Yoshimi, T., Yoshihara, I., Inagami, T. and et al. (1991) Atrial natriuretic peptide and brain natriuretic peptide coexist in the secretory granules of human cardiac myocytes. *Am J Hypertens*, **4**, 909-912.

Navarro, L., Dunoyer, P., Jay, F., Arnold, B., Dharmasiri, N., Estelle, M., Voinnet, O. and Jones, J.D. (2006) A plant miRNA contributes to antibacterial resistance by repressing auxin signaling. *Science*, **312**, 436-439.

Navarro, L., Zipfel, C., Rowland, O., Keller, I., Robatzek, S., Boller, T. and Jones, J.D. (2004) The transcriptional innate immune response to flg22. Interplay and overlap with Avr gene-dependent defense responses and bacterial pathogenesis. *Plant Physiol*, **135**, 1113-1128.

Nawrath, C. and Metraux, J.P. (1999) Salicylic acid induction-deficient mutants of *Arabidopsis* express *PR-2* and *PR-5* and accumulate high levels of camalexin after pathogen inoculation. *Plant Cell*, **11**, 1393-1404.

Nelissen, H., Fleury, D., Bruno, L., Robles, P., De Veylder, L., Traas, J., Micol, J.L., Van Montagu, M., Inze, D. and Van Lijsebettens, M. (2005) The *elongata* mutants identify a functional Elongator complex in plants with a role in cell proliferation during organ growth. *Proc Natl Acad Sci U S A*, **102**, 7754-7759.

Nembaware, V., Seoighe, C., Sayed, M. and Gehring, C. (2004) A plant natriuretic peptide-like gene in the bacterial pathogen *Xanthomonas axonopodis* may induce hyper-hydration in the plant host: a hypothesis of molecular mimicry. *BMC Evol Biol*, **4**, 10.

Nemchinov, L.G., Shabala, L. and Shabala, S. (2008) Calcium efflux as a component of the hypersensitive response of *Nicotiana benthamiana* to *Pseudomonas syringae*. *Plant Cell Physiol*, **49**, 40-46.

Neuhaus, G., Bowler, C., Hiratsuka, K., Yamagata, H. and Chua, N.H. (1997) Phytochrome-regulated repression of gene expression requires calcium and cGMP. *Embo J*, **16**, 2554-2564.

Newman, I.A. (2001) Ion transport in roots: measurement of fluxes using ion-selective microelectrodes to characterize transporter function. *Plant Cell Environ*, **24**, 1-14.

Newton, R.P., Kingston, E.E., Evans, D.E., Younis, L.M. and Brown, E.G. (1984) Occurrence of guanosine 3',5'-cyclic monophosphate (cyclic GMP) and associated enzyme systems in *Phaseolus vulgaris* L. *Phytochemistry*, **23**, 1367-1372.

Newton, R.P., Roef, L., Witters, E. and Van Onckelen, H. (1999) Cyclic nucleotides in higher plants: the enduring paradox. *New Phytol.*, **143**, 427-455.

Newton, R.P. and Smith, C.J. (2004) Cyclic nucleotides. *Phytochemistry*, **65**, 2423-2437.

Ng, C.K., Carr, K., McAinsh, M.R., Powell, B. and Hetherington, A.M. (2001) Drought-induced guard cell signal transduction involves sphingosine-1-phosphate. *Nature*, **410**, 596-599.

Ng, C.K. and McAinsh, M.R. (2003) Encoding specificity in plant calcium signalling: hot-spotting the ups and downs and waves. *Ann Bot (Lond)*, **92**, 477-485.

Ng, C.K.Y. and Hetherington, A.M. (2001) Sphingolipid-mediated Signalling in Plants. *Ann Bot (Lond)*, **88**, 957-965.

Nicol, F., His, I., Jauneau, A., Vernhettes, S., Canut, H. and Hofte, H. (1998) A plasma membrane-bound putative endo-1,4-beta-D-glucanase is required for normal wall assembly and cell elongation in *Arabidopsis*. *Embo J*, **17**, 5563-5576.

Nilson, S.E. and Assmann, S.M. (2007) The control of transpiration. Insights from *Arabidopsis*. *Plant Physiol*, **143**, 19-27.

Niu, X., Bressan, R.A., Hasegawa, P.M. and Pardo, J.M. (1995) Ion Homeostasis in NaCl Stress Environments. *Plant Physiol*, **109**, 735-742.

Nussenzveig, D.R., Lewicki, J.A. and Maack, T. (1990) Cellular mechanisms of the clearance function of type C receptors of atrial natriuretic factor. *J Biol Chem*, **265**, 20952-20958.

O' Conner, T.R., Dyreson, C. and Wyrick, J.J. (2005) Athena: A resource for rapid visualization and systematic analysis of *Arabidopsis* promoter sequences. *Bioinformatics*, **21**, 4411-4413.

Ohta, M., Guo, Y., Halfter, U. and Zhu, J.K. (2003) A novel domain in the protein kinase SOS2 mediates interaction with the protein phosphatase 2C ABI2. *Proc Natl Acad Sci U S A*, **100**, 11771-11776.

Olszewski, N., Sun, T.P. and Gubler, F. (2002) Gibberellin signaling: biosynthesis, catabolism, and response pathways. *Plant Cell*, **14 Suppl**, S61-80.

Ostergaard, L. and Yanofsky, M.F. (2004) Establishing gene function by mutagenesis in *Arabidopsis thaliana*. *Plant J*, **39**, 682-696.

Pandey, K.N. (2005) Biology of natriuretic peptides and their receptors. *Peptides*, **26**, 901-932.

Parinov, S. and Sundaresan, V. (2000) Functional genomics in *Arabidopsis*: large-scale insertional mutagenesis complements the genome sequencing project. *Curr Opin Biotechnol*, **11**, 157-161.

Parker, G., Schofield, R., Sundberg, B. and Turner, S. (2003) Isolation of *COV1*, a gene involved in the regulation of vascular patterning in the stem of *Arabidopsis*. *Development*, **130**, 2139-2148.

Parker, J.E., Holub, E.B., Frost, L.N., Falk, A., Gunn, N.D. and Daniels, M.J. (1996) Characterization of *eds1*, a mutation in *Arabidopsis* supressing resistance to *Peronospora parasitica* specified by several different *RPP* genes. *Plant Cell*, **8**, 2033-2046.

Paul, A.K., Marala, R.B., Jaiswal, R.K. and Sharma, R.K. (1987) Coexistence of guanylate cyclase and atrial natriuretic factor receptor in a 180-kD protein. *Science*, **235**, 1224-1226.

Pejchalova, K., Krejci, P. and Wilcox, W.R. (2007) C-natriuretic peptide: an important regulator of cartilage. *Mol Genet Metab*, **92**, 210-215.

Pennisi, E. (2000) Plant genomics. *Arabidopsis* comes of age. *Science*, **290**, 32-35.

Penson, S.P., Schuurink, R.C., Fath, A., Gubler, F., Jacobsen, J.V. and Jones, R.L. (1996) cGMP Is Required for Gibberellic Acid-Induced Gene Expression in Barley Aleurone. *Plant Cell*, **8**, 2325-2333.

Persson, S., Wei, H., Milne, J., Page, G.P. and Somerville, C.R. (2005) Identification of genes required for cellulose synthesis by regression analysis of public microarray data sets. *Proc Natl Acad Sci U S A*, **102**, 8633-8638.

Petersen, M., Brodersen, P., Naested, H., Andreasson, E., Lindhart, U., Johansen, B., Nielsen, H.B., Lacy, M., Austin, M.J., Parker, J.E., Sharma, S.B., Klessig, D.F., Martienssen, R., Mattsson, O., Jensen, A.B. and Mundy, J. (2000) *Arabidopsis* Map Kinase 4 negatively regulates systemic acquired resistance. *Cell*, **103**, 1111-1120.

Pfeiffer, S., Janistyn, B., Jessner, G., Pichorner, H. and Ebermann, R. (1994) Gaseous nitric-oxide stimulates guanosine-3',5'-cyclic monophosphate (cGMP) formation in spruce needles. *Phytochemistry* **36**, 259–262.

Pharmawati, M., Billington, T. and Gehring, C.A. (1998a) Stomatal guard cell responses to kinetin and natriuretic peptides are cGMP-dependent. *Cell Mol Life Sci*, **54**, 272-276.

Pharmawati, M., Gehring, C.A. and Irving, H.R. (1998b) An immunoaffinity purified plant natriuretic peptide analogue modulates cGMP levels in the *Zea mays* root stele. *Plant Sci*, **137**, 107–115.

Pharmawati, M., Maryani, M.M., Nikolakopoulos, T., Gehring, C.A. and Irving, H.R. (2001) Cyclic GMP modulates stomatal opening induced by natriuretic peptides and immunoreactive analogues. *Plant Physiol. Biochem.*, **39**, 385−394.

Pharmawati, M., Shabala, S.N., Newman, I.A. and Gehring, C.A. (1999) Natriuretic peptides and cGMP modulate K^+, Na^+, and H^+ fluxes in Zea mays roots. *Mol Cell Biol Res Commun*, **2**, 53-57.

Piggott, L.A., Hassell, K.A., Berkova, Z., Morris, A.P., Silberbach, M. and Rich, T.C. (2006) Natriuretic peptides and nitric oxide stimulate cGMP synthesis in different cellular compartments. *J Gen Physiol*, **128**, 3-14.

Pittman, J.K. and Hirschi, K.D. (2003) Don't shoot the (second) messenger: endomembrane transporters and binding proteins modulate cytosolic Ca^{2+} levels. *Curr Opin Plant Biol*, **6**, 257-262.

Polisensky, D.H. and Braam, J. (1996) Cold-shock regulation of the *Arabidopsis TCH* genes and the effects of modulating intracellular calcium levels. *Plant Physiol*, **111**, 1271-1279.

Potter, L.R., Abbey-Hosch, S. and Dickey, D.M. (2006) Natriuretic peptides, their receptors, and cyclic guanosine monophosphate-dependent signaling functions. *Endocr Rev*, **27**, 47-72.

Potter, L.R. and Hunter, T. (2001) Guanylyl cyclase-linked natriuretic peptide receptors: structure and regulation. *J Biol Chem*, **276**, 6057-6060.

Potters, G., Pasternak, T.P., Guisez, Y., Palme, K.J. and Jansen, M.A. (2007) Stress-induced morphogenic responses: growing out of trouble? *Trends Plant Sci*, **12**, 98-105.

Potthast, R. and Potter, L.R. (2005) Phosphorylation-dependent regulation of the guanylyl cyclase-linked natriuretic peptide receptors. *Peptides*, **26**, 1001-1008.

Qiu, Q.S., Guo, Y., Dietrich, M.A., Schumaker, K.S. and Zhu, J.K. (2002) Regulation of SOS1, a plasma membrane Na^+/H^+ exchanger in *Arabidopsis thaliana*, by SOS2 and SOS3. *Proc Natl Acad Sci U S A*, **99**, 8436-8441.

Qiu, Q.S., Guo, Y., Quintero, F.J., Pardo, J.M., Schumaker, K.S. and Zhu, J.K. (2004) Regulation of vacuolar Na^+/H^+ exchange in *Arabidopsis thaliana* by the salt-overly-sensitive (SOS) pathway. *J Biol Chem*, **279**, 207-215.

Quesada, V., Ponce, M.R. and Micol, J.L. (2000) Genetic analysis of salt-tolerant mutants in *Arabidopsis thaliana*. *Genetics*, **154**, 421-436.

Rafudeen, S., Gxaba, G., Makgoke, G., Bradley, G., Pironcheva, G., Raitt, L., Irving, H. and Gehring, C. (2003) A role for plant natriuretic peptide immuno-analogues in NaCl- and drought-stress responses. *Physiol. Plant.*, **119**, 554–562.

Rall, T.W., Sutherland, E.W. and Berthet, J. (1957) The relation of epinephrine and glucagon to liver phosphorylase. *J. Biol. Chem.*, **224**, 1987–1995.

Redman, J.C., Haas, B.J., Tanimoto, G. and Town, C.D. (2004) Development and evaluation of an *Arabidopsis* whole genome Affymetrix probe array. *Plant J*, **38**, 545-561.

Reggiani, R. (1997) Alteration of Levels of Cyclic Nucleotides in Response to Anaerobiosis in Rice Seedlings *Plant Cell Physiol*, **38**, 740-742.

Rep, M., Dekker, H.L., Vossen, J.H., de Boer, A.D., Houterman, P.M., Speijer, D., Back, J.W., de Koster, C.G. and Cornelissen, B.J. (2002) Mass spectrometric identification of isoforms of PR proteins in xylem sap of fungus-infected tomato. *Plant Physiol*, **130**, 904-917.

Rhee, S.Y., Beavis, W., Berardini, T.Z., Chen, G., Dixon, D., Doyle, A., Garcia-Hernandez, M., Huala, E., Lander, G., Montoya, M., Miller, N., Mueller, L.A., Mundodi, S., Reiser, L., Tacklind, J.,

Weems, D.C., Wu, Y., Xu, I., Yoo, D., Yoon, J. and Zhang, P. (2003) The *Arabidopsis* Information Resource (TAIR): a model organism database providing a centralized, curated gateway to *Arabidopsis* biology, research materials and community. *Nucleic Acids Res*, **31**, 224-228.

Richards, A.M. (2004) The natriuretic peptides in heart failure. *Basic Res Cardiol*, **99**, 94-100.

Richards, H., Das, S., Smith, C.J., Pereira, L., Geisbrecht, A., Devitt, N.J., Games, D.E., van Geyschem, J., Gareth Brenton, A. and Newton, R.P. (2002) Cyclic nucleotide content of tobacco BY-2 cells. *Phytochemistry*, **61**, 531-537.

Riechmann, J.L., Heard, J., Martin, G., Reuber, L., Jiang, C., Keddie, J., Adam, L., Pineda, O., Ratcliffe, O.J., Samaha, R.R., Creelman, R., Pilgrim, M., Broun, P., Zhang, J.Z., Ghandehari, D., Sherman, B.K. and Yu, G. (2000) Arabidopsis transcription factors: genome-wide comparative analysis among eukaryotes. *Science*, **290**, 2105-2110.

Robert-Seilaniantz, A., Navarro, L., Bari, R. and Jones, J.D. (2007) Pathological hormone imbalances. *Curr Opin Plant Biol*, **10**, 372-379.

Robison, G.A., Butcher, R.W. and Sutherland, E.W. (1971) *Cyclic AMP*. New York: Academic Press.

Roelofs, J., Smith, J.L. and Van Haastert, P.J. (2003) cGMP signalling: different ways to create a pathway. *Trends Genet*, **19**, 132-134.

Rosado, A., Schapire, A.L., Bressan, R.A., Harfouche, A.L., Hasegawa, P.M., Valpuesta, V. and Botella, M.A. (2006) The *Arabidopsis* Tetratricopeptide Repeats Containing Protein TTL1 Is Required for Osmotic Stress Responses and ABA Sensitivity. *Plant Physiol*, **142**, 1113–1126.

Rubio, F., Flores, P., Navarro, J.M. and Martinez, V. (2003) Effects of Ca^{2+}, K^+ and cGMP on Na^+ uptake in pepper plants. *Plant Sci*, **165**, 1043-1049.

Ruggiero, B., Koiwa, H., Manabe, Y., Quist, T.M., Inan, G., Saccardo, F., Joly, R.J., Hasegawa, P.M., Bressan, R.A. and Maggio, A. (2004) Uncoupling the effects of abscisic acid on plant growth and water relations. Analysis of *sto1*/*nced3*, an abscisic acid-deficient but salt stress-tolerant mutant in *Arabidopsis*. *Plant Physiol*, **136**, 3134-3147.

Rus, A., Lee, B.H., Munoz-Mayor, A., Sharkhuu, A., Miura, K., Zhu, J.K., Bressan, R.A. and Hasegawa, P.M. (2004) AtHKT1 facilitates Na^+ homeostasis and K^+ nutrition in planta. *Plant Physiol*, **136**, 2500-2511.

Rus, A., Yokoi, S., Sharkhuu, A., Reddy, M., Lee, B.H., Matsumoto, T.K., Koiwa, H., Zhu, J.K., Bressan, R.A. and Hasegawa, P.M. (2001) AtHKT1 is a salt tolerance determinant that controls Na^+ entry into plant roots. *Proc Natl Acad Sci U S A*, **98**, 14150-14155.

Ryals, J.A., Neuenschwander, U.H., Willits, M.G., Molina, A., Steiner, H.Y. and Hunt, M.D. (1996) Systemic Acquired Resistance. *Plant Cell*, **8**, 1809-1819.

Saleki, R., Young, P.G. and Lefebvre, D.D. (1993) Mutants of *Arabidopsis thaliana* Capable of Germination under Saline Conditions. *Plant Physiol*, **101**, 839-845.

Sambrook, J., Fritsch, E.F. and Maniatis, T. (1989) *Molecular cloning: a laboratory manual*. Cold Spring Harbor, New York: Cold Spring Harbor Press.

Sampedro, J. and Cosgrove, D.J. (2005) The expansin superfamily. *Genome Biol*, **6**, 242.

Sanan-Mishra, N., Pham, X.H., Sopory, S.K. and Tuteja, N. (2005) Pea DNA helicase 45 overexpression in tobacco confers high salinity tolerance without affecting yield. *Proc Natl Acad Sci U S A*, **102**, 509-514.

Sanders, D., Pelloux, J., Brownlee, C. and Harper, J.F. (2002) Calcium at the crossroads of signaling. *Plant Cell*, **14 Suppl**, S401-417.

Schechter, L.M., Roberts, K.A., Jamir, Y., Alfano, J.R. and Collmer, A. (2004) *Pseudomonas syringae* type III secretion system targeting signals and novel effectors studied with a Cya translocation reporter. *J Bacteriol*, **186**, 543-555.

Schmid, M., Davison, T.S., Henz, S.R., Pape, U.J., Demar, M., Vingron, M., Scholkopf, B., Weigel, D. and Lohmann, J.U. (2005) A gene expression map of *Arabidopsis thaliana* development. *Nat Genetics*, **37**, 501-506.

Scholl, R.L., May, S.T. and Ware, D.H. (2000) Seed and molecular resources for *Arabidopsis*. *Plant Physiol*, **124**, 1477-1480.

Schulz, S. (2005) C-type natriuretic peptide and guanylyl cyclase B receptor. *Peptides*, **26**, 1024-1034.

Schweitz, H., Vigne, P., Moinier, D., Frelin, C. and Lazdunski, M. (1992) A new member of the natriuretic peptide family is present in the venom of the green mamba (*Dendroaspis angusticeps*). *J Biol Chem*, **267**, 13928-13932.

Schwessinger, B. and Zipfel, C. (2008) News from the frontline: recent insights into PAMP-triggered immunity in plants. *Curr Opin Plant Biol*, **11**, 389-395.

Scrase-Field, S.A. and Knight, M.R. (2003) Calcium: just a chemical switch? *Curr Opin Plant Biol*, **6**, 500-506.

Seki, M., Narusaka, M., Ishida, J., Nanjo, T., Fujita, M., Oono, Y., Kamiya, A., Nakajima, M., Enju, A., Sakurai, T., Satou, M., Akiyama, K., Taji, T., Yamaguchi-Shinozaki, K., Carninci, P., Kawai, J., Hayashizaki, Y. and Shinozaki, K. (2002) Monitoring the expression profiles of 7000 *Arabidopsis* genes under drought, cold and high-salinity stresses using a full-length cDNA microarray. *Plant J*, **31**, 279-292.

Seo, M., Peeters, A.J., Koiwai, H., Oritani, T., Marion-Poll, A., Zeevaart, J.A., Koornneef, M., Kamiya, Y. and Koshiba, T. (2000) The *Arabidopsis aldehyde oxidase 3* (*AAO3*) gene product catalyzes the final step in abscisic acid biosynthesis in leaves. *Proc Natl Acad Sci U S A*, **97**, 12908-12913.

Seo, P.J., Lee, A.K., Xiang, F. and Park, C.M. (2008) Molecular and functional profiling of *Arabidopsis* pathogenesis-related genes: insights into their roles in salt response of seed germination. *Plant Cell Physiol*, **49**, 334-344.

Serrano, R., Mulet, J., Rios, G., Marquez, J., de Larrinoa, I., Leube, M., Mendizabal, I., Pascual-Ahuir, A., Proft, M., Ros, R. and Montesinos, C. (1999) A glimpse of the mechanisms of ion homeostasis during salt stress. *J Exp Bot*, **50**, 1023-1036.

Serrano, R. and Rodriguez-Navarro, A. (2001) Ion homeostasis during salt stress in plants. *Curr Opin Cell Biol*, **13**, 399-404.

Shabala, L., Cuin, T.A., Newman, I.A. and Shabala, S. (2005a) Salinity-induced ion flux patterns from the excised roots of *Arabidopsis sos* mutants. *Planta*, **222**, 1041-1050.

Shabala, S. (2000) Ionic and osmotic components of salt stress specifically modulate net ion fluxes from bean leaf mesophyll. *Plant Cell Environ*, **23**, 825-837.

Shabala, S. (2003) Regulation of potassium transport in leaves: from molecular to tissue level. *Ann Bot (Lond)*, **92**, 627-634.

Shabala, S. and Cuin, T.A. (2008) Potassium transport and plant salt tolerance. *Physiol Plant*, **133**, 651-669.

Shabala, S., Cuin, T.A. and Pottosin, I. (2007) Polyamines prevent NaCl-induced K^+ efflux from pea mesophyll by blocking non-selective cation channels. *FEBS Lett*, **581**, 1993-1999.

Shabala, S., Demidchik, V., Shabala, L., Cuin, T.A., Smith, S.J., Miller, A.J., Davies, J.M. and Newman, I.A. (2006) Extracellular Ca^{2+} ameliorates NaCl-induced K^+ loss from *Arabidopsis* root and leaf cells by controlling plasma membrane K^+ -permeable channels. *Plant Physiol*, **141**, 1653-1665.

Shabala, S. and Newman, I.I. (1999) Light-induced changes in hydrogen, calcium, potassium, and chloride ion fluxes and concentrations from the mesophyll and epidermal tissues of bean leaves. Understanding the ionic basis of light-induced bioelectrogenesis. *Plant Physiol*, **119**, 1115-1124.

Shabala, S. and Shabala, L. (2002) Kinetics of net H^+, Ca^{2+}, K^+, Na^+, NH^{+4}, and Cl^- fluxes associated with post-chilling recovery of plasma membrane transporters in *Zea mays* leaf and root tissues. *Physiol Plant*, **114**, 47-56.

Shabala, S., Shabala, L., Van Volkenburgh, E. and Newman, I. (2005b) Effect of divalent cations on ion fluxes and leaf photochemistry in salinized barley leaves. *J Exp Bot*, **56**, 1369-1378.

Shabala, S.N. and Lew, R.R. (2002) Turgor regulation in osmotically stressed *Arabidopsis* epidermal root cells. Direct support for the role of inorganic ion uptake as revealed by concurrent flux and cell turgor measurements. *Plant Physiol*, **129**, 290-299.

Shabala, S.N., Newman, I.A. and Morris, J. (1997) Oscillations in H^+ and Ca^{2+} Ion Fluxes around the Elongation Region of Corn Roots and Effects of External pH. *Plant Physiol*, **113**, 111-118.

Shang, Y., Li, X., Cui, H., He, P., Thilmony, R., Chintamanani, S., Zwiesler-Vollick, J., Gopalan, S., Tang, X. and Zhou, J.M. (2006) RAR1, a central player in plant immunity, is targeted by *Pseudomonas syringae* effector AvrB. *Proc Natl Acad Sci U S A*, **103**, 19200-19205.

Sharma, Y.K., Leon, J., Raskin, I. and Davis, K.R. (1996) Ozone-induced responses in Arabidopsis thaliana: The role of salicylic acid in the accumulation of defense-related transcripts and induced defense. *Proc Natl Acad Sci U S A*, **93**, 5099-5104.

Shi, H., Ishitani, M., Kim, C. and Zhu, J.K. (2000) The *Arabidopsis thaliana* salt tolerance gene *SOS1* encodes a putative Na^+/H^+ antiporter. *Proc Natl Acad Sci U S A*, **97**, 6896-6901.

Shi, H., Kim, Y., Guo, Y., Stevenson, B. and Zhu, J.K. (2003) The *Arabidopsis SOS5* locus encodes a putative cell surface adhesion protein and is required for normal cell expansion. *Plant Cell*, **15**, 19-32.

Shi, H., Quintero, F.J., Pardo, J.M. and Zhu, J.K. (2002a) The putative plasma membrane Na^+/H^+ antiporter SOS1 controls long-distance Na^+ transport in plants. *Plant Cell*, **14**, 465-477.

Shi, H., Xiong, L., Stevenson, B., Lu, T. and Zhu, J.K. (2002b) The *Arabidopsis salt overly sensitive 4* mutants uncover a critical role for vitamin B6 in plant salt tolerance. *Plant Cell*, **14**, 575-588.

Shi, H. and Zhu, J.K. (2002) *SOS4*, a pyridoxal kinase gene, is required for root hair development in *Arabidopsis*. *Plant Physiol*, **129**, 585-593.

Shin, R. and Schachtman, D.P. (2004) Hydrogen peroxide mediates plant root cell response to nutrient deprivation. *Proc Natl Acad Sci U S A*, **101**, 8827-8832.

Shinozaki, K. and Yamaguchi-Shinozaki, K. (1997) Gene Expression and Signal Transduction in Water-Stress Response. *Plant Physiol*, **115**, 327-334.

Shinozaki, K. and Yamaguchi-Shinozaki, K. (2000) Molecular responses to dehydration and low temperature: differences and cross-talk between two stress signaling pathways. *Curr Opin Plant Biol.*, **3**, 217-223.

Sindic, A., Hirsch, J.R., Velic, A., Piechota, H. and Schlatter, E. (2005) Guanylin and uroguanylin regulate electrolyte transport in isolated human cortical collecting ducts. *Kidney Int*, **67**, 1420-1427.

Sindic, A. and Schlatter, E. (2005) Mechanisms of actions of guanylin peptides in the kidney. *Pflugers Arch*, **450**, 283-291.

Slusarenko, A.J. and Schlaich, N.L. (2003) Downy mildew of *Arabidopsis thaliana* caused by *Hyaloperonospora parasitica* (formerly *Peronospora parasitica*). *Mol. Plant Pathol.*, **4**, 159-170.

Smyth, D.R., Bowman, J.L. and Meyerowitz, E.M. (1990) Early flower development in *Arabidopsis*. *Plant Cell*, **2**, 755-767.

Smyth, G.K. and Speed, T.P. (2003) Normalization of cDNA microarray data. *Methods*, **31**, 265-273.

Sondergaard, T.E., Schulz, A. and Palmgren, M.G. (2004) Energization of transport processes in plants. roles of the plasma membrane H^+-ATPase. *Plant Physiol*, **136**, 2475-2482.

Spiteri, A., Viratelle, O.M., Raymond, P., Rancillac, M., Labouesse, J. and Pradet, A. (1989) Artefactual origins of cyclic AMP in higher plant tissues. *Plant Physiol*, **91**, 624-628.

Spoel, S.H., Koornneef, A., Claessens, S.M., Korzelius, J.P., Van Pelt, J.A., Mueller, M.J., Buchala, A.J., Metraux, J.P., Brown, R., Kazan, K., Van Loon, L.C., Dong, X. and Pieterse, C.M. (2003) NPR1 modulates cross-talk between salicylate- and jasmonate-dependent defense pathways through a novel function in the cytosol. *Plant Cell*, **15**, 760-770.

Suarez-Rodriguez, M.C., Adams-Phillips, L., Liu, Y., Wang, H., Su, S.H., Jester, P.J., Zhang, S., Bent, A.F. and Krysan, P.J. (2007) MEKK1 is required for flg22-induced MPK4 activation in *Arabidopsis* plants. *Plant Physiol*, **143**, 661-669.

Sudoh, T., Minamino, N., Kangawa, K. and Matsuo, H. (1988) Brain natriuretic peptide-32: N-terminal six amino acid extended form of brain natriuretic peptide identified in porcine brain. *Biochem Biophys Res Commun*, **155**, 726-732.

Sudoh, T., Minamino, N., Kangawa, K. and Matsuo, H. (1990) C-type natriuretic peptide (CNP): a new member of natriuretic peptide family identified in porcine brain. *Biochem Biophys Res Commun*, **168**, 863-870.

Suga, S., Nakao, K., Itoh, H., Komatsu, Y., Ogawa, Y., Hama, N. and Imura, H. (1992) Endothelial production of C-type natriuretic peptide and its marked augmentation by transforming growth factor-beta. Possible existence of "vascular natriuretic peptide system". *J Clin Invest*, **90**, 1145-1149.

Sunarpi, Horie, T., Motoda, J., Kubo, M., Yang, H., Yoda, K., Horie, R., Chan, W.Y., Leung, H.Y., Hattori, K., Konomi, M., Osumi, M., Yamagami, M., Schroeder, J.I. and Uozumi, N. (2005) Enhanced salt tolerance mediated by AtHKT1 transporter-induced Na^+ unloading from xylem vessels to xylem parenchyma cells. *Plant J*, **44**, 928-938.

Sunkar, R., Kaplan, B., Bouche, N., Arazi, T., Dolev, D., Talke, I.N., Maathuis, F.J., Sanders, D., Bouchez, D. and Fromm, H. (2000) Expression of a truncated tobacco NtCBP4 channel in transgenic plants and disruption of the homologous *Arabidopsis* CNGC1 gene confer Pb^{2+} tolerance. *Plant J*, **24**, 533-542.

Surplus, S.L., Jordan, B.R., Murphy, A.M., Carr, J.P. and Mackerness, A.-H. (1998) Ultraviolet-B-induced responses in *Arabidopsis thaliana*: the role of salicylic acid and reactive oxygen species in the regulation of transcripts encoding photosynthetic and acidic pathogenesis-related proteins. *Plant Cell Environ*, **21**, 685-694.

Suwastika, I.N. and Gehring, C.A. (1998) Natriuretic peptide hormones promote radial water movements from the xylem of *Tradescantia* shoots. *Cell. Mol. Life Sci.*, **54**, 1161–1167.

Suwastika, I.N. and Gehring, C.A. (1999) The plasma membrane H^+-ATPase from *Tradescantia* stem and leaf tissue is modulated in vitro by cGMP. *Arch Biochem Biophys*, **367**, 137-139.

Suwastika, I.N., Toop, T., Irving, H.R. and Gehring, C.A. (2000) In situ and in vitro binding of natriuretic peptide hormones in *Tradescantia multiflora*. *Plant biol.*, **2**, 1-3.

Suzuki, H., Xia, Y., Cameron, R., Shadle, G., Blount, J., Lamb, C. and Dixon, R.A. (2004) Signals for local and systemic responses of plants to pathogen attack. *J Exp Bot*, **55**, 169-179.

Swindell, W.R. (2006) The association among gene expression responses to nine abiotic stress treatments in *Arabidopsis thaliana*. *Genetics*, **174**, 1811-1824.

Szepesi, A., Csiszar, J., Gemes, K., Horvath, E., Horvath, F., Simon, M.L. and Tari, I. (2009) Salicylic acid improves acclimation to salt stress by atimulating abscisic aldehyde oxidase activity and abscisic acid accumulation, increases in Na^+ content in leaves without toxicity symptoms in *Solanum lycopersicum* L. *J Plant Physiol*, **166**, 914-925.

Szmidt-Jaworska, A., Jaworski, K., Tretyn, A. and Kopcewicz, J. (2003) Biochemical evidence for a cGMP-regulated protein kinase in *Pharbitis nil*. *Phytochemistry*, **63**, 635-642.

Szmidt-Jaworska, A., Jaworski, K., Tretyn, A. and Kopcewicz, J. (2004) The involvement of cyclic GMP in the photoperiodic flower induction of *Pharbitis nil*. *J Plant Physiol*, **161**, 277-284.

Takei, Y. (2001) Does the natriuretic peptide system exist throughout the animal and plant kingdom? *Comp Biochem Physiol B Biochem Mol Biol*, **129**, 559-573.

Takei, Y., Takahashi, A., Watanabe, T.X., Nakajima, K. and Sakakibara, S. (1991) A novel natriuretic peptide isolated from eel cardiac ventricles. *FEBS Lett*, **282**, 317-320.

Takei, Y., Takano, M., Itahara, Y., Watanabe, T.X., Nakajima, K., Conklin, D.J., Duff, D.W. and Olson, K.R. (1994a) Rainbow trout ventricular natriuretic peptide: isolation, sequencing, and determination of biological activity. *Gen Comp Endocrinol*, **96**, 420-426.

Takei, Y., Ueki, M. and Nishizawa, T. (1994b) Eel ventricular natriuretic peptide: cDNA cloning and mRNA expression. *J Mol Endocrinol*, **13**, 339-345.

Talke, I.N., Blaudez, D., Maathuis, F.J. and Sanders, D. (2003) CNGCs: prime targets of plant cyclic nucleotide signalling? *Trends Plant Sci*, **8**, 286-293.

Tamura, K., Dudley, J., Nei, M. and Kumar, S. (2007) MEGA4: Molecular Evolutionary Genetics Analysis (MEGA) software version 4.0. *Mol Biol Evol*, **24**, 1596-1599.

Tao, Y., Xie, Z., Chen, W., Glazebrook, J., Chang, H.S., Han, B., Zhu, T., Zou, G. and Katagiri, F. (2003) Quantitative nature of *Arabidopsis* responses during compatible and incompatible interactions with the bacterial pathogen *Pseudomonas syringae*. *Plant Cell*, **15**, 317-330.

Tester, M. and Davenport, R. (2003) Na^+ tolerance and Na^+ transport in higher plants. *Ann Bot (Lond)*, **91**, 503-527.

Tian, D., Traw, M.B., Chen, J.Q., Kreitman, M. and Bergelson, J. (2003) Fitness costs of *R*-gene-mediated resistance in *Arabidopsis thaliana*. *Nature*, **423**, 74-77.

Toop, T. and Donald, J.A. (2004) Comparative aspects of natriuretic peptide physiology in non-mammalian vertebrates: a review. *J Comp Physiol [B]*, **174**, 189-204.

Torres, M.A. and Dangl, J.L. (2005) Functions of the respiratory burst oxidase in biotic interactions, abiotic stress and development. *Curr Opin Plant Biol*, **8**, 397-403.

Torres, M.A., Jones, J.D. and Dangl, J.L. (2006) Reactive oxygen species signaling in response to pathogens. *Plant Physiol*, **141**, 373-378.

Toufighi, K., Brady, S.M., Austin, R., Ly, E. and Provart, N.J. (2005) The Botany Array Resource: e-Northerns, Expression Angling, and promoter analyses. *Plant J*, **43**, 153-163.

Trajanovska, S., Inoue, K., Takei, Y. and Donald, J.A. (2007) Genomic analyses and cloning of novel chicken natriuretic peptide genes reveal new insights into natriuretic peptide evolution. *Peptides*, **28**, 2155-2163.

Tran, L.S., Urao, T., Qin, F., Maruyama, K., Kakimoto, T., Shinozaki, K. and Yamaguchi-Shinozaki, K. (2007) Functional analysis of AHK1/ATHK1 and cytokinin receptor histidine kinases in response to abscisic acid, drought, and salt stress in *Arabidopsis*. *Proc Natl Acad Sci U S A*, **104**, 20623-20628.

Trewavas, A.J. and Malho, R. (1997) Signal Perception and Transduction: The Origin of the Phenotype. *Plant Cell*, **9**, 1181-1195.

Trewavas, A.J., Rodrigues, C., Rato, C. and Malho, R. (2002) Cyclic nucleotides: the current dilemma! *Curr Opin Plant Biol*, **5**, 425-429.

Tsuda, K., Sato, M., Glazebrook, J., Cohen, J.D. and Katagiri, F. (2008) Interplay between MAMP-triggered and SA-mediated defense responses. *Plant J*, **53**, 763-775.

Tsugane, K., Kobayashi, K., Niwa, Y., Ohba, Y., Wada, K. and Kobayashi, H. (1999) A recessive *Arabidopsis* mutant that grows photoautotrophically under salt stress shows enhanced active oxygen detoxification. *Plant Cell*, **11**, 1195-1206.

Tusher, V.G., Tibshirani, R. and Chu, G. (2001) Significance analysis of microarrays applied to the ionizing radiation response. *Proc Natl Acad Sci U S A*, **98**, 5116-5121.

Tyerman, S.D. and Skerrett, I.M. (1999) Root ion channels and salinity. *Scientia horticulturae*, **78**, 175-235.

Underwood, W., Melotto, M. and He, S.Y. (2007) Role of plant stomata in bacterial invasion. *Cell Microbiol*, **9**, 1621-1629.

van der Weele, C.M., Spollen, W.G., Sharp, R.E. and Baskin, T.I. (2000) Growth of *Arabidopsis thaliana* seedlings under water deficit studied by control of water potential in nutrient-agar media. *J Exp Bot*, **51**, 1555-1562.

van Loon, L. and van Strien, E. (1999) The families of pathogenesis-related proteins, their activities and comparative analysis of PR-1 type proteins. *Physiol. Mol. Plant Pathol.*, **55**, 85-97.

van Loon, L.C., Rep, M. and Pieterse, C.M. (2006) Significance of inducible defense-related proteins in infected plants. *Annu Rev Phytopathol*, **44**, 135-162.

Van Volkenburgh, E. (1999) Leaf expansion - an integrating plant behaviour. *Plant Cell Environ*, **22**, 1463-1473.

Vanacker, H., Lu, H., Rate, D.N. and Greenberg, J.T. (2001) A role for salicylic acid and NPR1 in regulating cell growth in *Arabidopsis*. *Plant J*, **28**, 209-216.

Ventura, A., Kawakoshi, A., Inoue, K. and Takei, Y. (2006) Multiple natriuretic peptides coexist in the most primitive extant ray-finned fish, bichir Polypterus endlicheri. *Gen Comp Endocrinol*, **146**, 251-256.

Verslues, P.E., Agarwal, M., Katiyar-Agarwal, S., Zhu, J. and Zhu, J.K. (2006) Methods and concepts in quantifying resistance to drought, salt and freezing, abiotic stresses that affect plant water status. *Plant J*, **45**, 523-539.

Verwoerd, T.C., Dekker, B.M. and Hoekema, A. (1989) A small-scale procedure for the rapid isolation of plant RNAs. *Nucleic Acids Res*, **17**, 2362.

Very, A.A. and Sentenac, H. (2002) Cation channels in the *Arabidopsis* plasma membrane. *Trends Plant Sci*, **7**, 168-175.

Very, A.A. and Sentenac, H. (2003) Molecular mechanisms and regulation of K^+ transport in higher plants. *Annu Rev Plant Biol*, **54**, 575-603.

Vesely, D.L., Douglass, M.A., Dietz, J.R., Gower, W.R., Jr., McCormick, M.T., Rodriguez-Paz, G. and Schocken, D.D. (1994) Three peptides from the atrial natriuretic factor prohormone amino terminus lower blood pressure and produce diuresis, natriuresis, and/or kaliuresis in humans. *Circulation*, **90**, 1129-1140.

Vesely, D.L. and Giordano, A.T. (1991) Atrial natriuretic peptide hormonal system in plants. *Biochem Biophys Res Commun*, **179**, 695-700.

Vesely, D.L., Gower, W.R., Jr. and Giordano, A.T. (1993) Atrial natriuretic peptides are present throughout the plant kingdom and enhance solute flow in plants. *Am J Physiol*, **265**, E465-477.

Vlot, A.C., Klessig, D.F. and Park, S.W. (2008) Systemic acquired resistance: the elusive signal(s). *Curr Opin Plant Biol*, **11**, 436-442.

Voegele, R.T. and Mendgen, K. (2003) Rust haustoria: nutrient uptake and beyond. *New phytol*, **159**, 93-100.

Vollmar, A.M. (2005) The role of atrial natriuretic peptide in the immune system. *Peptides*, **26**, 1086-1094.

Volotovski, I.D., Dubovskaya, L.V. and Molchan, O.V. (2003) Photoreceptor phytochrome regulates the cyclic guanosine 3',5'-monophosphate synthesis in *Avena sativa* L. cells. *Bulg. J. Plant Physiol.*, **29**, 3-12.

Volotovski, I.D., Sokolovsky, S.G., Molchan, O.V. and Knight, M.R. (1998) Second messengers mediate increases in cytosolic calcium in tobacco protoplasts. *Plant Physiol*, **117**, 1023-1030.

Wagner, T.A. and Kohorn, B.D. (2001) Wall-associated kinases are expressed throughout plant development and are required for cell expansion. *Plant Cell*, **13**, 303-318.

Walters, D.R. and McRoberts, N. (2006) Plants and biotrophs: a pivotal role for cytokinins? *Trends Plant Sci*, **11**, 581-586.

Wang, D., Amornsiripanitch, N. and Dong, X. (2006) A genomic approach to identify regulatory nodes in the transcriptional network of systemic acquired resistance in plants. *PLoS Pathog*, **2**, e123.

Wang, D., Pajerowska-Mukhtar, K., Culler, A.H. and Dong, X. (2007a) Salicylic acid inhibits pathogen growth in plants through repression of the auxin signaling pathway. *Curr Biol*, **17**, 1784-1790.

Wang, D., Weaver, N.D., Kesarwani, M. and Dong, X. (2005) Induction of protein secretory pathway is required for systemic acquired resistance. *Science*, **308**, 1036-1040.

Wang, Y., Chen, X. and Xiang, C.-B. (2007b) Stomatal Density and Bio-water Saving. *J Integrative Plant Biol*, **49**, 1435-1444.

Wang, Y.H., Gehring, C., Cahill, D.M. and Irving, H.R. (2007c) Plant natriuretic peptide active site determination and effects on cGMP and cell volume regulation. *Funct Plant Biol*, **34**, 645-653.

Warren, R.F., Henk, A., Mowery, P., Holub, E. and Innes, R.W. (1998) A mutation within the leucine-rich repeat domain of the *Arabidopsis* disease resistance gene *RPS5* partially suppresses multiple bacterial and downy mildew resistance genes. *Plant Cell*, **10**, 1439-1452.

Weigel, R.R., Bauscher, C., Pfitzner, A.J. and Pfitzner, U.M. (2001) NIMIN-1, NIMIN-2 and NIMIN-3, members of a novel family of proteins from *Arabidopsis* that interact with NPR1/NIM1, a key regulator of systemic acquired resistance in plants. *Plant Mol Biol*, **46**, 143-160.

Weigel, R.R., Pfitzner, U.M. and Gatz, C. (2005) Interaction of NIMIN1 with NPR1 modulates *PR* gene expression in *Arabidopsis*. *Plant Cell*, **17**, 1279-1291.

Weiler, E.W., Kutchan, T.M., Gorba, T., Brodschelm, W., Niesel, U. and Bublitz, F. (1994) The *Pseudomonas* phytotoxin coronatine mimics octadecanoid signalling molecules of higher plants. *FEBS Lett*, **345**, 9-13.

Wenzel, C.L., Hester, Q. and Mattsson, J. (2008) Identification of genes expressed in vascular tissues using NPA-induced vascular overgrowth in *Arabidopsis*. *Plant Cell Physiol*, **49**, 457-468.

Werner, J.E. and Finkelstein, R.R. (1995) *Arabidopsis* mutants with reduced response to NaCl and osmotic stress. *Physiol. Plant.*, **93**, 659–666.

Wettenhall, J.M. and Smyth, G.K. (2004) limmaGUI: a graphical user interface for linear modeling of microarray data. *Bioinformatics*, **20**, 3705-3706.

Whalen, M.C., Innes, R.W., Bent, A.F. and Staskawicz, B.J. (1991) Identification of *Pseudomonas syringae* pathogens of *Arabidopsis* and a bacterial locus determining avirulence on both *Arabidopsis* and soybean. *Plant Cell*, **3**, 49-59.

Wildermuth, M.C., Dewdney, J., Wu, G. and Ausubel, F.M. (2001) Isochorismate synthase is required to synthesize salicylic acid for plant defence. *Nature*, **414**, 562-565.

Wohlbach, D.J., Quirino, B.F. and Sussman, M.R. (2008) Analysis of the *Arabidopsis* histidine kinase ATHK1 reveals a connection between vegetative osmotic stress sensing and seed maturation. *Plant Cell*, **20**, 1101-1117.

Wright, C.A. and Beattie, G.A. (2004) *Pseudomonas syringae* pv. *tomato* cells encounter inhibitory levels of water stress during the hypersensitive response of *Arabidopsis thaliana*. *Proc Natl Acad Sci U S A*, **101**, 3269-3274.

Wu, S.J., Ding, L. and Zhu, J.K. (1996a) *SOS1*, a genetic locus essential for salt tolerance and potassium acquisition. *Plant Cell*, **8**, 617-627.

Wu, Y., Hiratsuka, K., Neuhaus, G. and Chua, N.H. (1996b) Calcium and cGMP target distinct phytochrome-responsive elements. *Plant J*, **10**, 1149-1154.

Wu, Y., Kuzma, J., Marechal, E., Graeff, R., Lee, H.C., Foster, R. and Chua, N.H. (1997) Abscisic acid signaling through cyclic ADP-ribose in plants. *Science*, **278**, 2126-2130.

Xiong, L., Lee, B., Ishitani, M., Lee, H., Zhang, C. and Zhu, J.K. (2001) FIERY1 encoding an inositol polyphosphate 1-phosphatase is a negative regulator of abscisic acid and stress signaling in *Arabidopsis*. *Genes Dev*, **15**, 1971-1984.

Xiong, L., Lee, H., Ishitani, M., Tanaka, Y., Stevenson, B., Koiwa, H., Bressan, R.A., Hasegawa, P.M. and Zhu, J.K. (2002a) Repression of stress-responsive genes by FIERY2, a novel transcriptional regulator in *Arabidopsis*. *Proc Natl Acad Sci U S A*, **99**, 10899-10904.

Xiong, L., Schumaker, K.S. and Zhu, J.K. (2002b) Cell signaling during cold, drought, and salt stress. *Plant Cell*, **14 Suppl**, S165-183.

Xiong, L. and Zhu, J.-K. (2002a) *Salt tolerance*. Rockville, MD: American Society of Plant Biologists.

Xiong, L. and Zhu, J.K. (2002b) Molecular and genetic aspects of plant responses to osmotic stress. *Plant Cell Environ*, **25**, 131-139.

Yalpani, N., Enyedi, A., Leon, J. and Raskin, I. (1994) Ultraviolet light and ozone stimulate accumulation of salicylic acid, pathogenesis related proteins and virus resistance in tobacco. *Planta*, **193**, 372-376.

Yoshida, R., Umezawa, T., Mizoguchi, T., Takahashi, S., Takahashi, F. and Shinozaki, K. (2006) The regulatory domain of SRK2E/OST1/SnRK2.6 interacts with ABI1 and integrates abscisic acid (ABA) and osmotic stress signals controlling stomatal closure in *Arabidopsis*. *J Biol Chem*, **281**, 5310-5318.

Yoshioka, K., Moeder, W., Kang, H.G., Kachroo, P., Masmoudi, K., Berkowitz, G. and Klessig, D.F. (2006) The chimeric *Arabidopsis* CYCLIC NUCLEOTIDE-GATED ION CHANNEL11/12 activates multiple pathogen resistance responses. *Plant Cell*, **18**, 747-763.

Zarate, S.I., Kempema, L.A. and Walling, L.L. (2007) Silverleaf whitefly induces salicylic acid defenses and suppresses effectual jasmonic acid defenses. *Plant Physiol*, **143**, 866-875.

Zhang, X., Dai, Y., Xiong, Y., DeFraia, C., Li, J., Dong, X. and Mou, Z. (2007) Overexpression of *Arabidosis MAP kinase kinase 7* leads to activation of plant basal and systemic acquired resistance. *Plant J*, **52**, 1066-1079.

Zhu, J., Fu, X., Koo, Y.D., Zhu, J.K., Jenney, F.E., Jr., Adams, M.W., Zhu, Y., Shi, H., Yun, D.J., Hasegawa, P.M. and Bressan, R.A. (2007) An enhancer mutant of *Arabidopsis salt overly sensitive 3* mediates both ion homeostasis and the oxidative stress response. *Mol Cell Biol*, **27**, 5214-5224.

Zhu, J.K. (2001) Cell signaling under salt, water and cold stresses. *Curr Opin Plant Biol*, **4**, 401-406.

Zhu, J.K. (2002) Salt and drought stress signal transduction in plants. *Annu Rev Plant Biol*, **53**, 247-273.

Zhu, J.K. (2003) Regulation of ion homeostasis under salt stress. *Curr Opin Plant Biol*, **6**, 441-445.

Zhu, J.K., Liu, J. and Xiong, L. (1998) Genetic analysis of salt tolerance in *Arabidopsis*. Evidence for a critical role of potassium nutrition. *Plant Cell*, **10**, 1181-1191.

Zimmermann, P., Hirsch-Hoffmann, M., Hennig, L. and Gruissem, W. (2004) GENEVESTIGATOR. *Arabidopsis* microarray database and analysis toolbox. *Plant Physiol*, **136**, 2621-2632.

Zipfel, C., Robatzek, S., Navarro, L., Oakeley, E.J., Jones, J.D., Felix, G. and Boller, T. (2004) Bacterial disease resistance in *Arabidopsis* through flagellin perception. *Nature*, **428**, 764-767.